

DAMAGE BOOK

UNIVERSAL
LIBRARY

OU_156657

UNIVERSAL
LIBRARY

OUP—2273—19—11—79—10,000 Copies.

OSMANIA UNIVERSITY LIBRARY

Call No. 539.1

Accession No. 29433

Author C 815

cornwall, D. Others.

Title

This book should be returned on or before the date last marked below

THE SCIENCE AND ENGINEERING OF NUCLEAR POWER

by

Charles D. Coryell	H. H. Goldsmith
Martin Deutsch	Clark Goodman
Robley D. Evans	H. W. Ibser
Bernard T. Feld	John W. Irvine, Jr.
F. L. Friedman	W. J. Ozeroff
E. R. Gilliland	Victor F. Weisskopf
E. P. Wigner	

Edited by

Clark Goodman

Published by
ADDISON-WESLEY PRESS INC.
←
Cambridge 42, Mass.

Copyright 1947

Printed in U.S.A.

PREFACE

This publication and the second volume now in preparation contain the essentials of a series of seminars initiated at the Massachusetts Institute of Technology in October, 1946. The objective is to present the fundamentals of chain-reacting systems in terms that are understandable to the non-specialist, particularly to engineers interested in the industrial applications of nuclear energy. Progress in this field requires the coordinated effort of many branches of science and engineering, particularly during the next several years. Gradually, the responsibility will devolve to a new breed of specialists, already dubbed nuclear engineers. It is anticipated that collaborative publications of this type will assist materially in these developments.

Some words of explanation and apology are in order. By limiting consideration to declassified information or that available in the open literature, a number of prominent gaps remain. Likewise, only prewar values can be given for certain of the more important nuclear constants. Nevertheless, the free exchange of ideas which an unclassified publication makes possible should more than compensate for these limitations.

The material contained in this volume has been submitted to the U. S. Atomic Energy Commission for review by its Declassification Office and the Commission has approved publication from the standpoint of security. It should be understood that this approval relates only to security and involves no opinion as to the accuracy of the information contained in the book or as to any other matters.

An attempt has been made to systematize the notation of the various authors, but this has not been entirely successful. When multiple notation occurs, specific definitions are included in each chapter. In order to expedite publication, incomplete references and acknowledgments have been

made. However, it should be obvious that the bulk of the scientific and technical information has been drawn from many sources. The individual authors claim originality largely in the manner of presentation.

For permission to include previously published material, acknowledgment is made to the American Chemical Society for Figures 1-31 and 7-2; to the National Research Council of Canada for Figures 8-11, 8-12 and 8-13; to the Journal of Applied Physics for Chapter 4; to The Physical Review for Figures 9-3 and 9-4; and to the Reviews of Modern Physics for the cross section curves in Appendix C. The isotope chart, Figure 1-6, was kindly furnished by Dr. E. Segré. Appendix A is included through the courtesy of Dr. H. A. Bethe.

Mr. P. H. Lund and Mrs. Grace Rowe contributed much of the original drafting work. The secretarial assistance of Mrs. Charlotte Nichols, Miss Estelle Jenney, and Miss Ruth Deininger is gratefully acknowledged. Mrs. Olga Crawford and Mr. James Sterling have been unusually helpful in the editorial preparation of the material. Without the generous support and encouragement of Professors J. C. Slater and J. R. Zacharias, it would not have been possible to conduct the seminars on which these chapters are based.

Cambridge, Mass.
September, 1947.

Clark Goodman

TABLE OF CONTENTS

Chapter		Page
1	Fundamentals of Nuclear Physics by Robley D. Evans	1
2	The Fission Process by Martin Deutsch	75
3	Neutron Diffusion by Victor F. Weisskopf	87
4	Nuclear Chain Reactions by E. P. Wigner	99
5	Elementary Pile Theory by F. L. Friedman	111
6	The Application and Experimental Basis of Pile Theory by Bernard T. Feld	187
7	Chemistry of the Fission Process by Charles D. Coryell	231
8	Control and Operation of a Pile by W. J. Ozeroff	251
9	Construction of Nuclear Reactors by Clark Goodman	273
10	Heat Transfer by E. R. Gilliland	323
11	Heavy Elements and Nuclear Fuels by John W. Irvine, Jr.	353
Appendix A	Table of Precise Masses	379
Appendix B	Loss of Energy in Elastic Collisions	386
Appendix C	Neutron Cross Sections of the Elements by H. H. Goldsmith, H. W. Ibser, B. T. Feld	387
	List of Illustrations	503
	Index	

CHAPTER 1
FUNDAMENTALS OF NUCLEAR PHYSICS
by
Robley D. Evans

1-1 Size of Nuclei

It will be recalled that atoms have diameters of about 10^{-8} cm and are composed of one or more electrons surrounding a central core or nucleus. These electrons are bound inside the atom by the electrostatic attraction of their negative charge for the positive charge of the nucleus. As we shall see, the binding energy of these atomic electrons is much less than that between the particles in the nucleus (nucleons) and, in fact, is usually negligible in most considerations in nuclear physics. In spite of the continued statements found in elementary physics textbooks, it has been definitely established that there are no electrons in nuclei (${}^7_1\text{N}^{14}$ outstanding example). All nuclei consist of two types of particles of nearly equal mass, neutrons and protons. In terms of modern theory, these two particles represent different quantum states of a single fundamental particle, the nucleon.

A neutron has no electric charge; a proton has a positive charge, equal in magnitude but opposite in sign to that of an atomic electron. The simplest nucleus - that of hydrogen ${}_1^1\text{H}^1$ - consists of a single proton. All other nuclei contain a mixture of neutrons and protons, with the proportion of neutrons increasing with the atomic weight of the nucleus. The largest naturally occurring nucleus is that of ${}_{92}^{238}\text{U}$, which contains 92 protons and $238 - 92 = 146$ neutrons. The diameter of this nucleus is only about 7 times the diameter of its individual nucleons.

Between ${}_1^1\text{H}^1$ and ${}_{92}^{238}\text{U}^{238}$ there are a large number of species of nuclei, as indicated in Figure 1-1. In spite of the rather broad variation in the number of neutrons and protons, all of these nuclei have nearly the same nuclear density ρ (about 10^{14} grams per cc). While there are some periodicities in nuclear characteristics, these are completely independent of and much less pronounced than the chemical periodicities of atoms.

1-2 Nuclear Charge Z

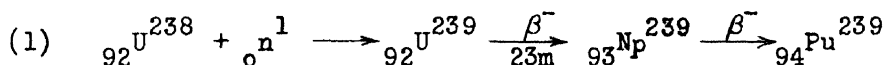
The nuclear charge, or atomic number Z , equals the number of protons in the nucleus. This important integral quantity may be determined in a variety of ways, among the more important of which are: (a) Moseley K and L

Figure 1-1. Naturally Occurring Nuclei. In this diagram the vertical scale is the number of "binding" neutrons B in the nucleus which is equivalent to $A - 2Z$, where A is the mass number. The horizontal scale is the atomic number Z which equals the number of protons in the nucleus. The squares represent naturally occurring stable nuclei, while the circles represent naturally occurring radioactive nuclei. An average curve through the tabulated nuclei follows roughly the relation, $B \propto A^{5/3}$.

Other charts of nuclei have different coordinates which emphasize other properties. $A - Z$ is often plotted versus Z . Less frequently, A is plotted against Z . Once the coordinates are ascertained, the various relationships become clear.



x-ray spectra, (b) Rutherford alpha-ray scattering experiments, and (c) the displacement law. Important examples of the displacement law are the nuclear transitions that take place following radiative capture of neutrons by ${}_{92}\text{U}^{238}$:



The nuclear charge Z which equals 92 in uranium, as indicated by the subscripts, changes to 93 upon the emission of a negative beta ray (β^-), thereby resulting in the formation of a nucleus of the element neptunium (Np). This nucleus, in turn, spontaneously emits a β^- resulting in a nucleus of plutonium (Pu) with $Z = 94$. Since neutrons (${}_0\text{n}^1$) have zero nuclear charge, their $Z = 0$. The superscripts are the mass number A discussed below. Since the mass of a beta ray is very small compared to the mass of a nucleon, A does not change during the emission of a β^- .

1-3 Mass Number A

The number of nucleons in a nucleus is represented by the integral mass number A . As seen in Figure 1-1, some 275 species of stable nuclei are known. With the exception of $A = 5$ and $A = 8$, all values of A from 1 to 209 are represented by known stable nuclei. With the exception of elements $Z = 43$ and $Z = 61$, stable nuclei with atomic numbers from 1 to 83 inclusive are found in nature. Nuclei of the same Z but different A are called isotopes. Since isotopes are different forms of the same element, they have essentially the same chemical properties, and hence cannot be separated by chemical methods. The proportion of the different isotopes of a given element can be determined either from band spectra, hyperfine structure, or by means of mass spectrometers. The latter also provide a precise method of determining the relative mass, i.e., the atomic weight, of the individual isotopes of many elements.

A useful relation for estimating a nuclear radius R is:

$$(2) \quad R = 1.5 \times 10^{-13} A^{1/3} \text{ cm } (\pm \sim 10\%)$$

The radius as here defined is the distance at which the nuclear Coulombian repulsion for positively charged particles just equals the nuclear attractive force that sets in at such small distances.

1-4 Isotopic Mass M

The exact mass of a neutral atom M is one of the most important quantities in nuclear physics. It is referred to an arbitrary assignment* of ${}_8\text{O}^{16} = 16.00000$. The differences in mass of nuclei enter into many computations, and it is desirable to know the individual nuclear masses to five or six decimal places.

The mass of deuterium ${}_1\text{H}^2$ is well established from doublet measurements in mass spectrometers. Using the Einstein relation:

$$(3) \quad \Delta E = (m - m_0)c^2 = \Delta mc^2$$

and measurements of the kinetic energy of protons emitted in the following nuclear reaction:



the mass M_n of the neutron has been determined with considerable accuracy.

Conversion factors and numerical values are as follows:

1 amu (atomic mass unit) = 931 Mev (million electron volts)

1 ev (electron volt) = 1.60×10^{-12} erg

1 Mev (million electron volt) = 1.60×10^{-6} erg

1 watt = 6.25×10^{12} Mev/sec

$m_0c^2 = 0.51$ Mev, = 0.00055 amu (where $m_0 \equiv$ rest mass of an electron)

In nuclear reactions such as (4) the Q value is the kinetic energy of the disintegration products in excess of the kinetic energy of the incident particles. Neutral atomic masses are generally used instead of nuclear masses in calculating Q values, since the electronic masses on each side of the reaction balance out, except when positrons (β^+) are emitted. In (4):

$$\begin{aligned} \text{mass of } {}_1\text{H}^2 &= 2.01472 \\ \text{mass of } {}_1\text{H}^1 &= \underline{1.00813} \\ {}_1\text{H}^2 \text{ minus } {}_1\text{H}^1 &= 1.00659 \\ Q &= -2.18 \text{ Mev} = \underline{-0.00234} \\ \therefore \text{mass of } {}_0\text{n}^1 &= 1.00893 \end{aligned}$$

*Unfortunately, in addition to the physical scale of atomic weights as defined above, there is also a chemical scale based on the natural mixture of oxygen isotopes $\text{O} = 16.0000$. Throughout these notes, atomic weights are given on the physical scale. For purposes of conversion: physical mass = $1.00027 \times$ chemical mass.

1-5 Total Angular Momentum

The total angular momentum quantum number I of a nucleus, taken about its internal axis, is the vector sum of the orbital angular momentum ℓ and spin angular momentum s of each proton and neutron in the nucleus. The manner in which the values of ℓ and s are added depends on the type of interaction or coupling assumed between the particles. But I is always a positive quantity or zero. The total nuclear angular momentum is $(h/2\pi)\sqrt{I(I+1)}$, and its maximum observable component in any direction, such as along an external magnetic field, is $I(h/2\pi)$.

For present purposes the important consideration is that angular momentum is always conserved in nuclear transitions. The vector difference between the initial value I and the final value I' must be possessed by a particle or quantum absorbed or emitted in the transition.

1-6 Parity

The parity of a system of elementary particles is a fundamental property of the motion according to the wave-mechanical description, but it has no simple analogue in ordinary mechanics.

The physical description of a particle or system of particles cannot depend, for example, on whether we are right-handed or left-handed. Hence the absolute value of the wave function ψ must be the same in coordinates (x, y, z, s) as in the coordinates $(-x, -y, -z, s)$ -- three spatial and one spin. This transformation of coordinates is equivalent to "reflecting the particle at the origin" in the (x, y, z) system, an operation which must either leave the wave function unchanged, or only change its sign, so that its squared absolute value remains unaltered in either case.

To a good approximation ψ is the product of a function depending on space coordinates and a function depending on spin orientation. When reflection of the particle at the origin does not change the sign of the spatial part of ψ , the motion of the particle is said to have even parity. When reflection changes the sign of the spatial part of ψ , the motion of the particle is said to have odd parity. It can be shown that the spatial part of ψ , on reflection of the particle, does not change sign, if ℓ is even, but does change sign if ℓ is odd. Hence for a particle with an even value of ℓ the motion has even parity, and with an odd value of ℓ the motion has odd parity.

For a system of particles the wave function becomes approximately the product of the wave functions (or a linear combination of such products) for the several particles, $\psi = \psi_1 \psi_2 \psi_3 \dots$. Hence the parity of a system of particles such as a nucleus will depend on the parity of the motion of its individual particles.

Visualizing reflection of the system as the successive individual reflection of each particle, one at a time, we conclude that a system will have even parity when the sum of the numerical values of ℓ for all its particles $\Sigma \ell$ is even, and odd parity when $\Sigma \ell$ is odd. A system containing any number of even parity particles and an even number of odd parity particles will have even parity. A system with any number of even parity particles and an odd number of odd parity particles will have odd parity. The intrinsic parity of a single elementary particle (proton, neutron, electron, photon, neutrino) is even, since $\ell = 0$ for the isolated particle.

Parity is always conserved. Thus the parity of a system (e.g., a nucleus) can only be changed by the capture of photons or particles having odd total parity (intrinsic parity plus parity of motion with respect to the initial system), or by the emission of photons or particles having odd total parity.

The selection rules for all nuclear transitions involve a statement of whether or not the nucleus changes parity as a result of the transition. Thus the notation "yes" denotes that the nuclear parity changes (from even to odd, or from odd to even); hence that the emitted or absorbed particles or quanta have odd total parity. For example an emitted quantum, having $\ell = 1$ with respect to the emitting nucleus, will have odd parity, and can be emitted only if the nuclear parity changes. Similarly the selection rule "no" means that the initial and final nucleus have the same parity (both even, or both odd). An emitted quantum, having $\ell = 0$, or 2, with respect to the emitting nucleus, will have even parity, and can only be emitted if the nuclear parity does not change.

1-7 Statistics of Nuclei

The concept of statistics arises from considerations of the effect on the wave function of the interchange of all the coordinates of two identical particles.

In the Fermi-Dirac statistics: (1) the Pauli Exclusion Principle holds, and the number of particles per quantum state is limited to one, (2) the wave function of the system of particles is "antisymmetrical", that is, it changes sign when all the coordinates (three spatial and one spin) of any pair of identical particles are interchanged. It is found experimentally that all "fundamental" particles - positron, electron, proton, neutron, neutrino - obey Fermi-Dirac statistics, as do also all nuclei of odd mass number A ; e.g., H^1 , Li^7 , F^{19} , Na^{23} , etc.

In the Einstein-Bosé statistics: (1) two or more particles may be in the same quantum state, (2) the wave function is "symmetrical", that is, it does not change sign when all the coordinates of any pair of identical particles are interchanged. All nuclei having even mass number A , have Einstein-Bosé statistics; e.g., H^2 , C^{12} , N^{14} , O^{16} , etc.

Due to the conservation of angular momentum, all systems having an odd number of particles will also have an odd half-integer total angular momentum ($1/2, 3/2, 5/2, \dots$). Similarly, all systems having an even number of particles will have even half-integer total angular momentum ($0, 1, 2, \dots$). Thus we have, in tabular form:

<u>Mass Number</u>	<u>Nuclear Angular Momentum</u>	<u>Statistics</u>
Odd	$1/2, 3/2, 5/2, \dots$	Fermi-Dirac
Even	$0, 1, 2, \dots$	Einstein-Bose

1-8 Magnetic Dipole Moment

We may obtain a physical understanding of the orbital part of the magnetic dipole moment, due to a single moving particle such as a proton, by considering the proton as moving in a plane circular orbit. Then in two dimensions, the orbital angular momentum $Mr^2\omega = \ell h/2\pi$ (M = mass of the particle, r = radius of the circular orbit, ω = angular velocity). The circular motion of a charge e (electrostatic units) is equivalent to a circular current $i = e\omega/2\pi c$ (electromagnetic units), and acts as a magnetic shell with a classical magnetic dipole moment $\mu_\ell = i\pi r^2$. Eliminating i and r^2 , we obtain

$$\mu_\ell = \frac{\ell eh}{4\pi Mc} = \ell \mu_0$$

where

$$\mu_0 = eh/4\pi Mc$$

is the nuclear magneton. From this elementary derivation, the complete

analogy between the nuclear magneton and the Bohr magneton for orbital atomic electrons is evident. The only difference is that the nuclear magneton involves the proton mass M and is therefore about 1840 times smaller than the Bohr magneton, which contains the electron mass.

The magnetic moment is taken as positive if its direction with respect to the angular momentum vector corresponds to the rotation of a positive electrical charge.

The magnetic dipole moment associated with the spin of the elementary particles cannot be derived in this simple fashion, because the distribution of electricity in the particles is unknown. The magnetic moment for the spinning elementary particle must be obtained from experiment. Whereas the magnetic moment of the electron is minus one Bohr magneton, in agreement with the Dirac electron theory, the magnetic moment of the proton has the anomalous value of 2.7896 nuclear magnetons. Therefore, the Dirac theory cannot be applied to the proton. The magnetic moment of the free neutron is $-1.9103 \mu_0$.

1-9 Electric Quadrupole Moment

We can visualize the atomic nucleus as an approximately spherical assembly of neutrons (charge, zero) and protons (charge, $+e$). If the charge due to the protons is not perfectly symmetrically distributed, the nucleus will possess a net electric quadrupole moment. Both positive and negative nuclear quadrupole moments are to be expected. Positive moments correspond to an elongation of the nuclear charge distribution along the axis of nuclear angular momentum I (cigar-shaped distribution). Negative quadrupole moments correspond to a flattened or oblate distribution of positive charge (plate-like distribution).

The value of the nuclear electric quadrupole moment, q , is the time average of the position of one asymmetric proton with respect to the (z) axis of total nuclear angular momentum I ; that is:

$$q = \langle 3z^2 - r^2 \rangle_{av}$$

where r is the radial distance of the proton from the center of the nucleus. Then q has the dimensions of cm^2 , and is usually of the order of magnitude of the square of the nuclear radius, say 10^{-26} to 10^{-24} cm^2 , corresponding to the asymmetric placement of one or, at most, a few protons in heavy nuclei. The electric quadrupole moment of the deuteron is $0.278 \times 10^{-26} \text{ cm}^2$.

1-10 Binding Energy E

In the simplest terms, the binding energy E of a nucleus can be thought of as the amount of work necessary to pull the nucleus apart into its individual neutrons and protons. Conversely, E is the energy given off in assembling the nucleus from separate neutrons and protons. In the foregoing notation E is given by

$$(5) \quad E = Zm_H + (A - Z)m_n - M$$

where $m_H \equiv$ the mass of a neutral hydrogen atom (1.00813) and $m_n \equiv$ the mass of a neutron (1.00893). Introducing a quantity known as the packing fraction P , defined as

$$(6) \quad P = (M - A)/A; \quad \text{or} \quad M = A(1 + P)$$

and substituting the precise experimental values for m_H and m_n

$$(7) \quad E/A = (Z/A)(m_H - m_n) + (m_n - 1) - P$$

$$= -0.00080Z/A + 0.00893 - P \quad \text{amu}$$

The ratio E/A is the average binding energy per nuclear particle, generally expressed in Mev/nucleon. The value of E/A as a function of A follows a curve of the form given in Figure 1-2. If the forces between nucleons were long-range, e.g., inverse-square, the total binding energy would be proportional to A^2 , and E/A would be proportional to A . The average binding energy per nucleon is approximately constant, showing that the important forces between nucleons are short-range exchange forces. There is evidence for forces of mutual polarization, or van der Waal's forces, as well as Coulomb repulsion between protons, and a marked deficiency of total binding energy in the lighter nuclei having a larger surface per unit volume. The lighter nuclei show marked periodicities in E/A , with maximum values at $A = 4, 8, 12, 16$, etc., showing the existence of Pauli four-shells and the saturated character of a nuclear sub-unit containing 2 neutrons and 2 protons. The marked variations in E/A among the lightest nuclei represent possible sources of nuclear energy. The energy released in nuclear fission, to be discussed in detail later, is seen to arise from the difference in binding energy between heavy and middle weight nuclei, which amounts to about 1 Mev per nucleon, or about 200 Mev per fission.

The binding force between any two nucleons is a short-range, non-gravitational, nonelectric force, known as the "specifically nuclear force." One fairly successful theoretical description of the observed force is in terms of an exchange force described by a meson potential of the form

$$U = (A/r)e^{-r/a}$$

where U is the potential energy between two nucleons at a separation r , A is a constant, and the "range" of the force is $a = \hbar/\mu c \approx 2 \times 10^{-13}$ cm for a meson mass μ equal to about 200 times the rest-mass of an electron.

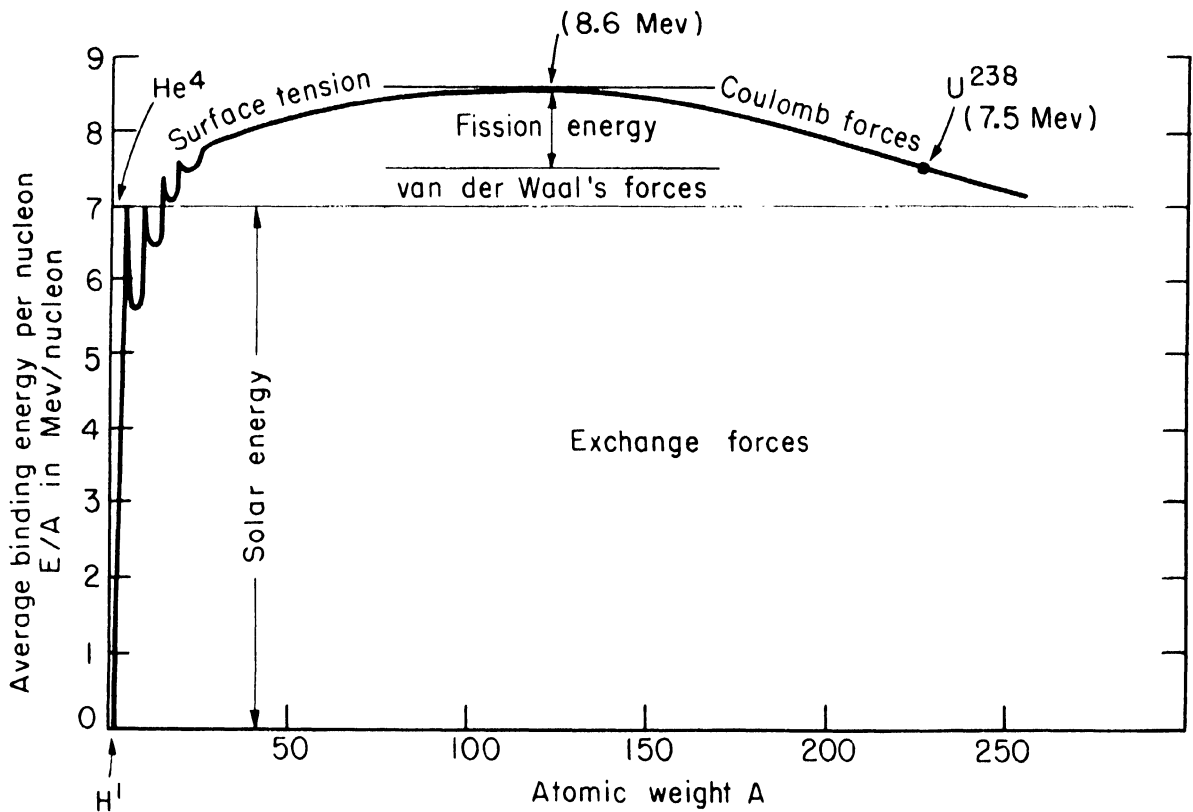


Figure 1-2. Binding Energy of Nuclei. The main features in the variation of the average binding energy per nucleon E/A and the nature of the nuclear forces which they suggest are indicated schematically. Numerical values for a range of nuclei are:

Nucleus	n	H ¹	H ²	H ³	He ³	He ⁴	A ⁴⁰ - Sn ¹²⁰	U ²³⁸
E	0	0	2.18	8.3	7.5	28.2		1780
E/A	0	0	1.09	2.8	2.5	7.0	~8.6	7.5

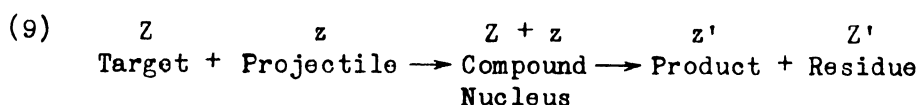
The magnitude of the attractive force (p, n) between a proton and a neutron is greater in the triplet state when the spins of the p and n are parallel $(p \uparrow \uparrow n)$, than in the singlet state when the spins are antiparallel $(p \uparrow \downarrow n)$, as is shown by the fact that the ground state of the deuteron is the triplet state. The attractive force between two neutrons (n, n) or between two protons (p, p) can only be a singlet force, with the spins of the two nucleons antiparallel, because the Pauli exclusion principle forbids the triplet state for identical particles. Considerations of the measured binding energy of H^3 and He^3 show that $(n, n) = (p, p)$. Comparisons of the scattering of fast neutrons in hydrogen and fast protons in hydrogen show that the $(p \uparrow \downarrow n)$ singlet force equals the (p, p) singlet force. Thus we have: $(p \uparrow \uparrow n) > (p \uparrow \downarrow n) = (p, p) = (n, n)$.

1-11 Nuclear Reactions

At distances r , large compared to the nuclear radius R , positively-charged particles such as protons, $({}_1H^1)^+$, deuterons $({}_1H^2)^+$, and alphas $({}_2He^4)^{++}$ experience a Coulombian repulsion according to the familiar relationship

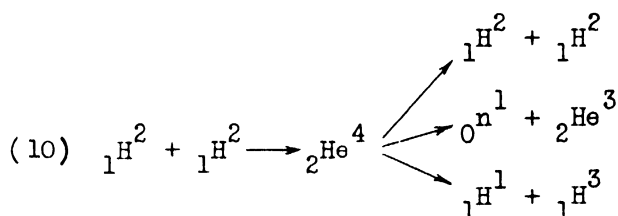
$$(8) \quad F = zeZe/r^2$$

where z and Z represent the atomic number of the projectile particle and target nucleus respectively, F is the force and e is the magnitude of the unit electric charge (4.80×10^{-10} esu or 1.6×10^{-19} coulomb). If the projectile particle has sufficient kinetic energy, it penetrates inside the nuclear radius, where it experiences the strong, short-range attractive force. The projectile coalesces momentarily with the target nucleus, forming an excited compound nucleus. In general, the lifetime of the compound nucleus is very short ($\leq 10^{-11}$ seconds), and the composite splits into a product particle and a residual nucleus which may or may not be identical with the incident projectile particle and target nucleus. If these are identical, the process is called scattering, which may be either elastic or inelastic, depending on whether the product particle leaves the target nucleus in an unexcited or excited state respectively. Schematically, the reaction can be represented as:



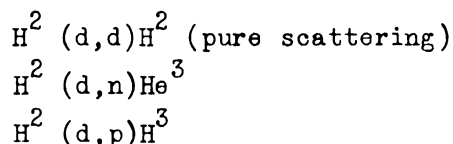
It has been established from cloud chamber photographs that both momentum and total energy are conserved in individual collisions.

The following are important examples of reactions that take place in cyclotrons, linear accelerators, and other high energy machines using deuterons as projectiles. The target nuclei are previous projectile deuterons that have become imbedded in the metallic target surface during the previous bombardment.



There are three possible modes of splitting of the highly-excited compound nucleus ${}_2\text{He}^4$. The first mode results in scattering, while the other two form new products and new residue nuclei. Under controlled conditions this reaction provides a convenient intense source of essentially monoenergetic neutrons when a narrow angle of the secondary beam is selected. The three modes of the reaction compete with one another. In general, the proportion of each is dependent on a number of factors, including the energy of the projectile particles, the Q value and angular momentum change of each mode, and the distribution of energy levels in the compound nucleus.

A condensed method of writing nuclear reactions is more commonly used. For example, the above three reactions would be:



In the parentheses, $d \equiv \text{H}^2$ a deuteron and $p \equiv \text{H}^1$ a proton. The subscripts are omitted because the chemical symbol gives a unique assignment of Z.

1-12 Potential Barrier

In the d on d reactions considered above, the projectile and the target are equal in mass. Hence the compound nucleus will receive a velocity equal to exactly half the velocity of the projectile particle. When viewed in the ordinary laboratory coordinates, the motion of the product and

residue particles will be strongly influenced by the motion of the compound nucleus. In terms of the center of mass system of coordinates, the compound nucleus is at rest. Similarly, if the mass of the target nucleus is much greater than that of the projectile particle, the velocity of the compound nucleus is generally small enough to be neglected. Nuclear potential barriers, as considered here, refer to a center-of-mass or heavy-target set of coordinates.

Figure 1-3 gives a qualitative representation of the potential energy U of a positively-charged (ze) particle in the field of a nucleus of charge $+Ze$.

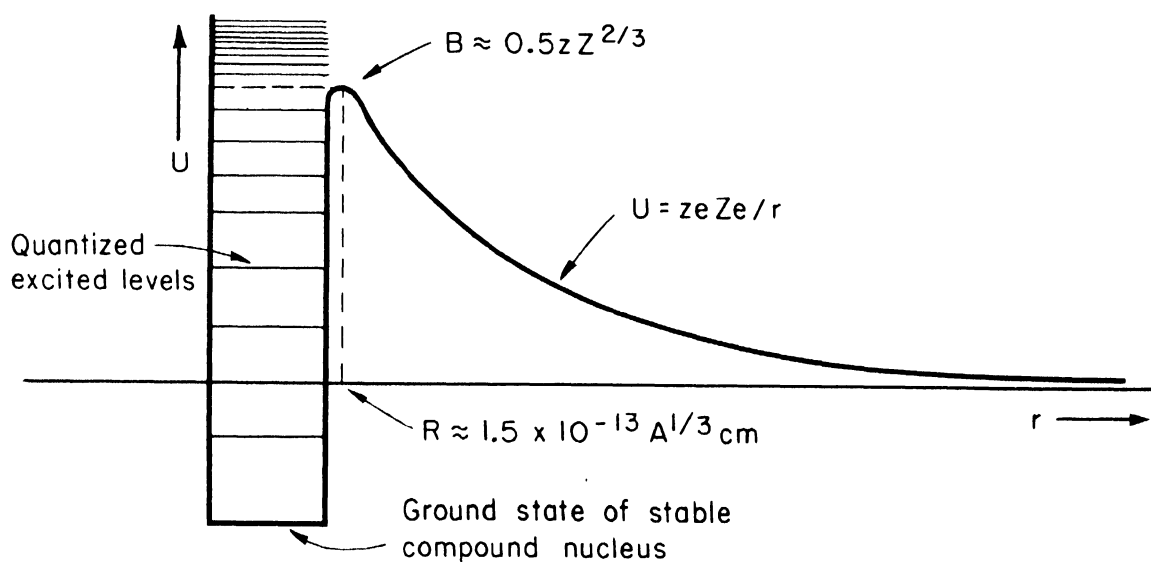


Figure 1-3. Nuclear Potential Barrier for Positively-Charged Particles

It is seen that for distances r greater than the previously defined nuclear radius R , the potential is that of a Coulombian field, i.e., inversely proportional to r . For distances less than R , the potential decreases rapidly to a fixed negative value representing the ground state of the stable compound nucleus (assuming it has a stable ground state). Inside this potential hole of the nucleus are numerous quantized excited energy levels above the ground state.

The wave properties of nuclear particles make it possible for the incident particle to penetrate the potential barrier or, conversely, for a similar particle to escape from inside the nucleus, even though the energy

is less than the barrier height B .^{*} If the energy of the incident particle is much less than B , the probability P for this penetration is

$$(11) \quad P = (k/v^2) \exp - (4\pi e^2 zZ/hv)$$

where $k \equiv$ a constant and $v \equiv$ the velocity of the incident particle. This expression indicates the importance of the parameters z , Z , and v .

In contrast to charged particles, neutrons experience no repulsion in the vicinity of nuclei. The potential is essentially negative out to large values of r and follows roughly the shape shown in Figure 1-4.

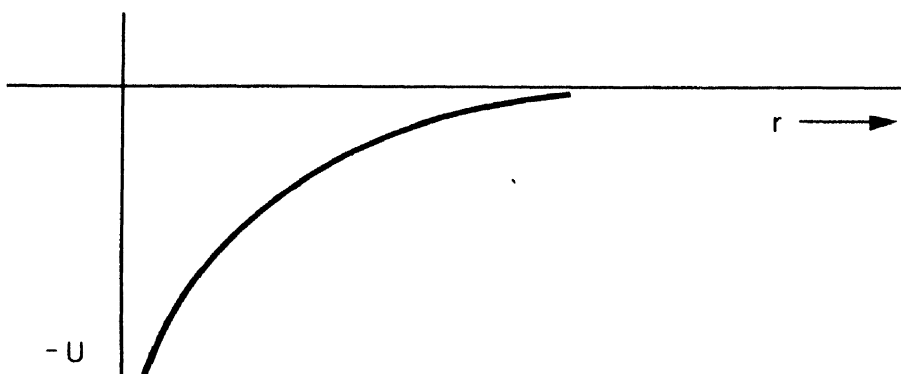


Figure 1-4. Nuclear Potential for Neutrons

1-13 Nuclear Cross Sections

Instead of complex probability relationships, the interactions between projectile particles and nuclei are expressed very simply in terms of nuclear cross sections. The meaning of cross section is best understood in terms of an example. If we imagine** a beam of neutrons incident from the left on a nucleus A , as shown in Figure 1-5, a certain fraction of the neutrons will be removed from the beam by A .

By definition the fraction of neutrons, contained in 1 cm^2 of the beam, that is intercepted by the single nucleus A is called the total cross section σ of A for such neutrons. The atomic electrons play no role in these interactions. Scattering and absorption are the most common types of interaction

^{*} B is about 0.5 Mev for protons or deuterons on hydrogen and about 10 Mev for protons on uranium.

^{**}It is more exact to consider the neutrons as comprising a plane wave with deBroglie wave length $\lambda = h/mv$.

between nuclei and neutrons. The separate cross sections for these two processes are designated σ_s and σ_a . If no other important interactions take place, $\sigma = \sigma_s + \sigma_a$. At a later time other cross sections, such as those for fission σ_f , inelastic scattering σ_s (inel) and transport σ_{tr} , will be defined. The dimensions for each of these, as the name implies, is an area per nucleus, usually $\text{cm}^2/\text{nucleus}$. Because most of these cross sections are about $10^{-24} \text{ cm}^2/\text{nucleus}$ in magnitude, this area has been dubbed the "barn", i.e., 1 barn = $10^{-24} \text{ cm}^2/\text{nucleus}$. The size of nuclear cross sections cannot be predicted from the present theoretical knowledge but are obtained from a variety of experimental determinations. As examples of the large differences that can exist between similar nuclei:

$$\sigma_a({}_1\text{H}^1) = 0.31 \text{ barn and } \sigma_a({}_1\text{H}^2) = 0.00065 \text{ barn for thermal neutrons.}$$

In pile theory it is convenient to use a macroscopic cross section Σ instead of the nuclear or microscopic cross section σ . Physically, Σ is the cross section per cc of the material and is simply:

$$\Sigma = \sigma N \left(\frac{\text{cm}^2}{\text{nucleus}} \times \frac{\text{nuclei}}{\text{cm}^3} \right)$$

where N is the number of nuclei/cc which equals the number of atoms/cc. The dimension of Σ is that of a reciprocal length, cm^{-1} , which is equivalent in the case of absorption to a linear absorption coefficient. It is also seen that $1/\Sigma$ has the dimension of a length, cm, which can be identified as a mean-free-path λ .

When applied to a target of thickness x , the emergent intensity I is related to the incident intensity I_0 , usually in neutrons/ $\text{cm}^2 \text{ sec}$, by

$$(12) \quad I = I_0 e^{-x\Sigma} = I_0 e^{-x/\lambda}$$

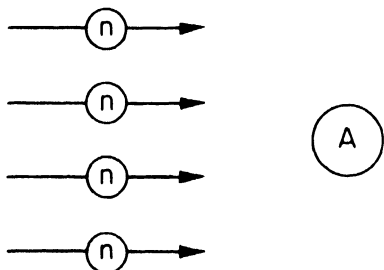


Figure 1-5. Schematic diagram of neutron beam incident on nucleus A.

For example, arsenic is monoisotopic (As^{75}) with a $\sigma = 4.6$ barns, density $\rho = 4.7$ grams/cc. Hence, $N = 0.0377 \times 10^{24}$ atoms/cc and $\Sigma = \sigma N = 4.6 \times 10^{-24} \times 0.0377 \times 10^{24} = 0.174 \text{ cm}^{-1}$. Therefore, $I/I_0 = e^{-0.174x} \approx 1 - 0.174x$ for small thicknesses. It is seen that a sheet of arsenic 1 mm in thickness attenuates a thermal neutron beam by about 1.7 per cent. Because of the much larger cross section of cadmium, $\sigma = 2500$ barns, a thickness of 1 mm attenuates a thermal neutron beam by nearly 100 per cent, i.e., is essentially "black" to thermal neutrons.

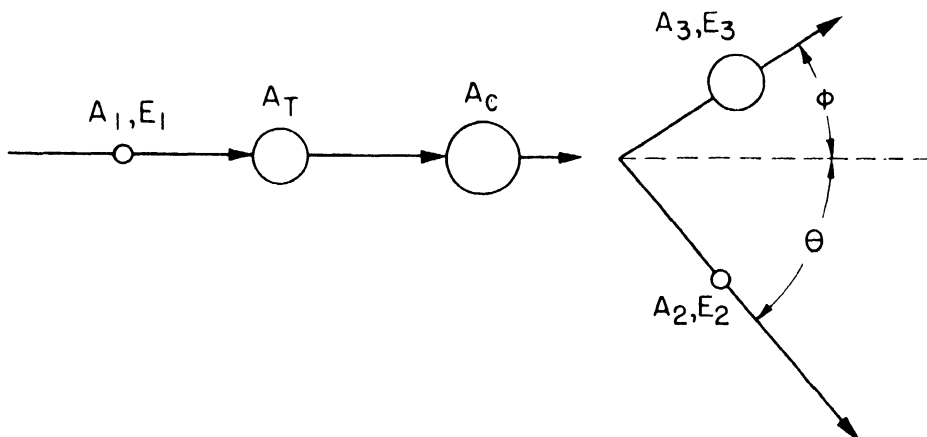
1-14 Nuclear Q Values

In Section 1-4 the Q value of a nuclear reaction was defined as the kinetic energy of the disintegration products in excess of the kinetic energy of the incident particles. Q can also be considered as the energy given to the reaction by the net change in rest mass. Hence, this reaction energy can be computed from knowledge of exact masses or, conversely, precise determinations of isotopic masses may be obtained from disintegration data. Since such considerations are important in problems associated with nuclear reactors, the general relations are summarized below with the previous d on d reactions cited as numerical examples.

$A_T, A_C, A_1, A_2, A_3 \equiv$ mass number of target, compound, projectile, product and residue nuclei respectively.

$E_1, E_2, E_3 \equiv$ kinetic energy of projectile, product and residue nuclei respectively.

$M_T, M_1, M_2, M_3 \equiv$ exact masses of target, projectile, product, and residue nuclei respectively.



$$E = \frac{1}{2} A v^2$$

$$p = A v = \sqrt{2AE}$$

$$(13) \quad \begin{aligned} \sqrt{2A_1 E_1} &= \sqrt{2A_2 E_2} \cos \theta + \sqrt{2A_3 E_3} \cos \phi \\ 0 &= \sqrt{2A_2 E_2} \sin \theta - \sqrt{2A_3 E_3} \sin \phi \\ E_1 + Q &= E_2 + E_3 \end{aligned}$$

$$(14) \quad Q = \left[(M_1 + M_T) - (M_2 + M_3) \right] c^2$$

$$(15) \quad Q = E_2 \left(1 + \frac{A_2}{A_3} \right) - E_1 \left(1 - \frac{A_1}{A_3} \right) - \frac{2 \sqrt{A_1 A_2 E_1 E_2}}{A_3} \cos \theta$$

E_2 greatest for $\theta = 0$; least for $\theta = 180^\circ$ (backward)

$$\text{e.g.} \quad {}_1\text{H}^2 + {}_1\text{H}^2 \longrightarrow {}_1\text{H}^1 + {}_1\text{H}^3 + Q$$

$$\begin{array}{rcl} \text{H}^2 & = & 2.01472 \\ \text{H}^2 & = & 2.01472 \\ \hline 2\text{H}^2 & = & 4.02944 \\ \text{H}^3 + \text{n} & = & 4.02518 \\ \hline Q & = & 0.00426 \left(\frac{931 \text{ Mev}}{\text{amu}} \right) = 3.96 \text{ Mev} \end{array} \quad \begin{array}{rcl} \text{H}^3 & = & 3.01705 \\ \text{H}^1 & = & 1.00813 \\ \hline \text{H}^3 + \text{H}^1 & = & 4.02518 \end{array}$$

$$\text{and e.g.} \quad {}_1\text{H}^2 + {}_1\text{H}^2 \longrightarrow \text{n} + {}_2\text{He}^3 + Q$$

$$A_1 = 2 \quad A_T = 2 \quad A_2 = 1 \quad A_3 = 3$$

$$\begin{array}{rcl} \text{H}^2 & = & 2.01472 \\ \text{H}^2 & = & 2.01472 \\ \hline 2\text{H}^2 & = & 4.02944 \\ \text{He}^3 + \text{n} & = & 4.02604 \\ \hline Q & = & .00340 \left(\frac{931 \text{ Mev}}{\text{amu}} \right) = 3.16 \text{ Mev} \end{array} \quad \begin{array}{rcl} \text{He}^3 & = & 3.01711 \\ \text{n} & = & 1.00893 \\ \hline \text{He}^3 + \text{n} & = & 4.02604 \end{array}$$

From Equation (15), at an angle $\theta = 90^\circ$ with the direction of the incident particles, the second of these reactions gives a monochromatic neutron source with $E_2 = f(\theta, E_1)$ given by:

$$\begin{aligned}
 (16) \quad E_n = E_2 &= \frac{A_3}{A_3 + A_2} \left[Q + \frac{A_3 - A_1}{A_3} E_1 \right] \\
 &= \frac{3}{3 + 1} \left[3.16 + \frac{3 - 2}{3} E_1 \right]
 \end{aligned}$$

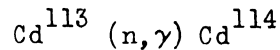
or if $E_1 = 2.58$ Mev, $E_2 = 3$ Mev. It is seen that the neutrons emitted from the target at 90° have more kinetic energy than the incident deuterons. In the forward direction the neutron energies will be larger than, and in the backward direction less than, 3 Mev.

1-15 Types of Nuclear Reactions

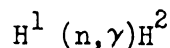
In the summary below nuclear reactions are systematized according to the projectile particle producing the reaction. Only those types are included for which two or more examples are known - more generally, 50 to 100 examples may be well established. Also all reactions are excluded which consist simply of capture and remission and are therefore of the character of elastic or inelastic scattering.

Neutron Reactions

(n, γ) The simplest type is that in which a neutron is captured and no heavy particle is emitted, but instead a gamma ray (γ) is emitted to conserve mass-energy. This reaction is extremely common in all types of chain-reacting systems, especially those containing slow neutrons. A few examples are:

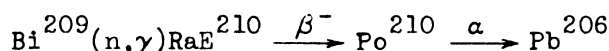


As seen in Figure 1-6, Cd has an unusually large absorption cross section σ_a of 2500 barns per average nucleus. It has recently been established that practically the entire absorption is attributable to the isotope $A = 113$, which has an abundance of 12.3 per cent. Hence $\sigma_a(\text{Cd}^{113}) = 20,000$ b. Because of this reaction Cd is a useful material in control rods and for slow neutron shielding.



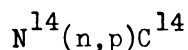
This reaction has a cross section $\sigma_a = 0.31$ barn and occurs in appreciable amounts in all reactors in which water is used as a coolant (as in the Hanford piles), as a moderator (as in the Los Alamos water boiler), or

in shielding material (as in the concrete of the Clinton pile). With thermal neutrons the gamma ray energy is 2.18 Mev.



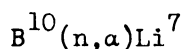
Although the absorption cross section σ_a is only about 0.016 barn for Bi, this reaction would produce significant amounts of RaE and hence Po if Bi were used as a coolant in a slow neutron reactor. The α rays from the Po (half-period 140 days) would continue to produce heat in the coolant for some time after a shut down. In fact, if separated from the Bi, Po could be used as an external heat source producing about 1/30 watt per curie or about 100 horsepower per pound. The short half-period of 140 days reduces its potential usefulness as a concentrated power source.

(n,p) Reactions of this type are more common among the elements of low Z rather than high Z. Although most (n,p) reactions have a negative Q value, $Q = +0.6$ Mev for $\text{N}^{14}(\text{n},\text{p})$, and the reaction is observed with thermal neutrons. An important example is:



This reaction has a cross section of about .02 barns for neutrons of energy between 200 and 500 kev. The C^{14} is β^- radioactive and is finding a number of applications as a radioactive tracer. It is evident that this reaction is prominent in the physiological effects produced when neutrons are absorbed in biological tissues. However, for present purposes, the main interest is that an appreciable absorption of neutrons results from this reaction in air-cooled piles (such as the graphite-uranium unit at the Clinton Laboratories).

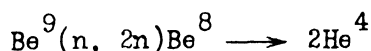
(n, α) Like the preceding reaction, this type is more common among the light elements. In heavy elements, the coulomb barrier for α emission makes the reaction improbable except for fast neutrons. The reaction



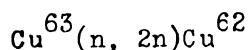
has a cross section of about 4000 barns for neutrons of .025 Mev and is inversely proportional to $\sqrt{E_n}$. From thermal neutrons, the α ray is emitted with an energy of about 2.1 Mev, which is sufficient to make detection by ionization methods relatively simple. Hence, this reaction is widely used

in slow neutron detectors such as BF_3 gas-filled proportional counters and B_4C -lined ionization chambers. Since B^{10} has an abundance of 18.4 per cent in B, the use of the separated isotope increases the sensitivity of such detectors by a factor of about 5.

(n, 2n) If the incident neutrons have sufficient energy, two neutrons may be emitted from the compound nucleus. This effect contributes a small increment in the neutron multiplication of a beryllium-moderated reactor by the following reactions:

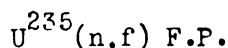


The threshold of this reaction is about 1.8 Mev. This reaction and a similar one,



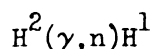
can be used for the detection of high energy neutrons. The threshold of the latter is about 12 Mev.

(n,f) Of course the most important type of neutron reaction is that which results in fission (designated as f). The classic example is:



in which F.P. represents the host of fission products that may be formed by the reaction. The details of this and similar reactions will be the subject of several subsequent discussions.

(γ ,n) The photodisintegration of nuclei resulting in neutrons can be expected in essentially all nuclei, provided the energy of the incident gamma rays is sufficiently large. A practical example is



which has a threshold of 2.18 Mev. Similar to the (n,2n) reaction on Be, this reaction contributes a small increment in the neutron multiplication of a heavy-water (deuterium oxide) moderated reactor such as the one at Chalk River, Ontario, Canada.

Reactions Involving Charged Particles

There are a large number of nuclear reactions produced by energetic charged particles. Since none of these is of direct interest in nuclear

power reactors, the more important types are merely listed.

(p,γ)	$(d,n); (d,H^3)$	(α,n)
(p,n)	$(d,p); (d,\alpha)$	(α,p)
(p,α)	$(d,2n)$	

It is to be noted that certain of these are equivalent to each other and to neutron reactions considered above as far as a given transmutation is concerned:

$$(n,2n) \equiv (\gamma,n) \equiv (d,H^3); \quad (d,2n) \equiv (p,n)$$

1-16 Charts of Nuclear Reactions

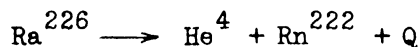
Two types of isotope charts are included in these notes. Figure 1-1 tabulates stable and naturally radioactive isotopes on an $A-2Z$ versus Z diagram, while Figure 1-6 is an $A-Z$ versus Z plot. It is both instructive and useful as a mnemonic aid to learning the transitions on these charts that correspond to the various type reactions considered above. For this purpose an enlarged section of Figure 1-1 is included as Figure 1-7. A few selected reactions are symbolized on this chart -- others may be added as desired. A similar diagram with the coordinates of Figure 1-6 can easily be drawn and will be found useful in becoming acquainted with this chart.

1-17 Principles of Radioactivity

In contrast with the nuclear disintegrations and transmutations that have been considered previously, radioactive processes are delayed, but spontaneous, nuclear transformations. Such processes can be divided into five types, each characterized by the radiation emitted.

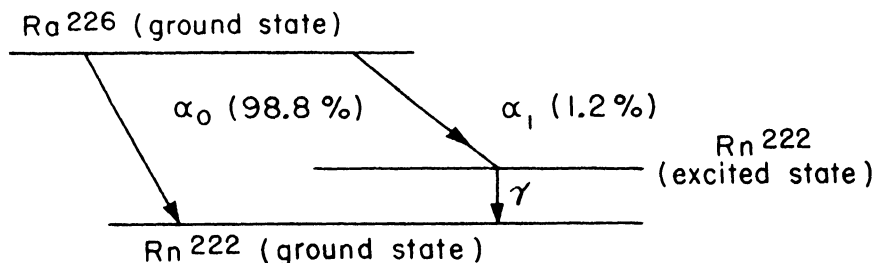
Alpha Decay

Nearly all alpha-ray emitters are found among the heavy elements in the three naturally occurring series headed by U^{238} , U^{235} and Th^{232} , shown schematically in Figure 1-8. A familiar example is the decay of radium:



Because the alpha particle (He^4) has a mass (4) that is appreciable compared to the residue nucleus (222), the Q value of this reaction includes not only the kinetic energy of the He^4 but also that of the Rn^{222} recoil, which accounts for about 2 per cent of the total energy. In addition, other energy relations must be considered, and these are most conveniently visualized in

terms of a nuclear energy level diagram based on an arbitrary vertical energy scale such as the following:



$$\alpha_0 = 4.878 \text{ Mev} = (\alpha_1 + \gamma) = (4.694 + 0.184) \text{ Mev*}$$

It is seen that a small proportion (1.2%) of the radium nuclei decay in two steps, by emission of a somewhat lower energy alpha (α_1) followed almost instantaneously by a gamma ray. Nuclear gamma rays invariably arise from transitions from excited states to lower energy states.

Activity Units

A curie is the quantity of radon (0.66 mm^3 at 0°C and 760 mm) in radioactive equilibrium with 1 gram of radium. The International Radium Standards Commission in 1930 recommended extending the curie unit to include the equilibrium quantity of any decay product of radium, such as polonium. Thus "1 curie Po" is $2.24 \times 10^{-4} \text{ gm}$ of Po, or the amount which has the same rate of emission of α particles as 1 gm of radium. The absolute disintegration rate of radium has been the subject of many measurements by a number of methods giving individual values between 3.40 and 3.72, with some indication in the more recent measurements that the true value probably lies in the neighborhood of $3.67 \pm 0.03 \times 10^{10}$ α particles per second per gram of radium. The Commission recommended the use of the arbitrary value 3.7×10^{10} until such time as agreement on the third decimal place could be reached.

The Commission expressed its opposition to extension of the curie unit to radioactive substances outside the radium family. Following the discovery of artificial radioactivity, the curie unit came into general unofficial use as a description of the disintegration rate, but in the case of isotopes which emit gamma radiation the curie was sometimes used to denote a

*These energies include the contributions from recoils.

Figure 1-6. Segré Chart.

This diagram contains a fairly complete summary of some of the more important properties of nuclei, both stable and radioactive. The chart has been reproduced in sections which overlap to some extent along the horizontal axis of atomic number Z . There is also some purposeful duplication along the vertical axis of $A-Z$ (the number of neutrons in the nucleus). With this set of coordinates, the atomic numbers A lie along diagonals indicated by the arrows. An explanation of the classification, abbreviations, and symbols is given at the lower right of the chart.

(Fold-in Chart at Back of Book)

gamma-ray emission producing the same ionization as the gamma rays from 1 curie of radon. These contradictory and conflicting uses of the curie unit, together with the uncertainty concerning the absolute disintegration rate of radium, have led to much confusion. Because it is now possible to measure the absolute disintegration rate of those radioactive isotopes whose decay schemes are known, the Committee on Radioactive Standards of the National Research Council and the National Bureau of Standards have recommended the use of 1.0×10^6 disintegrating atoms per second; called 1 rutherford (rd), as an unambiguous activity unit.

In interpreting the current literature the following definitions should be used:

$$1 \text{ curie} = 3.7 \times 10^{10} \text{ disintegrating atoms per second}$$

$$1 \text{ rd} = 10^6 \text{ disintegrating atoms per second}$$

Thus:

$$37 \text{ rd (rutherfords)} = 1 \text{ mc (millicurie)}$$

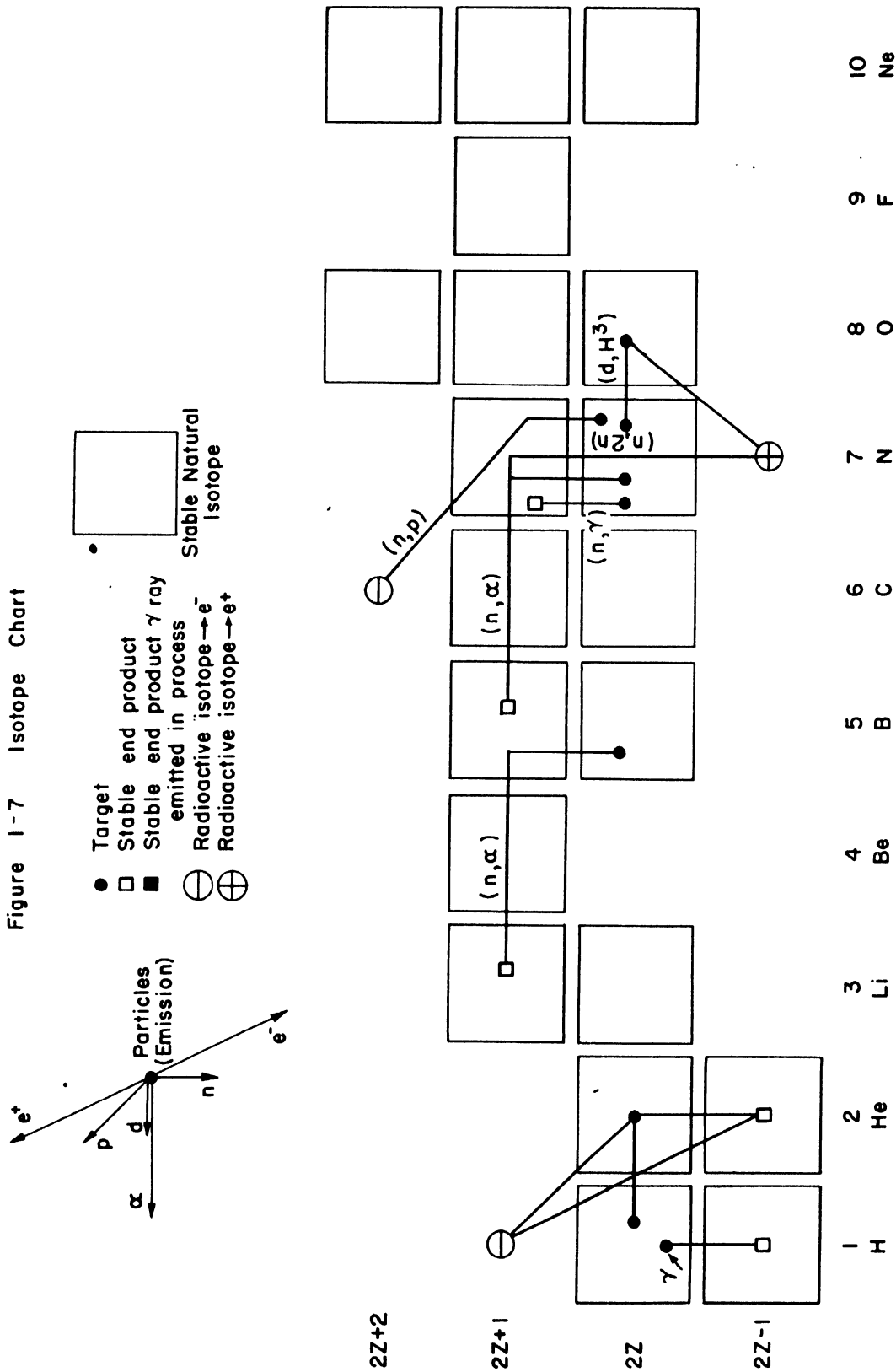
In the case of polonium it is strictly correct to speak of a curie of activity. Then 1 curie emits:

$$\begin{aligned} 3.7 \times 10^{10} \frac{\alpha}{\text{sec}} \times 5.401 \frac{\text{Mev}}{\alpha} \times 1.60 \times 10^{-6} \frac{\text{erg}}{\text{Mev}} \times \frac{1 \text{ watt sec}}{10^7 \text{ erg}} \\ = \frac{1}{30} \text{ watt} = 23.5 \text{ gm calories/hr} \end{aligned}$$

1-18 β^- Decay

The radioactive decay of an element of atomic number Z and mass number A by emission of a negative beta particle β^- results in an increase in Z by one unit without a change in A : $(Z)^A \longrightarrow (Z + 1)^A$. This transformation results when a neutron changes into a proton in the nucleus. To conserve mass-energy, angular momentum, and statistics, an hypothetical particle ν , called the neutrino, must be formed simultaneously with the beta particle in the region immediately surrounding the nucleus*: $(n \longrightarrow p) + \beta^- + \nu$. The neutrino must have zero charge, zero rest mass, a spin of $\frac{1}{2}$ ($h/2\pi$) and Fermi-Dirac statistics.

*As stated in Section 1-1, there are no electrons in nuclei. Hence electrons cannot be emitted directly from nuclei. The electrons, both + and -, that are seen in beta decay are the consequence of the transformations but do not pre-exist in the radioactive nuclei.



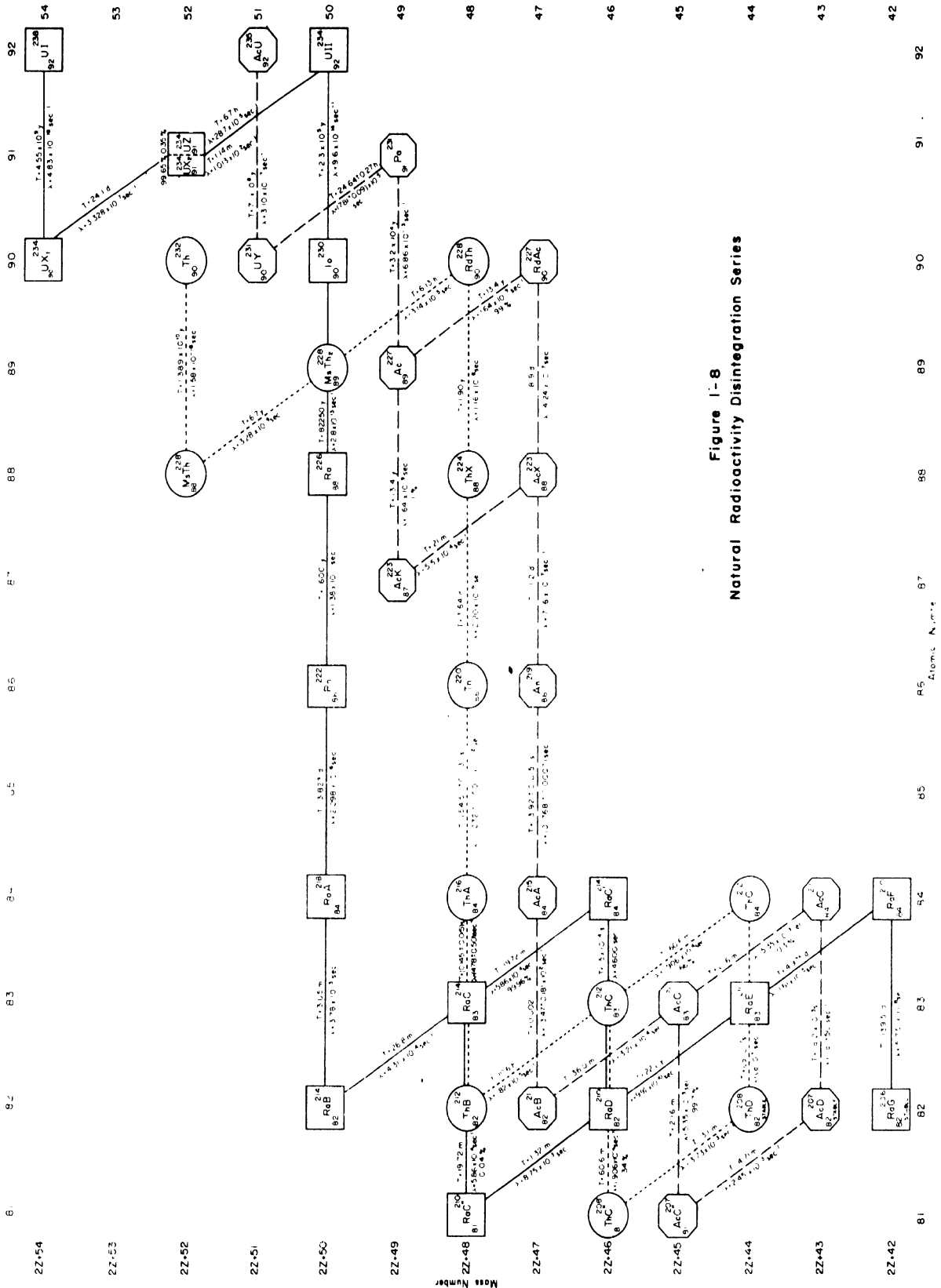


Figure 1-8
Natural Radioactivity Disintegration Series

Because the change involves three bodies, i.e., nucleus $(Z + 1)^A$, β^- and ν , the energy E_{β^-} of an individual β^- may be any value from essentially zero to a definite maximum E_{\max} set by the Q of the reaction. Hence the number of beta particles per unit energy interval dN/dE forms a continuous spectrum of the form given in Figure 1-9.

It is of interest that the peak of this curve occurs at an energy of somewhat less than $E_{\max}/3$. The average energy E_{av} , is approximately equal to $E_{\max}/3$, being between 0.2 and 0.4 E_{\max} for essentially all β^- emitters. The shape of the curve depends on Z and the degree of forbiddenness of the transition. Only one substance, namely RaE, has been investigated sufficiently to give a precise location of $E_{av} = 0.28 E_{\max}$. The value of E_{av} for RaE was determined by calorimetric measurements.

Any radioactive transition may leave the residual nucleus in an excited state from which it passes to the ground state by one or more gamma-ray transitions. Figure 1-10 illustrates one particular beta-ray spectrum that is of special interest in the design and operation of nuclear reactors. The fission product Br^{87} (mass assignments somewhat uncertain), with a half-period of 55.6 seconds, decays by the emission of three competitive β^- rays. The decay may end in (a) the radioactive ground state of Kr^{87} from which the nucleus later decays by β^- emission into stable Rb^{87} , (b) an excited level of Kr^{87} from which it decays by gamma emission to the ground state of Kr^{87} , or (c) a highly-excited level of Kr^{87} from which it may decay either by emission

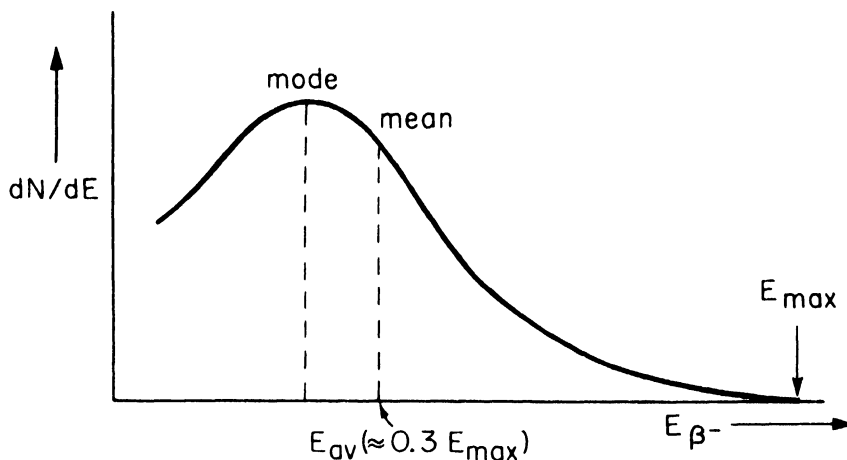


Figure 1-9. Typical β^- Spectrum.

of gamma rays to lower states of Kr^{87} or by the emission of a neutron to end in stable Kr^{86} . The latter is an example of delayed neutron emission by fission products. There are several other instances of this type among the fission products. In each case the rate of emission of the neutron is controlled by the rate of decay of a preceding level, in this case Br^{87} . As discussed in detail later, these delayed neutrons afford a very important means of controlling chain-reacting systems.

The emission of negatrons or β^- rays is the result of an excess of neutrons in the nucleus, that is, the nucleus lies above the general curve of stability about which the stable nuclei cluster as shown in Figure 1-1. Since the fission process invariably results in products with excess neutrons, these decay by emission of β^- s (and occasionally n's). There are no positron emitters among the fission products. The emission of positrons or β^+ rays is the result of a deficiency of neutrons, i.e., an excess of protons.

1-19 β^+ Decay and Annihilation Radiation

Positron decay results in a decrease in Z by one unit without any change in A : $(Z)^A \rightarrow (Z-1)^A$. This transformation results when a proton changes into a neutron in the nucleus. For the same reasons as in β^- decay,

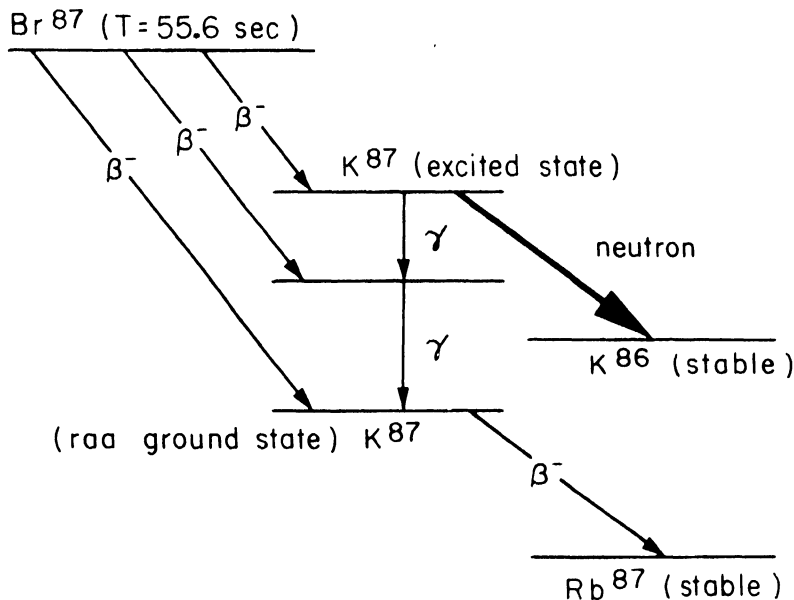


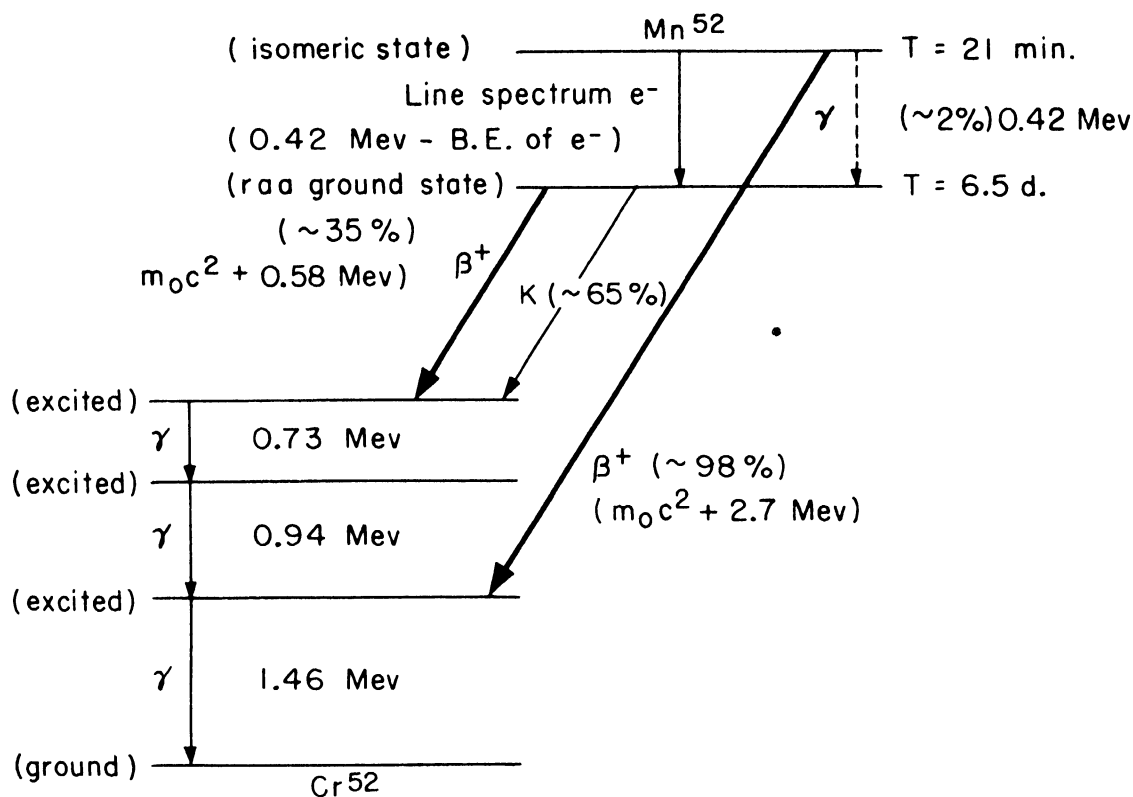
Figure 1-10. Energy Levels in Beta-Ray Spectrum of Br^{87} .

a neutrino is formed: $(p \rightarrow n) + \beta^+ + \nu$. The positron spectrum is similar to that of Figure 1-9 with a definite maximum energy E_{\max} and an average value at about the same position.

The as yet unpublished energy level diagram of Mn^{52} , recently obtained by Osborne and Deutsch, is given as Figure 1-11 not only to illustrate positron decay but also to show the other two types of radioactivity, electron capture and isomeric transition.

Mn^{52} has a radioactive ground state which decays by positron emission with a half-period of 6.5 days to a rather highly-excited state of Cr^{52} . The E_{\max} of these positrons is 0.58 Mev. When this kinetic energy is added to the $m_0 c^2 = 0.51$ Mev required to produce the positron rest mass, a total change in nuclear energy of 1.09 Mev is indicated. This change is followed by three successive gamma rays in cascade with energies of 0.73 Mev, 0.94 Mev and 1.46 Mev respectively, ending in the ground state of Cr^{52} . This type of diagram is characteristic of many positron spectra -- some, of course, show branching at the radioactive ground state with positron emission to other excited levels in the residual nucleus.

A free positron strongly attracts all the electrons in its vicinity and hence ionizes the material through which it is projected in exactly the same amount as would an electron of the same energy. When the positron's velocity is suitably reduced by these repeated energy losses, it may fail to escape from an attracted electron. The two then combine, annihilating each other. In this annihilation process, energy, momentum, and electrical charge must be conserved. The conservation of charge (zero before and after the collision) is satisfied by the disappearance of the two particles. Their energy is given up in the form of gamma rays, called the annihilation radiation. As the positron usually has nearly zero kinetic energy when it submits to annihilation, the total energy of the gamma rays in this case will be $2 mc^2 = 1.02$ Mev. This cannot be emitted as a single quantum because nothing remains after the annihilation to absorb the momentum $h\nu/c$ of such a single quantum. The energy is therefore divided between two quanta of equal energy $h\nu = mc^2 = 0.51$ Mev, and equal momentum $h\nu/c$, travelling in opposite directions away from the scene of the annihilation. The simultaneous emission of two quanta, each of 0.51 Mev energy, per annihilation has been confirmed by coincidence counter observations.

Figure 1-11. Energy Level Diagram of Mn^{52} .1-20 Electron Capture

Another process of radioactive decay is the capture by a nucleus of orbital electrons from the atom in which the nucleus is contained. Although L, M, etc., electrons are captured in some cases, the most common procedure is the capture of the innermost, or K, electrons. For this reason the process is often designated as K or K-capture (see Figure 1-6).

In Mn^{52} some 65 per cent of the nuclei in the ground state decay by this process to the uppermost excited level of Cr^{52} . Thus the result is similar to positron emission in that the change is $(Z)^A \rightarrow (Z-1)^A$ and neutrinos are emitted: $(p + e^- \rightarrow n) + \nu$. However, there are two important differences. The emission of positrons is accompanied by a continuous spectrum of neutrinos, while electron capture results in a line spectrum of neutrinos. As with other neutrinos, these have been studied extensively but have never been detected directly. However, the expected recoil of the residual nucleus following ν emission in electron capture transitions, has been observed. Because electron capture removes an inner atomic electron, the process is followed by the emission of the characteristic x-rays and Auger electrons of the

product atom. Since no other radiations appear, the process is identified and its competitive proportion is measured by means of these x-rays.

1-21 Isomeric Transition

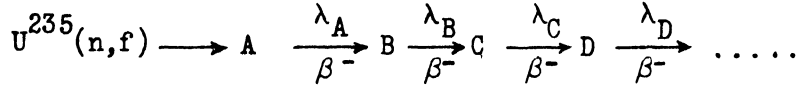
The fifth type of radioactive change takes place when a nucleus transforms from a metastable excited state of measurable lifetime to ground state with the emission of a gamma ray or an internal conversion electron. Competitive beta-ray emission from the excited level is sometimes observed. De-excitation by emission of a gamma ray or of an electron does not involve any change in the number of protons or neutrons in the nucleus but only a readjustment of their configuration. The ground state and excited state are called isomers of the same nucleus and the transition between is, therefore, called an isomeric transition designated as I.T. The symbol e^- is reserved in Figure 1-6 and elsewhere to designate internal conversion electrons emitted in isomeric transitions.

If the energy of excitation is greater than the binding energy of the atomic electrons, which is generally the case, the conversion electron will be ejected with a kinetic energy in the laboratory coordinates equal to the nuclear excitation energy minus the electronic binding energy. In the case of Mn^{52} (Figure 1-11) the line spectrum of electrons has an energy of 0.42 Mev - E.

The 21 min. isomer of Mn^{52} also decays by gamma-ray emission (0.42 Mev) to the ground state of Mn^{52} and by positron emission directly to the lower excited level of Cr^{52} . The predominance of the latter ($\sim 98\%$ by β^+) is very unusual, since most isomeric transitions go mainly by e^- or γ emission rather than by positron or electron beta-ray emission. The competition between e^- and γ emission is dependent primarily on the difference in angular momentum between the two isomeric states. The internal conversion (e^-) is more probable than γ emission if Z is large; if the energy of excitation is small, and if the nuclear angular momentum difference is large.

1-22 Radioactive Series Relations

As mentioned previously, the fission fragments lie well above the region of stability, and decay by a series of β^- (and occasionally n) transformation until a stable form is attained. Figure 1-10 describes a portion of one series. In general terms, this process can be represented as:



where B, C, D ... represent successive types of atoms formed by β^- decay from a particular fission fragment A; and $\lambda_A, \lambda_B, \lambda_C, \lambda_D \dots$ represent the decay constants for each of the designated steps. A given λ is the probability that the atom will decay in unit time and is independent of the age of the individual atom. Thus in a group of atoms of type A, all alike and A of them, the number which decay - dA in a time dt is given by $-dA = \lambda_A A dt$. Hence the fraction of atoms A/A_0 remaining after a time t is

$$(17) \quad A/A_0 = e^{-\lambda_A t}$$

when A_0 represents the number of atoms of type A present at time $t = 0$. It follows directly that the corresponding ratio of activities is given by

$$(18) \quad \lambda_A A / \lambda_A A_0 = e^{-\lambda_A t}$$

which has the form of Figure 1-12. The half-period T_A is the time required for the activity to decrease to one-half the initial value. τ_A is the mean life of the atoms A. It can be shown that $\tau_A = 1/\lambda_A$, and that $\tau_A \lambda_A A_0$ (the cross-hatched area) equals the area under the exponential curve, that is, the total number of atoms A_0 decaying.

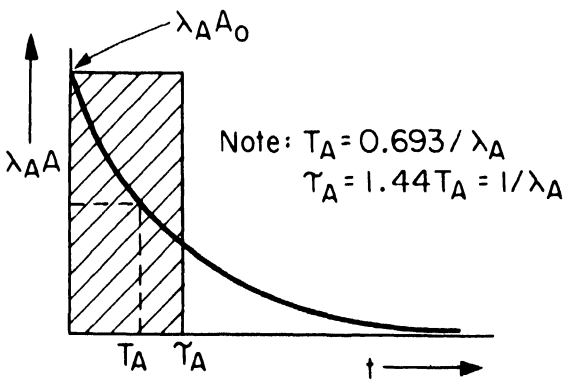


Figure 1-12. Exponential Decrease of Activity $\lambda_A A$ with Time t.

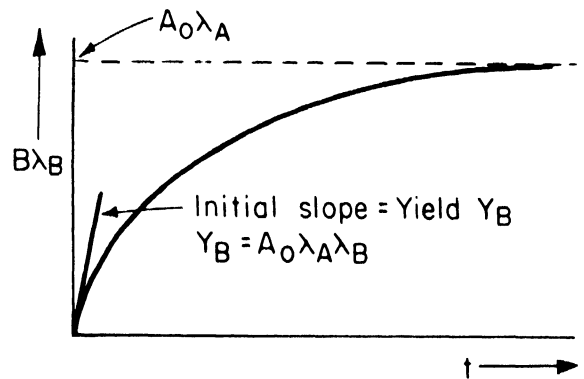


Figure 1-13. Exponential Build-Up $A \longrightarrow B$ when $\lambda_B \gg \lambda_A$.

If atoms A decay into radioactive atoms of the type B, the activity of the latter can be shown to be

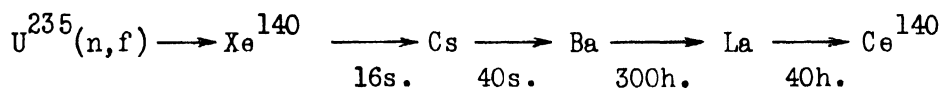
$$(19) \quad B\lambda_B = \left[\lambda_B \lambda_A A_0 / (\lambda_B - \lambda_A) \right] \left(e^{-\lambda_A t} - e^{-\lambda_B t} \right); \text{ if } B = 0 \text{ at } t = 0.$$

If $\lambda_B \gg \lambda_A$, that is, if the parent is long-lived and the daughter is short-lived, this expression reduces to the familiar exponential build-up

$$(20) \quad B\lambda_B = A_0 \lambda_A \left(1 - e^{-\lambda_B t} \right)$$

shown in Figure 1-13.

As an example, consider the fission product series:



and assume that after a given period of neutron bombardment the slug of uranium is dissolved and A_0 atoms of Ba^{140} are separated at time $t = 0$. The activity of the Ba^{140} (atoms A) and of the La^{140} (atoms B) will then follow Equations (18) and (19) as shown in Figure 1-14. The activity of La^{140} builds up from an initial value of zero until at time t_1 its activity equals that of Ba^{140} . At t_1 only:

$$(21) \quad A\lambda_A = B\lambda_B = A_0 \lambda_A e^{-\lambda_A t_1}$$

where

$$(22) \quad t_1 = \left[1/(\lambda_B - \lambda_A) \right] \ln (\lambda_B/\lambda_A) = 134 \text{ h. for } Ba \longrightarrow La \longrightarrow.$$

After a time $t \gg \tau_A$ or τ_B the activity of La^{140} is always slightly greater (~15%) than that of Ba^{140} -- a condition known as transient equilibrium exists:

$$(23) \quad B\lambda_B/A\lambda_A = \lambda_B/(\lambda_B - \lambda_A) = 1.15$$

The areas under the two curves in Figure 1-14 must be equal, since each represents the total number of atoms that decay from $t = 0$ to $t = \infty$ and one La^{140} is formed by the decay of each Ba^{140} .

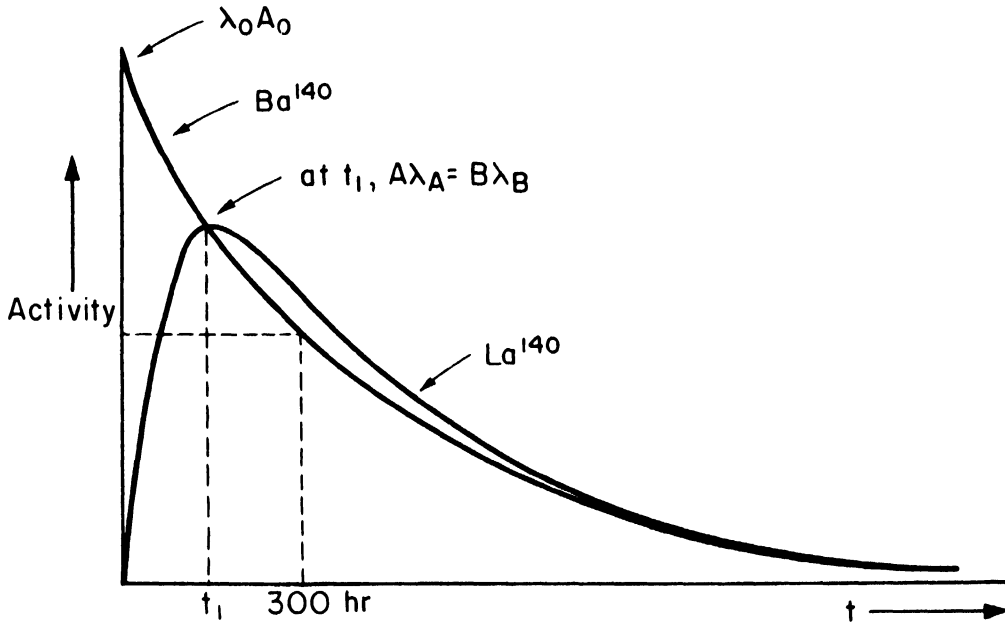


Figure 1-14. Activity Relations between Ba^{140} and La^{140} .

1-23 Width of Nuclear Energy Levels

The transition probability and the mean lifetime of excited states of nuclei are commonly expressed in terms of the "width" of the nuclear energy level. In nuclear physics, the concept of level width has the same origin and interpretation as the level widths of atomic spectroscopy. The Heisenberg uncertainty principle gives a general relationship between the uncertainty ΔE in energy and the concomitant uncertainty Δt in time:

$$(24) \quad \Delta E \Delta t = h/2\pi \equiv \hbar$$

Thus a nuclear level having a very short mean lifetime is correspondingly poorly defined in energy while a long-lived nuclear state will be very sharply defined in energy. The uncertainty in time Δt is taken as equal to the mean life τ of the state, while the corresponding uncertainty in energy ΔE is called the level width Γ . Then Equation (24) becomes:

$$\Gamma \tau = \hbar$$

or

$$(25) \quad \Gamma = \hbar/\tau = \hbar\lambda$$

and the level width Γ is proportional to the decay probability, λ . If $\lambda_1, \lambda_2, \lambda_3 \dots$ are partial decay constants, corresponding to various competitive modes of decay (e.g., β^+ and electron capture in the 6.5d level of Mn^{52} ; Figure 1-11) then the corresponding "partial level widths" are $\Gamma_1 = \hbar\lambda_1$; $\Gamma_2 = \hbar\lambda_2$; etc., and the total level width is the sum of the partial widths:

$$(26) \quad \Gamma = (\Gamma_1 + \Gamma_2 + \Gamma_3 + \dots) = (\lambda_1 + \lambda_2 + \lambda_3 + \dots)\hbar = \lambda\hbar$$

Thus the total width of a nuclear level, which is proportional to the total probability of decay of the excited level, depends on the configuration of all the lower lying levels to which transformations are possible. If the excited state tends to decay rapidly, then Γ is large and the energy of the level is poorly defined. The physical significance of the width of nuclear resonance levels will be discussed more fully in Section 1-27.

It is customary to express Γ in electron volts, hence with λ in sec^{-1} . we need

$$\begin{aligned} \hbar &= h/2\pi = 6.6 \times 10^{-27} \text{ erg sec}/2\pi \times 1.6 \times 10^{-12} \text{ (erg/ev)} \\ &= 0.65 \times 10^{-15} \text{ ev sec} \end{aligned}$$

For example, the 6.5 day Mn^{52} level of Figure 1-11 has the following characteristics:

$$\begin{aligned} T &= 6.5 \text{ days} \\ \tau &= 1.44 \times 6.5 \times 24 \times 3600 = 8.1 \times 10^5 \text{ sec} \\ \lambda &= 1/8.1 \times 10^5 \text{ sec} = 1.23 \times 10^{-6} \text{ sec}^{-1} \\ \Gamma &= 0.65 \times 10^{-15} \text{ ev sec}/8.1 \times 10^5 \text{ sec} = 8 \times 10^{-22} \text{ ev} \end{aligned}$$

Normally, the width of excited levels such as those in Cr^{52} (see Figure 1-11), from which ~ 1 Mev γ rays are emitted, is about 0.01 to 0.001 ev. Such states, therefore, have mean lives of the order of

$$\tau = \hbar/\Gamma = 0.65 \times 10^{-15} \text{ ev sec}/0.01 \text{ ev} = 0.65 \times 10^{-13} \text{ sec}$$

In the wave model of a radiating nucleus, the mean life τ is the duration of the electromagnetic pulse of γ radiation emitted, and therefore describes the length τc of the wave train emitted. The corpuscular counterpart of the wave

model simply identifies τ as the ordinary mean life in a large ensemble of identical excited states in a group of atoms. Thus if there are N_0 excited nuclei at time $t = 0$, the number N remaining untransformed at time t is $N = N_0 e^{-\lambda t} = N_0 e^{-t/\tau}$.

1-24 Interaction of Radiation with Matter

The fission of 1 kg of U^{235} , to take a purely arbitrary amount, results in about 989 grams of fission products, 10 grams of neutrons, 700 milligrams of kinetic energy (mass-energy equivalent) and an additional 100 milligrams of energy as radiation, largely from radioactive decay products.

The nature of the fission products will be presented in a later section on radiochemistry. The interactions of neutrons with matter are discussed in general terms in this section but will be considered in detail under pile theory. The absorption of the kinetic energy of the fission fragments and the interactions of the radioactive radiations (gamma, beta, alpha and neutrino) with matter are of fundamental importance in the design and engineering of nuclear reactors. For example, it follows directly from such considerations that an intensely radioactive coolant in a heat exchanger will not produce any appreciable amount of radioactivity in the secondary cooling medium.

Gamma Rays

Gamma rays are emitted (a) during fission, (b) from the radioactive fission products, (c) from (n, γ) reactions, and (d) from induced radioactivity in materials of construction. By definition, γ rays are emitted by nuclei; all other high energy electromagnetic radiations associated with nuclear and electronic interactions are called x-rays. The dualistic nature of wave and corpuscular properties is particularly evident in this high energy electromagnetic radiation.

Gamma rays diverge from the emitting nucleus like a radio or radar pulse from an antenna. At any point in space, the electromagnetic wave train is a short pulse having a velocity* $c = 3 \times 10^{10}$ cm/sec and frequency ν sec⁻¹, hence wave length $\lambda = c/\nu$. The duration of the pulse can be identified with the mean life against γ emission of a typical single nuclear state and can be estimated from $\Gamma = \hbar/\tau$. With $\Gamma \approx 10^{-3}$ ev, $\tau \approx 0.6 \times 10^{-12}$ sec is a repre-

*Because there is no dispersion, group and phase velocity are equal.

sentative emission time. The length of the corresponding wave train is $\ell \approx c\tau = 0.2$ mm. The formation of a wave train of finite length with a localized maximum amplitude defining the position of the photon implies a Fourier superposition of monochromatic wave trains of infinite extent, having wave lengths slightly different from λ . Thus there is an indeterminacy in λ , which can be shown to be identical with the general form of the Heisenberg Uncertainty Principle $\Delta x \Delta p = h/2\pi = \hbar$. The energy and momentum of the photon associated with or represented by the electromagnetic wave, are $E = h\nu$ and $p = h\nu/c$ respectively. Hence, taking the maximum uncertainty Δp as the entire momentum $p = h\nu/c$, the minimum uncertainty in position of the photon is $(\Delta x)_{\min} = (h/2\pi)/(h\nu/c) = \lambda/2\pi = \lambda$.

The relation between wave length λ and energy E in Mev is:

$$(27) \quad \lambda = \frac{1238.}{E} \times 10^{-13} \text{ cm}$$

Thus for $E = 1$ Mev, $\lambda = 1238 \times 10^{-13}$ cm. Since nuclear gamma rays have energies between about 0.05 and about 3 Mev, with the majority between 0.5 and 1.5 Mev, the gamma ray wave lengths are much greater than nuclear or electronic dimensions (R and r_0 are $\approx 10^{-13}$ cm).

The directional distribution of the gamma-ray wave amplitude ψ or the intensity I ($\propto \psi^2$) is characteristic of an oscillating electric dipole, quadrupole, etc., or of an oscillating magnetic dipole, quadrupole, etc. Actually the electric quadrupole radiation ($k \equiv \vec{I} - \vec{I}' = 2$, "no" change in parity) is the most common type of nuclear gamma ray. The electric dipole moments are usually negligible, due to symmetry of charge distribution, but electric quadrupole moments may be relatively large.

For purpose of visualization, a gamma-ray photon may be represented diagrammatically as in Figure 1-15. The shaded area represents the general location of the photon from the uncertainty principles. The electric vector \vec{E} and the magnetic vector \vec{H} are at right angles to each other and to the Poynting vector of energy flow \vec{S} . The single quantum has a plane of polarization which rotates about \vec{S} with an angular momentum or spin of $h/2\pi$. The wave length λ gives a clue as to the types of interaction to be expected.

The three most prominent modes of interaction are photoelectric effect, Compton effect, and pair production. These are discussed in detail below. In a rigorous treatment, three others must be included:

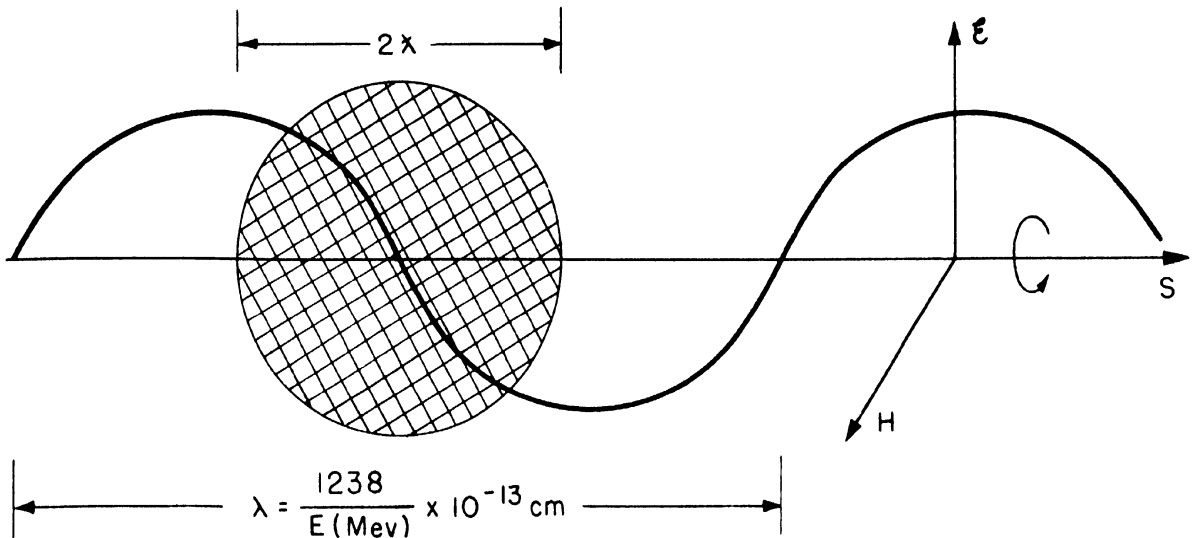


Figure 1-15. Schematic Representation of a Gamma-Ray Photon.

(a) Formation of isomeric nuclear levels. The excited state may be sufficiently long-lived to be observed by isomeric transitions of the type discussed in Section 1-21.

(b) Photodisintegration of nuclei. In heavier elements the energy required to knock out a neutron is the order of 8 Mev, the binding energy of a nucleon. As considered in Section 1-15, the threshold for certain light elements may be much less (2.18 Mev for $H^2(\gamma, n)$ and 1.63 Mev for $Be^9(\gamma, n)$).

(c) Coherent or Bragg Scattering. This effect is important in the low-energy field. The Bragg reflection angle of rock salt for 0.5 Mev gamma rays is about 15 minutes of arc. Hence, coherent scattering is in general unimportant -- the angles are small and the intensities are small for high-energy nuclear gamma rays.

Photoelectric Effect. In the photoelectric effect, the gamma ray interacts as a wave with the entire struck atom. Momentum and energy are conserved and the general result is that a single atomic electron somewhere in the atom (generally a K or L electron) receives all of the energy of the photon in one encounter. The electron is ejected from the atom with an energy $E_{\text{photo}} = h\nu - B$, i.e., the energy of the incident photon $h\nu$ diminished by the binding energy B of the electron in the atom. The effect is described diagrammatically in Figure 1-16. The shaded circle represents the atom from which an electron e^- is ejected. For low-energy gamma rays, the

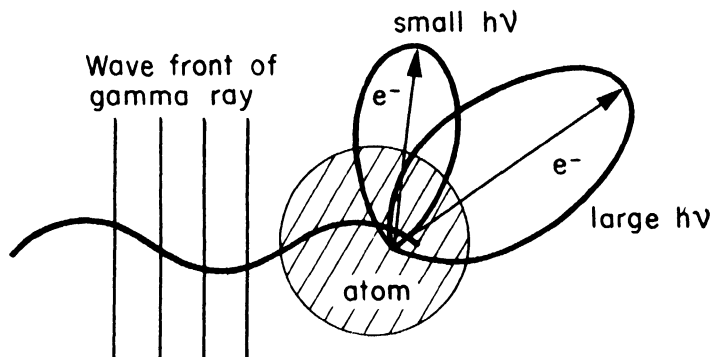


Figure 1-16. Photoelectric Effect.

photoelectrons tend to come out at right angles to the incident direction of the gamma rays. This angular distribution can be visualized as the effect of the electric vector \mathcal{E} in Figure 1-15. For high-energy gamma rays, the photoelectrons tend to come out in a more forwardly direction, which becomes almost directly forward for very high-energy gamma rays. This forward motion can be thought of as resulting from the momentum transfer of the incident photon combined, of course, with the backward momentum which the atom takes as a whole. Alternatively, this forward motion can be considered to be the result of the Lorentz force of the H component of the electromagnetic wave.

Following photoelectric emission, the atom emits characteristic x-rays and Auger electrons as the electronic energy levels are refilled. It is evident that monoenergetic gamma rays produce line spectra of photoelectrons.

The atomic cross section for the photoelectric absorption τ_A has received considerable theoretical attention, but as yet no completely satisfactory general theory has resulted. Roughly,

$$(28) \quad \tau_A \simeq \text{const} (1/h\nu)^{2.8} Z^4 \text{ cm}^2$$

Numerically τ_A has such values that photoelectric absorption is dominant in heavy elements, such as Pb, below an energy of about 0.5 Mev. The Z^4 dependence results in negligibly small values of τ_A for light elements, such as Al. The linear absorption coefficient $\tau = \tau_A N \text{ cm}^{-1}$, where N = number of atoms/cc. Numerical values for τ of Pb are plotted in Figures 1-17 and 1-18 for two ranges of gamma-ray energy. To estimate τ for other materials, use these figures for Pb and correct for density ρ , atomic weight W , and atomic number Z by:

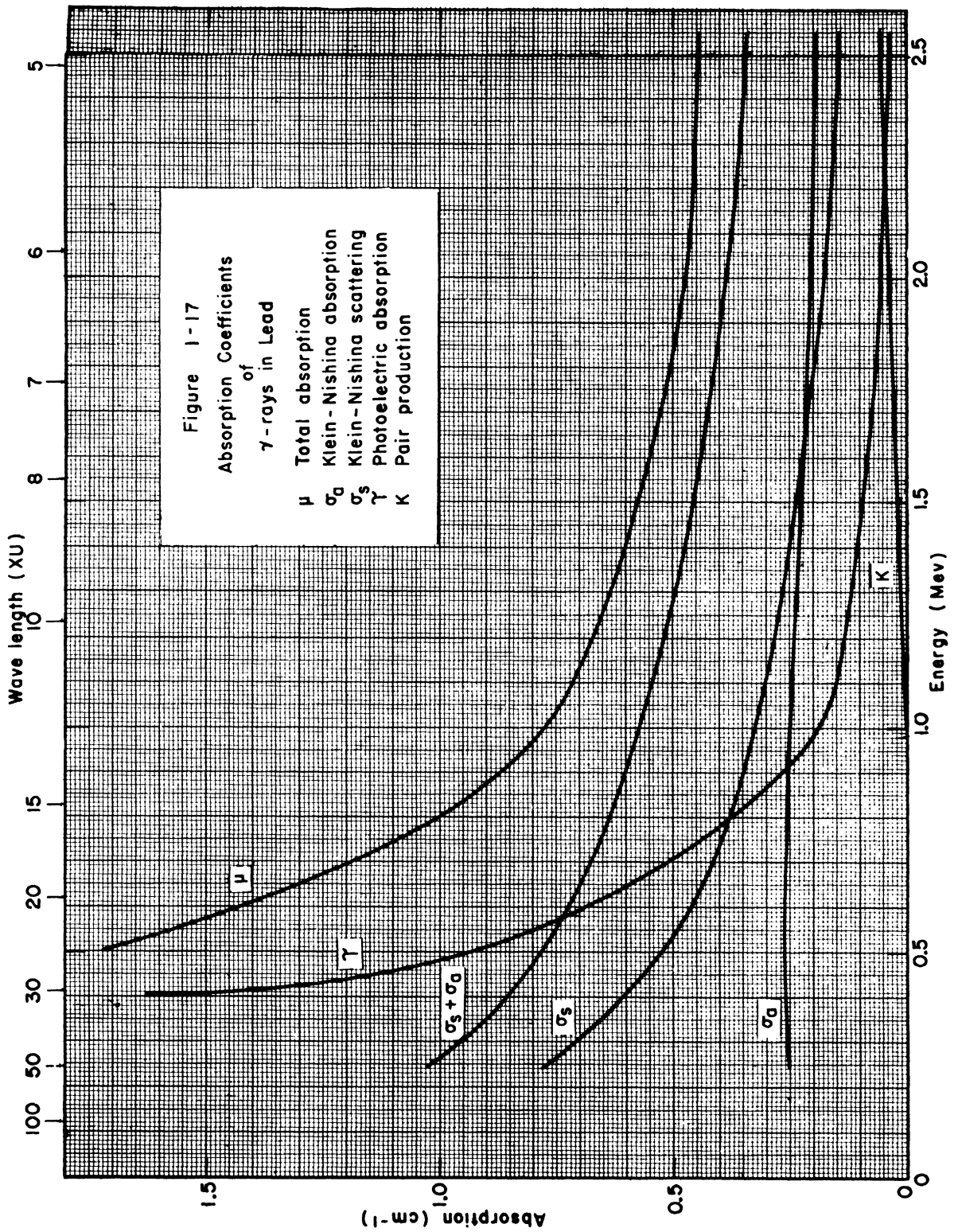


Figure 1-17

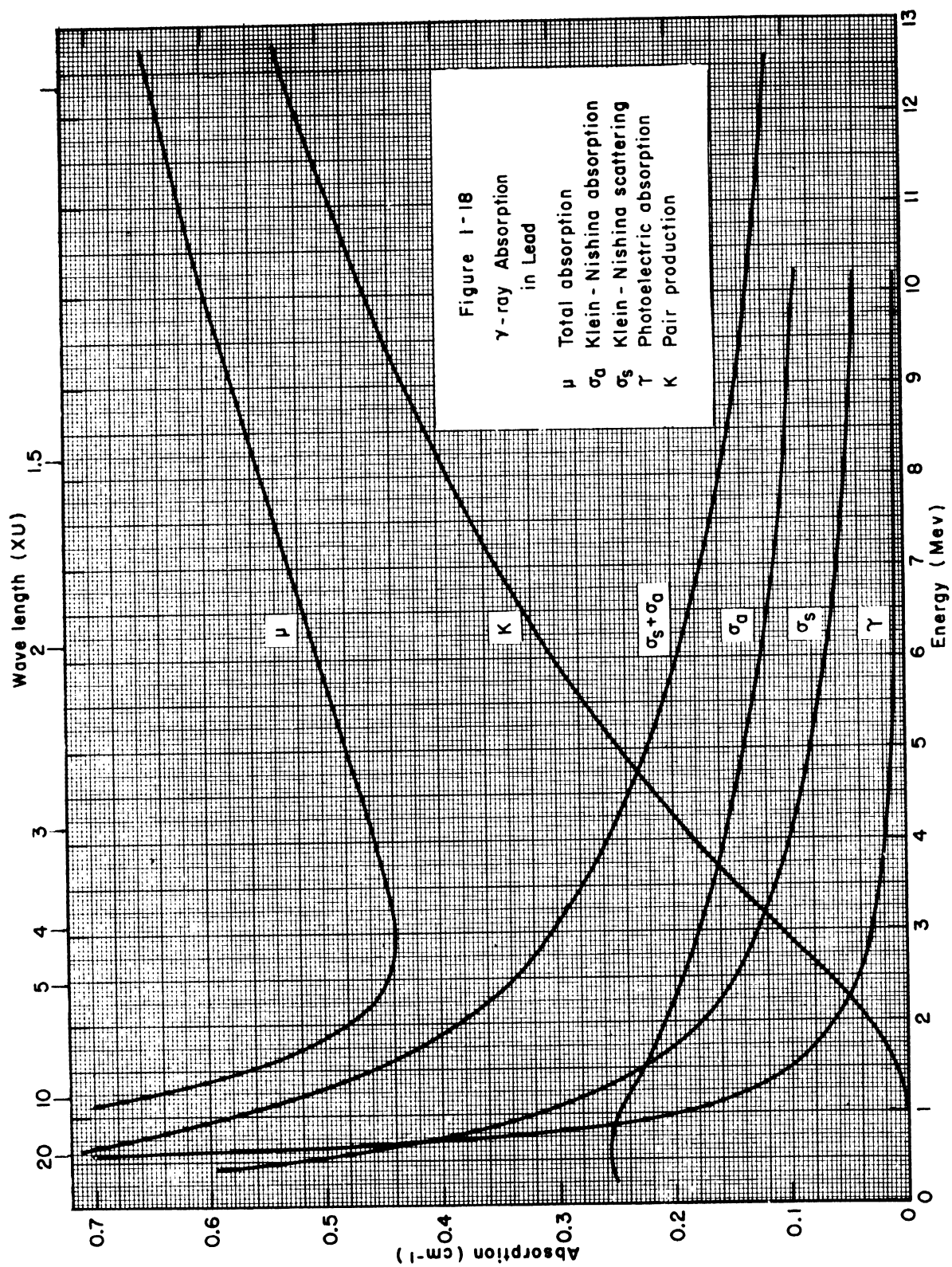


Figure 1-18

$$(29) \quad \tau = \tau_{\text{Pb}} (\rho/11.3)(207.2/W)(Z/82)^4$$

Compton Effect. In contrast with the photoelectric effect, the Compton Effect is an elastic collision between a gamma-ray quantum and a single electron. Momentum and energy are conserved -- the electron generally being considered as unbound. The details of this interaction have been analyzed quite completely by Klein and Nishina and can be considered as rather thoroughly understood. Experiments have been made up to energies of 17 Mev, and the agreement with theory is excellent. Figure 1-19 is similar to the original diagram used by A. H. Compton to explain the original interpretation of this effect. The incident quantum $h\nu$ gives up a portion of its energy E_0 to the electron e^- , which flies off at an angle ϕ with the direction of the incident quantum. The degraded radiation $h\nu'$ is observed at an angle θ given in the relation:

$$(30) \quad h\nu' = \frac{m_0 c^2}{(1 - \cos \theta + \frac{m_0 c^2}{h\nu})}$$

The change in wave length is given by the familiar expression:

$$(31) \quad \lambda' - \lambda = (h/m_0 c)(1 - \cos \theta) = \lambda_0(1 - \cos \theta)$$

where the Compton wave length $\lambda_0 = 24.7 \times 10^{-11}$ cm = 24.7 XU, i.e., the

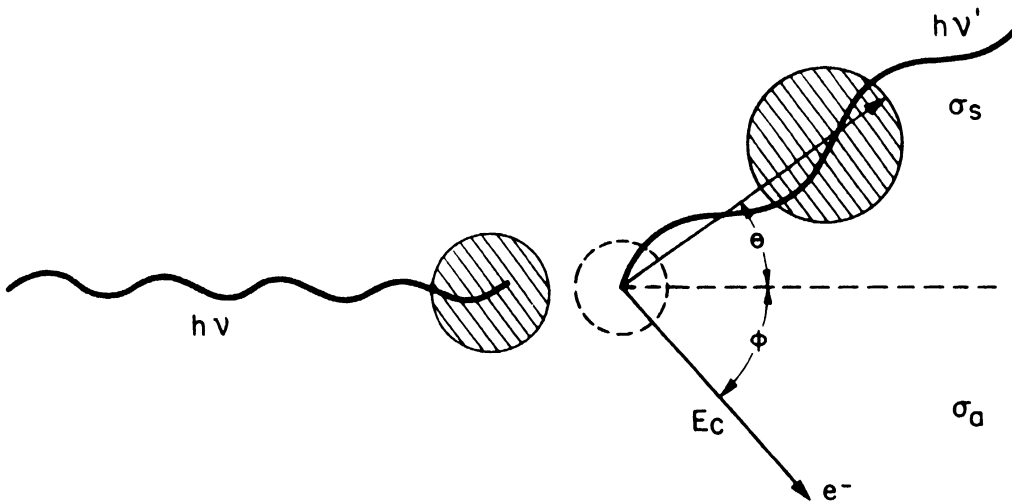


Figure 1-19. Schematic Diagram of Compton Collision.

wave length of a 0.51 Mev quantum. For $h\nu \gg m_0 c^2$, $h\nu' \rightarrow 0.51$ Mev at $\theta = 90^\circ$ and $h\nu' \rightarrow 0.25$ Mev at $\theta = 180^\circ$. The degraded radiation goes on to indulge in further interactions and generally ends in a photoelectric encounter.

The Compton electrons of energy $E_c = h\nu - h\nu'$ have a continuous distribution in energy from zero up to a maximum (at $\phi = 0^\circ$, $\theta = 180^\circ$) of

$$(32) \quad (E_c)_{\max} = h\nu / (1 + m_0 c^2 / 2h\nu)$$

which for $h\nu \gg m_0 c^2$ is given by

$$(33) \quad (E_c)_{\max} \approx h\nu - \frac{m_0 c^2}{2} = h\nu - 0.25 \text{ Mev}$$

The electronic cross section ${}_e\sigma$ for the Compton process is composed of two parts, the cross section for scattering ${}_e\sigma_s$ and the cross section for absorption ${}_e\sigma_a$. The latter accounts for the energy taken out of the gamma-ray beam and put into kinetic energy of motion of the electron which, as far as the gamma ray is concerned, is an absorption process. At an energy of 1.6 Mev, ${}_e\sigma_s = {}_e\sigma_a = 0.08$ barn per electron, while below 1.6 Mev ${}_e\sigma_s > {}_e\sigma_a$ and above 1.6 Mev ${}_e\sigma_a > {}_e\sigma_s$. The total electronic cross section is ${}_e\sigma = {}_e\sigma_s + {}_e\sigma_a$, which in turn is related to the total linear coefficient σ as

$$(34) \quad \sigma = \sigma_s + \sigma_a = ({}_e\sigma_s + {}_e\sigma_a)(\rho NZ/W)$$

Numerical values for σ_s , σ_a and $(\sigma_s + \sigma_a)$ for Pb are included in Figures 1-17 and 1-18 and for Al in Figure 1-20. To estimate σ for other materials, the values given for Pb can be corrected for density ρ , atomic weight W , and atomic number Z by the relation

$$(35) \quad \sigma = \sigma_{\text{Pb}} (\rho/11.3)(207.2/W)(Z/82)$$

A similar expression can be used with the values given for Al (2.68×10^{24} electrons/cc Pb and 0.78×10^{24} electrons/cc Al).

Pair Production. As the name implies, a gamma ray may produce an electron pair, that is, a negative electron e^- and a positive electron or positron e^+ . This interaction is between a gamma-ray quantum and a nucleus. According to present theory, the incoming quantum is completely absorbed in

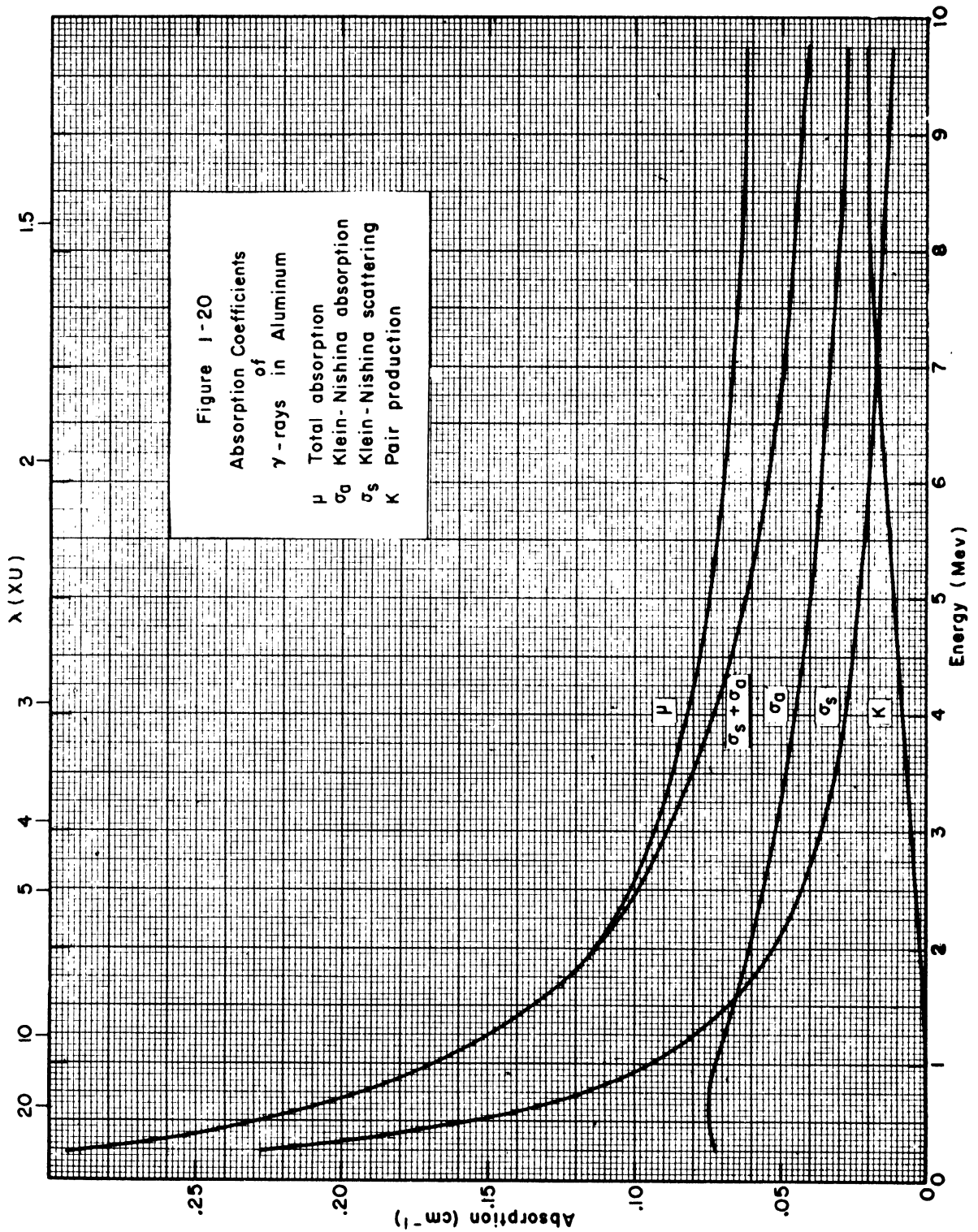


Figure 1-20

the region of the nuclear Coulomb field, but not "in" the nucleus. It lifts an electron e^- from a negative energy state and gives it sufficient kinetic energy to escape from the attractive nuclear field. The hole in the energy continuum is identified as the positron e^+ . The electron pair (e^+ , e^-) and the residual nucleus form a three-body system which conserves energy and momentum (see Figure 1-21). Since the charges on the two particles e^+ and e^- are equal in magnitude but opposite in sign, charge is also conserved in the process. The total energy of the quantum appears as kinetic energy of the three bodies, e^+ , e^- , and nucleus, plus the mass energy $2m_0c^2$. Hence, the cross section for this interaction is zero for energies less than $2m_0c^2 = 1.02$ Mev.

Pair production is important for high energies and for heavy elements -- it is equal in importance to the Compton coefficient for Pb at 4.75 Mev. Above this energy, pair production becomes predominant. The nuclear cross section κ_A is given by an expression of the form:

$$(36) \quad \kappa_A = Z^2 F(h\nu),$$

where $F(h\nu) \approx \text{const } (h\nu - 2m_0c^2)$

hence $F(h\nu) = 0$ at $h\nu = 2m_0c^2$

Numerical values of the corresponding linear absorption coefficients κ for Pb and Al are given in Figures 1-17, 1-18, and 1-19. The value for any other absorber may be obtained from the value for Pb, κ_{Pb} by

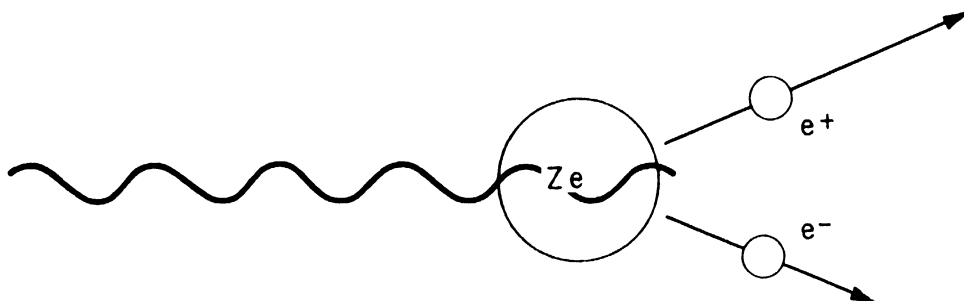


Figure 1-21. Pair Production Process. The longer vector for e^+ symbolizes that there is a slight tendency to emphasize the energy of the positron over that of the e^- because of the effect of the Coulomb field of the nucleus on the newly created particles.

$$(37) \quad \kappa = \kappa_{\text{Pb}}(\rho/11.3)(207.2/w)(Z/82)^2$$

The total absorption coefficient μ is the sum of photo τ , Compton σ , and pair κ ,

$$(38) \quad \mu = \tau + \sigma + \kappa$$

and has a high value at low energy because of the importance of photo, and rises at high energies because of the importance of pair production. These relationships are clearly demonstrated in the curve of μ_{Pb} in Figure 1-18. It is seen that the values of μ_{Pb} above 0.44 cm^{-1} are double valued in the gamma-ray energy. Hence, care must be taken in using lead for energy determinations by absorption measurements. This precaution is particularly true in copper, since μ_{Cu} is essentially constant (about 0.28 cm^{-1}) for all gamma rays above an energy of 6 Mev.

The intensity of a collimated gamma-ray beam I after traversing a thickness x of material in the direction of the incident beam of intensity I_0 is given by the familiar expression

$$(39) \quad I = I_0 e^{-\mu x} \approx I_0 e^{-(\mu/\rho)w}$$

The latter form, involving the mass absorption coefficient (μ/ρ) in cm^2/gm and the thickness of absorber $w = \rho x$ in gm/cm^2 , is particularly useful for medium energies (~ 0.5 to 1.5 Mev) in heavy elements and over a wider range in elements of low Z , since the Compton effect predominates and the following simplifications can be employed:

$$(40) \quad dI = I\mu dx \approx I\sigma dx = I_0 \sigma (\rho NZ/w) dx \\ \approx I_0 \sigma (\text{const}) \rho dx = I(\mu/\rho)(\rho dx)$$

since $Z/w \approx 1/2$ and the mass absorption coefficient $\mu/\rho = \sigma NZ/w$ is approximately independent of Z .

Hence

$$(41) \quad dI \approx I(\mu/\rho)(\rho dx)$$

which is nearly independent of the Z of the absorber.

Electrons

Aside from the annihilation phenomenon for e^+ from pair production and β^+ from the radioactive decay of nuclei, positrons and negative electrons (negatrons) behave identically in their interaction with matter. Their static corpuscular properties are:

$$\text{Charge: } e = \pm 4.80 \times 10^{-10} \text{ esu} = 1.60 \times 10^{-19} \text{ coulomb}$$

$$\text{Mass: } m_0 = 0.9 \times 10^{-27} \text{ gm (rest mass)}$$

$$\text{Radius: } r \approx e^2/m_0 c^2 = 2.8 \times 10^{-13} \text{ cm}$$

In general the dynamic properties of electrons in nuclear physics must be considered relativistically because the energies are usually much higher than the rest energy of the electron. Hence:

$$\text{Relativistic mass: } m = m_0 / \sqrt{1 - v^2/c^2}$$

(see insert in Figure 1-22 for $\beta = v/c$ versus energy E in Mev).

$$\text{Kinetic energy: } T = mc^2 - m_0 c^2$$

$$\text{Momentum: } p = mv = (1/c) \sqrt{T(T + 2m_0 c^2)}$$

$$H\rho = (10^4/3) \sqrt{E(E + 1.02)}$$

Where $H \equiv$ magnetic field strength in gauss and $\rho \equiv$ radius of curvature in cm for electron of energy E Mev moving in this magnetic field in a plane normal to the direction of the field, $c \equiv$ velocity of light in cm/sec. Values of the momentum measured in terms of $H\rho$ may be obtained for all values of energy from essentially 0 up to 35 Mev by reference to Figure 1-22. Both sets of coordinates are to be multiplied by the factor shown adjoining the appropriate curve. Thus electrons with an energy of 3.0 Mev (3.0×1) have a momentum of 11,500 gauss cm ($11,500 \times 1$). While electrons with an energy of 30 Mev (3.0×10) have a momentum of 101,000 gauss cm ($10,100 \times 10$).

It is often convenient to consider the ratio of the total energy to the rest energy:

$$W^2 \equiv (mc^2/m_0 c^2)^2 = (1 + T/m_0 c^2)^2 = 1 + (p/m_0 c)^2$$

which reduces to $W^2 = 1 + \eta^2$, where $\eta = H\rho/1700$ and $W = 1 + E/0.51$.

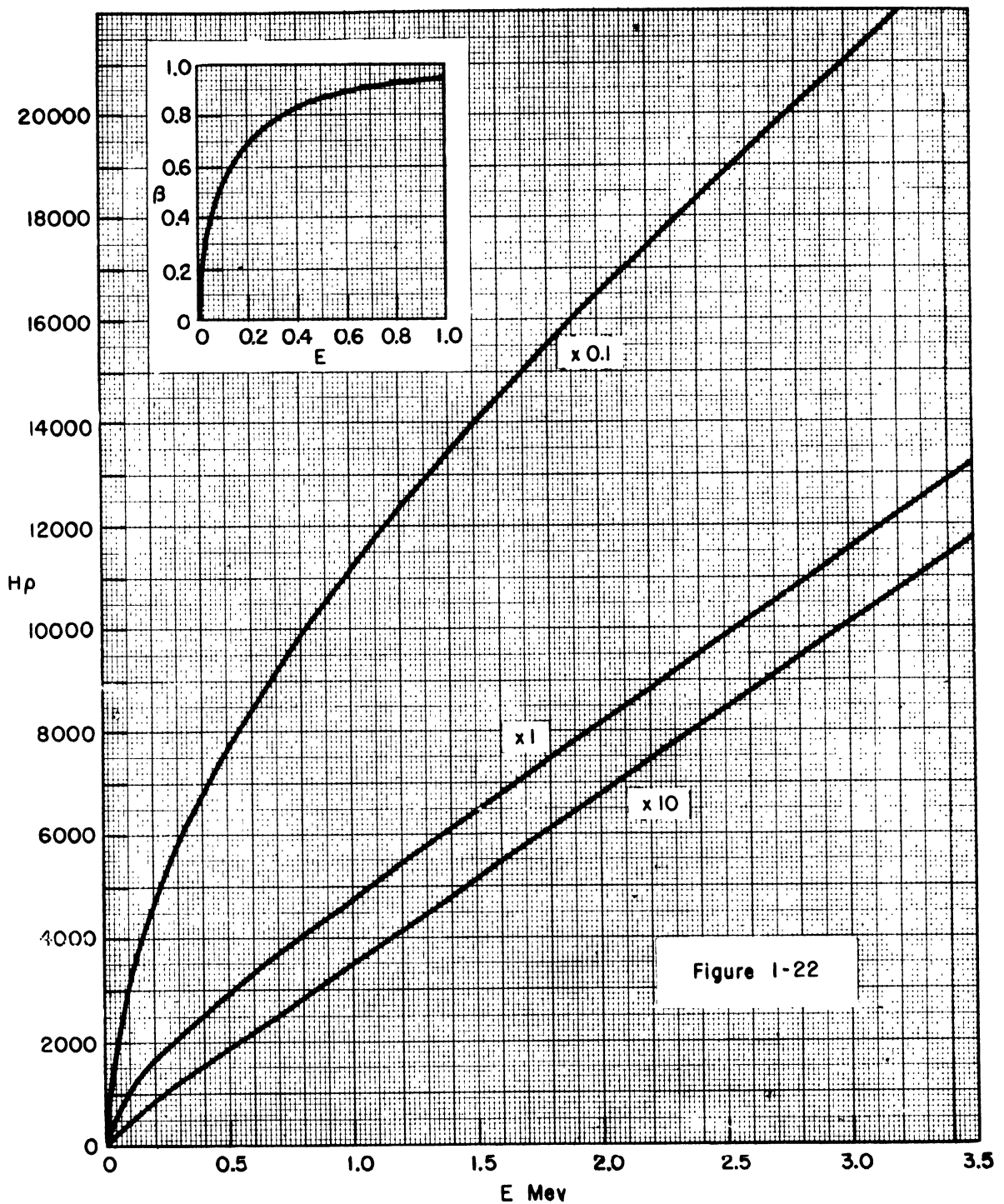


Figure 1-22.

Another dynamic characteristic of considerable importance is the de Broglie wave length $\lambda = h/p$. The following table gives the wave length for electrons for a series of values of energy and momentum:

E(in Mev)	0.01	0.05	0.10	0.50	1.0	2.0	10.	1000.
p(in 10^{-17} gm cm/sec)	0.54	1.23	1.80	4.65	7.6	13.2	56.	5400.
λ (in 10^{-11} cm)	123.	54.	37.	14.3	8.7	5.0	1.18	0.012

It is seen that for energies of 0.01 to 0.05 Mev, the wave length ranges from 0.123 Å to 0.054 Å, which is very large compared to nuclear dimensions. These wave lengths account for the diffraction of such electrons by atoms in crystals and for their usefulness in electron microscopes. At the very high energies the wave lengths are comparable to the diameters of nuclear particles (n or p), i.e., 1.2×10^{-13} cm at 1000 Mev (1 Bev). It has been suggested by Slater that such electrons, which may soon be available from high voltage machines, may have their greatest use in diffraction studies within nuclei.

Elastic Scattering. Electrons are scattered appreciably by both atomic electrons and atomic nuclei. When an electron of rest mass m_0 and velocity v passes through an atom, the interaction of its charge with the central field of the nucleus causes the electron to be deflected or scattered. For each atom the integrated probability of scattering through a given angle is proportional to $(Ze^2/m_0 v^2)^2 (1 - v^2/c^2)$, i.e., the cross section for scattering of electrons of a given energy by nuclei is $\sigma_A' \propto Z^2$. The scattering of electrons by atomic electrons involves a special theoretical treatment based on the wave mechanical resonance principles describing the interaction of two identical particles. In this case the cross section is $\sigma_A \propto Z$. Hence, for electrons of the same energy, $\sigma_A'/\sigma_A \approx Z$. Thus the two effects are of nearly equal importance in hydrogen ($Z = 1$), while for medium or heavy elements the scattering is mostly nuclear; in Au only about 1 per cent of the total scattering is caused by atomic electrons.

The other important interactions of electrons with matter are the inelastic processes: nuclear excitation, radiation, and ionization.

Nuclear Excitation. As mentioned previously, electrons cannot exist in nuclei. However, it is possible for a fast-moving electron to interact

directly with a nucleus, lifting the whole ensemble to an excited and perhaps isomeric meta-stable state. The electron then departs, deprived of some of its kinetic energy. As predicted theoretically, the cross sections for nuclear excitation by electrons are quite small ($\sim 10^{-9}$ barn). The excited state may disintegrate by neutron emission, and non-capture disintegration by electrons has a cross section of $\sim 10^{-7}$ barn for ~ 2 Mev electrons on Be^9 .

Radiation. The continuous x-ray spectrum or Bremsstrahlung is a familiar example of the conversion of electron energy into quanta of radiation as a result of inelastic scattering of electrons by the Coulomb field of atomic nuclei in the target. In the low-energy domain, this process represents only a small portion of the total energy losses, as the electron loses much more energy by ionization than by radiation. However, high energy β rays may lose very significant amounts of energy by radiation in traversing heavy materials, since this loss increases linearly with the kinetic energy E as well as with Z^2 :

$$(42) \quad (dE/dr)_{\text{rad'n}} \propto NZ^2 E/m_0^2$$

A radiated quantum may have any energy up to a maximum value equal to the incident energy of the electron. The quantum energy equals the kinetic energy lost by the electron. In theory, the radiative process is the inverse of pair production -- incident electrons produce radiation or incident radiation produces electron pairs.

Ionization. The basic mechanism for loss of energy by ionization is the same for electrons and heavy charged particles (Section 1-25). If the moving electron interacts electrostatically with an atomic electron with sufficient intensity and duration, the atomic electron may be removed, leaving a positive ion and a free electron. These separated electric charges are called an ion pair, regardless of whether the electron remains free or becomes attached to a neutral atom forming a negative ion. On the average, the energy required to produce one ion pair in air is 32.5 ev or $\sim 30,000$ ion pairs/Mev.

The ionization losses for low energy electrons having up to about one Mev of energy are given by a relation of the form:

$$(43) \quad (dE/dr)_{\text{ions}} \propto NZ/v^2 \quad (\text{low energy})$$

whence for monoenergetic electrons $dE = \text{const.} (NZdr) = (\rho mE/W)dr \approx \text{const.} (\rho dr)$.

Thus the average range of electrons, if measured in terms of gm/cm^2 of material traversed, is approximately independent of Z . The path of an individual electron in an absorber, however, is generally tortuous rather than straight, particularly at moderate and low energies.

At higher energies (above the minimum expected at $3m_0c^2$) theory predicts that the ionization losses should rise very slowly (by only 60 per cent between 3 and $1000 m_0c^2$), approximately in proportion to the logarithm of the energy.

As noted above, the radiative losses depend upon the rest mass m_0 of the swiftly-moving electron, whereas the ionization losses do not. Furthermore, in contrast with ionization processes, the energy losses by quantum radiation occur in a small number of collisions, in each of which a relatively large proportion of the electron's total energy is lost. Therefore the radiative loss for an individual electron may be much less or much greater than the average loss for the distance traversed. This is equivalent to saying that the straggling of radiative energy losses is very great. The observed straggling will, of course, be due to both radiative and ionization losses.

The ratio of radiative to ionization losses for electrons is approximately

$$(44) \quad (dE/dr)_{\text{rad}} / (dE/dr)_{\text{ion}} = EZ / 1600 m_0 c^2$$

where E is energy in Mev. As a rough rule of thumb, the two effects are equal (each about 1.6 Mev/mm Pb) in lead ($Z = 82$) for $E = 10$ Mev. At higher energies, such as are met in cosmic-ray electrons, the radiative losses become predominant, and the total observed losses are in agreement with the predicted sum of the ionization and radiative losses.

Absorption. In the foregoing considerations, the distances traversed by the electrons refer to the actual path. Because of the many deflections suffered, the total length of the path through an absorber may be from 1.5 to $4\times$ the actual thickness of absorber. Thus range measurements, except in a cloud chamber arranged to photograph the entire path, have none of the definiteness attached to range observations on heavy particles considered in Section 1-25. Nevertheless, careful observation of the effects of various absorbing foils on electrons of known energy and homogeneity can be used to define a practical extrapolated or maximum range for electrons.

In spite of variations in the form of the absorption curves, the thickness of material required to reduce the ionization or counting to essentially zero is a fairly definite observable quantity. Reproducible results are obtained in the case of initially homogeneous electrons by extrapolating the approximately linear middle portion of the absorption curve, until it cuts the value assigned to background effects. Thus the extrapolated range R_0 for homogeneous electrons is obtained as in Figure 1-23.

All available data on the extrapolated ranges of homogeneous beta rays are presented in Figure 1-24. From 0.5 to 3 Mev these data on line spectra may be represented within about +5 per cent by the linear relationship $R_0 = 0.52 E - 0.09$, where E is in Mev and R_0 is in gm Al/cm^2 .

Extrapolated ranges have also been measured for very low energy electrons in aluminum. These results are also plotted in Figure 1-24 for homogeneous beta rays from 0.01 to 0.15 Mev. Because of the greater ionization and scattering losses at such low energies, these ranges are much smaller than those for higher energies but can be represented between $E = 0.03$ and 0.15 Mev by $R_0 = 0.15 E - 0.0028$.

The distribution of electron energies is continuous, with a definite maximum value E_m , for both radioactive beta-ray spectra and for Compton recoil electrons. The shape of the absorption curves for continuous spectra differs markedly from that for line spectra. Because the lower energy electrons are most rapidly absorbed, the absorption curves for continuous spectra fall off

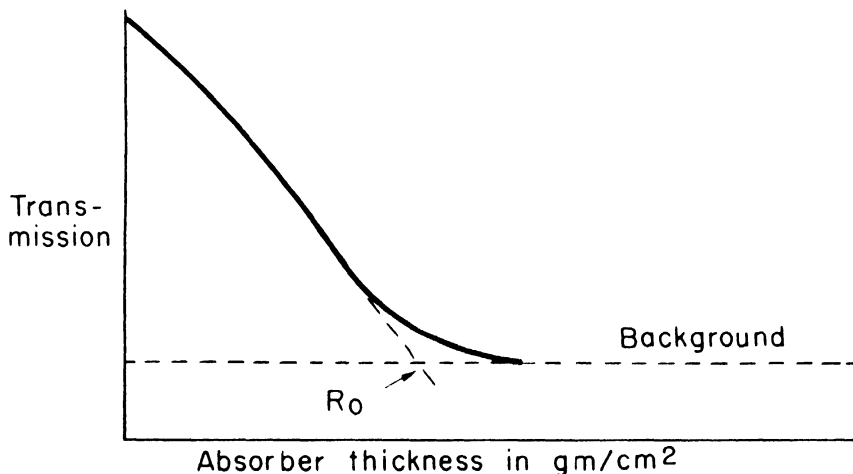


Figure 1-23. Typical Absorption Curve for Homogeneous Electrons.

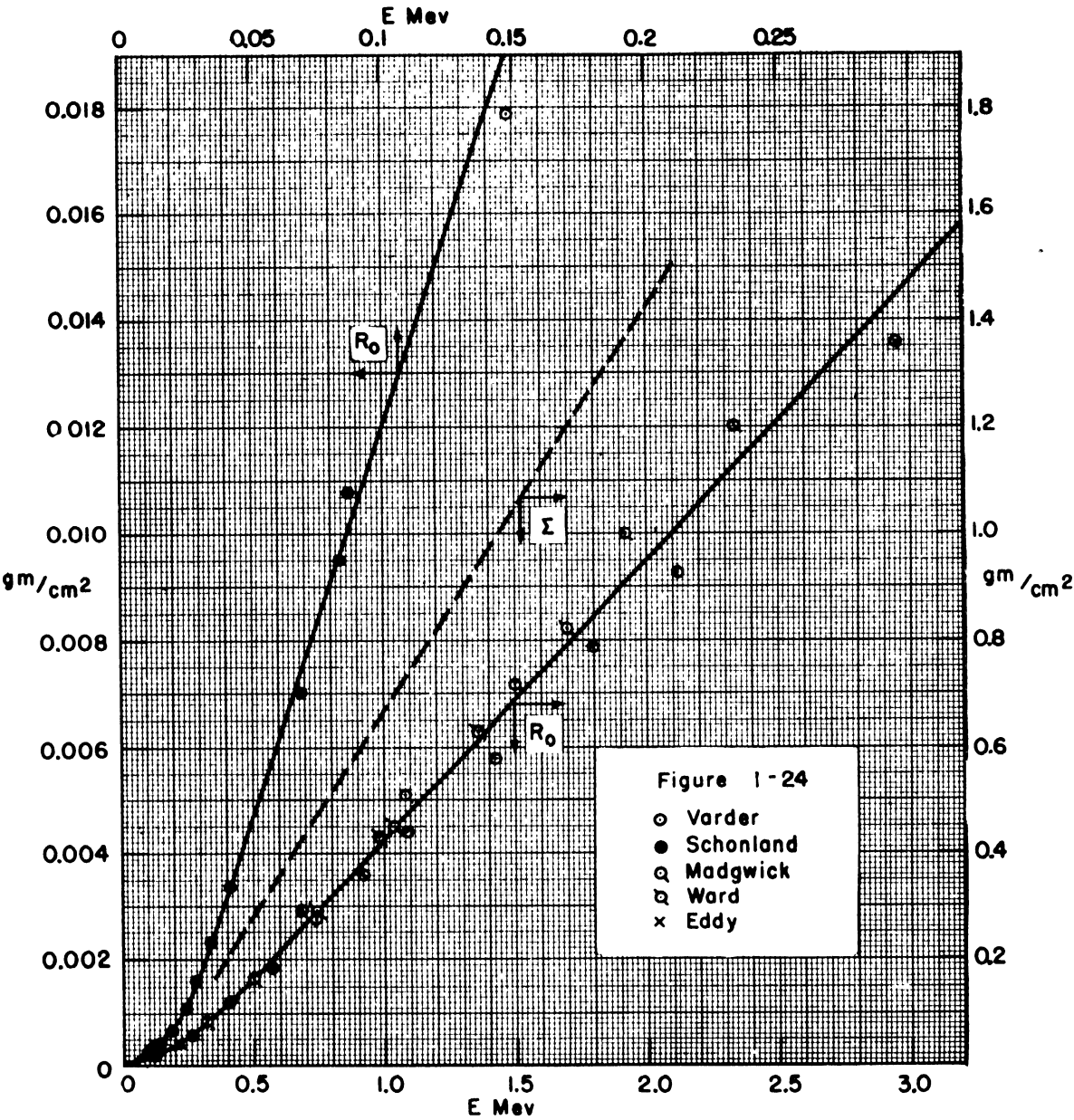


Figure 1-24.

more rapidly than those for line spectra. For radioactive beta-ray spectra, the absorption curve obtained in ionization measurements is often nearly exponential over the majority of its length, and can then be represented approximately by: $I/I_0 = e^{-\mu x}$, where I/I_0 is the fraction of the initial ionization measured after the beta rays have passed through x cm of absorbing material, and $\mu \text{ cm}^{-1}$ is the apparent absorption coefficient for the particular spectrum. If $d \text{ gm per cm}^3$ is the density of the absorber, it is found experimentally that the mass absorption coefficient μ/d is nearly independent of the atomic weight of the absorber, rising only slightly with increasing atomic number. A plot of all known values of μ/d against the maximum energy of the beta-ray spectrum E_m shows that within a probable error of about 0.2 Mev, the following empirical relationship describes these data: $\mu/d = 22/E_m^{1.33}$, where E_m is in Mev, and μ/d is measured in cm^2 per gm of aluminum. Then the absorber thickness D required to reduce I/I_0 to 0.5 is approximately:

$$(45) \quad D = \frac{0.693}{(\mu/d)} = 0.032 E_m^{1.33}$$

where the half-value thickness D is in gm per cm^2 of aluminum, or some neighboring light element. In computing I and I_0 , the background must first be deducted from all readings.

Because the shape of the absorption curve will depend somewhat on geometrical conditions, more reproducible results may be obtained by observing the thickness of absorber required to stop the beta rays of highest energy. This maximum thickness is called the maximum range, R_m . The definition of maximum range is illustrated by Figure 1-25. In the case of several radioactive substances, relatively reliable measurements are available on both the maximum range and the observed maximum energy as determined from magnetic spectrograph measurements. These data are plotted on Figure 1-26. A straight line through these points is given by

$$(46) \quad R_m = 0.54 E_m - 0.15$$

which is valid, within the known uncertainties, for maximum energies E_m near the 1 to 3 Mev domain.

A correction must be made if the beta-ray source has finite thickness, due to the absorption of beta rays within the source itself. For sources

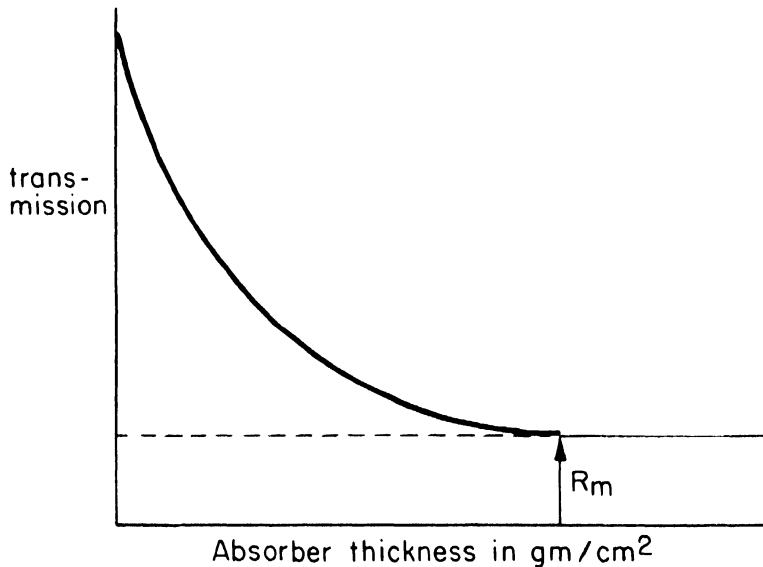


Figure 1-25. Typical Absorption Curve for Continuous Spectra.

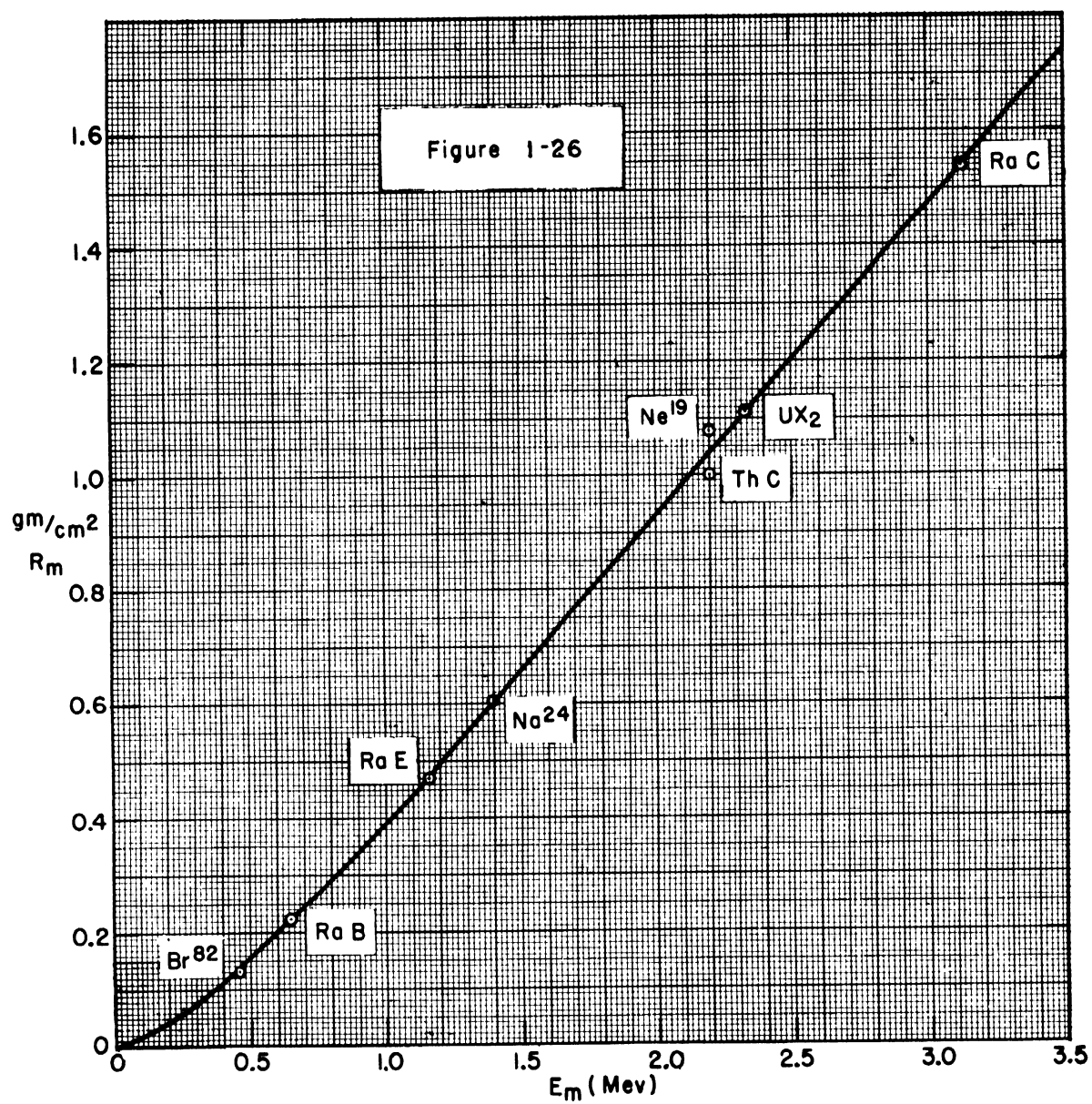
thinner than $R_m/4$, it is sufficient to add one-third of the source thickness, in gm per cm², to the observed maximum range R_m before determining E_m by Equation (46).

Neutrinos

Very little can be said about the interaction of neutrinos with matter, since these particles have never been observed directly. From the attempts that have been made, lower limits can be set for some of the physical constants. For example, from the failure to observe ionization when a known number of neutrinos pass through a known volume of gas, it is established that the mean free path for ionization is $> 3 \times 10^5$ km of air. Therefore the magnetic dipole moment of the neutrino is $< 1/5500$ Bohr magneton. It will be recalled that two-thirds of the radioactive energy of beta decay is associated with the neutrinos. It is a little unfortunate that this energy cannot be captured. The flux of neutrinos escaping from a pile operating at 200,00 kw is $\sim 10,000$ kw.

1-25 Interaction of Protons (p), Deuterons (d), and Alpha Particles (α) with Matter

With respect to the so-called heavy nuclear particles, p, d, and α , it will be recalled that these are all stripped atoms. The alpha particle, for instance, is simply a helium nucleus (${}_2\text{He}^{4+}$) with both atomic electrons absent, while the proton and deuteron are hydrogen nuclei (${}_1\text{H}^{1+}$) and (${}_1\text{H}^{2+}$) respectively.



The masses are of the order of the masses of atoms, that is, of atomic mass units per particle. Consequently, the rest energy M_0c^2 is of the order of magnitude of 1000 Mev. The kinetic energies of these particles are generally much lower, 0 to 10 Mev, and therefore their motion and interactions can be treated nonrelativistically. For example, an α of KE = 2.07 Mev has a velocity of 10^9 cm/sec or $\beta = v/c = 1/30$.

The nuclear disintegrations produced by p, d, and α were considered briefly in Section 1-15. It was observed that there is inelastic scattering and there is competition between the various modes of disintegration. These interactions, in general, have small cross sections because of the Coulomb barrier which must be overcome by these charged particles in order to penetrate a nucleus. The radiative losses, which are important in the interaction of light particles such as electrons with matter, are substantially absent in this energy domain for the p, d, and α because of their large rest masses. It will be recalled from Section 1-24 that the radiative losses are inversely proportional to the square of the rest mass. Hence for these particles the effects are $\sim 10^{-6}$ that for electrons. This leaves two important interactions for these particles, (1) the nuclear scattering and (2) the ionization effects or interaction with atomic electrons.

Elastic Nuclear Scattering. The classical theory for nuclear scattering as developed by Rutherford and by Darwin involves the simple picture of a heavy target nucleus with charge (Ze) toward which is directed at a velocity V a heavy particle of mass M which is \ll the mass of the struck particle. The Coulomb interaction results in a deflection of the incoming particle through an angle ϕ , and it can be shown that the fraction n/n_0 deflected through more than the angle ϕ is given by:

$$(47) \quad n/n_0 = (N\pi t/4)(Ze)^2(ze)^2 \left[\cot^2(\phi/2) \right] / (MV^2/2)^2$$

in which $N \equiv$ number of scattering centers or nuclei per cm^3 , $t \equiv$ the thickness of the foil in cm. The important factor to be considered, for it enters very strongly in the case of the fission particles, is the variation with charge. It is seen that the magnitude of the scattering to be expected is proportional to the square of the charges of the struck nuclei $(Ze)^2$ and to the square of the charges of the moving nuclei $(ze)^2$ and inversely proportional to the square

of the energy of the latter $(MV^2/2)^2$. If the struck particle is not infinitely massive compared with the moving particle, corrections need to be made in Equation (47), for the most part replacing the mass by the reduced mass of the system. Such corrections obviously must be made in the case of fission particles.

Ionization. In the ionization of matter by swiftly-moving heavy particles; alpha particles for example, the theory is fairly good in the high velocity domain and can be used for interpolation between measured points and for extrapolation somewhat beyond these values. The theory was originally due to Bethe in the case of hydrogen. He made some modifications of his own later on, and then a similar treatment was developed by Bloch using the Thomas-Fermi model of the atom. An alpha particle of charge ze is considered (either as a corpuscle or wave) to be moving with a velocity V by an atom of nuclear charge Ze surrounded by Z electrons. In the case of hydrogen, one writes the Schrödinger equation for the potential between the nucleus and its one atomic electron, puts in perturbation terms for the interaction between the alpha particle and the nucleus and between the alpha particle and the electron, uses the Born approximation and obtains a solution of this character:

$$(48) \quad dT/dr = (4\pi e^2/m_0)(ze/V)^2 NZ \ln 2m_0 V^2/J$$

where the loss in kinetic energy per unit of path is dT/dr , the rest mass of the struck electron is m_0 , the number of atoms per cm^3 is N , the geometric mean ionization potential for all possible excited levels of the atom is J . J is approximately αZ and equals about 98 ev for air. The numerator of the \ln term, $2m_0 V^2$, represents the maximum kinetic energy that can be given to the light particle by the head-on collision of an alpha particle. Hence $2m_0 V^2$ is the maximum energy of the δ rays, i.e., the more energetic electrons that are seen springing out the side of alpha particle tracks in cloud chamber photographs. Using nonrelativistic kinetic energy and rearranging Equation (48) to obtain an integration of dr from the beginning of the range at the point of emission of the alpha particle from the nucleus to its final range R in the absorber,

$$(49) \quad R = \int_0^R dr = (m_0/4\pi e^2)(M/z^2) \int_{V_0}^0 \left[V^3/NZ \ln (2m_0 V^2/J) \right] dV$$

This integral cannot be evaluated all the way from the initial velocity V_0 to the end of the range when the velocity is zero, but can be evaluated to some arbitrary critical velocity V_c greater than $J/2m_0$. This mathematical failure is equivalent to the failure at these lower velocities of the Born approximation and physically is equivalent to the condition that the kinetic energy of the moving particle is no longer large compared to the binding energy of the inner electrons, such as the K and L electrons. This effect is especially pronounced in heavy elements.

Theory and experiment are in excellent agreement above a velocity V of about 8×10^8 cm/sec. The ranges vary with velocity for alpha particles as shown in Figure 1-27, which is approximately as $R \approx k V^3$.

Because of statistical fluctuations in both the number of ionizing collisions and in the energy transferred per collision, any group of originally monokinetic alpha rays will have a statistical distribution of residual velocities at any distance from the source, and a distribution of ultimate ranges about the most probable value, called the mean range. This straggling of ranges is illustrated in Figure 1-28.

The air-mm used in Figure 1-27 means a path equivalent to one mm of dry air at 15°C and 760 mm pressure. It is a standard of ranges for swiftly-moving charged particles throughout nuclear physics. Thus the ranges R for particles like protons and deuterons can be had from the known ranges R_α for

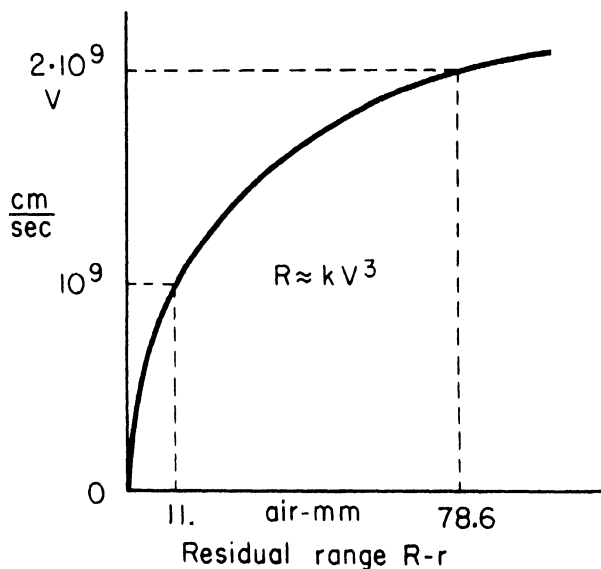


Figure 1-27. Range-Velocity Relation for Alphas.

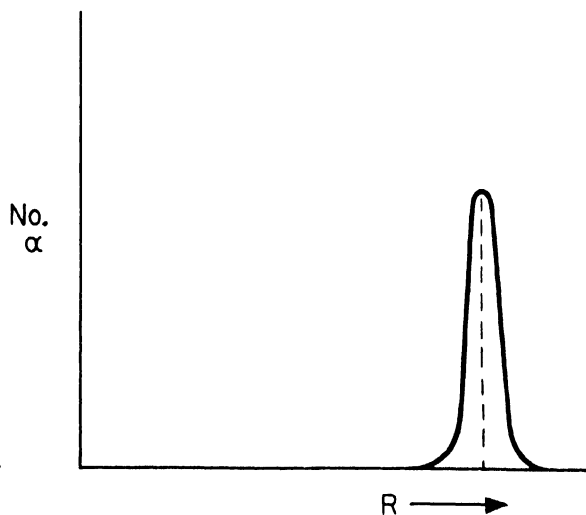


Figure 1-28. Statistical Straggling of Alphas.

alphas from the relationship M/z^2 which is ≈ 1 for alphas, ≈ 1 for protons and ≈ 2 for deuterons: $R = R_\alpha(M/z^2)$ for the same V_0 . There is a small correction of 2 air-mm which must be subtracted from this calculated range in the case of protons because the influence of capture and loss of e^- on the range is less for protons than for α rays.

The experimentally observed loss of energy per unit length of path for alphas is shown in Figure 1-29. The energy loss is expressed in ion-pairs per air-mm which can be converted to Mev/air-mm through the relationship that, on the average, 32.5 ev are required to produce one ion-pair in air. The residual range $R-r$ as used in both Figure 1-27 and Figure 1-29 is the remaining path length to be travelled after the particle has gone a distance r . For large residual range, when the particle still has most of its energy, the curve of energy loss follows the prediction of Equation (48). At a value of $R-r \approx 4$ air-mm (for which $dT/dr \approx 6600$ ion-pair/air-mm, $V \approx 6 \times 10^8$ cm/sec and $E \approx 0.75$ Mev), the specific ionization departs from the predicted value and decreases rapidly to zero at $R-r = 0$. The reason for this is the capture and loss of electrons on the moving particle. Even at high velocity an alpha particle occasionally captures an electron from the atoms through which it moves, becoming He^+ instead of He^{++} for a short while. However, this effect increases markedly at low velocities. At the peak of Figure 1-29, which could be called a Bragg curve for a single particle, the average charge $ze \approx 1.5e$ instead of $2e$. In the remaining 4 air-mm of travel, the alpha particle on the average

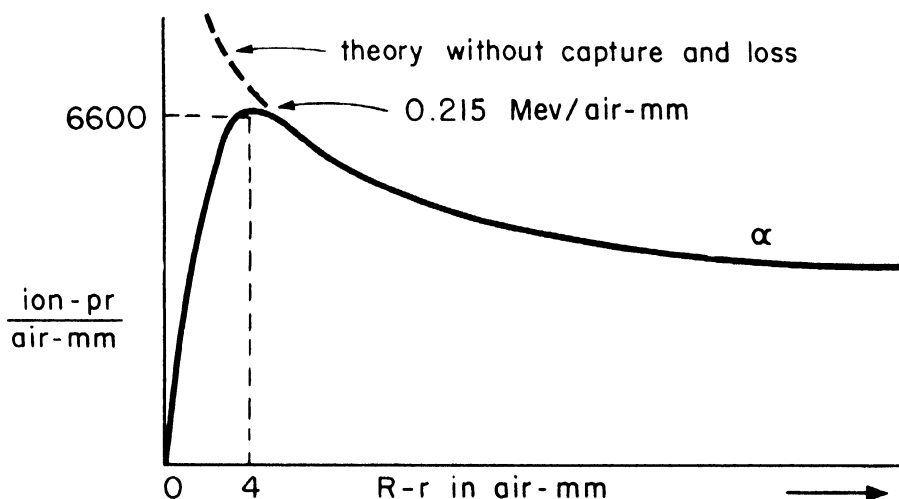


Figure 1-29. Specific Ionization by Alphas.

exchanges an electron with the medium more than 1000 times, i.e., the mean-free-path for capture and loss is very short. This effect is even more pronounced in the fission fragments.

With respect to the ranges of particles of this character in materials other than air, the originally empirical Bragg-Kleeman Rule, which now has some basis in theory, states that the length L of the path in the medium is related to the range R_a in air as

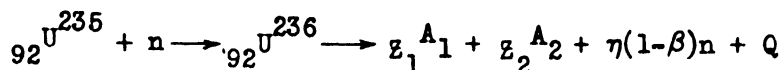
$$(50) \quad L = R_a (\rho_a / \rho) \sqrt{A/A_a} = 3.2 \times 10^{-4} (R/\rho) \sqrt{A}$$

where $A \equiv$ mass number of material, $A_a \equiv$ mean mass number of air, and ρ, ρ_a are respective densities. Substituting for A_a and ρ_a , it is seen that for alphas of 7 Mev, for which $R_a \approx 6$ cm of air, the path length in ordinary solids is 30 to 40 microns. Unlike the case for electrons, the ranges cannot be written simply in gm/cm^2 for all materials. In addition to $\rho L (\text{gm/cm}^2)$, there is a variation with \sqrt{A} ; i.e., $\rho L / \sqrt{A} \approx \text{const.}$ Figure 1-30 gives the range energy relationship for alpha particles on three separate curves. The solid lines are in accord with the theory in which J has been matched by taking known values for alpha-ray ranges in air; J turns out to be 98 ev in air. The ranges shown are in air-cm at 15°C and 760 mm Hg pressure.

As seen in Figure 1-29, there is intense ionization along the path of the alpha ray. This dense, columnar ionization produces chemical changes in many materials and distorts the lattice structure of crystalline solids. For example, the luminosity of a radium-bearing watch dial fades within a few months because of this effect, not due to the decay of the radium. The fission fragments can be expected to be even more damaging. For this reason studies of the effects of radiation on materials of construction in nuclear reactors are of major engineering importance.

1-26 Interaction of Fission Particles with Matter

In general terms, the fission of ^{235}U can be written as



where the light and heavy fission fragments will be designated as A_1 and A_2 respectively. The average number of neutrons per fission is η , which lies somewhere between 2 and 3 (estimated from pre-1941 literature). A small

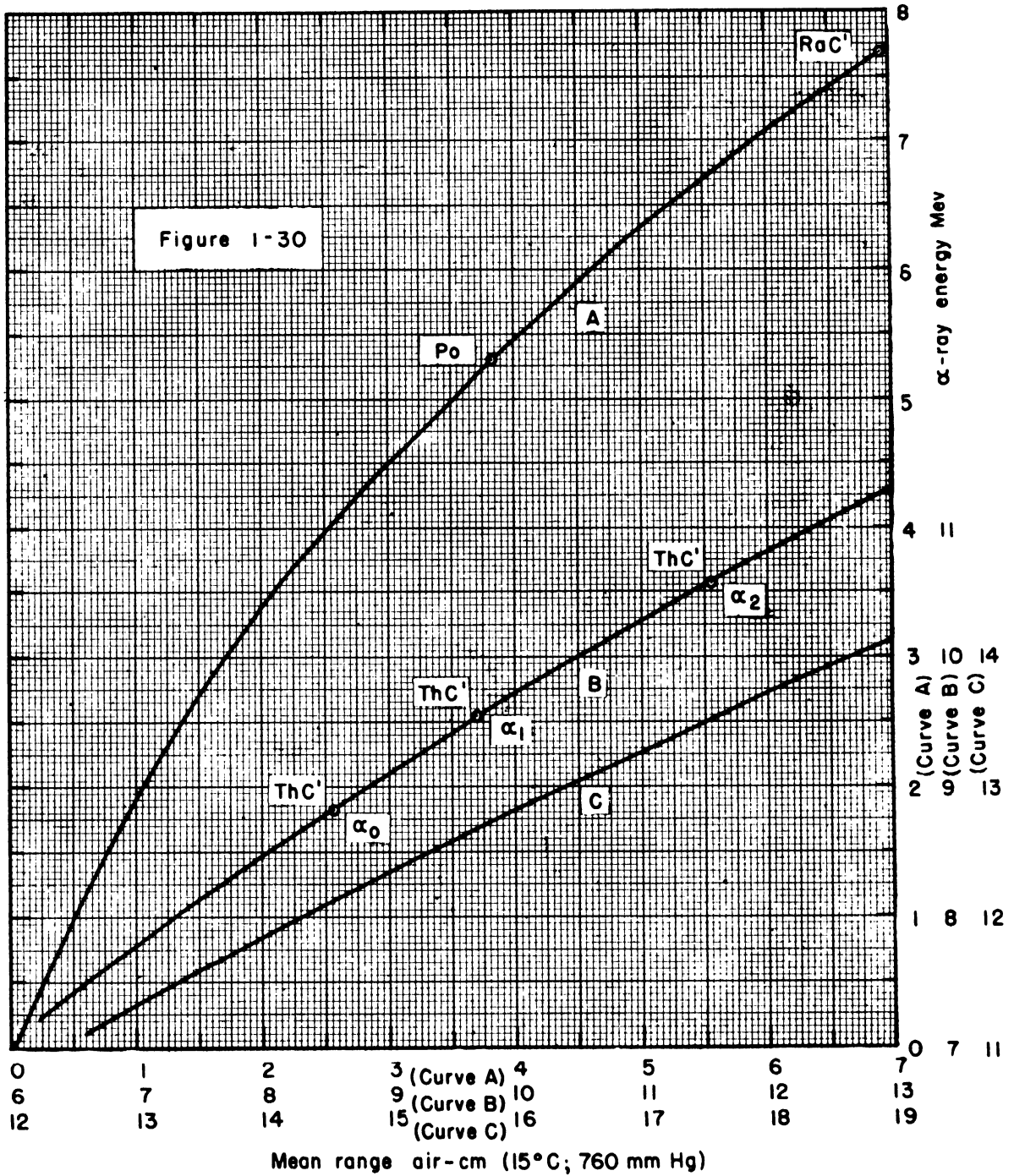


Figure 1-30.

fraction $\beta (\approx 0.006)$ of these neutrons are delayed (e.g., see Figure 1-10) but the majority $\eta(1-\beta)$ of the neutrons per fission are emitted promptly.

The original compound nucleus may be thought of as elongating and splitting into two parts with charges Z_1 and Z_2 , masses A_1 and A_2 , and velocities of recession from their center of mass V_1 and V_2 . Assuming, for the moment, that the neutrons are emitted from the fragments rather than simultaneously with fission, conservation of momentum requires that $A_1V_1 = A_2V_2$. Therefore, $(A_1V_1)^2/2 = (A_2V_2)^2/2$ or $A_1E_1 = A_2E_2$. Hence, the total energy, $E_1 + E_2 = E_1(1 + A_1/A_2)$, can be measured from the energy of the light fragment and knowledge of the ratio of the masses A_1/A_2 , which is generally <1 .

The total energy of fission Q not only can be estimated from the binding energy curve of Figure 1-2, but also can be found from the electrostatic energy of repulsion between the two fragments: $Q \approx Z_1Z_2e^2/r \approx 200$ Mev for $r = 1.5 \times 10^{-12}$ cm, distance between centers of the two fragments assumed spherical and just touching. Calorimetric and ionization measurements (assuming 32.5 ev/ion pr) give $Q \approx 160$ Mev for the most probable fragments.

There is a statistical distribution of the masses such that $(A_1 + A_2)$ generally equals 234 or 233, depending on the number of prompt neutrons. The distribution of these fission products (F.P.) is as indicated in Figure 1-31. The fission yields in log % have modal values, or most probable values, $A_1 \approx 95$ and $A_2 \approx 139$. The yields decrease rapidly at high and low A to about 10^{-5} per cent for $A_1 \approx 72$ and $A_2 \approx 162$. The total fission energy depends to some extent on the particular values of A_1 and A_2 , since these determine the positions of the fission fragments on the binding energy curve.

The most probable values of the important properties of the fission fragments of U^{235} , as given in the unclassified references cited, are listed in Table 1-1.

The most probable values of A in amu are ~ 95 and ~ 139 as seen in Table 1-1. The most probable values of Z are rather uncertain, the values $Z_1 \approx 38$ and $Z_2 \approx 54$ are based on the assumption that the nuclear charge is proportional to the total number of particles, i.e., $Z/A = \text{const}$. The energy, again corresponding to the most probable mode of disruption, is $E_1 \approx 97$ Mev and $E_2 \approx 65$ Mev. In spite of these high energies, because of the large masses, the corresponding initial velocities V_0 are not as large as have been considered for alpha particles. The magnetic rigidity at the moment of splitting

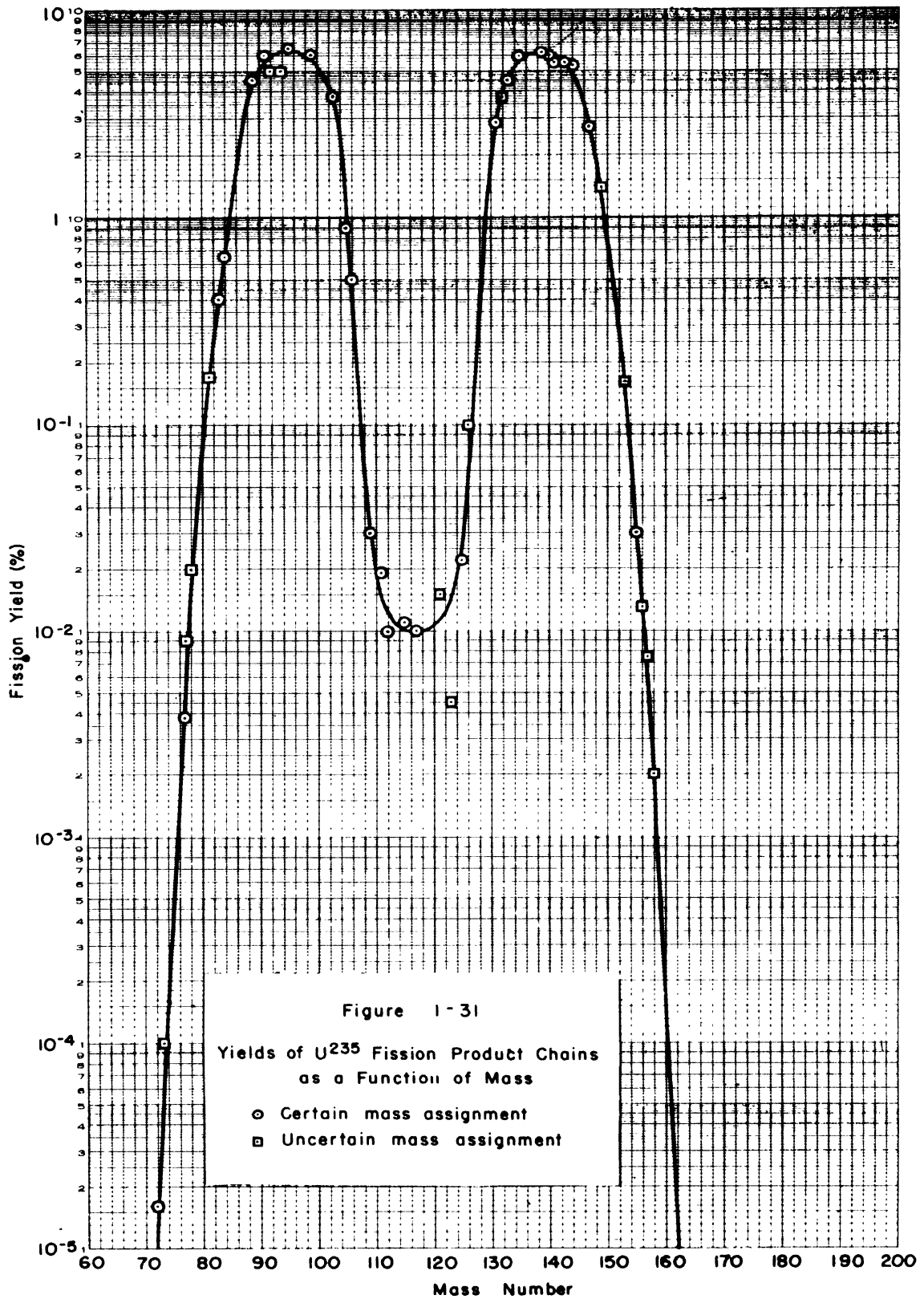


TABLE 1-1

	Light Fragment A_1	(ref.)	Heavy Fragment A_2
A amu	~95	(1)	~139
Z	~38 (Sr)	(2)	~54 (Xe)
E Mev	97	(3)	65
$V_0 \frac{\text{cm}}{\text{sec}}$	1.4×10^9	(4)	0.93×10^9
$(H\rho)_0$ gauss-cm	6.5×10^5	(5)	5.9×10^5
(ionic charge) ₀	20 e	(6)	22 e
R_{mean}	25. air-mm	(4)	19. air-mm

(1) Plutonium Project Report J. Am. Chem. Soc. 68, 2411-2442 (1945). (2) if Z/A is const. (Bohr.) (3) If $E_1 A_1 = E_2 A_2$ and $E_1 + E_2 = 162$ Mev (Bohr). (4) Bøggild et al. Kgl. Danske 1940. (5) Lassen PR 69, 137 (1946); and $Z_1(H\rho)_1 = Z_2(H\rho)_2$ (=MV). (6) Lassen PR 68, 1426 (1945).

$(H\rho)_0$ is nearly 1000 times that usually encountered for beta rays. Hence, very intense magnetic fields are required to deflect these particles. The cyclotron in Copenhagen has been used to produce neutrons from Be (d,n) which induce fission in uranium placed close to the internal Be target. The fission fragments have then been studied by means of the magnetic deflection in the field of the cyclotron. The most probable value of 6.5×10^5 gauss-cm for the light fragment was derived from these measurements. The value for the heavy fragment was then calculated. The initial ionic charge is extremely important in the fission process. It is seen that, unlike the alpha particle which is emitted with its two electrons stripped off, the fission fragments retain a significant fraction of the atomic electrons of the compound atom. Contrary to any theories thus far proposed, the heavier fragment has a higher initial ionic charge. The mean range cannot be calculated from the two-body theory used for alpha particles, since the fission fragments have many electrons attached as they move through matter. The values given are based entirely on experimental observations.

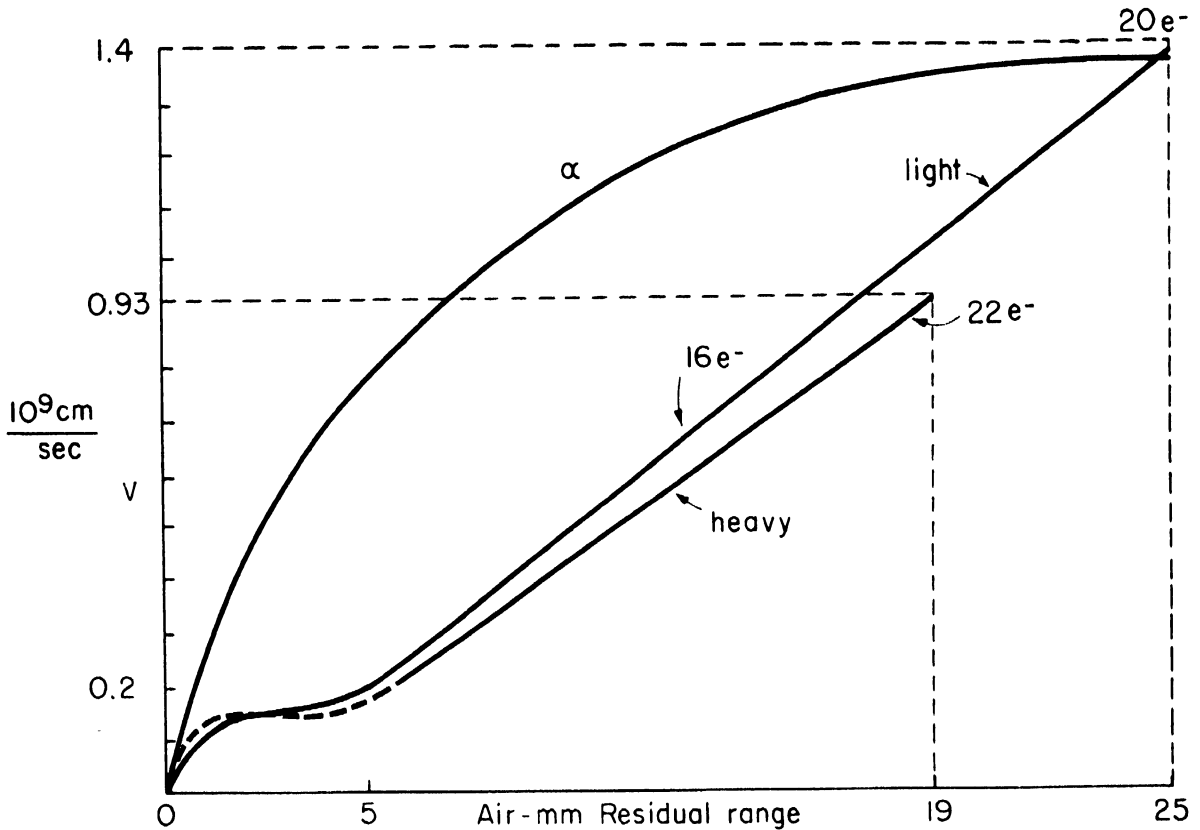


Figure 1-32. Range-Velocity Relationship of Fission Fragments.

Instead of the relationship $R \approx k V^3$ for alphas, as illustrated in Figure 1-27 and repeated for comparison in Figure 1-32, the fission fragments have unique range-velocity characteristics. As this figure shows, the range (~ 25 air-mm) of the most probable light fragment is nearly the same as that for an alpha particle of the same initial velocity, 1.4×10^9 cm/sec, while the range of the heavy particle is substantially greater than for an alpha of the same velocity. The decline in velocity with decreasing residual range is very different, being nearly linear down to about 0.2×10^9 cm/sec at 5 air-mm for both the light and heavy fission fragments. This effect is solely the result of capture and loss of electrons by the highly-charged particles which at the instant of splitting are about 20 times and 22 times ionized respectively. As their velocity decreases, the charge also decreases. Hence the specific ionization dT/dr along their paths decreases almost linearly with their range, as seen in Figure 1-33. Thus the upper part of the range-velocity relationships for fission fragments is very similar to the front face of the

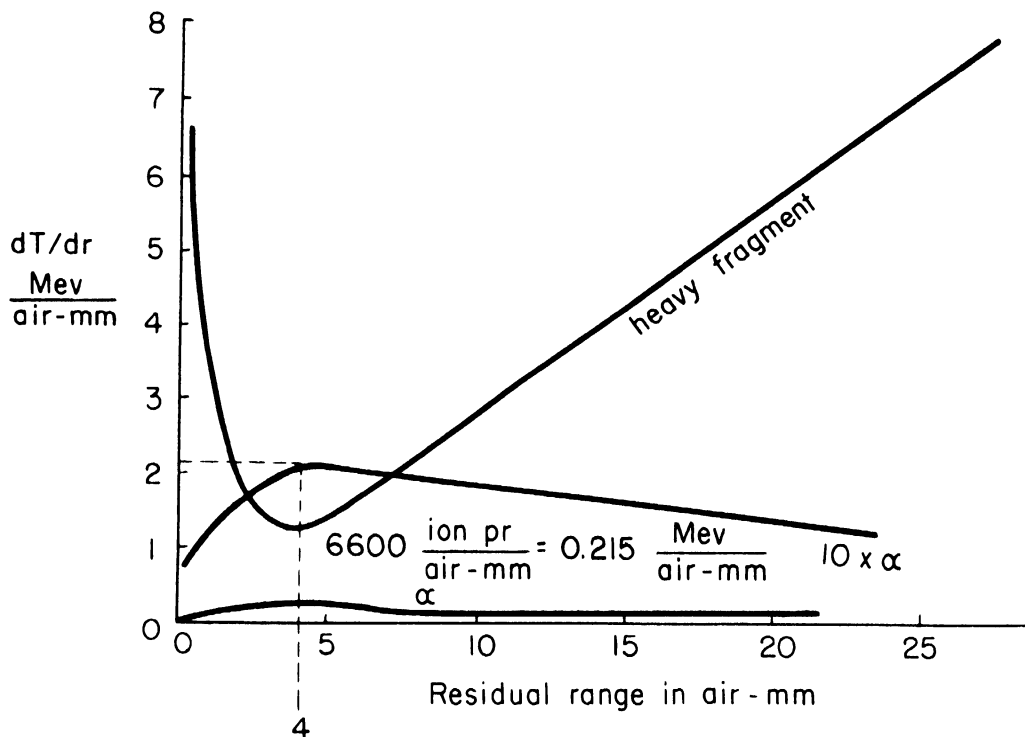


Figure 1-33. Rate of Energy Loss as a Function of Range. The curve for a heavy fission fragment is compared with that of an alpha particle (magnified for clarity).

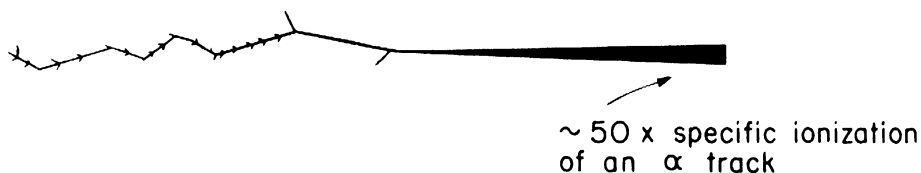


Figure 1-34. Schematic Drawing of Fission Track as Seen in a Cloud Chamber.

Bragg curve for an alpha particle, except that in the latter the effect takes place in the last 4 mm of the alpha track.

At a velocity of about 0.2×10^9 cm/sec, which corresponds approximately to that of the most loosely bound electrons in the neutral atom, the fission fragments lose energy at a much slower rate than at any other part of the range, giving rise to almost flat plateaus in the curves of Figure 1-32 and a minimum in the curve of Figure 1-33.

Below a velocity of about 0.2×10^9 cm/sec, the effect of nuclear collisions becomes increasingly important, resulting in marked curvatures of the path and a rapid increase in the rate of energy loss, as seen in Figure 1-33. The knock-on atoms of the absorber, which correspond to the knock-on electrons

or δ rays produced by alpha particles, appear as dense spurs along the fission tracks, shown schematically in Figure 1-34. A great deal of energy is lost by a fission fragment in each of these elastic nuclear collisions. The velocity-range relationships for the fission fragments are determined by measurements on cloud chamber photographs of these secondary particles. The number of nuclear collisions per fission track ranges from 0 up to about 9, with a mean of about 2. Hence the straggling in range of fission fragments is very large. The average number of branches with lengths between the limits corresponding to energies E_1 and E_2 has been given by Bohr [Phys. Rev. 59, 270 (1941)] as:

$$(51) \quad \omega/\Delta x = 2\pi N(Z_e/V)^2 \left[(Z_a e)^2/M \right] \left[(1/E_1) - (1/E_2) \right]$$

where Z_e is the nuclear charge of the fragment whose velocity is V , $Z_a e$ and M are the charge and mass of the knock-on nuclei, N is the number of these nuclei per cm^3 , and Δx is the interval of range. This formula holds in a region where both energy limits represent values which can actually be attained by the struck nuclei, consistent with the requirements of conservation of energy and momentum.

1-27 Neutron Interactions

The neutron is a particle of zero charge ($Z = 0$), hence can be considered as having an atomic number 0 in the periodic system of the elements. The rest mass m of the neutron (1.00893 amu) is only slightly larger than that of the proton (1.00758). The neutron has a negative dipole moment ($\mu = -1.91\mu_0$), an angular momentum or spin $I = 1/2$ and Fermi-Dirac statistics.

For a neutron moving with velocity V , the wave length $\lambda = h/mV = h/\sqrt{2mE} = 0.286/\sqrt{E(\text{ev})}$ Angstroms. Thus for a neutron of energy 1 ev, $\lambda = 0.286\text{\AA}$, which is atomic in size. Hence, beams of such neutrons can be diffracted by crystals in spectrometers that are very similar to those used for x-rays (either transmission or reflection). By this means it is possible to obtain beams of monoenergetic neutrons.

The only known sources of neutrons are from nuclei which have undergone a change, usually as the result of a collision with a particle or quantum. Most neutrons are emitted with energies of about 1 Mev or more. Since all nuclei, with the possible exception of He^4 , have measurable neutron cap-

ture cross sections, free neutrons in matter are quickly slowed down and captured; for example, the mean life for neutrons in paraffin is $\sim 10^{-4}$ sec. The major capture in this case is by $H^1(n, \gamma)H^2$. Because of the mass difference, it is energetically possible for a neutron to change to a proton, $n \rightarrow p^+$. From theoretical considerations, it has been predicted that the half-period for this beta decay of the free neutron is ~ 30 min. Experiments testing this prediction are in progress at the Clinton Laboratories and elsewhere.

The interactions of neutrons with matter are all of a nuclear character. There are no interactions between neutrons and electrons. The various type reactions for neutrons have been summarized in Section 1-15. Following neutron capture in target nuclei of low Z and hence low Coulomb barrier, the (n, α) and (n, p) reactions are more likely, while for high Z the (n, γ) reaction is more probable. There can also be both elastic and inelastic scattering (n, n) processes.

Elastic Scattering. In the absence of substances with large inelastic or capture cross sections, the slowing down of the fast, fission neutrons ($\gtrsim 1$ Mev) is largely by elastic collisions with the surrounding nuclei. A series of successive elastic collisions takes place in which a neutron loses a fraction of its energy at each collision with the nuclei of the moderator. It can be shown from Equation (52) below that the average residual energy of a neutron after striking hydrogen (H^1), for example, is $1/e$ of the initial energy. As derived below, the fractional energy loss per collision declines rather rapidly with increasing atomic weight. Hence heavy elements are not good choices as moderators for slow neutron reactors.

From the Q equation (Equation (15), p.17) with $Q = 0$, which obtains in an elastic collision, $A_1 = A_2 = m = \text{mass of the neutron}$, $A_3 = A = \text{mass of target nucleus}$, $E_1 = E_0 = \text{initial kinetic energy of neutron}$, and $E_2 = E = \text{final kinetic energy of scattered neutron}$, it is shown in Appendix B that for the head-on collision, in which $\theta = 0$ and $E = E_{\min}$, the energy lost by the neutron is:

$$(52) \quad E_0 - E_{\min} = E_0 \left\{ 1 - \left[(A - m)/(A + m) \right]^2 \right\} = E_0 (1 - \alpha)$$

where

$$\alpha = \left[(A - m)/(A + m) \right]^2 = E_{\min}/E_0$$

Thus the maximum fractional loss of kinetic energy in one collision is

$$(E_o - E_{\min})/E_o = \left\{ 1 - \left[(A - 1)/(A + 1) \right]^2 \right\} = (1 - \alpha)$$

Values of $(1 - \alpha)$ for a broad range of nuclei are given in Table 1-2. This table also includes values for the mean logarithmic energy loss in one collision ξ and the average number of collisions ν required to slow down a 1 Mev neutron to thermal energy (by definition $E_{\text{th}} = (1/2)m V_{\text{th}}^2 = kT$; for $T \approx 293^\circ\text{K}$, $E_{\text{th}} = 0.025 \text{ ev}$, $\lambda_{\text{th}} = 1.8 \text{ \AA}$, $V_{\text{th}} = 2200 \text{ meters/sec}$). From its definition, $\xi = \text{average of } (\ln E_o - \ln E)$ over the range E_{\min} to E_o ,

$$(53) \quad \xi = \frac{1}{E_o(1 - \alpha)} \int_{\alpha E_o}^{E_o} \ln(E_o/E) dE = \frac{1}{E_o(1 - \alpha)} \left[E \ln E_o - E \ln E \right]_{\alpha E_o}^{E_o}$$

$$(54) \quad \xi = 1 + \left[\alpha/(1 - \alpha) \right] \ln \alpha \approx 2/(A + 2/3) \text{ for } A \gg 1$$

$$(55) \quad \nu = (1/\xi) \ln E_o/E_{\text{th}} = (1/\xi) \ln 4 \times 10^7 = 17.5/\xi$$

When high energy neutrons are produced continuously in an extended but non-infinite and heterogeneous medium (such as in a graphite-uranium reactor), the resulting elastic collisions (and a small amount of capture) can be shown to produce a number-energy distribution that is like a Maxwellian distribution characteristic of the absolute temperature T of the moderator (thermal distribution) plus a $1/E$ tail at high energies. A curve of this type is shown in Figure 1-35, in which the fraction $N(V)/N$ of neutrons within a given velocity range V to $V + dV$ is plotted against the velocity V . The peak of this curve occurs at the modal velocity, 2200 m/sec, characteristic of thermal neutrons at 15°C .

TABLE 1-2

A	H ¹	H ²	He ⁴	Be ⁹	C ¹²	O ¹⁶	U ²³⁸
(1 - α)	1	0.88	0.40	0.36	0.27	0.22	0.0085
ξ	1	0.72	0.43	0.35	0.16	0.12	0.0084
ν	18	24	41	50	110	145	2100

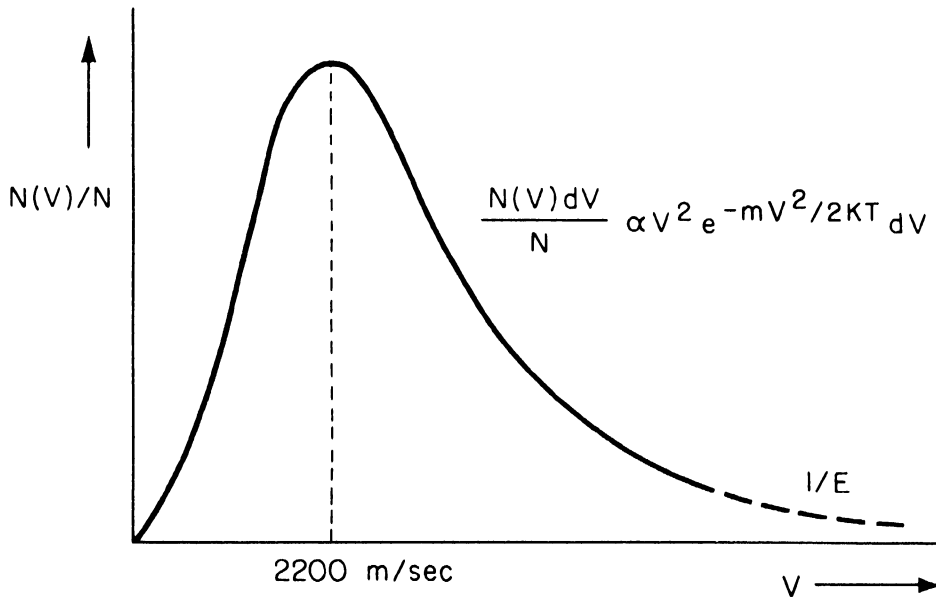


Figure 1-35. Maxwellian Distribution of Thermal Neutrons.

Dispersion Theory for Single Resonance Levels. By analogy with the theory of optical dispersion, the modes of interaction of neutrons, particularly those of thermal energy, with nuclei can be described. A neutron of energy E , wave length λ , and minimum position indeterminacy $\lambda/2\pi = \lambda = h/2\pi p$ combines with a nucleus A forming a compound nucleus $A+1$ in an excited state. This ensemble of nucleons can have a number of quasi-stationary states, different from the ground state and even above the dissociation limit, because of the many-body composition of nuclei. Hence there are virtual excited levels in the compound nucleus $A + 1$ with average spacings of several hundred kilovolts near the ground state and of about 100 ev at excitation energies of about 8 Mev, that is, in the neighborhood of the dissociation energy.

The compound nucleus then has a number of probabilities λ_i of transition to lower-lying levels:

elastic re-emission of n	$(n, n);$	$\lambda_n;$	$\Gamma_n = \hbar \lambda_n \sim 10^{-3} \text{ ev}$
γ emission to one or more lower states	$(n, \gamma);$	$\lambda_\gamma;$	$\Gamma_\gamma = \hbar \lambda_\gamma \sim 0.1 \text{ ev}$
α emissions	$(n, \alpha);$	$\lambda_\alpha;$	$\Gamma_\alpha = \hbar \lambda_\alpha$
p emissions	$(n, p);$	$\lambda_p;$	$\Gamma_p = \hbar \lambda_p$
<hr/>			
Total:	$\lambda_t;$	Γ	$= \hbar \lambda_t$

The quantities Γ_i represent the partial width, usually expressed in ev, of the energy level for various possible modes of de-excitation. Thus the total width Γ of a level in the compound nucleus is the sum of all the partial widths:

$$(56) \quad \Gamma = \Gamma_n + \Gamma_r$$

where $\Gamma_r = \Gamma_\gamma + \Gamma_\alpha + \Gamma_p$. The total width Γ is proportional to the total probability of decay of the excited level and depends on the configuration of all the lower-lying levels to which transformations are possible. Experimentally, it is found that $\Gamma_n \ll \Gamma_r$, that is, the compound nucleus has a large damping and the probability of elastic re-emission of the neutron (n, n) is thus made very small.

Under the restrictions that $\lambda \gg$ nuclear radius, and central collisions (s wave capture) only, and considering only a single resonance level, Breit and Wigner have shown that the nuclear cross section for neutron capture σ_c can be represented by the relation

$$(57) \quad \sigma_c = \pi \lambda^2 \Gamma_r \Gamma_n / \left[(E - E_0)^2 + \Gamma^2/4 \right]$$

and the cross section for elastic scattering of neutrons is

$$(58) \quad \sigma_s = \pi \lambda^2 \Gamma_n \Gamma_n / \left[(E - E_0)^2 + \Gamma^2/4 \right]$$

from which, by Equation (56), the total cross section σ_t is given as

$$(59) \quad \sigma_c + \sigma_s = \sigma_t = \pi \lambda^2 \Gamma_n \Gamma / \left[(E - E_0)^2 + \Gamma^2/4 \right]$$

But Γ_n varies with the amplitude of the neutron wave at the surface of the nucleus considered either in capture or emission, hence Γ_n is proportional to the neutron velocity V :

$$(60) \quad \Gamma_n = C'V = C\sqrt{E}; \quad \lambda = D/\sqrt{E}$$

$$(61) \quad \sigma_c = \pi \frac{D^2}{E} \cdot \frac{C\sqrt{E} \Gamma_r}{(E - E_0)^2 + \Gamma^2/4}$$

At $E = E_0$:

$$(62) \quad \sigma_c = \sigma_0 = \pi CD^2 \Gamma_r / \sqrt{E_0} (\Gamma^2/4)$$

hence, in general,

$$(63) \quad \sigma_c = \sigma_0 \sqrt{E_0/E} / \left\{ \left[(E - E_0)/(\Gamma/2) \right]^2 + 1 \right\}.$$

It will be noted that this expression is similar in form to the equation for the antenna current in a highly-damped (low Q) radio receiver, as well as to equations in the theory of optical dispersion.

The maximum cross section σ_0 occurs when the incident neutron has exactly the kinetic energy $E = E_0$ necessary to form the quasi-stationary excited state of the compound nucleus. If E_0 is in the thermal range, the excited state has an excitation energy of about the average binding energy per nucleon, say 8 Mev. It can be seen that for reasonably sharp resonances, where $\Gamma \ll E_0$, the width Γ corresponds physically to the full width of the resonance curve at half-maximum, i.e., $\sigma_c = \sigma_0/2$ for $E - E_0 = \pm \Gamma/2$.

For very broad resonances, it follows directly that if $\Gamma \gg (E - E_0)$,

$$(64) \quad \sigma_c = \sigma_0 \sqrt{E_0} / \sqrt{E}$$

hence

$$\sigma_c \propto 1/V$$

which is the usual $1/V$ relationship for a broad level with high probability of capture of slow neutrons. In general,

$$(65) \quad \sigma_c \propto (1/V) \Gamma_r / \left[(E - E_0)^2 + \Gamma^2/4 \right]$$

These phenomenological relationships are useful in understanding the variation of cross section with energy of a number of important substances used in nuclear reactors. The general shape of the curves for fuel materials U^{238} and U^{235} and for detection and control materials B^{10} and Cd^{113} are shown in Figures 1-36 to 1-39.

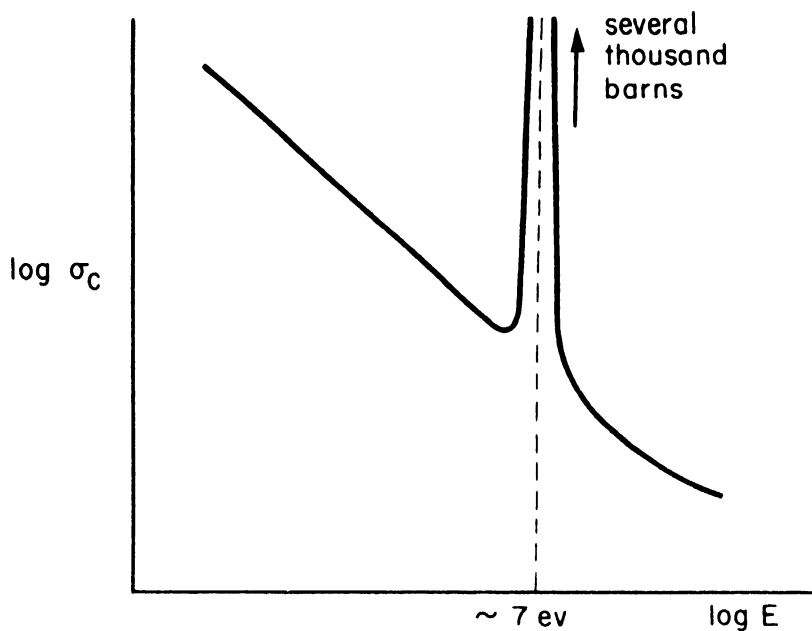


Figure 1-36. Capture Cross Section of $U^{238} (n, \gamma)$, showing essentially $1/v$ relationship plus large resonance at ~ 7 electron volt energy.

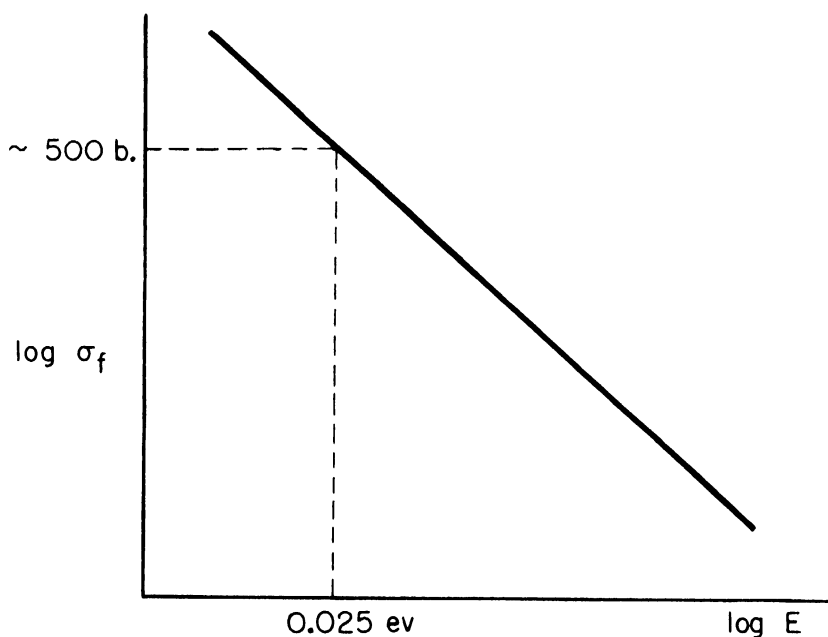


Figure 1-37. Fission Cross Section of $U^{235} (n, f)$, showing essentially $1/v$ relationship (approximate value shown for $k T$ neutrons based on averages from pre-1941 literature).

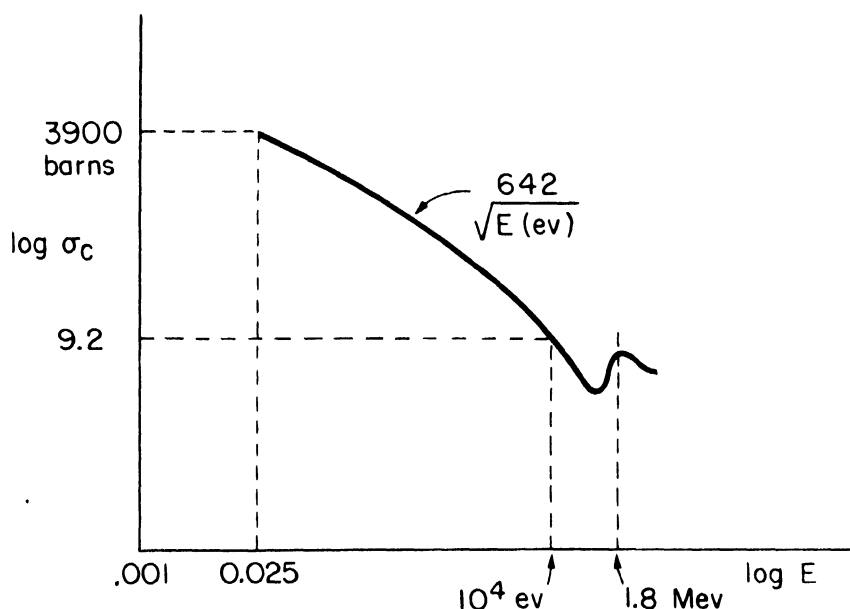


Figure 1-38. Capture Cross Section of B^{10} (n, α). Except for the small resonance at 1.8 Mev, this absorption is essentially $1/\sqrt{E}$ below about .1 Mev. B^{10} has an abundance of 18.4% in boron, thus the separated isotope for which the curve is drawn has an absorption of 5.43 times that of the natural element.

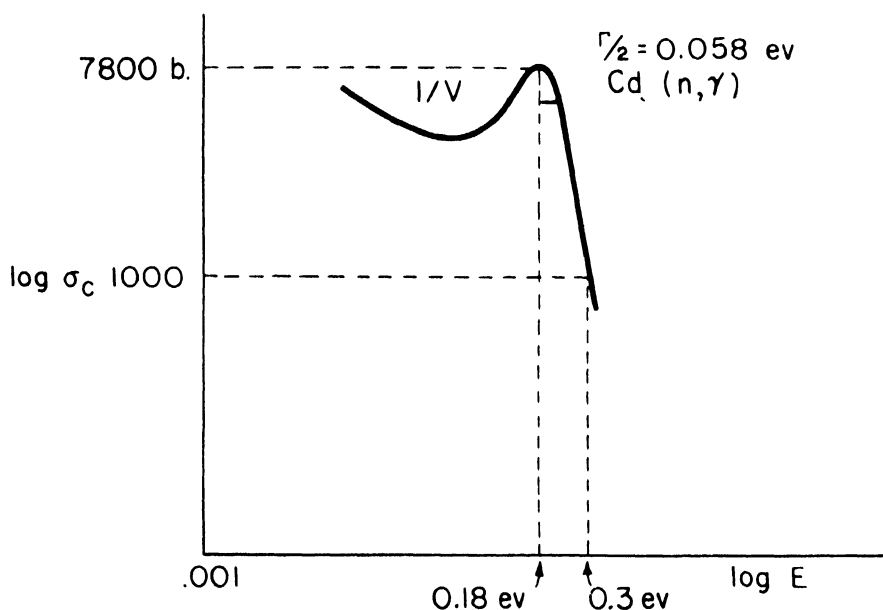


Figure 1-39. Capture Cross Section of Cd (n, γ). This element shows a large resonance absorption at .18 ev. The Γ of this peak is .116 ev. Below about .025 ev the absorption follows $1/V$. It is evident that only a few tenths of a millimeter of cadmium greatly attenuates all neutrons of energy below 0.3 ev. Such neutrons are known as C neutrons.

CHAPTER 2

THE FISSION PROCESS*

by

Martin Deutsch

2-1 Semi-Empirical Relations

In the absence of adequate theoretical knowledge concerning nuclear forces, it is necessary to rely almost completely on empirical relations for nuclear binding energies. As discussed in Section 1-3, the nuclear radius R is related to the atomic weight A for medium weight and heavy nuclei as $R = 1.5 \times 10^{-13} A^{1/3}$ cm. Thus the average density of nucleons in most nuclei is nearly constant. It also seems likely that the density is essentially uniform throughout a single nucleus. As seen in Figure 1-2, except for the lightest elements, the binding energy per nucleon E/A follows a smooth curve over a broad range of A . The specifically nuclear forces contribute the bulk of the effect. In light nuclei, which contain a relatively large surface per unit mass, the binding energy per particle is less than for nuclei of medium A . This decrease in binding with area is attributed to the smaller binding of the surface particles as compared to the particles inside a nucleus where each nucleon is completely surrounded by others. Since surface is $\propto R^2$, the effect must be proportional to $A^{2/3}$ and be of opposite sign to the saturating forces which are $\propto A$.

Above an A of ~ 120 , the increase in E/A resulting from the decrease in surface area per particle is offset by the increase in the Coulomb repulsion between the protons. If it is assumed that the charge Z is uniformly distributed throughout a spherical nucleus, the energy will be given by: $(3/5)e^2 Z^2/R \approx (3/5)e^2 Z^2/A^{1/3} \times 1.5 \times 10^{-13}$.

Combining the three factors considered thus far and introducing the semi-empirical constants a_1 , a_2 , and a_3 :

$$(2-1) \quad E/A = a_1 - a_2/A^{1/3} - a_3 Z^2/A^{4/3}$$

In addition to the foregoing, other bits of information about nuclei indicate that certain correction terms should be added to this expression.

*This discussion has leaned rather heavily on the lectures given by E. Fermi in the fall of 1945 as part of the program of the Los Alamos University.

For example, in light nuclei the number of protons and the number of neutrons are nearly the same, i.e., $(A - Z) \approx (Z)$. In accord with the conclusions from scattering experiments cited in Section 1-10, this condition indicates the approximate equality of (n, n) and (p, p) nuclear forces. If the total effect of the latter is decreased by the Coulomb repulsion in heavy nuclei, it is to be expected that the most stable heavy nuclei would contain more neutrons than protons. This slight excess of neutrons over protons in stable nuclei is evident in Figure 1-1.

If it is assumed that except for the Coulomb forces the most stable configuration is $(A - Z) = Z$, then a curve of binding energy E versus Z would have a maximum at $Z = A/2$ and would be less for either $Z < A/2$ or $Z > A/2$. It seems reasonable to assume that the change in binding energy associated with this departure from $Z = A/2$ is, to a first approximation, proportional to $(Z - A/2)^2/A$.

An additional correction results from the observation that the most stable nuclei tend to have both Z and $(A - Z)$ even. Slightly less stability occurs for either $[Z \text{ odd}, (A - Z) \text{ even}]$ or $[Z \text{ even}, (A - Z) \text{ odd}]$ while least stability occurs for $[Z \text{ odd}, (A - Z) \text{ odd}]$. It has been suggested that the nucleons tend to fill the lowest nuclear energy levels and that strong forces exist between pairs of neutrons or protons that can fill the same level. The purely empirical term δ is used below to express this effect.

Instead of continuing to express these factors in terms of the binding energy, it is somewhat more convenient to consider the precise atomic mass M which will be a function of Z and A in which the masses of the free neutrons and protons are decreased by the various binding energy terms expressed in atomic mass units:

$$(2-2) \quad M = 1.00893 (A - Z) + (1.00812) Z - a_1 A + a_2 A^{2/3} \\ + a_3 Z^2/A^{1/3} + a_4 (Z - A/2)^2/A + \delta$$

To obtain a_4 , set $(dM/dZ) = 0$. The resulting equation

$$(2-3) \quad Z_A = A (.00081 + a_4)/(2a_4 + .001254A^{2/3})$$

gives Z_A , i.e., the most stable Z for any A , when $a_2 = .000627$, which fol-

laws from elementary electrostatics, is used. When fitted to the curve of stable isotopes, $a_4 = 0.083$, hence

$$(2-4) \quad Z_A = A / (1.981 + .015A^{2/3})$$

By fitting Equation (2-2) to the known data for nuclear masses, $a_1 = 0.01504$ and $a_2 = 0.014$. While δ is given empirically as:

$$\delta = \begin{cases} 0 & \text{for } A \text{ odd} \\ \mp (.036/A^{3/4}) & \text{for } A \text{ even} \end{cases} \begin{cases} Z \text{ even} \\ Z \text{ odd} \end{cases}$$

Hence:

$$(2-5) \quad M = .99389 A - .00081 Z + .014 A^{2/3} + .000627 Z^2/A^{1/3} \\ + .083 (Z - A/2)^2/A + \delta$$

An example of the application of Equation (2-5) is the calculation of the binding energy of a neutron to U^{235} :

$$\begin{aligned} M(U^{235}) &= 235.11240 && (\text{from (2-5)}) \\ M(n) &= \underline{1.00893} \\ M(U^{235} + n) &= 236.12133 \\ M(U^{236}) &= \underline{236.11401} && (\text{from (2-5)}) \\ \text{Binding energy} &= .00732 \text{ amu} = 6.81 \text{ Mev} \end{aligned}$$

Similarly, binding energies of a neutron to U^{236} , U^{237} , and U^{238} , would be 5.51, 6.56, and 5.31 Mev respectively. This information is closely connected to the ability of slow neutrons to cause fission of these various isotopes.

Equation (2-5) describes quite well the atomic masses of stable isotopes throughout the periodic table. It can be used to predict the most stable Z . This formula also gives fairly reliable values for the energy release in beta decay. It is also quite useful in calculating the energy release in other nuclear changes.

2-2 Nuclear Fission

It is evident from Figure 1-2 that because of the greater Coulomb repulsion, heavy nuclei have less binding energy per particle than nuclei of medium A. Were this curve drawn precisely, it would show that it is energetically possible for all nuclei above $A \approx 100$ to transform into middle-sized nuclei. When large nuclei break into two such fragments, the process is called nuclear fission. Since fission does not occur below $A \approx 220$, the question is, in what circumstances is this breaking up possible?

The energy released in the symmetrical fission of an atom $M(A, Z)$ would be

$$(2-6) \quad E_o = M(A, Z) - 2 [M(A/2, Z/2)]$$

An approximate curve of E_o in Mev versus A is given in Figure 2-1. The energy released E_o begins to have a positive value at $A \approx 85$ and increases as shown for larger A. The reason that only the heaviest nuclei undergo fission is that there is an activation energy for this reaction, i.e., a certain activation energy is required to initiate the process. This condition is illustrated schematically in Figure 2-2.

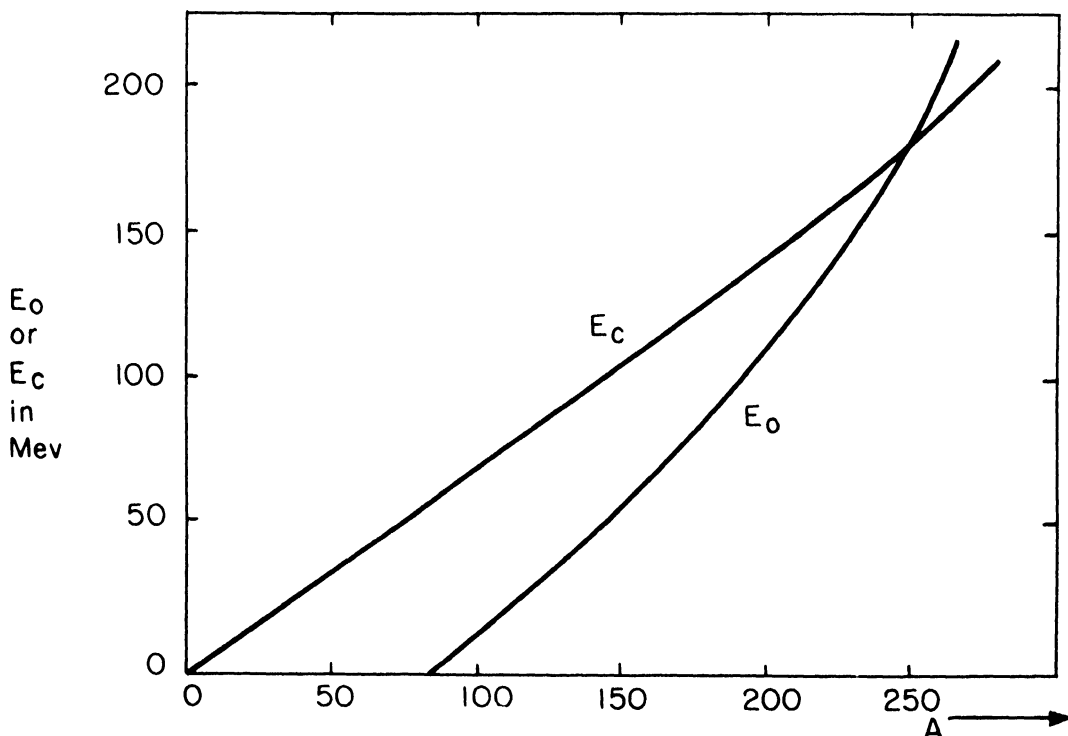


Figure 2-1. Coulomb Energy E_c and Symmetrical Fission Energy E_o versus A.

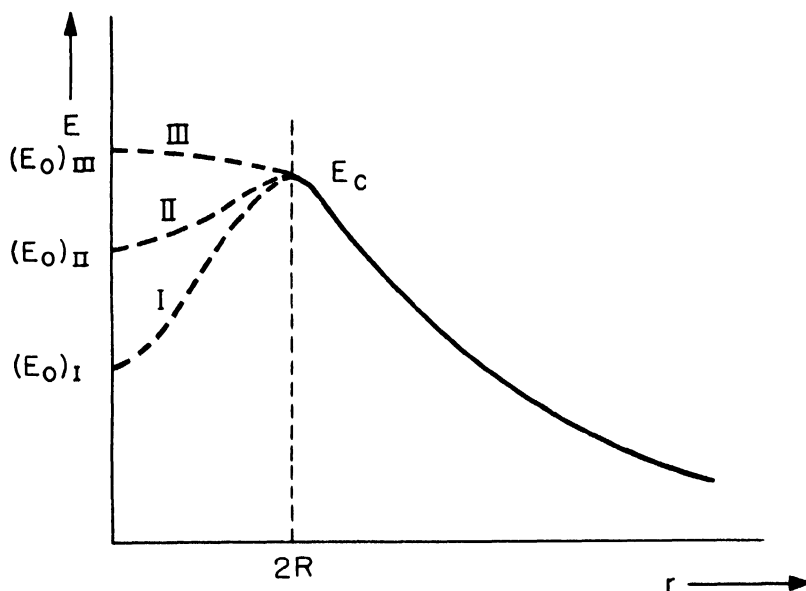


Figure 2-2. Nuclear Energy E as a Function of Distance r between Fission Fragments.

If E represents the potential energy of the nucleus (or the fragments) as a function of distance r between the centers of the two parts, it is evident that for large r , the energy is simply the electrostatic energy resulting from the mutual repulsion of the two positively-charged nuclear fragments. The value of E in this region is $(Ze/2)^2/r$, hence increases as the distance between the two like fragments is decreased. The energy at $r = \infty$ is considered zero. At $r \leq 2R$, that is, twice the radius of each fragment assumed to be spherical, the energy will no longer be simply Coulombian, since there will be other forces between the fragments. The curve must pass through the point corresponding to the energy of the coalesced nucleus E_0 , when $r = 0$.

Three possibilities are shown in Figure 2-2. Stable nuclei with A somewhat > 100 are of type I, with $E_0 < E_c$, the Coulomb energy at $r = 2R$. The variation of E_c with A is shown in Figure 2-1. The difference $E_c - E_0$ for such nuclei is about 50 Mev and is known as the energy barrier height against splitting. Nuclei like uranium, thorium, plutonium, etc., would be of type II in which $E_c - E_0$ is about 6 Mev. For still heavier nuclei E_0 may be $> E_c$ as in type III. This condition obtains above about $A = 250$, as shown in Figure 2-1. Such nuclei would certainly undergo fission spontaneously, hence could not exist for long in nature. The nonexistent transuranic elements are presumably of this type.

On a classical basis, nuclei of type II are entirely stable. However, quantum mechanically there is a certain probability that such nuclei will undergo spontaneous fission; the probability increases rapidly with decreasing $(E_c - E_0)$. Only in the case of A greater than about 220 is the barrier height small enough for spontaneous fission to occur with any reasonable probability. For instance, U^{238} undergoes spontaneous fission at the rate of about 20 disintegrations per gram per hour. The corresponding half-period for this process is about 10^{17} years.

2-3 Liquid-Drop Model

Previous sections have shown that if energy is fed into nuclei, various changes take place. It seems reasonable to suppose from Figure 2-2 that if an energy $\geq E_c - E_0$ were fed into the corresponding stable nucleus, fission might take place. The liquid-drop model which has been the basis for most of the foregoing discussion in this section has had a rather spectacular success in predicting the shape of the dotted curves in Figure 2-2. The original nucleus, i.e., $r = 0$ in Figure 2-2, is assumed to be spherical. When energy is fed into this nucleus, it starts deforming or vibrating like a drop of liquid. Assuming that the sphere becomes slightly ellipsoidal ($r = \epsilon$, with $\epsilon \ll R$) and that the nuclear density does not change, the two major changes will be in the surface energy and the Coulomb energy. The surface energy will be changed in proportion to the increase in surface area. The elongation of the nucleus pulls the protons apart, which causes a decrease in their mutual repulsion. The two effects cancel each other to some extent, but in sufficiently heavy nuclei with large Z , the energy is decreased by deformation, as shown in curve III, Figure 2-2. Such spherical nuclei are unstable and spontaneous fission takes place with the slightest change. Calculations by Bohr and Wheeler indicate that the relation $Z^2/A < \text{about } 45$ must obtain to avoid having a nucleus disintegrate almost immediately by spontaneous fission. The highest value of this ratio for any element that occurs in nature to any extent is ~ 36 for U. As previously indicated, U^{238} does undergo appreciable spontaneous fission. Hence, even at $Z^2/A \approx 36$, the energy barrier is somewhat transparent.

2-4 Induced Fission

The necessary excitation energy $E_0 - E_0$ required to induce fission in nuclei of type II can be provided in several forms. Electrons, protons, deuterons, alpha particles, gamma rays, and neutrons have been shown to produce fission in different nuclei under various conditions. Only neutrons and, to a lesser extent, gamma rays are of interest in this regard in nuclear reactors.

The threshold energy for fission induced by electromagnetic radiation (photofission) is ~ 5 Mev, being somewhat less for A even (such as U^{238}) than for A odd (such as U^{235}). Since very few of the fission or fission product gamma rays have energies > 5 Mev, photofission does not account for a significant proportion of fissions produced in nuclear reactors.

The most important process is neutron-induced fission. Neutrons contribute both their kinetic energy and their binding energy to the nucleus. As computed in Section 2-1, the binding energy is between ~ 5 and 7 Mev for the heaviest nuclei. Reference to these values indicates that because of the δ term in Equation (2-5), the binding energy of neutrons to nuclei of odd A-Z (such as U^{235} and U^{237}) is larger than for even A-Z (such as U^{236} and U^{238}). Thus fission with thermal neutrons (very low contribution of kinetic energy) is more prevalent in nuclei with an odd number of neutrons (A-Z odd). Thus thermal neutrons on U^{235} contribute an excitation energy of 6.8 Mev which is sufficient to carry the compound nucleus U^{236} over the potential barrier and produce fission. On the other hand, thermal neutrons on U^{238} contribute an excitation energy of only 5.3 Mev, which is insufficient to carry the compound nucleus U^{239} over its potential barrier. To cause fission in U^{238} , the neutrons must have about 1 Mev of kinetic energy in addition to their binding energy.

2-5 Symmetry of Fission Process

In the foregoing discussion of the fission process, essentially symmetrical fission has been assumed, that is, $(Z, A) \rightarrow 2(Z/2, A/2)$. From present theory this process is very probable. However, as indicated in the previous chapter, exactly symmetrical fission is either very rare or nonexistent. Only by chemical studies of the fission products has evidence for symmetrical fission been found (small amounts of $^{46}_{46}\text{Pd}$ among F.P. of $^{92}_{92}\text{U}$). The pronounced asymmetry of the process is not yet understood.

2-6 Energy and Mass of Fission Fragments

The best published determinations of the energy and mass of the fission fragments are by Jentschke (Zeit. f. Physik 120, 165-184, 1943). The apparatus used is shown schematically in Figure 2-3.

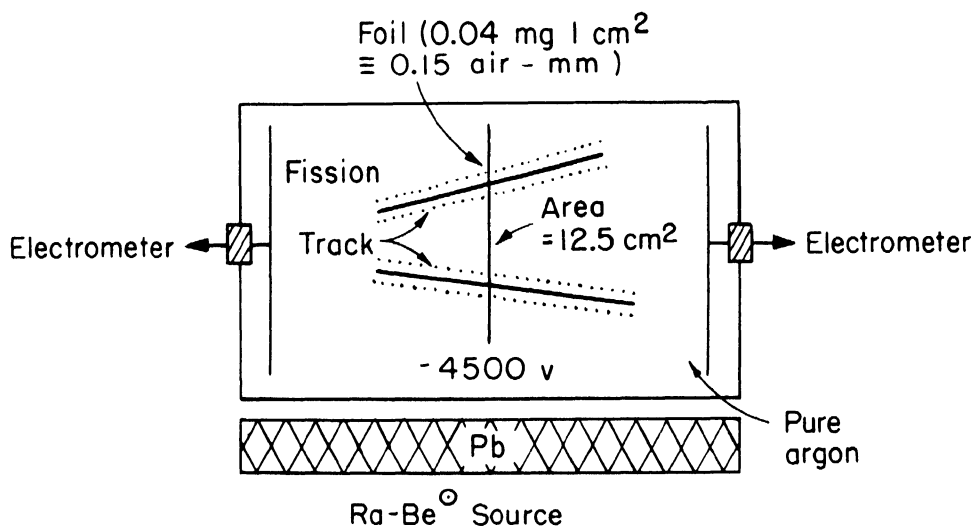
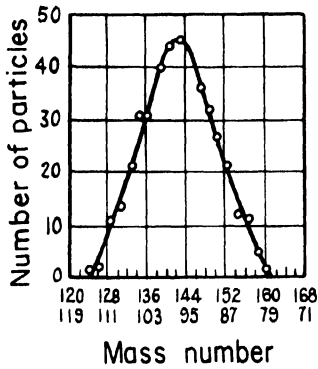
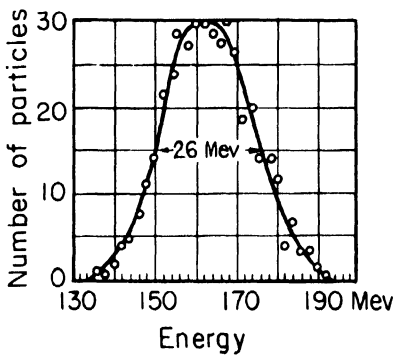


Figure 2-3. Ionization Chamber Used for Measurement of Fission Fragments.

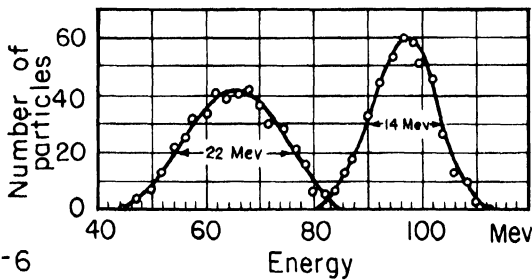
The ionization produced by the two fission fragments that appear simultaneously in the two halves of the ionization chamber when a fission occurs in the thin U or Th foil is collected in the electrostatic field and measured by the calibrated electrometers. It was assumed throughout these measurements that the energy required to produce an ion-pair in argon is the same as that for alpha particles, i.e., 27.5 ev/ion pair, and that the total energy is proportional to the total ionization. Neglecting the loss of mass by emission of prompt neutrons from the fragments, from conservation of momentum $M_1 V_1 = M_2 V_2$. Therefore, $E_1/E_2 = M_1 V_1^2 / M_2 V_2^2 = M_2/M_1$. Hence, not only can the total energy $E_1 + E_2$ for each fission be determined but also the proportion of energies and masses can be deduced. Figure 2-4 gives the distribution of masses for both the light and heavy fragments from U^{238} bombarded by fast neutrons. Cd shielding was used to filter out the slow neutrons. The statistical distribution of the total energy for the same conditions is shown in Figure 2-5, while the curves for the separate groups of fragments are given in Figure 2-6. Similar curves to the above are given for U^{235} , bombarded by slow neutrons, in Figures 2-7, 2-8, and 2-9. The



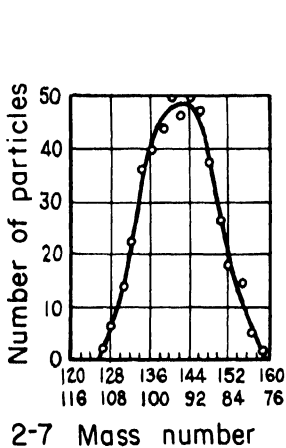
2-4



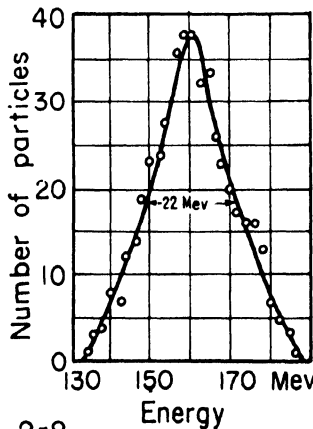
2-5



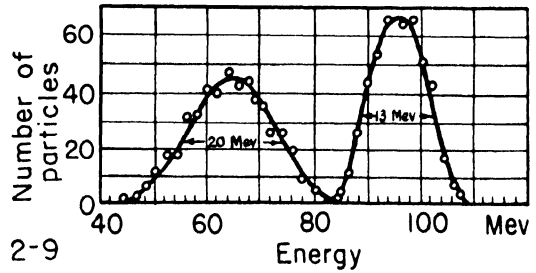
2-6



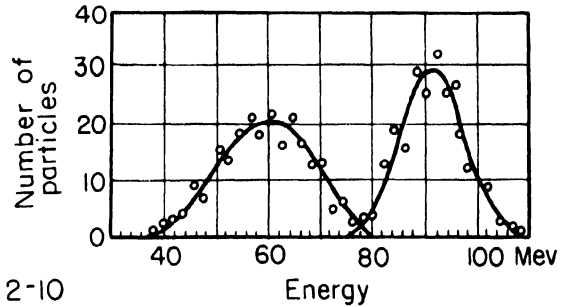
2-7 Mass number



2-8



2-9



2-10

Figure 2-4. Distribution of masses produced in the fission of U^{239} . Irradiation of U^{238} by fast Rn-Be neutrons.

Figure 2-5. Statistical distribution of the sum of the kinetic energies of the two fragments in the fission of U^{239} .

Figure 2-6. Energy distribution of the heavy and light fragments in the fission of U^{239} .

Figure 2-7. Distribution of masses produced in the fission of U^{236} . Irradiation of normal uranium with predominantly thermal neutrons.

Figure 2-8. Statistical distribution of the sum of the kinetic energies of the two fragments in the fission of U^{236} .

Figure 2-9. Energy distribution of the heavy and light fragments in the fission of U^{236} .

Figure 2-10. Distribution of masses produced in the fission of Th^{233} . Irradiation of Th^{232} by fast Rn-Be neutrons.

number-energy distribution for the two groups from Th^{232} bombarded by fast neutrons is given in Figure 2-10. A more recent and more precise distribution of the fission fragments from U^{236} as determined by Coryell, et al, was given in Figure 1-31.

2-7 Source of Prompt Neutrons

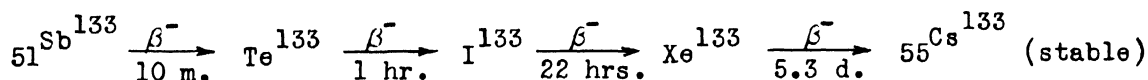
Although the splitting of a heavy nucleus has been likened to the splitting of a liquid drop, the prompt fission neutrons apparently are not produced during the actual nuclear splitting as are the tiny droplets that often accompany the rupture of a liquid drop, as seen in flash photographs. Instead, it appears much more likely that these neutrons are emitted from the highly-excited fission fragments immediately after splitting has taken place. It is clear from previous discussions that the binding energy of the last neutron in a fission fragment is much less than the average binding energy per particle. Since there is usually more energy of excitation in each fission fragment than corresponds to the binding energy of the last neutron, emission of neutrons by the fission fragments is very probable. In fact, on the average, somewhat more than one neutron is emitted per fission fragment (number of neutrons per fission event averages between 2 and 3).

If equipartition of energy among the nuclear particles is assumed, the observed energy distribution of the prompt neutrons would consist of a superposition of a Maxwellian distribution plus a translational component resulting from the motion of the fragments. A distribution of this type fits fairly well the continuous distribution in energy that is observed. However, it is not to be interpreted from these brief comments that the fission process is fully understood. Much experimental and theoretical work remains to be done in this field.

2-8 Energy Balance

From the foregoing curves, it is seen that the average total kinetic energy of the two fission fragments from U^{236} is about 160 Mev. In addition, the prompt neutrons have kinetic energies totaling about 5 Mev. If the energy of excitation of the fission fragment immediately after its formation is insufficient to cause neutron emission, the nucleus may lose energy by the emission of prompt gamma rays. On the average, about 5 Mev of energy is released in this form. Since the fission fragments are invariably radio-

active, there is additional energy released as β^- , γ , and neutrino radiation. On the average, each fission fragment emits 3 betas. The radioactive energy, about 20 Mev, is released over a period of time following fission. The rate of decay in nearly every fission product chain is greater at the beginning than toward the end. For example,



slows down from $T \leq 10 \text{ m.}$ for Sb^{133} to $T = 5.3 \text{ d.}$ for Xe^{133} . There is, of course, some dependence in this regard upon odd and even values of Z and A .

The prompt neutrons plus the fraction of a per cent of delayed neutrons eventually are absorbed either in other fissionable nuclei or in materials of construction. The binding energy of these neutrons ($\sim 10 \text{ Mev}$) is released either in the form of gamma radiation or of beta rays from radioactive decay. While of minor significance in the total energy release (about 5%), the energy associated with these stray neutrons becomes of importance if they are absorbed in other than useful parts of a nuclear reactor. Thus the total average energy released in all of the important forms is summarized in Table 2-1.

TABLE 2-1
FISSION ENERGY BALANCE

Fission fragments	$\sim 160 \text{ Mev}$
Prompt neutrons	~ 5
Prompt gammas	~ 5
Radioactive series	~ 20
Absorbed neutrons	~ 10
Total	$\sim 200 \text{ Mev}$

2-9 Delayed Neutrons

The mechanism of the emission of delayed neutrons has been discussed in Chapter 1, in which the emission from Kr^{87} was used as an example. In the case of U^{235} , at least five different delayed neutron periods have been identified thus far. The proportion of these, as compared to the total number of neutrons emitted (prompt + delayed) are given in Table 2-2. The first two periods are rather well verified, while the shorter ones are as yet not precisely measured.

TABLE 2-2
DELAYED NEUTRONS

<u>Half-Period</u>	<u>Percentage</u>
55.6 sec.	.02
22.0	.14
4.51	.18
1.53	.20
.42	<u>.07</u>
Total	.61

There are also gamma rays of the same period associated with these neutrons.

2-10 Types of Fission

In addition to neutron-induced fission, other radiations have been used. Photofission produced by high energy gamma rays causes the splitting of the target nucleus. Spontaneous fission without any initial change in A also occurs in some nuclei (for example, U^{238}). In either fast or slow neutron fission, the splitting nucleus is one unit heavier than the target nucleus (for example, U^{236} upon bombarding U^{235}). In the case of deuteron induced fission of U^{235} , it is not certain whether the splitting nucleus is Np^{237} or U^{236} . In the latter case, the deuteron would not enter the U^{235} nucleus but would be disintegrated at the nuclear barrier with the absorption by U^{235} of the neutron portion and repulsion of the proton. Further experimental work is needed to settle this question.

CHAPTER 3

NEUTRON DIFFUSION

by

Victor F. Weisskopf

3-1 Elementary Theory

It is clear that the diffusion of neutrons is of fundamental importance in any problem of nuclear power. In moving from the source to the point at which they are utilized, the neutrons must penetrate matter, and in this process they undergo quite a number of changes. It is of interest to consider what laws and regularities can be formulated for a motion of this type. The mechanics of the penetration of neutrons through matter is very similar to the diffusion processes in gases. The neutrons emerge from the sources, collide with nuclei in the surrounding material, and suffer changes in direction and speed of a statistical nature. The process is much the same as the diffusion of one gas in another. It is, however, more similar to the diffusion of electrons in gases, for in diffusing through a material of moderate atomic weight ($A \gg 1$, i.e., non-hydrogenous), a neutron undergoes the major change in direction, velocity, and momentum upon collision with one of the atoms. The nucleus of the struck atom does not change much, because it is much heavier than the neutron. This constitutes a characteristic difference from the diffusion of gases and makes the calculation of neutron diffusion somewhat easier.

Although many important problems in nuclear reactors are concerned with the diffusion in hydrogenous (or very low A) materials where the momentum exchanged between the neutron and the light nucleus must be considered, the present discussion is restricted to the simpler conditions. The more complicated problem will be considered in subsequent sections.

The following simplifying assumptions will be made:

- (1) There is no energy (or momentum) transfer from the neutron to the nucleus with which it collides.
- (2) All neutrons considered have the same velocity (a scalar) and this velocity remains the same before and after the collision.*
- (3) All cross sections (scattering, absorption, transport, etc.) remain constant.**

*The slowing down is an important feature that is deferred for later consideration.

**This condition follows directly from the second assumption since, as previously considered, the cross sections are generally dependent on the neutron velocity.

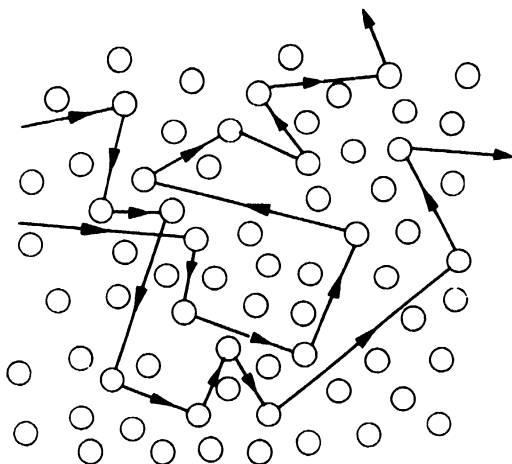


Figure 3-1. Schematic Representation of Neutron Diffusion through a Material.

The process of diffusion can then be represented schematically as in Figure 3-1. Atomic nuclei are distributed in a statistical manner throughout the medium being bound in place by electrostatic forces.*

The neutrons diffuse through the material, changing direction each time they collide with a nucleus, resulting in a statistical distribution of particles. An important concept in the description of this process is the mean-free-path λ , which is the average distance between two collisions. This quantity, of course, depends on the cross section of the nuclei in the elementary manner:

$$(3-1) \quad \lambda = 1/N\sigma$$

where N is the number of nuclei per cm^3 and σ is the cross section. In other words, the larger the cross section for collision, the greater is the chance for a collision and hence the shorter the mean-free-path.

Another important quantity is the neutron current S . Imagine a neutron distribution $n(x)$ which depends only on one coordinate x and which is essentially linear in x over distances of the order λ :

$$(3-2) \quad \lambda^2 \frac{d^3 n}{dx^3} \ll \frac{dn}{dx} \quad **$$

*Although the lattice structure of materials must be considered in some instances, for purposes of simplification this effect is neglected.

**The second derivative does not contribute to the current at all.

Consider a surface element perpendicular to the x -direction. If the neutron distribution $n(x)$ were a constant ($\frac{dn}{dx} = 0$), there would be an equal number of neutrons crossing this element from both sides. If there are more on one side, more neutrons will come from this side. The neutrons come on the average from a distance λ_t , when λ_t is the so-called transport mean-free-path. The difference S between the number of neutrons crossing a unit surface per second from one side and from the other is given by

$$S = \frac{\lambda v}{3} \frac{dn}{dx}$$

The factor $1/3$ comes from the fact that roughly $1/3$ of the neutrons move perpendicular to the surface; $2/3$ move parallel. The magnitude S is the net current through the surface. After generalizing this to any given direction, we get for the current

$$(3-3) \quad S = -D \text{ grad } n$$

where $D \equiv$ the diffusion constant is given by

$$D = \frac{\lambda_t v}{3}$$

This expression is correct only if $n(x)$ is such that Equation (3-2) is fulfilled.

The quantity λ_t requires some detailed explanation. It is the distance which a neutron travels on the average in the direction of its initial motion. This distance is one mean-free-path λ , only if after a collision the direction of motion is completely undetermined. If the collision mechanism is such that there is a predominance of scattering in a given direction, for example, in the forward direction, the value of λ_t is somewhat greater than for purely isotropic scattering. Conversely, if back scattering predominates, λ_t should be somewhat less than for isotropic scattering. The transport mean-free-path λ_t is the average distance in the initial direction that a neutron would travel after an infinite number of collisions. It is this mean-free-path that is suitable for specifying the neutron current as in Equation (3-2). It is easily shown that*

* $\lambda \cos \varphi$ is the average projection of the free flight of the neutron after the first collision on the direction of flight before the collision. $\lambda \overline{\cos \varphi^2}$ is the projection of the next flight on the original direction, etc.

$$\begin{aligned}
 \lambda_t &= \lambda + \lambda \overline{\cos \theta} + \lambda (\overline{\cos \theta})^2 + \text{-----} \\
 &= \lambda (1 + \overline{\cos \theta} + (\overline{\cos \theta})^2 + \text{-----}) \\
 &= \lambda / (1 - \overline{\cos \theta}) = 1/\overline{N\sigma_t}
 \end{aligned}$$

$$(3-4) \quad \sigma_t = \sigma (1 - \overline{\cos \theta})$$

where $\overline{\cos \theta} \equiv$ the average cosine of the scattering angle relative to the initial direction, σ and $\sigma_t \equiv$ the scattering and transport cross sections respectively.

Neutron scattering cross sections are not spherically symmetric. Almost all elements favor forward scattering to some extent, especially at high energies. Hence, in general, $\overline{\cos \theta}$ is positive, $\lambda_t > \lambda$, and $\sigma_t < \sigma$. The foregoing quantities will be used to formulate approximate relations for the diffusion of neutrons in matter.

Neutrons can be produced by a source or by a fission process which happens to occur at a given point. Neutrons can disappear by being captured by an absorber at a point. The neutron density can change by a change in the current S . Thus the equation of continuity at a point is:

$$(3-5) \quad dn/dt = q - a - \text{div } S$$

where:

q = the source density per cm^3 per second which may be from fissionable material

a = the number of absorptions per cm^3 per second, and

$\text{div } S$ = the divergence or change in current (either $+$ for a source or $-$ for a sink)

Combining (3-2) and (3-5):

$$(3-6) \quad dn/dt = q - a + \text{div } D \text{ grad } n$$

Since it has been assumed that λ_t and v do not change throughout the medium, therefore

$$(3-7) \quad dn/dt = q - a + D \nabla^2 n$$

The absorption is proportional to the neutron density and inversely proportional to their mean life for absorption τ_0 , hence $a = n/\tau_0$. If fission is the source of production, q is also proportional to n , inversely proportional to τ_0 , and proportional to the fraction of absorptions which produce fission. Since η neutrons are produced on fission

$$(3-8) \quad q = \frac{n}{\tau_0} \frac{\sigma_f}{\sigma_a} \eta$$

The mean life is related to the absorption cross section, σ_a , as

$$(3-9) \quad \tau_0 = \frac{1}{N\sigma_a v}$$

by elementary statistical theory; and σ_f is the fission cross section.

3-2 Application to Infinite Mass Containing a Point Source

By considering an infinite mass of a very heavy material such as Pb, the assumptions on which the foregoing relations were derived are more nearly fulfilled. In such a medium, the neutrons lose only a small amount of energy in a collision. In Pb, $A \approx 207$, a neutron loses about $2/A \approx 0.01$ of its energy per collision. The source is assumed to be very small in size but of appreciable intensity (for example, a Ra-Be source). The neutrons are emitted equally in all directions, collide with the lead nuclei and undergo a diffusion process. The average density n as a function of the distance r from the source is obtained for the steady state ($dn/dt = 0$) as the solution of Equation (3-7) reduced to:

$$(3-10) \quad \nabla^2 n - n/\tau_0 D = 0$$

It is to be noted that $q = 0$ throughout the medium except in the immediate vicinity of the source, i.e., where $r \approx 0$. If $n = u/r$

$$(3-11) \quad (d^2 u/dr^2) - u/\tau_0 D = 0$$

which has the simple solution $u = Ce^{-r/L}$, where $L = \sqrt{D\tau}$ or $n = (C/r)e^{-r/L}$. The quantity L is to be identified as the diffusion length. The positive exponential, which is also a solution of Equation (3-9), has no physical significance, since u would go to infinity at $r = \infty$.

It is to be noted that for no absorption, $\sigma_a = 0$, which is approximated by Pb, since it has such a small absorption, $L = \infty$ and $n = C/r$. Thus, because of the diffusion effect, the neutron density decreases as $1/r$ instead of as $1/r^2$ for the case of a vacuum in which the neutrons travel in straight lines away from the source. The constant C depends on the source strength Q as follows:

$$(3-12) \quad Q = \int_{\text{Surface}} S r^2 \sin \theta d\theta d\phi = \frac{DC}{L} \int_{\text{Surface}} e^{-r/L} \sin \theta d\theta d\phi$$

where the integration of the current is over the total surface of a small sphere surrounding the small source. Therefore

$$(3-13) \quad Q = 4\pi DC/L \quad \text{or} \quad C = LQ/4\pi D$$

and n can be written explicitly as

$$(3-14) \quad n = (LQ/4\pi Dr) e^{-r/L}$$

3-3 Dimensional Considerations

In the immediate vicinity of the source, the first collisions of neutrons occur on the average at a distance $r = \lambda$. If the source is considered as surrounded by a concentric sphere of radius small compared to λ , for example, $r = \lambda/10$, within this sphere very few initial collisions will take place. Hence, the solution of n within this sphere will contain a term which varies as $1/r^2$; while for small distance Equation (3-14) indicates a variation as $1/r$. The explanation of this paradox is that the diffusion theory is not an exact treatment of this case. A further assumption was implicit in the original conditions under which the diffusion theory was derived, namely, that the region in which diffusion theory holds is always at least λ_t away from any sharp discontinuity of either the density or the distribution of sources. Here, consequently, we cannot trust diffusion theory at distances from the isolated source which are less than λ_t . Neither can diffusion theory be trusted within distances of the order of λ_t from a boundary at which the properties of the medium change radically (Section 3-4) or anywhere in a system which is not large compared with λ_t .

Since many of the interesting problems in neutron physics involve distances of the order of a mean-free-path, care must be taken in the use

of diffusion equation. For example, in the calculation of the critical mass of pure fissionable material, the radius is just of the order of the mean-free-path. Thus, for this and many related problems, more powerful methods must be used. However, it is true that even in these problems, the diffusion equation gives a fair approximation if it is used in the correct manner.

3-4 Neutron Distribution

We now consider the neutron distribution in more detail. We will be interested not only in the neutron density (number per cm^3) but also in the distribution as to their direction of motion. Let us, for the sake of simplicity, assume that all magnitudes depend only on one coordinate x . Let us define $n(x, \mu) d\mu dx$ as the number of neutrons in the interval between x and $x + dx$, whose velocity includes an angle θ with the x -axis, so that $\cos \theta$ is between μ and $\mu + d\mu$ ($\mu = \cos \theta$). We then get

$$(3-15) \quad n(x) dx = dx \int_{-1}^{+1} n(x, \mu) d\mu$$

It is further assumed that the dependence of n on μ is a simple one which allows the expansion

$$(3-16) \quad n(x, \mu) = n_0(x) + \mu n_1(x) + \text{-----}$$

and that the dependence on angle is sufficiently small so that only the first spherical harmonic is included. The higher harmonics give a more refined neutron distribution, but these fine details are neglected in this simplified treatment.

The two constants, with respect to μ , $n_0(x)$ and $n_1(x)$ can then be determined. By substituting Equation (3-16) in Equation (3-15) and integrating, the second term drops out, leaving $n(x) = 2n_0$, from which $n_0 = n(x)/2$. From Equation (3-3):

$$(3-17) \quad S = -D(dn/dx)$$

while from Equation (3-2) it is

$$\begin{aligned} S &= \int_{-1}^{+1} n(x, \mu) \mu v d\mu = \left[(n_0(x) \mu^2 v/2) + (n_1(x) \mu^3 v/3) \right]_{-1}^{+1} \\ &= (2/3) n_1(x) v \end{aligned}$$

hence

$$n_1 = -(3D/2v) \, dn/dx$$

These relations can then be applied to the characteristic problem of an infinite, nonabsorbing half-space (Figure 3-2) containing neutron sources that are remote from the plane boundary at $x = 0$ between the material and a vacuum. For this one dimensional case $\nabla^2 n = 0$, hence $n = Ax + B$ and the slope of the neutron density $dn/dx = A$.

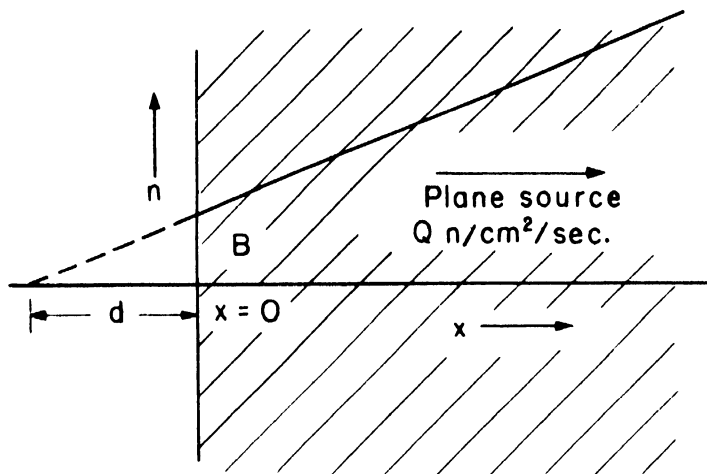


Figure 3-2. Neutron Distribution in Nonabsorbing Half-Space.

The current $S = -D(dn/dx) = -DA$. The value of B is the neutron density at the interface $x = 0$ which is determined as follows. The number of neutrons emerging into the vacuum per second at $x = 0$ is:

$$(3-18) \quad Z = \int_{+1}^0 n(x, \mu) \mu v d\mu = -v \left(\frac{n_0(x)}{2} - \frac{n_1(x)}{3} \right)$$

This is equal to

$$Z = -v \frac{n(0)}{4} - \frac{D}{2} \left(\frac{dn}{dx} \right) \quad \text{at } x = 0$$

This number Z should be equal to S , the net flow, since there is no flow back from the vacuum. Therefore, after putting $n = Ax + B$, we get:

$$(3-19) \quad -DA = -\frac{vB}{4} - \frac{DA}{2} \quad \text{or} \quad \frac{B}{A} = \frac{2D}{v}$$

From the geometry of Figure 3-2, $d = B/A$, therefore

$$(3-20) \quad d = 2D/\bar{v} = 2/3 \lambda_t$$

A more exact solution gives the important relation

$$(3-21) \quad d = 0.71 \lambda_t$$

This length is called the extrapolated endpoint of the neutron distribution.

According to the foregoing approximate methods, the neutron density decreases to a definite value at the boundary and then falls to zero outside. In the vacuum, the density must be infinitely smaller than in the diffusing medium, for in the medium a single neutron passes back and forth many times through a given point, whereas in the vacuum a neutron retains the velocity with which it emerges and therefore does not return. Therefore, the ratio of the density in the medium to the density in the vacuum equals the number of times a neutron goes back and forth through one volume element. If the mean-free-path is very small compared to the linear dimensions, as is assumed here, this ratio is a very large number.

While the more exact treatment shows a slightly rounded curve instead of an abrupt decrease in neutron density at the boundary, the approximate result is in remarkably good agreement with the facts. It is also of interest to note that Equation (3-21) is also applicable to the case of an absorbing medium. Instead of a linear decrease in n , there will be an exponential decrease. Also, the mean-free-path is somewhat smaller in an absorbing medium.

3-5 Critical Mass

Based on the assumptions stated in Section 3-1, the resulting elementary neutron diffusion theory will be applied to calculate the critical radius R of a sphere of fissionable material. This sphere will be of just the right size to maintain a chain reaction, that is, just as many neutrons are lost as are recreated by fission. The losses are by emergence to the outside and by absorption, which will be proportional to the nuclear absorption cross section σ_a .

Referring to the stationary state equation given previously,

$$(3-22) \quad (\lambda \bar{v}/3) \nabla^2 n - (n/\tau_0) + q = 0$$

and substituting the production $q = \frac{n}{\tau_0} \frac{\sigma_f}{\sigma_a} \eta$

the following is obtained

$$(3-23) \quad \nabla^2 n + \mathcal{K}_0^2 n = 0$$

where

$$(3-24) \quad \mathcal{K}_0^2 = \left(\frac{3}{\lambda v} \right) \frac{1}{\tau_0} \left(\frac{\sigma_f \eta}{\sigma_a} - 1 \right).$$

This equation can be further simplified by using $\lambda = 1/\Sigma \sigma$ total and $\sigma_a - \sigma_f = \sigma_c$, the cross section for capture not leading to fission.

In these expressions λ represents the mean-free-path between collisions of all types, absorption, scattering, fission, etc. Thus,

$$(3-25) \quad \mathcal{K}_0^2 = (3/\lambda^2) f$$

where

$$f = \left\{ \left[(\eta-1)\sigma_f - \sigma_c \right] / \sigma_{\text{total}} \right\}$$

The term f is the important quantity in determining the critical mass. It represents the excess number of neutrons created per collision. The magnitude of f is classified information. Assuming the values for f and λ are known, and considering spherical geometry for which $n = u(r)/r$

$$(3-26) \quad (d^2 u / dr^2) + \mathcal{K}_0^2 u = 0$$

The boundary conditions are: $u = 0$ at $r = 0$; $u = 0$ at $r = R + 2\lambda/3 = R^*$. The approximation is made here that the actual radius R must be increased by an amount $2\lambda/3$ to obtain the extrapolated minimal radius R^* at which the neutron density falls to zero, as was found before. This extrapolation was actually derived for plane geometry, but it can be applied with a fair reliability to spherical geometry. The solutions are of the form

$$(3-27) \quad u = \sin \mathcal{K}_0 r$$

in which $\sin \mathcal{K}_0 R^* = 0$ if $R^* = \pi / \mathcal{K}_0 = \pi \lambda / \sqrt{3f}$, hence $R = (\pi \lambda / \sqrt{3f}) - 2\lambda/3$. It is to be noted that if $\sigma_f \approx \sigma_{\text{total}}$ and $\eta \approx 2$, then $f \approx 1$, $R^* \approx 1.8\lambda$ and

$R \approx \lambda$. Hence, the linear dimensions being considered in this case are of the order of the mean-free-path which does not comply with the assumptions on which the theory is based. Therefore, this is only an approximation, but more exact considerations indicate that the results are not very seriously in error.

3-6 Effect of Reflector

One way of reducing the size of the critical mass as calculated for a bare sphere is to surround the fissionable material with a reflector, preferably composed of a material that has $\sigma_a = 0$. In this way there would be no absorption losses in the reflector, but there is the further advantage that it is easier to calculate. In addition to assuming $\sigma_a = 0$, the reflector is considered infinite in radius. Although there will be no absorption losses in this reflector, there will be some losses of neutrons, because there is a finite probability that once a neutron gets into the reflector it will not get back to the sphere of fissionable material.

In the reflector, $f = 0$ and $\nabla^2 n = 0$. In the reflector, the boundary condition is $n = 0$ at $r = \infty$; and consequently, $n = c/r$. Putting $u_2 = rn$, in the reflector, then $u_2 = c$ and $\frac{du_2}{dr} = 0$.

$u_1 = r$ times the neutron density in the sphere containing fissionable material, as given by Equation (3-27). This solution must be joined to u_2 at the boundary between the active material and the reflector, with the appropriate boundary conditions. These are that the neutron density and neutron flux must both be continuous across the boundary. Assuming the mean-free-path in the reflector equals that in the active zone

$$(3-28) \quad \cos \mathcal{K}_0 R = 0; \quad \text{and} \quad \mathcal{K}_0 R = \frac{(2m + 1)\pi}{2}$$

The smallest R for which Equation (3-28) is satisfied is obtained when $m = 0$; hence the critical radius for this case is $R = \pi/2\mathcal{K}_0$, or $R = R^*/2$. Thus, the use of such a reflector results in a very substantial saving in fissionable material, since the critical volume will be only somewhat more than one-eighth that for the bare sphere.

CHAPTER 4

NUCLEAR CHAIN REACTIONS

by

E. P. Wigner*

4-1 Elementary Theory

The great surprise about nuclear chain reactions was the ease with which they could be established. A paper by Szilard in January 1940 described a workable arrangement. Our own early work in this field was not based on Szilard's paper, but on Fermi's work, the concepts of which are less intricate than Szilard's. Ideas similar to Fermi's were developed also by others, notably v. Halban; moreover, the whole work was duplicated, apparently without any major deviation, by the German nuclear physicists.

In a chain reaction of the kind considered by us, uranium nuclei undergo fission and liberate neutrons. These neutrons are first fast but are soon slowed down by the moderator which, in our case, is carbon (graphite). After being slowed down, the neutrons still diffuse around for a period of time before being absorbed. Most of them are absorbed by uranium, which then undergoes fission and emits the neutrons of the next generation. The ratio of the number of neutrons in one generation to the number of neutrons of the preceding generation is called the multiplication constant and is usually denoted by k . Fermi's theory divides the problem of multiplication constants and critical sizes into two parts. The first problem is the calculation of the multiplication constant in an infinite medium, k_{∞} , which is usually referred to briefly as the multiplication constant. It depends only on the geometry and the materials of the chain-reacting system and gives the ratio of the numbers of neutrons in successive neutron generations under the assumption that the same materials, arranged in the same geometry, extend all over infinite space.

The second problem is the calculation of a critical length which does not depend on the inner structure of the chain reacting unit but only on its size and shape. This critical length, or its reciprocal \mathcal{H} , permits one to calculate, from k_{∞} , the second kind of multiplication constant, k_{eff} . This

*This is a slightly abbreviated version of a paper which appeared in the Journal of Applied Physics, Vol. 17, p.857, November 1946, and is included here with the permission of Dr. Wigner.

gives the ratio of the numbers of neutrons in successive generations in a finite pile. This second kind of multiplication constant is, of course, the relevant one from a practical point of view. It depends not only on the materials and their arrangement into a lattice which determine k_{∞} , but depends also on the actual extension of the lattice, i.e., the size and shape of the pile. In a steadily running pile, k_{eff} is always 1 and it exceeds 1 only when the power of the pile is increased, e.g., during startup, and then only very little. The k_{eff} is always smaller than k_{∞} because in an actual, finite pile some of the neutrons of every generation diffuse out of the pile and do not contribute to the next generation. No such "leakage" exists in an infinite pile.

It would seem that only the effective multiplication constant has real significance but it turns out that the calculation of k_{∞} is an almost necessary preliminary for the calculation of k_{eff} .

I will sketch only the calculation of k_{∞} , which is already given in principle in the Smyth report. In order to calculate the number of neutrons of the next generation, one may start at the birth of one neutron. This occurs in the uranium lumps and the neutron has, originally, considerable velocity. As a result, it will be able to induce fission not only in the U^{235} nuclei but, what is more important because of their larger numbers, also in the U^{238} atoms. Competing with this process are the process of inelastic scattering by U atoms by which the original neutrons may be slowed to a velocity below the fission threshold^{(1)*} of U^{238} , and the process of escape of the neutrons from the U lump into the moderator.

The importance of fast fission was recognized by Szilard and his collaborators. The rest of the factors making up k_{∞} were all recognized before and are contained also in Fermi's considerations.

Let us assume that the original neutron generates $\epsilon - 1$ further neutrons by fast fission. From Fermi**, $\epsilon - 1 \approx .03$, so that we arrive with $\epsilon \approx 1.03$ neutrons just below the fission threshold. Most of these neutrons diffuse out into the moderator and are slowed down to thermal energies. Some of them occasionally enter the uranium and are absorbed there by one of the

*Superiors in parentheses refer to bibliography at end of this chapter.

**Fermi, Science 105, 28 (Jan. 10, 1947).

numerous resonance levels of the U^{238} . These absorptions do not lead to fission and constitute an actual loss of neutrons. The importance of this process was recognized by N. Bohr and others in 1940. Only when the neutron has lost sufficient energy to be below the lowest resonance level of U^{238} -- which is, according to data in the literature⁽²⁾, at about 5 ev -- is it safe from this fate. The probability that a neutron will escape resonance capture is usually denoted by p . It is a number smaller than 1. As a result of the resonance absorption, we arrive with ϵp neutrons below the energy of 5 ev instead of the ϵ neutrons which we had just below the fast fission threshold.

It would lead too far to describe the actual calculation of p . Among all the processes which contribute to the chain reaction, the resonance absorption is the only one which was not really understood when we started our work. S. M. Dancoff and I were the ones who were most interested in the physical principles which determine the resonance absorption of macroscopic bodies, but ideas similar to ours were developed also by others. The actual calculation of p was described by R. F. Christy, A. M. Weinberg, and myself, although many others, including H. L. Anderson, contributed to it. The material constants necessary for the calculation were measured by Creutz, Jupnik, Snyder, and R. R. Wilson in Princeton, and later by Mitchell's group at the University of Indiana.

We now have ϵp neutrons with an energy below the resonance levels of uranium. According to theory, they will be slowed down to thermal energies by the moderator. After that, they will be absorbed, some of them by the moderator and the impurities present in the pile, some of them by the uranium. Fermi denotes this last fraction by f , so that, altogether, ϵpf thermal neutrons are absorbed by the uranium, giving

$$(4-1) \quad k = \epsilon pf\eta$$

secondary neutrons, η being the number of fission (fast) neutrons produced in the uranium per thermal neutron absorbed. The principles for the calculation of the "thermal utilization" f were established independently by Fermi, Placzek, and our group. The formulae which we used were derived by Christy, Mrs. Monk, Plass, and myself in a way which is similar to the calculation of wave functions in metals by the cellular method.⁽³⁾

On the whole, the calculation of the multiplication constant for an infinite lattice is quite "straightforward" and one of the great surprises of the Plutonium Project was how easy it was. Mr. G. N. Plass and myself happened to be the ones who attempted to calculate the "optimal lattice" (i.e., the lattice with the highest k_{∞}) early in 1942. Although the physical constants were not known too accurately at that time, the dimensions we obtained (later incorporated in the first chain reacting unit) are now believed to give a k_{∞} just 1/2 per cent short of the k_{∞} of the real optimal lattice. We are quite convinced that any reasonably competent people would have arrived at the same results. In later years, computations of k_{∞} were much facilitated by diagrams prepared for this purpose by Mrs. Monk and Mrs. Uchiyama, under Professor Wheeler's direction. The calculation of k_{∞} was extended to all sorts of lattices, containing heavy and ordinary water, etc. Most of this work was done by A. M. Weinberg and his collaborators, Mrs. Monk, Mr. Plass, Mrs. Uchiyama, Mr. Stephenson, and others. Qualitatively, the results were quite similar for all systems considered.

In spite of this, the properties which make a lattice optimal are not very simple. One may note that it is good if the high energy neutrons remain in the uranium to give a high ϵ . On the other hand, it is best if the lower energy (resonance) neutrons keep out of the uranium as much as possible so that p may remain reasonably close to 1. Again, the thermal neutrons should return to the uranium to give a high f -- as close to 1 as possible. These conflicting requirements determine the geometry of the optimal lattice, i.e., give the ratio of the amounts of moderator and uranium as well as the lattice constant. However, even relatively large deviations from the optimal dimensions do not decrease k_{∞} to a very great extent.

The foregoing describes the calculation of k_{∞} . Although Fermi has given a method for calculating k_{eff} from k_{∞} , I will not give his method here but will turn to the more advanced theory which permits a direct calculation of k_{eff} .

4-2 More Detailed Theory

The more detailed theory of chain reactions should provide more accurate methods both for the calculation of k_{∞} and also for the calculation of k_{eff} . However, as far as k_{∞} is concerned, only few improvements were

made. None of these improvements occurred in the calculation of ϵ and p , only one occurred in the calculation of f .

The behavior of "thermal" neutrons in a moderator-uranium lattice is far from simple. Evidently, it would take infinitely many collisions to establish real thermal equilibrium between the neutrons and the moderator, and in a well-designed lattice the neutrons will be absorbed by the uranium after a relatively small number of collisions. As a result, the energy spectrum of the neutrons will remain quite complex and their average energy will stay considerably above $\frac{3}{2}kT$. This average energy will be different even at different points of the lattice. The actual energy distribution will be influenced by the absorbing power of the material as well as by its moderating power. The latter is influenced in turn by the atomic weight of the moderator, by Fermi's chemical binding effect and by the crystalline nature of the moderator, which gives a considerable anisotropy to the scattered (refracted) neutrons.

The only serious attempt to take these factors (excepting the crystal effect) into account is due to E. Teller and his collaborators, mainly N. Metropolis and P. Morrison. A more rigorous but much more formal attempt later by J. E. Wilkins and myself did not contribute much to the qualitative picture. Wick has reported some work which he did on this problem. Teller's work gave, at least, an approximate measure for the difference in the effective temperature of the neutrons and the moderator. In spite of this, we are far from having an adequate knowledge of the energy spectrum of the neutrons in a chain-reacting unit.

Moreover, the problem of calculating f remains far from being simple even if the energy spectrum of the neutrons is known. It is, in fact, quite complicated even if one assumes that all the neutrons have the same energy. The reason for this is that the ordinary diffusion theory proves to be quite inadequate. G. Placzek carried out the most accurate calculations for the diffusion of monoenergetic neutrons. Some of his results were obtained also by German and Italian theorists⁽⁴⁾ and published. Our work along this line was not pushed with much vigor because we were, perhaps, too well aware of the inadequacy of the model which uses monoenergetic neutrons. Actually, there is evidence that the errors in our primitive diffusion equations are quite substantial and in the direction indicated by Placzek's work.

There is no relevant difference between the fast effect in a finite and infinite lattice. However, the probability p that a neutron with an energy just below fission threshold should become a thermal neutron is smaller in a finite lattice than in an infinite one because in addition to being captured by the uranium, some neutrons will be lost from a finite lattice by "leaking" (diffusing) out of it. This leakage was calculated by Fermi and his co-workers⁽⁵⁾ even before fission was discovered. For a finite lattice, their work gives

$$(4-2) \quad p_{\text{eff}} = p \exp(-\tau \mathcal{K}^2)$$

where τ is one-sixth the mean square distance, in an infinite lattice, between the point where the neutron originated and the point where it becomes thermal. The quantity \mathcal{K}^2 is the ratio $-\Delta n/n$, where n is the average of the neutron density over a lattice cell and will be discussed presently.

According to Equation (4-2), the effective p is smaller than it would be for the constant n of an infinite lattice, i.e., for $\mathcal{K} = 0$. The leakage depends on the "age" τ , which in its turn increases with increasing mean-free-path of the neutrons in the moderator and with the number of collisions which are necessary to slow down the neutrons to thermal energies. The quantity τ , and hence the leakage, is smallest in a water-moderated pile and much greater in a graphite-moderated pile.

Just as the fraction of neutrons which slowed down to thermal energies in the pile is, because of the leakage, smaller in a finite than in an infinite pile, so is the fraction of thermal neutrons absorbed by the uranium decreased by the escape of some of the thermal neutrons from the pile. The equation analogous to Equation (4-2) is

$$(4-3) \quad f_{\text{eff}} = f(1 + L_p^2 \mathcal{K}^2)^{-1}$$

The significance of \mathcal{K} in Equation (4-3) is the same as in (4-2), that of L_p^2 similar to that of τ in (4-2): L_p^2 is one-sixth of the mean square distance in an infinite lattice between the point where the neutron becomes thermal to the point to which it has diffused when it gets absorbed. L_p is also called the diffusion length of thermal neutrons in the lattice because the n decreases with an exponential relaxation distance L_p

$$(4-4) \quad n \sim \exp(-x/L_p)$$

in a region in which no thermal neutrons are produced.

G. N. Plass has shown, by means of a calculation which is similar to Bardeen's work⁽⁶⁾ on metallic wave functions, that

$$(4-5) \quad L_p^2 = L_m^2(1-f)$$

is a very good approximation for L_p if L_m is the diffusion length in the pure moderator, without uranium lumps.

The condition that a lattice can maintain a chain reaction at a steady rate is that $k_{\text{eff}} = 1$, i.e., that

$$(4-6) \quad k_{\text{eff}} = \epsilon p_{\text{eff}} f_{\text{eff}} \eta = 1$$

Using the expressions (4-2) and (4-3), this becomes

$$\epsilon p f \eta \exp(-\tau \mathcal{H}^2) (1 + L_p^2 \mathcal{H}^2)^{-1} = 1$$

or, by Equation (4-1)

$$(4-7) \quad k_{\infty} = (1 + L_p^2 \mathcal{H}^2) \exp(\tau \mathcal{H}^2)$$

an equation essentially identical to one obtained by Fermi.

This last equation can be considered to be an equation for \mathcal{H} which, in its turn, will be seen to depend only on the size and shape of the pile. Hence Equation (4-7) gives us the size of a pile if its shape and internal structure, in particular its infinite multiplication constant k_{∞} , are given.

The connection between the quantity \mathcal{H} and the size and shape of the pile is established by the classical equation

$$(4-8) \quad \Delta n + \mathcal{H}^2 n = 0$$

in which the average neutron density n is subject to the boundary condition that it vanish at the outer boundaries of the pile. It is well known that Equation (4-8) allows a solution only for definite, discrete values of \mathcal{H}^2 which depend on the size and shape of the region on the boundary of which n has to vanish, i.e., on the size and shape of the pile. Only for the smallest of these \mathcal{H}^2 is n positive throughout and this smallest \mathcal{H}^2 is the one which

occurs in Equation (4-7). Equation (4-8) gives an effective dimension \mathcal{R}^{-1} to every size and shape and Equation (4-6) shows how this effective dimension affects the effective multiplication constant. If the \mathcal{R} of the pile, as defined by Equation (4-8), is larger than the solution of Equation (4-7), the pile is under critical, its effective multiplication constant being smaller than 1. If the solution of Equation (4-7) is larger than the \mathcal{R} satisfying Equation (4-8), the pile is above critical.

The quantity n to which Equation (4-8) applies is the average neutron density, the average to be taken over a cell. Evidently an equation applying to such an average as does Equation (4-8) can be accurate only if this average does not change too rapidly from cell to cell. The relation of the n of Equation (4-8) to the actual neutron density is similar to the relation of the macroscopic density of bodies to their rapidly fluctuating density as given by their atomistic structure. The theory of Equation (4-8) is therefore called the macroscopic pile theory, while the quantities of Equations (4-1) to (4-7) are concepts of the microscopic pile theory. Actually, Equation (4-8) is only the simplest equation of macroscopic pile theory, which applies if the spatial variation of the neutron density is independent of energy. This is an important particular case but does not hold in general. For instance, most control rods absorb only low energy, thermal neutrons. The surface of a control rod is, therefore, a boundary where the density of thermal neutrons vanishes. However, the density of fast neutrons does not vanish at the surface of the control rod and the densities of fast and of slow neutrons are not proportional any more. Problems of this nature call for more complicated equations than (4-8). The most important results toward the solutions of these problems are due to Messrs. F. L. Friedman, A. M. Weinberg, and J. A. Wheeler.

Even the simple Equation (4-8) raises a number of interesting problems. If the shape of the pile is at all complicated -- which is almost invariably the case if the chain reacting material is liquid -- the solution of Equation (4-8) could be obtained only by perturbation methods. Some of these show a remarkable similarity to the Rayleigh-Schrodinger method, with which we are familiar from its application to quantum-mechanical problems. We owe many interesting results on Equation (4-8) to Messrs. F. Murray, L. W. Nordheim, and H. Soodak.

A good part of the work in this connection is too special to be taken up in detail. In my opinion, a good deal of work remains to be done in this field. In particular, the behavior of "thermal" neutrons in the pile and the transition from fast to thermal energies requires further clarification both from the experimental and from the theoretical side. But there remain interesting details to be worked out in almost any part of the theory. There are, also, some problems which have already commanded considerable attention but which I have not even touched. Chief among these is the change in neutron densities with time if Equations (4-6), (4-7) are not exactly fulfilled and the pile is either below or above critical. Messrs. R. F. Christy, L. W. Nordheim, and J. E. Wilkins were particularly active in this field.

4-3 Effect of Radiation on Matter

The radiation densities, both γ and neutron, are higher in a plutonium producing pile than can be maintained outside the pile for extended periods. The effect of these radiations on the structure of materials was one of our early concerns from the theoretical point of view. The experimental work was carried out in the Chemistry Division. Dr. M. Burton reported at the Atlantic City meeting of the American Chemical Society about his, his collaborators', and Dr. J. Franck's work on the subject. On the theoretical side, M. Goldberger, R. S. Mulliken, and F. Seitz shared my interest in the subject, which still has some aspects about which we cannot talk freely.

Clearly, the collision of neutrons with the atoms of any substance placed into the pile will cause displacements of these atoms. If the substance is a chemical compound, the displacement will result in chemical changes which were, of course, investigated before chain-reacting units came into being and are summarized, e.g., in the booklet of Lind.⁽⁷⁾ All these changes are much more intense in the pile, owing to the more intense radiation. But substantial effects can be expected in elementary substances also. The matter has great scientific interest because pile irradiation should permit the artificial formation of displacements in definite numbers and a study of the effect of these on thermal and electrical conductivity, tensile strength, ductility, etc., as demanded by theory. One may expect that studies of the solid state, particularly of the structure sensitive properties, will be greatly stimulated by the additional experimental facility given by the pile.

Before a final interpretation of the experimental results can be made, our knowledge of the ranges of low energy ions will have to be extended. It is on this subject that most of Messrs. Goldberger's and Seitz's work was concentrated. A good deal of the rest of our work was speculation which will either be confirmed or refuted by future experiments.

4-4 Theoretical Physics

The theoretical work of the group fell into two categories: help with the evaluation and planning of experimental work, and real theoretical work. Into the first category falls the work of Messrs. Cahn, Schweinler, Weinberg, and others on the so-called pile oscillator. This is an instrument which permits an absorber of known or unknown neutron-absorbing characteristics to be put into periodic motion in the pile. The oscillation of the neutron absorber causes intensity waves to spread all over the pile. These waves are similar to the temperature waves in the earth, generated by the daily and yearly heat fluctuations of the heat input on the earth's surface. The amplitude and wave length of the waves permits one to evaluate the characteristics of the neutron-absorbing oscillators and of properties of the pile.

The work on neutron diffraction received considerable attention on the part of Goldberger and Seitz. They interpreted and extended Weinstock's results⁽⁸⁾ considerably and took into account phenomena not previously considered. Their work is being continued by Mr. M. Moshinsky in Princeton.

As a last example, I would like to mention Dancoff's work on short-range α -particles. This work actually started because of some acute problems which were practically forgotten by the time Dancoff took over. He noticed that the intensity of short range α 's is often anomalous in the light of Gamow's theory⁽⁹⁾, which stipulates that the α -particle is emitted by an excited residual nucleus. Dancoff investigated several other mechanisms, among which the excitation of the residual nucleus by the α -particle after it has already penetrated the potential barrier seems to be the most important. These theoretical investigations have now received added interest in view of Chang's⁽¹⁰⁾ experimental results. Chang has discovered Dancoff's mechanism independently.

Bibliography

- (1) Haxby, Shoupp, Stephens, and Wells, Phys. Rev. 57, 1088A (1940); 58, 199A (1940).
- (2) H. L. Anderson, Phys. Rev. 57, 566 (1940).
- (3) Cf. e.g., F. Seitz, The Modern Theory of Solids (McGraw-Hill Book Co., Inc., New York, 1940), Chap. IX.
- (4) G. C. Wick, Zeits. f. Physik 121, 702 (1943).
- (5) E. Fermi and F. Rasetti, Ricerca Scient. 9, 472 (1938); G. Placzek, Phys. Rev. 69, 423 (1946).
- (6) J. Bardeen, Phys. Rev. 49, 653 (1936). Cf. also ref. 3.
- (7) Cf. e.g., S. C. Lind, Chemical Effects of α Particles and Electrons (Chemical Catalogue Company, New York, 1928).
- (8) R. Weinstock, Phys. Rev. 65, 1 (1944).
- (9) Cf. G. Gamow, Structure of Atomic Nuclei (Clarendon Press, Oxford 1937), p. 104 ff.
- (10) W. Y. Chang, Phys. Rev. 69, 60 (1946).

CHAPTER 5
ELEMENTARY PILE THEORY

by
F. L. Friedman

I. INTRODUCTION

5-1 General

The theoretical and experimental work which lies in back of these notes on the theory of a chain-reacting pile was performed in the course of the last seven years by an enormous staff of scientists and technicians working on the wartime atomic energy project. It is therefore almost impossible to single out a few names for credit. The largest part of the theoretical work was performed in Chicago in the theoretical group working under Professor E. P. Wigner. Other work has been done both by the British and at the Los Alamos laboratory. More recently, theoretical work has also gone on at the Clinton Laboratories. Some of the earliest theoretical work and a great deal of the experimental background is due to Professors E. Fermi and L. Szilard and their collaborators at Columbia and Chicago.

The pile theory to be considered is applicable to a rather narrow range of possible piles -- namely, those which operate with thermal neutrons. These piles are relatively large, compared to a bomb, at least, hence certain approximations are possible which do not apply in general. The preceding diffusion analysis summarized by Weisskopf is applicable in these cases.

In the following discussion, a number of elementary models, which are quite unrealistic, are used to introduce the fundamental concepts and show how and when these concepts become important in pile theory.

The problems of pile theory may be classified in the following scheme:

1. Time behavior of reactors
2. Critical size for chain reaction
 - a. Assuming knowledge of relative concentrations of all constituents
 - b. Determination of optimal conditions and concentrations for various designs
3. Experiments to determine relevant properties and to check the theory

4. "Special" problems (e.g., controls, reflectors)

5. Operational problems

Although we do not treat all of these problems, it may be useful to keep this classification in mind.

5-2 Summary of Symbols and Definitions

A	Mass of nucleus in units of the neutron mass.
A_i	Activation. It is a measure of the radioactivity produced in a detector by neutron bombardment; i refers to the "type" of neutron involved.
A_f	Fast neutron activation.
A_r	Resonance neutron activation.
A_{th}	Thermal neutron activation
β	Fraction of fission neutrons which are delayed.
β_i	Fraction of fission neutrons which are delayed of type i .
c	Density of delayed neutrons (latent neutron density).
c_i	Density of delayed neutrons of type i (latent neutron density of type i).
d	The extrapolation distance = the distance beyond the physical boundary of a medium in which neutrons diffuse at which a linear extrapolation of the diffusion solution for the neutron density becomes zero.
D	Diffusion constant, connects flux, ϕ , with gradient of n ($\bar{\phi} = -D\nabla n$).
ϵ_c	Efficiency of counter in a particular geometrical arrangement.
η	Number of neutrons released per fission.
$\eta(1-\beta)$	Number of neutrons released immediately on fission.
$\eta\beta$	Number of neutrons released as delayed neutrons per fission.
ηf	Number of neutrons produced per thermal neutron absorbed, usually $= k/p$.
ηfp	Number of neutrons which would return around the cycle of slowing down, thermal diffusion, capture, and fission -- per neutron starting in an infinite medium; usually $= k$.

η_u	Number of neutrons released per capture in ordinary uranium (more generally per capture in all but the moderator material)
f	Thermal utilization = fraction of all thermal neutron captures taking place in fissionable isotopes.
f_u	Fraction of all thermal neutron captures taking place in natural uranium -- or more generally, in any material not considered to be the moderator material.
I_j	The relative resonance integral for an atom of type j . The integral over the resonance absorption cross section divided by thermal capture cross section.

$$\left(I_j = \int \frac{\sigma_{rj}}{\sigma_{oj}(\text{th})} \frac{dE}{E} \quad \text{where the integral is taken over the resonance region} \right)$$

k	Number of neutrons completing the cycle of slowing down thermal diffusion, capture, fission -- measured just after the fission per one starting from fission; usually = ηfp .
$k\beta$	" k delayed" -- number of neutrons getting around cycle with a wait as delayed (latent) neutrons.
$k(1-\beta)$	" k prompt" -- number of neutrons getting around the cycle which avoid a wait as latent (delayed) neutrons
k_{eff}	Number of neutrons actually getting around the cycle in a finite system. The effects of leakage are included.
$k_e = k_{\text{excess}}$	Number of neutrons minus one actually getting around the cycle. (In a finite system, the effects of leakage are included.)
\mathcal{K}^2	A characteristic geometrically determined constant such that if the space variation of every neutron density satisfies $\Delta S + \mathcal{K}^2 S = 0$, the boundary conditions are satisfied for a chain reactive unit (unless $\mathcal{K}^2 = \mathcal{K}_0^2$ the neutron densities in the reactor are functions of time).
\mathcal{K}_0^2	A characteristic constant of a homogeneous medium such that if every neutron density has a space variation given by S where $\Delta S + \mathcal{K}_0^2 S = 0$, there is no time variation of the neutron densities in an infinite region (critical conditions).
\mathcal{K}_{ij}^2	The \mathcal{K}^2 corresponding to the ij harmonic. When $\Delta S + \mathcal{K}^2 S = 0$, the boundary conditions can be satisfied by a sequence of eigenfunctions and eigen-values $S_{ij}, \mathcal{K}_{ij}^2$. This sequence is called a sequence of harmonics. The indices are used to label the elements in the sequence.

ℓ_f	Fraction of neutrons which stay in a finite system during the slowing-down process (computed as if resonance capture were absent).
ℓ_{th}	Fraction of neutrons which stay in a finite system during thermal neutrons.
L	Thermal diffusion length ($L^2 = \frac{\overline{r^2}}{6}$, $L^2 = D\tau_0$).
L_0	Thermal diffusion length in pure moderator.
L_f	Analogue of L for slowing down process
	$L_f^2 = \frac{\overline{r^2}}{6} = \int_E^{E_{fiss}} \frac{1}{3(\sigma N)^2} \frac{dE}{\xi E}$
M^2	$L^2 + L_f^2$, called migration area.
n	Density of neutrons (usually thermal neutrons; occasionally, when specified, of other velocities per unit $\ln E$ interval).
N_i	Density of nuclei of type i .
p	Probability that a neutron escapes resonance absorption during slowing down in an infinite medium.
q	Slowing-down density = number of neutrons slowing down through a given energy per unit volume and unit time.
Q	Source strength (neutrons per unit time; for a plane source, neutrons per unit time and unit area).
$\overline{r^2}$	Mean square distance from source point to absorption point for thermal neutrons or to point at which neutron becomes thermal for fast neutrons.
R_{ij}	The relaxation distance of the ij harmonic. In a moderating column $\frac{1}{R_{ij}^2} = \frac{1}{L^2} + \mathcal{H}_{ij}^2$.
σ	Cross section (total).
σ_c	Capture cross section.
σ_f	Fission cross section.
σ_a	Activation cross section in sections on activation; sometimes used elsewhere as $\sigma_0 + \sigma_f$, the total absorption cross section.

$\sigma_s N_s \xi_s$	Slowing-down power = scattering cross section per unit volume times the average $\ln E$ loss per collision.
τ	Pile period.
τ_a	Decay period of radioactive nucleus formed by activation through neutron capture.
τ_d	Mean life of delayed neutrons.
τ_i	Mean life of delayed neutrons of type i.
τ_j	j^{th} characteristic period of the pile.
τ_o	Mean life of thermal neutrons against capture.
$\bar{\theta}$	Mean slowing down time to top of $1/v$ region.
ξ	Mean logarithmic energy loss per collision

$$\overline{(\ln E_{\text{in}}/E_{\text{out}})}_{1 \text{ coll}}$$

5-3 Review of Relevant Concepts from Nuclear Physics

A great many properties of nuclei have been discussed in previous chapters. Fortunately, of these, only a few are of importance in describing a nuclear chain-reacting system. The following is a list of the more important properties:

1. The number of neutrons released on fission. Undoubtedly this quantity is not a constant. However, we are only interested in its average value. This value is clearly greater than 1. Otherwise, as we shall see, it would be impossible to run the Hanford piles or explode a bomb. According to the Smyth Report, its value is somewhere between 1 and 3. We shall denote it by the symbol η .

2. Delayed neutrons associated with fission. Most of the neutrons produced on the fission of nuclei appear at once. Some, however, are delayed, appearing first some time after the fission has taken place.

3. The cross section for the production of fission by the capture of a neutron in a fissionable nucleus, such as U^{235} or Pu^{239} . This cross section, which we shall denote by the symbol σ_f , is a function of the energy of the neutrons which are captured.

4. The cross sections for capture of neutrons in other nuclei. These are also functions of neutron energy and will be denoted by σ_o . In order to keep our ideas more definite, we may occasionally use the cross section for absorption in the resonance region, by which we mean the cross section of absorption evaluated in a certain range of energies not far above the energy at thermal equilibrium. It will be denoted by σ_r .

5. Cross sections for scattering by all the nuclei present, σ_s . In general, these also are functions of the neutron energy.
6. The average logarithmic energy loss suffered by a high-energy neutron in colliding with a nucleus, ξ .
7. Although we can hardly consider the numbers of nuclei of various types as properties of the nuclei, the proportions in which we mix nuclei and the total numbers present are always important data.

Even though we have eliminated such constants as the magnetic and quadrupole moments, this list is still too long. Consequently, we shall develop the theory of chain-reacting piles by practicing on a simpler model in which only a few of the essential quantities are involved and in which the relevant cross sections are important at only a single energy.

II. THE CLOSED BOX OF THERMAL NEUTRONS

5-4 The Homogeneous Closed Box with Monokinetic Neutrons

The imposing title of this section is merely a technical description for a simple model. In this model, all neutron energies are those of thermal equilibrium. The neutrons released by fission come out in thermal equilibrium with the medium and they remain in equilibrium until their death either by capture to create another fission or by capture in nonfissionable nuclei. The box is closed by walls which are perfectly reflecting. No neutrons are lost in the walls or leak out of the box.

We shall now define the thermal utilization, f ; this is the fraction of all neutrons captured which are captured in fissionable nuclei. It is clear that ηf is then the number of neutrons produced per neutron absorbed. If no neutrons escape from our box and if

$$\eta f = 1$$

the total number of neutrons inside will remain constant. Nevertheless, fissions will go on and energy will be released. The rate of fission is determined by

$$(5-1) \quad n v \sigma_f N_f V$$

where n is the neutron density, v is the velocity of the neutrons in thermal equilibrium, N_f is the density of fissionable nuclei, and V is the volume of the box. We need only multiply this expression by the average energy released per fission to find the power level at which our reactor is running.

(It should be remarked that $v\sigma_f$ is approximately constant over a reasonable temperature range. It may also be useful to know that 3×10^{10} fissions per second is approximately 1 watt.)

If $\eta f < 1$, the box progressively empties, while if $\eta f > 1$, the box fills up with neutrons. In both cases the power is proportional to the density of neutrons, and falls or rises with the number of neutrons.

It only remains to calculate f , the thermal utilization, from the known values in our list of fundamental constants. Just as (5-1) gives the rate of fission

$$(5-2) \quad nv(\sigma_f N_f + \sigma_c N_c)V$$

gives the rate of capture of neutrons as a result of all processes. Consequently,

$$(5-3) \quad f = \frac{\sigma_f N_f}{\sigma_f N_f + \sigma_c N_c}$$

It is interesting to note that $\sigma_s N_s$ does not appear anywhere in the theory.

5-5 Time Dependence of the Neutron Density (no delayed neutrons)

The rate at which the box empties or fills with neutrons depends on something in addition to the value of ηf . Some sort of characteristic time is required. For example, if we could state that a neutron lives just $\bar{\tau}$ long, then the neutron density in the box would change by the factor ηf each $\bar{\tau}$, and we could write

$$(5-4) \quad n = n_0 e^{\ln(\eta f)t/\bar{\tau}}$$

We might tentatively identify $\bar{\tau}$ with $\frac{1}{v(\sigma_f N_f + \sigma_c N_c)}$, which must be a mean lifetime for the neutrons, assuming that none is delayed.

In order to get the time dependence more accurately, we note that, when there are no delays

$$(5-5) \quad (\eta f - 1)nv(\sigma_f N_f + \sigma_c N_c)V = \frac{\partial n}{\partial t} V$$

is the rate of increase of neutrons present, and consequently the neutron density is given by

$$(5-6) \quad n = n_0 e^{(\eta f - 1)t/\tau_0}$$

and

$$(5-7) \quad 1/\tau_0 = v(\sigma_f N_f + \sigma_c N_c)$$

Our first guess, given by formula (5-4), is not too bad as long as $|\eta f - 1| \ll 1$. Again we note the absence of scattering properties and of the volume of the box. τ_0 , however, depends on the absolute density, whereas f only depends on the relative densities of the constituents.

5-6 Time Dependence of the Neutron Density when Delayed Neutrons are Considered

We have committed many sins of omission in the above analysis. We shall now generalize our model through successive steps so as to bring it into better accord with these facts. First we shall consider the effect of the delayed neutrons; then we shall consider the effects introduced by allowing the energy of fission neutrons to take its proper value; and finally we shall rub off the ideal nuclear paint which forms the reflecting walls.

When we cause a large number of fissions at a given instant and observe the neutron emission for some time thereafter, we find that most of the neutrons appear at once. However, some neutrons continue to show up for a long time afterwards. The frequency with which these delayed neutrons appear can be analyzed as a function of time into a sum of descending exponentials. This analysis has been presented in an earlier lecture. If we call the neutrons associated with a given descending exponential, let us say the i^{th} exponential, neutrons of type i , we are confronted with a half-dozen different types of delayed neutrons. Since in this section we are, at best, considering a simplified model, we can get a good idea of the effect of delayed neutrons on the time variation of the neutron density by considering only one type of delayed neutron. This fictitious type decays away with the mean life τ_d , and on the average the fraction β of all the neutrons released in fission are of this type.

In the new model, with the delayed neutrons, formula (5-1) still gives the rate of fission. However, only $(1 - \beta)$ of all the neutrons produced per fission appear in our box immediately. These we call the prompt neutrons; there are now $\eta f(1 - \beta)$ of them per absorption instead of ηf , as was the case in our previous model. The other β arrive gradually. Before they appear, we may call them latent neutrons; and at any time, aside from the

ordinary free neutrons, we should find a certain number of latent neutrons in the pile. If we attempt to rewrite (5-5), we will have to take into consideration not only the decrease in prompt neutrons by the factor $(1 - \beta)$ but also the rate at which latent neutrons are transformed into free neutrons. This rate is given by

$$(5-8) \quad \frac{c}{\tau_d}$$

where c is the density of latent neutrons. (Equation (5-8) can easily be verified by setting up the equation for the decay of latent neutrons after a single fission

$$(5-9) \quad \frac{c}{\tau_d} + \frac{\partial c}{\partial t} = 0$$

The solution of this equation exhibits characteristic exponential decay which we are attempting to introduce into the theory.) We are now in a position to improve Equation (5-5)

$$(5-5a) \quad \frac{n [\eta f (1 - \beta) - 1]}{\tau_o} + \frac{c}{\tau_d} = \frac{\partial n}{\partial t}$$

is our improved result.

Despite the improvement, we are unable to find the time behavior from Equation (5-5a) alone because of the introduction of the unknown c . We therefore look around for another equation which will determine c . The rate of creation of latent neutrons is

$$nv(\sigma_f N_f + \sigma_o N_c) V \eta f \beta$$

and the rate at which they turn into free neutrons is given by (5-8). Consequently, we may write

$$(5-5b) \quad \frac{n \eta f \beta}{\tau_o} - \frac{c}{\tau_d} = \frac{\partial c}{\partial t}$$

Both (5-5a) and (5-5b) obtain simultaneously, and our problem is to solve the pair simultaneously.

Before investigating the general solution, let us ask what happens when $\eta f = 1$. Then by adding the two equations we discover that

$$(5-10) \quad n + c = \text{constant}$$

By substituting for c in (5-5a), it is possible to determine the variation of n . As expected, one possible answer, of which there are two, is that n is a constant. The question arises: What is the significance of the other answer? In order to see the significance, let us consider what happens in our box when we start it off by injecting a batch of free neutrons. At this moment there are no latent neutrons, but as time goes on latent neutrons are created as the free neutrons are absorbed. Since the total number of latent and free neutrons remains constant, the number of free neutrons must decrease as the number of latent neutrons increases. Eventually, as is shown by the existence of the infinite period associated with n equals constant, an equilibrium division between n and c will be obtained (more exactly, such an equilibrium is approached exponentially as time goes on).

We shall now look at some of the features of the general solution of Equations (5-5a) and (5-5b). As a result of previous experience, we may expect the time dependence to be given an exponential, say $e^{t/\tau}$. Assuming

$$(5-11) \quad n = n_{o1} e^{t/\tau_1} + n_{o2} e^{t/\tau_2}$$

$$(5-12) \quad c = c_{o1} e^{t/\tau_1} + c_{o2} e^{t/\tau_2}$$

and substituting in Equations (5-5a) and (5-5b), we obtain

$$(5-5a') \quad n_{oj} \frac{\eta f(1-\beta)-1}{\tau_o} + \frac{c_{oj}}{\tau_d} = \frac{n_{oj}}{\tau_j}$$

$$j = 1, 2$$

$$(5-5b') \quad n_{oj} \frac{\eta f \beta}{\tau_o} - \frac{c_{oj}}{\tau_d} = \frac{c_{oj}}{\tau_j}$$

The solution of these equations gives the following formula for τ_j .

$$(5-13) \quad \frac{1}{\tau_j} = \frac{1}{2} \left\{ \omega(-) \pm \sqrt{\omega^2(+) + \frac{4\eta f \beta}{\tau_o \tau_d}} \right\}$$

where

$$\omega(\pm) = \left[\frac{\eta f(1-\beta)-1}{\tau_o} \pm \frac{1}{\tau_d} \right]$$

or its equivalent

$$(5-13') \quad \frac{1}{\tau_j} = \frac{1}{2} \left\{ \omega(-) \pm \sqrt{\omega^2(-) + \frac{4(\eta f - 1)}{\tau_o \tau_d}} \right\}$$

and also determines the associated ratio

$$(5-14) \quad \frac{n_{oj}}{c_{oj}} = \frac{\tau_o}{2\eta f \beta} \left\{ \omega(+) \pm \sqrt{\omega^2(+) + \frac{4\eta f \beta}{\tau_o \tau_d}} \right\}$$

or

$$= \frac{\tau_o}{2\eta f \beta} \left\{ \omega(+) \pm \sqrt{\omega^2(-) + \frac{4(\eta f - 1)}{\tau_o \tau_d}} \right\}$$

If we call the ratios

$$(5-14') \quad \frac{n_{oj}}{c_{oj}} \equiv a_j$$

we are enabled to rewrite Equation (5-11)

$$(5-11') \quad n = c_{o1} a_1 e^{t/\tau_1} + c_{o2} a_2 e^{t/\tau_2}$$

In (5-11') and (5-12) only c_{o1} and c_{o2} are not already determined from our fundamental data. The values of these constants will be fixed by the initial conditions. That is to say, if $n(0)$ and $c(0)$ are the values of n and c at $t = 0$:

$$(5-15) \quad n(0) = c_{o1} a_1 + c_{o2} a_2$$

$$c(0) = c_{o1} + c_{o2}$$

Suppose, for example, that there are no neutrons present in our box at time zero, but that for some reason a single fission then takes place. If we want to find the future behavior of the neutron densities, we can start out by writing the particular forms of Equation (5-15) for this case. They are:

$$(5-16) \quad \eta(1-\beta)/V = c_{o1} a_1 + c_{o2} a_2$$

$$\eta\beta/V = c_{o1} + c_{o2}$$

By a small amount of algebra, we can find the following equations for c_{o1} and c_{o2} .

$$(5-16a) \quad c_{o1} = \frac{\eta}{V} \frac{(1-\beta) - \beta a_2}{a_1 - a_2}$$

$$c_{o2} = \frac{\eta}{V} \frac{(1-\beta) - \beta a_1}{a_2 - a_1}$$

In order to finish up our problem, we introduce the additional assumption that

$$\eta f = 1$$

Whenever $\eta f = 1$, we shall have

$$(5-17) \quad a_1 = -1, \quad a_2 = \frac{\tau_o}{\beta \tau_d}$$

$$\frac{1}{\tau_1} = -\frac{\beta}{\tau_o} + \frac{1}{\tau_d}, \quad \frac{1}{\tau_2} = 0$$

and applying these results to the present example

$$(5-18) \quad n \frac{V}{V_i} = \frac{1-\beta - \tau_o/\tau_d}{1 + \tau_o/(\beta \tau_d)} e^{-\left(\frac{\beta}{\tau_o} + \frac{1}{\tau_d}\right)t} + \frac{\tau_o/(\beta \tau_d)}{1 + \tau_o/(\beta \tau_d)}$$

$$c \frac{V}{\eta} = \frac{\tau_o/\tau_d - (1-\beta)}{1 + \tau_o/(\beta \tau_d)} e^{-\left(\frac{\beta}{\tau_o} + \frac{1}{\tau_d}\right)t} + \frac{1}{1 + \tau_o/(\beta \tau_d)}$$

which gives the desired complete description for the time dependence.

To show the general nature of this type of solution, we note that the exponentials will eventually drop away and we are left with certain constant values for the free and latent neutron densities. The ratio between these constant values is the equilibrium distribution between free and latent neutrons. It is also easy to check that if one exponential corresponds to an increasing density, the other corresponds to a falling density in such a way that the sum of the free and latent densities is constant. Here, since

β is small compared to one (As we know, it is approximately 1/2 per cent) and since τ_o/τ_d is also small in a realistic case, the coefficient of the exponential is positive for free and negative for latent neutrons.

We must say a little bit about τ_o/τ_d just to get an impression of the order of magnitude. A review of the information on delayed neutrons shows that to invent one delayed neutron period to represent them all, we have to take the one period of the order of 10 seconds. On the other hand, τ_o depends on how we build the system. Of all the quantities which we discussed in the preceding sections, this is the only quantity which depends on the absolute densities involved. If we build a box with practically no density at all, in an absolute sense, it would take the neutrons an essentially infinite time to find any material in which to be absorbed. τ_o would become extraordinarily large. In practical systems, then, we make it as an assertion that the densities will be held high enough so that τ_o will be very small compared to the delayed neutron periods. Then our statements about the coefficients of the exponentials are justified.

We have just worked out Equations (5-13) and (5-14) for the case $\eta f = 1$. It is also easy to write down the answers if $\beta = 0$ or if $\eta f = 0$. For $\beta = 0$, we have

$$\frac{1}{\tau_1} = \frac{\eta f - 1}{\tau_o}, \quad a_1 = \infty$$

(5-19)

$$\frac{1}{\tau_2} = -\frac{1}{\tau_d}, \quad a_2 = \frac{\tau_o}{(\eta f - 1)\tau_d + \tau_o}$$

For $\eta f = 0$, we have

$$\frac{1}{\tau_1} = -\frac{1}{\tau_o}, \quad a_1 = \infty$$

(5-20)

$$\frac{1}{\tau_2} = -\frac{1}{\tau_d}, \quad a_2 = \frac{\tau_o}{\tau_d - \tau_o}$$

Previously, when we investigated the case $\beta = 0$, we obtained only one period, and when there is no reproduction, it might appear that there is no problem at all. Strangely enough, in each case we get a couple of periods and associated densities. The reason we get these is that we set up our problem in such a way as to satisfy initial conditions. For example, even though our medium is not reproducing, our initial conditions may force upon us neutron densities, and the array of periods and ratios leads to the description of what happens to those neutron densities in a medium which does not reproduce at all.

These results are straightforward. A far more important result can be found by considering what happens when

$$\eta f(1 - \beta) - 1 \gg 4 \frac{\tau_0}{\tau_d}$$

In that case

$$(5-21) \quad \frac{1}{\tau_1} \approx \frac{\eta f(1 - \beta) - 1}{\tau_0} \gg \frac{4}{\tau_d}$$

From Equation (5-21) it follows that after a short time the neutron density and the power level must be rapidly rising. Since τ_0/τ_d is usually extremely small, we should attempt to build reactors in which we can be sure that at all times

$$(5-22) \quad \eta f(1 - \beta) < 1$$

This eliminates the possibility of leaving the delayed neutrons completely behind and of having the neutron level rise on a purely prompt neutron cycle. Since

$$\beta \approx .005$$

we find that it is wise to keep

$$(5-22a) \quad \eta f < 1.005$$

On the other hand, in a practical reacting system, we want to make $\eta f > 1$ at some times in order to get our neutron density to rise to the level of standard operations. We are therefore interested in finding the values of τ when

$$(5-23) \quad |\eta f - 1| \ll 1, \quad \eta f(1 - \beta) - 1 < 0$$

and (of necessity)

$$\beta \ll 1.$$

For example, let us assume as a sufficiently stringent safety condition that

$$(5-24) \quad |\eta f(1 - \beta) - 1| \gtrsim |\eta f - 1|$$

Then, using (5-13'), we find as a good approximation for the periods

$$(5-25) \quad \frac{1}{\tau_1} \approx \frac{\eta f(1 - \beta) - 1}{\tau_0} - \frac{1}{\tau_d}$$

$$\frac{1}{\tau_2} \approx \frac{\eta f - 1}{\tau_0 - [\eta f(1 - \beta) - 1] \tau_d}$$

Here τ_1 is always a falling period, but τ_2 is a rising period when $\eta f > 1$ and falling when $\eta f < 1$. If we can control ηf , then, we can make the pile rise or fall. From (5-24) and (5-25) it follows that the periods are safe; that is to say, no rising period for the reaction is permitted which is faster than τ_d . Recalling that $\tau_d \approx 10$ sec, we see that the pile will not rise at an uncontrollably fast rate.

Let us summarize the mathematical discussion of time behavior. We found that if the excess number of neutrons in one generation, $\eta f - 1$, is not very great (i.e., if it is only of the order of or somewhat less than the number of delayed neutrons, $\eta f \beta$, created in one generation) no long-run, fast rising period is present. In fact, we found a slow rising period and another period which is falling. The behavior of the neutron density, however, is slightly complicated because the densities associated with the various periods may combine in such a way that this apparently falling period actually leads to a transient rise. The transient period can be quite fast, for either rising or falling density. It is the response of the prompt neutrons to changes, let us say, in the excess reproduction per cycle.

For example, suppose that, from a steady state, a quick change is somehow induced in the pile, the neutron density will follow this change as

best it can with the prompt neutrons. If ηf goes up, the density will promptly go up. If ηf goes down, it will promptly go down. In neither direction, however, can the density get very far, because it is limited by the delayed neutrons. They are running on the old level. To a rising density they do not contribute enough and to a falling density they contribute too many neutrons to allow a fast period to survive long. As the transient levels off, the delayed neutrons come in; the period from then on is largely controlled by the delay periods. It becomes the slow period, the safe period, which is really rising when $\eta f > 1$.

The transient rise is usually extremely short. Therefore a crude way of analyzing these problems is to throw away the transient (as unobservable) and to deal only with the density associated with the long period. That associated density we can compute mathematically and in many pile problems this is all that is required. The transient is then represented merely by a jump.

5-7 Controlling the Chain-Reacting Box; Oscillation Method

Most of the time so far we have been talking about chain-reacting boxes whose properties are fixed. In such a box a rising neutron density will continue to rise indefinitely or a falling one will continue to fall. Our boxes would clearly be much more useful if we were able to control the time behavior of the neutron density to suit ourselves. In order to do this, it is necessary to have at least one of the properties at our disposal.

We can easily keep for ourselves the power of controlling f by leaving space inside the reacting box, into which we can introduce or from which we can take out thermal absorber. (Of course, in order to keep our simple theory, the introduction or removal must be done uniformly throughout the box.) Nonfissionable absorber which is placed in the pile will essentially make the thermal utilization smaller by increasing the denominator in formula (5-3) without changing the numerator. Conversely, on taking out some absorber, ηf will become bigger. By this method, we can control $\eta f - 1$. Other methods of controlling the chain-reacting box which do not require a change in f will be discussed later. They arise when we deal with the modifications involved in the theory of a pile from which the neutrons are allowed to leak out.

When $\eta f - 1$ is changed rapidly by successively putting in and taking out absorber, the transient jumps described in the preceding section will occur in rapid succession. On the other hand, for sufficiently rapid oscillation about a mean value, the delayed neutrons will not follow but will act as if the pile were in a steady state. This oscillation method has been put to good use in separating the part of ηf which goes with the delayed neutron action, $\eta f \beta$, from the part which goes with prompts, $\eta f(1 - \beta)$. It can also be employed to measure the absorption cross section of the oscillating material. Both applications are discussed in later sections.

5-8 Measurement of $\eta f - 1$

Occasionally throughout these lectures it will be interesting to discuss not merely the problem of designing a chain-reacting unit from a known set of nuclear constants, but also a problem, which in some sense is the inverse problem, that of determining some of the constants in the theory from the behavior of a reacting unit or from an independent experiment. The constants which we can thus determine are not usually fundamental nuclear constants like cross sections. Rather, they are combination constants like f , the thermal utilization, or τ_0 , which involves cross sections, densities and neutron velocity. So far we have predicted the combination constants from fundamental data. Our values may be in error and it is good to check them. Consequently, let us now assume that we have constructed a chain-reacting unit on the basis of approximate values of the relevant nuclear constants and set out to determine $\eta f - 1$ from the behavior of our reactor.

It is easy to rework formula (5-13') into

$$(5-13a) \quad \eta f - 1 = \tau_0 / \tau_j + \frac{\eta f \beta \tau_d}{\tau_j + \tau_d}$$

This formula is particularly useful since, as we just showed, the safe rising periods for a reactor are sufficiently long that the first term on the right can be neglected by comparison with the second. For reasons which we shall come to in a later section, the same thing can often be said for safe falling periods. In any case, for a practical reactor we should be able to put ourselves in this situation. It is then possible to write

$$(5-13a') \quad \frac{\eta f - 1}{\eta f} \approx \beta \frac{\tau_d}{\tau_j + \tau_d}$$

which will be valid to a very good approximation. From (5-13a') we are able to determine $\eta f - 1$ by measuring the actual time behavior of our reactor. Only the properties of the delayed neutrons need be known in addition.

Of course, (5-13a) can be solved explicitly for ηf , but when a long period is employed, (5-13a') is quite adequate. More important when we introduce the consideration of finite size by rubbing off the ideal nuclear paint, the simple solution for ηf is no longer maintained, while the analogue of (5-13') is still valid.

III. THE CLOSED BOX WITH NEUTRONS OF ALL ENERGIES

5-9 The Slowing Down of Neutrons without Resonance Capture

Earlier we promised to bring our crude model into better accord with reality by allowing the fission neutrons to be released at their rightful energy. (This energy is of the order of a million electron volts.) In order to perform an analysis of the new situation, it will be necessary to introduce some more of the fundamental nuclear properties from our list of Section 5-3. We shall proceed in two steps: first, assuming that there is no resonance absorber present, and later, introducing modifications which arise when resonance absorber must be considered.

If it were true that both σ_f and σ_c were proportional to $1/v$ throughout the whole energy spectrum, changing the energy of the neutrons released in fission would have no effect whatsoever on our analysis. However, if it were true that σ_f , σ_c suddenly dropped to zero above a certain critical velocity v_c , the time taken by the neutrons to slow down from the velocity at which they are emitted in fission to the critical velocity should be added in some way to the characteristic time which they live before absorption in the $1/v$ region. Let us investigate the manner in which this slowing down time should be added to the mean life against "thermal" capture by returning to a model in which we forget that any of the neutrons are delayed. Suppose that we know the frequency distribution of neutrons entering the $1/v$ region as a function of time after their release in fission. Let us call this distribution $K(\theta)$, and assume that we have normalized $K(\theta)$ so that

$$(5-26) \quad \int_0^{\infty} K(\theta) d\theta = 1$$

If we define $q(t)$ as the number of neutrons slowing into the $1/v$ region per unit time and unit volume, we can write for $q(t)$

$$(5-27) \quad q(t) = \eta f v (\sigma_c N_c + \sigma_f N_f) \int_0^t n(t') K(t - t') dt'$$

while the analogue of Equation (5-5) becomes

$$(5-5c) \quad q(t) - nv (\sigma_c N_c + \sigma_f N_f) = \frac{\partial n}{\partial t}$$

Combining these two equations, we obtain

$$(5-5c') \quad \frac{\eta f}{\tau_0} \int_0^t n(t') K(t - t') dt' - \frac{n}{\tau_0} = \frac{\partial n}{\partial t}$$

From our previous experience, we are led to seek a solution of (5-5c') of the form

$$n = n_0 e^{t/\tau}$$

and in turn we obtain a new characteristic equation

$$(5-28) \quad \frac{\eta f}{\tau_0} \int_0^t e^{-\theta/\tau} K(\theta) d\theta - \frac{1}{\tau_0} = \frac{1}{\tau}$$

This equation may be solved under various assumptions as to the form of $K(\theta)$. For example, if $K(\theta) = \delta(\theta - \theta_0)$, we obtain

$$(5-28') \quad \frac{\eta f e^{-\theta_0/\tau} - 1}{\tau_0} = \frac{1}{\tau} \quad \text{for } t > \theta_0$$

More generally, we may expand θ/τ under the integral and obtain

$$(5-28a) \quad \frac{\eta f (1 - \frac{\bar{\theta}}{\tau} + \frac{1}{2} \frac{\bar{\theta}^2}{\tau^2} - \dots) - 1}{\tau_0} = \frac{1}{\tau}, \quad \bar{\theta}^n \equiv \int_0^\infty \theta^n K(\theta) d\theta$$

for all values of t sufficiently large that $K(t)$ is essentially zero. This procedure is a practical one, since all neutrons slow down in a very short time after their release in the fission process (or when $\beta \neq 0$ by turning

from latent into free neutrons). For the same reason, the series $1 - \frac{\bar{\theta}}{\tau} + \frac{1}{2} \frac{\bar{\theta}^2}{\tau^2} - \dots$ will converge rapidly for all values of τ of practical interest. It is therefore possible to make an accurate approximation for τ by

$$\frac{1}{\tau} = \frac{\eta f e^{-\bar{\theta}/\tau} - 1}{\tau_0} \quad \text{or} \quad \frac{1}{\tau} \approx \frac{\eta f - 1}{\tau_0 + \eta f \bar{\theta}}$$

We have been claiming that $\bar{\theta}$ is small, for example, compared to τ_0 . (Since $\bar{\theta}$ depends on velocity and on the absolute density, τ_0 is the only legitimate comparison standard.) Let us now attempt to calculate $\bar{\theta}$ in terms of more fundamental nuclear constants. In order to make this calculation, we shall assume that as the neutrons slow down, they do so by making elastic collisions with the scattering nuclei in the box. The law of scattering will be such that the scattering is isotropic in the center of gravity system of neutron and nucleus. When this is the case, the neutrons bounce down the energy scale, losing, on the average, the same fraction of their energy at each collision. The quantity ξ measures this fractional loss. It is defined by $\xi = \left\{ \left(\ln \frac{E_{\text{in}}}{E_{\text{out}}} \right)_{\text{averaged over one collision}} \right\} = \left(\ln \frac{E_{\text{in}}}{E_{\text{out}}} \right)_{1 \text{ coll}}$, where E is the neutron energy, and in accordance with the assumptions we have just made can be shown to be given by

$$(5-29) \quad \xi = 1 - \frac{(A - 1)^2}{2A} \ln \frac{A + 1}{A - 1}$$

where A is the mass of the recoiling nucleus in units of neutron mass.

The average time between collisions at a given energy is given by

$$\Delta t = \frac{1}{\sigma_s N_s v}$$

and the change in energy in the collision is given by

$$\Delta E = \xi E$$

Consequently,

$$(5-30) \quad \frac{\Delta E}{E \Delta t} = \xi \sigma_s N_s v$$

Upon adding up all the collisions, we obtain rather closely

$$(5-30a) \quad \bar{\theta} = \int_{v_c}^{v \text{ fissions}} \frac{dE}{\xi \sigma_s N_s v E} = 2 \int_{v_c}^{v \text{ fissions}} \frac{dv}{\xi \sigma_s N_s v^2}$$

In order to get an approximate evaluation of this integral, we shall assume that σ_s is a constant. Since the largest contribution to the integral arises in the region where v is near v_c , we may pick the value of σ_s at v_c without making a substantial error. With this assumption, we get

$$(5-30a') \quad \bar{\theta} = \frac{2}{\xi \sigma_s N_s v_c}$$

This formula shows that the major fraction of the time is consumed in making the last few collisions when the neutron is travelling slowly. Carrying out the comparison with τ_o , we obtain the approximate formula

$$(5-31) \quad \frac{\bar{\theta}}{\tau_o} \approx \frac{2 v (\sigma_c N_c + \sigma_f N_f)}{\xi \sigma_s N_s v_c}$$

In this formula v_c may be chosen realistically to be several times v , the mean value of the velocity for neutrons in thermal equilibrium. For most of the materials which do the major part of the slowing down in chain-reacting systems ξ is greater than its value for carbon, while for carbon a simple calculation shows that ξ is .158. $\bar{\theta}/\tau_o$ is then determined to be

$$(5-31') \quad \frac{\bar{\theta}}{\tau_o} \lesssim \frac{\sigma_c N_c + \sigma_f N_f}{\sigma_s N_s} \approx \frac{1}{f} \frac{\sigma_f N_f}{\sigma_s N_s}$$

since the scattering cross section (except for hydrogen, when the whole analysis is not very good) is usually approximately the same at v and v_c . Again substituting the values of our fundamental nuclear constants and the proportions found in "practical" reacting systems, we find that $\bar{\theta}/\tau_o \ll 1$, as previously assumed. In fact, we may usually go back to using τ_o alone, rather than correcting for $\bar{\theta}$ in the formulae for the time variation of neutron densities.

This result is really a definition, rather than a conclusion. If we put a very large amount of thermally fissionable material into the reacting box, we will make the numerator in (5-31) large. At the same time, we must take out most of the scattering material or at least dilute it in order to get the additional fissionable material in, thus making the denominator of (5-31) small and violating the inequality (5-31'). In slightly different words, if there is a lot of fissionable material and very little light, scattering, moderating material in the box, neutrons will not slow down quickly and once they get thermal they will be captured immediately. In such a system the neutrons are travelling quite fast, and a great deal of fissionable material is present. We are therefore going away from the thermal pile toward the fast neutron action of the bomb. In writing down inequality (5-31') for "practical" cases, we are essentially restricting the area of discussion to thermal piles. At the end of the next section we shall make further remarks on the realistic nature of the assumptions employed in this section.

5-10 The Slowing Down of Neutrons, Resonance Capture Considered

The presence of resonance capture in the energy region above thermal energies (see Section 1-27) will decrease the number of neutrons which become thermal as compared with the number of neutrons which start the slowing down process after fission. Let us call the ratio of the number of neutrons arriving at the top of the $1/v$ region to the number of neutrons starting to slow down after being released on fission, p , the resonance escape probability. To find the slowing down density $q(t)$ at the top of the $1/v$ region, we must multiply the right-hand side of Equation (5-27) by the factor p . This essentially replaces ηf by ηfp in all the formulae where ηf occurs. For example, when $\eta fp = 1$, $1/\tau = 0$.

A review of our work will show that in computing the characteristics of our chain-reacting boxes, the combination ηf always occurs together; neither η nor f occurs by itself. In the future the product ηfp will occur and no one of η , f , and p will occur by itself. We therefore define

$$(5-32) \quad k \equiv \eta f p$$

and in the future any further analogues of ηfp we shall also call k . k is the reproduction constant; it tells us the number of neutrons which return

to fission energies (through the process of fission) for each neutron which starts out at that energy. This number is counted over one cycle: that is, slowing down, thermal diffusion, and capture to create the new neutrons by means of the fission process.

In order to calculate p , we will have to make use of our knowledge of the cross sections for resonance capture and of the density of resonance absorbing nuclei present in the box. We also need the scattering cross section and the density of scattering nuclei; in particular, we want the value of the scattering cross section in the energy region of the resonance absorption. In this energy region, the chance that a neutron will survive a single collision is given by

$$(5-33) \quad 1 - \frac{\sigma_r N_r}{\sigma_r N_r + \sigma_s N_s}$$

This is also the probability that the neutron will be slowed down as a result of the collision and, if this occurs, the neutron loses on the average the amount of energy given by $\Delta E = \xi E$. The next collision takes place (on the average) at the energy $E(1 - \xi)$, and it follows that the probability of surviving two collisions is (closely)

$$(5-33') \quad \left(1 - \frac{\sigma_r(E) N_r}{\sigma_s(E) N_s + \sigma_r(E) N_r} \right) \left(1 - \frac{\sigma_r(E(1-\xi)) N_r}{\sigma_s(E(1-\xi)) N_s + \sigma_r(E(1-\xi)) N_r} \right)$$

Since the neutron again loses energy, we see that by repeating our multiplications a sufficient number of times we will compute the probability of escaping resonance capture on slowing down through the whole resonance region.

Actually, the neutrons do not bounce along hitting only the average energy values; and in considering a large group of neutrons, we substitute for the spread in energy the concept of a fractional collision which reduces the energy by $\Delta E = \xi E/n$, while giving a survival probability of

$$\left(1 - \frac{\sigma_r N_r}{\sigma_r N_r + \sigma_s N_s} \right)^{1/n}$$

As n becomes large, the neutrons will hit all energies in better correspondence with the actual facts. Also, as n becomes large, the probability of survival may be rewritten as

$$(5-33a) \quad p = e^{-\frac{\sigma_r N_r}{\sigma_r N_r + \sigma_s N_s} \frac{1}{n}}$$

It follows that

$$(5-34) \quad p = e^{-\int \frac{\sigma_r(E) N_r}{\sigma_r(E) N_r + \sigma_s(E) N_s} \frac{dE}{\xi E}}$$

if the integral is taken all over the energy region of resonance absorption. (Our procedure is essentially an analogue of the change of $e^{\ln(\eta f)t/\tau}$ into $e^{(\eta f-1)t/\tau_0}$ in Section 5-5.)

At the end of the last section we promised to make some remarks justifying the assumptions employed. The main point to note is that the top of the $1/v$ region will be set by the position of the lowest resonance absorption. Since we do not build piles of materials with resonances in the thermal region, the top of the $1/v$ region is normally at many times thermal energy. It is often set by the characteristic resonance of Uranium 238, which is usually present. In that case, v_0 is probably over ten times thermal equilibrium velocity. Also, since we are dealing with thermal piles, the neutrons which go around the cycle are almost exclusively those which get into thermal equilibrium -- well into the $1/v$ region. Consequently, our calculations of the cycle time $\tau_0 + k\bar{\theta}$ is essentially correct. If for some reason the fission cross section competes favorably with the resonance absorption (for example, if resonance absorption is absent), the neutrons which cycle at this higher energy region do so in a shorter time than we have assumed, and the cycle time is less lengthened by the introduction of the slowing down than predicted by our calculation. There is one chance for trouble. If the $1/v$ region does not extend to the energy at which the chemical binding freezes our scattering nuclei, our calculation of $\bar{\theta}$ is inapplicable. In this case a much more complicated calculation must be indulged in, but the result, that $\bar{\theta}$ is small compared to τ_0 , is maintained.

We should also say a word about the validity of formula (5-34). Our arguments in deriving this formula were plausible rather than rigorous. For example, if σ_r were infinite over a range of energies greater than the possible energy loss of a neutron as a result of a single collision, p should be zero. However, formula (5-34) predicts an appreciable survival. Formula (5-34) can be shown by rigorous arguments to be correct when $\sigma_r N_r \ll \sigma_s N_s$ or when the width of the resonance becomes very small compared to the average energy jump. In most practical work (5-34) will give an accurate answer.

It is interesting to note that since the introduction of slowing down problems in Section 5-9 the scattering properties of our reactor have entered the theory. They come in both the calculation of the slowing down time and the resonance escape probability. They enter because the rate of slowing down depends not only on ξ but also on the frequency of collisions. The product which occurs, $\sigma_s N_s \xi_s$, is often called the slowing down power of the scattering material. It may be viewed as a macroscopic absorption cross section (see Section 1-13) for fast neutrons. Just as $nv\sigma_c N_c$ is the rate at which neutrons leave the thermal region by capture in nonfissionable isotopes $nv\sigma_s N_s \xi_s$ is the rate at which neutrons pass out of a higher energy region by slowing down (Here nv is defined per unit $\ln E$). In a later, more realistic version of the theory, the scattering properties will enter for a different reason and in that case they will not always enter in combination with ξ as they do here.

5-11 Measurement of p , the Resonance Escape Probability

We have just seen that the introduction of resonance absorber to our ideal chain-reacting box changes ηf everywhere in the theory to ηfp . Mentally, at least, we are able to measure p and consequently

$$\int \frac{\sigma_r N_r}{\sigma_s N_s + \sigma_r N_r} \frac{dE}{E}$$

by introducing resonance absorber into the box. To do this measurement, we observe the changes in the time behavior of the neutron density and from them we infer the change in k . The ratio of k before and after the introduction of resonance absorber is exactly p .

In practice, using a nuclear chain reaction may be a bit expensive and wasteful, particularly if the introduction of resonance absorber de-

creases k so much that the reactor is no longer workable. We shall, therefore, describe a somewhat cheaper method for measuring p .

In this method we employ three new instruments: a neutron source which emits neutrons at some energy not far above that at which resonance absorption takes place, an ideal resonance detector which becomes radioactive as the result of its own ability to capture neutrons in a very low energy resonance, and a block of scattering material. The ideal resonance detector must have its resonance absorption at an energy which is lower than the resonance absorption of the material we are investigating. With these instruments we make two measurements. First, we measure the activation of the detector inside the block of scattering material at a short distance from the source. Then we introduce some of the resonance absorber whose effect we want to measure and repeat the experiment. The ratio of activations in the first and second experiments gives p for the scattering material employed and the concentration of resonance absorber introduced.

In describing the measurement of p , the scattering properties enter; and the density of scattering nuclei is a relevant quantity. If, however, p has been measured for one density of scattering nuclei and one density resonance absorbing nuclei and ξ is known for the scattering nuclei, by use of formula (5-34) the p 's can be computed for other proportions and densities of scattering and resonance absorbing nuclei. In fact, it can be computed for other scattering substances for which the values of ξ and σ_s are known.

5-12 Measurement of f , the Thermal Utilization

In order to measure f , we introduce two new pieces of equipment: the ideal thermal detector and the standard box. The ideal thermal detector is an instrument which tells, usually by radioactivation, the density of thermal neutrons in which it has been placed. It is sensitive to nothing but thermal neutrons. The standard box is also simple. It contains no fissionable material and usually no resonance absorber, but otherwise it exactly resembles the box which we have been employing to produce our chain reaction. It contains exactly the same density of the same scattering nuclei and the same density of the same thermally absorbing nuclei.

It is useful in the laboratory since it provides, for example, a method for the intercomparison of neutron sources and a convenient place in

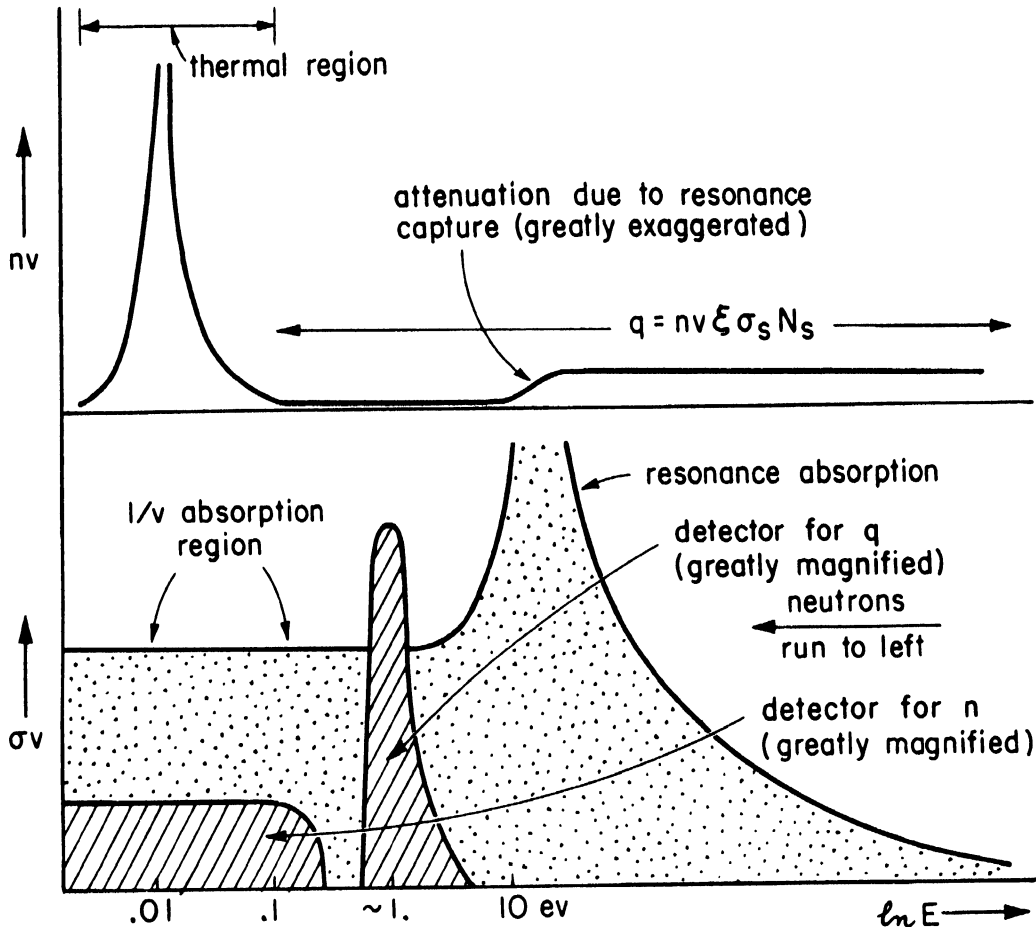


Figure 5-1. Schematic Neutron Densities and Absorption Cross Sections (both are multiplied by v , the neutron velocity). The characteristics of an ideal resonance detector (detector for q) are: (1) it is sensitive to neutrons only in a narrow range of energies; (2) the energy range of sensitivity is lower than all resonance energies of interest, but high compared with thermal equilibrium energy. Consequently, the neutrons in thermal equilibrium, in the Maxwell distribution (see upper half of figure and Section 5-13) do not affect it. It therefore measures q after resonance escape.

The characteristic of an ideal thermal neutron detector is that its activation is proportional to n , the neutron density, throughout the energy region of thermal equilibrium. It must therefore be a $1/v$ absorber, throughout this region.

The neutrons in thermal equilibrium constitute almost all neutrons in the $1/v$ region for the piles which we discuss. We shall often use a crude classification of neutrons into neutrons in thermal equilibrium and neutrons which are slowing down, rather than the classification into neutrons in the $1/v$ region and those with higher energies.

which to "keep" a standard thermal neutron density. In this section we shall confine our interest in the standard box to the measurement of f .

Inside the box we place a neutron source, either the one used in the last experiment for the measurement of p or, more conveniently, let us say, a Ra-Be source. We measure the activation both of the ideal resonance detector and of the ideal thermal detector. Since all the neutrons from the source slow down through the energy region in which the ideal resonance detector is sensitive in just the same way as they do in the chain-reacting box, the activation of the ideal resonance detector is proportional to $q(t)$, the number of neutrons becoming thermal per unit volume and unit time with the same proportionality constant which holds between the activation and $q(t)$ if we place the same detector in the chain-reacting box. The thermal neutron detector, of course, is given an activation proportional to the density of thermal neutrons in the standard box or the reacting box, depending only on its location.*

In the reacting box, the densities measured by the two ideal detectors are independent of the position of the detectors in the box, while in the standard box the densities measured are functions of position. In order to get rid of the space dependence, we shall move the detectors around inside the standard box and compute the average activations which in turn reflect the average densities.

Now in the reacting box, where no source is introduced, Equation (5-5c) obtains. On the other hand, in the standard box

$$(5-35) \quad \bar{q} = \bar{n} v \sigma_c N_c$$

*If a different moderator from that in the reacting box were used in the standard box, the ideal resonance detector would measure something proportional to q but with differing proportionality constants in the two boxes. Resonance detectors (in fact) are sensitive to the neutron density at the energy of the resonance which leads to activation, and therefore activation is proportional to $q/N_s \sigma_s \phi_s$: i.e., to q divided by the slowing down power. Also, even though the thermal neutron detector measures n irrespective of the medium in which it is placed, a different moderator would, in general, have a different thermal absorption. Thus, although theoretically feasible, the measurement of f would be far less direct, without our particular standard box.

where \bar{q} and \bar{n} are the space averages. Let us define R by

$$(5-36) \quad R \equiv \frac{\bar{q}\bar{n}}{(q - \frac{\partial n}{\partial t}) \bar{n}}$$

From (5-5c) and (5-35) it follows that

$$(5-37) \quad R = \frac{\sigma_c N_c}{\sigma_c N_c + \sigma_f N_f} = 1 - f$$

Now, if we are fortunate or foresighted, we have adjusted the constants of the reacting box in such a way that $\frac{\partial n}{\partial t} = 0$. (In practice this adjustment, as we will see in a later section, is possible without changing either η or f .) When the adjustment has been made, (5-37) becomes

$$(5-37') \quad R = \frac{(\bar{q}/\bar{n})}{(q/n)} = 1 - f$$

As we have seen, $\frac{\bar{q}}{q} = \frac{\bar{A}_r}{A_r}$, where \bar{A}_r is the activation of the ideal resonance detector in the standard box averaged all over the volume of the box, and A_r is the activation of the same detector in the reacting box. If we also define \bar{A}_{th} and A_{th} in the analogous manner, we find the following formula for f , in terms of the activations which we measure with the detectors:

$$(5-38) \quad f = 1 - \frac{\bar{A}_r A_{th}}{A_r \bar{A}_{th}}$$

IV. THE PILE WITH THERMAL NEUTRONS

5-13 Homogeneous Thermal Neutron Pile; Critical Size

We shall now return to the homogeneous closed box with monokinetic neutrons. By rubbing off the ideal nuclear paint, we open up the box. Neutrons which formerly hit the ideal nuclear paint and bounced back into the box now leak out. The neutron density at the edge of the box falls down. The outflow from the box will decrease the number of neutrons which go the full distance around the cycle from fission to fission. We might, therefore, change the reproduction constant k from ηf to $\eta f \ell$ (or from $\eta f p$ to $\eta f p \ell$ when

resonance capture enters into the theoretical picture) where ℓ is the probability that the neutron has not leaked out in the course of the cycle. Since ℓ should be computed for all neutrons which start out from fission, no matter at what position in the box fission takes place, we expect that ℓ will be a function of the size and shape of the box.

Rather than modify our definition of k to include the leakage and thus involve the shape and size, we shall continue with the definition of k which involves only the intrinsic properties of the constituents of the pile. We shall bring in the leakage considerations explicitly.

In Section 3-4 it is shown that the flux of neutrons through a unit area, ϕ , is given by

$$(5-39) \quad \phi = -D \frac{\partial n}{\partial s}$$

where $\frac{\partial n}{\partial s}$ is the derivative along the normal to the surface in the direction of the flux. It is also shown that

$$(5-40) \quad D \approx \frac{v}{3\sigma_s N_s}$$

where isotropic scattering is assumed and $\sigma_s N_s \gg \sigma_c N_c + \sigma_f N_f$. Under these conditions, and assuming that there are no delayed neutrons, the equation of continuity

$$(5-41) \quad -\operatorname{div} \vec{\phi} + (\text{source density}) = \frac{\partial n}{\partial t}$$

becomes

$$(5-42) \quad \Delta n + \frac{\eta f - 1}{D\tau_0} n = \frac{\partial n}{D\partial t}$$

where

$$\Delta u \equiv \frac{\partial^2 u}{\partial x^2} + \frac{\partial^2 u}{\partial y^2} + \frac{\partial^2 u}{\partial z^2}$$

When a single type of delayed neutron is considered, (5-42) becomes

$$(5-42a) \quad \Delta n + \frac{\eta f(1 - \beta) - 1}{D\tau_0} + \frac{\lambda}{D\tau_d} = \frac{\partial n}{D\partial t}$$

Equation (5-42a) takes the place of Equation (5-5a), and Equation (5-5b) remains valid without change when we investigate time dependence of the neutron density in the pile.

In a stationary state the delayed neutrons are in equilibrium:

$$\frac{c}{D\tau_d} = \frac{\eta f \beta}{D\tau_o}$$

Therefore, to find the size of a pile which will just maintain a chain reaction, we need only investigate (5-42) with $\frac{\partial n}{\partial t} = 0$.

Calling

$$(5-43) \quad \mathcal{H}_o^2 \equiv \frac{\eta f - 1}{D\tau_o},$$

Equation (5-42) is seen to be

$$(5-44) \quad \Delta n + \mathcal{H}_o^2 n = 0$$

We shall call \mathcal{H}_o^2 and any generalizations of the combination $\frac{\eta f - 1}{D\tau_o}$ which we may define in the future, the negative Laplacian, and sometimes merely the "Laplacian." \mathcal{H}_o^2 is a property of the medium at a given point. It depends on the diffusion coefficient in the medium, the mean life against thermal capture, and the reproductive properties considered as if the medium were infinite. Although we shall relate it immediately to the critical dimensions through Equation (5-44), it has nothing to do in this definition with geometric considerations of critical size.

The mathematical treatment of Equation (5-44) is well known for many geometries. For example, with "cubic" symmetry the solution of (5-44) is given by

$$(5-45) \quad n = n_o \sin \gamma x \sin \gamma y \sin \gamma z, \quad 3\gamma^2 = \mathcal{H}_o^2$$

The length of the side of the cubic lattice cell is

$$(5-46) \quad a = \frac{\pi}{\gamma} = \frac{\pi \sqrt{3}}{\mathcal{H}_o} = \frac{\pi \sqrt{3D\tau_o}}{\sqrt{\eta f - 1}}$$

On the other hand, we know that the neutron density in our pile extrapolates to zero a very short distance beyond the surface. In Section 3-4, it is shown that at the edge of the pile the boundary condition on the neutron density is

$$(5-47) \quad -\frac{\partial \ln n}{\partial s} = \frac{1}{d} \approx \frac{\sigma_s N_s}{.71}$$

where $\frac{\partial \ln n}{\partial s}$ means the derivative in the direction of the outward normal to the surface of the pile. It follows that a pile which is cubic in shape will be in the stationary state ($\frac{\partial n}{\partial t} = 0$), as we have assumed, if the length of its sides is given by

$$(5-48) \quad a_c = a - 2d$$

Since we can re-define our pile to include the extrapolation region around its boundaries (this is the region between the boundary of the pile and a fictitious boundary, a distance d beyond the physical boundary of the pile), we shall always confine ourselves to determining a and its analogues: that is to say, to determining the extrapolated boundaries of the pile. Before building any piles, however, it is better to take into consideration the difference between a and a_c .

In this section we have picked as an example only a cubic pile. The results, however, are easily modified to take account of other geometric shapes. Formula (5-46) for the critical dimension always turns up in the form

$$(5-46a) \quad a = \frac{G}{\mathcal{K}_0} = \frac{G \sqrt{D\tau_0}}{\sqrt{k-1}}$$

where G depends only on the geometric shape and \mathcal{K}_0 involves neither shape nor size. For a cylinder, for example, the critical radius is given by

$$(5-46a') \quad a = \frac{\sqrt{\pi^2 \rho^2 + \mu^2}}{\mathcal{K}_0} \quad \text{where } \mu = 2.4048$$

is the first zero of the Bessel function J_0 and ρ , the ratio of radius to height, is a shape factor. Again for the critical radius of a sphere we obtain (see Section 3-5)

$$(5-46a'') \quad a = \frac{\pi}{\mathcal{K}_0}$$

As might be expected, the volume of the critical sphere is less than the volume of any other pile with the same nuclear properties and densities. For example, the ratio of the volume of the cube to the volume of the sphere when each is critical is given by

$$\frac{\text{Vol}_o}{\text{Vol}_s} = \frac{3^{5/2}}{4\pi} \approx 1.24$$

Unfortunately, spheres are not easily engineered. Later, however, we shall discover other methods of approaching the minimum amounts of the valuable materials used in the construction of piles. (Some remarks on the use of reflectors have already been made in Section 3-6.)

Aside from constructing spherical piles, in order to minimize the amount of material used we should clearly increase the density of the materials employed. In the formula which relates the critical size to the nuclear properties, formula (5-43), the combination $D\tau_o$ is the source of the dimension of length. Of course, $D\tau_o$ has the dimensions $[L^2]$. Let us call it L^2 . If we substitute for D and for τ_o the values given in (5-40) and in (5-7), we find that L^2 is

$$(5-49) \quad L^2 \equiv D\tau_o \approx \frac{1}{3\sigma_s N_s (\sigma_c N_c + \sigma_f N_f)}$$

If the proportions of the constituent materials remain the same, we see from formula (5-49) that L^3 is inversely proportional to the cube of the density. Since the volume is proportional to L^3 , the total mass is inversely proportional to the square of the density.

5-14 Temperature Dependence and Velocity Distribution

In Equation (5-49) v , the velocity of the neutrons, is implicit in the cross sections. Often σ_s is approximately constant, while both σ_c and σ_f vary as $1/v$. In any case, since the dimension of the pile is proportional to L , in order to find the real physical dimensions we must understand how to compute v . This sensitivity to v is a new phenomenon in our theory and is characteristic of the finite size. Crudely speaking, v is the velocity of neutrons in thermal equilibrium. This crude concept is good enough to establish a temperature dependence of the critical dimension. v rises with the square root of the temperature, and for $1/v$ absorbers but constant scat-

tering cross sections the critical dimension rises with the square root of v . The critical size is consequently proportional to the three-fourths power of the absolute temperature.

For a more exact determination of the velocity v of the thermal neutrons, we must take into account the fact that the neutrons have a velocity distribution which is given by the well-known formula due to Maxwell. The velocities, therefore, must be averaged over the Maxwell distribution. The question of what kind of average to perform may be settled by going back to Equation (5-42), in which the only place that the velocity appears is in the first term. (For a $1/v$ absorber, the second term, which contains $\nu\sigma_o, \nu\sigma_f$, is, of course, independent of the velocity of the neutrons.) Hence, the average value of v appropriate to our formula is

$$(5-50) \quad \bar{v} = \frac{\int v M(v) dv}{\int M(v) dv}$$

where $M(v)$ is the Maxwellian distribution function giving the number of neutrons per unit velocity interval.*

5-15 Time Behavior of the Homogeneous Thermal Neutron Pile - (No Delayed Neutrons)

If we build our pile, and pile means extrapolated pile, with dimensions bigger than a , the average leakage around the cycle will be decreased. Extra neutrons will remain inside on each cycle and the neutron density will rise; if we build it smaller, the neutron density will fall. The time behavior, as we saw earlier, is also a function of the reproduction properties of the materials in the pile. We must, therefore, be able to relate the size and the reproduction characteristics through their influence on the time behavior. Equations (5-44) and (5-46) form such a relation for the special case

*For general applicability, the above considerations assume that the distribution of neutrons after collisions in the thermal region is always Maxwellian. Otherwise, if high-velocity neutrons remain high and low-velocity neutrons remain low despite collisions, the preferential absorption of low-velocity neutrons makes a unique \bar{v} impossible in many situations. In tracing a given batch of neutrons as a function of time, higher velocity neutrons live longer. They also travel farther. Consequently, regions into which neutrons diffuse contain, on the average, higher velocity neutrons than the regions from which they diffuse.

of a stationary state. To obtain more general relations of this type for the time behavior of piles either smaller or larger than the so-called critical size, we must return to (5-42a).

As a first simple case, we omit delayed neutrons and employ only Equation (5-42). To solve Equation (5-42), let us assume that $n = ST$, where S is a function of the coordinates only; T is a function of time only. Equation (5-42) then separates, and we find that $T = T_0 e^{t/\tau}$ where τ is a constant and the equation for S is

$$(5-44a) \quad \Delta S + \mathcal{K}^2 S = 0, \quad \mathcal{K}^2 = \mathcal{K}_0^2 - \frac{1}{D\tau}$$

Here \mathcal{K}^2 is determined by the boundary conditions: that is, by the size and shape of the pile.

Equation (5-44a) has solutions which are formally the same as those of Equation (5-44). For a cubic pile, therefore, we may write

$$(5-45a) \quad n = n_0 \sin \gamma x \sin \gamma y \sin \gamma z e^{t/\tau}, \quad 3\gamma^2 = \mathcal{K}_0^2 - \frac{1}{D\tau}$$

The boundary condition that the neutron density vanishes on the extrapolated surfaces of the pile determines that for a pile of this type in which the length of the sides is r ,

$$(5-51) \quad \mathcal{K}^2 = 3 \left(\frac{\pi}{r} \right)^2 = \mathcal{K}_0^2 - \frac{1}{D\tau} \quad \text{or}$$

$$\frac{1}{\tau} = \frac{\eta f - 1 - 3(\pi/r)^2 D\tau_0}{\tau_0}$$

Equation (5-51) is merely the result of working out the details in Equation (5-44a). Either (5-44a) or (5-51) is the desired relation between the time behavior, the size, and the intrinsic properties of the medium. Equation (5-51), of course, merely applies to cubic piles, while Equation (5-44a) is the general result. Any size and shape may be introduced into (5-44a) by determining \mathcal{K}^2 from the boundary conditions.

Another general form of (5-44a), the analogue of the second equation (5-51), is

$$(5-44b) \quad \frac{1}{\tau} = \frac{\eta f - 1 - \mathcal{K}^2 L^2}{\tau_0}$$

This form is the generalization of Equations (5-6) and (5-19) for finite size. It is also, as is (5-44a), the generalization of (5-44) for arbitrary time behavior. As the pile period becomes infinite, we see that \mathcal{K}^2 becomes \mathcal{K}_0^2 and that the actual size approaches the critical size.

We can identify $\mathcal{K}^2 L^2$ quite generally with the number of thermal neutrons leaking out of the pile per thermal neutron captured inside. The leakage of thermal neutrons per unit time is $-D \int \nabla n \cdot d\vec{S}$ where the integral is to be taken all over the surface of the pile. On applying Gauss' lemma, we transform the leakage into the volume integral over the pile:

$$\frac{-D\tau_0}{\tau_0} \int \Delta n \, dV = L^2 \mathcal{K}^2 \int \frac{n}{\tau_0} \, dV.$$

Since

$$\int \frac{n}{\tau_0} \, dV$$

is the absorption rate for the whole pile, $\mathcal{K}^2 L^2$ is the leakage per absorption. From this result, the interpretation of (5-44b) is obvious.

For future use, we shall also compute the fraction of the neutrons entering the thermal energy region inside the pile which end their life there. It is the ratio of absorptions in the pile to absorptions plus leakage, and is therefore

$$(5-52) \quad \ell_{th} = \frac{1}{1 + \mathcal{K}^2 L^2}$$

This is the fraction of neutrons which escape thermal leakage. Written in terms of ℓ_{th} (5-44b) becomes

$$(5-44c) \quad \frac{1}{\tau} = \frac{\eta f \ell_{th} - 1}{\tau_0 \ell_{th}}$$

As expected, $\eta f \ell_{th} = 1$ for critical conditions.

We shall postpone further discussion of the relations connecting size and shape with intrinsic properties and time behavior until the theory of the finite pile has been developed to include slowing down effects. Then we shall develop still more general relations which also take account of the delayed neutrons.

V. THE PILE WITH NEUTRONS OF ALL ENERGIES

5-16 The Slowing Down of Neutrons in a Pile

In Section 5-9 we discussed the slowing down of neutrons. There we were interested in the length of time it took the neutrons to go from fission energies to the top of the $1/v$ region. In Section 5-10 the resonance capture was considered. The arguments and the results of both these sections remain valid, whether resonance capture is present or not, for those neutrons which would remain inside of a pile in the absence of resonance capture. Since the neutrons that leak out are of no further interest to us as far as the computation of critical size or time dependence is concerned, we can take over the results of Sections 5-9 and 5-10 bodily. There is, however, another very important aspect of the slowing down process which concerns us when we allow the neutrons in the pile to be released on fission with their real energies. Before they become thermal, these neutrons may have traveled quite a long distance, and the space distribution of the neutrons as they slow down is of primary concern in finding the critical size.

We may look at the travels of the neutrons in slowing down as a diffusion and merely add the mean square distance which the neutrons diffuse in slowing down to the mean square distance which they travel while in thermal equilibrium. This way of looking at things is a little bit crude, but should give us a first approximation to the real situation. Our first problem, then, is to calculate the mean square distance.

If we consider a point source of thermal neutrons located in an infinite region in which $\eta = 0$ but all the other properties are the same as in the pile, we find that

$$(5-53) \quad L^2 = \frac{\overline{r^2}}{6}$$

where $\overline{r^2}$ is the mean square distance away from the point source at which neutrons are absorbed. In fact, the equation for the diffusion of thermal neutrons may be written

$$(5-54) \quad \Delta n - \frac{n}{L^2} = 0$$

and (5-53) is easily verified from the point source solution of this equation. Since adding $\overline{r^2}/6$ consistently is as good as adding $\overline{r^2}$, we may confine our attention to L^2 and its analogue for the slowing down process.

Let us now look back on formula (5-49). If we multiply on the right side of Equation (5-49), both numerator and denominator by $\sigma_s N_s$, we see that we can write for L^2

$$(5-49') \quad L^2 = \frac{N}{3(\sigma_s N_s)^2}$$

where N is the number of collisions before capture. (This is a familiar result in other fields of diffusion theory: e.g., Brownian motion.) Similarly, we may assume that one-sixth the mean square distance in slowing down is given by

$$(5-55') \quad \frac{\overline{r_f^2}}{6} = \frac{\ln(E_{fiss}/E_{thermal})}{3(\sigma_s N_s)^2 \xi}$$

where we have computed the number of collisions by dividing logarithmic energy loss into the total logarithmic energy span to be covered and have assumed that the scattering cross section is not a function of energy. This analogue of L^2 for the slowing down process we call L_f^2 . L_f^2 is sometimes known as the Fermi age. The reasons for the choice of the name "age" will soon become apparent; however, we shall usually call L_f^2 the fast migration area in analogy with L^2 , the thermal diffusion area. A more rigorous calculation considering the energy dependence of σ_s gives

$$(5-55) \quad L_f^2 = \int_{E_{th}}^{E_{fiss}} \frac{dE}{3(\sigma_s N_s)^2 \xi E}$$

Let us define M^2 , which we shall call the total migration area, as the sum of L^2 and L_f^2 . If we substitute M^2 for L^2 in (5-42) or in (5-43), we essentially substitute M for L in all the formulae for the critical dimensions, acting as if a single diffusion took place. This procedure cannot be completely accurate, since, in general, the spatial distribution of neutrons captured at thermal energy around a point source of fast neutrons is not of the same form as that around a thermal neutron source. In order to refine the treatment, we need to know more about the space distribution of q , the slowing down density around a point source.

Such special distributions can be determined experimentally for various sources, including fission sources. The experiments can be performed by using the ideal resonance detector in a large block of the scattering material, and the fission source can be created by running an intense beam of thermal neutrons through the large block, in the center of which a small amount of fissionable isotope has been placed. In general, the shape of the special distribution near the source is found to be roughly Gaussian. The details depend both on the source and on the slowing down material. Hydrogenous materials are the greatest exception to our qualitative statement. The region which can be considered to be Gaussian is very small, and it might be said that an exponential would give a better fit to the data. Typical shapes for the slowing down distribution are shown in Figure 5-2 on the following page.

If we integrate the slowing down distribution over all space, we must find all neutrons except those which disappear in resonance capture. We shall now define q to be the slowing down density that would be present if we forgot about resonance capture. The real source of thermal neutrons is then pq . With this definition, a unit source of neutrons will lead to a normalized distribution

$$(5-56) \quad 1 = \int q(x,y,z) dx dy dz$$

In the case of a Gaussian, the normalization condition gives us

$$(5-57) \quad q = \frac{e^{-\frac{x^2 + y^2 + z^2}{4 L_f^2}}}{(4\pi)^{3/2} L_f^3} = \frac{e^{-\left(\frac{r}{2 L_f}\right)^2}}{(2\sqrt{\pi} L_f)^3}$$

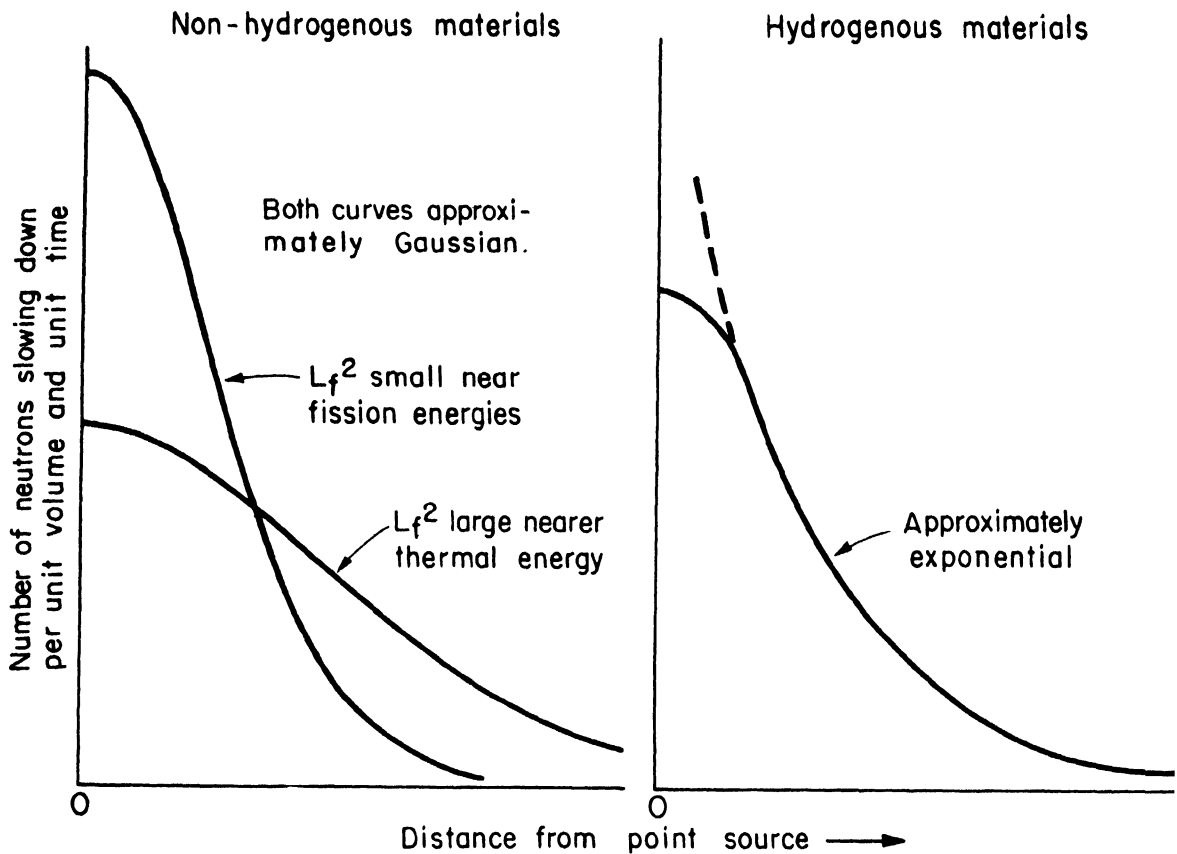


Figure 5-2. Typical Curves of the Spatial Distribution of Neutrons Slowing Down from a Point Source.

This is the standard form for the slowing down distribution which is to be employed here to investigate the influence of slowing down more accurately, but it should be remembered that this form is not universally applicable. In graphite, for example, the slowing down distribution from a Ra-Be source is reasonably well represented by a superposition of three such standard distributions, each with a different value for L_f^2 . (See Table 5-1.)

There are theoretical reasons for expecting the Gaussian form in the slowing down distribution and also for expecting the exceptional slowing down distribution obtained in hydrogenous materials. If the number of collisions which the neutron undergoes in slowing down is large, and the free path is always small compared with L_f , it follows from the theory of random flights that the slowing down distribution must be Gaussian. However, we would only expect a single Gaussian to apply to those neutrons which started out at exactly the same energy and underwent exactly the same number of collisions.

If the number of collisions is large, the correlation between energy and number of collisions is very good; but most sources do not emit monokinetic neutrons. Consequently, it is not surprising to find that a superposition of Gaussians is a better representation than a single Gaussian, when the spectrum of emitted neutrons is not monokinetic.

An essentially exponential behavior must, of course, be expected far from any source. The neutrons remaining fast at large distances from a source have either made an abnormally large number of forward scattering collisions or have traveled for long distances without collision. The fraction of neutrons which have made no collisions will only decrease exponentially

TABLE 5-1*
ANALYSIS OF RADIUM-BERYLLIUM SOURCE

L_f^2 in Graphite		Per cent Associated Source Strength
<u>Indium Resonance</u>	<u>Iodine Resonance</u>	
130 cm ²	54	15.0
340	268	69.3
815	736	15.7

rather than in Gaussian fashion. Exponential behavior must, therefore, be observable at large distances. Nevertheless, for slowing down in nonhydrogenous materials, a single Gaussian adjusted to give the correct value of $r^2/6$ is often an excellent approximation to the actual spatial distribution. The spread in energy in the neutrons emitted from the source is either not too great or accidentally compensated, and the number of collisions is sufficiently large that the exponential tail is of little importance. For example, for a single Gaussian to represent the slowing down distribution from a fission source in graphite of density 1.6 gms per cm³, Fermi gives $L_f \approx 17.3$ cm.**

*Data taken from E. Fermi: Neutron Physics, February 5, 1946.

**E. Fermi, Science 105, No. 2715, January 10, 1947.

In hydrogen, a neutron can lose essentially all of its energy in a single collision. Also, the cross section of hydrogen rises steeply as the energy of the neutron falls. Consequently, the largest fraction of the distance traveled by neutrons in hydrogenous media is likely to be traveled in the first or the first and second flights. The restrictions under which the Gaussian distribution for the slowing down is to be expected are all violated. On the other hand, the fact that only the first couple of collisions made by the neutron have much importance in determining its final position, implies that some sort of exponential distribution will obtain at any considerable distance from the source.

If we look at L_f as a function of the lower limit of the integral in (5-55), (5-57) gives the slowing down distribution as a function of both space and energy around a point source. We also recognize that (5-57) is a point source solution of the differential equation

$$(5-58) \quad \Delta q = \frac{\partial q}{\partial (L_f^2)}$$

This differential equation, which is derivable either from the theory of random flights or by a simple argument which we will give in the next paragraph, is formally identical with the equation of heat conduction. L_f^2 in (5-58) plays the same role that time does in the heat equation. For this reason L_f^2 has been called by Fermi the age, and we may occasionally call it the Fermi age.

To derive Equation (5-58), we consider the equation of continuity in four dimensions, x, y, z , and $\ln E$. The density of neutrons per unit volume in this space is called n . The net number of neutrons entering a volume element by translation in space x, y, z , is given by $D\Delta n dx dy dz d\ln E$ and the net number entering the volume by translation in log energy is given by

$$\frac{\partial (nv\zeta\sigma_s N_s)}{\partial \ln E} dx dy dz d\ln E$$

Consequently, the equation of continuity reads

$$(5-59) \quad D\Delta n + \frac{\partial (nv\zeta\sigma_s N_s)}{\partial \ln E} = \frac{\partial n}{\partial t}$$

On identifying $nv\xi\sigma_s N_s$ with q , we can rewrite (5-59)

$$(5-59a) \quad \frac{D\Delta q}{v\xi\sigma_s N_s} + \frac{\partial q}{\partial \ln E} = \frac{\partial q}{v\xi\sigma_s N_s \partial t}$$

from which (5-58) follows when $\frac{\partial q}{\partial t} = 0$ by using the differential of (5-55).

In determining the characteristic size of a pile, we shall usually employ Equation (5-58) or its solution (5-57) to give the description of the slowing down process.

In applying this slowing down description, some care must be exercised. If we obtain L_f^2 by definition from (5-59a), we have

$$L_f^2 = \int \frac{D \, dE}{v\xi\sigma_s N_s E}$$

In obtaining (5-55) then, $\sigma_s N_s$ enters once in the slowing down power $\xi\sigma_s N_s$ and once from $1/D = 3\sigma_s N_s/v$; consequently, we should really have a transport cross section in place of one of these scattering cross sections. Since high energies are involved in L_f^2 , it is particularly clear that the transport cross section will have to be used, for at high energies anisotropic (forward) scattering is theoretically expected and experimentally found not only because the center of gravity system of coordinates moves in the experimental system but also because higher angular momenta participate in the scattering process. Also, at sufficiently high energies, where the scattering is anisotropic in the center of gravity system, our derivation of ξ must also be improved, and in the more refined calculation ξ will become a function of energy.

Rather than develop the theory to include the needed refinements at high energies, we shall use it as it stands under the assumption that L_f^2 will be filled in from experimental data. The experimental data will then not only give a rigorous treatment to the high energy refinements but will also show us when necessary that deviations from Gaussian shape require even more radical revisions in our description.

By modifying Equation (5-59) to include absorption (adding $\sigma_a N_a nv$ to the right-hand side), we can derive a version of (5-58) which includes a treatment of the resonance escape probability, and from which we may com-

pute not q but pq . This derivation implies a continuous picture, that is, a picture of continuous collisions; therefore, we expect it to give a somewhat cruder approximation for p than we obtained in Section 5-10. The formula obtained for p by modifying (5-59) is

$$(5-34') \quad p = e^{-\int \frac{\sigma_r N_r}{\sigma_s N_s} \frac{dE}{\xi E}}$$

This formula is very similar to (5-34). The only difference is in the denominator of the integral. In (5-34) the integral is

$$\int \frac{\sigma_r N_r}{\sigma_r N_r + \sigma_s N_s} \frac{dE}{\xi E}$$

It is not surprising that a completely different treatment gives a different result. We have already discussed the limitations of formula (5-34) in Section 5-10. Since the method of derivation in neither case is rigorous, it may be worth discussing (5-34').

One of the tests which we applied to (5-34) is to allow the cross section for resonance capture to become infinite over such a wide range of energies that the resonance escape probability should fall to zero. Unfortunately, it does not. Here, if we apply the same test to (5-34'), the resonance escape probability will fall to zero. However, we come upon a new difficulty. The resonance escape probability not only falls to zero when it should, but it also falls to zero when it should not. Indeed, it will fall to zero if the resonance absorption cross section becomes infinite at any energy. Therefore, for narrow resonances of great height, formula (5-34') is not as good as formula (5-34). Both formulae reduce to the same thing and to the correct limit when the resonance absorption ($\sigma_r N_r$) is small compared with the scattering ($\sigma_s N_s$).

It is clear why this continuous collision treatment fails for high, narrow resonances. Each collision produces only an infinitesimal change in neutron energy. Each neutron will therefore make a collision in the high resonance and will consequently be lost, contrary to the actual fact. Since we may be interested in high resonances but certainly not in those for which p is near zero, the error in the continuous treatment is likely to be serious, while (5-34) is usually a reasonable approximation. We shall therefore

adopt the procedure of combining the resonance escape probability as calculated in Section 5-10 with the slowing down description on the completely continuous picture rather than carrying the continuous picture through to the extent of including resonance capture.

5-17 The Critical Size of a Pile

The problem of finding the critical size of the chain-reacting unit has now been reduced to the problem of finding the simultaneous solution of two differential equations. These two equations are Equation (5-58) for the slowing down of neutrons and the thermal diffusion equation given below:

$$(5-60) \quad D \Delta n + p q - \frac{n}{\tau_0} = 0$$

The two equations are interconnected, that is to say, the slowing down density enters the thermal diffusion equation and the thermal neutron density is connected with the initial condition for the slowing down equation by the following relation:

$$(5-61) \quad \frac{n}{\tau_0} \eta f = q \text{ when } L_f^2 = 0$$

In attempting to solve these equations simultaneously, we pay no attention to the delayed neutrons; we need to pay no attention to them if we are only looking for the critical size. In this case the rates at which neutrons feed in and out of the latent type are always exactly equal. Of course, when the pile is not in a stationary state (that is, when it is not exactly of critical dimension), it is necessary to modify the equations in order to bring in the effect of the delayed neutrons on the time behavior. For the moment, we shall only handle the case of exact criticality.

We shall attempt to find a solution in the form

$$q = S(x, y, z) H(L_f^2)$$

$$n = S(x, y, z)$$

where

$$(5-44) \quad \Delta S + \kappa_0^2 S = 0$$

In this case, Equation (5-58) yields us

$$(5-58') \quad -\mathcal{H}_0^2 = \frac{\partial H}{\partial (L_f^2)}$$

which has the solution

$$H = H_0 e^{-\mathcal{H}_0^2 L_f^2}$$

Upon substituting into (5-60) and (5-61), we obtain

$$(5-60') \quad D\mathcal{H}_0^2 + p H_0 e^{-\mathcal{H}_0^2 L_f^2} - \frac{1}{\tau_0} = 0$$

and

$$(5-61') \quad \frac{\eta f}{\tau_0} = H_0$$

On combining these two relations, our final result is

$$(5-62) \quad (1 + \mathcal{H}_0^2 L^2) = k e^{-\mathcal{H}_0^2 L_f^2}$$

This equation is often called the characteristic equation determining the critical size. It is so called because it determines \mathcal{H}_0^2 , and at the same time Equation (5-44) relates \mathcal{H}_0^2 to the actual critical dimension.

When

$$\mathcal{H}_0^2 (L^2 + L_f^2) \ll 1$$

the characteristic equation can be simplified to read

$$k = (1 + \mathcal{H}_0^2 L^2)(1 + \mathcal{H}_0^2 L_f^2 + \text{-----})$$

and it then follows that \mathcal{H}_0^2 is given by

$$(5-63) \quad \mathcal{H}_0^2 \approx \frac{k - 1}{L^2 + L_f^2} = \frac{k - 1}{M^2}$$

This is the result for \mathcal{R}_0^2 that was obtained by adding together the mean squares in our very crude treatment in the last section. We now see that this result is obtained here whenever $|k-1| \ll 1$. The details which we promised to consider, namely, the details of the Gaussian shape, have all been put into the new characteristic equation, (5-62).

Suppose now that instead of the Gaussian we use as a description for the slowing down a diffusion, not dissimilar from the thermal diffusion. Such a diffusion will give a certain type of exponential as a point source solution and may then be appropriate for hydrogenous substances. In order to write down the equations, we assume that there is not only a thermal density n but also a fictitious density for fast neutrons which we symbolize by n_f . We also invent a mean life for fast neutrons which we symbolize τ_f and a diffusion coefficient D_f . Let us proceed without defining τ_f and D_f too closely. After we have proceeded a short way, it will become clear that we do not need to know the exact values for D_f and τ_f but only for the product $D_f \tau_f$, which must be L_f^2 . The two diffusion equations which we use are

$$D_f \Delta n_f + \frac{k}{p} \left(n / \tau_o \right) - \frac{n_f}{\tau_f} = 0$$

(5-64)

$$D \Delta n + p \left(n_f / \tau_f \right) - n / \tau_o = 0$$

The source density of fast neutrons is determined by the rate of absorption of thermal neutrons in the same volume, and the source of thermal neutrons is likewise related to the rate of absorption in the fast group. Since the major resonance effects will be found in the epithermal region, we assume all the resonance absorption takes place in passing from the fast to the thermal neutron group. Consequently, the thermal source density is $p n_f / \tau_f$ and the fast source must be $(k/p)(n / \tau_o)$.

Using the same S as before, we try to find a solution of (5-64) in the form $n_f = A_f S$ $n = S$.

On substituting in (5-64), we obtain the algebraic equations

$$(\mathcal{R}_0^2 D_f + \frac{1}{\tau_f}) A_f = \frac{k}{p} \frac{1}{\tau_o}$$

(5-64')

$$(\mathcal{R}_0^2 D + \frac{1}{\tau_o}) = (p / \tau_f) A_f$$

If these two equations are multiplied together, we obtain another characteristic equation for the determination of the critical size:

$$(5-65) \quad (1 + \alpha_o^2 L^2)(1 + \alpha_o^2 L_f^2) = k$$

Here the symmetry between fast and thermal neutrons is obvious and we can identify

$$\ell_f = \frac{1}{1 + \alpha_o^2 L_f^2}$$

as the probability that a neutron shall remain in the pile during the slowing down process. (We recall that

$$\ell_{th} = \frac{1}{1 + \alpha_o^2 L^2}$$

See Section 5-15, Equation (5-52).)

Again we should note that under the same conditions as in our last case we are able to obtain the simple form

$$(5-63) \quad \alpha_o^2 \approx \frac{k - 1}{M^2}$$

Of course, it is no accident that this simple form always arises. Let us consider a general description of the slowing down, one which may be determined purely empirically. For this purpose we define $K(\rho)$, the slowing down density from a point source at a distance ρ . We assume that $K(\rho)$ has been normalized so that it will give over all space just one neutron per unit time. The total number of neutrons which are slowing down is given by Q where Q is the source strength in neutrons per unit time. We are now in a position to modify the equation for thermal diffusion of neutrons in such a way that it becomes the integral equation

$$(5-66) \quad D\Delta n + \frac{k}{\tau_o} \int n(x', y', z') K \left(\sqrt{(x-x')^2 + (y-y')^2 + (z-z')^2} \right) dx dy dz$$

$$- \frac{n}{\tau_o} = 0$$

The integral term in this equation takes account of the source density of thermal neutrons. It already contains the interconnection between the absorption and the source strength for fast neutrons.

In order to solve the integral equation, we make an expansion for $n(x', y', z')$ as it appears under the integral

$$n(x', y', z') = n(x, y, z) + x \frac{\partial n}{\partial x} + y \frac{\partial n}{\partial y} + z \frac{\partial n}{\partial z} + \frac{x^2}{2} \frac{\partial^2 n}{\partial x^2} + xy \frac{\partial^2 n}{\partial x \partial y} + \text{-----}$$

On integrating over this expansion term by term and assuming at the same time that the space dependence of the neutron density is given by S , we obtain a generalized expression for the characteristic equation in the form

$$(5-67) \quad (1 + \mathcal{L}_0^2 L^2) = k(1 - \mathcal{L}_0^2 L_f^2 + \text{-----})$$

where

$$L_f^2 = \overline{\rho^2}/6 \quad \text{and} \quad \overline{\rho^2} = 4\pi \int \zeta^2 K(\zeta) \zeta^2 d\zeta$$

It is clear that as k approaches one, the neutron density flattens out. Only the first few terms of the Taylor expansion are necessary because the first few terms give a sufficiently good approximation for $n(x', y', z')$ at all values of $K(\sqrt{\quad})$, which are substantially different from zero. Consequently, we again find, quite generally this time, that \mathcal{L}_0^2 is given by

$$(5-63) \quad \mathcal{L}_0^2 \approx \frac{k-1}{M^2}$$

as long as $|k-1|$ is small.

Since there was a good deal of difficulty and question about whether piles would run at all with natural uranium, $k-1$ cannot be terribly big; this approximation is therefore valuable.* As k becomes larger, it is necessary

*According to the Smyth report, Appendix 4, with a lattice of uranium rods in graphite, $k = 1.07$ may be achieved. The lattice is resorted to in order to increase the reproduction constant above that obtainable in a homogeneous mixture. Some discussion of the advantages of lattices will be given later.

to improve the approximation for \mathcal{K}_0^2 by solving the appropriate characteristic equation in a more rigorous fashion, for example, by trial and error or by expansion in power series in the variable $k-1$.

Since our formulations for the problem of critical size differ essentially only in the description applied to the slowing down process, we may be able to summarize them in a simple form by writing

$$(5-68) \quad 1 + \mathcal{K}_0^2 L^2 = k \ell_f$$

We may call this equation the general characteristic equation, just as the one before, and in this equation we are permitted to calculate ℓ_f by any method we choose. ℓ_f always means the fraction of neutrons which stay in the pile during the slowing down process, calculated as if there were no resonance capture. We can abbreviate (5-68) as

$$(5-68a) \quad k \ell_f \ell_{th} = 1$$

where ℓ_{th} may also be calculated by any method. (The result

$$\ell_{th} = \frac{1}{1 + \mathcal{K}_0^2 L^2}$$

will be obtained as long as a thermal diffusion description is used.)

When we know \mathcal{K}_0^2 from any of the equations summarized in (5-68), we can find the critical size from the interconnections (5-46, 5-46a, etc.) given in Section 5-13. Although the relations between a , k , and L must now be considered as special cases, the equations given there between a and \mathcal{K}_0 still obtain.

Of the equations for \mathcal{K}_0^2 which we have developed, Equation (5-62) is usually the most reliable. It is not always possible, however, to apply the analysis employed in deriving it in the simplest fashion. For example, Equation (5-65) and the associated treatment which was given as a possible approximation for finding \mathcal{K}_0^2 for hydrogenous systems is sometimes applied to nonhydrogenous systems, because of its greater simplicity. This simplicity is not important if we are considering a single homogeneous region as we have been doing so far, but becomes significant in more complicated problems

in which the pile considered is composite (i.e., contains regions of differing characteristics). As we shall see later, there are then rather few problems which can be solved in a finite time by continuing to use the continuous collision slowing down treatment in composite systems; many that can be solved by extending the method of interconnected diffusion equations.

5-18 Comments on L^2 , f , and η for the Computation of Pile Size

It is important to note that the L^2 in a chain-reacting system is different from the L^2 measured by observing the neutron distribution in pure moderating (slowing down) material. (The measurement of L^2 in moderating blocks is discussed in a later section.) For example, if L_o^2 is the diffusion length in the moderating material

$$L_o^2 = \frac{1}{3\sigma_{cm}N_m\sigma_{sm}N_m}$$

where N_m is the density of moderator nuclei; σ_{cm} and σ_{sm} , their capture and scattering cross section. In the pile, on the other hand,

$$L^2 = \frac{1}{3(\sigma_{cm}N_m + \sigma_{fm}N_f + \sigma_{co}N_o)(\sigma_{sm}N_m + \sigma_{sf}N_f + \sigma_{so}N_o)}$$

where σ_{co} , σ_{so} , and N_o refer to any substances other than fissionable materials which may be introduced in building the pile. If the scattering per unit volume remains the same in the pile as in pure moderator

$$(5-69) \quad L^2 = L_o^2 (1 - f_u)$$

where f_u is the thermal utilization in everything but moderator: i.e., the fraction of all thermal neutron captures which take place in any nuclei but those for which L_o^2 is measured. It is

$$(5-3a) \quad f_u = \frac{\sigma_{fm}N_f + \sigma_{co}N_o}{\sigma_{fm}N_f + \sigma_{co}N_o + \sigma_{cm}N_m}$$

When only fissionable nuclei distinguish the pile from the moderator, $f_u = f$. When other new nuclei are also present in the pile, f_u can be measured by the experiment described earlier for measuring f . In order to mea-

sure f rather than f_u , it is necessary to poison the standard box with the same other new nuclei which enter the pile. If these new nuclei are essentially tied up with the fissionable nuclei as U-238 with U-235, the poisoning may be extremely difficult. Instead of measuring f , then, we prefer to measure f_u .

With formula (5-69), L^2 is easily found from L_o^2 (see Table 5-2 for typical values of L_o^2). If we measure f_u , however, in order to find k we

must either assume that we know $\frac{\sigma_f N_f}{\sigma_f N_f + \sigma_{oo} N_o}$ or measure the number of neu-

trons released per capture in all but the moderator materials. The product

$\frac{\sigma_f N_f \eta}{\sigma_f N_f + \sigma_{oo} N_o}$ is the number of neutrons released per nonmoderator capture.

Whether found experimentally or computed from fundamental data, we shall call it η_u . Whenever convenient, we may now compute k as

$$(5-32a) \quad k = \eta_u f_u p$$

TABLE 5-2*
TYPICAL THERMAL DIFFUSION LENGTHS

Moderator	Density (gms/cm ³)	L_o (cm)
H ₂ O	1.0	2.85
D ₂ O	1.1	> 100
Be	1.8	31
C	1.62	50.2

5-19 Temperature Considerations

In Section 5-14 we found that it is necessary to consider the energy spectrum of the thermal neutrons and the energy variation of the cross sections in order to find an appropriate value for L^2 . We also established a temperature dependence for L^2 based on the variation of the mean thermal neutron velocity assuming thermal equilibrium. In Section 5-14 thermal

*Data taken from E. Fermi: Neutron Physics, February 5, 1946.

equilibrium was closely enforced because, in the model employed there, the neutrons emitted in fission are emitted in the equilibrium distribution.

When the slowing down of neutrons from true fission energies is included in our picture of the pile, the neutrons approach thermal equilibrium from higher energies by making collisions with the nuclei of the moderating materials in the pile. The situation is more difficult to analyze. If the neutron capture cross sections were infinitesimal, thermal equilibrium would be essentially complete; but as the neutrons in practical piles make only a limited number of collisions on the average, the "thermal" neutron spectrum is shifted to a higher apparent temperature than that of the pile materials. (The Maxwell velocity distribution will be approximately maintained if the capture cross sections are not too great.) Such apparent thermal neutron temperature shifts have been observed. Consequently, we believe that the L^2 appropriate to the actual operation of a chain reaction is somewhat larger than is computed on the basis of strict thermal equilibrium.

As the neutrons slowing down in a pile penetrate into the energy region below one volt, the nuclei in the pile cease to act as individuals. The chemical binding forces freeze them together with a strength comparable to the neutron energy, and the mechanisms of neutron energy loss become complex. We may expect that the slowing down power of the moderating materials in the pile will fall off, and that the apparent temperature shift will be enhanced due to the decreased rate of slowing down in the epithermal energy region. In any case, except for a gaseous pile, an accurate estimate of the temperature shift will involve a fairly complete knowledge of the characteristics of either solids or liquids and must depend on relatively complicated calculations.

The ordinary temperature effect on L^2 , of course, is still present. Since L_f^2 has a much weaker and probably opposite temperature dependence, the temperature effect on the migration area, M^2 , is not the same, and the temperature effect on the characteristic pile area, $1/\kappa_0^2$, is even less closely related to the temperature effect on L^2 . To estimate the effect of a change in operating temperature on the critical size of a pile, we should consider the effects on the density of the materials, on the mean velocity of thermal neutrons, and on f (or f_u and η_u) if the cross sections are not all $1/v$. We should then compute L^2 , L_f^2 , and k ; and finally obtain κ_0^2 from the appropriate characteristic equation.

5-20 The Time Behavior of Noncritical Piles

Any one of the three treatments of Section 5-17 may be extended to include the time behavior when the pile is not critical. For the sake of simplicity, we shall only detail a single one of the three type treatments. We shall take for our example the Gaussian case.

In order to treat the Gaussian case, it is necessary for us to return to Section 5-16 and to extend a derivation of Equation (5-58) to include an actual time variation as well as an energy and a space variation. We did actually include such a time variation in our derivation. However, we threw it away at the last minute. When we keep it, we may write

$$(5-58a) \quad \Delta q = \frac{\partial q}{\partial (L_f)^2} + \frac{\partial q}{D \partial t}$$

In conformity with the treatment given in Sections 5-17 and 5-14, we shall attempt to solve this equation by the separation

$$(5-70) \quad q = TSH, \Delta S + \mathcal{X}^2 S = 0$$

where, as in (5-44a), \mathcal{X}^2 is geometrically determined through application of the boundary conditions. As a result of our previous experience, we may immediately write

$$(5-71) \quad T = T_0 e^{t/\tau}$$

In these circumstances, we obtain for H the following equation

$$\left[\mathcal{X}^2 + \frac{1}{D\tau} \right] H = \frac{\partial H}{\partial (L_f)^2}$$

and

$$(5-58a') \quad H = H_0 e^{-\mathcal{X}^2 L_f^2} e^{-\bar{\theta}/\tau}$$

where $\bar{\theta}$ is a function of L_f^2 .

Employing Equations (5-69) and (5-70) to determine the form of the left-hand side, the time dependent thermal diffusion equation

$$(5-60a) \quad D\Delta\eta - \frac{n}{t_0} + pq = \frac{\partial n}{\partial t}$$

can be written

$$(5-60a') \quad (1 + \kappa^2 L^2 + \frac{\tau_0}{\tau}) = \frac{qp}{n} \tau_0$$

The equation for the interconnection of the initial condition of the slowing down density with the thermal density must now include the delayed neutrons; that is to say, we must also include the rate at which latent neutrons of various types become free. When this is done, the interconnection equation reads

$$(5-61a) \quad \frac{k}{p} \frac{(1 - \beta)n}{\tau_0} + \sum \frac{c_i}{\tau_i} = q \quad \text{when } L_f^2 = 0$$

The subscript i refers to the various latent neutron types.

Since the latent neutron densities have entered our last equation, in order to have a complete set of equations, it is necessary to write down the connection between the latent neutron densities and the thermal neutron density. Assuming that the nuclei from which delayed neutrons originate do not move about, these relations are (cf. Equation 5-5b'):

$$(5-72) \quad c_i \left(\frac{1}{\tau_i} + \frac{1}{\tau} \right) = \frac{k}{p} \frac{n c_i}{\tau_0}$$

Upon combining all these equations, we can eliminate all the densities and obtain a new characteristic equation which is

$$(5-13c) \quad \left(1 + \kappa^2 L^2 + \frac{\tau_0}{\tau} \right) = k \left[1 - \beta + \sum \frac{\beta_i \tau}{\tau_i + \tau} \right] e^{-\kappa^2 L_f^2} e^{-\theta/\tau}$$

In this equation, if we interpret the 1 on the left as one thermal neutron absorption, $\kappa^2 L^2$ is the associated thermal neutron leakage (see Section 5-14), and τ_0/τ is the rate of rise of the thermal neutron density in

units of the thermal neutron absorption rate. The left side must, therefore, equal the rate of production of thermal neutrons in the same units.

On the right-hand side we obtain the production of thermal neutrons by adding together those which were produced as prompt neutrons and those which were produced on fission as latent neutrons.

The term $k(1 - \beta) e^{-\lambda_f^2 L_f^2} e^{-\bar{\theta}/\tau}$ is the rate in units of the thermal neutron absorption rate at which prompt neutrons become thermal. In this term, $\frac{k}{p}(1 - \beta)$ is the prompt neutron production, and $p e^{-\lambda_f^2 L_f^2} = p l f$ is the fraction which arrives at thermal energies inside the pile. The factor $e^{-\bar{\theta}/\tau}$ occurs because the prompt neutrons now becoming thermal were produced as the result of absorptions at a time $\bar{\theta}$ ago when the absorption rate was lower or higher by this factor. The other terms on the right side are all of the form

$$(5-73) \quad \frac{k\beta_1\tau}{\tau_1 + \tau} e^{-\lambda_f^2 L_f^2} e^{-\bar{\theta}/\tau}$$

Each such term represents the rate (per thermal neutron capture) at which neutrons once delayed as latent neutrons of type i now reach thermal energies. These neutrons turned from latent to free neutrons a time $\bar{\theta}$ ago, but were produced over a range of times still further in the past. The rate of production per present thermal neutron capture was $k\beta_1 e^{-\frac{t + \bar{\theta}}{\tau}}$ for a time $t + \bar{\theta}$ ago, and the rate of transformation to free neutrons of the latent neutrons produced at $t + \bar{\theta}$ was

$$k\beta_1 e^{-\frac{t + \bar{\theta}}{\tau}} \left(\frac{e^{-t/\tau_1}}{\tau_1} \right) \text{ at a time } \bar{\theta} \text{ ago.}$$

Upon integrating over t from zero to infinity -- all the relevant past time -- we obtain (5-73).

With a little algebra, Equation (5-13c) can be transformed to

$$(5-13d) \quad k l_f l_{th} - 1 = k l_f l_{th} \sum \frac{\beta_1 \tau_1}{\tau_1 + \tau} + \frac{\tau_0 l_{th}}{\tau} + (e^{\bar{\theta}/\tau} - 1) + (e^{\bar{\theta}/\tau} - 1) \frac{\tau_0}{\tau} l_{th}$$

Similarly, from the model in which two coupled diffusion equations are employed

$$(5-13e) \quad k \ell_f \ell_{th} - 1 = k \ell_f \ell_{th} \sum \frac{\beta_i \tau_i}{\tau_i + \tau} + \frac{\tau_o \ell_{th} + \tau_f \ell_f}{\tau} + \frac{\tau_o \tau_f \ell_f \ell_{th}}{\tau^2}$$

as the symmetry of the model would lead us to expect. For this purpose, τ_f must be considered as a real time and may be identified with $\bar{\theta}$. When $\tau \gg \frac{\tau_f}{\theta}$, $e^{\bar{\theta}/\tau} - 1 = \bar{\theta}/\tau$, showing the close relationship of the two results.

In Equation (5-13d) the exponential dependence on $\bar{\theta}$ (and also the exponential leakage factor, ℓ_f) arises from the strict correlation of time and energy in the continuous slowing down theory as contrasted with the exponential frequency distribution in the coupled diffusion model. In Equation (5-13e) the appearance of ℓ_f in the combination $\tau_f \ell_f$ on the coupled diffusion model is associated with the decreasing probability as a function of time that a neutron which remains in the fast group shall become thermal inside the pile. In the continuous slowing down picture, Equation (5-13d), where there is only one lifetime, $\bar{\theta}$, for slowing down, this factor is absent.

In any case, as $\tau \rightarrow \infty$ we find

$$(5-68a) \quad k \ell_f \ell_{th} = 1$$

determining the critical size. Also, as long as $\bar{\theta} \ll \tau_o \ell_{th}$ and τ , and thermal neutrons are handled by a diffusion model

$$(5-13f) \quad k_{eff} - 1 = k_{eff} \sum \frac{\beta_i \tau_i}{\tau_i + \tau} + \frac{\tau_o \ell_{th}}{\tau}$$

where $k_{eff} = k \ell_f \ell_{th}$.

In defining k_{eff} , the effective reproduction constant, as $k \ell_f \ell_{th}$, we have finally made the modification of the definition of the reproduction constant to include leakage effects which is mentioned as a possibility at the beginning of Section 5-13. Since we know how to relate the actual size and shape of a pile to k_{eff} , at this point the characteristic equation for critical size, $k_{eff} = 1$, and Equation (5-13f) are abbreviations rather than definitional identities.

Equation (5-13f) is the generalization of (5-13a) and (5-44c). Since for long periods, $k_{\text{eff}} \approx 1$ and $k_{\text{eff}} - 1 \approx \frac{\sum \beta_i \tau_i + \tau_0 \ell_{\text{th}}}{\tau} \approx \frac{C_1}{\tau}$, $1/\tau$ is a good measure of $k_{\text{eff}} - 1$. Since $1/\tau$ is an inverse time, (5-13f) is often called the inhour equation. $k_{\text{eff}} - 1$ is sometimes called k_e , the excess reproduction constant, and in this notation, according to Nordheim

$$(5-13g) \quad k_e/k_{\text{eff}} = C_1 (\text{Inhour}) = C_1 \left[\frac{54}{\tau} + \frac{33}{\tau + 0.7} + \frac{1139}{\tau + 6.5} + \frac{1793}{\tau + 34} + \frac{585}{\tau + 83} \right]$$

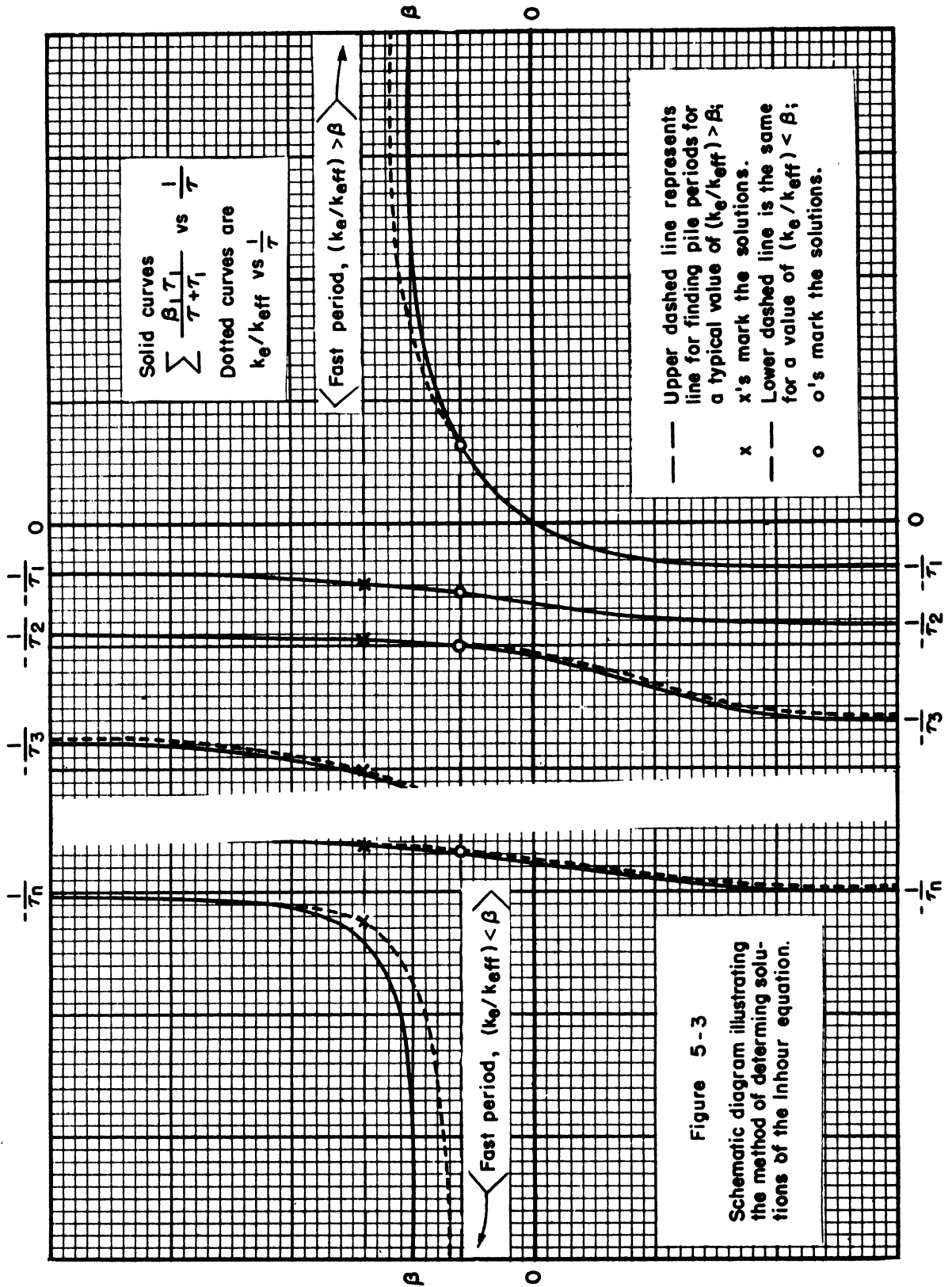
where the period is to be measured in seconds, and C_1 is a constant. Here the inhour is used as a unit of "reactivity", and is defined in such a way that a period of one hour corresponds to one inhour.* k_e is essentially proportional to the reactivity in inhcur, since for long periods $k_{\text{eff}} \approx 1$. The constant C_1 is easily computed by comparing (5-13g) with (5-13f). It is $\sim 2.5 \times 10^{-5}$.

Equation (5-13f) is an equation of $n + 1$ the degree, where n is the number of delayed neutron periods and the 1 comes in because of the fact that we have essentially a fundamental cycle time for undelayed neutrons which manage never to get into a latent group at all. We, therefore, find $n + 1$ periods. In order to see what these periods are, we shall examine (5-13f) in the form

$$k_e/k_{\text{eff}} = \sum \frac{\beta_i \tau_i}{\tau_i + \tau} + \frac{\tau_0 \ell_{\text{th}}}{\tau k_{\text{eff}}}$$

The sum $\sum \frac{\beta_i \tau_i}{\tau_i + \tau}$ is plotted schematically in Figure 5-3 (solid curves). So that the fast periods are essentially out at infinity, and the desirable periods, the slow ones, are in the middle of the figure, it is plotted as a function of $1/\tau$. As $1/\tau$ becomes zero, the neglected terms in (5-13f) become small compared to the sum plotted. (We assume that $\tau_0 \ell_{\text{th}} \ll \sum \beta_i \tau_i$.) There-

*In (5-13g) the normalization actually employed is asymptotic in character. As the period increases, the reactivity in inhcur becomes equal to the period in hours. For a period of one hour, the reactivity differs from one inhour by about 1/2%.



fore, in the central region of the figure, this graph is substantially an accurate plot of the whole right-hand side of the "inhour" equation. Consequently, much information about the solutions of (5-13f) can be obtained just by looking at this graph. If we go far enough out from the central region, we must also consider the effect of the other terms on the right side of (5-13f). The term $(\tau_o l_{th})/(\tau k_{eff})$ is the first one to add in. We must add for it, in first approximation, a line of low (positive) slope going through zero. (Where the absolute value of the resulting graph is not small compared to 1, higher approximations or different methods of attack are needed to account for the fact that k_{eff} changes.) When this term (and the first approximation to the terms including the mean slowing down time from Equation (5-13d) or (5-13e)) is added, instead of going asymptotically to the value β , as $(1/\tau) \rightarrow \infty$, the graph of the left-hand side of the inhour formulae goes down very slowly, while on the right it goes up very slowly (dotted line in Figure 5-3). We now get the $n + 1$ solutions for τ , and by inspection we find that one τ is unavoidably a fast period. The other periods, as we see, can be depended on to be slow enough for safety.

Although there is a very fast period, if we obtain it on the left side of the figure it is a descending one. It represents the prompt neutron effect which we described in Section 5-6. This fast period allows us to follow fluctuations, but will never kill us because it is always of an essentially negative character. It will always damp itself out. To be sure that the fast period (i.e., $|\frac{1}{\tau}|$ large) is a descending one, we must know that the right side (and therefore the left side also) of the inhour equation is less than β . This is the condition: $k_e/k_{eff} < \beta$. If, on the other hand, $k_e/k_{eff} > \beta$, we obtain a fast period on the right-hand side of Figure 5-3. It is a fast rising one, and leads to disaster. In terms of this diagram, then, we have shown that the condition for safe operation is

$$\frac{k_e}{k_{eff}} < \beta$$

or

$$k_{eff}(1 - \beta) < 1$$

This is exactly the same condition that we gave in Section 5-6, Equation (5-22), generalized so that leakage is also considered. In order to make the energy release in a pile rise, k_{eff} must be greater than 1. Therefore, safe condi-

tions in bringing a pile up to standard operation require

$$0 < k_e/k_{eff} < \beta$$

When the periods have been found from any of the Equations (5-13), it is then possible to go back to the equations which connect the densities and find the ratios for the various densities which are to be associated with the given periods. The evaluation of the ratios was done in detail in Section 5-6 for the simple model; to evaluate ratios here is merely long-winded, but not more complicated. When the inhour formula is used to determine the period, we find that just enough ratios are determined to give all the ratios of the latent neutron densities and the free neutron density, but there are not enough ratios to distinguish in the initial conditions between those neutrons which are slowing down and those which are thermal. This is not surprising because we have made the time for slowing down so short that neutrons during the slowing down process are already to be considered as thermal neutrons. If we want to make further distinctions in the initial conditions, it is necessary to go back to the more exact forms of the characteristic equation. We then obtain an infinite sequence of solutions by means of which we hope to represent the initial condition applying to the slowing down densities as well as to all the other densities.

Just as we viewed (5-13a) in Section 5-8, Equation (5-13f) can be looked at as a method of finding k_e or k_{eff} in terms of the time behavior of a pile. If we measure the time behavior and fit it to the right side of the equation, we can determine k_e/k_{eff} . The method for the measurement of k given in Section 5-8 is really a method for the measurement of k_e or k_{eff} .

So far, we have assumed that the energies of the neutrons released promptly on fission and of the delayed neutrons are identical. If the energies are different, different β 's and different L_f^2 's and ℓ_f 's must be associated with the various neutron types. Since the slowing down time is small enough to be neglected, the differences in slowing down times will not interest us. We should, however, investigate the modifications which are introduced by considering various ℓ_f 's.

If ℓ_{fp} denotes the fraction of prompt neutrons staying in the pile during slowing down (computed as if there were no resonance capture) and ℓ_{fi}

are the corresponding fractions for the free neutrons which arise from the various latent neutron types,

$$(5-74) \quad \ell_f \equiv (1 - \beta) \ell_{fp} + \beta \ell_{fd}$$

$$\text{with} \quad \ell_{fd} \equiv \sum \beta_i \ell_{fi} / \beta$$

With these definitions and some algebra, we find that

$$(5-13h) \quad k_e = k_{\text{eff}} \sum \left(\frac{\beta_i \tau_i}{\tau + \tau_i} \right) \left(\frac{\ell_{fi}}{\ell_f} \right) + \frac{\tau_0 \ell_{th}}{\tau} + \dots$$

When the various L_f^2 's are known separately, (ℓ_{fi}/ℓ_f) may be computed and (5-13h) employed. For large piles, however, as \mathcal{R}^2 becomes zero, (ℓ_{fi}/ℓ_f) becomes 1 no matter what energies of emission are associated with the various types of neutrons, and (5-13h) becomes identical with our other equations (5-13).

For example, suppose that $k = 1.11$. Then $\ell_f > .9$. Even if the fast migration area for neutrons slowing down after delay in the i^{th} latent group is only one-half of the average fast migration area,

$$\frac{\ell_{fi}}{\ell_f} = \ell_f^{-\frac{1}{2}} < \frac{1}{.95}$$

Therefore, (ℓ_{fi}/ℓ_f) is between 1.00 and 1.05. If thermal neutrons also leak out of the pile, as they do, the range of (ℓ_{fi}/ℓ_f) above 1.00 is more restricted, and if the fast migration areas differ less radically, this range is still further cut down. We conclude, therefore, that when $|k - 1| \ll 1$, we need not go to the refinement of (5-13h). As k becomes large, however, or, more accurately, as ℓ_f becomes smaller, the differences in the various ℓ_{fi} and ℓ_{fp} may become significant.

A slight modification of the safety condition for pile operation with rising power levels may also be derived from a consideration of the various ℓ_f 's. Since it is rising prompt neutron reproduction which we wish to avoid, in place of $k_{\text{eff}} (1 - \beta) < 1$, we should write

$$k_{\text{eff}} (1 - \beta) \frac{\ell_{fp}}{\ell_f} < 1$$

Using (5-74), this condition becomes either

$$k_{\text{eff}} \left(1 - \beta \frac{\ell_{fd}}{\ell_f}\right) < 1$$

or

$$k_e < \frac{\beta \frac{\ell_{fd}}{\ell_f}}{1 - \beta \frac{\ell_{fd}}{\ell_f}} = \frac{\beta \frac{\ell_{fd}}{\ell_{fp}}}{1 - \beta}$$

in place of $k_e < \frac{\beta}{1 - \beta}$.

Since ℓ_{th} and (ℓ_{f1}/ℓ_f) enter the inhour equation, it is no longer possible to eliminate the size and shape of the pile from one side of the equation; k_e cannot be found merely in terms of the time behavior. It is for this reason we did not push (5-13a) to a formal solution for k_e .

VI. SPECIAL TOPICS

5-21 Preliminary Remarks on Controls, Absorbers, and Reflectors

In the last section we obtained relations between the intrinsic properties, the size and shape, and the time behavior of piles. The introduction of absorbing material into a pile will also affect the critical size or time behavior. If the absorbing material is introduced uniformly, it is simplest to view these changes as the result of changes in the reproduction constant and migration areas. If, on the other hand, the absorber is introduced in a small region, it may be convenient to isolate that region from the rest of the pile. Boundary conditions can be found connecting the neutron densities in the pile with those in the isolated region, and the changes in time behavior (or critical size) may be computed by considering the changed size and shape of the pile: that is to say, by considering the changes in \mathcal{K}^2 .

The insertion or removal of localized absorbing material changes \mathcal{K}^2 without changing the intrinsic properties in the body of the pile; so also does a variation in the overall size or shape. Consequently, it is possible, by thus controlling \mathcal{K}^2 , to bring a pile to a stationary state without chang-

ing its thermal utilization. The method for measuring f , described in Section 5-12, can be employed without the aid of luck and without accurate building and rebuilding of the pile, by using localized absorbers to attain a stationary state. Such localized absorbers are usually employed in the form of rods which can be inserted in or withdrawn from the pile.

The theory of the effectiveness of such control rods is an excellent example of the problems which may be approached by use of the idea of geometric change. Suppose that a control rod of perfect neutron absorber is introduced along the axis of a cylindrical pile. When the control rod is in place, the neutron densities must extrapolate to zero a short distance inside the control rod as well as a short distance outside the external boundary of the pile. In Figure 5-4 the spatial distribution of the neutron density is plotted along a radius of the pile for the two cases of the original pile and the pile with the control rod inserted. Since the new boundary put in along the axis of the pile has the effect of increasing κ^2 , the insertion of the control rod causes all the periods, as given by the inhour formula, to shift to the left on Figure 5-3. If the original pile is in a stationary state, the pile power level will fall when the control rod is inserted.

That the pile power level will fall in these circumstances is clear ab initio. The introduction of absorber robs the pile of neutrons which

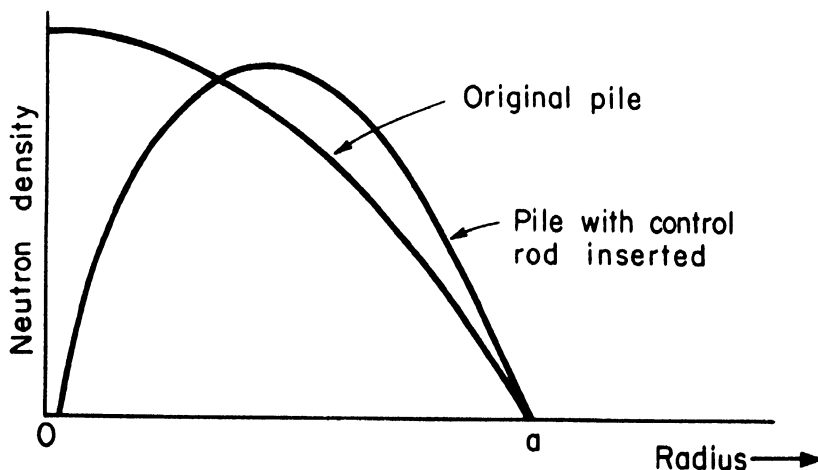


Figure 5-4. Neutron Density Distributions in a Cylindrical Pile.

are necessary to maintain the reproductive cycle. It is, however, not possible to compute the time behavior from a naive consideration of the absorption of neutrons in the control rod. Since the whole spatial distribution of neutrons is changed by the presence of the control rod, not only is a leakage into the control rod produced, but also the leakage of neutrons to the outside is changed. The picture of geometric changes considers both effects at once.

For weak absorbers localized in the pile, the picture of geometric change is not so obvious. We expect that the spatial distribution of neutrons is hardly disturbed and that the capture of neutrons in the extra absorbing material is given by $\int n v \sigma_{ce} N_e dV$, where $n v$ is the original neutron density and σ_{ce} , N_e refer to the extra absorbing material. Although we are correct, let us look at the problem more closely.

For example, we consider a pile in which the neutrons are always in thermal equilibrium, and there are no delayed neutrons. If it is in a stationary state (cf. Section 5-13),

$$(5-75) \quad \Delta n + \frac{(k-1)}{L^2} n = 0$$

When weak absorber is also present, we have instead

$$(5-76) \quad \Delta n' + \frac{(k-1)}{L^2} n' - \frac{n' \sigma_{ce} N_e v}{D} = \frac{\partial n'}{D \partial t}$$

where n' is the modified spatial distribution.

On multiplying (5-75) by n' and (5-76) by n and subtracting (5-76) from (5-75), we obtain

$$\nabla \cdot (n' \nabla n - n \nabla n') + n n' \frac{\sigma_{ce} N_e v}{D} = - \frac{n}{D} \frac{\partial n'}{\partial t} = - \frac{n n'}{D} \frac{1}{\tau}$$

Integrating over the whole pile, the first term drops, since both n and n' vanish on the surface. Therefore

$$(5-77) \quad \int_{\text{pile}} n n' \frac{\sigma_{ce} N_e v}{D} dV \quad \Bigg/ \quad \int_{\text{pile}} \frac{n n'}{D} dV = - \frac{1}{\tau}$$

On the other hand, suppose that by any geometric change, we change \mathcal{L}^2 in the pile from \mathcal{L}_0^2 to \mathcal{L}^2 . Then Equation (5-44a), Section 5-14, gives

$$D(\mathcal{L}^2 - \mathcal{L}_0^2) = -\frac{1}{\tau}$$

By an appropriate choice of \mathcal{L}^2 , we can make the periods given by (5-77) and (5-44a) equal. This choice is

$$(5-78) \quad \mathcal{L}^2 = \mathcal{L}_0^2 + \frac{\int_{\text{pile}} \frac{n n'}{D} \sigma_{ce} N_e dV}{D \int_{\text{pile}} \frac{n n'}{D} dV}$$

Since the absorber is weak, $n' \approx n$, and we finally obtain

$$(5-79) \quad \mathcal{L}^2 = \mathcal{L}_0^2 + \frac{\int_{\text{pile}} n^2 \frac{\sigma_{ce} N_e v}{D} dV}{\int_{\text{pile}} n^2 dV}$$

Equation (5-79) is the first order perturbation theory result, well known in quantum theory from the Schrödinger perturbation theory. Whether this result is valid or not, we are on sure ground for any absorber up to Equation (5-78). The effect of any absorber may therefore be assimilated to a change in geometry.

Since the effects of absorber and of change in geometry can be interconverted, and since the change in time behavior of a pile as the result of introducing absorbing material is a measure of the absorption introduced, absorption is sometimes measured in inhours at a standard position in a pile. In our simple example, Equation (5-77) gives the pile period when the extra absorber is in place. The period is infinite when the extra absorber is absent. With $n' \approx n$, for weak absorber, and localization of the extra absorber in a small region V_e where $n \approx n_e$

$$(5-77') \quad -\frac{1}{\tau} = \frac{n_e^2 \sigma_{ce} v N_e V_e}{\int_{\text{pile}} n^2 dV}$$

By naively balancing the extra absorption rate against the rate of change of the total number of neutrons in the pile, we would obtain the erroneous result

$$(5-77 \text{ wrong}) \quad -\frac{1}{\tau} = \frac{n_e \sigma_{ce} v N_e V_e}{\int_{\text{pile}} n dV}$$

(This naive attack can be corrected easily, as we shall see at the end of the next section.)

The geometry, i.e., the boundary conditions, and therefore \mathcal{K}^2 , is obviously changed by surrounding a pile with a reflecting layer of scattering nuclei. Some of the neutrons which leak out of the pile instead of staying outside bounce back in. They act approximately as if they came from an extension of the reproducing region. The pile size is effectively increased, and \mathcal{K}^2 is decreased. A subcritical pile may, therefore, be brought to a stationary state, or the power level of a pile of critical size may be made to rise by placing a neutron reflector around it. An example of the change in critical size effected by a reflector is given for a simple model in Section 3-6.

The general problems of controls, pile perturbation theory, and reflectors are more difficult than we have pretended in this section. Absorbers are not found black to neutrons of all energies. Actual control rods may be highly absorbing at thermal neutron energies but are likely to have no significant effect on high energy neutrons. The geometry may be effectively altered for thermal neutrons, but apparently unchanged from the viewpoint of other neutrons. It is therefore necessary to find the effective geometry change, the change in \mathcal{K}^2 , by gluing together different geometries for fast neutrons and thermal neutrons. Since the behavior of fast neutrons and of thermal neutrons has been described by different equations, we can introduce different boundary conditions on the solutions in correspondence with the different geometries.

Similarly, in the reflector problem, the differences in the slowing down characteristics of pile and reflector are hardly expected to be similar to the differences at thermal neutron energies. The presence of fissionable material in the pile leads to desirable thermal absorption. A reflector, on the other hand, is selected to scatter neutrons back into the pile. Neutron

absorption in the reflector is a loss. In practice, then, the properties of the reflector are likely to be radically different from those of the pile at thermal energy, while they may be quite similar at higher energies. Again we must use a set of boundary conditions between pile and reflector rather than a single condition.

Pile perturbation theory, which we developed slightly in discussing weak absorbers, must be adapted to consider perturbing influences not only as a function of position, but also as a function of energy. It must also be extended to include reflectors.

There are complications of a different type. One is illustrated by the reflector problem. Neutrons which spend a large fraction of their lives in the reflector may have a different mean life from neutrons which stay in the pile. We may therefore expect further changes in the description of the time behavior when reflectors are used.

5-22 Harmonic Expansions

The equation

$$(5-80) \quad \Delta S + \mathcal{K}^2 S = 0$$

with the appropriate boundary conditions, can be solved for many values of \mathcal{K}^2 . So far we have used but a single value of \mathcal{K}^2 , and we have assumed that whenever S equals zero, we have located one of the boundaries of the pile, or possibly of one of the images. This procedure gives a unique solution for S , the space variation of the neutron density in a pile of a given dimension. We must, however, examine all the solutions, S_m of (5-80). Since they meet the boundary conditions, it is possible that the neutron density is

$$(5-81) \quad S = \sum_m B_m S_m$$

rather than the single S_m , say S , we have used.*

*We disregard the possibility, raised in the last section, that the boundary conditions may change with energy. Returning to simple piles, $\Delta S_m + \mathcal{K}_m^2 S_m = 0$ and the set of \mathcal{K}_m^2 , S_m are so determined that the S_m are all zero at any point on the extrapolated boundaries of the pile. They may, however, have other zeros which are not located on the pile boundaries.

Let us arrange the \mathcal{R}_m^2 in ascending order, and call the S_m in this order the successive harmonics in the neutron density. To each harmonic (\mathcal{R}_m^2, S_m) there corresponds a characteristic time behavior. Equations (5-13) of Section 5-20 determine a set of associated periods, τ_{mj} , and from the initial conditions and the τ_{mj} the neutron densities associated with the various periods may be found. The neutron densities are now broken down as

$$n = \sum_{m=1}^{\infty} \sum_{j=1}^{n+1} n_{mj} e^{t/\tau_{mj}} S_m(x, y, z)$$

(5-82) and

$$c_i = \sum_{m=1}^{\infty} \sum_{j=1}^{\infty} i_{mj}^c e^{t/\tau_{mj}} S_m(x, y, z)$$

where the n_{mj} and i_{mj}^c are constants. The ratios i_{mj}^c/n_{mj} (we call them i_{mj}^a) are fixed by equations corresponding to (5-72). Then

$$n_m(0) = \sum_{j=1}^{n+1} n_{mj}$$

(5-83) and

$$i_m^c(0) = \sum_{j=1}^{n+1} i_{mj}^a n_{mj}$$

are found from the initial spatial distributions. Finally, from (5-83), the n_{mj} and i_{mj}^c are determined.

Upon referring to the inhour equation and to Figure 5-3, we see that as \mathcal{R}^2 increases, each of the periods decreases. Consequently, as time goes on, the higher harmonics disappear with respect to the lower ones, and finally only the lowest harmonic is of significance in a pile. It is this

lowest harmonic which has been taken by us as a unique solution. There are, however, cases, particularly when independent sources are present, in which the higher harmonics maintain a certain significance. For example, if any permanent sources of neutrons are present, and if the effective reproduction constant is less than one, the higher harmonics should always be taken into account. In the next section, we shall consider just such an example.

In the last section, we found that an incorrect result is obtained by balancing the rate of change of the neutron density against the capture in extra-absorbing material placed in an original critical pile. The trouble arises because leakage is not correctly accounted for. Let us, therefore, fit the sink into the pile with the correct boundary conditions.

To meet the boundary conditions, we can use an harmonic expansion. If the functions S_n form a complete orthogonal set in which any density distribution in the pile may be expanded, a unit point source at r_0 is represented by

$$(5-84) \quad \sum \left(S_n(r_0) S_n(r) / \int_{\text{pile}} S_n^2(r) dV \right)$$

Since we are considering only weak absorbers, the neutron density distribution in the pile, which, in general, is

$$n = \sum a_n S_n(r)$$

is closely given by $S_1(r)$, the lowest harmonic. The sink at the extra absorber is, therefore

$$\sigma_e N_e v S_1(r_e) V_e \sum \left(S_n(r_e) S_n(r) / \int_{\text{pile}} S_n^2(r) dV \right)$$

and the rate of absorption of the lowest harmonic due to the presence of the sink is

$$\sigma_e N_e v V_e S_1^2(r_e) S_1(r) / \int_{\text{pile}} S_1^2(r) dV$$

Since the S_n are orthogonal, this is the only harmonic which we can match with the approximate neutron density $S_1(r)$; consequently we find

$$\frac{\partial S_1(r)}{\partial t} = -\sigma_e N_e v V_e \frac{S_1^2(r_e)}{\int_{\text{pile}} S_1^2(r) dV} S_1(r)$$

and to the extent that $S_1(r)$ represents the whole neutron density,

$$(5-77') \quad \frac{1}{\tau} = -\frac{n_e^2 \sigma_e N_e v V_e}{\int_{\text{pile}} n^2 dV}, \text{ the correct result.}$$

5-23 The Approach to Critical Conditions

In practice, when building a pile it is unwise to construct the whole chain-reacting system first, and later sit down to see what is going on. Instead, the pile is built bit by bit in order that we may observe the approach to the critical condition. To observe this approach to the critical condition, we must first make a few computations to see how the neutron density acts as we increase the size of the pile.

Suppose that we place a source in the center of a very small cubic pile. For simplicity, we shall choose our neutron source to be a point source of thermal neutrons of strength Q neutrons emitted per unit time. This pile is smaller than the critical dimension, but we shall gradually increase its size until it runs. As we build the pile, we shall observe the neutron density in the stationary state at every size. Let us examine such a stationary state.

When no independent source is present, the thermal diffusion equation, the interconnection relations, and the slowing down description -- on the model of continuous collisions, for example -- may be combined in an overall pile equation

$$(5-85) \quad \left[L^2 \Delta + k \sigma_f^L \Delta^2 - 1 \right] \frac{n}{\tau_0} = 0$$

for a stationary state. When $\Delta n + \mathcal{L}^2 n = 0$, Equation (5-85) becomes Equation (5-62). When there is also a permanent source of thermal neutrons present, (5-85) must be modified to include the source. It becomes

$$(5-85a) \quad - \left[L^2 \Delta + k e^{L_f^2 \Delta} - 1 \right] \frac{n}{\tau_0} + Q = 0$$

If we expand both n and Q in a complete set $S_{ijk}(x,y,z)$ of orthogonal functions satisfying (5-80) and the boundary conditions, on carrying out the operations indicated we obtain

$$(5-85a') \quad \left[-\mathcal{L}_{ijk}^2 L^2 + k e^{-\mathcal{L}_{ijk}^2 L_f^2} - 1 \right] \frac{n_{ijk}}{\tau_0} + Q_{ijk} = 0$$

where

$$n = \sum n_{ijk} S_{ijk}(x,y,z)$$

$$Q = \sum Q_{ijk} S_{ijk}(x,y,z)$$

Therefore

$$\frac{n}{\tau_0} = \sum \frac{Q_{ijk} S_{ijk}(x,y,z)}{1 + \mathcal{L}_{ijk}^2 L^2 - k e^{-\mathcal{L}_{ijk}^2 L_f^2}}$$

(5-86)

$$= \sum \frac{Q_{ijk} \ell_{th_{ijk}}}{1 - k_{eff_{ijk}}} S_{ijk}(x,y,z)$$

since $\frac{1}{1 + \mathcal{L}_{ijk}^2 L^2}$ is ℓ_{th} and $e^{-\mathcal{L}_{ijk}^2 L_f^2}$ is ℓ_f when $n = S_{ijk}$. (Of course,

Equations (5-85a') and (5-86) may be obtained from an analysis parallel to that given in Section 5-17 in deriving (5-62).)

If $Q(x,y,z)$ is a point source of strength Q at (x_0, y_0, z_0)

$$(5-84') \quad Q_{ijk} = Q S_{ijk}(x_0, y_0, z_0) / \int S_{ijk}^2(x,y,z) dx dy dz$$

In a cubic pile, where the length of the extrapolated sides is r , the functions

$$S_{ijk} = \sin \frac{i\pi x}{r} \sin \frac{j\pi y}{r} \sin \frac{k\pi z}{r}; \quad i, j, k \text{ integers}$$

form a complete orthogonal set satisfying (5-80) and the boundary condition that $S = 0$ on the planes $x = 0$, $y = 0$, $z = 0$, $x = r$, $y = r$, and $z = r$. The corresponding α_{ijk}^2 are

$$\alpha_{ijk}^2 = \left(\frac{\pi}{r}\right)^2 [i^2 + j^2 + k^2]$$

$$\text{and } \int S_{ijk}^2 dx dy dz = \left(\frac{r}{2}\right)^3 \text{ for all } (i, j, k).$$

In these coordinates the center of the pile is at $(\frac{r}{2}, \frac{r}{2}, \frac{r}{2})$. For a source at the center:

$$Q_{ijk} = 0 \text{ if } i, j, \text{ or } k \text{ is even.} \quad \left(\begin{array}{l} \text{The harmonics } S_{ijk} \\ \text{with any index even} \\ \text{have no amplitude} \\ \text{at the source and} \\ \text{are therefore ab-} \\ \text{sent.} \end{array} \right)$$

$$Q_{ijk} = Q \left(\frac{2}{r}\right)^3 \text{ for } i, j, \text{ and } k \text{ all odd.}$$

Consequently

$$(5-86') \quad \frac{n}{\tau_0} = Q \left(\frac{2}{r}\right)^3 \sum \frac{\ell_{th_{ijk}}}{1 - k_{eff_{ijk}}} S_{ijk}(x, y, z)$$

where $i, j, k = \text{odd integers.}$

If the pile is almost of critical size, $1 - k_{eff_{111}}$ is almost zero, but the other denominators in (5-86') are appreciable. Below critical, but near it, only the first harmonic is of major importance. n/τ_0 is then given by the first term in (5-86'): i.e.,

$$(5-86'') \quad n/\tau_0 \approx Q \left(\frac{2}{r}\right)^3 \frac{\ell_{th_{111}}}{1 - k_{eff_{111}}} S_{111}(x, y, z)$$

When r reaches the critical dimension a , the pile rides up on this lowest harmonic. The other harmonics, however, are still tied to the source and are consequently left behind.

Since as r approaches a ,

$$\mathcal{L}_{111}^2 - \mathcal{L}_0^2 = 3\pi^2 \left(\frac{1}{r^2} - \frac{1}{a^2} \right) \approx 6\pi^2 \frac{a-r}{a^3}$$

we find that

$$\frac{\ell_{th_{111}}}{1 - k_{eff_{111}}} = \frac{a^3}{6\pi^2 (a-r) (L^2 + L_f^2 k_e^{-\mathcal{L}_0^2 L_f^2})}$$

or

$$(5-86''a) \quad (a-r)n = \frac{4Q\tau_0}{3\pi^2 (L^2 + L_f^2 k_e^{-\mathcal{L}_0^2 L_f^2})} S_{111}(x,y,z)$$

The difference between a and r (that is, the distance away from critical conditions) is measured by a constant divided by the thermal neutron density. If we construct a graph of $1/n$ as a function of r while we build a pile, we are able to extrapolate this graph to the place at which $1/n$ becomes zero some time before we actually reach it. The place at which $1/n$ becomes zero is the critical dimension.

It should be mentioned that this type of procedure can be applied whether or not we build up our pile in a completely symmetric fashion. It is, in fact, more usual in practice to build one dimension almost complete and then extend the pile only in another direction.

To show that when r approaches a the higher harmonics in the expansion n/τ_0 become negligible by comparison with n_{111} , let us consider the next harmonics. They are $(3,1,1)$, $(1,3,1)$, and $(1,1,3)$; and all of them are equal. Also

$$\mathcal{L}_{311}^2 = \mathcal{L}_{131}^2 = \mathcal{L}_{113}^2 = \frac{11}{3} \mathcal{L}_{111}^2 \approx \frac{11}{3} \mathcal{L}_0^2$$

near critical conditions. When $\mathcal{L}_0^2 L_f^2 \ll 1$, it is easy to evaluate

$$\frac{\ell_{th_{311}}}{1 - k_{eff_{311}}}$$

it is approximately

$$\frac{\ell_{th_{311}}}{1 - k_{eff_{311}}} \approx \frac{1}{8/3 \mathcal{L}_o^2 M^2} = \frac{a^2}{8\pi M^2}$$

Also, when $\mathcal{L}_o^2 L_f^2 \ll 1$

$$\frac{\ell_{th_{111}}}{1 - k_{eff_{111}}} = \frac{a^3}{6\pi^2 (a - r) M^2}$$

(5-87) and

$$\frac{n_{311}}{n_{111}} = \frac{3}{4} \frac{a - r}{a}$$

Clearly, then, n_{311} disappears by comparison with n_{111} as critical conditions are approached.

If there is no reproduction in the pile but somehow the other properties, including $(\sigma_o N_o + \sigma_f N_f)$, are unchanged, the coefficient n_{ijk}/τ_o of the (i,j,k) harmonic is

$$\frac{n_{ijk}}{\tau_o} = Q \left(\frac{2}{r} \right)^2 \ell_{th_{ijk}}$$

The reproduction increases the (i,j,k) harmonic by the factor

$$a_{ijk} \equiv \frac{1}{1 - k_{eff_{ijk}}}$$

This harmonic amplification factor due to the reproduction is sometimes useful, especially when the pile is almost critical. For example, in the range

in which only the first harmonic is of significance, $l_{th_{111}}$ is approximately constant $\left(l_{th_{111}} = \frac{1}{1 + \mathcal{L}_o^2 L^2} \right)$ and

$$(5-88) \quad \frac{n(1)}{n(2)} = \frac{1 - k_{eff_{111}}^{(2)}}{1 - k_{eff_{111}}^{(1)}} = \frac{a_{111}(1)}{a_{111}(2)}$$

for two different almost critical values of r .

CHAPTER 6

THE APPLICATION AND EXPERIMENTAL BASIS OF PILE THEORY

by

Bernard T. Feld

I. Application of Elementary Pile Theory in the Design of a Power Pile

6-1 General Considerations

In order to review the ideas developed in the preceding lectures and to illustrate how they might be applied, we shall undertake to design a pile. We shall assume the availability of sufficient quantities of enriched uranium and of graphite to do the job. The uranium is assumed to be enriched to an atomic ratio $\frac{N(U^{235})}{N(U^{238})} = \frac{1}{50}$. This uranium is mixed uniformly with graphite and the mixture pressed to a density of 1.6 gms/cm^3 . (As will be seen, we are interested only in mixtures containing a small fraction of uranium, so that the mixture should physically resemble pure graphite.)

It must be pointed out at the onset, and emphasized throughout, that this paper does not represent an attempt to reproduce the work done on the Manhattan project. Only nuclear design problems will be considered; there will be no attempt to build into the pile any provision for removing heat, nor will any other engineering problems be given serious consideration. In order to be able to substitute numbers into the formulae, it is necessary to assume values for the nuclear constants involved. To prevent this example from being completely fantastic, we have chosen, at random, constants from the prewar published literature, without prejudice as to whether these constants agree or disagree with those measured in the Manhattan project laboratories.

It is worth emphasizing again that the pile here designed has no resemblance to any actual pile, living or unborn.

6-2 The Nuclear Constants

Uranium (U^{235})

$\sigma_f = 500 \times 10^{-24} \text{ cm}^2$ A rough average of all the prewar values; previously given in Professor Evans' paper (page 73)

$\sigma_s = 15 \times 10^{-24} \text{ cm}^2$ Assumed equal to that for U^{238} .

$$\eta = 2.3$$

Zinn and Szilard, Phys. Rev. 56, 619 (1939).

Delayed Neutrons

β_i	τ_i	
.0002	80.2 sec	Fermi - lectures in nuclear physics given at Los Alamos, declassified (Table 2-2)
.0014	31.7 "	
.0018	6.51 "	
.0020	2.21 "	
.0007	.61 "	
$\sum \beta_i = .0061$		

Uranium (U^{238})

$$\sigma_s = 15 \times 10^{-24} \text{ cm}^2$$

Goldsmith, Cohen, and Dunning,
Phys. Rev. 55, 1124 (1939).

$$\sigma_o = 2 \times 10^{-24} \text{ cm}^2$$

σ_r - the measurements of Anderson (Phys. Rev. 57, 566 (1940)) indicate a resonance at 5 ev. In order to find σ_r , we shall assume that the resonance cross section is given by the Breit-Wigner formula

$$\sigma_r = \frac{\pi \hbar^2}{m^2 v^2} \frac{\Gamma_n \Gamma_\gamma}{(E - E_r)^2 + \frac{\Gamma^2}{4}}$$

where

$$\hbar = 1.05 \times 10^{-27} \text{ erg-sec}$$

$$E_r = 5 \text{ ev}$$

$$m = 1.66 \times 10^{-24} \text{ gm}$$

$$\Gamma = \Gamma_n + \Gamma_\gamma$$

$$v = \text{neutron velocity in cm/sec}$$

$$\Gamma_\gamma = .15 \text{ ev}$$

$$E = \text{neutron energy in ev}$$

$$\Gamma_n = 10^{-4} \text{ ev}$$

The last two constants are typical of the values found in (n, γ) resonances involving heavy elements.

From these constants, it is possible to calculate

$$\int_{1 \text{ ev}}^{\infty} \sigma_r \frac{dE}{E} = 44 \times 10^{-24} \text{ cm}^2$$

Since U^{238} is a heavy element, and heavy elements are known to have (n, γ) resonances spaced at intervals of $\sim 10 - 30$ ev, it is reasonable to assume that higher resonances also contribute to the above resonance integral. Since the magnitude of the contribution of higher resonances falls off inversely with their energy, we shall assume (in a completely arbitrary fashion) that all of the higher resonances, lumped together, double the above value of the integral, and take

$$\int_{1 \text{ ev}}^{\infty} \sigma_r \frac{dE}{E} = 88 \times 10^{-24} \text{ cm}^2$$

Graphite (C)

$$\sigma_s = 4.8 \times 10^{-24} \text{ cm}^2 \quad \text{Segre chart (following page 22)}$$

$$\sigma_o = .005 \times 10^{-24} \text{ cm}^2 \quad \text{Fermi lecture (cited above). Also Segre' chart.}$$

ξ = the average logarithmic energy loss

$$= 1 - \frac{(A-1)^2}{2A} \ln_e \frac{A+1}{A-1}$$

$$= 1 - \frac{(11)^2}{24} \ln_e \frac{13}{11} = .158$$

$N(C)$ = the number of carbon atoms per cm^3

$$= \frac{1.6}{12} \times 6 \times 10^{23} = 8 \times 10^{22}$$

6-3 The Calculation of $k = f p \eta$

(1) The thermal utilization (fraction of all the thermal neutrons captured by U^{235} in an infinite medium) is:

$$(6-1) \quad f = \frac{N(U^{235}) \sigma_f(U^{235})}{N(U^{235}) \sigma_f(U^{235}) + N(U^{238}) \sigma_o(U^{238}) + N(C) \sigma_o(C)}$$

where N is the number of atoms per cm^3 .

This expression can be simplified by dividing numerator and denominator by the numerator:

$$f = \frac{1}{1 + \frac{N(U^{238})}{N(U^{235})} \frac{\sigma_o(U^{238})}{\sigma_f(U^{235})} + \frac{N(C)}{N(U^{235})} \frac{\sigma_o(C)}{\sigma_f(U^{235})}}$$

$$f = \frac{1}{1 + 50 \cdot \frac{2}{500} + 50 \cdot \frac{N(C)}{N(U^{238})} \cdot \frac{.005}{500}} = \frac{1}{1.2 + 5 \times 10^{-4} R}$$

where $R = \frac{N(C)}{N(U^{238})}$ = the ratio of carbon to U^{238} atoms in the mixture.

(2) The resonance escape probability is:

$$(6-2) \quad p = e^{-\int \frac{\sigma_r(U^{238}) N(U^{238})}{\sigma_r(U^{238}) N(U^{238}) + \sigma_s(C) N(C)} \frac{dE}{\xi E}}$$

Under the assumptions $\sigma_r(U^{238}) N(U^{238}) \ll \sigma_s(C) N(C)$ and $\sigma_s(C)$ and ξ are independent of E , the expression for p reduces to

$$p = e^{-\frac{1}{\xi \sigma_s(C)} \int \sigma_r(U^{238}) \frac{dE}{E} - \frac{116}{R}} = e$$

(3) The value of $k = fp\eta$ is now determined if R (the ratio of carbon to U^{238} atoms in the mixture) is given. From the form of the expression for f and p , it is clear that, as R becomes large, p approaches 1 and f approaches 0. Conversely, as R becomes small, p approaches 0 and f approaches 0.835. The ratio of carbon to uranium for the mixture is the one parameter at our disposal, and we should therefore choose a value of R which will yield a k

greater than 1. Since the exponential (from which p is calculated) is a function which varies rapidly with the value of the exponent, we should confine our choice of R to values between 10^2 and 10^3 . Table 6-1 gives the values of f , p , and k for a number of values of R in this range.

TABLE 6-1
CALCULATION OF k

<u>R</u>	<u>f</u>	<u>p</u>	<u>$k = fp\eta$</u>
3×10^2	.741	.679	1.158
5×10^2	.690	.793	1.258
8×10^2	.625	.865	1.244
10×10^2	.588	.890	1.202

The values calculated above indicate that k has its maximum value for R between 5×10^2 and 8×10^2 . Since the k 's calculated are already sufficiently greater than 1 to assure us of the possibility of obtaining a chain-reacting pile of manageable size, we shall not attempt to obtain the highest possible value of k , but will choose, rather arbitrarily, a mixture with $R = \frac{N(C)}{N(U^{238})} = 500$. For this mixture, then, the system has the following properties:

$$f = .690, p = .793, \eta = 2.3 \text{ and } k = 1.258$$

6-4 The Calculation of Critical Size

The critical size of a chain-reacting system (pile) with a given k is obtained from the following equation (when graphite is the moderating medium; when hydrogenous slowing down materials are used, the proper formula is given on page 158).

$$(6-3) \quad (1 + \mathcal{L}_0^2 L^2) = k e^{-\mathcal{L}_0^2 L_f^2}$$

where \mathcal{L}_0^2 is related to the critical size for a particular geometric configuration. Thus, for a cubic pile:

$$(6-4a) \quad \mathcal{H}_o^2 = \frac{3\pi^2}{a^2}$$

where a is the length of an edge; for a spherical pile:

$$(6-4b) \quad \mathcal{H}_o^2 = \frac{\pi^2}{S^2}$$

where S is the radius of the critical sphere.

To obtain the value of \mathcal{H}_o^2 , it is necessary, first, to calculate L^2 and L_f^2 .

(1) The calculation of L^2 , the thermal diffusion area

$$(6-5) \quad L^2 = \frac{1}{3 \left[\sigma_s(C)N(C) + \sigma_s(U)N(U) \right] \left[\sigma_o(C)N(C) + \sigma_o(U^{238})N(U^{238}) + \sigma_f(U^{235})N(U^{235}) \right]}$$

$$= \frac{1}{3 \sigma_s(C) \sigma_o(C) (N(C))^2 \left[1 + \frac{1}{R} \frac{\sigma_s(U)}{\sigma_s(C)} \right] \left[1 + \frac{1}{R} \frac{\sigma_o(U^{238})}{\sigma_o(C)} + \frac{1}{R} \frac{N(U^{235})}{N(U^{238})} \frac{\sigma_f(U^{235})}{\sigma_o(C)} \right]}$$

We note that L^2 depends inversely on $N(C)^2$ [$N(C) = 8 \times 10^{22}$], and hence decreases with increasing density of the graphite. Substituting the values of the constants, together with $R = 500$, gives $L^2 = 358 \text{ cm}^2$.

(2) The calculation of L_f^2 , the slowing down area (all constants are assumed independent of neutron energy):

$$(6-6) \quad L_f^2 = \frac{\ln \frac{E_{fiss}}{E_{th}}}{3 \xi \sigma_s(C)N(C) \left[\sigma_s(C)N(C) + \sigma_s(U)N(U) \right]}$$

$$= \frac{\ln \frac{E_{fiss}}{E_{th}}}{3 \xi \sigma_s^2(C)N^2(C) \left[1 + \frac{1}{R} \frac{\sigma_s(U)}{\sigma_s(C)} \right]}$$

Substituting the constants given above, plus the values

$$E_{fiss} \cong 10^6 \text{ ev and } E_{th} \cong \frac{1}{40} \text{ ev}$$

we obtain $L_f^2 = 242 \text{ cm}^2$.

(3) The critical size:

It is now possible to solve the critical size equation for \mathcal{K}_0^2 . This is a transcendental equation; perhaps the easiest method of solving it is by trial and error. In order to orient ourselves, we may first solve the approximate equation

$$(6-3a) \quad \mathcal{K}_0^2 \approx \frac{k-1}{M^2}$$

where $M^2 = L^2 + L_f^2 = 600 \text{ cm}^2$ = the migration area. This equation holds for $k - 1 \ll 1$; since this condition does not really obtain in our case ($k - 1 = .258$), the solution will only serve to obtain a starting point for the trial and error solution of Equation (6-3).

$$\mathcal{K}_0^2 \approx \frac{.258}{600} = 4.3 \times 10^{-4} \text{ cm}^{-2}$$

With this as a starting point, we obtain from Equation (6-3) after very few trials and errors:

$$\mathcal{K}_0^2 = 4.00 \times 10^{-4} \text{ cm}^{-2}$$

Hence, for a cubic pile, the critical side is

$$a = \sqrt{\frac{3\pi^2}{\mathcal{K}_0^2}} = 272 \text{ cms}$$

and for a sphere, the critical radius is

$$S = \sqrt{\frac{\pi^2}{\mathcal{K}_0^2}} = 157 \text{ cms}$$

These critical dimensions include the "extrapolated length", i.e., these are the dimensions at which the neutron density may be said to fall to 0. The actual size of the pile (side of the cube or diameter of the sphere) is smaller than the above dimensions by twice the extrapolation distance, $d = \frac{.71}{N_s \sigma_s} = 1.8 \text{ cm}$. Hence the actual side of the critical cube is

$$a_0 = 272 - 3.6 = 268.4 \text{ cm}$$

and for the critical sphere:

$$S_0 \cong 157 - 2 = 155 \text{ cm}$$

6-5 Provision for Excess k

If we build a pile to exactly the critical dimensions, it will maintain whatever neutron density is present, but it will give no provision for increasing the neutron density. In order to be able to cause the neutron density to rise, so that the power produced may be increased, it is necessary to build a pile larger than the critical size. With such a pile, it is possible to control the neutron density by the insertion or removal of additional neutron absorbers (control rods). Thus, by removing the control rods, the pile will become supercritical and the neutron density will rise; by inserting the control rod, the pile may be made subcritical, and the neutron density caused to fall. For one particular position of the control rod the pile will be just critical, and the neutron level will maintain itself; the pile will then run at constant power.

We have seen that a certain fraction (0.6%) of the fission neutrons are emitted after a delay of the order of seconds. Hence, the period of exponential rising or falling of the neutron density can be made fairly long, and the pile can be controlled with ease provided the excess k (designated as k_e) is never allowed to become greater than this fraction. Hence, in building a pile larger than the critical size, we must be careful that k_e is never greater than .006.

For complete safety, let us build our pile with $k_e = .003$. The excess k is given by the expression

$$(6-7) \quad k_e = k - k_c = \frac{-\mathcal{K}_f^2 L^2}{(1 + \mathcal{K}_f^2 L^2)} - 1 = .003$$

where \mathcal{K}^2 is connected with the pile size by Equations (6-4), with \mathcal{K}^2 replacing \mathcal{K}_0^2 .

Equation (6-7) can be solved by using the method of trial and error and bearing in mind that since the actual size is to be greater than the critical size, $\mathcal{K}^2 < \mathcal{K}_0^2$. For $k_e = .003$, we obtain

$$\mathcal{K}^2 = 3.946 \times 10^{-4} \text{ cm}^{-2} = \frac{3\pi^2}{(a')^2}$$

$$a' = 273.8 \text{ cms}$$

Subtracting off 2d, we obtain for the actual side of our super-critical cube

$$a_o' = 270.2 \text{ cm}$$

compared to 268.4 cm for a just-critical pile.

The difference between a_o' and a_o is 1.8 cm in about 270, or .67%. Thus, the margin between a just-critical and a safely super-critical pile is quite small. It should hardly be necessary to emphasize the need for extreme care, in the construction of a pile, not to exceed the limit of safe operation ($k_e < .006$).

In addition, it should be stated that the critical size of the pile calculated above could have been reduced by surrounding the pile with a reflector, say pure graphite. The theory of the critical dimensions of a pile with reflector will be treated in future lectures; we merely point out that it may be possible to achieve a substantial saving of fissionable material by the use of reflectors. (Sections 3-6 and 5-21.)

6-6 Amounts of Materials Required

Knowing the volume of the pile and the density of the graphite-uranium mixture, it is easy to calculate the amounts of the various materials going into our pile. Since

$$R = \frac{N(C)}{N(U^{238})} = 500$$

$$\frac{Wt(C)}{Wt(U^{238})} = \frac{N(C) \times 12}{N(U^{238}) \times 238} = 25$$

$$\frac{Wt(C)}{Wt(U^{235})} = 25 \times 50 = 1250$$

The total weight of the pile is

$$(a_o')^3 \times 1.6 = 31.8 \text{ metric tons} = 35.2 \text{ short tons}$$

From this:

$$\begin{aligned} \text{Wt. of Carbon} &= 31.8 \times \frac{25}{26} = 30.6 \text{ metric tons} \\ &= 35.2 \times \frac{25}{26} = 33.8 \text{ short tons} \end{aligned}$$

$$\text{Wt. of } U^{238} = \frac{31.8}{26} = 1.22 \text{ metric tons}$$

$$= \frac{35.2}{26} = 1.35 \text{ short tons}$$

$$\text{Wt. of } U^{235} = \frac{1.22}{50} \times 10^3 = 24.4 \text{ kg}$$

$$= \frac{1.35 \times 2000}{50} = 54.0 \text{ lbs}$$

6-7 Power Considerations

The power developed in the pile is proportional to the average neutron flux, $\bar{n}\bar{v}$, and to the total number of U^{235} nuclei present. Since 3×10^{10} fissions/sec = 1 watt, the power in watts (P) is given by the expression

$$(6-8) \quad P = \frac{\bar{n}\bar{v} \sigma_f(U^{235}) N(U^{235}) V}{3 \times 10^{10}} \text{ watts}$$

Substituting

$$V = (a_0')^3 = 1.99 \times 10^7 \text{ cm}^3$$

$$N(U^{235}) = \frac{N(C)}{50 \times 500} = 3.2 \times 10^{18} \frac{\text{atoms}}{\text{cm}^3}$$

$$\sigma_f(U^{235}) = 500 \times 10^{-24} \text{ cm}^2$$

$$\bar{n}\bar{v} = .94 \times 10^6 \text{ neutrons/cm}^2, \text{ sec, watt.}$$

For thermal neutrons, the average velocity

$$\bar{v} \cong 2 \times 10^5 \text{ cm/sec}$$

and, thus, the average density of neutrons is

$$\bar{n} \cong 5 \text{ neutrons/cm}^3, \text{ watt}$$

In a cubic pile, the neutron density has its maximum, n_0 , at the center and falls to zero just outside the pile. In terms of the peak neutron density,

$$(6-9) \quad n = n_0 \cos \frac{\pi x}{a} \cos \frac{\pi y}{a} \cos \frac{\pi z}{a}$$

(the origin is taken at the center and the coordinate axes parallel to the edges of the pile). Averaging over the cube, we obtain

$$(6-9') \quad \bar{n} = \frac{8}{\pi^3} n_0 ; \quad n_0 = 3.9 \bar{n}$$

For our pile, this gives

$$n_0 \bar{v} = 3.7 \times 10^6 \frac{\text{neutrons}}{\text{cm}^2, \text{sec, watt}}$$

$$n_0 \cong 18 \frac{\text{neutrons}}{\text{cm}^3, \text{watt}}$$

At a power of 1 watt, 3×10^{10} U^{235} nuclei undergo fission each second. In one year, the consumption of U^{235} is $3 \times 10^{10} \times 3.15 \times 10^7 = 9.5 \times 10^{17} \frac{\text{atoms}}{\text{year, watt}}$. Since the total number of U^{235} atoms in the pile is 6.4×10^{25} , the rate of depletion of U^{235} is

$$100 \times \frac{9.5 \times 10^{17}}{6.4 \times 10^{25}} = 1.5 \times 10^{-6} \% \text{ per year per watt}$$

6-8 Time Behavior of the Pile

We have designed our pile so that with all control rods removed, it will rise with a period determined primarily by the delayed neutrons. It is instructive to calculate the period associated with the prompt neutron multiplication. The mean life of thermal neutrons in the pile, τ_0 , is given by the expression

$$(6-10) \quad \tau_0 = \frac{1}{v \left[\sigma_f(U^{235}) N(U^{235}) + \sigma_o(U^{238}) N(U^{238}) + \sigma_o(C) N(C) \right]}$$

$$\tau_0 = .00215 \text{ sec. (for } v = 2 \times 10^5 \text{ cm/sec)}$$

For a pile of infinite size, the neutron density is given by the expression

$$(6-11) \quad n = n_0 e^{(k_p - 1)t/\tau_0}$$

The period (time for an e-fold increase in neutron density) is

$$\begin{aligned} \tau &= \frac{\tau_0}{k_p - 1} \\ (6-11a) \quad &= \frac{2.15 \times 10^{-3}}{0.252} = .0085 \text{ sec} \end{aligned}$$

Hence, a very large pile would be extremely difficult to control.

In the theory used above, we have consistently neglected the slowing down time $\bar{\theta}$, compared to τ_0 . To see if this was justified, let us calculate $\bar{\theta}$:

$$(6-12) \quad \bar{\theta} \approx \frac{2}{\xi^0 \Sigma_s v_c}$$

where v_c is approximately the velocity corresponding to the lowest resonance of U^{238} , which occurs at a neutron energy of about 5 ev. Hence

$$\frac{v_c}{v} = \sqrt{\frac{5}{1/40}} = 14.1$$

and

$$\bar{\theta} \approx \frac{2}{.158 \times 5 \times 10^{-24} \times 8 \times 10^{22} \times 14.1 \times 2 \times 10^5}$$

$$\bar{\theta} \approx .000011 \text{ sec} \ll \tau_0$$

Having designed the pile so that the shortest period τ_m is determined by the delayed neutrons, we can calculate the value of τ_m from the in-hour equation

$$(6-13) \quad \frac{k_0}{k_0 - 1} = \frac{\tau_0}{\tau_{ke} - \lambda_{Lf}^2} + \sum_i \frac{\beta_i \tau_i}{\tau + \tau_i}$$

when $k_0 = 0.003$ and the values of β_i and τ_i are given in Section 6-2.

$$(6-13a) \quad \frac{.003}{1.003} = \frac{.00215}{1.14 \tau_m} + \sum_i \frac{\beta_i \tau_i}{\tau_m + \tau_i}$$

This equation is most easily solved either by a graphical method or by trial and error. The solution turns out to be $\tau_m \cong 9$ sec. This is the shortest possible period with which the pile can rise; hence the pile can always be kept under control.

6-9 Conclusion

These illustrative calculations have been made to demonstrate the application of elementary pile theory to the design of chain-reacting units. Many important factors have been neglected; for instance, no provision has been made for possible changes in the value of k as the pile temperature changes. Nor has any attempt been made to embody any engineering features into the design; for example, the removal of the power developed. The design of a more practical unit is left as an exercise for the reader.

II. Experimental Basis of Pile Theory

The Detection of Charged Particles

The preceding chapters contain what might be called the heart of pile theory. Problems of critical size, the time behavior of the neutron density, etc., have been discussed and some of the considerations which determine the choice of materials and of concentrations in the design of an actual pile have been set forth. The models which have been developed are often fairly complicated, although there is nothing really deep or difficult in the treatment.

From time to time there have been described rather idealized experiments. It is now time to check up on the theory in a more realistic fashion. It will turn out that this check-up can be used not merely to verify the general correctness of the theory developed, but also to improve upon the detail of theoretical prediction by an adjustment of the constants so that the greatest amount of data is fitted inside the theoretical framework.

In order to handle adequately the experimental problem, it is necessary to have a reasonably good idea of the instruments used in experimentation. It is therefore our intention to give a brief discussion of most of the instruments employed in real experiments. As we proceed with the description of the instruments, we shall describe sample experiments in

which they are used. These sample experiments are also chosen for their usefulness in the development of the nuclear energy field.

6-10 The Ionization Process

A charged particle, on passing through matter, loses energy mainly by the processes of ionization. The rate at which the energy is lost depends on the charge and mass of the particle as well as on its velocity; the total energy lost is, of course, the initial energy of the particle. The distance the particle goes before losing all of its energy (the range of the particle) is thus determined by the type of particle (charge and mass) and the initial energy of the particle. Range-energy relationships have been discussed in previous chapters (Chapter 1, Sections 1-25 and 1-26).

6-11 The Scintillation Method

One of the first methods used to detect charged particles consisted in allowing them to fall on a screen having a high efficiency for conversion of the energy of ionization into visible radiation. Whenever and wherever a flash of light (scintillation) was observed on the screen, it could be inferred that a charged particle had hit the screen. Such fluorescent screens (zinc sulphide was, and still is, mainly employed as the fluorescent material) were used by Lord Rutherford and his co-workers in their classic experiments on the scattering of alpha particles. Fluorescent screens are now extensively employed for the detection of electrons in cathode ray tubes. (An obvious extension of this technique is used in the production of the visible images observed on television screens.)

6-12 The Photographic Method

Photographic plates may also be used to make visible the effects of ionization. When a charged particle moves through a photographic emulsion, the ionization in its wake sensitizes some of the grains; upon developing the emulsion, a line appears along the track of the particle. The use of photographic plates for the detection of charged particles introduces the possibility of measuring more than the mere presence of the particle. From the length of the track (and the density of the emulsion) we have a measure of the range (and, thus, of the energy) of the particle, if we know the identity of the particle. The relative spacing of developable grains in the

track gives a measure of the nature of the particle, since the closeness of sensitized grains depends on the density of ionization, which in turn depends on the mass and charge of the ionizing particle. Thus, a combined measurement of the range and density of ionization can identify the particle and yield a measure of its energy.

Photographic emulsions have been developed which have a threshold of sensitivity such that the ionization due to electrons will not leave a developable track, while the greater specific ionization due to heavy particles (say, protons or alpha particles) will result in a line on the developed plate. Thus, heavy particles may be observed in the presence of a large background of gamma or beta radiation, which would render ordinary photographic plates uniformly black. Recently, emulsions have been produced which will respond only to the dense ionization of fission fragments, while lighter particles produce no effects. Such plates, impregnated with uranium and exposed to thermal neutrons, have been used to study the fission process. Their great advantage lies in the fact that the presence of the large alpha particle background due to the natural radioactivity of uranium and its decay products does not disturb the observation of the tracks due to fission fragments.

One of the most useful applications of photographic plate detection of ionizing radiation is in the health-monitoring business. Ordinary photographic film is sensitive to γ and β radiation, and exposure to such radiation results in a uniform blackening of the film. The amount of blackening is determined by the sensitivity of the film and the total amount of radiation to which it has been exposed. Thus, individuals who are subject to exposure to ionizing radiations can carry on their persons strips of film. After a suitable period of exposure, the film can be developed and the total amount of radiation to which the person has been subjected can be determined by a simple comparison of the blackness of the developed film with samples of identical film exposed to known amounts of radiation. Due to the wide range of sensitivity obtainable in different films, such radiation monitors can be made to cover a very wide range of possible exposures.

6-13 The Cloud Chamber Method

In actual practice, the measuring of tracks formed in the emulsion of a photographic plate is very laborious, since it involves searching for and measuring each track under a microscope. Mainly for these reasons, the photographic plate technique is seldom used for observing charged particles. Instead, an instrument is widely used which allows for the visual observation of charged particle tracks in a gas, where the range is much greater and the measuring much simpler. Such a device is the Wilson Cloud Chamber.

In the operation of a cloud chamber, a gas, saturated with water or alcohol vapor, is suddenly expanded; the saturated vapor will then condense, provided that there are present, in the gas, centers around which the condensation can take place. Such nuclei of condensation are provided by ions which are present at the time of the expansion. Thus, if a charged particle has traversed the chamber shortly before the expansion, its track will be observed as a line of droplets. The track can be photographed, the range and density of ionization observed, and the particle thus identified.

The photographic plate technique has the one advantage that plates sensitive only to certain particles can be employed, while cloud chambers are sensitive to all charged particles; cloud chambers, on the other hand, are considerably more flexible instruments. For instance, it is possible to apply a magnetic field in the region of the cloud chamber to measure the curvature of the track and, thus, to obtain a measure of the momentum of the charged particle which, together with a measurement of the range, completely identifies the particle in a much more satisfactory fashion than the simultaneous (difficult) measurement of density of ionization and range. In addition, it is possible to arrange that the cloud chamber be expanded only after a particle in which we are interested has passed through, thus eliminating the necessity for studying many pictures in order to observe one interesting track.

6-14 The Electroscope

The first instrument developed to detect charged particles by electronic means was the electroscope. Such instruments can be made simple and rugged and are still extensively used in radioactivity measurements.

We shall briefly describe a simple electroscope, discussed and dem-

onstrated in all elementary physics courses. This instrument is a condensor, one of the elements of which ends in a pair of gold leaves, as pictured in Figure 6-1.

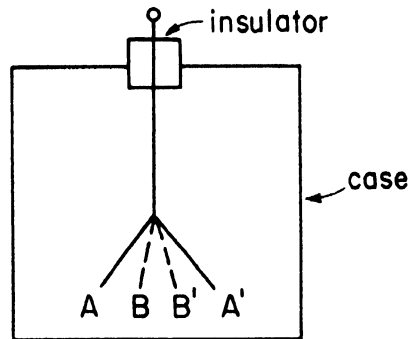


Figure 6-1.

The case serves as the second element of the condensor. When the two elements are connected across a source of potential difference, they become oppositely charged; the gold leaves (A and A') separate, due to the electrostatic repulsion of like electrical charges. If, now, the source of potential difference is removed and the gas in the condensor is ionized, charges opposite to those accumulated migrate to the elements of the condensor, the net charge on the elements and the potential difference between the elements decrease, and the leaves collapse to, say, positions B and B'. The separation of the gold leaves is a measure of the potential difference between the elements. The rate of collapse of the gold leaves is a measure of the rate at which the gas in the chamber is being ionized and, thus, of the intensity of the ionizing radiation. Such an instrument is very useful in the detection and intensity measurement of γ and β radiation.

Electroscopes have been developed in which the moving element is considerably more sensitive to small changes in potential difference than the one described above. One such (the Lauritsen electroscope) uses as the moving element a very light quartz fibre. This instrument can be made small and sturdy enough to be carried around in the pocket, like a fountain pen, and is very useful as a health monitoring instrument, to measure the total amount of radiation to which the carrier has been exposed over periods of the order of days.

Electroscopes can also be made to operate in conjunction with extremely sensitive voltmeters (Lindemann electrometer), and these are among the most sensitive ionization detectors at our disposal.

6-15 Ionization Chambers

In the main, charged particles are most easily detected by the use of gas-filled "ionization chambers" and their accompanying (now) standard electronic circuits. A simple ionization chamber is shown in Figure 6-2. The charged particle ionizes the gas in the chamber. Due to the difference in potential between the electrodes of the chamber, a current flows. This current produces a potential at point A, proportional to the magnitude of the current, which is detected by the vacuum tube and amplified by the electronic detector.

Such a chamber is most useful in measuring the intensity of beams of electrons or gamma rays. If the intensity of the beam is increased, the ionization in the chamber increases and the current to the plates increases.

Single particles may also be detected in an ionization chamber if the ionization pulse due to a single particle is great enough to give an observable current. This criterion is usually obeyed in the case of heavy particles. (Because heavy particles have much shorter range than electrons of the same energy, they can be stopped in the gas of the chamber.) It is thus possible to observe the pulse due to the stopping of a fission fragment in the gas. If one of the plates is coated with uranium, slow neutrons may be observed by the pulses resulting from capture of slow neutrons by U^{235}

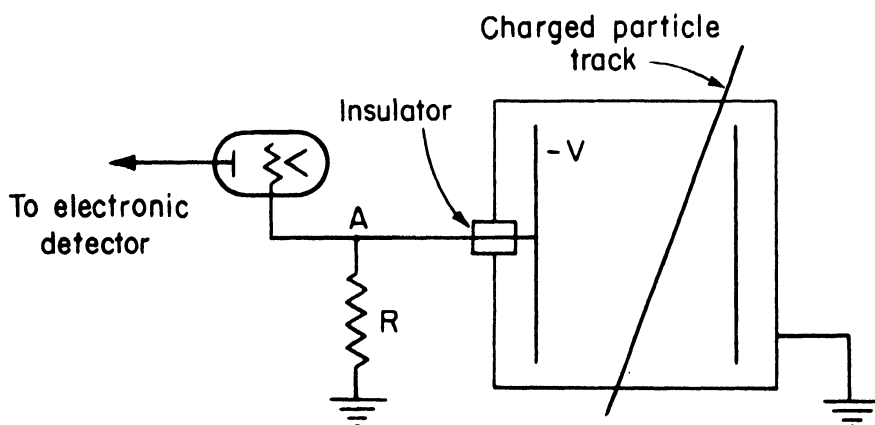


Figure 6-2.

leading to the production of fission fragments which penetrate into the gas. The number of such pulses observed per unit time is then proportional to the intensity of the slow neutron beam impinging on the uranium. An ionization chamber used in this way is called a "fission chamber." Fast neutrons may also be detected in a fission chamber because of the fact that they can produce fission in U^{238} . Thus, a fission chamber in which uranium depleted in the U^{235} isotope is used, or from which slow neutrons are eliminated by surrounding the chamber with cadmium or boron, can be used as a detector of fast neutrons.

Another method of detecting slow neutrons is by filling an ionization chamber with a boron-containing gas. The absorption of a neutron by the B^{10} isotope results in the emission of an energetic alpha particle which can then be detected by its ionization. If the chamber contains only enough gas so that a small fraction of the impinging neutrons is absorbed, the number of pulses, or the total current, depends on the cross section of boron for the particular neutrons in the beam. Since the cross section of boron for slow neutron capture obeys a $1/v$ law, the efficiency of such a chamber for neutron detection is inversely proportional to the velocity of the neutrons. If, on the other hand, the amount of boron is such that all of the impinging neutrons are absorbed (this implies a large chamber, made smaller by the use of the separated B^{10} isotope), then the efficiency of the detector will be independent of the energy of the slow neutrons and, in fact, equal to one. Most boron-filled chambers have efficiencies lying between the two extremes discussed above.

When an ionization chamber is used to detect pulses due to individual charged particles, a measure of the energy of the particle may be obtained from the total ionization in (or the height of) the pulse. In such uses, however, the geometrical shape and size of the chamber are of great importance. If, for instance, the linear dimensions of the chamber are comparable to the range of the charged particles, many of the particles will produce part of their ionization in the walls of the chamber, and the pulse heights will no longer be a measure of the energy of the particle. This difficulty may be minimized by using large chambers and by increasing the pressure of the gas in the chamber. (Still, it will always be necessary to apply a cor-

rection for the fraction of particles ending their paths in the wall of the chamber.) Another difficulty encountered in this use of "pulse ionization chambers" is the fact that the shape and height of the pulses are usually strongly dependent on the position in the chamber at which the ionization occurs. This difficulty in the measurement of particle energies has been overcome by the technique of placing a grid at an appropriate position between the plates of the chamber. The presence of the grid (for reasons which we shall not go into at this point) tends to equalize pulses of the same energy originating in different parts of the chamber.

6-16 Proportional Counters

Pulse ionization chambers are most conveniently employed when the particle energies are quite large (fission fragments or high energy alpha particles). For particles of low energy, the pulses resulting from a single particle are usually too small to be observed (or accurately measured) above the "noise" background due to random fluctuations in the electronic elements. In such cases, the particle pulses may be amplified in the ionization chamber by employing fields strong enough to produce additional ionization in the chamber gas, due to electrons originally freed by the charged particle. In parallel plate chambers (of the type discussed in the preceding section) the required uniformity of the electric field demands exceedingly careful machining of the plates, while the voltages required to produce such strong electric fields are excessively high. A simple modification may be used to overcome these difficulties.

In the chamber shown in Figure 6-3, the plates are concentric cylinders. (A wire is used for the anode.) The electric field in such a chamber is nonuniform, increasing towards the wire like $1/r$. (r is the perpendicular distance from the center of the wire.) Thus, even with the employ-

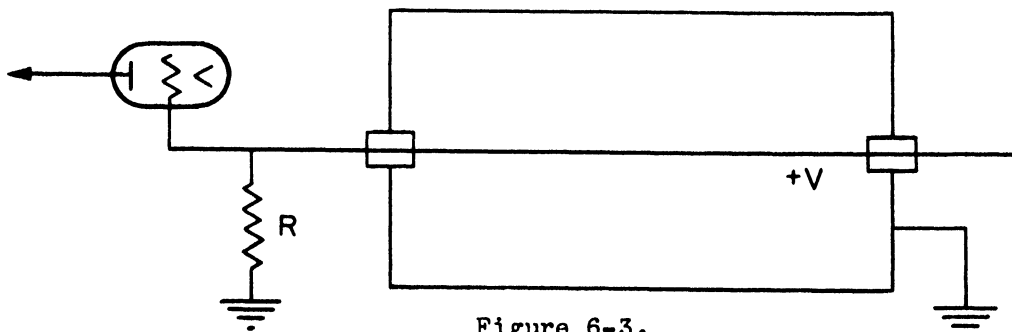


Figure 6-3.

ment of moderate potential differences, the field in the vicinity of the wire is sufficient to produce an observable pulse. In the chamber shown, it will be noted that the electrons are collected (by the anode) to produce the pulses. This technique has the advantage, over the collection of the positive ion current, that the electrons are lighter and hence move faster (through the same potential drop) and are more rapidly collected than are the positive ions. Hence, by cutting down the collection time, the frequency with which particles may be counted is increased and the "resolving time" of the system is decreased. This improvement is very useful when one wishes to count pulses resulting from a high flux of ionizing particles, or when one wishes to resolve events separated by very short times. The resolving time of such counters may be made smaller than a microsecond (compared to $\sim 10^{-5}$ sec for positive ion collection).

The pulse heights in such systems are still proportional to the original ionization produced by the charged particles as long as moderate multiplication ($\lesssim 100$) is employed. Such counters are known as "proportional counters." They are often filled with a boron-containing gas for the detection of slow neutrons, or with hydrogen for the detection of fast neutrons.

In the latter case, the neutrons are detected by the fact that they can give up, in a collision with a proton, a large fraction of their original energy. The recoil proton is then detected by its ionization, and the original neutron energy obtained from the energy given to the recoil proton by applying the laws of conservation of energy and momentum (provided that the angle between the neutron and recoil proton is known).

Since such a measurement requires an accurate knowledge of the direction of the original neutron and of the recoil proton, before the neutron energy can be ascertained, the proportional counters used are never as simple as the one drawn above. In practice, the best measurements of neutron energy by the proton recoil method have employed argon-filled chambers in which the recoil protons originate from a thin paraffin radiator placed at one end of the chamber. The neutron beam is first collimated, so that the original neutron direction is accurately known. The counter is divided into several parts by the insertion of a number of diaphragms with holes in them to allow the passage of a beam of protons moving along the direction of the wire. The

several parts are operated as separate counters and an electronic coincidence circuit registers only such pulses as occur simultaneously in a sequence of counters (starting from the paraffin radiator). In this way the angle of recoil is specified, and the range is measured by counting the number of segments through which the protons penetrate. This method, although it results in an accurate measure of the energies of the impinging neutrons, suffers from the fact that only a very small fraction of all of the recoil protons are measured; hence, it can only be employed when very high neutron fluxes are available.

Other techniques have been worked out for measuring fast neutron energies by observing proton recoils in a proportional counter, but it can be stated as a rather general rule that any system which is devised to use a larger fraction of the proton recoils (than the one described above) does so at the expense of introducing less resolution in the neutron energies measured.

Proportional counters are also employed in the accurate measurement of the energies of alpha particles emitted in natural and artificial radioactivity.

6-17 Geiger-Mueller Counters

Let us consider an experiment in which the pulse heights, due to particles (say, electrons) of a given energy impinging on the counter at a given point from a given direction, are measured as a function of the potential difference between the electrodes. Curves of the nature of those shown in Figure 6-4 may be observed (differing in detail from counter to counter).

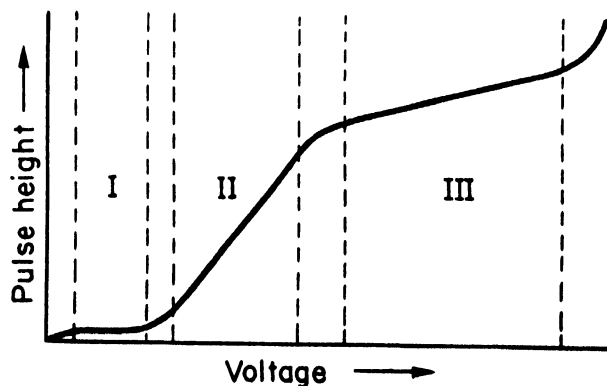


Figure 6-4

In region I, the ionization chamber region, all of the electrons are collected, there is no electron multiplication, and the pulse height is independent of the voltage. In region II the magnification is small (up to ~ 100) and essentially independent of the original particle energy, and the final pulse height is proportional to the original particle energy (for constant voltage). In this range of voltages the counter behaves as a proportional counter. In region III the magnification in pulse height is large, and no longer linear with increasing voltage. Almost all particles going through the sensitive region of the counter produce large pulses. A counter operating in this voltage range is called a Geiger-Mueller or Geiger counter.

Although the mechanism of operation of Geiger counters is not completely understood, it is known that the ionization produced by a single charged particle causes a discharge between the electrodes, which can be quenched by a suitable circuit or by the use of a suitable (self quenching) gas; mixtures of argon and alcohol have been extensively used to fill Geiger counters, although other gases are frequently employed. In the region to the right of III, the voltage is so high that a discharge, once set up, perpetuates itself and a single ionizing particle will result in a large number of pulses.

In practice, the best operating voltage of a Geiger counter is found by exposing it to a source of electrons (the energy distribution is practically immaterial) and plotting a curve of pulse rate versus voltage, as shown in Figure 6-5. Region II is the proportional counter range. In region III, the Geiger counter range, the pulse rate is almost independent of voltage (increasing by a few per cent per 100 volt increase for a good counter). The operating voltage is usually chosen somewhere around the middle of the "plateau" in region III.

Geiger counters are most extensively used in the detection of electrons in problems where the number of particles striking the counter (rather than their energies) is of greatest interest. It should be noted that the use of a Geiger counter does not preclude a measurement of the energy of the impinging particle. Energies may be found by obtaining an absorption curve, wherein the number of particles reaching the counter is determined as a function of the thickness of absorber placed between the source of particles and the counter.

The efficiency of a Geiger counter for detecting electrons is approximately 100 per cent, provided that the electron has enough energy to pene-

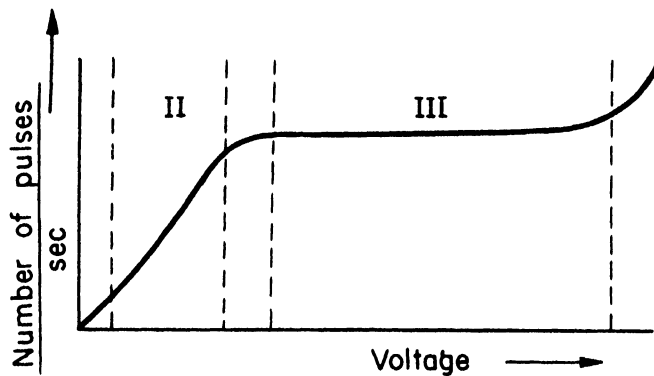


Figure 6-5

treat the wall of the counter. For detecting low energy electrons, counters with thin windows may be employed, or the source of electrons may be placed inside the counter.

Gamma rays and x-rays (photons) may also be detected by the use of Geiger counters, although the efficiency for their detection is usually quite small (~ 1 per cent). The detection of photons is based on their ability to produce recoil electrons in the walls of the counter (by the processes of Compton recoil or photoelectric effect); the electrons are then detected. Since the probability for a photon to produce a recoil electron is strongly dependent on the energy of the photon, the efficiency of a Geiger counter for photon detection is thus also strongly dependent on the photon energy. The efficiency for photon detection is also a function of the material out of which the counter wall is made. By a suitable choice of material for the walls, counters may be obtained whose efficiency for photon detection is quite high (~ 10 per cent) and for which the curve of efficiency of detection versus photon energy is predictable.

III. Neutron Detection and Neutron Flux Measurement by the Radioactivation of Foils

6-18 The Radioactivation of Foils in a Pure Thermal Neutron Density

Consider a thin foil of a pure isotope placed in a region in which there exists a density, n , of thermal neutrons, neutrons of no other energy being present. By "thin" is meant that only a small fraction of the neutrons traversing the foil are absorbed. In such a foil the rate of production of active nuclei is given by

$$n \nu \sigma_a N_a V$$

where σ_a is the cross section for neutron absorption leading to activation per nucleus, N_a is the number of nuclei (atoms) per unit volume, and V is the total volume of the foil. If the active nuclei thus produced disintegrate with a mean life τ_a , the equation which expresses the rate of change of active nuclei while the foil remains in the thermal neutron flux, nv , is

$$(6-14) \quad nv\sigma_a N_a - \frac{N}{\tau_a} = \frac{\partial N}{\partial t}$$

In this equation N is the number of active nuclei per unit volume. The general solution of this equation is

$$(6-15) \quad N = nv\sigma_a N_a \tau_a (1 - e^{-t_e/\tau_a}) + N_0 e^{-t_e/\tau_a}$$

We have now written t_e for the time that the foil remains in the thermal neutron flux (exposure time) and N_0 for the initial density of active nuclei in the foil. If $t_e \gg \tau_a$, we obtain the "saturated" density of active nuclei, which is given by

$$(6-15') \quad N = nv\sigma_a N_a \tau_a$$

This expression also follows from Equation (6-14) by considering that after a long exposure time an equilibrium condition obtains, wherein active nuclei are formed as fast as they decay, and $\frac{\partial N}{\partial t} = 0$.

On the other hand, if $t_e \ll \tau_a$, we obtain

$$(6-15'') \quad N = nv\sigma_a N_a t_e + N_0 (1 - t_e/\tau_a)$$

In standard practice, in order to simplify the analysis, it is usual to use foils for which N_0 is sufficiently small that the second term on the right-hand side of Equation (6-15) will always be negligible compared to the first term for the exposure times contemplated. (Another possible working condition is given by

$$(6-16) \quad n v \sigma_a N_a \tau_a \gg N_0$$

In this case the number of active nuclei minus N_0 is exactly the same as it is in the case in which N_0 is completely negligible.)

In order to measure the number of active nuclei produced by our exposure to thermal neutrons, we need to measure the rate of disintegration or the total number of disintegrations in the foil in a given time. It is possible to obtain a measure of the activation of the foil by placing it in a standard geometry near a standard Geiger-Mueller counter. If it takes a time t_w after exposure to move the foil into the standard geometry and to start the count, the number of active nuclei at the time that the count is started is given by

$$(6-17) \quad N = n v \sigma_a N_a \tau_a (1 - e^{-t_e/\tau_a}) e^{-t_w/\tau_a}$$

If we count for a time t_c , the total number of disintegrations is therefore given by

$$(6-18) \quad \int_{t_w}^{t_w+t_c} N \frac{dt}{\tau_a} = n v \sigma_a N_a \tau_a (1 - e^{-t_e/\tau_a}) e^{-t_w/\tau_a} (1 - e^{-t_c/\tau_a})$$

This number is not, however, the number of counts recorded by the Geiger-Mueller counter. The number of counts recorded is less by a factor ϵ_c , which represents the efficiency of the counter for counting a disintegration in the foil placed in a given geometry. Let us now define A by the following equation:

$$(6-19) \quad A \equiv \frac{C}{(1 - e^{-t_e/\tau_a}) e^{-t_w/\tau_a} (1 - e^{-t_c/\tau_a})} = \epsilon_c n v \sigma_a N_a \tau_a V$$

in which C is the number of counts recorded. A is then a measured activation which takes into account the whole experimental setup. It is a function only of:

- (1) The counter and foil geometry (\mathcal{E}_0)
- (2) The particular foil employed ($\sigma_a N_a \tau V$)
- (3) The flux of neutrons in which it was exposed ($n\nu$)

By using the same foil, counter, and geometry, we can intercompare neutron fluxes. By measuring A with the same foil, in the same flux, using the same counter, but in different geometries, we can standardize our geometry factors. By measuring a sequence of foils exposed in the same flux and counted on the same counter in the same geometry, we can standardize the foils, finding the so-called foil factors. In order to guard against errors due to changes in the counter, it is useful to maintain a standard thermal neutron flux. Employing this flux with a given foil and geometry, it is possible to watch for any changes in the counter efficiency and to correct for them if they occur. Only one measurement of an absolute neutron flux is then needed to reduce all our measurements to absolute terms.

It is not necessary to restrict our treatment to the thin foils which we have considered so far. If the foils employed are thick, the theory which we have developed is not rigorous. A correction which accounts for the shielding of one atom, which might be activated, by other atoms in the foil must be introduced. However, for relative measurements it is not necessary to introduce this correction explicitly into the theory since it may be lumped into the foil factors. On the other hand, it is not desirable to use extremely thick foils which absorb a large number of neutrons. If this is done, the neutron flux being measured is perturbed by the presence of the foil. When this perturbation is sufficiently large to change the experimental conditions in other parts of the experiment, we may fail to measure what we are attempting to determine. It is not a question of using infinitesimal foils, because the perturbation involved usually does not affect the measurement through the decrease in neutron density at the position of the foil itself, but usually enters only when the perturbation is sufficiently large to extend to other parts of the experimental setup.

It is also not necessary to restrict ourselves to foils which contain only a single isotope. If more than one isotope is present, it is necessary to modify the equation which gives the activation by considering the activations produced by the various isotopes. We then have a sequence of activation cross sections and a sequence of nuclear densities for the vari-

ous isotopes leading to a sequence of equations like (6-14), one for each isotope. If the periods of the active nuclei produced on exposure to neutrons are the same, this modification is of no consequence. On the other hand, if the periods differ, it is necessary to concentrate on one of them. Various methods may be employed to sort out a single period. Often the beta rays emitted in radioactive disintegrations are of different range, and a single period may be sorted out by an absorption method. Again, it is possible that the periods are sufficiently different that the radioactive decay pattern may be analyzed as a function of time to determine the various periods which enter. This type of analysis is performed in a standard fashion by taking a series of measurements of the decay rate as a function of time; different exposure times may be used to accentuate the different periods.

The recorded count C which enters Equation (6-19) may have to be corrected for a background count. Such a background count always exists, even in the best shielded counters; but in experiments involving the neutron fluxes produced in piles (even those run at low power) the problem is usually shifted to that of finding a time of exposure t_e and a counting time t_c such that the count due to the foil is much larger than the background count normally present. For accurate work, or for any work at low neutron fluxes, it is necessary to measure the background and to subtract this from the count as actually recorded by the Geiger-Mueller counter.

If neutrons of velocities other than thermal velocity are present, we can expect that a real foil will not simply ignore them. It would be desirable to eliminate their influence by finding a filter which screens out all high energy neutrons. Unfortunately, no such practical filter exists. Fast neutrons penetrate any reasonable thickness of any known material. In the next section, we shall describe a simple technique for eliminating the effects of fast neutron activation when we want to measure the effect due only to thermal neutrons.

6-19 The Cadmium Difference Method

We are able to get around the problem of finding a fast neutron filter if we are able to find a slow neutron filter. Such a filter is cadmium. By measuring with a foil, say indium, first covered with cadmium and second, uncovered, we are able to measure first an activation which depends on the fast neutrons present, and second, an activation which depends on all the

neutrons present. We denote these activations, respectively, by A_f and $A_f + A_{th}$. The difference, A_{th} , of these two measurements is a measure of the thermal neutron flux in the region which is shielded from activation when the cadmium surrounds the foil. The absorption of cadmium is such that fast neutrons penetrate through a cadmium sheet, but thermal neutrons are absorbed almost completely. Consequently, A_{th} can be associated with the thermal neutron activation discussed in the last section.

The crude cadmium difference scheme just outlined can be refined by making a series of measurements with differing thicknesses of cadmium around the foil. From such a series of measurements it is possible to make a good estimate of the decrease in the resonance activation (high energy activation) of the foil as a result of the presence of cadmium and also of the leakage of thermal neutrons through the cadmium filter. In this way, an extremely accurate estimate of both A_f and A_{th} can be made. In practice, this procedure is used to approximate the ideal thermal detector which was employed in the ideal experiments of earlier sections.

6-20 Resonance Activation as a Measure of the Slowing Down Density

In order to obtain an accurate measure of the slowing down density, q , at a given energy, it would be desirable to have a foil consisting of nuclei which have a sharp absorption resonance in the energy region in question and no absorption elsewhere throughout the energy spectrum. In practice, it is possible to find detectors which have essentially only one sharp resonance. However, even these detectors have the property of mixing in a measurement of the thermal neutron density with their measurement of the neutron flux in the resonance region. By covering such detectors with cadmium, however, it is possible to eliminate the thermal neutron effect almost completely and, as was pointed out in the last section, by employing different thicknesses of cadmium it should be possible to get an accurate measurement of the resonance activation of the foil.

Employing, then, the methods of the last two sections, such cadmium-covered foils should yield a resonance activation, A_r , which is given by

$$(6-20) \quad A_r = \xi_0 \int n v \sigma_a N_a \frac{dE}{E} \tau_a V$$

In this equation, the integral is to be taken over the resonance region of the detector material. Also, nv is the neutron flux per unit logarithmic energy interval in the resonance region. This nv can be related to the slowing down density q by:

$$(6-21) \quad q = nv\sigma_s N_s \xi$$

If we use this formula to introduce q into Equation (6-20), we obtain for A_r

$$(6-20a) \quad A_r = \xi_c q \frac{\sigma_a(th)N_a}{\sigma_s N_s \xi} I_a \tau_a V$$

$$\text{where } I_a = \int \frac{\sigma_a(E)}{\sigma_a(th)} \frac{dE}{E}$$

and $\sigma_a(E)$ is the resonance activation cross section, which is a function of the neutron energy, E .

Equation (6-20a) shows that A_r depends not only on the variables (1) and (2), as was the case for the thermal neutron activation, and on q , but also upon the characteristics of the moderator--in particular, upon the so-called slowing down power, $\sigma_s N_s \xi$. We find, therefore, that it is only possible to intercompare slowing down densities in this simple fashion when the moderator is always the same or when the slowing down powers of the moderators employed are well known. Fortunately, the scattering cross sections of moderators can be measured with comparative ease. The nuclear density can be measured with no trouble at all. And there is now reason to believe that the average logarithmic decrement in energy per collision, ξ , can be predicted from the theory with substantial accuracy.

IV. Application of Measuring Techniques

6-21 Measurement of Pile Power Levels

The ionization chambers and counters described in Sections 6-15, 6-16, and 6-17 are employed for making the measurements required in building and operating a chain-reacting unit. The total power developed in a pile of uniform composition is proportional to the neutron density integrated over the volume of the pile; to a good approximation, the space distribution of neutrons in a pile is determined only by the geometry of the pile. Therefore, it is

sufficient, in order to find the power developed, to measure the neutron density at one point in the pile. To do this, we may place a boron-filled ionization chamber of known efficiency at some point in the pile. The ionization produced in this chamber can be continuously observed, so that we can obtain a continuous record of the power at which the pile is operated.

If the pile is operated over a very wide range of power levels, we cannot reasonably expect that a single ionization chamber will cover the entire range. If the sensitivity is such that easily measurable currents are obtained at the highest neutron fluxes, then the current from the ionization chamber at low power levels will be too small to be detected. If, on the other hand, the chamber is designed to give measurable currents at very low power levels, then at high power levels the response of the chamber will no longer increase with neutron flux, but will "saturate." Hence, in practice, a number of ionization chambers of different sensitivities are distributed at various places in the pile, so that at any power level there will be at least one ionization chamber of known efficiency capable of yielding a value of the neutron flux in the pile.

In an early section it was pointed out that the criticality of a chain-reacting unit may be increased or decreased by subtracting from the pile or adding to the pile neutron absorbing material. In practice, the control of a chain-reacting unit is usually achieved through the motion into or out of the pile of a rod of material of high neutron absorption cross section, such as cadmium or boron. We leave the development of the theory of "control rods" to a later section, and merely point out that if a pile is just critical when a control rod is inserted a given distance into the pile, then the neutron density may be made to increase by withdrawing, slightly, the control rod from the pile, so that the fraction of neutrons absorbed by the rod is decreased. Likewise, to decrease the neutron density, the control rod is pushed further into the pile. Thus, while the control rod is being moved in and out of the pile and the power level varied to obtain a desired value, the ionization chambers in the pile will provide a means for obtaining a continuous record of the power, and will therefore give the operator the information which he requires for the manipulation of the control rod.

6-22 Measurement of η

In developing the theory of a chain-reacting unit, we have assumed that η , the number of neutrons released per fission, is known. The value of η may be obtained by the following experiment. An ionization chamber, in which one of the plates is coated with a thin layer of uranium (say, U^{235}), is placed in a flux of thermal neutrons. If the thickness of the uranium layer is very much less than the range of a fission fragment, a pulse will result for each fission that occurs, since one of the fragments will always emerge from the plate into the gas. Thus, the rate at which fissions are occurring in the chamber may be measured.

The number of neutrons emitted per unit time can also be measured. In order to make this measurement, we place the fission chamber inside a large block of moderating material--paraffin (or water) and graphite are most commonly used. The neutrons are slowed down by the moderator, and since the moderating materials have negligible neutron capture cross sections above thermal energies, all of the neutrons eventually reach thermal energy, where they are captured by the moderating material. (The leakage is negligible if the block is large enough.) The number of neutrons becoming thermal at any point in the block can be measured by observing the activity induced in an ideal resonance detector. In practice, indium, surrounded by cadmium, is used as the resonance detector, since such a detector is almost entirely activated by neutrons at the energy of the indium resonance (1.4 ev). If the efficiency of the detector is known (i.e., the number of neutrons passing through the indium resonance energy per cm^3 and second corresponding to a given activation of the detector), we obtain the rate of neutron emission from the uranium by integrating the indium activity over the volume of the block. That is: if Q is the rate of neutron emission from the U and A_r , the activity of the indium detector as a function of the distance, r , from the fission chamber, then

$$(6-22) \quad Q = 4\pi \int_0^\infty A_r r^2 dr$$

where B is a number which converts the indium resonance activation, A_r , into q , the number of neutrons per cm^3 and sec passing through the indium resonance energy.

Before describing the method for measuring B , it should be pointed out that the above experiment implies that we have a pure thermal neutron source, so that indium resonance activation can only result from fast neutrons produced in fission of the uranium. Almost-pure thermal neutron sources are obtainable from the "thermal columns", which can be attached to piles. A thermal column is a long block of moderating material (say, graphite), one end of which is next to an operating pile. The neutrons leaving the pile and entering the thermal column have an appreciable fast neutron component; but if the column is long enough, practically all of the neutrons will have been moderated to thermal energy by the time they emerge from the other end. It is possible to correct for the small fraction of fast neutrons present in the beam by repeating the experiment described above, except that the fission chamber is surrounded by cadmium. If the indium resonance activity, in this case, is A_r' , then $A_r - A_r'$ is a correct measure of the number of neutrons resulting, at the distance r from the chamber, from the fission of U^{235} by thermal neutrons, and

$$(6-22a) \quad Q = B \cdot 4\pi \int_0^{\infty} [A_r - A_r'] r^2 dr$$

For the measurement of B , it is only necessary to have a source whose rate of fast neutron emission is constant, and known (and, say, equal to Q_1). The fission chamber is replaced by this source, the thermal neutron flux turned off, and A_{1r} measured in the same block, using the same detectors. Then

$$(6-22') \quad Q_1 = B \cdot 4\pi \int_0^{\infty} A_{1r} r^2 dr$$

and

$$(6-23) \quad Q = Q_1 \cdot \frac{\int_0^{\infty} [A_r - A_r'] r^2 dr}{\int_0^{\infty} A_{1r} r^2 dr}$$

The integrations are usually performed graphically. The number of neutrons emitted per fission is now directly obtainable:

$$(6-24) \quad \eta = Q/F$$

F is the number of fission pulses per unit time occurring in the chamber without the cadmium covering, minus the corresponding fission rate with cadmium around the chamber (see the first paragraph of this section).

6-23 Calibration of Neutron Sources

There remains, still, the problem of measuring the rate of neutron emission from a single, constant source. (For if one Q_1 is determined, all Q 's can be found.) An absolute source calibration has been obtained as follows: the source is put at the center of a mass of slowing down material (say, a tank of water) so large that all of the neutrons are slowed down and absorbed in the moderating material, and the number leaking out the ends is negligible. The size of the water tank required for such an experiment can be reduced to manageable proportions by adding boron to the water to hasten the absorption of the neutrons. If, then, the macroscopic absorption cross section, $N\sigma_c$, of the material is known (N is the number of absorbing atoms per cm^3 , and σ_c the absorption cross section per atom) and the neutron density, $n(r)$, measured, the total number of neutrons absorbed is

$$(6-25) \quad 4\pi \int_0^{\infty} N\sigma_c n(r) r^2 dr = Q_1$$

where v is the velocity of the neutrons. It should be pointed out that if the absorbing material obeys a $1/v$ law (like hydrogen and boron), the velocity of the neutrons need not be known, since $\sigma_0 = \alpha/v$ and $v\sigma_0 = \alpha =$ a constant independent of v . This is true, provided that the detector used to measure n also obeys a $1/v$ law. Such a detector is, for instance, a small boron-filled proportional counter. If such a counter, in which the amount of boron is accurately known, is used for a detector, the number of pulses per second, P , is a direct measure of the neutron density n , since

$$(6-26) \quad P = nv \frac{\alpha_B}{v} N_B$$

(N_B = number of boron atoms in the chamber and $v\sigma_0$ (boron) = α_B). From the definition of α , α_B and by combining (6-25) and (6-26), we find

$$(6-25a) \quad Q_1 = \frac{Na}{N_B \alpha_B} \cdot 4\pi \int_0^\infty P(r) r^2 dr$$

Although such an experiment for the measurement of Q_1 is in principle quite straightforward, it requires, in practice, great care and ingenuity to obtain an accuracy of better than 10%.

In the above description the only physical constants which we have assumed are the absorption cross sections of boron and hydrogen (together with the fact that these cross sections obey the $1/v$ law). For the sake of logical completeness, a description of methods of measuring neutron cross-sections follows.

V. Measurement of Neutron Cross Sections

6-24 Survey of Cross Section Results*

The most straightforward method for measuring nuclear cross sections for neutrons is by a "transmission experiment." In such an experiment a beam

*The author is indebted to H. H. Goldsmith for the critical compilation and analysis of neutron cross sections upon which many of the generalizations contained in this and the following sections are based.

of neutrons is allowed to fall on a slab of thickness t and density N (N = the number of atoms/cm³ in the slab) of the material under investigation and the attenuation of the beam observed, by comparing the reading of a detector with and without the material in the path of the beam. If I equals the intensity transmitted through the material, and I_0 equals the intensity without the material in the beam, then

$$I = I_0 e^{-N\sigma t}$$

where σ = the total atomic cross section for neutron absorption and scattering.

A number of points should be noted: (1) The above formula holds only in the case of "good geometry", i.e., when the distances from source to slab and slab to detector are large compared to the dimensions of the slab and detector. (2) The cross section measured is the total cross section for all nuclear processes. In the case of boron and other materials of high absorption cross section, the total cross section is primarily due to absorption ($\sigma = \sigma_c$). In the case of some other materials, like Bi, the total cross section is almost entirely due to scattering ($\sigma = \sigma_{sc}$). In the case of most materials, the total cross section is the sum of absorption and scattering cross sections ($\sigma = \sigma_c + \sigma_{sc}$). (3) The cross sections for different processes exhibit different energy dependences. Scattering cross sections are almost always constant in the low energy region (unless "crystal effects" are present). The most important exception to this rule is hydrogen, in which the scattering cross section decreases from ~80 barns for very slow neutrons to 20.8 barns for neutrons of 1 ev energy. Most absorption cross sections obey a $1/v$ law. However, many nuclei exhibit absorption resonances in the low energy region. For instance, the neutron absorption cross section of indium has a value of ~200 barns at 1/40 ev, obeys roughly a $1/v$ law in the thermal neutron region, and then rises to a value of ~30,000 barns at the peak of the resonance, at ~1.4 ev. Cadmium, with an absorption resonance at .08 ev, has an absorption cross section for thermal neutrons which does not even faintly resemble a $1/v$ law.

Thus, it is important to know the energy of the neutrons used in a transmission measurement of the total cross section. If a heterogeneous energy distribution is employed in the neutron beam, the cross section measured is an average over the energy distribution of the beam, and is quite

difficult to interpret in terms of the various cross sections involved and their energy dependence, unless these factors are known beforehand. It is therefore highly desirable, in cross section measurements, to use beams of single, known energies, and to be able to vary the neutron energies used. Devices for providing a homogeneous neutron beam of known and variable energy are called neutron "velocity selectors." They will be described in the next section.

As a result of many investigations of total cross sections as a function of neutron energy for many materials, the following generalizations can be made:

(1) Most nuclei have a total neutron cross section in the thermal neutron energy region, made up of a constant scattering cross section and an absorption cross section varying as $1/v$.

(2) Many neutron resonances are observed. The width at half maximum of most neutron resonances is about 0.1 ev. As far as neutron resonances are concerned, nuclei can be divided roughly into three classes: (a) Atomic weight 0-100: there are very few resonances in the region 0-100 ev. (b) Atomic weight 100-200: many resonances are encountered. The average distance between neutron resonances for a given nucleus is ~ 30 ev, but the resonances are distributed in a random fashion. (c) Atomic weight > 200 : most nuclei exhibit neutron resonances, with an average spacing of ~ 30 ev. However, there are some striking exceptions in which no resonances have been observed up to 100 ev; such nuclei, like Bi and Pb, exhibit abnormally low neutron absorption cross sections.

6-25 Velocity Selectors

Three types of velocity selectors are most commonly used in cross section measurements. They are: (1) the mechanical velocity selector, (2) the "time of flight" velocity selector, and (3) the crystal spectrometer. In the following sections these instruments will be described and compared. In comparing velocity selectors, we shall pay particular attention to several characteristics. The first is the "range", which is simply the neutron energy region covered by the velocity selector. The second is the "resolution" of the velocity selector. The resolution is a measure of the spread in energies in the monoenergetic neutron beam emerging from the velocity selector. The resolution, we shall see, depends on the neutron energy, and the spread in neutron energies increases (in any velocity selector) with the energy of the neutron beam. Another characteristic of the whole system of source, velocity selector, and detector is the total neutron intensity, in a given energy

range, as seen by the detector. This property depends on source, selector, and detector, but is essentially correlated with the neutron source in conjunction with which the velocity selector can operate. Thus, a velocity selector which can be used with a pile is capable of yielding a much greater neutron intensity at a given energy than a velocity selector used in conjunction with a cyclotron.

(1) The Mechanical Velocity Selector

The earliest mechanical neutron velocity selectors employed the same principle as was used by Fizeau in his classic measurement of the velocity of light. However, this design is not the most efficient to use on neutrons.

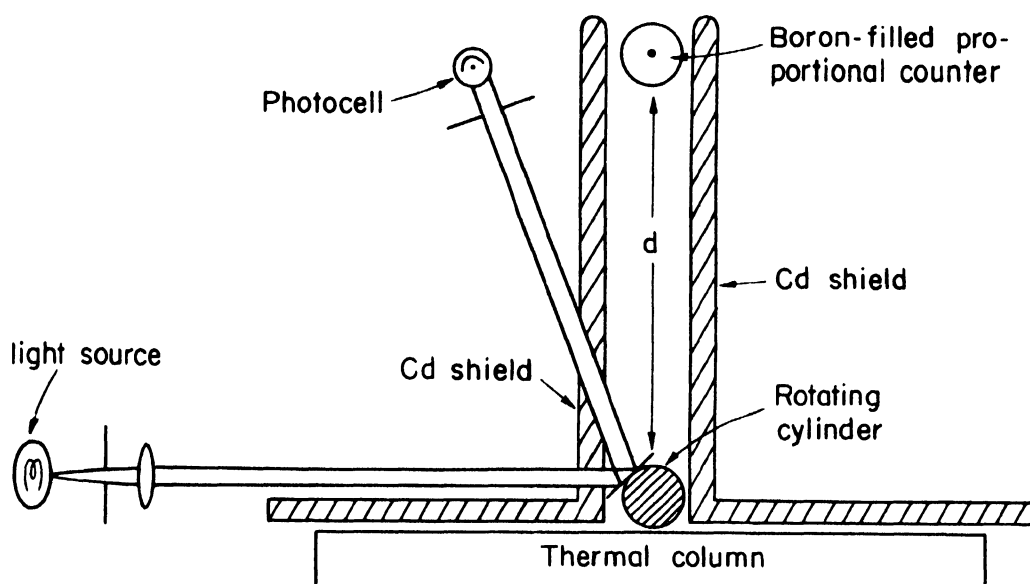


Figure 6-6

Figure 6-6 illustrates a more convenient mechanical selector built and operated by Fermi and his co-workers at the Argonne Laboratories.

The rotating cylinder next to the thermal column consists of alternate thin laminations of aluminum and cadmium, so that slow neutrons can get through the cylinder only when the direction of the layers is parallel to the beam (or perpendicular to the top surface of the thermal column). A mirror, attached to it, rotates with the cylinder so that a beam of light is reflected into a photocell once during each revolution of the cylinder. The time in the cycle at which this reflection takes place is adjustable. The photocell is coupled to the boron-filled proportional counter in such a way

that the counting rate is recorded only when light falls on the photocell. Thus, by varying the position of the mirror, the time, τ , elapsing between the transmission of neutrons through the cylinder and their detection may be varied. Hence, of the multitude of neutron velocities in the beam, only those are detected whose velocity is equal to d/τ . By placing a slab of scattering and absorbing material in the beam (halfway between cylinder and counter), the total cross section of neutrons of a given velocity ($v = d/\tau$) can be measured. This velocity selector works well for neutrons of low energy, up to about .2 ev, but for neutrons of higher energies the energy spread increases, since the maximum speed at which the cylinder can be rotated is limited.

(2) The Time-of-Flight Velocity Selector

The time-of-flight velocity selector is based on the possibility of modulating a source or beam of ions in such a way that the ions fall on a target in short bursts, lasting only a few microseconds. Thus, neutrons may be produced in short bursts. However, this velocity selector can be used only in conjunction with instruments in which the neutron beam is produced by a beam of ions falling on a target. Thus, a cyclotron or linear accelerator is used as the neutron-producing instrument.

The detector is then placed at a distance d from the source and also modulated so that it is sensitive only during a short interval separated from the period of neutron production by the variable time τ .

The neutrons produced by positive ion beams are usually of rather high energies, so that if we wish to have a source of slow neutrons it is necessary to slow the burst of neutrons down by passing them through a slab of paraffin. Fortunately, the time for slowing down in paraffin is short (compared to the times of flight, τ , of interest). Nonetheless, the spread in the slowing down times for different neutrons sets a limitation on the shortest time interval that can be used. The source intensity and detector sensitivity are shown in Figure 6-7.

The velocity of neutrons detected is, then, given by $v = d/\tau$. Since τ is variable, the neutron velocity to which the selector is sensitive is also variable. Again, by placing a slab of material halfway between source and detector, the total cross section of the material can be measured as a function of neutron velocity. Such instruments have been constructed which

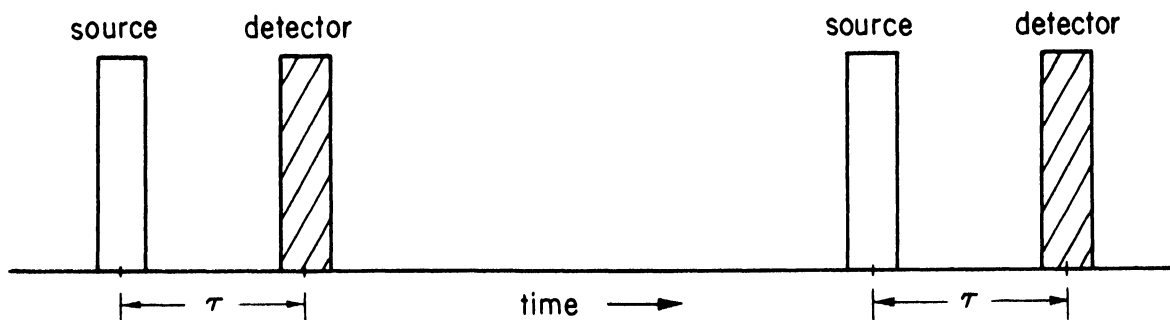


Figure 6-7

have a range up to about 10,000 ev, although the resolution decreases with increasing neutron energy, and is about equal to the neutron energy at an energy somewhere between 100 and 1000 ev, the limiting energy differing from instrument to instrument.

(3) The Crystal Spectrometer Velocity Selector

This selector is based upon the wave properties of slow neutrons. According to the laws of quantum mechanics, a particle of velocity v can be said to behave as a wave of wave length λ , where

$$\lambda = \frac{h}{mv}$$

m = the mass of the neutron = 1.66×10^{-24} gms

h = Planck's constant = 6.62×10^{-27} erg-sec.

From the above relationship, we can see that neutrons of thermal energies ($v \approx 2 \times 10^5$ cm/sec) have an associated wave length

$$\lambda = \frac{6.6 \times 10^{-27}}{1.66 \times 10^{-24} \times 2 \times 10^5} \approx 2 \times 10^{-8} \text{ cm}$$

This wave length is of the same order as the wave lengths of x-rays, and also of the distance between planes in a crystal, so that we should expect interference effects when neutrons are reflected from crystals, in much the same way as x-ray interference patterns are obtained on reflection from crystals. Thus, if a beam of slow neutrons, of wave length λ , is reflected from the surface of a crystal, we should expect reflection maxima at angles given by the Bragg relationship.

$$n\lambda = 2d \sin \theta$$

n = an integer (1, 2, 3,)

d = the distance between crystal planes

θ = the angle of incidence and reflection

From these considerations it follows that if a beam of neutrons of heterogeneous energies is allowed to fall on the face of a crystal, most of the reflected neutrons will have a velocity

$$v = \frac{nh}{2md \sin \theta}$$

Thus a crystal can be used in conjunction with the neutrons coming from a pile to provide monokinetic beams of neutrons, the velocity of which can be varied by varying the angle of incidence of the neutron beam. An experimental setup for such a velocity selector is shown in Figure 6-8.

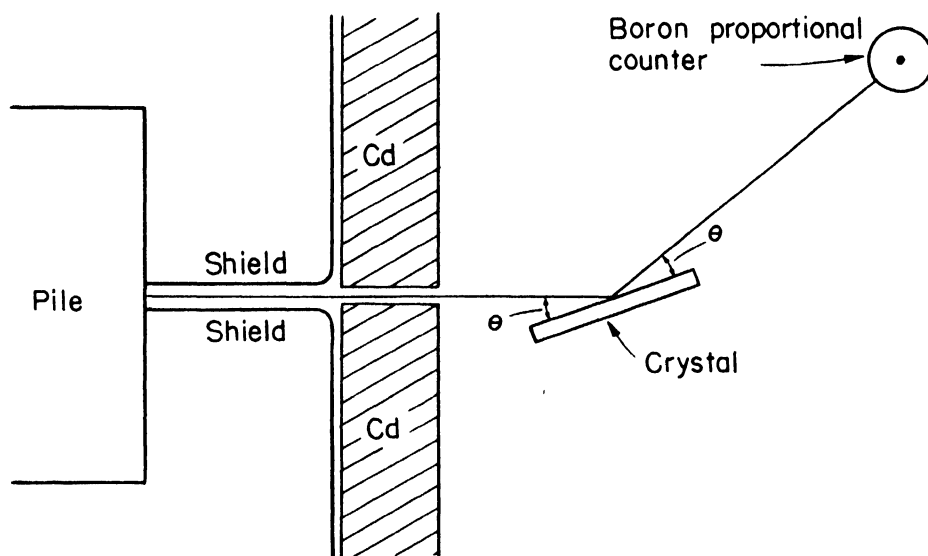


Figure 6-8

Again, by placing the material under investigation between the crystal and the detector, the total cross section of the material can be measured as a function of neutron velocity. The crystal spectrometer is limited to neutrons of energies between $\sim 0.01 - 100$ ev because at high velocities the angles of incidence become very small and at large angles (low velocities) higher order reflections for the neutrons most abundant in the thermal distribution (energy ~ 0.025 ev) make the reflected beam polykinetic.

Table 6-2 compares the three velocity selectors described above with regard to the three criteria discussed at the beginning of the section on velocity selectors.

TABLE 6-2

<u>Selector</u>	<u>Range</u>	<u>Resolution</u>				<u>Neutron Source</u>
		<u>.025 ev</u>	<u>1 ev</u>	<u>10 ev</u>	<u>100 ev</u>	
Mechanical	0-.2 ev	~.005 ev	---	---	---	pile, Ra-Be and paraffin
Time of flight	0-10,000 ev	~.001 ev	~.1 ev	~1 ev	~20 ev	cyclotron, linear accelerator
Crystal	.01-100 ev	~.001 ev	~.5 ev	~10 ev	---	pile

The mechanical velocity selector is seen to be useful only at low neutron energies. The time of flight and crystal spectrometer velocity selectors are about equally good up to ~.05 ev, after which the crystal spectrometer resolution becomes rapidly worse, while the time of flight selector maintains a fairly good resolution up to about 10-50 ev.

6-26 Special Techniques

A number of specialized techniques have been developed for detecting neutrons of certain definite energies, and these are worth mentioning at this point. One of these is the use of resonance detectors to select neutrons of a definite energy. Thus, if a heterogeneous neutron beam impinges on a slab of material, and the detector is, let us say, a foil of indium surrounded by Cd, then the cross section measured is primarily that for neutrons of the indium resonance energy, or ~1.4 ev. Thus, by the use of this detector, cross sections of various materials for 1.4 ev can be measured. Other resonance detectors can be used to measure cross sections for different neutron energies. This technique has been developed by many experimenters, mainly by Goldhaber and his collaborators. The weakness of this technique is that it is difficult to correct for the effects of other resonances occurring at energies higher than the main resonance energy of the detector.

Neutrons of very low energy can be obtained, and used to measure cross sections, in the following fashion: A beam of thermal neutrons im-

pinges on the bottom of a long, thin column of a polycrystalline material, such as graphite. The material contains many small crystals, randomly oriented. The beam of neutrons, on traversing the material, encounters crystals at all angles, so that, eventually, all neutrons will suffer Bragg reflections and will be knocked out of the beam. However, for those neutrons of long wave length

$$\lambda \geq 2d$$

the only angle at which the Bragg condition can be satisfied is $\theta = 0^\circ$. These neutrons will thus not be reflected by the small crystals in the material and will traverse the material without very great attenuation. Hence, the neutrons emerging from the top of a long column of polycrystalline material will mostly have wave lengths $\lambda > 2d$, or very low energies. If graphite is the material used, $2d$ corresponds to neutron energies of .0015 ev, so that the "cold neutrons" emerging from the top of the column will mostly have energies less than .0015 ev. This beam can be used to measure the total cross section of various materials for neutrons of very low energy.

6-27 Sorting Out the Cross Sections

The methods described in the previous sections all involve measurements, by the "transmission method", of the total cross section. As described in Section 6-24, the total cross section consists of different parts (i.e., scattering and absorption) which are characterized by different dependences on the energy of the impinging neutron beam. It is possible to take advantage of the different energy dependence of scattering and absorption cross sections to sort out these effects in a measurement of the total cross section. For instance, if on analyzing a curve of total cross section vs. neutron velocity it is found that the curve can be represented by a constant plus a $1/v$ term, then the constant part can be associated with the scattering cross section and the $1/v$ part with the absorption. Likewise, if the curve can be described by a constant plus a Breit-Wigner resonance term, the resonance term is associated with absorption and the constant with scattering. (It should be noted that whenever the absorption has a resonance peak, the scattering also has a resonance peak; however, the magnitude of the resonance scattering cross section can usually be shown to be small compared to the resonance absorption cross section, so that the total cross

section in a resonance is usually essentially equal to the absorption cross section.)

Because of the crystal effects described in Sections 6-25 and 6-26, it is obvious that, depending on the crystalline nature of the scattering material employed in a transmission experiment, an energy dependence may be introduced into the scattering cross section (Bragg reflections) which is not at all a nuclear effect, but rather an effect of the particular lattice configuration of the scattering material. Hence, particular care must be exercised in the performance and interpretation of experiments designed to measure total (or scattering) cross sections for slow neutrons.

In the case of measurements of scattering cross sections, it is not necessary to depend completely on transmission measurements of total cross section and the interpretation thereof. One can measure, directly, scattering cross sections by placing the detector at some other angle (say, 90° rather than 0°) from the incident beam and observing directly the neutrons scattered from the incident beam into the detector. Such a measurement depends on the possibility of getting neutron beams containing a large flux of neutrons; but such beams are available from piles.

In the case of absorption cross sections, these can sometimes be measured directly in cases where the absorption of a neutron leads to the production of a radioactive isotope, the radioactivity of which can then be detected in, say, a Geiger counter. If the substance is put into a known flux of neutrons of known velocity (flux = nv), the rate of activation is $nv\sigma_a N$ (where N is the number of absorbing atoms per cm^3) and, if the period of exposure is long compared to the decay period of the radioactive isotope produced, the rate of radioactive decay immediately upon removal of the material from the neutron flux is equal to $nv\sigma_a N$. Thus, it is only necessary to know the efficiency of the Geiger counter geometry (and the decay period) to obtain a value of σ_a . (See Section 6-18 for the formulae.)

CHAPTER 7

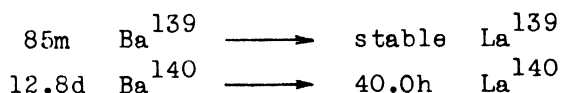
CHEMISTRY OF THE FISSION PROCESS

by

Charles D. Coryell

7-1 Identification of the Fission Products

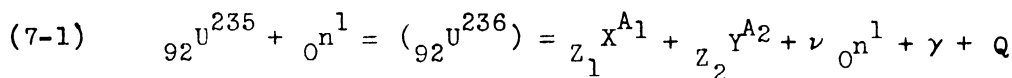
The fission process was discovered by O. Hahn and F. Strassmann (Naturw. 27, 11 (1939)) as a result of painstaking radiochemical studies of several of the radioactive species produced by the interaction of neutrons with uranium. Hahn and Strassmann showed that several activities previously thought to be Ra species decaying to Ac were inseparable from Ba on fractionation under conditions that lead to considerable separation of authentic Ra isotopes. These include activities now known as:



Hahn and Strassmann were, in their first paper, loath to accept all the consequences of their findings, but they did point out that one of the sulfide precipitable activities (67h Mo⁹⁹) might be Mo, and that the sum of the masses for active Ba and active Mo might be equal to that of U.

Adequate confirmation of the occurrence of this important reaction came promptly from the observation of the enormous energy release in fission and from the identification of some 50 isotopes of different intermediate elements within a year.

The fission process may be represented as:



Symbols X and Y represent the light and heavy fission product atoms, ν the number of neutrons released, γ the release of γ -rays at the instant of fission, and Q the kinetic energy of the fission product atoms and fission neutrons. From a consideration of the neutron content of fissionable nuclei and of stable elements in the range $30 < Z < 60$ it is predicted that the primary fission fragments X and Y will undergo together some six β decays before the nuclei become stable.

A large body of useful information has been obtained from the chemical separation of the fission products (including the active descendants of the primary species) and from the characterization of individual active species. Fission product activities have been found for all elements from $_{30}\text{Zn}$ to $_{63}\text{Eu}$, with masses identified ranging from 72 to 158. Attention is drawn to the comprehensive tabulation of the physical data on all recognized fission products, issued by the Plutonium Project in the J.A.C.S. 68, 2411-43, (1946) and also in Rev. Mod. Phys. 18, 513-44 (1946). There are listed in this survey, with extensive documentation to the open literature and Project reports, critical evaluations of all information on the half-life, decay process, discovery in fission, yield in U^{235} fission, energetics of particle and electromagnetic radiation, mass assignment and chain relationships. Data are included on 162 cases of β^- emission (6 having daughters emitting neutrons), on 11 of isomeric transition, on 7 stable isotopes of Kr and Xe identified mass spectrographically, and on 22 nuclei whose presence is inferred from radiochemical evidence, a total of 202 different nuclear species.

In the course of the investigation of the occurrence of fission products, chemical procedures had to be developed for the isolation of each one of the elements in high radiochemical purity (free from contamination with the activities of other fission elements). In the studies of 49h Zn^{72} , for instance, decontamination from gross fission product activity by a factor of $\sim 10^9$ was required. Chemical procedures were developed for the relatively rapid quantitative analysis for major fission product activities in a variety of chemical mixtures.

7-2 Determination of Fission Yields

The fission yield of a given fission product is defined as the fraction of fissions leading to the nucleus in question by direct formation and by the decay of precursors. Absolute fission yields have been established for a number of prominent chains in the fission of U^{235} by pile neutrons. The general principle involves the simultaneous irradiation of a thin sample m_1 of fissile material in a fission chamber A and a larger sample m_2 in the same neutron field, from which quantitative isolation and measurement of one or more of the fission products is subsequently carried out. The apparatus is given schematically in Figure 7-1.

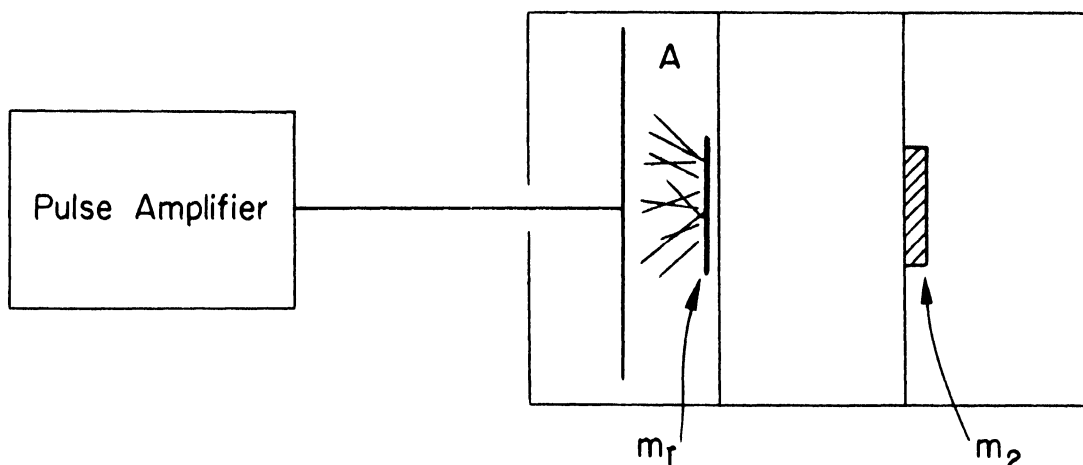


Figure 7-1 Apparatus for Fission Yield Determinations (Schematic)

The fission chamber has a geometry of essentially 2π , and therefore has an efficiency of 1.00 for counting fissions occurring in a foil of thickness much less than the range of fission recoils.

The fission counting rate C_f , determined during the irradiation, is given by the equation.

$$(7-2) \quad C_f = k_f \Sigma_f m_1 (nv)$$

where k_f is the efficiency of fission counting (1.00), Σ_f is the fission cross section per gm of the fissile material, m_1 is the mass in the fission chamber, and nv is the neutron flux.

At the conclusion of an irradiation of time T , the larger sample of mass m_2 is dissolved, a known mass is added of the element whose fission isotopes are being studied, to act as carrier during the chemical purification and from whose observed recovery the chemical yield y_c of the radioactive species can be determined, and the beta counting rate C_β is determined at time t after conclusion of the irradiation. The beta counting rate is given by the equation:

$$(7-3) \quad C_\beta = k_\beta y_c \Sigma_f m_2 (nv) y (1 - e^{-\lambda T}) e^{-\lambda t}$$

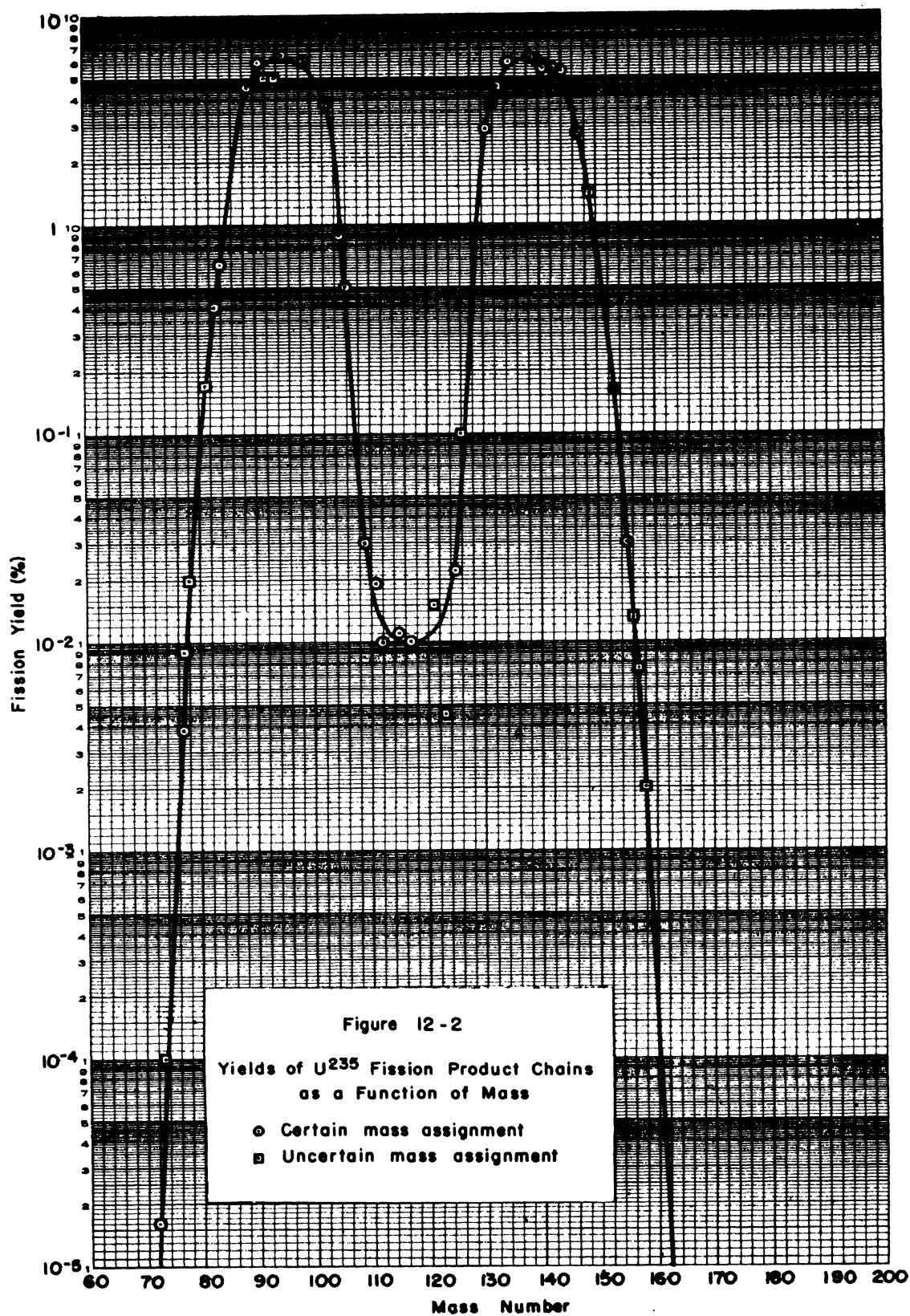
where k_β is the efficiency of β -counting (generally standardized by quantitative correlation of UX_2 β -counting against U α -counting or RaE β -counting against the derived RaF (Po^{210}) α -counting), λ is the decay constant for the species being counted, and y is the fission yield. The terms Σ_f and nv are eliminated between Equations (7-2) and (7-3), and all terms other than y are measurable. In Equation (7-3) it is assumed that the species being studied is a primary fission product, or that its precursors have half-lives small compared to its own; suitable corrections can be made if these conditions are not met.

If the fission yield of one fission product is known, that of others can be determined by reference with it by determination of C_β , k_β , and λ for each. Careful extrapolations of the β absorption curves of the two species to zero net absorber are used to achieve comparable values of k_β . The ^{140}Ba has been selected as a convenient fission product for reference, using the fission yield of 6.1% determined by M. L. Freedman and D. W. Engelkemeir (Plutonium Project Report CC-1331, Feb. 1944). Obviously the determination of absolute fission yields is based on the determination of absolute β -counting with thin sample and a thin window Geiger counter.

7-3 General Features of the Yield-Mass Curve

Fission yields have been determined for the last or the next to the last active members of 44 different chains. The curve for the fission yield as a function of mass number of the chain is given in the Plutonium Project release (loc. cit.) and is presented here as Figure 7-2. Grummitt and Wilkinson of the National Research Council of Canada have published a similar curve (Nature, 158, 163 (1946) based on their absolute fission yields which is in agreement with this curve within the limits of experimental error. Relative values of the fission yield as a function of the mass have also been determined by Jentzschke (Z. f. Physik, 120, 165-84 (1943) from the ratio of the energies of the two fission fragments (see Figure 2-5). This curve is in good agreement with that determined radiochemically, but is of lower dispersion and range.

There are several important characteristics of the yield-mass distribution (Figure 7-2). The definition of the fission products into light and heavy groups is very pronounced: over 95% of the fissions fall in the



mass range 83-105 (light) and 129-151 (heavy) for which the individual yields at a given mass are in excess of 0.5%. The most probable masses are 95 and 139. The probability of any nearly symmetrical fission (~ 117 and ~ 117) is only 0.01%. No satisfactory theoretical explanation for the asymmetric nature of the fission process has yet been developed.

The curve shows no significant difference between odd masses and even masses. Since the fission neutrons are thought to be expelled after the separation of the main fragments, and since nuclei of even proton number Z and even neutron number $A-Z$ are stabler than those of even Z and odd $A-Z$ or of odd Z and even $A-Z$, which are in turn stabler than those of odd Z and odd $A-Z$, by spin coupling energies of ~ 1 Mev, it might have been thought that there would be some difference in yields of even and odd masses.

Only one point falls far from the smooth curve through the points, that of 0.0044% for ^{123}Sn . It is probable that this nucleus is isomeric with an undetected one of yield $\sim 0.012\%$, decaying independently so that the sum of the yields for nuclei of mass 123 is $\sim 0.016\%$, as expected from the curve.

The fission yield varies so rapidly with the mass (about 3-fold per mass unit at either side of the curve) for most of the masses that the fission yield can be used effectively to estimate the mass assignment. All mass numbers from 75 to 159 should have yields greater than $10^{-3}\%$. One or more members have been identified for about 75 of the 85 chains expected in this yield range.

The smooth curve in Figure 7-2 is an empirical one drawn symmetrically around mass 117, the symmetrical character being self-revealing. The area under the whole curve is found to be 197%, in excellent agreement with the predicted area of 200%. Although the excellence of this agreement may be adventitious, it serves to give confidence to the techniques of absolute β counting underlying the determination of fission yield.

7-4 Statistical Survey of the Fission Products

If there were a unique primary nuclear charge associated with each mass number A of the fission products, which in the subsequent decay to stable end products is displaced about three units (average for light and heavy group), it would be expected that there would be over 250 radioactive fission products

of fission yield in excess of $10^{-3}\%$. It is quite probable that there is a statistical distribution of primary charge in fission around a most probable value Z_p for each A value, so that the total number of fission products is probably considerably greater than 250. Indeed, several chains are known with five or more radioactive members (cf. Table II of the Plutonium Project survey, loc. cit.). Three nuclei, $34h \text{ Br}^{82}$, $19.5d \text{ Rb}^{86}$, and $13d \text{ Cs}^{136}$ are found in low yield among the fission products; these are shielded nuclei (they have one less neutron than corresponds to a stable nucleus) so they are presumably formed directly in fission with a high value of the nuclear charge and their partners presumably have a very low value and great chain length.

Many of the fission products have half-lives so short that direct study of the activities has not yet been possible, and indirect evidence for their occurrence is generally not available unless they are noble gases, that can rapidly be separated from the fission material, or have noble gas precursors. It is probable, however, that the search is nearly complete for all fission products of half-life greater than 3 hours and yield in excess of 0.01%, although much needs to be done still in the characterization of many of the activities.

The distribution of the half-lives of the recognized fission products is given in Figure 7-3, where the histogram shows the distribution in number of fission products having a half-life T within the range of 0.5 in $\log T$, plotted against $\log T$. The shortest half-life depicted is that for the 0.05s delayed neutron emitter, and the longest is for $4 \times 10^6 \text{ y } \text{Tc}^{99}$. The natural activity $6.3 \times 10^{10} \text{ y } \text{Rb}^{87}$ is shown as a block with abscissa off-scale on the right; this nucleus is certainly formed in fission. Indirect evidence also shows that five other very long-lived fission products are formed, but direct information has not been obtained on these, which are given in the figure as a block without specific abscissa. They are listed in Table 7-1, together with estimated limits on their half-lives if it be assumed that their β rays could be counted with reasonable efficiency. It seems unlikely that a 2.5m activity in neutron activation ascribed to Zr^{93} is correctly identified. The nucleus Sm^{151} may also be in this class, but evidence for its activity comes only from mass-spectrographic sources.

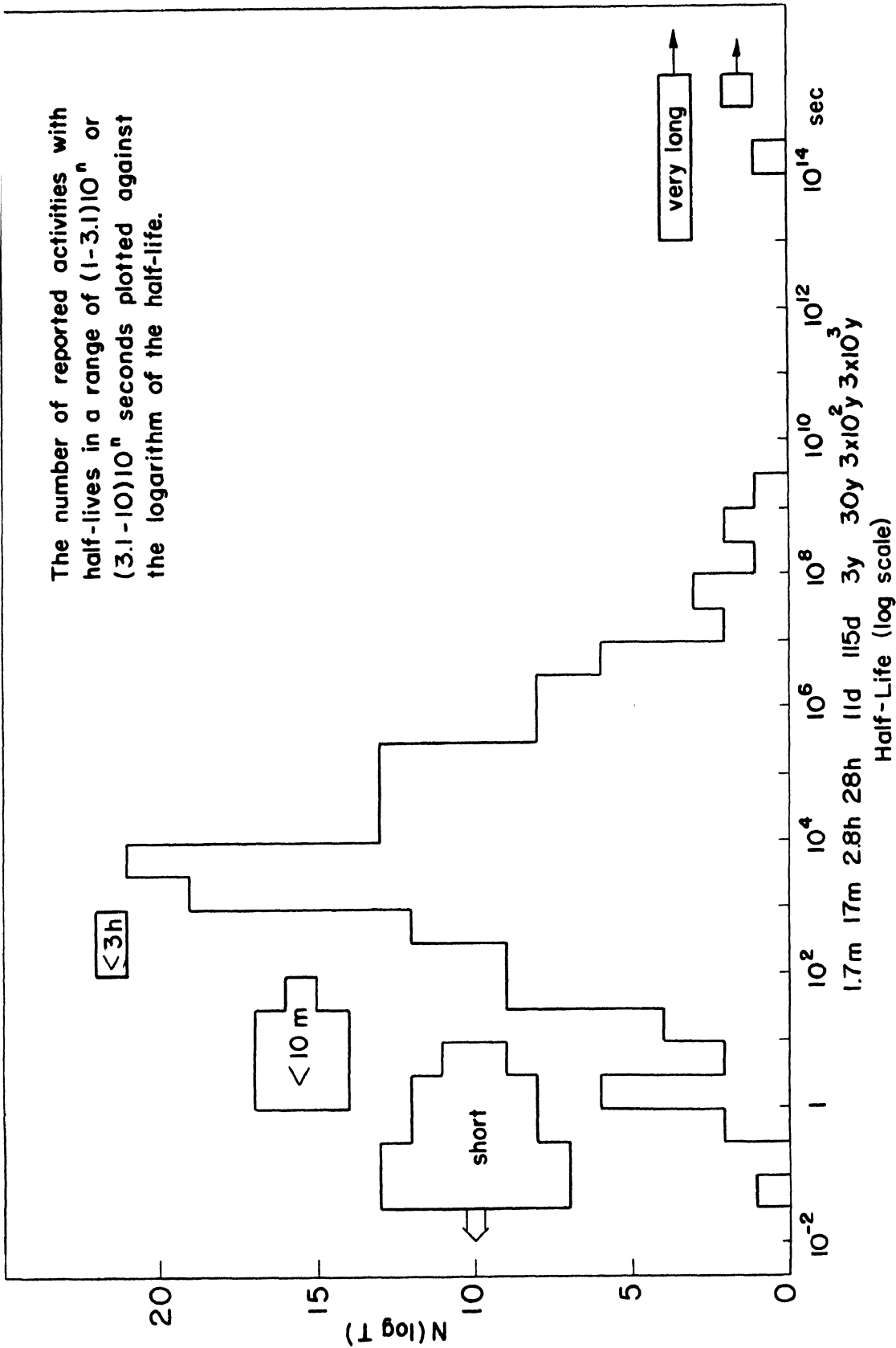


Figure 7-3
Distribution of half-lives of fission products

On the short half-life side in Figure 7-3 there is presented a block for the 22 short activities known to occur as a result of rapid separation of given elements (mostly Kr and Xe) and the identification of long-lived descendants.

TABLE 7-1
VERY LONG-LIVED NUCLEI PRODUCED IN FISSION

<u>Nucleus</u>	<u>Estimated Half-life</u>	<u>Estimated Fission Yield (%)</u>
Se ⁷⁹	$>7 \times 10^6 \text{ y}$	0.04
Zr ⁹³	long	6
Pd ¹⁰⁷	$>10^8 \text{ y}$	0.1
I ¹²⁹	very long	1.0
Cs ¹³⁵	$>2 \times 10^4 \text{ y}$	6

In addition direct searches for precursors of certain fission products have given evidence that certain activities must have upper limits of half-life around 10m (8) or 3h (2), which are also shown as blocks without specific abscissa.

The assembly of the fission products can serve as an extensive body of substances to check relationships among unstable nuclei. The decay schemes of a number have been fairly well worked out, and those of many others are accessible to study. Attempts to correlate the logarithm of the half-lives with the logarithm of the β decay energies show a broad spread of points, without apparent grouping around curves as predicted by simple theory and represented by the Sargent relations. The total decay energies provide an opportunity to check the validity of current theories of nuclear stability (cf. Section 2-1 of these notes), and study of the phenomenon of delayed neutron emission occurring with six fission products may cast light on the problem of neutron binding. In general it is found that the parabolic energy-charge equation is in reasonable agreement with the great body of observations, but the energetics of the neutron emission processes for the 55.6s Br and the 22s I are difficult to correlate with the mass assignments 87 and 137 proposed (Snell, Lvinger, Wilkinson, Meiners, and Sampson, Phys. Rev. 70, 111 (1946)).

7-5 Quantities of Fission Products Produced

The conventional value for the energy release in fission is taken as 200 Mev. This value consists of the kinetic energy of the fission fragments (~ 160 Mev), of the fission neutrons (~ 5 Mev), the energy of the prompt γ rays (~ 4 Mev), the energy given off by the absorption of the neutrons (~ 9 Mev, dependent on the manner of absorption of the neutrons), and 22 ± 3 Mev radioactive decay energy of the fission products. About half of this last figure is emitted as neutrino energy, not absorbed terrestrially, and the remainder is emitted as β and γ energy, dissipated over a long period of time.

On this conventional basis, the number of fissions per sec yielding one watt is:

$$(7-4) \quad \frac{1}{200} \frac{\text{fissions}}{\text{Mev}} \times \frac{\text{Mev}}{1.6 \times 10^{-6} \text{ erg}} \times \frac{10^7 \text{ erg}}{\text{watt-sec}} = 3.1 \times 10^{10} \frac{\text{fissions}}{\text{watt-sec}}$$

This figure is generally rounded off to 3×10^{10} . Correspondingly 1 megawatt-day (10^3 Kwd) corresponds to the consumption of the following amount of fissile material (U^{235}):

$$(7-5) \quad \frac{3.1 \times 10^{10} \text{ fissions}}{\text{watt-sec}} \times \frac{10^6 \text{ watts}}{\text{megawatt}} \times \frac{8.64 \times 10^4 \text{ sec}}{\text{day}} \times \frac{235 \text{ gm}}{\text{gm-atom}} \\ \times \frac{\text{gm-atom}}{6.02 \times 10^{23} \text{ fissions}} = \frac{1.0 \text{ gm}}{\text{megawatt day}}$$

The activity of radioactive materials is commonly expressed in curies C where one curie is 3.70×10^{10} disintegrations per second (dis/sec). The activity A_1 of a given radioactive species of fission yield y_1 and decay constant λ_1 (equal to $0.693/T_{1/2}$ is the half-life) produced in a system of fission rate f per sec in time of operation T is:

$$(7-6) \quad A_1(\text{dis/sec}) = f y_1 (1 - e^{-\lambda_1 T})$$

if the species is formed directly in fission or if all of its precursors are of very much shorter life. This result may be expressed in curies at a power level of P watts as:

$$(7-7) \quad A_1 \text{ (curies)} = \frac{3 \times 10^{10} \text{Py}_1}{3.7 \times 10^{10}} \left(1 - e^{-\lambda_1 T} \right)$$

The equation for the production in time of operation T of an activity A_2 of a secondary species of decay constant λ_2 formed from the decay of a primary fission product of fission yield y_1 and decay constant λ_1 is:

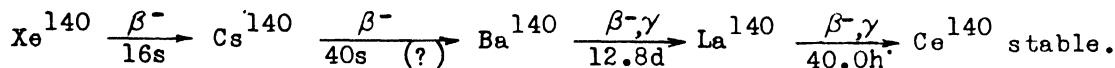
$$(7-8) \quad A_2 \text{ (dis/sec)} = fy_1 \left(1 - \frac{\lambda_1 e^{-\lambda_2 T} - \lambda_2 e^{-\lambda_1 T}}{\lambda_1 - \lambda_2} \right)$$

If the primary product of disintegration rate A_1^0 is isolated and purified, the activity of the secondary species will grow in the preparation according to the following law:

$$(7-9) \quad A_2 \text{ (dis/sec growth)} = \frac{A_1^0 \lambda_2}{\lambda_2 - \lambda_1} \left(e^{-\lambda_1 t} - e^{-\lambda_2 t} \right)$$

where t is the time elapsed since the purification operation. The total amount of secondary material available after any period T of fission operation and t of subsequent shutdown (radioactive "cooling") is given by the obvious combination of Equation (7-8) multiplied by the decay factor $e^{-\lambda_2 t}$ plus Equation (7-9) with A_1^0 taken from Equation (7-7).

As an example we may consider the amount of 12.8d Ba^{140} produced in a chain-reacting system. The chain in question is:



(These and other data on the fission products are taken from the survey issued by the Plutonium Project, J.A.C.S. 68, 2411-43 (1946), also Rev. Mod. Phys. 18, 513-44 (1946)). After a time of operation T , great compared to the half-life $T_{1/2}$ of the Ba^{140} (which can obviously be considered to be a primary fission product), the activity A_{Ba} has reached the constant value, called the saturation value. If we calculate the activity in curies produced in a

reactor or portion of a reactor operating at a conventional power of 10^3 KW, we find that the activity for the observed fission yield of 6.1% is:

$$(7-10) \quad A_{\text{Ba}} = \frac{3 \times 10^{16} \times 0.061}{3.7 \times 10^{10}} = 50,000 \text{ C}$$

Corresponding large activities of all other major fission products are produced at this relatively low nuclear power level.

The La^{140} comes to saturation at an activity equal to that of the Ba^{140} . After shutdown, the activity of the secondary substance decays more slowly than that of the primary until, after a time, it comes to a constant relative activity, exceeding its longer-lived parent in activity by the factor $\lambda_2/(\lambda_2 - \lambda_1) = (T_{1/2})_1 / ((T_{1/2})_1 - (T_{1/2})_2)$, equal in this case to 1.15. After 12.8 days of cooling there would remain 25,000 C of Ba^{140} and 29,000 C of La^{140} .

Significant masses of individual fission product elements are obviously produced in large-scale operations. The mass of each element will include the stable isotopes formed as the result of decay of short-lived fission product chains, plus a calculable amount of the activities of half-life comparable to the cooling period, plus the amount of any isotope of half-life long compared to the operating and cooling time. The mass of stable or long-lived isotope formed as the result of 1 gm of fission is $Ay/235$ where A is the atomic weight and y the fission yield. It is to be noted that this corresponds to the production of 0.025 gm of $4 \times 10^6 y \text{ Tc}^{99}$ and 0.016 gm of $3.7y \text{ Ba}^{147}$ per gm of fission. Neither of these two elements (43 or 61) has been found in nature. The presence of weighable amounts of the fission elements must be taken into account in planning chemical procedures for processing.

7-6 Radioactive Power Dissipation by the Fission Products

Since the half-lives and radiation energies are known for virtually all significant fission products of half-life in excess of ~ 3 hrs, the total decay energy $E(T, t)$ for any times of operation T and cooling t of the fission products can be calculated from the summation:

$$(7-11) \quad E(T, t) = k f \sum_i y_i E_i \left(1 - e^{-\lambda_i T} \right) e^{-\lambda_i t}$$

where k is the constant converting Mev dis/sec to heat, and E_i is the energy of the γ radiation or the average energy of β radiation (about $1/3$ of the value of the maximum energy recorded in tables). In applying Equation (7-11), cases of short-lived daughters are handled by adding their decay energies to those of the parent using its decay constant and fission yield, and cases where $\lambda_2 \approx \lambda_1$ are ignored (the only prominent case is that of $65d \text{ Zr}^{95} \rightarrow 35d \text{ Cb}^{95}$).

Because of the large number of fission products, empirical or statistical analysis of energy dissipation can be readily made. K. Way (Phys. Rev. 70, 115 (1946)) gives the following empirical equations for the dissipation in sensible energy from fission products, expressed in Mev per sec per fission for decay time τ in seconds:

$$(7-12) \quad E_\beta = 1.40 \tau^{-1.2} \quad 10 < \tau < 10^7 \text{ sec}$$

$$(7-13) \quad E_\gamma = 1.26 \tau^{-1.2}$$

These equations can be transformed to more practical ones by the conversion of time to days and power and fission to a macro scale:

$$(7-14) \quad E_\beta = \frac{1.40 \text{ Mev}}{\text{sec-fission}} \times \frac{1.6 \times 10^{-13} \text{ watt-sec}}{\text{Mev}} \times \frac{6.02 \times 10^{23}}{235 \text{ gm}} \times \frac{t^{-1.2}}{(8.64 \times 10^4)^{1.2}}$$

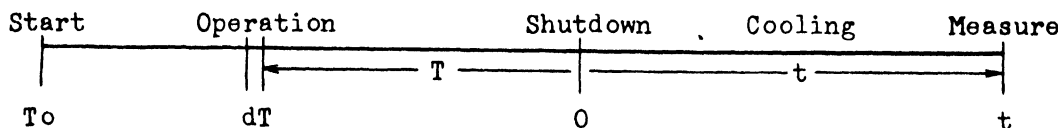
$$= 680 t^{-1.2} \frac{\beta \text{ watts}}{\text{gm fission}}$$

$$(7-15) \quad E_\gamma = 620 t^{-1.2} \frac{\gamma \text{ watts}}{\text{gm fission}}$$

$$(7-16) \quad E_\beta + E_\gamma = a t^{-1.2} = 1.3 \times 10^3 t^{-1.2} \frac{\beta + \gamma \text{ watts}}{\text{gm fission}}$$

These equations are presumed to be good within less than a factor of 2 for periods of time from 10^{-4} to 10^2 days.

These latter equations lend themselves to ready modification to take care of radioactive power dissipation after a finite period of fission. If the radioactive power equation is of the type of Equation (7-16), the contribution dE at the time of cooling t from the f fissions per unit time occurring in infinitesimal time dT at time T calculated backward



from shutdown is

$$(7-17) \quad dE = af(T + t)^{-1.2} dT$$

$$(7-18) \quad E(T, t) = af \int_0^{T_0} (T+t)^{-1.2} dT = \frac{af}{-0.2} \left[(t+T_0)^{-0.2} - t^{-0.2} \right]$$

Taking the value of a from Equation (7-16) the power dissipation in watts from 1 gm of fission products produced in operating times T of 0, 1, and 10 days is plotted in Figure 7-4 as a function of time of cooling t for periods from 0.1 to 60 days. Immediately after shut-down these curves should differ greatly in position, and that for $T = 1$ should lie higher than that for $T = 10$ by a factor of 10 (the ratio of the fission rates). By 0.1 day they differ successively by about a factor of 5. At greater times the short-lived fission products, in whose contributions they differ so much, have died out, and the curves come closer together, so that they are essentially together after about 50 days.

7-7 Some Factors Affecting Reprocessing of Pile Material

Some or all of the contents of a pile may need to be processed chemically for one or more of the following reasons: (1) It may be necessary to recover some fissile material such as Pu^{239} produced as a result of neu-

tron capture by one of the constituents of the nuclear fuel substance.

(2) Physical deterioration of the fuel material may make discharge necessary, and recovery of precious fuel economically desirable. (3) Recovery of unused

fuel substance or useful by-product from spent charge material may be desired.

(4) Long-lived or stable fission products may capture neutrons to such a degree as to threaten the neutron economy of the pile. For instance, Lapp, VanHorn, and Dempster (Phys. Rev. 70, 104 (1946)) have shown that Sm^{149} has a cross-section σ for neutron absorption of 53,000 barns (units of $10^{-24} \text{ cm}^2/\text{atom}$). Mass 149 has a fission yield y of 1.4%. The rate of formation of Sm^{149} is Σnv where Σ is the fission cross section of a unit of the pile and nv is the neutron flux (the effect of the 47h 61^{149} precursor is ignored). The rate of consumption of the Sm^{149} is $\sigma nv (\text{Sm})$ where (Sm) is the Sm concentration in atoms per unit of the pile.

The net equation for Sm formation is:

$$(7-19) \quad (\text{Sm}) = \frac{\Sigma y}{\sigma} (1 - e^{-\sigma nvt})$$

If the term nvt approaches infinity, it can be seen that the rate of neutron loss on Sm^{149} is Σnv , or the fraction of neutron loss is this term divided by the fission rate Σnv , numerically equal to y . The effect of neutron poisoning becomes apparent earlier the higher the neutron flux or power density. Similar equations hold for other fission products, but values of σ are lower for stable ones and generally unknown for active ones.

The chemical processing of pile materials will undoubtedly be inevitable in any extensive nuclear power program. The considerations of timing are a complicated function of a number of factors outside the scope of this lecture. In the following section there will be given a high spot survey of some of the problems caused by the tremendous radioactivity of the fission products and of accessory materials made radioactive in the neutron bath.

7-8 Some Consequences of High Activity

Any chemical operations on material which has undergone fission in a pile must be carried out by remote control because of the intense γ activity. The radiations from the chain $\text{Ba}^{140} - \text{La}^{140}$ discussed in Section 7-5 are

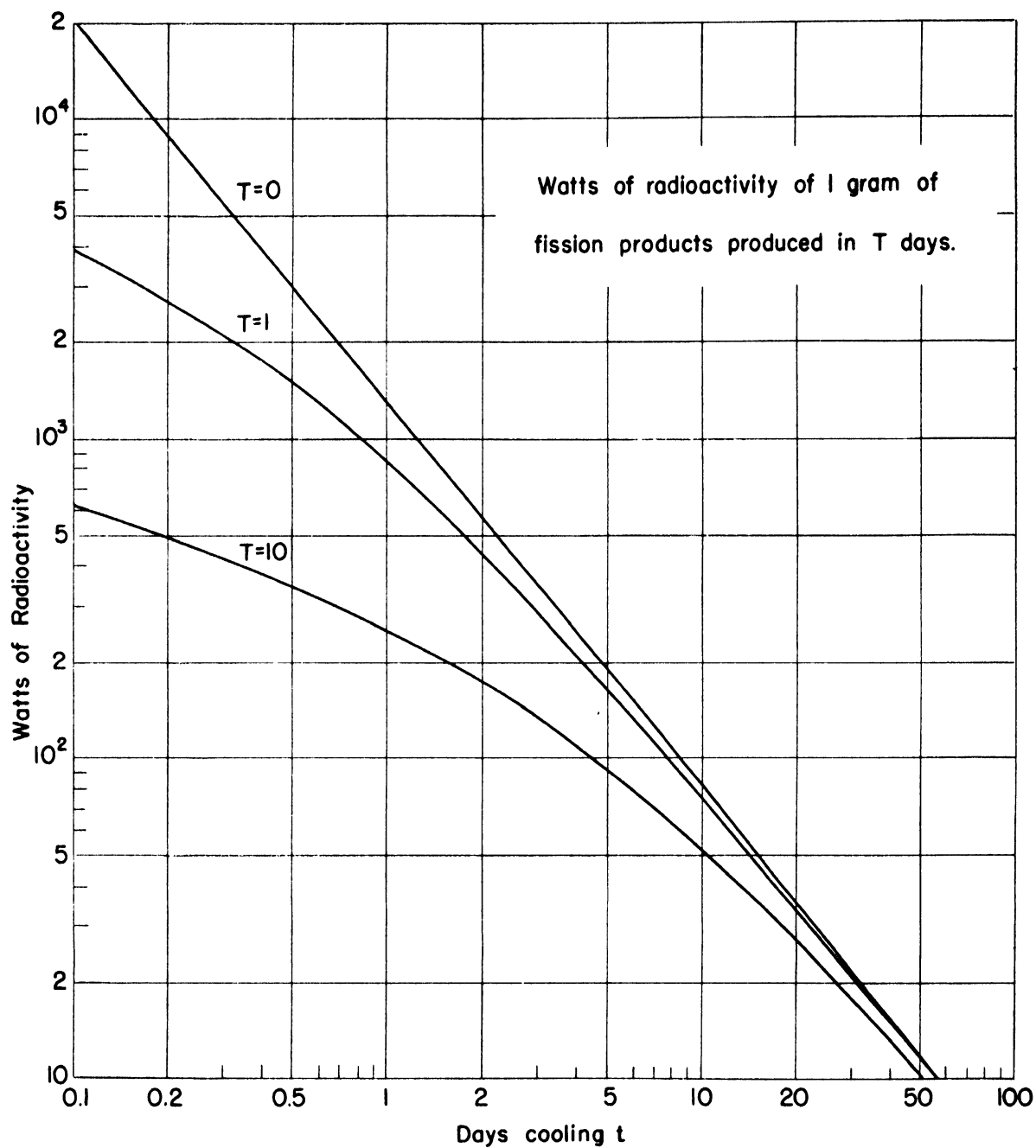


Figure 7-4
Radioactive power dissipation

among the most penetrating of those of fission products and may find considerable technological and medical use since they are not greatly different from those of the Ra family (RaC'). The Ba¹⁴⁰ decays ~75% with $\beta = 1.05$ Mev, and 25% with $\beta^- = 0.4$ and $\gamma = 0.54$ Mev. The secondary La¹⁴⁰ decays by the emission of a complex β spectrum: ~10% with $\beta^- = 2.1$, 70% with $\beta^- = 1.4$, and 20% with $\beta^- = 0.9$ Mev; and a complex γ spectrum: 5% with $\gamma = 2.3$, ~75% with $\gamma = 1.64$, ~12% with $\gamma = 0.85$, ~7% with $\gamma = 0.49$, and 1% with $\gamma = 0.33$ Mev.

The shielding requirements for La¹⁴⁰ may be discussed as representative of those required for safe operation on separations of pile products. The radiations from 1 C of a γ emitter of ~2 Mev energy produce a dosage at 1 meter of 1 r/hr, and the dosage from 1 C of La¹⁴⁰ is about the same. The thickness of Pb necessary to cut the intensity of such radiations 10-fold is 2 inches, that of concrete is ~8 inches. The tolerance dose for humans is generally taken as 0.1 r/day, or for an 8 hour shift, 12.5 mr/hr (milli-roentgens/hr). To cut the dose of the radiations from a 40,000 C source of La¹⁴⁰ to this tolerance level would require a wall of Pb 13 inches thick and a gross separation of 1 meter, or a wall of about 4 feet of concrete. Such a source would, as we have seen, be associated with pile material containing less than 1 gm of fission products.

Actually greater thickness of shielding than this is required to lower the γ background in operating areas to provide for sensitive detection of possible leaks and spills from the control panels of the remote control process and from analytical sampling operations.

The contribution to the activity of this particular chain can of course be lowered by holding the fission material in storage for longer periods of time before starting chemical operations. After some weeks the dominant γ activity comes from 65d Zr⁹⁵ of 6.4% fission yield and its daughter 35d Cb⁹⁵, each of which has γ radiation of ~0.8 Mev, which requires nearly as great shielding to lower the radiation level to tolerable values, and which tends to decay very much more slowly, particularly in view of the long half-life of the secondary activity. Other γ emitters are listed in part B of Table 7-2 in order of increasing half-life, together with their fission yields and a rough characterization of their decay energies.

TABLE 7-2
LONG-LIVED FISSION PRODUCTS OF TECHNOLOGICAL IMPORTANCE

<u>Activity</u>	<u>Fission Yield</u>	<u>β Energy</u>	<u>γ Energy</u>
<u>A. Activities that may be volatilized</u>			
5.3d Xe ¹³³	6	0.35	0.085, 0.03
8.0d I ¹³¹	2.8	0.6	0.367
42d Ru ¹⁰³ → 56m Rh ^{103*}	3.7	0.2	0.56
1.0y Ru ¹⁰⁶ → 30s Rh ¹⁰⁶	0.48	2.8, 3.9	0.3, 0.8 ^a
10y Kr ⁸⁵	0.24	0.74	none
<u>B. Long-lived $\beta + \gamma$ emitters</u>			
11.0d Nd ¹⁴⁷	2.6	0.4, 0.9	0.6
12.8d Ba ¹⁴⁰ → 40h La ¹⁴⁰	6.1	0.4, 1.0+1.4	0.4+0.8, 1.63, 2.3
15.4d Eu ¹⁵⁶	0.013	0.5, 2.4	2.0
28d Ce ¹⁴¹	6	0.55	0.2
32d Te ^{129*} → 70m Te ¹²⁹	0.19	1.8	0.3, 0.8
42d Ru ¹⁰³ → 56m Rh ^{103*}	3.7	0.2	0.56
65 Zr ⁹⁵ → 35d Nb ⁹⁵	~6.4	0.4+0.15	0.73+0.75
275d Ce ¹⁴⁴ → 17m Pr ¹⁴⁴	5.3	0.3+3.1	0.2, 1.2 ^a
1.0y Ru ¹⁰⁶ → 30s Rh ¹⁰⁶	0.48	2.8, 3.9	0.3, 0.8 ^a
2.7y Sb ¹²⁵	0.02	0.3, 0.7	0.6
33y Cs ¹³⁷	~6	0.5, 0.8	0.75
<u>C. Long-lived β emitters without γ radiation</u>			
13.8d Pr ¹⁴³	6	1.0	none
53d Sr ⁸⁹	4.6	1.50	none
57d Y ⁹¹	5.9	1.53	none
90d Te ^{127*} → 9.3h Te ¹²⁷	0.03	0.7	none
2y Eu ¹⁵⁵	~0.03	0.23	0.084
3.7y Bi ¹⁴⁷	2.6	0.2	none
25y Sr ⁹⁰ → 65h Y ⁹⁰	~5	0.6+2.2	none

a. Gamma Radiations present at low intensity.

In the process of dissolving fission material in acid the noble gases Kr and Xe are discharged, and under certain conditions an appreciable fraction of I and Ru may also be swept off. The isotopes of these elements of longest half-life are listed in Part A of Table 7-2.

The activities listed in Table 7-2 include all those recognized with fission yields in excess of 0.01% and with half-lives in the range from 10 days to 10^4 years. The longest-lived species (cf. Table 7-1) are not of technological importance since they are produced in low activity compared to the shorter-lived ones. For half-lives $T_{1/2}$ large in comparison to the operating time T , the activity produced is proportional to $yT/T_{1/2}$.

Shielding problems are not serious with the pure β emitters listed in part C of the table, but the activities represent a serious personnel hazard, and present the same general requirements in waste disposal.

In general, radioactive wastes from separation processes must be stored indefinitely in systems free from leaks if the activity is above some very low minimum discussed below. The activities induced in water or air coolant on passage through a pile are of much shorter half-life, and these wastes can be discharged into the surroundings after a relatively short hold-up for decay and careful monitoring.

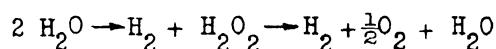
Animal tolerance to radiations is conventionally taken as 0.1 r for a 24 hour period, and 1 r is produced by the absorption of 5.2×10^{13} ev/gm in tissue under the assumption that 1 ion pair is produced for each 32 ev absorbed and that tissue absorbs 790 times as effectively as air at S.T.P. From these figures it can be seen that tolerance dosage will be 6.0×10^7 ev/gm-sec, a quantity produced by the radiations from 4×10^{-12} C/cm³ of an activity emitting γ rays of 1 Mev or β rays of 1 Mev average energy dispersed in the air surrounding the animal (solid angle 2π) or from 1.6×10^{-9} C/cm³ of activity of the same energy dispersed in the water surrounding the animal.

These figures are for general irradiation of any organ or of the whole body. If activities are ingested, it is probable that specific active elements will be concentrated in certain organs to give a higher radiation dose. Consequently the tolerance for certain elements will be much lower than that set by the general considerations given above. Examples of specific concentration have been noted with I from air or water in the thyroid, Na in fish, and Se and Te in plants, which might later be ingested by animals.

One expects chemical effects of the intense radiations associated with the pile operation or with separations of pile materials. The field of study of the interaction of extremely energetic radiations and fast particles with matter is known as radiation chemistry. The studies in this field include the studies of effects produced by α and β particles and γ rays (found in radioactivity), neutrons and fission recoils, and fast protons, deuterons, electrons, and x-radiations produced by various instrumental means. This field is a very important one both from the standpoint of fundamental research on the primary processes and from the empirical side with regard to behavior of structural materials, lubricants, insulators, solvents, and chemical changes in aqueous solutions.

Fission recoils and fast neutrons can have a pronounced disruptive effect on materials from momentum transfer. It has been found, for instance, that the electric resistance, the elasticity, and the heat conductivity of graphite all change with exposure to intense neutron radiation.

The high speed recoil atoms involved can, like β rays and the secondary electrons from γ rays, including those from slow neutron capture, cause profound disturbance due to the extensive ionization produced. It is found that the absorption of radiant energy to the extent of about 100 ev generally leads to the disruption or transformation of one or several molecules. In water and aqueous solution considerable decomposition occurs by the reactions:



It is found that heavy particles lead to greater decomposition than primary and secondary electrons because the higher local concentration of OH radicals in the first case leads to more H_2O_2 formation, and that the reaction is also favored by conditions leading to removal of the product gases. In the bombardment of hydrocarbons by electrons, unsaturation decreases the yield of gaseous products and increases the yield of polymer.

If we have a source of 50,000 C of radioactive material dissolved in say 500 liters of solution, and the average decay energy ($\beta + \gamma$) is 1 Mev, the solution will dissipate 3.7×10^{18} ev/l. This corresponds to the destruction of about 4×10^{21} molecules per liter per day or about 0.01 moles per liter per day. The radiation intensity from 1 l of this solution is 70 r/sec. Operations must be planned in the light of the physical and chemical implications of the high level of radiation intensity involved.

CHAPTER 8

CONTROL AND OPERATION OF A PILE

by

W. J. Ozeroff

8-1 Description of Pile

In this chapter we shall describe the engineering aspects of the control and operation of a chain-reacting pile. For this purpose we shall assume that we have before us a pile designed roughly as in Figure 8-1.

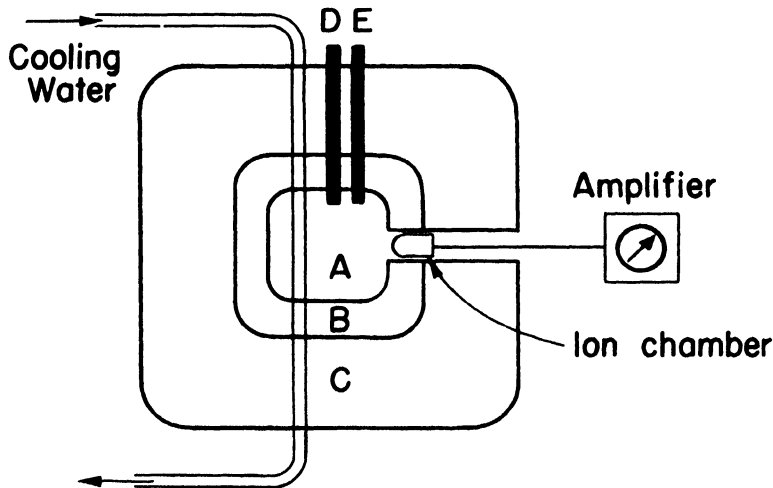


Figure 8-1.

Referring to this schematic diagram, the portion A is the reacting mixture (uranium and moderator) designed according to the recipe given by Dr. Feld in a previous chapter. In particular, the design is such that the period is not less than τ_d , (of the order of seconds). B is a reflector for thermal neutrons. This has been discussed by Professor Weisskopf in an earlier chapter. Briefly, its purpose is to reduce the critical size of A by reflecting back some of the neutrons that normally would leak away. C is a massive shell of some hydrogenous material, e.g., concrete, which absorbs neutrons that leak through the reflector. It is known as a biological shield, since its purpose is to reduce the radiation intensity around the pile to safe health levels. A cooling agent, which we shall assume to be water, is circulated through the reacting mixture. Since the cooling agent will absorb neutrons, it must be taken into account in the design of part A. D is a massive cadmium rod that can be moved up and down, known as the shut-

off rod. When it is dropped into position in A it insures, by a large safety factor, that no chain reaction can go on. By dropping it in, we may shut the pile down very quickly - as quickly, in fact, as we can get it in. Part A is so designed that K_{eff} will only be greater than one when D is completely withdrawn and E, the control rod, is partially withdrawn. The action of the control rod has been discussed by Dr. Feld. It is described in Figure 8-2, where we have plotted the neutron density against distance on a diameter of the reacting mixture A. The loss of neutrons at the boundaries (reflector and control rod) is the slope of the density curve at the boundary. It is obvious from the curves that as the control rod is raised, the loss into both boundaries decreases. Our pile is so designed that at some (nearly out) position of the control rod, $K_{\text{eff}} = 1$.

The neutron flux, and therefore the power, which is proportional to the neutron flux, depend on the position of the control rod. In Figure 8-3

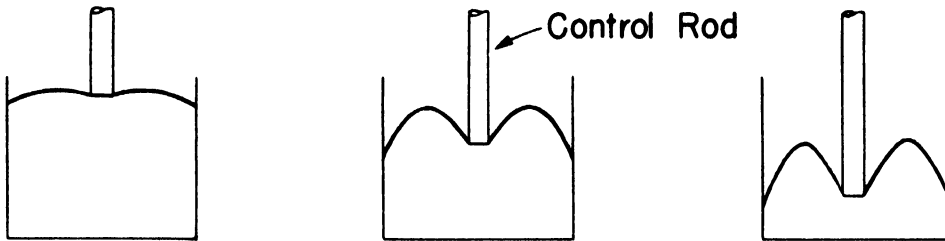


Figure 8-2.

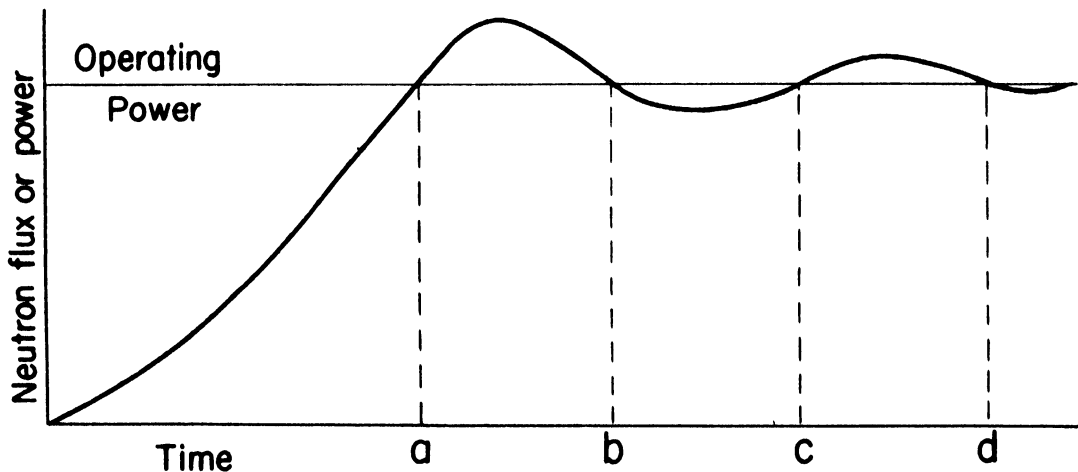


Figure 8-3.

* K_{eff} \equiv the effective reproduction constant of the nuclear reactor.

we have plotted the power of the pile as a function of time and position of the control rod (with the shut-off rod completely out). First we raise the rod to a position slightly too high. K_g will be greater than one and the power will rise. At time a we lower the rod, since we have almost reached the designed power and, if we have lowered it too much, the power will begin to fall. We raise it a bit at time b, and lower it a bit at time c, and so on, until we find the correct position for constant power (i.e., $K_g = 1$). As the pile warms up (because of the power produced by it), slight dimensional changes will take place. These will alter K_g and necessitate a slight readjustment in the control rod.

The control of a pile is, in principle, an exceedingly simple matter, since we have only one variable - the neutron flux. This is in contrast to an installation such as a steam plant, in which there are many variables (e.g., amount of coal, amount of air, etc.) In principle, then, we could have one instrument indicating the neutron flux, and this would be sufficient to operate the pile. In practice, however, certain problems arise which complicate the picture and these we now proceed to describe.

8-2 Scheme for the Operation of a Pile

Since the control and operation of the pile depend mainly on radiation measurements, we shall give first a general description of the instruments used. A more detailed description of typical instruments will be given later. All radiation measurements involve an ionization chamber. This is an instrument which gives a small current when exposed to the radiation. If the radiation level is very low, a few particles per second, the current consists of a series of discrete pulses. As the radiation level increases, these pulses come more and more frequently and finally merge into a direct current. We can measure the number of pulses with a linear amplifier and counting circuit and the D.C. current (which will be of magnitudes between 10^{-13} to 10^{-6} amperes) with either a galvanometer or an electronic D.C. amplifier.

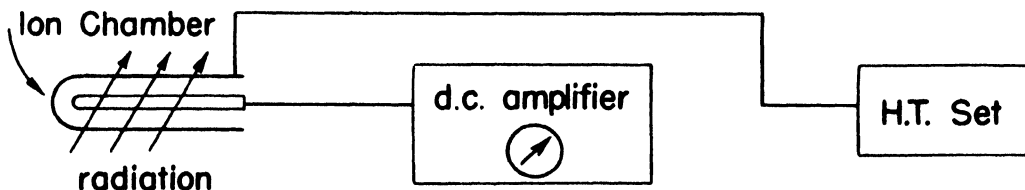


Figure 8-4.

Figure 8-4 is a schematic drawing of the fundamental instruments used for all purposes. As engineers, all we need to know about these is that if the chamber is placed in a radiation field, then the meter on the amplifier indicates the level, or intensity, of this field.

Having these instruments, we now turn to the problems of operating the pile. First of all, we must know the neutron flux, and so the power, in the reacting portion A. For this purpose, we install a chamber as shown in Figure 8-1. The reasons for putting it at the boundary, and not inside of the reacting mixture, are chiefly the practical ones that (a) the critical size is reduced and (b) the insulators of the chamber, which are at the back end, are exposed to less radiation than the active part of the chamber, because of the sharp falling off of neutron flux at the boundary. The D.C. amplifier meter will then indicate a current which is proportional to the power of the pile. On reference to Figure 8-3, it will be seen that a desirable feature of the amplifier would be to have the possibility of expanding the scale around the steady power level. This can be done by adding a second sensitive meter and operating it as a null instrument at this power level. Such a feature enables us to find the correct position for the control rod more easily than otherwise. It is useful (for legal as well as technical reasons) to record the neutron flux at all times. This can be done easily by feeding the output of the D.C. amplifier into a commercial pen recorder such as the Esterline-Angus 1 ma. recorder. For practical reasons (such as breakdown of insulation, death of electronic tubes, etc.), we should have two or three such instruments as well as a standby power system, in case the power from the 110 v. lines fails.

Secondly, we must have instruments which will drop the shut-off rods into the pile should the power go inadvertently to too high a level. Too much power might heat the pile excessively and cause mechanical damage. The chambers for this function are just like the former ones, but they feed into

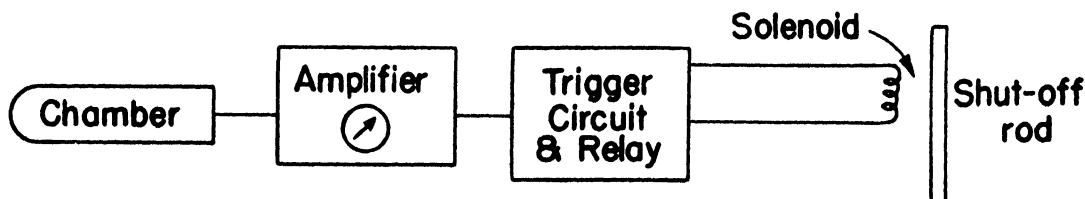


Figure 8-5.

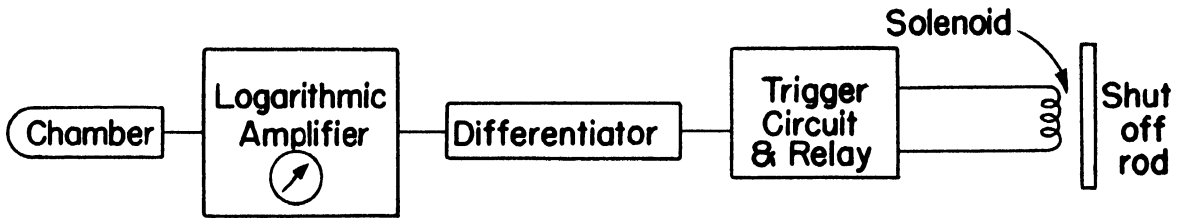


Figure 8-6.

two different kinds of circuits. The first type is shown schematically in Figure 8-5.

The trigger circuit opens a relay which drops the shut-off rod when the power reaches some predetermined value. A diagram of the second type is shown in Figure 8-6. This is known as a rate-of-rise shut-off, since it will shut down the pile if the rate of increase of power exceeds a certain value (e.g., doubling of power in 5 seconds). The operation is as follows: The chamber current is amplified logarithmically by a special amplifier so that its output voltage is, say, $K \log i$. This is differentiated by a resistance-condenser circuit so that the signal fed into the trigger circuit is V_t where

$$V_t = \frac{d(K \log i)}{dt} = \frac{K}{i} \frac{di}{dt}$$

That is, for example, we get equal V_t 's if the power begins to increase at some rate at 1 kilowatt, as if it began to increase at the same rate at 100 kilowatts. The trigger and relay are connected to the shut-off rod dropping mechanism. Because of the crucial importance of these two types of shut-off instruments, they should be designed with great care and all precautions should be taken to insure against their failure in operation. Some precautions will be discussed later.

Thirdly, we must monitor the cooling water to be sure that it contains no dangerous activities. This cooling water usually flows back into a river. (It might be added here that continuous recirculation is not practical, since impurities in it would become radioactive and this would present difficulties in servicing the pumps, etc.) Health authorities have placed rigorous limits on the amount of activity that may be dumped into rivers. The activity is the induced radioactivity in the impurities contained in the water. A simple scheme for monitoring the cooling water would be to place one or two chambers in the exit pipe and to use a recording amplifier, thus

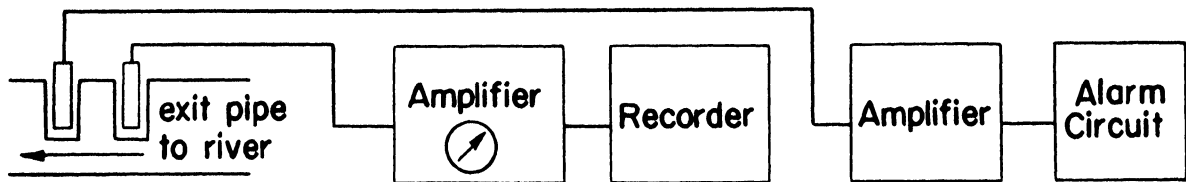


Figure 8-7.

keeping a record for legal purposes. The amplifiers should also have some warning device that would tell us when the water is too active. A block diagram is given in Figure 8-7.

Fourthly, we must monitor the cooling water for delayed neutrons. The reason for this is that, if our reactor is inhomogeneous, then most of the heat is produced in the uranium metal (since the fissions take place here) and so we must cool the metal. However, the water may carry some uranium away if there is a leak in the protective coating of the uranium lump. Such a leak represents a serious loss of fissionable material and the only way we can detect it is by the delayed neutrons. Since we want to detect the smallest leak possible, this means trying to measure as few neutrons as possible. Because of background, the lower limit is a few neutrons per minute. Here we use a neutron pulse chamber and a counting rate meter. The counting rate meter actuates a shut-off mechanism, when the rate is more than about 10 per minute. The chamber must be placed very near the point where the water leaves the pile, otherwise the delayed neutrons would have disappeared. The counting rate meter will be described later.

Up to now we have described the instruments necessary to run the pile and to maintain its "health." The final problem is the health of the personnel who operate the pile. In health physics the roentgen is used as a unit of X and γ -radiation, the maximum permissible dosage rate of these radiations being 0.1 roentgen per day. If a person plans to work for a period of 8 hours a day, the maximum permissible exposure in his working area is 12.5 milliroentgens per hour. The roentgen is defined as "that amount of X or γ -radiation such that the associated corpuscular emission (secondary electron radiation) per 0.001293 grams of air produces, in air, ions carrying one e.s.u. of quantity of electricity of either sign." A convenient unit in common use to describe the radiation dose from other types of radiation is the "roentgen equivalent physical" or the rep. It is equivalent to the roentgen since both a rep and a roentgen each produce about 83 ergs per gram of tissue. Neutrons

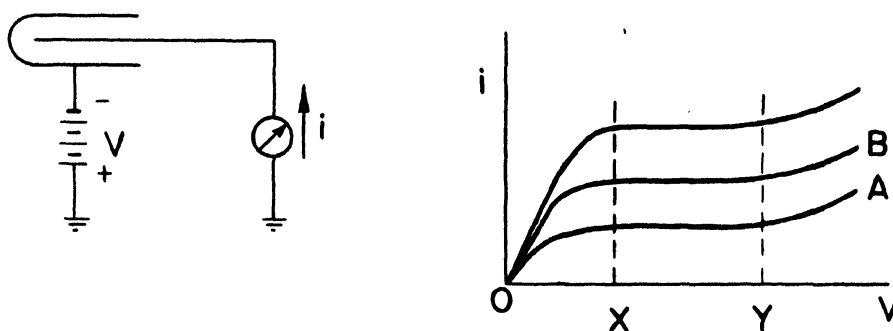


Figure 8-8.

are considered to be more harmful than gamma rays and the maximum permissible dose is 20 mrep per day for fast neutrons (± 200 fast neutrons/cm² sec for an 8 hr exposure per day) and 50 mrep per day for thermal neutrons (± 4500 thermal neutrons/cm² sec for an 8 hr exposure per day). Leaks in the biological shield, leaks through experimental and instrument holes, etc., of the pile may raise the radiation in the pile room to dangerous levels. For this reason we must continuously monitor the space around the pile with "health" instruments. These consist of slow neutron and γ -ray chambers with their associated amplifiers and alarm circuits, such that warning is given if there are either too many neutrons or too many γ -rays around.

8-3 Ionization Chambers*

An ionization chamber consists essentially of an outer (H.T.) electrode enclosing an inner well-insulated electrode, known as the collecting electrode. If we connect up such a chamber as shown in Figure 8-8 and, leaving the radiation intensity fixed, increase the voltage V , then the ionization current will vary as shown in curve A. In the region from 0 to X, the field is not strong enough to sweep out the ions before some of them recombine. From X to Y every ion created is collected by the more intense field. Beyond Y, the ions have so much energy that they themselves cause ionization and we have what is called gas amplification. On raising the radiation level and taking another voltage characteristic, we obtain curve B, etc. In the region X to Y, the ion current is directly proportional to the radiation in the chamber and is independent of V , the voltage on the chamber. For this reason, we operate all our chambers in this region, where the ion current is "saturated."

The factors that govern the design of an actual chamber for the pile are the following:

*The design of the two ionization chambers described here is due to H. Carmichael, N.R.C., Chalk River, Canada; C. R. Report July 30, 1946.

- (1) Saturation of the entire active volume of a chamber to insure linearity.
- (2) The radiation levels to be measured.
- (3) The pressure and kind of gas used to fill the chamber.
- (4) The minimum ion current necessary to operate a D.C. amplifier reliably.
- (5) The size of the instrument holes in the pile.
- (6) In the case of health chambers, a minimum equivalent volume of standard air to insure a representative picture of the intensity of radiation.

A discussion of all these factors is beyond our scope here. Moreover, a knowledge of these factors does not lead to any unique design of a chamber. In practice, a design is usually a compromise between desirable characteristics and practically obtainable ones. We shall therefore content ourselves with a detailed description of two chambers which have been used in pile operation. Both are neutron chambers, but one of them may be used for γ -rays also. Their sensitivity to neutrons is due to the presence in the chamber of the isotope B^{10} of boron, whose nucleus, on capturing a slow neutron, disintegrates into an α -particle and a Lithium nucleus with the release of 2.57 Mev of energy. This energy is shared by the two particles which fly apart in opposite directions. The boron can be introduced into the chamber either as a gaseous compound (e.g., BF_3), is filling the ion collecting space, or as solid B_4C or metallic B deposited on the walls of the electrodes. The ordinary boron, containing about 20% of the isotope B^{10} , is used here. If we could use the pure B^{10} isotope, an increase in sensitivity by a factor of 5 is possible.

The first chamber is the one used to measure the high neutron flux in the pile. It has boron-coated electrodes. There are two reasons why it was not gas filled: (1) an ion chamber containing BF_3 , subjected to the strong flux of slow neutrons in the pile, changes its sensitivity because the gas is gradually decomposed by the intense radiation and (2) saturation of a given ion current with BF_3 requires much higher voltages than with certain gases such as argon. We see, then, that it is preferable, where a large neutron flux is to be measured, to put the boron into the chamber in the form of a permanent layer on the wall of the electrode and to have the disintegration particles of B^{10} (α) Li^7 produce their ionization in argon. Since the range of the alpha is about 0.7 cm in standard air, the ionization in a chamber containing standard air will be confined to a region 0.7 cm distant from the boron coating. It is of advantage to keep the electrode separation as small

as possible for the following reasons: (a) the saturation characteristics of the chamber improve with decreasing separation and (b) the ratio of ion current due to neutrons, to ion current due to α -rays increases with smaller separation, since the latter is proportional to the separation.

The dependence of ion current on electrode separation and boron coat thickness is geometrical and may be inferred from the idealized picture in Figure 8-9. We shall assume that the ionizing particle has a range = 1 in both media, and that its ionization is constant along its path. This means using different normalized units of length in each medium. Now a particle, starting at A in II, at an angle θ , has a range in I equal to

$$1 - \frac{x}{\cos \theta}$$

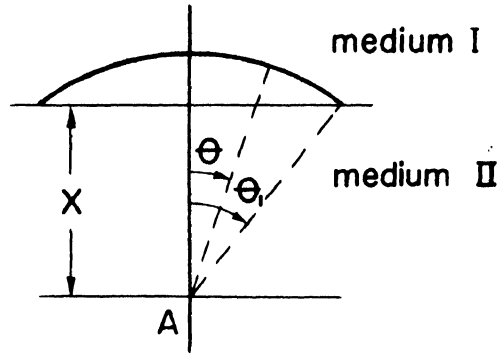


Figure 8-9.

The average range in I for particles starting at A is

$$\begin{aligned} & \int_0^{\theta_1} \left(1 - \frac{x}{\cos \theta}\right) 2\pi \sin \theta d\theta \bigg/ \int_0^{\pi} 2\pi \sin \theta d\theta \\ &= \left\{ -\cos \theta + x \log \cos \theta \right\} \bigg|_0^{\theta_1} \\ &= \frac{1}{2} (1 - x + x \log x) \text{ where } x = \cos \theta_1 \end{aligned}$$

This number represents the average track length in I for one disintegration at A in II. Now the average track length in I per disintegration in the layer dx of II is

$$\frac{1}{2} (1 - x + x \log x) dx$$

and the average track length in I per disintegration in the layer of II from $x = x$ to $x = 1$ is

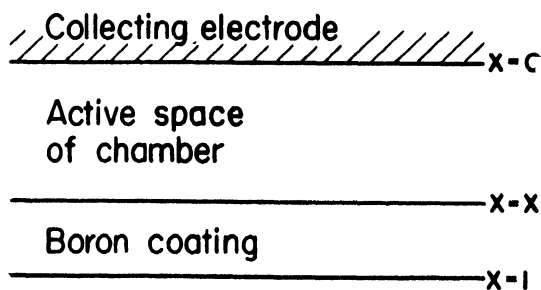
$$\int_x^1 \frac{1}{2} (1 - x + x \log x) dx = \frac{1}{2} \left(x - \frac{3x^2}{4} + \frac{x^2}{2} \log x \right) \bigg|_x^1$$

$$r_{av.} = \frac{1}{8} - \frac{x}{2} + \frac{3x^2}{8} - \frac{x^2}{4} \log x$$

This number represents the average fraction of the range of a particle due to a disintegration in that part of II from $x = x$ to $x = 1$, which lies in I.

We now apply this picture to determine (i) the electrode separation and (ii) the thickness of the boron coating.

(i) The electrode separation: To calculate the loss of ionization caused by the fact that part of the α tracks lie in the collecting electrode, we need consider only those α 's which come from distance 1 (in our length units) away. Thus only those α 's which come from a layer of boron of thickness $1 - x$ will be affected. The fractional loss per α is now given by



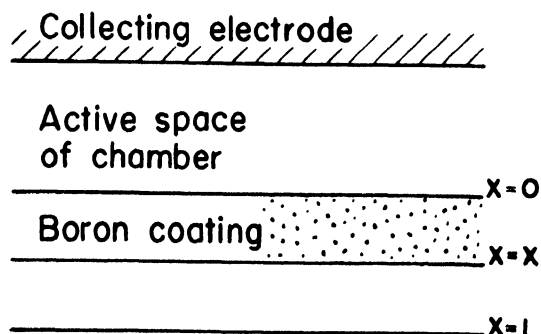
$$F = \left(\frac{1}{8} - \frac{x}{2} + \frac{3x^2}{8} - \frac{x^2}{4} \log x \right)$$

where x is the fraction:

$$x = \frac{\text{electrode separation}}{\text{range of } \alpha \text{ in ionizing gas}}$$

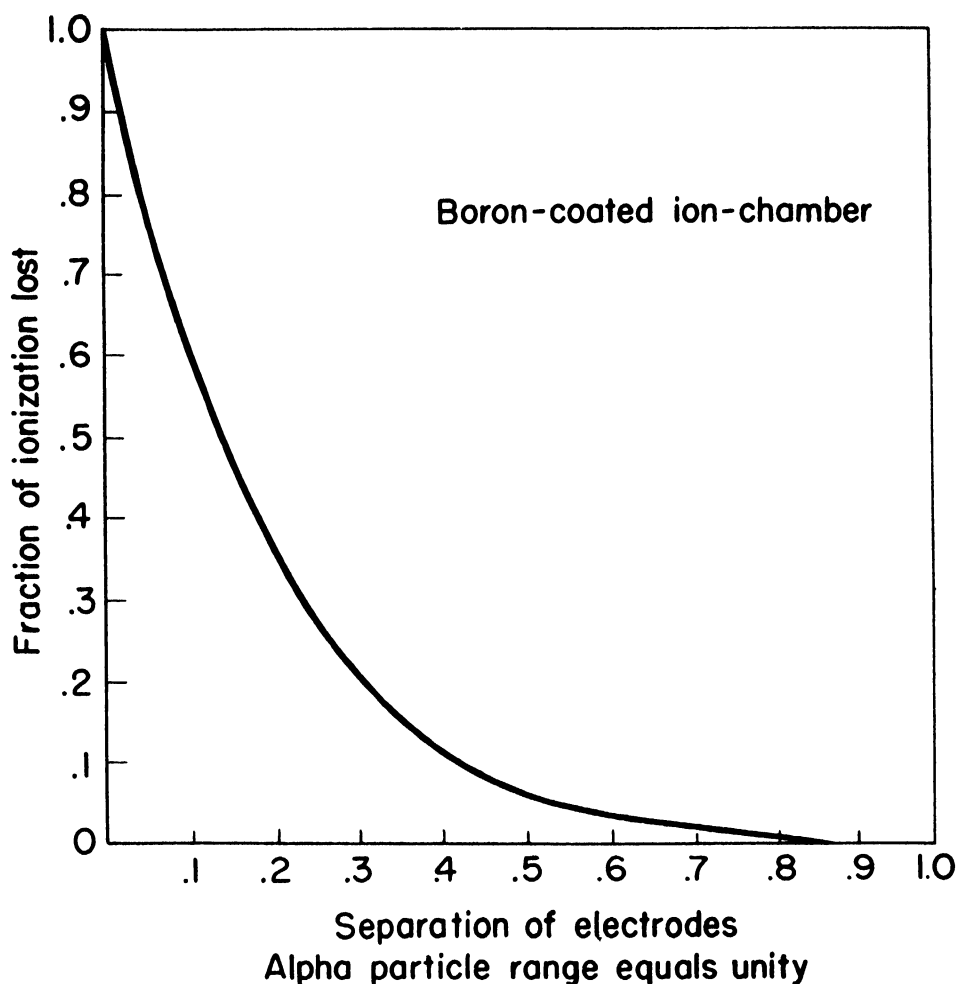
In Figure 8-10 we have plotted F against x . It will be seen that, even if the electrode separation is $1/2$ the range of the α , the loss of ionization is only about 6%.

(ii) Thickness of boron coating: If the boron coating is of thickness x (in our length units), then the ionization caused by α 's starting from the layer $x = x$ to $x = 1$ is lost (any α starting below $x = 1$ won't reach the ionizing space anyway). As before, this is just



$$F = \left(\frac{1}{8} - \frac{x}{2} + \frac{3x^2}{8} - \frac{x^2}{4} \log x \right)$$

where now $x = \frac{\text{thickness of boron coating}}{\text{range of } \alpha \text{'s in boron coating}}.$



Reproduced by permission of
H. Carmichael, Nat. Res. Council, Canada

Figure 8-10.

Thus we see, as before, that only 6% will be lost even if we make the thickness of the boron $1/2$ the range in boron of the α -particle.

The actual range of the boron disintegration α -particle in boron is 9.1×10^{-4} cm. Thus we may use a coat of about 5×10^{-4} cm. This corresponds to about 1 mg of boron/cm² of surface. A drawing of the chamber is given in Figure 8-11.

Other factors entering into the design of the chamber will not be discussed here. We shall describe a design that has been used in the pile at Chalk River, Canada. The design cannot be made unique and, for a given purpose, several designs may be satisfactory.

We proceed now to calculate the current to be expected from this chamber. The electrode separation here is 0.533 cm. The argon pressure, p , required to make 0.533 cm equal to half the range of the α -particle, is given by

$$p = \frac{\text{range of } \alpha \text{ in standard air}}{\text{stopping power of argon rel. to air}} \\ \times \text{pressure of st. air} \times \frac{1}{2 \times .533} \\ = \frac{0.7}{.914} \times 76 \times \frac{1}{2 \times .533} = 55 \text{ cm. of Hg at } 0^\circ\text{C.}$$

The stopping power of elements for α -particles is about proportional to $\sqrt{\text{at. wt.}}$

Next we calculate the current per sq. cm. of boron coating caused by the ionization produced in the collecting space by the disintegration α -particles and Li nuclei. The current due to the α -particles is given by:

$$i_\alpha = N \times F \times \frac{E_\alpha}{E_{ip}} \times i_{ip}$$

where N = no. of α -particles produced.

$$= (\text{neutron flux}) \times (\text{cross section of } B^{10}) \times (\text{No. of } B^{10} \text{ atoms in the absorption range of } \alpha\text{-particle in boron})$$

F = fraction of the energy of the α -particle which is expended in the argon.

E_α = energy of the α -particle.

E_{ip} = energy required to produce 1 ion pair.

i_{ip} = current per ion pair per sec.

The current due to the Li nuclei is given by a similar expression. Substituting in the equation, we find the total current to be

$$i/\text{cm}^2 = 5.33 \times 10^{-17} f \text{ amperes/cm}^2$$

where f = no. of neutrons/cm²/sec. The area of the electrode surface is 690 cm². Thus we get a total ion chamber current of $3.68 f \times 10^{-14}$ amperes. The experimental value is 10^{-14} f amperes. Most of the error is no doubt due to the idealized method in calculating wall losses.*

*Much more complete calculations for wall losses, etc., were done by R. D. Evans, Phys. Rev. 45, 29, (1934).

The second type of chamber is designed to measure much lower intensities of radiation. It is sensitive to γ -rays, fast or slow neutrons, depending upon the type of filling gas used. For γ -rays it is filled with argon, for slow neutrons with (BF_3) boron trifluoride, for fast neutrons H_2 , or helium. The chamber is made to stand pressures of filling gas up to 20 atmospheres. It may be used to control piles of low power, to monitor the cooling water, and to make health measurements in the pile room. The design of such a chamber depends on the list of factors given at the beginning of the discussion on ion chambers. A drawing of the chamber is given in Figure 8-12. The collecting electrode is made large to secure a strong and uniform collecting field. The shape and dimensions insure that when saturation field is established over the greater part of the collecting volume, there remain no regions of comparatively weak field still far from saturation. The weakest field is at the surface of the outer cylindrical electrode and this is made equal to the field at the apex of the spherical portion. At the other (insulator) end, the field is much stronger but this is of no consequence since, after saturation, the current does not depend on the field. Apart from the part of the design dictated by saturation requirements, the rest of the design depends on many practical factors, such as ease of construction, size of holes in the pile, etc. When this chamber is filled with BF_3 , it gives a current of the order of 10^{-11} amperes for a slow neutron flux of about $10^4/\text{cm}^2/\text{sec}$. This corresponds to 1/2 a tolerance dose of slow neutrons.

A word should be said here about the insulators on the chambers. They must have the following properties:

- (1) Mechanical strength to withstand high filling pressures and accidental knocks and jars.

- (2) High resistance (about $10^{15} \Omega$ or more). This must be maintained under adverse humidity conditions.

- (3) Absence of deterioration under intense radiation of neutrons, γ -rays, etc.

- (4) Maintenance of mechanical and electrical properties over long periods of time.

- (5) The insulator should be shielded from the field to minimize surface leakage.

The most suitable insulator material appears to be quartz.

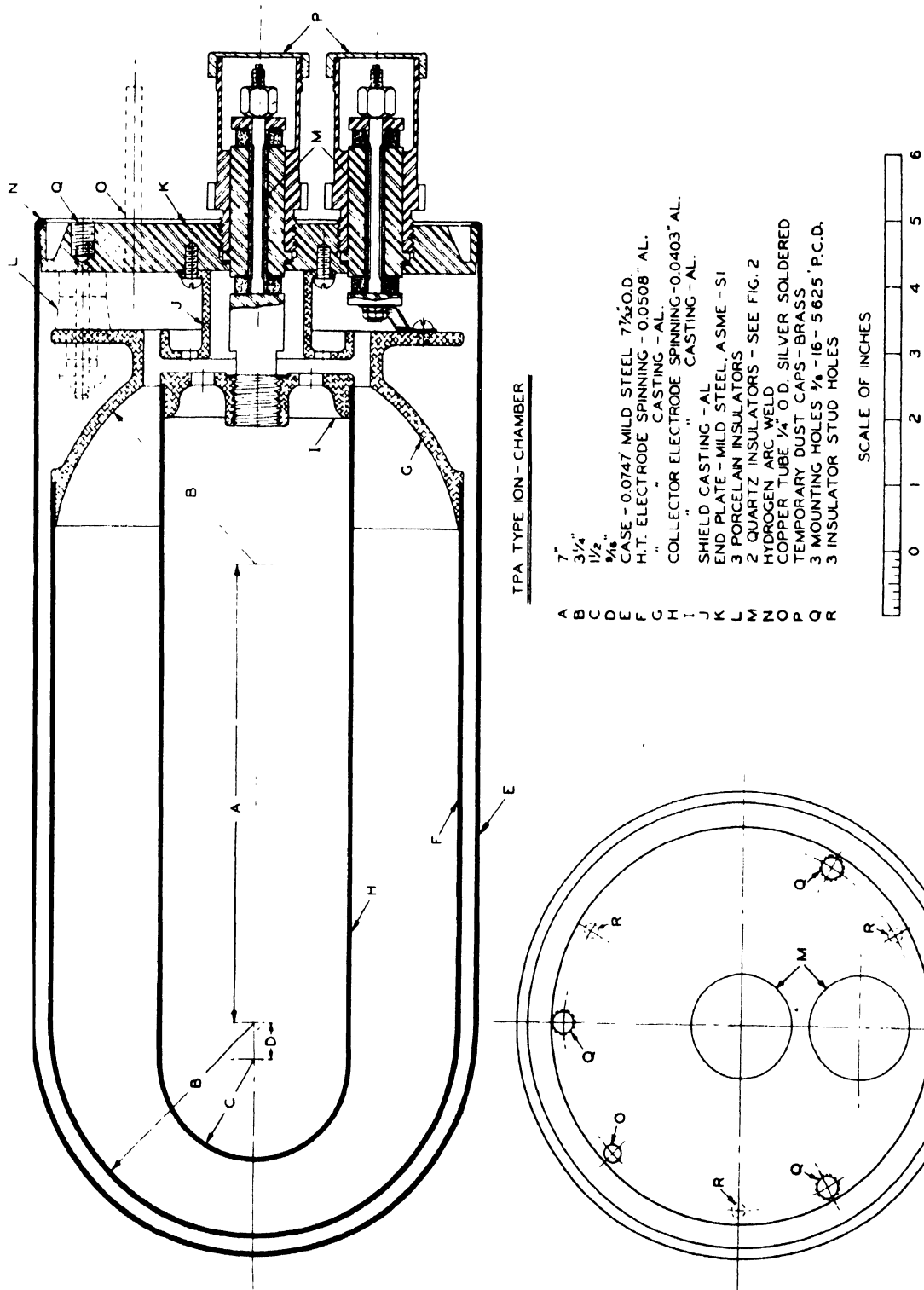


Figure 8-12

Reproduced by permission of
H. Carmichael, Nat. Res. Council, Canada

After the chambers are built, they must be calibrated with the radiation for which they are intended. This is easily done by using known sources of radiation and appropriate current measuring apparatus.*

8-4 D.C. Amplifiers

We have seen that the ionization chambers give currents in the range between 10^{-13} and 10^{-6} amperes for the radiation intensities that we shall measure. These currents must be measured and recorded and, in some cases, be made to control the relays in alarm and shut-off circuits. The most suitable instrument for these functions is the electronic directly-coupled amplifier. The only other possibility is to use electrometers or sensitive galvanometers in combination with recording cameras and photoelectric cells. But these instruments are not sufficiently rugged to be used in an industrial plant, such as the pile. A general requirement on all instruments is that they have errors not exceeding 2 or 3%.

Before going on to a description of the actual amplifiers used, we shall discuss briefly several factors that enter into the design of any low current amplifier.

(a) The grid current of the input tube must be at least 50 times less than the current we are measuring. This is necessary, since the grid current in most commercial receiving tubes is subject to violent fluctuations of the order of 50 or 60%. These fluctuations must then be 1 or 2% of the current measured. The causes of grid current are well known and the grid current may be reduced to about 10^{-13} or 10^{-14} amperes in some commercial tubes with sufficiently good insulation of electrodes by reducing filament and all other electrode voltages.** For example, a 954-type tube, with the following voltages and currents: $E_p \sim 8$ v., $i_p \sim 60$ μ a, $i_f \sim 120$ ma, $E_{g1} = 0$, $E_{g2} \sim 6$ v., $E_{g3} \sim 1$ v., has a grid current in the third (suppressor) grid of about 10^{-13} amperes. This grid may be used as a control grid. There are several tube types manufactured specifically for electrometer purposes, such as the FP54 and the VX124. These have grid currents of about 10^{-15} and 10^{-14} , respectively and, accordingly, may be used to measure smaller currents.

(b) Stability. For a purely engineering purpose, we require that the amplifier zero and sensitivity drifts be no more than 1 or 2% per week. Moreover, we require that the amplifiers operate out of 110-volt A.C. lines, which will fluctuate by about $\pm 15\%$. The first step toward stability is to use a very highly-stabilized power supply. There are several well-known circuits for such power supplies and, with some refinement, stabilization factors of the order of 5,000 to 10,000 are possible.

*See C. R. Tec 282, C. O. Peabody, Nat. Res. Council, Chalk River, Ontario, Canada.

**Gabus and Pool, R.S.I. 8, 196, (1937).

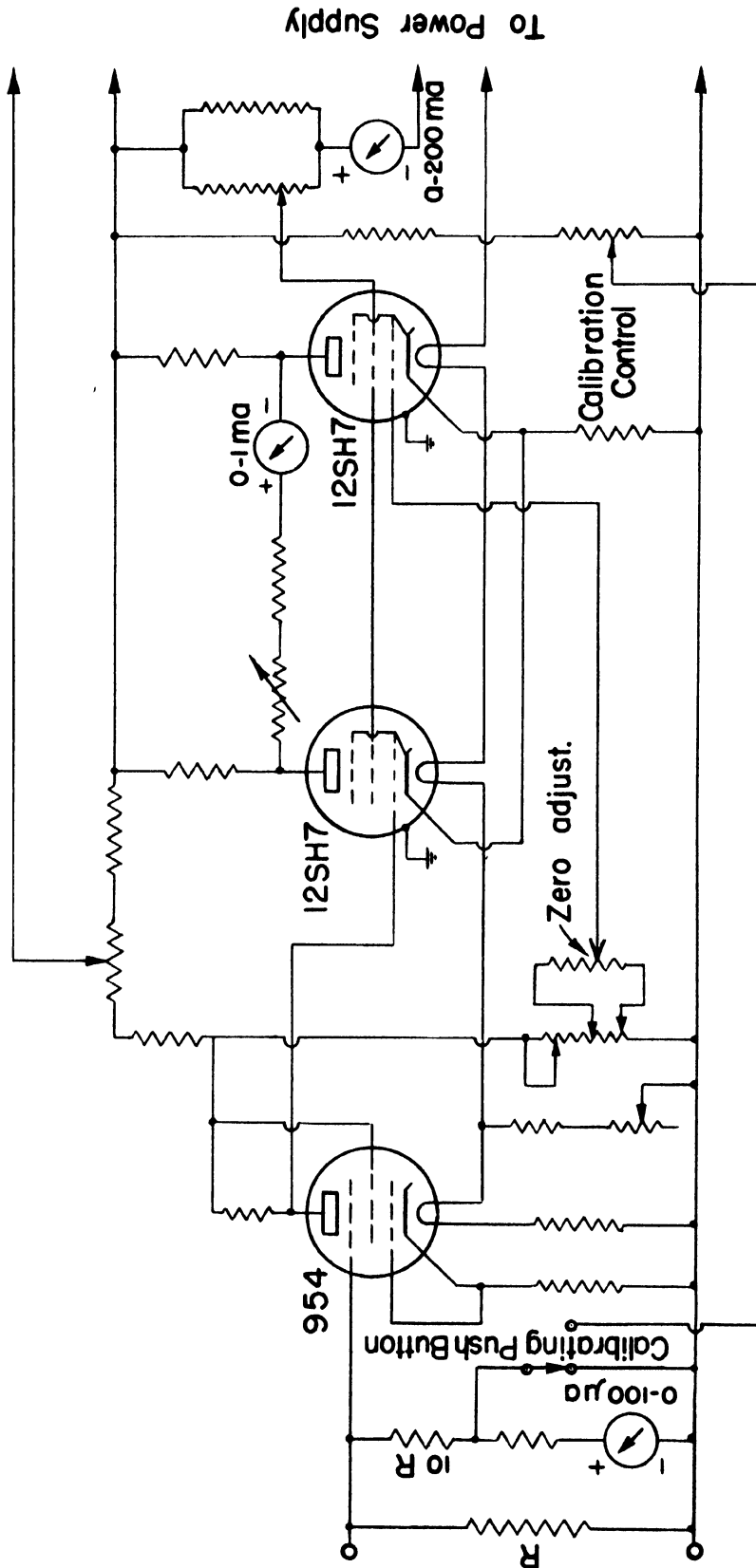


Figure 8-13
D C Amplifier

Secondly, since part of the drift is due to varying contact potentials at the input, and since this variation is of the order of millivolts, we design the amplifier so that 1 volt on the input grid corresponds to full scale.

Thirdly, wire-wound resistances are more permanent than commercial carbon resistances and so the former should be used at all critical parts of the circuit.

Fourthly, tubes are stabilized by aging them for 100 hours under the conditions in which they will operate in the amplifier.

And, finally, any residual drifts left may be reduced by proper design of the circuit. We shall see later that it is possible to design circuits such that, over a certain range, the output signal is independent of some supply voltage to which, normally, the signal may be sensitive.

(c) Dependability. The circuits should be designed so that if an amplifier for some reason ceases to operate properly, it will give warning of this condition.

(d) As far as possible, the amplifiers should be rugged and easy to adjust and service.

With these preliminary remarks, we pass on to a description of a D.C. amplifier that has been used in pile operation. A circuit diagram is given in Figure 8-13. The first stage is the low grid current electrometer tube, which here is a 954 acorn type. Two features of this stage are of interest: (1) The grid current is about 10^{-13} amperes so that, with 1-volt full-scale signal, we may use grid resistors up to 2×10^{11} and thus measure currents down to $\frac{E}{R} = \frac{1}{2 \times 10^{11}} = 5 \times 10^{-12}$ amperes full scale. (2) The circuit has a stabilizing feature. This can be explained as follows:

In Figure 8-14 we plot the plate current i_p against filament current. It will be seen that at $i_f \sim 120$ ma, the plate current is almost independent of i_f and this leads to a stable output voltage at the plate. The necessity for the extra stabilization of i_f is due to the fact that at low filament currents, small changes in i_f cause large changes in i_p . The second stage is a push-pull cathode coupled current

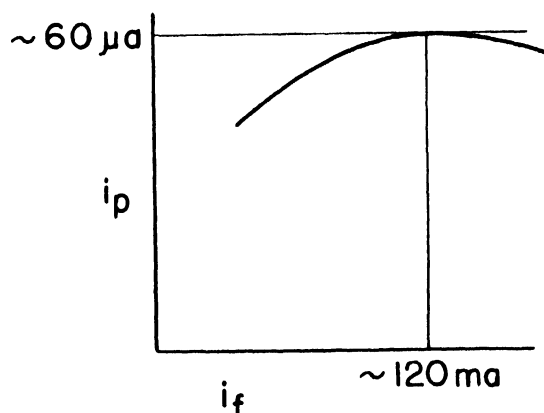


Figure 8-14.

amplifier which operates a 1 ma meter. The stability here is enhanced by the fact that the tubes are matched and therefore any supply voltage drifts affect them equally. The output voltage of the current amplifier is passed

on to the trigger circuit, which is of the conventional Schmidt type. The second tube of this stage contains the relay as a plate load. In this amplifier, the following precautions are taken against failures: (1) All the filaments are directly heated from the stabilized power supply and are connected in series. This insures that a warning is given if some filament burns out. (2) The relay has current in it in the no-alarm position. If the current is cut off for some reason (e.g., failure of tube), then the relay closes the alarm or shut-off contacts. (3) These amplifiers are "protectively" serviced and adjusted once a week and tubes are changed every 1000 hours of operation. Experience has shown that almost all failures can be prevented in this way.

The chamber is connected to the amplifier input through a shielded coaxial cable. This cable and its connectors must have the required insulation resistance of about 10^{15} ohms. Most cables are ruled out by this requirement and some of the remaining ones, e.g., polystyrene cables, are useless, since they have frictional electrostatic effects (these produce large spurious signals when the cable is moved or bent). The most satisfactory cable has been found to be solid copper coaxial, with isolantite insulating beads. The electrostatic frictional effect is very small here - largely owing to the rigidity of the cable.

The second instrument we describe is the logarithmic amplifier.* The principle of operation is as follows: If we connect a retarding voltage V_R between a large plane cathode and plate (see Figure 8-15), then the relation

*Meagher and Bentley, R.S.I. 10, 336 (1939).

*Nottingham, Phys. Rev. 49, 78 (1936)

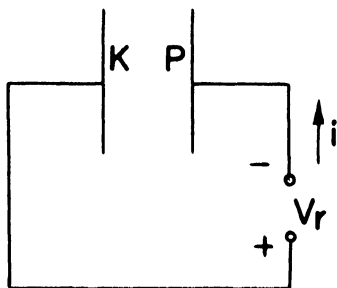


Figure 8-15.

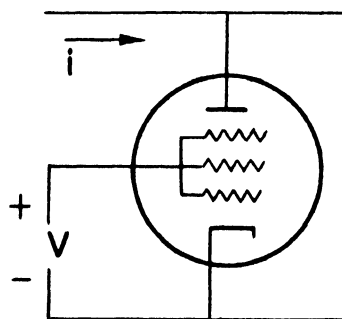


Figure 8-16.

between the current that flows and the retarding voltage is of the form:

$$V_R = -K \log i + b$$

where K and b are constants. Now it is possible to obtain the conditions represented in Figure 8-15 in commercial electronic tubes. This is done by connecting up the tube as shown in Figure 8-16. Here the grids are all tied together and a positive voltage is applied to them. The electrons, starting from the cathode, are accelerated through the grids and then enter the retarding field between the last grid and plate. In the case of a type 959 tube, connected up this way, it is found that the voltage at the plate, V , is related to the tube current i by an equation similar to the one above, namely,

$$V = -K \log i + b$$

The constant K is about .2 volts. Experimentally, this relation is found to hold for currents in the range 10^{-13} to 10^{-6} with deviations of a few per cent. If we now replace the input resistance of the D.C. amplifier which has a full-scale input of one volt, by the logarithmic tube, then we have a logarithmic amplifier which will measure currents over a range of $10^{1/.2} = 10^5$.

The final instrument is the counting rate meter.* The essentials of one type of counting rate meter are shown in Figure 8-17. The input pulses are first fed into a standardizing circuit, e.g., a biased multivibrator, which accepts pulses of any size and shape and transforms them into pulses of constant width and amplitude. These standard pulses are fed into the RC circuit through a diode arranged so that each pulse puts a constant charge q on the condenser C . If we start feeding in pulses at some rate, say n/sec , then the voltage on the resistance R is given by

$$V_R = V_{\infty} (1 - e^{-t/RC})$$

*Evans and Alder, R.S.I., 10, 332 (1939).

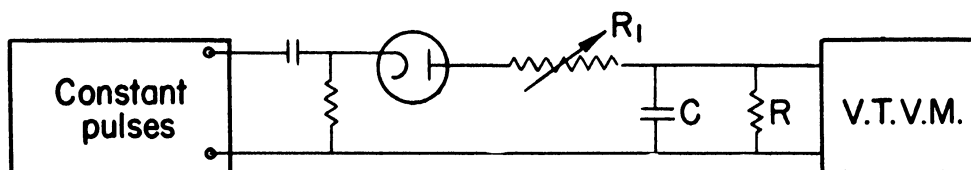


Figure 8-17.

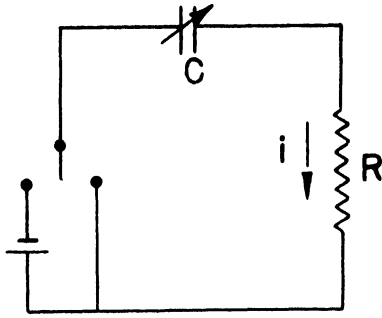


Figure 8-18.

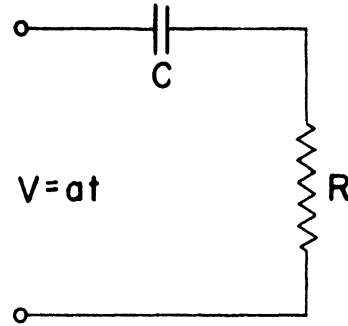


Figure 8-19.

where V_{∞} is the final voltage, determined by the condition that the charge which leaks through R per second is just equal to nq . That is,

$$V_{\infty} = nqR = iR$$

in the steady state. From this we see that V_{∞} , the steady state voltage on R , is proportional to n , the number of pulses per second. V_R is measured with a vacuum tube voltmeter.

Two features of this instrument are of interest: (1) It is possible to vary the range by varying R_1 (and so q) without changing the time constant RC , and (2) it is likewise possible to vary RC (by changing C) without varying the range. (This is useful in some investigations, since the time constant must bear a definite relation to the counting rate in order to minimize random fluctuations.)

Finally, we mention briefly here two methods of calibrating low current amplifiers. The problem of calibration reduces essentially to producing small known currents. This can be done with good accuracy in two ways:

(a) Referring to the circuit in Figure 8-18, if we first charge the condenser and then short circuit it and simultaneously begin reducing the capacity of C , so that $C_t = C_0 - at$, at such a rate that the voltage across R remains constant, then the current i is equal to $V_R \frac{dC}{dt}$. Both V_R and $\frac{dC}{dt}$ may be measured with good accuracy.

(b) In the circuit of Figure 8-19, we leave the condenser fixed but apply a linearly increasing voltage $V = at$. Under these conditions, the steady state current is given by $i = C \frac{dV}{dt}$ and again C and $\frac{dV}{dt}$ may be measured with accuracy. The second method admits of a useful application to the cal-

ibration of pile instruments. The condenser C is already in existence as the interelectrode capacity of the chamber (capacity between H.T. electrode and collecting electrode) and it has, in a good chamber, the requisite high insulation. All we need to do is to make the H.T. voltage rise at some known rate. Then, knowing the interelectrode capacity, the induced current in the amplifier input is $C \frac{dV}{dt}$. In this way, we calibrate the amplifier as well as check the whole system for faulty insulation.

CHAPTER 9

CONSTRUCTION OF NUCLEAR REACTORS

by

Clark Goodman

9-1 General Considerations

The preceding discussions have laid the experimental and theoretical foundation on which, in a general way, we should be able to design and build nuclear power reactors. The major problems involved are of an engineering nature, but of an unconventional type, which is beginning to be called "nuclear engineering." During its formative stage, nuclear engineering was devoted primarily to the development of explosives for military purposes. The emphasis has now shifted to the development of peacetime applications, particularly in the field of nuclear power. On the basis of the previous discussions, we will consider some of the problems involved in the construction of such power units. It should be stressed at the outset that most of the technological details that follow have been obtained either from the open literature or from declassified reports of the Manhattan Project. In all other instances, the suggestions are simple extrapolations which any technical person could make, using well-known principles.

(Table 9-1 summarizes some of the declassified information about the several nuclear reactors that have been built. The initial date refers to the date of the first operation, or the date of the explosion in the case of the five bombs.) It is not certain that the German pile ever attained the critical size. As discussed later, the reactors are considered to be of two classes: heterogeneous and homogeneous. In the latter, the fissionable material is uniformly distributed throughout the active portion of the reactor. For example, in the Los Alamos "water boiler," approximately 1 kg. of U^{235} , in the form of a soluble salt of enriched uranium, is dissolved in light water. Thus the fissionable material is dispersed throughout the moderator; the active portion being contained in a stainless-steel sphere about one foot in diameter surrounded by a reflector of BeO (Ref. 6 in Table 9-1).

(In heterogeneous units, the fissionable material is localized in lumps or rods forming a structured unit. For example, the Hanford piles contain solid cylindrical rods of ordinary uranium metal (clad with aluminum and cooled by an annulus of water) distributed in a symmetrical array throughout a graphite lattice.)

TABLE 9-1
SUMMARY OF NUCLEAR REACTORS
(described in open literature)

Location	Initial Dates	Class	Type	Fissionable Material	Moderator	Coolant	Power Developed or Energy Released	Ref.
Univ. Chicago (West Stands)	Dec. 2, 1942	Heter.	Thermal	U + U oxide (lumps)	Graphite	None	200 watts	(1)
Oak Ridge	Nov. 4, 1943	Heter.	Thermal	U (Al-clad rods)	Graphite	Air	>2000 kw.	(2)
Argonne	Spring 1943	Heter.	Thermal	U + U oxide (lumps)	Graphite	None	few kw.	(3)
Hanford (three)	Summer 1944-Spring 1945	Heter.	Thermal	U (Al-clad rods)	Graphite	Water	>10 ³ kw.	(4)
Argonne	May 15, 1944	Heter.	Thermal	U (rods)	D ₂ O	D ₂ O	>300 kw.	(5)
Los Alamos	1944 ?	Homo.	Thermal	Enriched U	H ₂ O	H ₂ O	10 kw.	(6)
Chalk River	Fall 1945	Heter.	Thermal	U (rods)	D ₂ O	D ₂ O	3.5 w.	
Alamogordo	July 16, 1945	Homo.	Fast	U-235 or Pu-239	None	None	>10 ⁵ tons TNT	(7)
Hiroshima	Aug. 6, 1945	Homo.	Fast	U-235 or Pu-239	None	None	>10 ⁵ tons TNT	(8)
Nagasaki	Aug. 9, 1945	Homo.	Fast	U-235 or Pu-239	None	None	>10 ⁵ tons TNT	(8)
Bikini (two)	July 1 and July 25, 1946	Homo.	Fast	U-235 or Pu-239	None	None	>10 ⁵ tons TNT	(8)
Haigerloch, Germany	?	Heter.	Thermal	U (2 tons)	D ₂ O (2 tons) C (10 tons)	?	?	(9)

References: Smyth Report: (1) 6.29 and appendix 4; (2) 6.44, 8.37, 8.43, 8.53; (3) 8.28; (4) 7.19, 8.53; (5) 8.27, 8.32; (7) Appendix 6; (6) R. F. Christy: Verbal report Chicago meetings, American Physical Society, July 1946; Abstract Bulletin American Physical Society, December 1946; (8) Chemical and Engineering News, pp. 1782-1786 (July 10, 1946); Life, pp. 25-29 (July 15, 1946); Power, pp. 83-91 (September 1946); (9) Quotation from W. Heisenberg, Boston Herald, February 24, 1947.

(Each of these two classes of reactors can be of three general types: fast, resonance (or epithermal), or thermal -- so named for the average velocity or energy of the neutrons that propagate the chain reaction.)

CLASS		TYPE
(composition and structure)		(energy or velocity of neutrons)
HOMOGENEOUS	}	FAST
HETEROGENEOUS		RESONANCE (OR EPITHERMAL)
		THERMAL

As discussed below, any of these types might be used to develop power.

9-2 Fission Process as a Source of Power

However, none of the chain-reacting units that have been built to date develops useful power. The heat from the piles is delivered at such a low temperature (less than 100° C. for water-cooled units and less than 150° C. for air-cooled units)* that it is of only limited usefulness. Inherently, there is no practical limit for the temperatures attainable in the fission process, as evidenced by the stellar temperatures of the "atomic" bomb. In fact, it follows from elementary thermodynamics that the fission particles fly apart with velocities corresponding to temperatures of many billion degrees.)

$$(9-1) \quad \text{K.E.} = \frac{1}{2} mv^2 = \frac{3}{2} kT = \frac{3}{2}(1.37 \times 10^{-16})T = 1.6 \times 10^{-6} E$$

$$(9-2) \quad \therefore T = 7.8 \times 10^9 (E) \quad T \text{ in } ^{\circ}\text{K}, E \text{ in Mev}$$

As given in Table 1-1, the most probable values of E for the fission fragments of U^{235} are 97 Mev for the light and 65 Mev for the heavy. Thus the fission energy is delivered at a very low level of entropy ΔS :

$$(9-3) \quad \Delta S = \Delta E/T$$

*Smyth Report, 8.43

corresponding to a highly available state. However, nuclear explosives are the only means thus far developed which take advantage of this low level of entropy. Even the most refractory materials (W, graphite, BeO , Al_2O_3 , MgO , UC_2 , UO_2 , ThO_2) melt or decompose at temperatures of only a few thousand degrees. Thus the atomic properties of structural materials impose very restrictive limits for useful applications of nuclear energy. In the deceleration of the fission fragments, much of the thermodynamic advantage of the fission process is lost. The highly available energy of the fission process almost immediately undergoes a large increase in entropy upon being transferred to the thermal agitation of the surrounding atoms. In brief, explosive reactors develop their energy at too high a temperature to be useful, while the physical properties of structural materials limit the temperature of power units to conventional engineering levels.

9-3 Impracticable Methods

Some highly impracticable schemes have been suggested in attempts to span this gap. Three of these will be considered briefly, not because they are to be taken seriously, but because they illustrate other limitations of the fission process. Figure 9-1 is a schematic cross section of a ram jet engine using a spherical nuclear reactor as a source of heat. The heat transfer is assumed to take place almost entirely by radiation from the high surface temperature T_s to the heavily smoke laden air which whizzes through the orifice surrounding the streamlined reactor. The smoke presumably is generated by conventional means and injected at the intake end of the ram jet. The particles which are heated by radiation almost immediately transfer their thermal energy to the adjoining air molecules. Greater surface for radiation could be provided by channels through the reactor, but these would substantially increase the size and decrease the neutron efficiency of the reactor. It is clear that any openings in the reactor which allow the passage of air will also provide ready egress for the neutrons. Upper limits for T_s are dictated by the melting or sublimation temperatures of the reflector materials. Limitations are also imposed by the oxidizing properties of materials which might otherwise appear promising. Thermal stresses would be excessive under the large temperature gradients. In brief, as Gilliland* has

*See Chapter 10.

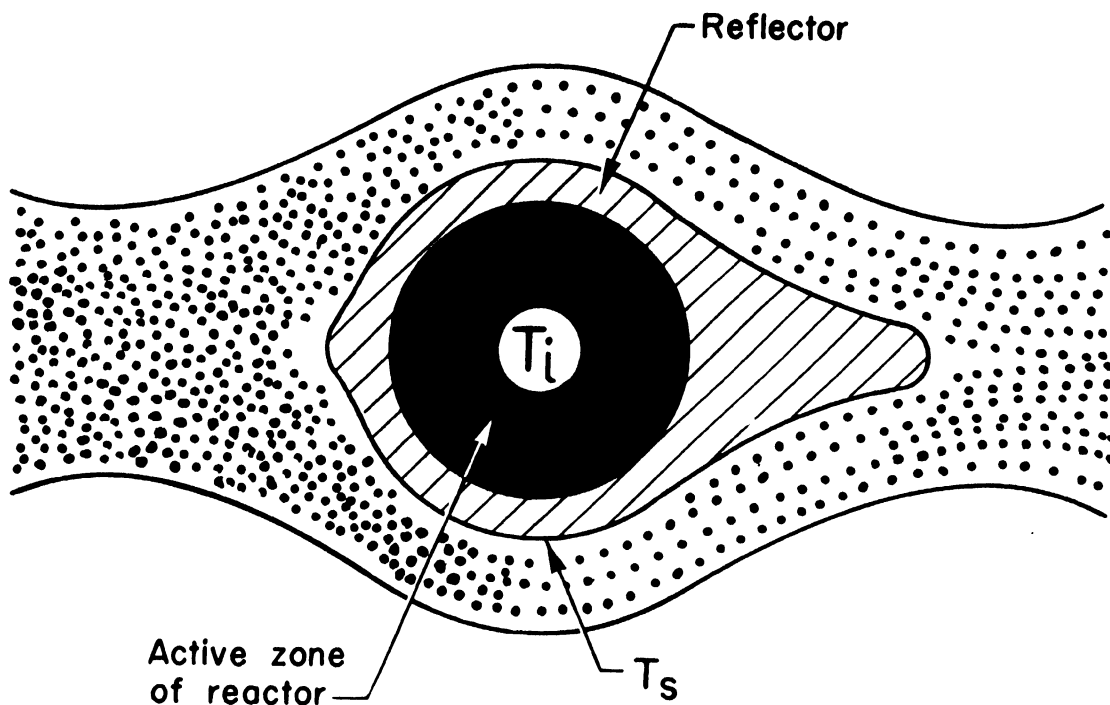


Figure 9-1. Hypothetical Ram Jet Engine. The similarity between the central sphere and the conventional eight ball is not intended to be symbolic.

shown, at the temperatures at present attainable, heat transfer by radiation is much less promising than by convection. However, the relative merits of possible combinations of materials for such a device are summarized in Table 9-2.

The second scheme, which is absurd, to say the least, proposes to use the recoil momentum of fission fragments to obtain a thrust $d(mv)/dt$. It is easy to show that this pseudo-rocket would be flea-powered. Figure 9-2 serves to illustrate this idea. Since most of the impulse will come from the rearward component of the momentum of the fission fragments which escape, it is important to know the range of fission fragments in solid materials. The cloud chamber studies of the Scandinavian trio, Bøggild, Brostrom, and Lauristen, discussed in Section 1-26, established mean ranges of 25 air-mm for the light fragments and 19 air-mm for the heavy fragments. Obviously, only a layer of solid material a few microns in thickness would be effective - all other fission fragments would be absorbed essentially in situ.

TABLE 9-2. SUMMARY OF MATERIALS OF CONSTRUCTION FOR HOMOGENEOUS NUCLEAR REACTORS THAT MIGHT OPERATE AT VERY HIGH TEMPERATURES (enriched uranium assumed in each case)

Type	Reactor		Reflector		Limitations
	Materials	M.P. °C	Materials	Max. T _s °C	
Fast*	U	1150	W	3370	Oxidation of W
Fast*	U+W	<3370	W	3370	Oxidation of W and U
Fast*	U	1150	C	3500	Oxidation of C
Fast*	U+Th	<1150	ThO ₂	> 3000	
Resonance	U+Ta	?	Ta	2800	Oxidation of Ta
Resonance	U+Re	<1150	Re	3400	Scarcity of Re
Resonance	U+Cu	<1150	MgO	2800	
Resonance	U+Cu	<1150	ThO ₂	>3000	
Resonance	U+MgO	?	MgO	2800	
Thermal	U+Be	<1150	BeO	2600	
Thermal	U+BeO	?	BeO	2600	Thermal stresses
Thermal	UC ₂	2260	C	3500	Oxidation of C
Thermal	U+C	?	MgO	2800	
Thermal	UO ₂	2500	MgO	2800	
Thermal	U+Be ₂ C	?	Be ₂ C	2100	Decomposition of Be ₂ C
Thermal	U+Al ₂ O ₃	?	Al ₂ O ₃	2500	

*Assumed to operate with molten core.

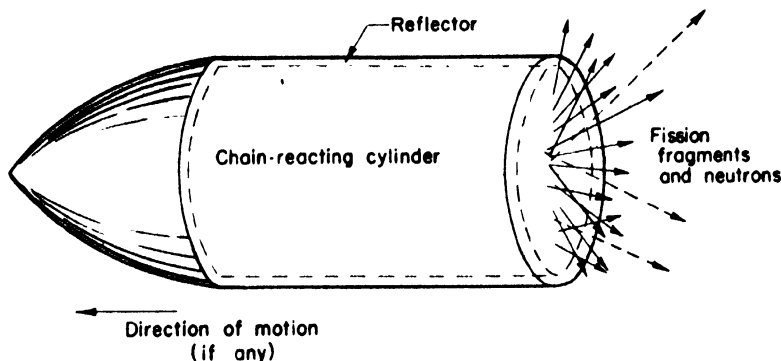


Figure 9-2. Nuclear-Powered Pseudo Rocket.

9-4. Range of Fission Fragments

Because the range of fission fragments is of general importance in the design of nuclear reactors, particularly in considering radiation effects and in determining the minimal thickness of cladding materials on fuel assemblies, two ingenious investigations of this problem will be reviewed at this time. In the first of these, Segre and Wiegand* performed two sets of measurements. A thin layer of U_3O_8 ($.085 \text{ mg/cm}^2$) enriched in U^{235} and deposited on a Pt disk was covered with various thicknesses of Al foil over which was placed a thick film of celluloid. The layered system was irradiated with a known flux of neutrons for a given period of time, and the beta-activity of the fission fragments collected in the celluloid was measured. If the fission fragments all had the same range, the curve of transmission versus thickness of Al (expressed in mg/cm^2) would be a straight line. Such is the case for Po alpha particles used for comparison. However, as discussed in Section 2-6, the fission fragments show considerable variation in mass and energy. Hence, the transmission follows the relationship shown graphically in Figure 9-3. Using the same deposits of U_3O_8 , the transmission of collodion, Al, Cu, Ag, and Au were measured with a H_2 -filled ionization chamber connected to a linear amplifier of constant amplification and bias. After applying a correction due to the minimal detectable range, the experimental results shown in Figure 9-4 yield the tabulated values of Table 9-3.

Although these observations cannot be compared directly with those

*Phys. Rev. 70, 810 (1946)

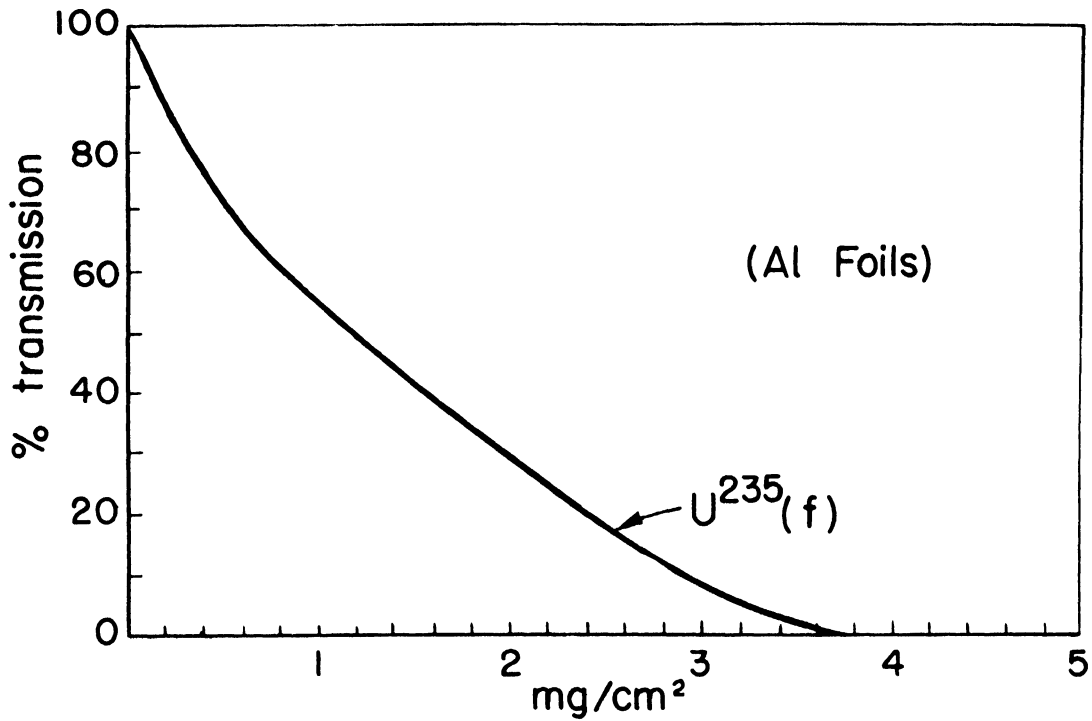


Figure 9-3. Transmission through Aluminum of Fission Fragments from U^{235} (from Segré and Wiegand)

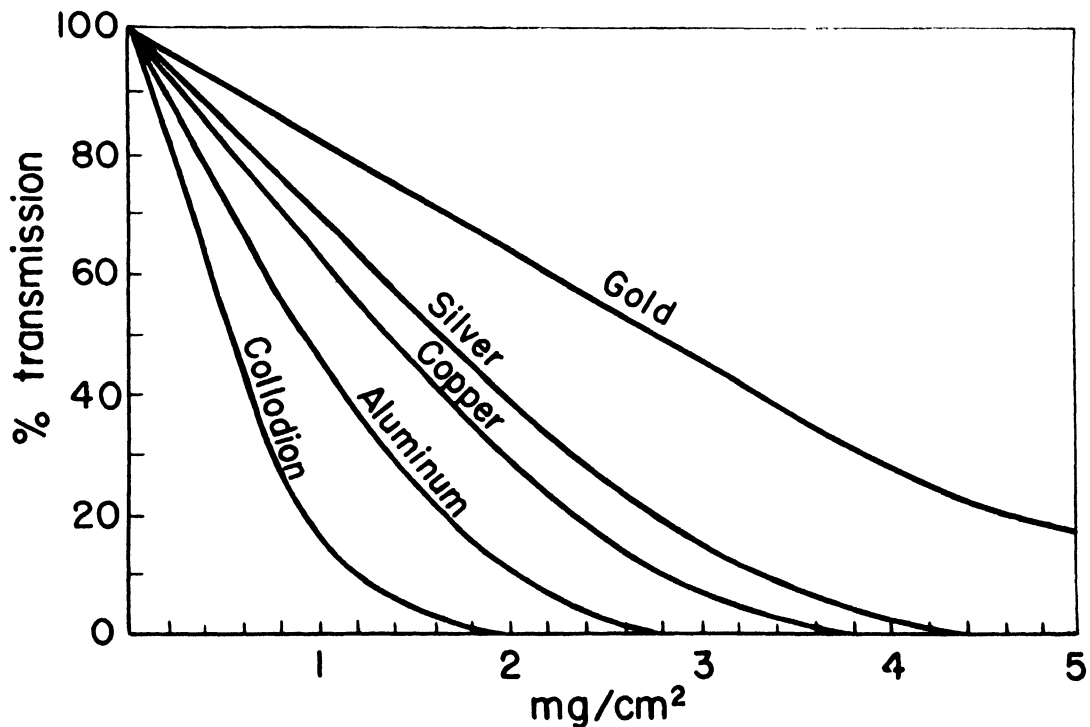


Figure 9-4. Transmission through Various Materials of Fission Fragments from U^{235} as Measured by Pulse Counting (from Segré and Wiegand)

TABLE 9-3
THICKNESS OF ABSORBER REQUIRED TO STOP 100 PER CENT
OF FISSION FRAGMENTS FROM U^{235}

<u>Absorber</u>	<u>Thickness of Absorber</u>		
	<u>mg/cm²</u>	<u>microns</u>	<u>mils</u>
Collodion ($C_{12}H_{17}O_{16}N_3$)	2.6	26	1.0
Aluminum	3.7	14	.55
Copper	5.2	5.8	.23
Silver	6.1	5.8	.23
Gold	11.14	5.8	.23
Uranium*	(12.6)	(6.7)	(.26)
U_3O_8	(10.0)	(14.)	(.55)

() Values in parentheses were computed -- others experimentally determined.

*Also found experimentally that 1 cm² of thick uranium gives recoil activity equivalent to 4.7 mg/cm² of thin uranium.

of Demers,* the results appear to be in general agreement. Demers measured the range of fission fragments in photographic emulsions by observing the length of tracks as compared to those of the 0.6 Mev protons from the reaction $N^{14}(n,p)C^{14}$ of thermal neutrons and nitrogen in the emulsion. A distribution in range of the fission fragments was observed with mean values as given in Table 9-4.

From Table 9-3 it is seen that only a fraction of a mil of metal cladding is sufficient to prevent the escape of fission fragments. If the cladding material has an undesirably large macroscopic capture cross-section but favorable corrosion properties, it may be advisable to use only slightly more than this minimal thickness (probably by electroplating). Otherwise, mechanical difficulties of fabrication may dictate the minimal thickness.

The same limitations of range that make the nuclear recoil rocket motor so completely impracticable also impose equally stringent limitations

*Phys. Rev. 70, 974 (1946)

TABLE 9-4
MEAN RANGES OF U^{235} FISSION
FRAGMENTS IN A PHOTOGRAPHIC EMULSION

	<u>Light Fragments</u>	<u>Heavy Fragments</u>	<u>Protons (0.6 Mev)</u>
R(air-mm)	23.9	18.7	10.6
R(microns)	14.4	11.2	6.34

for the fission emf device shown schematically in Figure 9-5. In this Rube Goldberg, the fission fragments are supposed to transfer their electrostatic charge against an opposing intense electric field between the inner solid, chain-reacting sphere and the outer concentric spherical shell. The space between the two electrodes, of course, must be highly evacuated to prevent ionization of the gas by the fission fragments. Even at a difference of potential of a million volts, the power that can be developed is negligibly small.

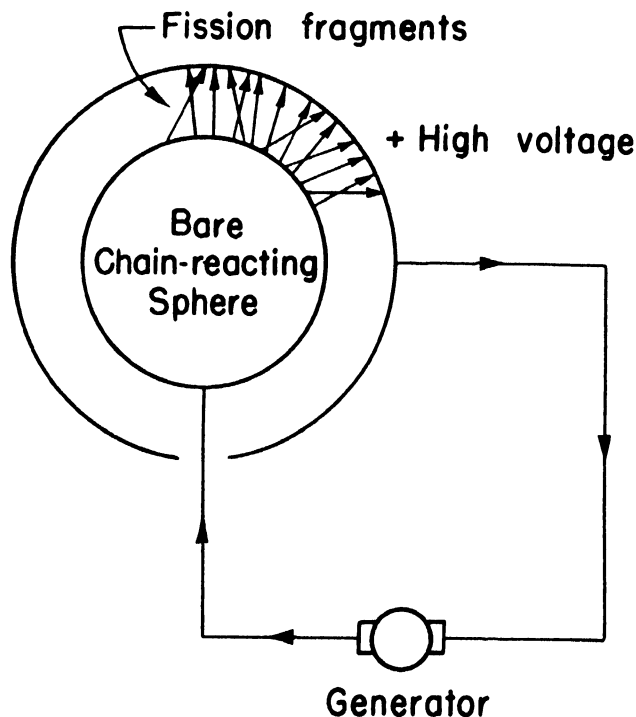


Figure 9-5. Hypothetical Fission EMF

9-5 Fundamental Aspects of Practical Methods

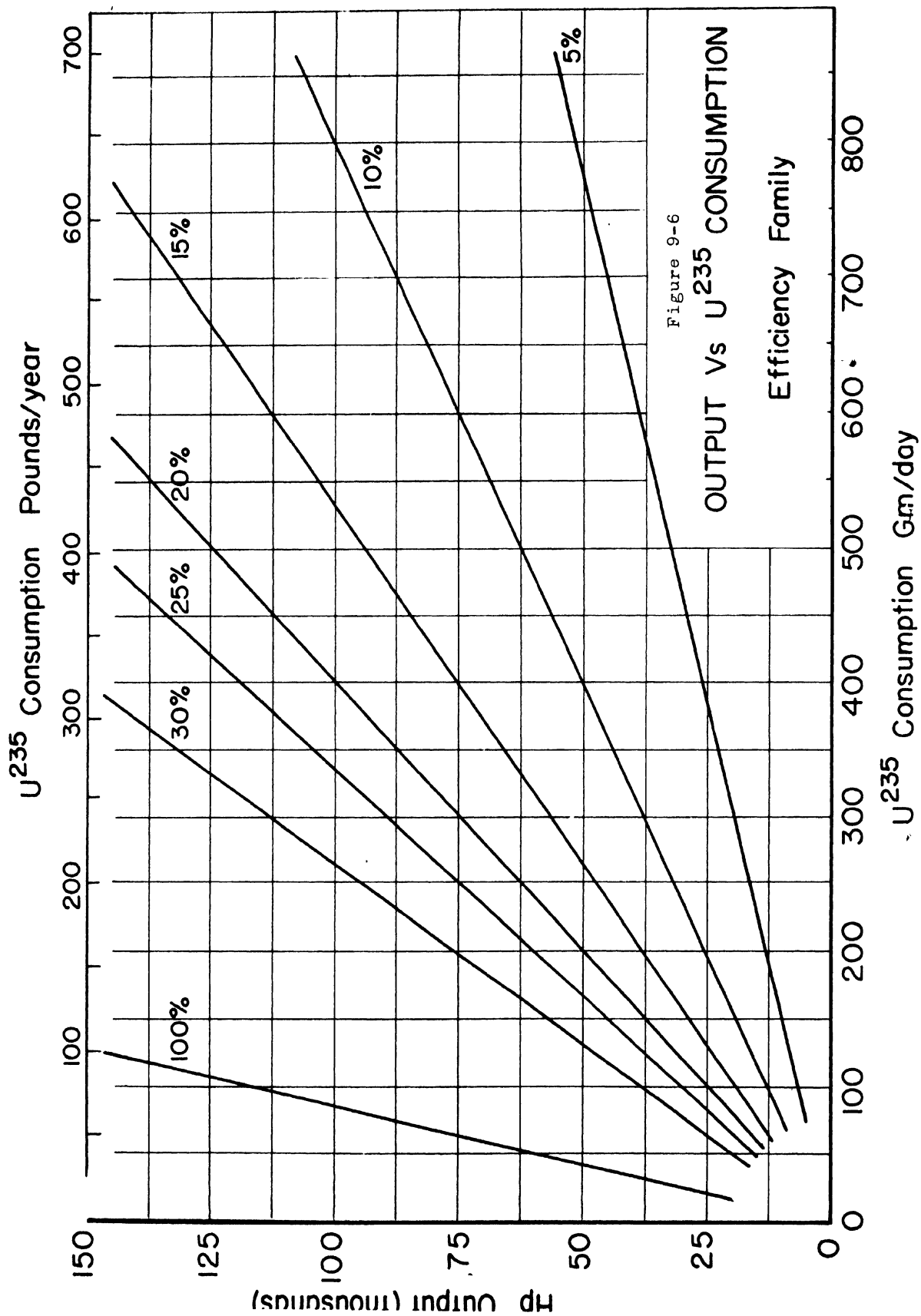
Returning to the realm of practicality, it appears for the present that all nuclear power units depend on: (a) the maintenance of a neutron chain reaction in fissionable material, (b) the inherent conversion of the fission and the fission product energy to relatively high entropy heat energy, and (c) the removal of this heat energy by raising the temperature of a fluid, followed by (d) the conversion of this heat energy into mechanical energy by conventional methods. Basically, therefore, a nuclear power reactor is simply a new type of heat source, inherently capable of delivering its energy at a very high temperature level, but, for practical reasons, limited to moderate temperatures, such as are encountered in other engines.

The major advantages which appear to make nuclear energy unique are: (1) the relatively small amounts of fuel expended and reaction products per unit of heat energy developed, (2) the lack of dependence on a source of oxygen or other oxidizing agent, (3) the potentially large power per unit weight, and (4) a possible economic advantage.

A quantitative example under item (1) was given in the hypothetical example of Section 6-7. The rate of consumption of U^{235} as fuel was 9.5×10^7 atoms* per watt-year which corresponds to 1.6 moles (360 grams) per megawatt-year, which is equivalent to 0.8 pound,* or 1.5 per cent of the U^{235} content, per megawatt-year. It is to be noted that this estimate considered only the total heat developed. Since nuclear power units, as now envisaged, will suffer from the same limitations in efficiency as other heat engines, the delivered horsepower probably will be less than 30 per cent of the heat power. Graphical relations, which include efficiency factors, are given in Figure 9-6 to facilitate rapid estimates of fuel consumption in nuclear power reactors. Item (2) follows directly from the nuclear nature of the chain reaction as contrasted with the atomic processes in chemical reactions. The realization of item (3) depends on either the use of remote control power plants, such as pilotless planes or the development of compact, light-weight shields. The question of the cost of nuclear power, included as a possible advantage under (4), has been considered at some length in a number of publications**

*Twice this number of atoms of radioactive fission products, but approximately equal in weight to the U^{235} consumed, are produced.

**Chem. Engineering, October 1946; Atomic Power 1, 3, (June 1946); "One World or None," 20-21, McGraw-Hill (1946).



without very convincing arguments pro or con. It is certain that for at least the next several years considerations other than economic will be predominant in the development of nuclear power.

9-6 Types of Reactors

In this section an attempt is made to extend previous considerations to include neutrons which cycle at energies above the thermal region. As before, a naive model will be chosen to illustrate the modifications introduced by this change in energy. Assume a mixture containing a ratio of fissionable nuclei to capturing nuclei per cm^3 given by $C = N_f/N_c$. For an infinite amount that is just chain-reacting, $k = 1$ and $C_\infty = (N_f/N_c)_\infty$. If the nuclei N_c are of low atomic weight and are sufficiently prevalent, the neutrons will cycle at thermal velocities and the previous simple relation for the reproduction factor will be applicable, $k = \eta pf = 1$.

However, if C_∞ is not $\ll 1$, or if the nuclei N_c are of moderate ($20 \lesssim A \lesssim 100$) or high ($A \gtrsim 100$) atomic weight, fissions may result before the neutrons have been thermalized, resulting in a mean value of the neutron energy in the epithermal region (between ~ 1 and $\sim 10^4$ ev) or in the fast region (between $\sim 10^4$ and $\sim 10^6$ ev). For reactors of these types, the reproduction factor k will be a function of the neutron energy designated as $k(E) = \eta(E)p(E)m(E)\epsilon(E)$. The term $\epsilon(E)$ is the fast-fission effect which will certainly be energy sensitive. For most considerations, $\epsilon(E)$ is only slightly > 1 , hence it will be considered to be a constant, ϵ . (Assumption a) In addition, it will be assumed (b) that there is no resonance capture ($\sigma_r = 0$), hence $p = 1$, and (c) that $\eta(E) = \eta = \text{const}$. The term "thermal utilization" is replaced by "metal utilization" designated by $m(E)$ and defined (d) as:

$$(9-4) \quad m(E) = \frac{N_f \int_{E_1}^{E_f} \sigma_f(E) dE}{N_f \int_{E_1}^{E_f} \sigma_f(E) dE + N_c \int_{E_1}^{E_f} \sigma_c(E) dE}$$

where the integrations are over the major portion of the energy region occupied by a continuous distribution of neutrons beginning at the upper limit of the fission energy E_f and extending down to a value E_1 at which the density is a small fraction of the maximum value. Hence,

$$(9-5) \quad C_{\infty} = \frac{\int_{E_1}^{E_f} \sigma_o(E) dE}{(\eta\epsilon - 1) \int_{E_1}^{E_f} \sigma_f(E) dE} = \left(\frac{N_f}{N_o} \right)_{\infty}$$

It is of interest to consider values of C_{∞} for which the variations of cross section with energy are known or can be postulated from physical reasoning.

If σ_o is linearly related to σ_f over the energy interval E_1 to E_f , i.e., $\sigma_f = \alpha \sigma_o$:

$$(9-6) \quad C_{\infty} = \frac{1}{\alpha(\eta\epsilon - 1)} \approx \frac{0.72}{\alpha}$$

for $\epsilon = 1.04$ and $\eta = 2.3$ as used in Section 6-2. An example for which this relationship would be approximately correct is a mixture of U^{235} and Li. Because of the low A of the latter and the $1/v$ variation of $\sigma_f(235)$ and $\sigma_o(Li)$, see Section 1-27 and Appendix C, α at 0.025 ev would be $\alpha = 500/73 = 6.85$, $\therefore C_{\infty} \approx .10 = N(235)/N(Li)$. Hence U^{235} would be present in an atomic abundance of 10 per cent and in a weight abundance of 79. per cent. Such a homogeneous mixture would be just chain-reacting for an infinite amount. For finite amounts of U^{235} , a smaller proportion of lithium would suffice to prevent a spontaneous chain reaction.

On the other hand, a homogeneous mixture of graphite and U^{235} would have an $\alpha = 500/.0045 = 1.1 \times 10^5$, $\therefore C_{\infty} = .65 \times 10^{-5} = N(235)/N(c)$. Hence, U^{235} would be present in an atomic abundance of only $.65 \times 10^{-3}$ per cent and in a weight abundance of 0.013 per cent. For a finite reactor, a larger proportion of U^{235} would be required, particularly if U^{238} were present as in the example of Section 6-3 in which $C_{\infty} = 1/50R = 4 \times 10^{-5}$.

If a diluent of medium or high atomic weight were mixed with the U^{235} instead of the low values assumed in the two foregoing examples, it is necessary to know the value of $\sigma_f(235)$ at higher than thermal energies. Unfortunately, no reliable measurements of this important relation are available in the open literature. Accordingly, it is necessary to estimate the value from the only accurate value of σ_f at higher energies that is available, namely, that of Np^{237} given in Appendix C. The important features of the curve are reproduced in Figure 9-7. It is seen that the fission threshold is at a neutron energy of ~ 0.35 Mev, and σ_f rises rapidly to a value of 1.4 barns at ~ 1.2 Mev and remains essentially constant for at least up to 3 Mev. The shaded area of Figure 9-7 corresponds to the shaded area of the energy curve of Figure 9-8. The latter is similar to Figure 2-2, E_0 corresponding to $(E_0)_{II}$ of the latter. The solid curve expresses the coulomb energy of mutual repulsion of the fission fragments (assuming symmetrical splitting) as a function of the distance of separation r between centers. E_c is the maximum potential energy at the critical distance of separation $r = 2R$, when the two fragments (each assumed to be spherical and of radius R) are just separated. E_0 is the energy of the coalesced nucleus, in this case considered to be ${}_{93}^{238}Np$.

The binding energy of a neutron to Np^{237} is 5.7 Mev as calculated from Equation (2-5), page 77. Since the fission threshold is ~ 0.35 Mev, this amount of kinetic energy must be given to the neutrons to excite the nucleus into the shaded area of Figure 9-8. Below this energy, the (n, γ) process occurs* instead of (n, f) . As additional kinetic energy is added, there is an increase in σ_f corresponding to an increase in the wave penetration of the potential barrier. At a kinetic energy of ~ 1.2 Mev, the excitation equals $E_c - E_0 \approx 6.9$ Mev. Additional kinetic energy does not result in an appreciable increase in σ_f .

For present purposes, these general considerations are of interest in attempting to predict $\sigma_f(U^{235})$ for fast neutrons. It is assumed that U^{236}

*Seaborg has recently reported (Science 104, 386, Oct. 25, 1946) a $\sigma_c(Np^{237})$ for (n, γ) of ~ 200 barns for thermal neutrons. He also states that a $\sigma_f(Np^{237})$ of $\sim .02$ barns has been observed by Ghiorso and Magnusson for thermal neutrons. The measurements of Frisch, et al, given in Appendix C, do not extend below 0.27 Mev.

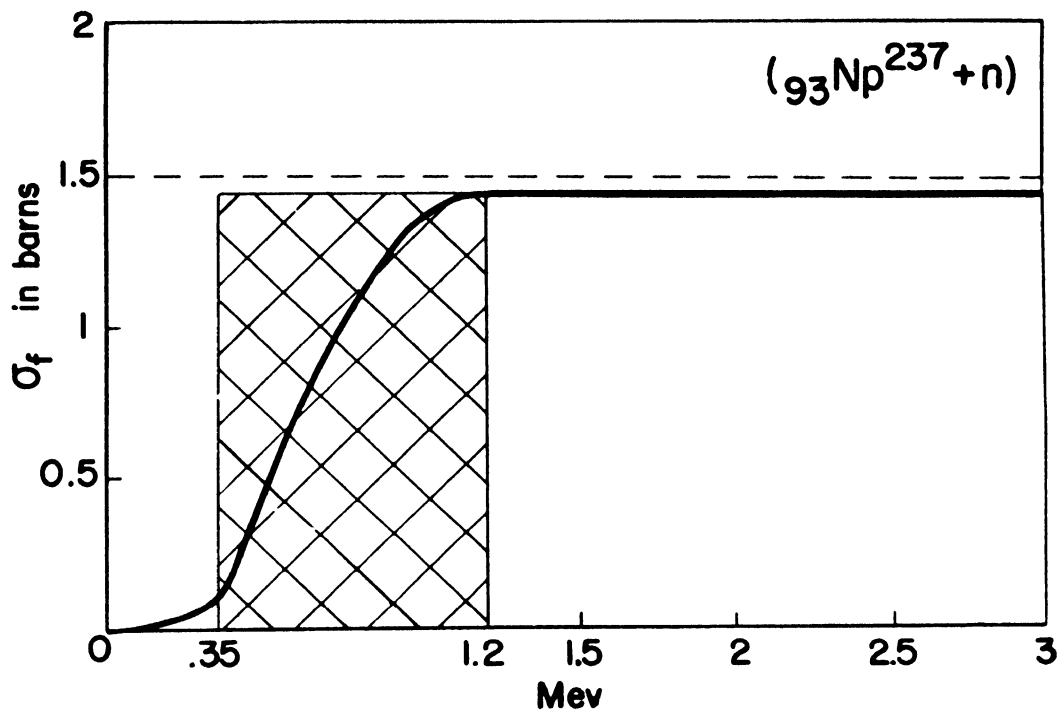


Figure 9-7. Cross-Section vs. Energy for Fission of ${}_{93}\text{Np}^{237}$ by Neutrons

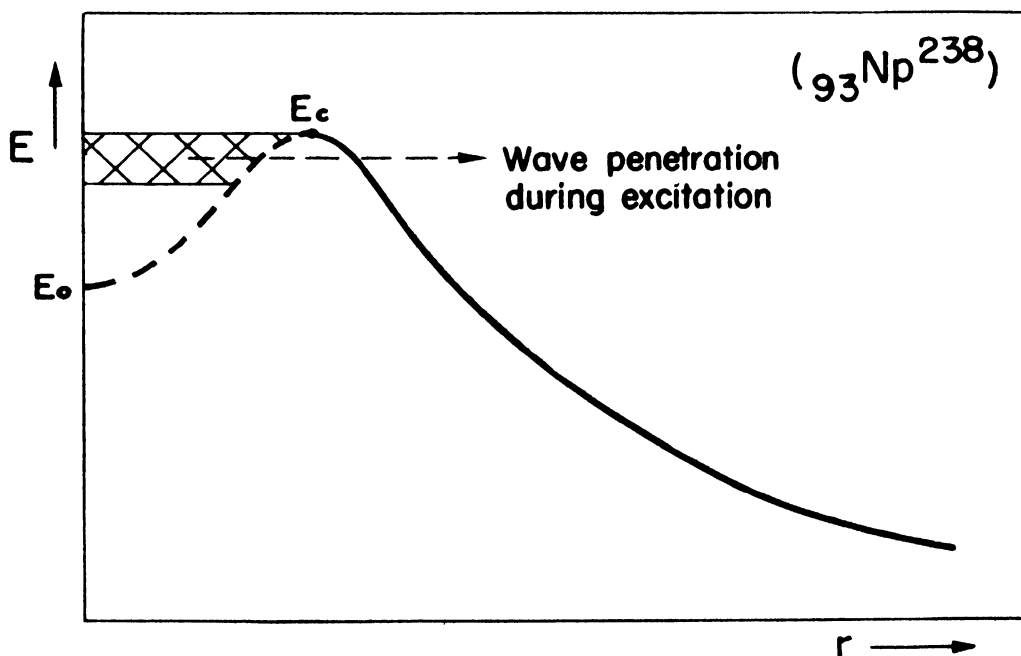


Figure 9-8. Qualitative Energy Relation for Symmetrical Fission of ${}_{93}\text{Np}^{238}$ as a Function of Distance of Separation r between Fragments

has a potential curve similar to Figure 9-8, but because of its even Z , as compared to odd Z for Np^{238} , the δ term in Equation (2-5) page 77, is negative. Hence $E_c - E_0 < 6.8$ Mev for U^{236} , since U^{235} is fissionable with thermal neutrons. The cross section $\sigma_f(\text{U}^{235}) \propto 1/\sqrt{E}$ in the thermal region, as expressed by the Breit-Wigner relation for very broad resonances, see Equations (6-3) and (6-4), page 72. A similar relation obtains for $\sigma_c(\text{B}^{10})$ from $\sim .01$ to ~ 1000 ev as shown in Appendix C. If the relation for $\sigma_f(\text{U}^{235})$ is applicable over a similar energy range, the fission cross section would be about 1 barn at 6000 ev (assuming $\sigma_f(\text{U}^{235}) = 500$ b. at 0.025 ev). Above this energy, it would be expected that the fission cross section levels off at a value somewhat less than that for Np^{237} above 1.2 Mev. Accordingly, it will be assumed in the subsequent discussion that the curve of $\sigma_f(\text{U}^{235})$ vs. $E(\text{ev})$ is given by Figure 9-9. The uncertainty of this reasoning and the qualitative nature of the conclusions are emphasized by the following statements of Fermi ("Neutron Physics" LADC 255, page 74 (1946)):

"The cross sections for capture and fission for the isotopes of uranium and plutonium that have so far been investigated show a rather complicated dependence on energy. For some isotopes the (n,f) cross section decreases with neutron energy, whereas for others it increases. Some isotopes show an (n,f) threshold, whereas some have an (n,f) cross section that follows the $1/v$ law at low energies. Pronounced resonances for capture are apparent at low neutron energies in isotopes like U^{238} . The resonances become less striking at higher energies where they tend to get smeared out."

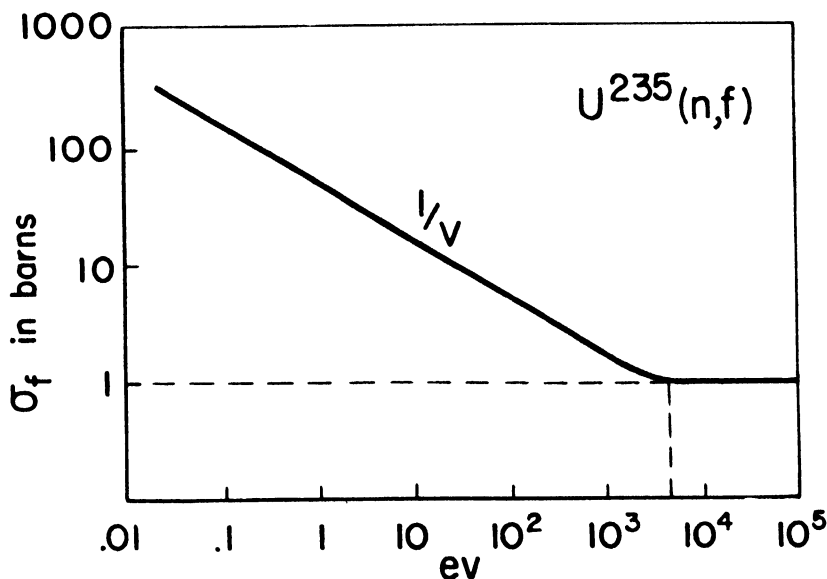


Figure 9-9. Assumed Fission Energy Relationship for U^{235} .

TABLE 9-5 SOME NUCLEAR PROPERTIES OF THE ELEMENTS

The macroscopic cross sections, $N\sigma$, enter many of the fundamental equations in the elementary theory of nuclear reactors. The density of nuclei per cc, N , (which of course equals the number of atoms per cc) is calculated from the simple relation $.602 \times 10^{24} \times \text{density}/\text{atomic weight}$. In such calculations it is convenient to express Avogadro's number and N as a decimal fraction $\times 10^{24}$, because when multiplied into the nuclear cross section, σ , in barns (10^{-24} cm^2) the exponents of 10 exactly cancel each other.

Even though the gaseous elements (He, N, O, F, Ne, etc.) are seldom used in the liquid or solid form, for purposes of comparison it is convenient to determine $N\sigma$ on this basis. Hence the densities listed for these elements are at impracticably low temperatures. On the other hand, the densities listed for a number of possible structural materials (Mg, Al, Fe, Cu, Zn) are at elevated temperatures that might be met in nuclear power reactors.

The nuclear cross sections are from the following declassified sources: $\sigma \equiv$ total and $\sigma_c \equiv$ capture, from Segre' chart* (Figure 1-6); $\sigma_s \equiv$ scattering** from M. Goldhaber and G. H. Briggs, Proc. Roy. Soc. (A) 162, 127 (1937) for Ti, Se, Sr, Br, Cb, Mo, Ru, Pd, Te, Ba at neutron energies absorbable in Cd, from J. Rainwater and W. Havens (Columbia Project) for Mn, Cr, Ni, Cu, Ge, Cd, Sn, Sb, Ta, Os, Pt, Tl, Pb, Bi, U^{238} at 1 ev and for Ag at 0-0.5 ev, W at 0.5 ev and Hg at 0-1 ev, and from N. E. Bradbury et al Phys. Rev. 52, 1023 (1937) for Co for neutron energies absorbable in Cd. In those cases in which σ is measured, it was possible either to subtract unambiguously a term proportional to $1/v$ (considered to be σ_c) or neglect σ_c as compared to σ . The σ_s (Cd) was determined as an additive term to the best-fitting Breit-Wigner resonance expression.

*It is to be noted that a number of inconsistencies exist in this chart between the values of σ_t for certain elements as indicated at the bottom of the vertical column and the values of σ_t and σ_c given for individual isotopes of known abundance. These inconsistencies introduce corresponding uncertainties in several of the tabulated values of σ_c and σ_s .

**As tabulated by H. Feshbach, D. C. Peaslee, and V. F. Weisskopf, Phys. Rev. 71, 152 (1947).

TABLE 9-5

SOME NUCLEAR PROPERTIES OF THE ELEMENTS

Atomic Number Z	Element	Density gms/cc @ T °C.	Chem. Atomic Weight	Nuclei per cc N X 10 ²⁴	Nuclear σ	Nuclear Cross Sections in barns σ _c	σ _s	Cross Section in cm ⁻¹ Nσ _c	Cross Section Nσ _s
1	H	0.0709	1.0078	.0424	20.	0.30	20.	.013	.85
2	He	0.126	4.003	.0190	1.5	0	1.5	0	.029
3	Li	0.53	6.940	.0459	66.3	64.	2.	2.9	.092
4	Be	1.8	9.02	.120	6.1	0.009	6.1	.0011	.73
5	B	2.3	10.82	.139	703.	700.	3.	97.	.42
6	C	1.62	12.01	.0805	4.84	0.0045	4.8	.00036	.39
7	N	0.808	14.008	.0347	11.75	1.75	10.	.061	.35
8	O	1.14	16.000	.0429	4.1	0.0016	4.1	.000068	.18
9	F	1.11	19.00	.0351	4.1	0.01	4.1	.00035	.14
10	Ne	0.9002	20.183	.0268	2.8		~2.5		.067
11	Na	0.93	22.997	.0243	4.	0.5	3.5	.012	.085
12	Mg	1.57	24.32	.0389	4.	0.4	3.6	.016	.14
13	Al	2.4	26.97	.0536	1.7	0.23	1.5	.012	.080
14	Si	2.4	28.06	.0515	1.95	0.25	1.7	.013	.088
15	P	1.745	30.98	.0339	10.3	0.31	10.	.01	.34
16	S	1.808	32.06	.0339	2.	0.53	1.5	.018	.051
17	Cl	1.557	35.457	.0264	<43.	33.	~10.	.87	~.26
18	A	1.402	39.944	.0211	2.53	0.62	1.9	.013	.040
19	K	0.83	39.096	.0128	3.7	2.2	1.5	.028	.019
20	Ca	1.55	40.08	.0233	9.93	0.43	9.5	.01	.22
21	Sc	2.5	45.10	.0334		22.		.74	
22	Ti	4.5	47.90	.0566	11.2	5.2	6.	.29	.34
23	V	5.68	50.95	.0704	>13.	5.	>8.	.35	>.56
24	Cr	7.14	52.01	.0822	6.5	3.	4.	.25	.33
25	Mn	7.2	54.93	.0789	15.2	12.8	2.4	1.01	.19
26	Fe	6.9	55.85	.0744	12.	2.5	11.	.19	.82
27	Co	8.9	58.94	.0909	38.	33.	5.	3.0	.45
28	Ni	8.90	58.69	.0913	17.4	4.4	18.	.40	1.6
29	Cu	8.3	63.57	.0786	11.2	4.	8.	.31	.63
30	Zn	6.7	65.38	.0617	4.85	1.25	4.2	.077	.26

TABLE 9-5 (Continued)

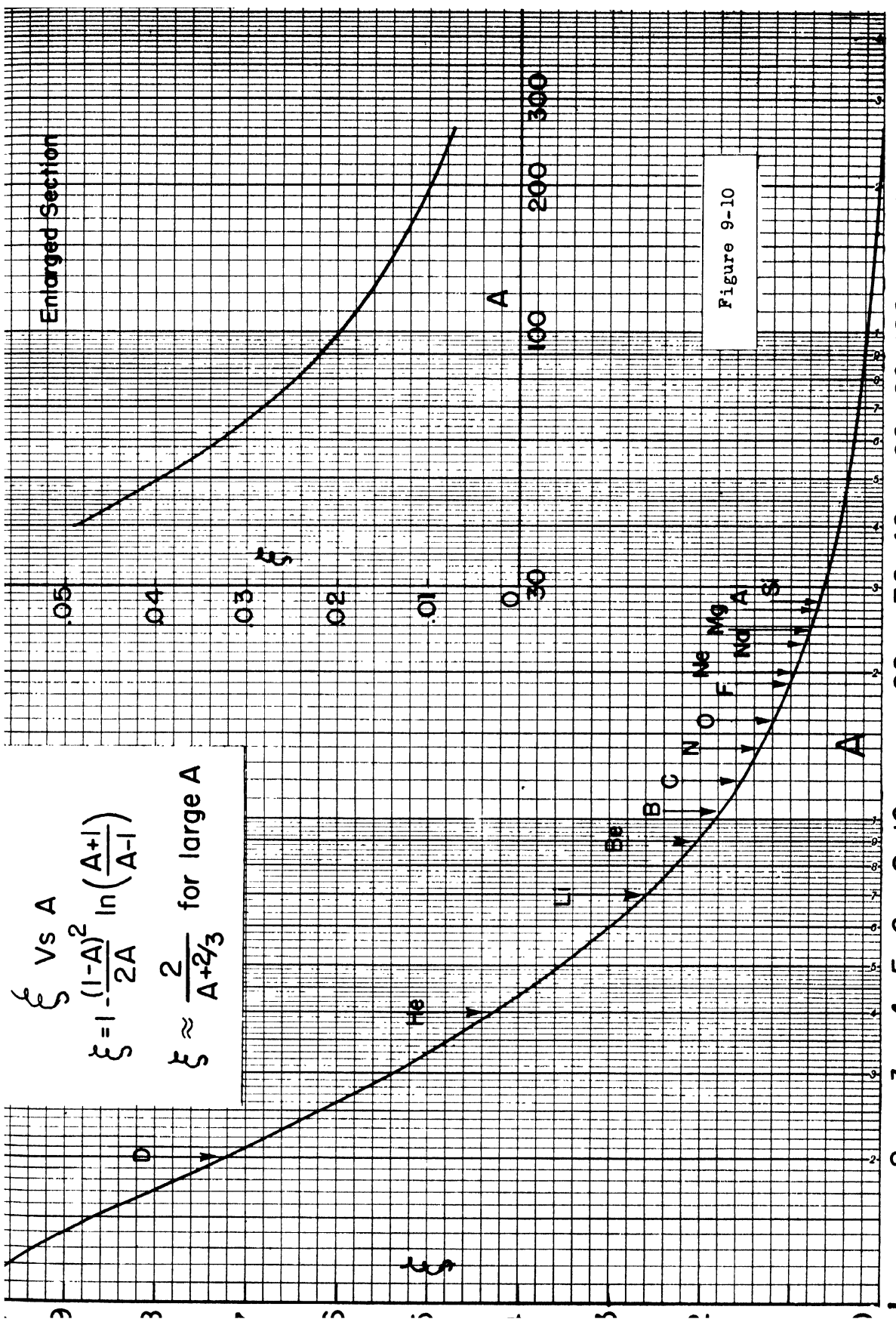
Atomic Number Z	Chem. Atomic Weight	Density gms/cc @ T °C.	Nuclei per cc $N \times 10^{24}$	Nuclear Cross Sections			Cross Section	
				σ	in barns σ_c	σ_s	$N\sigma_c$ in cm^{-1}	$N\sigma_s$
31 Ga	69.72	5.91	.0510	20.	2.3	18.	.12	.92
32 Ge	72.60	5.36	.0444	25.	~.6	22.	~.03	.98
33 As	74.91	2.0	.0161	12.6	5.6	7.	.09	.11
34 Se	78.96	4.50	.0343	28.	16.	10.	.55	.34
35 Br	79.916	3.119	.0235	9.5	7.	2.5	.16	.06
36 Kr	83.7	(2)	.0144	27.	.1	27.	.001	.39
37 Rb	85.48	1.53	.0104	12.	.5	11.	.005	.11
38 Sr	87.63	2.6	.0179	11.	1.5	10.	.027	.18
39 Y	88.92	5.51	.0373	15.	1.1	14.	.041	.59
40 Zr	91.22	6.4	.0422	6.9	>0.5	5.	>.021	.28
41 Nb	92.91	8.57	.0555	7.9	1.4	6.5	.078	.41
42 Mo	95.95	10.2	.0638		3.9		.25	
43 Tc	99.							
44 Ru	101.7	12.2	.0502	155.	150.	6.	7.4	.30
45 Rh	102.91	12.5	.0496	13.5	9.	5.	.58	.25
46 Pd	106.7	11.	.0639	66.4	58.5	4.5	3.3	.29
47 Ag	107.880	10.5	.0567	2507.2	2500.	6.6	115.	.37
48 Cd	112.41	8.6	.0461	194.	190.	5.3	7.3	.24
49 In	114.76	7.3	.0383	4.89	0.69	4.	.020	.15
50 Sn	118.70	5.750	.0292	9.	4.7	5.0	.155	.15
51 Sb	121.76	6.684	.0330	10.	5.	4.2	.14	.14
52 Te	127.61	(β)6.00	.0283	9.4	6.8	5.	.16	.07
53 I	126.92	4.93	.0234	35.		3.		
54 Xe	131.3	(2.7)	.0124	50.	41.		.35	.08
55 Cs	132.91	1.90	.0086	9.25	1.25	9.	.019	.12
56 Ba	137.36	3.5	.0153	25.	12.	13.	.32	.35
57 La	138.92	6.15	.0267	29.				
58 Ce	140.13	6.9	.0296	>25.				
59 Pr	140.92	6.50	.0278		90.		2.6	
60 Nd	144.27	6.90	.0288					
61 Pm	147.							
62 Sm	150.43	7.7	.0308	8000.			246.	
63 Eu	152.0			2500.				

TABLE 9-5 (Continued)

Atomic Number Z	Element	Density gms/cc @ T °C.	Chem. Atomic Weight	Nuclei per cc $N \times 10^{24}$	Nuclear Cross Sections in barns			Cross Section in cm ⁻¹ $N\sigma_c$ $N\sigma_s$	
					σ	σ_c	σ_s		
64	Gd		156.9			~38,000.			
65	Tb		159.2		15.				
66	Dy		162.46			850.			
67	Ho		164.94			65.			
68	Er		167.2			260.			
69	Tm		169.4			130.			
70	Yb		173.04		65.				
71	Lu		174.99						
72	Hf	11.4	178.6	.0384	130.	195.	10.	4.6	.38
73	Ta	16.6	180.88	.0552	24.5	120.	7.2	1.1	.40
74	W	19.3	183.92	.0631	20.9	16.	5.7	1.01	.36
75	Re	20.	186.31	.0691		130.		9.0	
76	Os	22.48	190.2	.0707	30.	20.	10.	1.41	.71
77	Ir	22.4	193.1	.0699		400.		27.9	
78	Pt	19.	195.23	.0586	21.5	10.8	12.	.63	.70
79	Au	19.3	197.2	.0589	101.	94.5	5.	5.57	.29
80	Hg	14.19	200.61	.0426	440.	425.	15.	18.1	.64
81	Tl	11.85	204.39	.0349	16.9	2.9	9.7	.101	.34
82	Pb	11.34	207.21	.0329	10.2	0.17	13.	.006	.43
83	Bi	9.8	209.00	.0282	8.9	0.016	9.2	.0005	.26
84	Po		210.						
85	At		211.						
86	Rn	4.40	222.	.0108					
87			223.						
88	Ra	5.0	226.05	.0133					
89	Ac		227.						
90	Th	11.5	232.12	.0290	16.	6.	~10.	.17	~.29
91	Pa		231.						
92	U	18.7	238.07	.0473	10.	~2.	8.2	.095	.39
93	Np		237.						
94	Pu		239.						
95	Am		241.						
96	Cm		242.						

In Equation (9-5) the proportion of fissionable nuclei depends on $\sigma_c(E)$, the capture cross section of the diluent. Some nuclear properties of the elements, including values of σ_c and $N\sigma_c$ at thermal energy, are given in Table 9-5. Copper ($Z = 29$) will be used as an example. This element has a number of desirable physical properties in addition to being readily available, but because of its relatively large capture cross section for thermal neutrons, $\sigma_c(\text{Cu}) = 4 \text{ b.}$, $\sigma_c(\text{Cu})N(\text{Cu}) = .31 \text{ cm}^{-1}$, copper cannot be used in any appreciable amount in thermal reactors. However, as the mean energy of the neutrons is increased, $\sigma_c(\text{Cu})$ decreases until it reaches a constant value of about 5×10^{-3} barns in the energy range of 10^3 to 10^6 ev where $C_\infty = N(\text{U}^{235})/N(\text{Cu}) \approx 4 \times 10^{-3}$.

In general, as the atomic weight (A) of the diluent increases, the mean energy at which the neutrons cycle increases. Except for the complications introduced by resonances and large inelastic scattering cross sections, the competitive processes are scattering, capture, and fission. To obtain a tangible notion of the relative importance of these, it is instructive to compare the mean-free-paths ($\lambda = 1/N\sigma$). For purely elastic scattering, the average number of collisions ν required to reduce the energy of a fission neutron by a factor of 10, i.e., from E_f to $E_f/10$, is $\nu = 2.3/\xi$, where ξ is the mean logarithmic energy loss per collision as defined in Section 5-9. For convenience, values of ξ for the full range of atomic weights may be obtained from Figure 9-10. It is seen that for Cu, $A = 64$, $\xi = .031$, hence $\nu = 74$. In the foregoing mixture of Cu and U^{235} , $N(\text{Cu})\sigma_s(\text{Cu}) \approx 0.6 \text{ cm}^{-1}$, hence $\lambda_s(\text{Cu}) \approx 1.7 \text{ cm}$. The mean-free-path to reduce the energy from 10^6 ev to 10^3 ev would be $3\nu\lambda_s = 380 \text{ cm}$. Because of the small concentration of U^{235} , the loss in energy by scattering from these nuclei is negligible. On the other hand, the fission mean-free-path $\lambda_f = 1/N(\text{U}^{235})\sigma_f(\text{U}^{235}) \approx 3 \times 10^3 \text{ cm}$, and the capture mean-free-path $\lambda_c = 1/N(\text{Cu})\sigma_c(\text{Cu}) \approx 4 \times 10^3 \text{ cm}$. Thus, while a neutron is moving a distance equal to one mean-free-path for fission, capture is approximately as probable as fission and a reduction in energy below 10^3 ev by elastic scattering is about ten times as probable as fission. Accordingly, most of the neutrons will be slowed down to such low velocities that a significant rise in $\sigma_c(\text{Cu})$ and $\sigma_f(\text{U}^{235})$ will result.



Assuming Figure 9-9 to apply for $\sigma_f(U^{235})$ and a constant $\sigma_0(\text{Cu})$, it is seen that at 10^2 ev $\sigma_f(U^{235}) \approx 5$ barns, $\lambda_f \approx 600$ cm and fission is about seven times as probable as capture and about two-thirds as probable as scattering. Under these conditions the reactor would probably operate in the resonance region with an energy interval similar to that shown on the right in Figure 9-12.

As A is increased, either by increasing the proportion of fissionable material or shifting to diluents of higher atomic weight, the mean neutron energy increases. With a material such as Bi ($A = 209$, $\xi = .0095$, $\nu = 240$) capture* is much less important, and a balance is maintained between a decrease in energy by scattering and fission capture. Thus $\lambda_s \approx 3$ cm and $\nu\lambda_s \approx 700$ cm. If most of the neutrons are to be captured by fissionable nuclei before being degraded in energy below about 10^4 ev, λ_f must $\approx 2\nu\lambda_s = 1400$ cm. Assuming $\sigma_f(U^{235}) \approx 1$ b. in this energy interval, $N(U^{235}) \approx .0007$; hence, $N(U^{235}) / N(\text{Bi}) \approx .025$. The neutron spectrum would be of the general shape designated "fast" in Figure 9-12 et seq.

All three of these types of reactors can be used for the development of power. By proper design the excess reactivity $k_e = (k_{\text{eff}} - 1)$, for each can always be kept less than the fraction of delayed neutrons β . Hence, the rate of change of power level will be dictated by the periods of the delayed neutrons, and the reactor will be controllable. It is evident that there are no elements with large capture cross section to use as control rods in fast reactors. As indicated in Appendix C, a few elements show resonance peaks up to about 300 ev which might be of value in the control of resonance reactors.

9-7 Methods of Control

Several methods may be used to control resonance and fast units. Selected fuel rods could be made adjustable in their depth of penetration in the active zone. An example of this type of control is shown in the schematic diagram Figure 9-11 of the first nuclear power plant at present in the design stage but soon to be constructed at the Clinton Laboratories in Oak Ridge. In a homogeneous reactor containing a solid fuel mixture, such as is shown

*In fact σ_0 (n, particle) may be $> \sigma_0$ (n, γ).

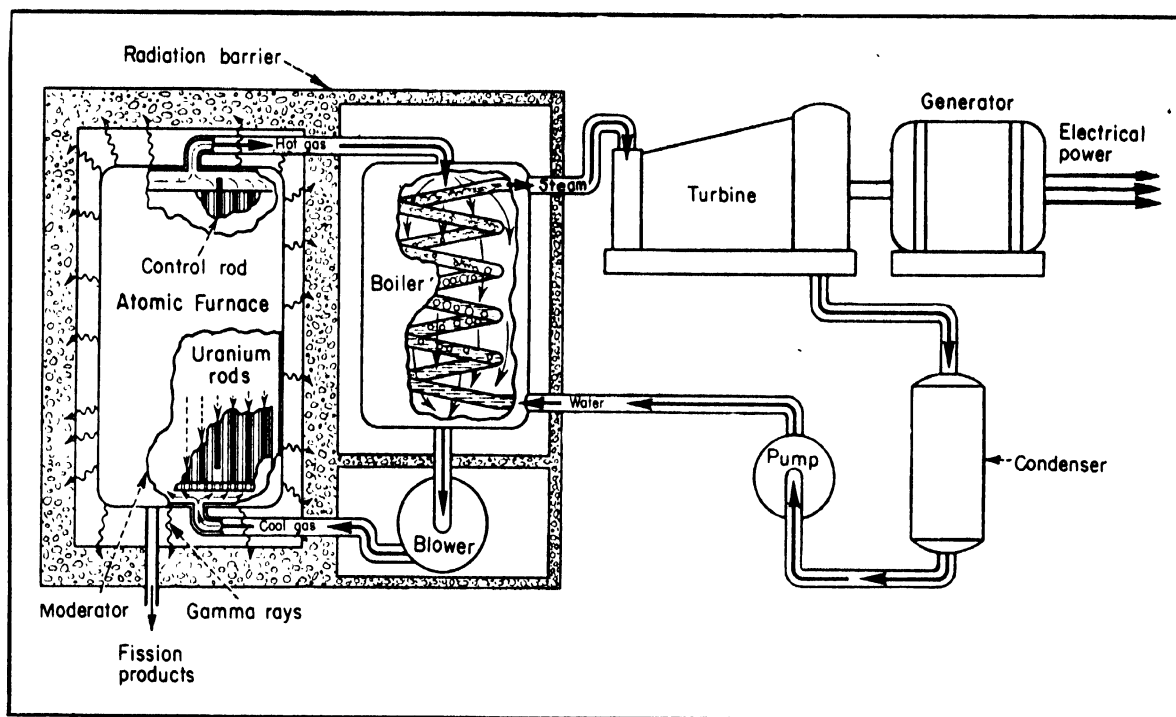


Figure 9-11. Schematic Diagram of Projected Oak Ridge Power Installation (War Dept. Release). The sketch indicates that the first nuclear power plant is scheduled to include all the components of a conventional power central station, i.e., heat source, boiler, turbine generator, and condenser. A gas, presumably He, CO₂, SO₂, or some other with low σ_c at thermal energies, is indicated as the coolant for this heterogeneous unit. This gas flows in cylindrical annuli about the uranium rods, one of which is shown partially withdrawn to serve as a control rod. The amount of shielding required around the boiler unit is purported to be only about one-third that around the "atomic furnace." In order to remove the fission products it would be necessary to remove the uranium rods and process chemically rather than by means of the idealized method indicated in the sketch.

in Figure 9-12, portions of the mixture could be made movable. However, this method of control involves a number of engineering difficulties in addition to being poor in neutron economy because of the introduction of gaps.

If the reactor has a negative temperature coefficient, i.e., $\Delta k = -f(T)$, control could be obtained by varying the flow of the coolant or liquid fuel. This method has a number of difficulties and would certainly require supplementary controls for start-up and safety. If the production of U²³³ or Pu²³⁹

is of interest, control rods containing Th or U^{238} might be used. These control rods would be removed periodically for chemical processing. It is also possible that elements possessing large $\sigma(n, \text{particle})$ for high energy neutrons could be used. For example, in Appendix C sulphur is seen to have a $\sigma(n, \alpha) = 0.1$ b. at 2.4 Mev and 0.4 b. at 5 Mev. Undoubtedly there are a number of other elements with similar cross sections at even more useful neutron energies. Of course, the familiar use of rods containing boron for the control of thermal reactors is based on this type of nuclear reaction. Obviously, considerable heat is produced in the control rod and some method for direct cooling must be provided.

As discussed in Sections 3-6 and 5-21, substantial increases in reactivity can be obtained by the use of reflectors. Consequently, the active region of any well-designed unit will be practically completely surrounded by a reflector. The ideal reflector would have essentially zero capture cross section. By introducing absorbing material in the form of movable rods or by making sections of the reflector movable, a very convenient means of control can be obtained without introducing openings in the active zone. Of course, these control materials, as well as those previously discussed, could be fluid rather than solid. For example, a safety control of mercury could be used for thermal reactors. In an emergency, means could be provided for allowing mercury to flow into openings in the reactor or in the reflector. After re-establishing other controls, the mercury could be drained off and returned to the original reservoir.

9-8 Homogeneous Reactors

Since homogeneous reactors are certainly simpler to construct than heterogeneous reactors, it is pertinent to ask why the large majority of those that have been built to date have been of the heterogeneous class. It will be noted in Table 9-1 that all of these heterogeneous units use ordinary uranium as fuel. Simple calculations prove that, with the exception of heavy water (D_2O), a homogeneous mixture of natural uranium cannot sustain a thermal chain reaction. It is also well established that an infinite amount of natural uranium metal is not chain-reacting. The latter necessarily would be of the fast type. Except for the definitions listed below, for simplicity and continuity the following computations use the same nuclear constants and notation of Sections 6-1 and 6-8.

$\sigma_c(D) \equiv$ the capture cross section of the diluent in barns

$\sigma_s(D) \equiv$ the scattering cross section of the diluent in barns

$N(D) \equiv$ the number of atoms of diluent per cc

$N(238) \equiv$ the number of atoms of U^{238} per cc

$N(235) \equiv$ the number of atoms of U^{235} per cc (in natural uranium
 $N(238) / N(235) = 139$)

The reproduction constant can be expressed as a function of the atomic ratio $R = N(D) / N(238)$ as follows:

$$(9-7) \quad k = \eta f p = \frac{2.3 \times 3.57}{5.57 + \sigma_c(D)R} e^{-\frac{88 \xi \sigma_s(D)R}{\xi \sigma_s(D)R}}$$

The optimum value of R corresponds to the maximum k obtained from $dk/dR = 0$,

$$(9-8) \quad \therefore \sigma_c(D)R^2 - \frac{88 \sigma_c(D)}{\xi \sigma_s(D)} R - \frac{(5.57)88}{\xi \sigma_s(D)} = 0$$

$$(9-9) \quad \text{Optimum } R \approx \frac{44}{\xi \sigma_s(D)} \left[1 \pm \sqrt{1 + \frac{\xi \sigma_s(D)}{4 \sigma_c(D)}} \right]$$

The negative root is a non-physical solution. For purposes of comparison in Table 9-6 are given values of the macroscopic cross sections $N\sigma_s$ and $N\sigma_c$, ξ , the slowing-down power $N\sigma_s \xi$, and the ratio of constants $\sigma_s \xi / \sigma_c$ under the radical sign which has been designated the "moderating ratio". Thus it is seen that, in general, the largest value of k in Equation (9-7) will result from the use of materials with the largest moderating ratio. Except for beryllium and graphite, all of the materials with large moderating ratios are gaseous in the elemental form at ordinary temperatures. Helium has the largest value, since it has essentially zero capture cross section. However, helium cannot be used because it forms no compounds. Oxygen has a rather large ratio. Hence the combinations H_2O , D_2O and BeO are among the best moderating materials as far as nuclear properties are concerned. In considering these compounds the value of ξ should be computed as follows:

$$(9-10) \quad \xi(D_2O) = \frac{2\sigma_s(D) \xi(D) + \sigma_s(O) \xi(O)}{2\sigma_s(D) + \sigma_s(O)}$$

in which D_2O is cited as an example. Using the foregoing relationships, the maximum values of k for the best moderating materials are given in Table 9-7.

To have a chain-reacting system, k must at least equal 1 for an infinite unit or be greater than 1 for a finite size. The reason for the interest in heavy water during the initial stages of work on nuclear energy in this country and abroad is evident from Table 9-7. D_2O is the only practical moderating material which will sustain a chain reaction with ordinary uranium; that is, uranium containing a ratio of $N(238)/N(235) = 139$. If the uranium were in the form of uranyl sulfate it could be dissolved in heavy water at the concentration required to give a ratio of $N(D_2O)/N(238) = 170$. A slight change in this concentration might be necessary to compensate for the small increase in neutron capture due to the sulphur which, from Table 9-5, has a macroscopic cross section $N\sigma_c = .018$. Computation of the critical size is left as an exercise for the reader.

As shown in the Segre Chart, Figure 1-6, deuterium (H^2) has a relative abundance of only 0.02 per cent in hydrogen. However, because of the proportionately large mass difference, these isotopes can be separated in large quantities fairly readily. The first supplies of deuterium were secured as a by-product of electrolysis. Fractionation factors of 10 to 20 may be obtained between the gas evolved at the cathode and the hydrogen remaining in the solution. Because of the large effect secured in a single unit, batch methods are more convenient than a cascade. Effective concentration of the isotopes of hydrogen, carbon and sulphur can be obtained from chemical exchange reactions. Thermal diffusion, centrifugation and electromagnetic methods may also be used. While all of these methods require large installations and are expensive to operate, the Chalk River and Argonne piles attest to the practicability of obtaining and using large volumes of pure heavy water. Of course, these reactors are of the heterogeneous class discussed in a subsequent section.

For the present Table 9-7 serves to emphasize that, with the possible exception of those containing D_2O , all of the homogeneous units to be considered must use a concentrated nuclear fuel, i.e., enriched uranium ($> 1\% U^{235}$) or its equivalent in U^{233} or Pu^{239} . In other words, nearly all of the homogeneous units to be discussed depend on primary fuel sources consisting

TABLE 9-6

COMPARISON OF LIGHT ELEMENTS AS MODERATORS

(The values given are for thermal energies)

Element	A	Cross Section (cm^{-1})		ξ	Slowing-down Power $N\sigma_s \xi$	Moderating Ratio $\frac{\sigma_s \xi}{\sigma_c}$
		Scattering $N\sigma_s$	Capture $N\sigma_c$			
H	1	.85	.013	1.	.85	65.
D	2	.10	.0000015	.72	.072	47,500.
He	4	.029	0.	.425	.0123	∞
Li	7	.092	2.9	.26	.024	.0083
Be	9	.73	.0011	.2	.146	133.
B	11	.42	97.	.17	.071	.00073
C	12	.39	.00036	.15	.058	162.
N	14	.35	.061	.13	.045	.74
O	16	.18	.000068	.12	.0215	316.
F	19	.14	.0023	.10	.014	6.1
Ne	20	.067	---	.095	.0064	---
Na	23	.085	.012	.083	.0071	.59
Mg	24	.14	.016	.080	.0112	.70
Al	27	.080	.012	.070	.0056	.47
Si	28	.088	.013	.070	.0062	.42
P	31	.34	.01	.06	.0204	2.04
S	32	.051	.018	.06	.00306	.17
Cl	35.5	.26	.87	.055	.0143	.0165
A	40	.040	.013	.050	.0020	.154
K	39	.019	.028	.050	.00095	.034
Ca	40	.22	.01	.050	.011	1.1

TABLE 9-7

COMPARISON OF OPTIMUM HOMOGENEOUS MIXTURES
OF NATURAL URANIUM AND MODERATING MATERIALS

Moderator	Optimum R	Maximum k
H ₂ O	5.7	.62
Be	340	.66
Graphite	440	.84
D ₂ O	170	1.33

either of isotope separation plants or of chain-reacting units, such as those at Hanford, for the production of Pu^{239} or U^{233} . Under these conditions a number of possible combinations of materials can be used in the construction of homogeneous reactors. For convenience these will be divided according to general physical properties with subdivisions based on neutron energy.

(a) Homogeneous solid fuel mixtures

If methods of fabrication could be worked out, the combinations of materials listed below would be particularly promising. The metallurgical feasibility of the alloys is not clear from the limited information in the open literature. Likewise the corrosive properties, failure under high temperature gradients, chemical reactivity with the fuel ingredients and a host of other important prerequisites are not well defined.

- (1) U or Pu alloys of high melting point
(Thermal: Be, Mg, Al)
(Resonance and fast: Cu, Fe, W, Ag, Zn, V, Th)
- (2) U or Pu metal dispersed in high melting point solid
(Thermal: graphite, BeO, MgO, Al_2O_3 , SiO_2 , Be_2C , SiC)
(Resonance or fast: CuO, Bi_2O_3 , Fe_2O_3 , PbO, ThO_2)
- (3) U or Pu compounds mixed with other substances (Thermal: UO_2 + graphite, BeO, MgO, Al_2O_3 , SiO_2 , Be_2C or SiC; UC_2 + graphite, BeO, Al_2O_3 , SiO_2 , Be_2C or SiC; US_2 + graphite)

In addition to the advantages discussed in the caption of Figure 9-12, the solid homogeneous mixture is simple in construction and may allow the use of oxides which are easier than the metals to produce and process. On the contrary, the necessity of removing all, or even a major part, of the active portion in order to refuel is a serious objection for many power applications.* Furthermore it is to be noted that reprocessing the active section required handling a large mass of materials (the fuel plus the diluent) in order to replace a relatively small percentage of depleted fuel. Since the completeness of recovery of the U or Pu is a major factor in the cost of any nuclear power unit, the presence of a large amount of diluent may not only be costly in terms of the diluent itself but also in the decreased recovery of fuel that it may impose.

*In the propulsion of ships this might not be considered a major limitation.

In any homogeneous unit, the heat is developed throughout the active section. Except for the discontinuities in the cooling ports, dQ/dt varies as a sinusoidal function along the axis and as a zero-order Bessel function along the radius of the cylindrical unit shown in Figure 9-12. This heat must flow by conduction through the mixture to the coolant. Unless the active section is composed of materials with a large thermal conductivity, a low thermal expansion and a large shearing strength, the solid mixture may rupture badly under the large temperature gradients required to deliver significant amounts of power. It is also important that these properties not deteriorate under the intense radiations which in this case consist of fission fragments, neutrons, beta rays and gamma rays. These requirements may reduce the choice of diluent, structural material and coolant in a list that is already abbreviated by the nuclear prerequisites.

(b) Homogeneous fluid fuel mixture

The only combinations of this type that are known to be feasible are the solutions. However, these are limited in temperature unless high pressures are used, and decomposition of the water would certainly introduce complications. Bubbling would affect the reactivity of the unit and make steady control difficult. Disposal of the H_2 and O_2 produced from H_2O and recombination of D_2 and O_2 produced from D_2O would be difficult though not impossible for most applications. Precipitation and corrosion would be important considerations at useful temperatures and pressures. With these limitations in mind, the following incomplete list is given of possible homogeneous fluid fuel mixtures:

- (1) U or Pu alloys of low melting point
(Thermal: Na)
(Resonance and fast: Hg, Pb, Bi, Sb, Tl)
- (2) U or Pu compounds in solution
(Thermal: carbonate, sulfate or possibly nitrate dissolved in H_2O or D_2O)
- (3) Slurries
(Thermal: UO_2 , UC_2 or possibly US_2 dispersed in H_2O or D_2O)
(Resonance or fast: UO_2 , UC_2 or possibly US_2 dispersed in Hg or in molten Pb, Bi, Pb-Bi, Sb, or Tl)

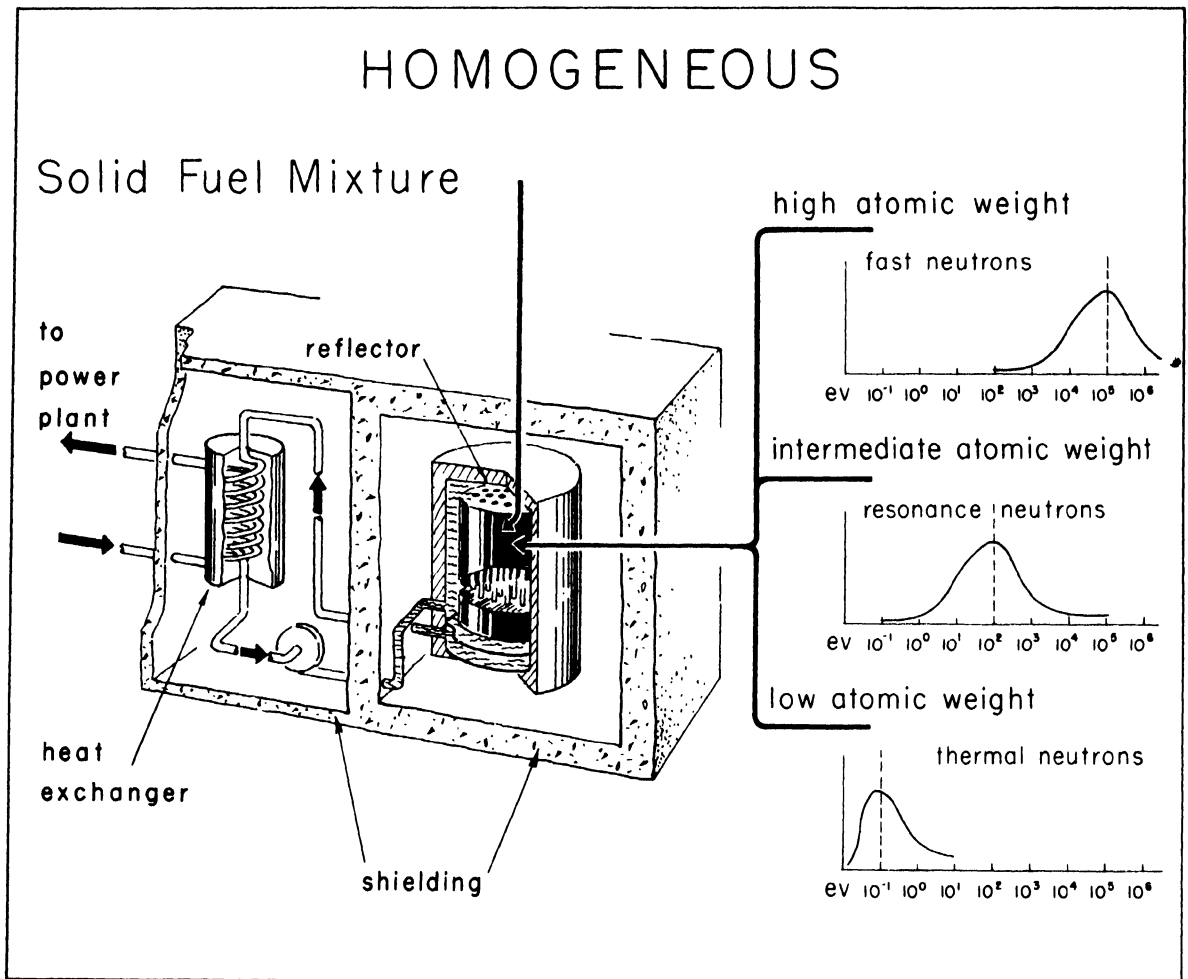


Figure 9-12. Schematic Diagram of a Homogeneous Reactor Containing a Solid Fuel Mixture. The cylindrical core or central section consists of a high-melting-point mixture of U or Pu and a selected diluent. An alloy or simple mechanical mixture of metal or compound with the diluent might be used. The type of the reactor is determined by the mean atomic weight of the mixture. The core could be fabricated in sections or as a subcritical whole. It should be possible to obtain sufficient excess reactivity for operation from the introduction of the coolant and the addition of the reflector. In the diagram above, the coolant might be either a liquid or a gas. In addition to the advantages to be gained in heat transfer by the use of a liquid, particularly a liquid heavy metal such as Hg, Bi or Pb, instead of a gas, such a coolant would (a) block the escape of neutrons from the cooling ports, (b) partially serve as a peripheral reflector, (c) absorb heat which would otherwise be lost to the reflector, (d) be preheated before entering the active section, and (e) act as a shield against the escape of gamma radiation. If in addition the coolant were selected from among those elements which have

(4) Gaseous mixture
(Thermal: $\text{UF}_6 + \text{F}_2$)

Essentially nothing is available in the open literature on low melting alloys of U and even less about Pu. The soluble compounds of U are well known. As reported in Section 11-3 the oxidation states of Pu in solution are VI, V, IV, and III with a shift in stability toward III as compared to Np and U. While the use of slurries would make simple the separation of the fissionable material from the diluent, coagulation or local concentrations of the active materials would certainly complicate control of the reactivity. The water slurries would be subject to decomposition problems to only a slightly smaller degree than for solutions. The only gaseous compound that seems at all reasonable is UF_6 . Fluorine would be added as additional moderator and to stabilize the molecular UF_6 , which would probably decompose under the intense radiation. The critical size of such a gaseous mixture would be substantially greater than for liquids or solids.

The use of a circulating fluid fuel mixture obviates many of the problems encountered in the solid mixture discussed above. The fission and radiation energy is converted to heat in the mixture which then circulates to the external heat exchanger where the heat is transferred to the secondary coolant (probably water and steam). Obviously, the use of a fluid fuel mixture provides greater opportunity for addition of fuel and removal of fission products during operation than does a solid reactor core. In fact, unless some ingenious method of construction were employed which allowed the replacement of sections of the active solid, it would be necessary to shut down the

Figure 9-12. Caption (Continued)

a low neutron cross section for transmutation to energetic gamma-radioactive products, the shielding of the heat exchanger and circulation system could be quite thin. Of course it is important to prevent contamination of the coolant by fission products and corrosion of the fuel mixture by the coolant. Hence the cooling channels would need to be lined with at least a thin layer of some resistant material. This requirement introduces complications in fabrication and efficient heat transfer.

No shielding is necessary for the secondary coolant which drives the power units, because the cross section for gamma-induced transmutations is exceedingly small. This factor is of considerable importance in nearly all nuclear power units since radioactive contamination of the power machinery would introduce serious problems in servicing and maintenance.

reactor, remove the entire central zone and replace it with a new unit whenever refueling was necessary. An alternate method is the use of a fusible mixture of fuel and diluent that remains in situ and through which pass tubes carrying a coolant such as might be used with the solid unit. The heat transfer coefficient for such a fluid mixture, particularly if it were a molten metal that wets the walls of the cooling tubes, may be unusually good. Portions of this fluid fuel mixture could be continuously or periodically removed for reprocessing while at the same time the correct amount of replacement fuel was added to the mixture. Thermal convection in the fluid should be of value in maintaining a uniform mixture provided there is no gravitational segregation of the heavy fuel atoms.

As indicated in Section 9-6, regardless of the type of reactor, control is maintained by the fraction β of the neutron flux contributed by the delayed emitters.* If an appreciable fraction of the delayed neutrons are emitted outside the active volume V_1 (see Figure 9-13) control may be difficult. At a rate of circulation, Q cm³/sec, which is very large, the concentration of fission products in the external volume V_0 (pipes, pumps and heat exchanger) will be essentially the same as in the active volume. In this case a fraction V_0/V_1 of the delayed neutrons will be emitted in V_0 . Hence, the effective fraction $\beta_{\text{eff}} = \beta(1 - V_0/V_1)$, and it is desirable to design the unit so as to keep V_0/V_1 as small as possible.** For $V_0/V_1 = 0.18$, $\beta_{\text{eff}} = 0.50$ per cent instead of 0.61 per cent (see Section 2-9). In the extreme case of moderate Q and sufficiently large V_0/V_1 such that practically all the delayed emitters removed from the active volume decay before returning to V_1 , it can be shown that

$$(9-11) \quad \beta_{\text{eff}} = \sum_i p_i / \left(\frac{T_i Q}{0.693 V_1} + 1 \right)$$

*These nuclei do not know whether they were formed in fast or thermal fission. Of course, it is more important in the case of fast than for thermal reactors to keep k_{eff} less than β if the unit is to be more controllable than a bomb.

**This prerequisite is likewise important in minimizing the total amount of fuel mixture required.

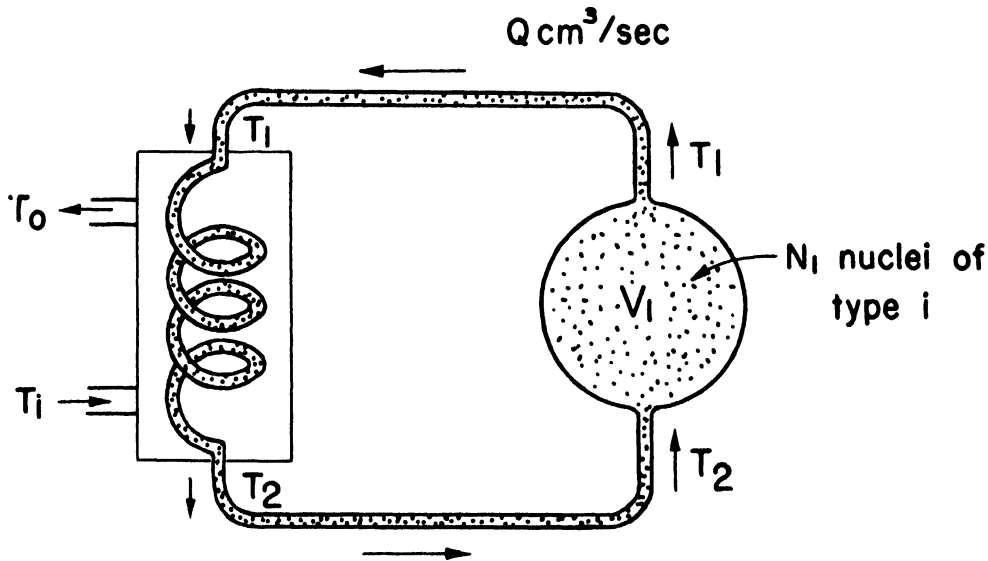


Figure 9-13. Diagram of Circulating Homogeneous Fluid Fuel.

where $p_i \equiv$ percentage of delayed neutrons of half-period T_i seconds. Using the values of P_i and T_i given in Section 2-9 the following minimal values of β_{eff} are obtained.

$Q/V_1 =$	0	.001	.01	.10	1.0
$\beta_{eff} \geq$.61	.60	.57	.36	.14

From these considerations plus engineering estimates made by Gilliland*, it is concluded that the β_{eff} of practical units would not be seriously less than β . Hence, the use of circulating fluid fuel mixtures is not limited by the loss of delayed neutrons.

The major disadvantages of this system are (a) the somewhat larger amount of fuel required, (b) the engineering difficulties of servicing and replacing pumps, pipes and heat exchangers that contain the highly radioactive fission products and (c) the substantially greater amount of shielding required. The intense gamma radiation and appreciable neutrons from the fission products, which circulate with the fuel, would require heavy shielding about the circulation system, heat exchanger, and pumps as shown in Figure 9-14. The long-lived nature of the gamma and beta activity makes servic-

*See Chapter 10.

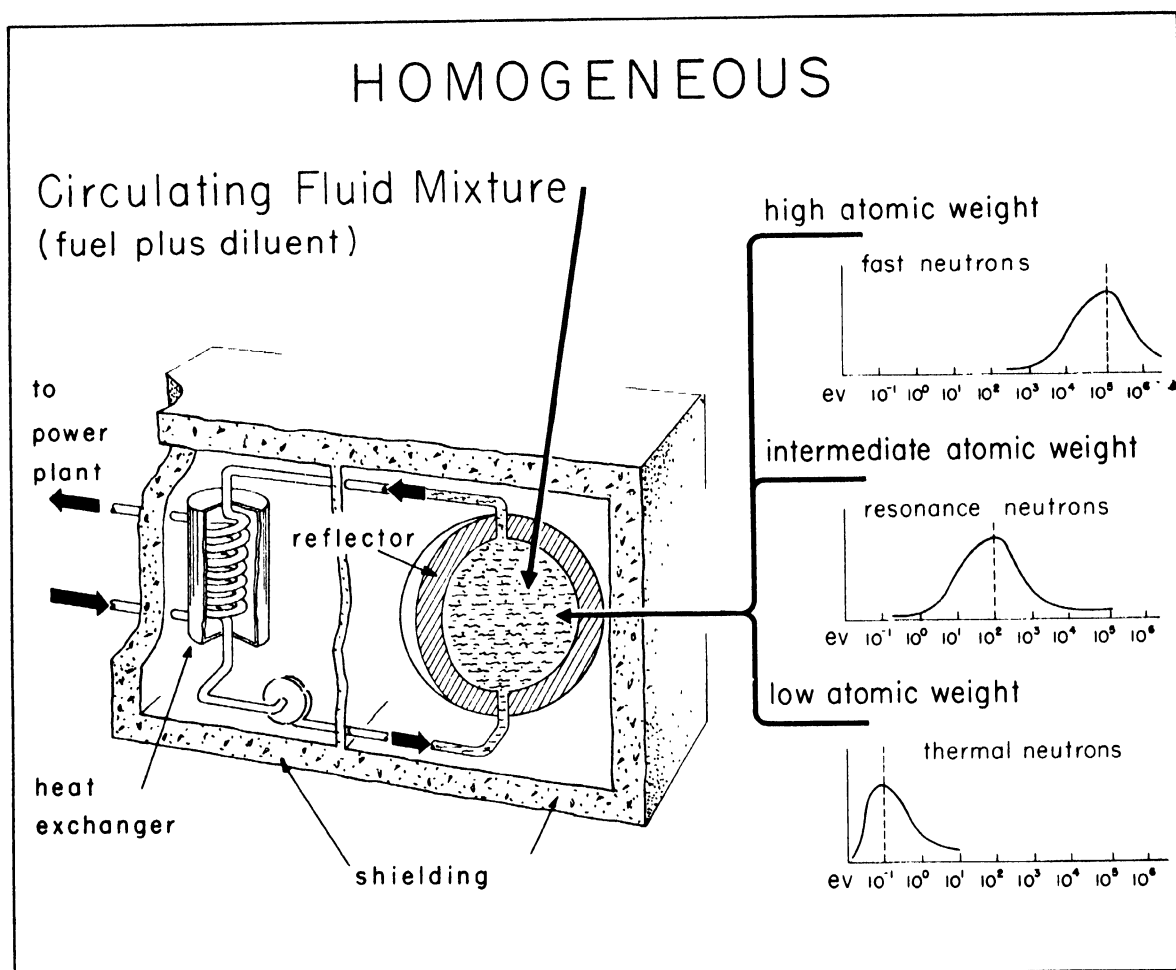


Figure 9-14 Homogeneous Reactor with Circulating Fuel Mixture. In this unit a fluid mixture of uranium or plutonium and a suitable diluent is pumped through a closed cycle consisting of a spherical reactor and a heat exchanger. If the reactor were cubical or cylindrical in shape, a somewhat larger volume of fuel mixture would be required (See Section 5-13). As discussed in Section 3-6 and 5-21 the use of a surrounding reflector substantially reduces the active volume. The mean atomic weight of the fuel mixture, and to a lesser extent the variation of σ_c with energy, determines the energy distribution of the neutrons in the reactor. Rough distribution curves for the three types of units are shown on the right.

Note heavy shielding (particularly against gamma radiation) is required about entire circulating system. Of course in practical installation shielding would directly adjoin reactor and heat exchanger. Likewise it would be necessary to have removable sections in order to gain access to both. Because of the delayed neutrons emitted by the fission products in the heat exchanger, some radioactivity will be induced in the secondary coolant. This effect complicates the servicing of the power machinery and would probably necessitate some gamma shielding of same.

ing of these parts nearly as difficult as repairs on the inner section of the reactor proper. The shielding and servicing problems are particularly acute in mobile units, such as could be used for ship propulsion, railway installations, and aircraft power units other than those that might be operated by remote control. Since the shield is like a thick skin about the active parts, the volume increases approximately as the square of the linear dimensions. The attenuation of gamma rays accompanying fission, plus those resulting from the fission products and from (n, γ) transitions in shielding materials, is about 10^{-x} where $x \approx$ feet of concrete or $10^{-x/5}$ where $x \approx$ cm of Pb.

9-9 Heterogeneous Reactors

In the preceding section it was shown that a homogeneous mixture of ordinary uranium and graphite cannot sustain a chain reaction. Yet it is well known that a combination of these ingredients can be made chain-reacting. Of course, the trick is to lump the uranium in the form of metal slugs (both spheres and cylinders have been used) and distribute them in a lattice array within the graphite. According to the Smyth Report, Section 2-10, "the high-speed fission neutrons, after being ejected from uranium and before reencountering uranium nuclei, would have their speeds reduced below the speeds for which non-fission capture is highly probable." Actually this description of the function of a lattice is incomplete. A more accurate description has been given by Fermi*:

"The resonance absorption which is responsible for the loss of neutrons during the slowing down has very sharp cross section maxima of the Breit-Wigner type. Therefore, if the uranium, instead of being spread through the graphite mass, is concentrated in rather sizable lumps, we will expect that the uranium in the interior of a lump will be shielded by a thin surface layer from the action of neutrons with energy close to a resonance maximum. Therefore, the resonance absorption of a uranium atom inside the lump will be much less than it would be for an isolated atom. Of course, self-absorption in a lump reduces not only the resonance absorption but also the thermal absorption of uranium. One can expect theoretically, however, and experiment has confirmed, that at least up to a certain size of lumps the gain obtained by reducing the resonance loss of neutrons overbalances by a considerable amount the loss due to a lesser absorption of thermal neutrons."

*Fermi, Science 105, 28 (Jan. 10, 1947).

Figure 9-15. Neutron Density Along the Diameter of a Spherical Reactor. The density n as a function of the radius r is given by $n = n_0 [\sin(\pi r/R)]/[\pi r/R]$ where n_0 is the density at the center and R is the radius of the sphere including the extrapolated spherical shell, i.e., $R_0 = R - d$. When surrounded by a reflector as in Figure 9-14, the distribution and hence the rate of heat production across the active zone can be considerably flattened. The density extrapolates to zero at a substantially larger distance beyond the boundary of the active volume.

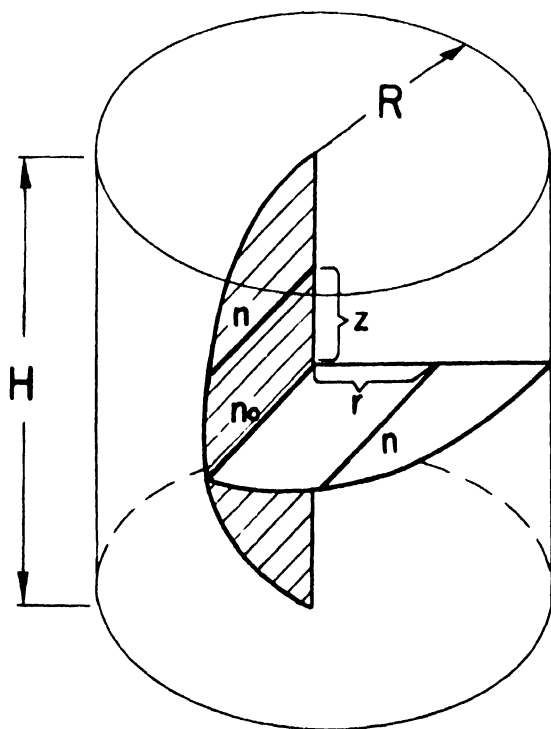
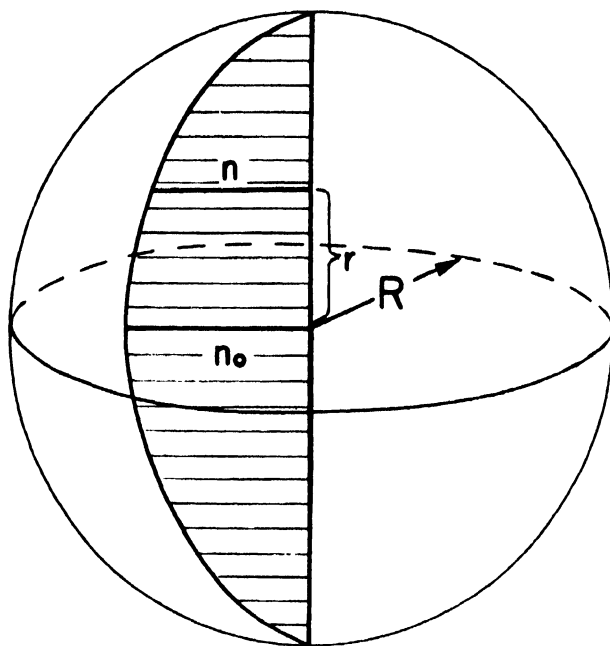


Figure 9-16. Neutron Density Along the Axis and Radius of a Right Circular Cylindrical Reactor. The density n as a function of the radius r and distance z from the center along the axis is given by:

$$n = n_0 J_0(2.4048r/R) \cos(\pi z/H)$$

where n_0 is the density at the center, J_0 is the first harmonic of the Bessel function of zero order, R is the radius of the cylinder including extrapolated cylindrical shell and H is the height including the extrapolated distance along the axis at each end. The cylinder of minimum volume is, of course, given by $R = 0.5413 H$. The use of a surrounding reflector (which may in part be the coolant), as in Figure 9-12, substantially reduces the active volume and flattens the neutron density distribution throughout the same.

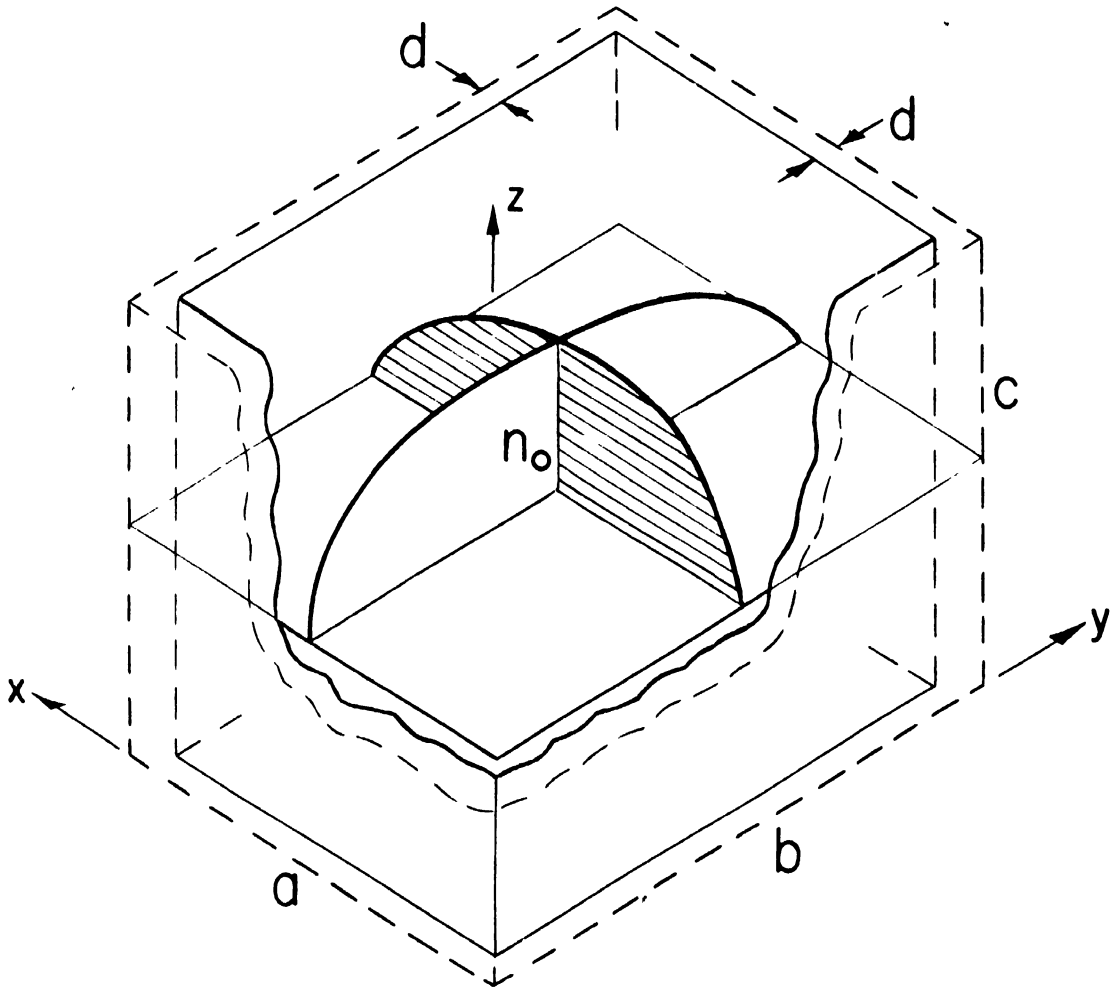


Figure 9-17 Neutron Density Along Major Horizontal Axes of a Rectangular Parallelepipedal Reactor. The density n as a function of the distances x , y and z along the edges from an outer corner of the extrapolated volume is given by:

$$n = n_0 \sin \frac{\pi x}{a} \sin \frac{\pi y}{b} \sin \frac{\pi z}{c}$$

where a , b and c are the outer dimensions as shown. There is, of course, a sinusoidal variation in n along the central z axis which could not be shown conveniently in this diagram. For the special case of a cube, $a = b = c$ and $a_0 = a - 2d \approx a - 1.42\lambda_g$ as discussed in Section 5-13.

In terms of the pile parameters, lumping results in a substantial increase in the resonance escape probability p while the thermal utilization f is decreased only slightly. The result is an increase in k from the maximum of 0.84, previously calculated for a homogeneous mixture of graphite and uranium, to the optimum value of 1.07 cited by Smyth for a heterogeneous system. The purpose of this section is to summarize the general effects produced by lumping insofar as this information has been declassified.

9-10 Distribution of Neutron Flux

The neutron density distribution has been discussed briefly in Sections 5-13 and 5-21. At steady state the first harmonic predominates. For the three common geometries shown in Figure 9-15 through 9-17, the distributions along the major axes are especially simple. The schematic three-dimensional drawings are intended to assist in the visualization of the neutron densities.

The cubical geometry will be used as illustrative of heterogeneous reactors in general. It will be recalled that the neutron density distributions shown in Figures 9-15 through 9-17 were derived for homogeneous systems. The question then arises, what are the distribution in heterogeneous units? Fortunately, it can be shown that in the first approximation the local variation due to the periodic structure of the lattice can be neglected when an equivalent homogeneous system is substituted for the heterogeneous system. Thus the problem can be simplified by dividing it into two parts. The macroscopic variations are represented by the smooth functions applicable to homogeneous mixtures, the densities being average values over the individual lattice cells. Superposed on these smooth relations will be local or microscopic variations over distances that are small compared to the dimensions of a lattice cell. Figure 9-18 illustrates the combined result for a cubical reactor.

The various processes that take place in a given cell will be reviewed by reference to Figure 9-20. Whenever a fission takes place in the fuel, an average of η neutrons are emitted with a continuous distribution of energy of the order of magnitude of 1 Mev as reported by Fermi*. There is a prob-

*Fermi, Science, 105, 27 (Jan. 10, 1947).

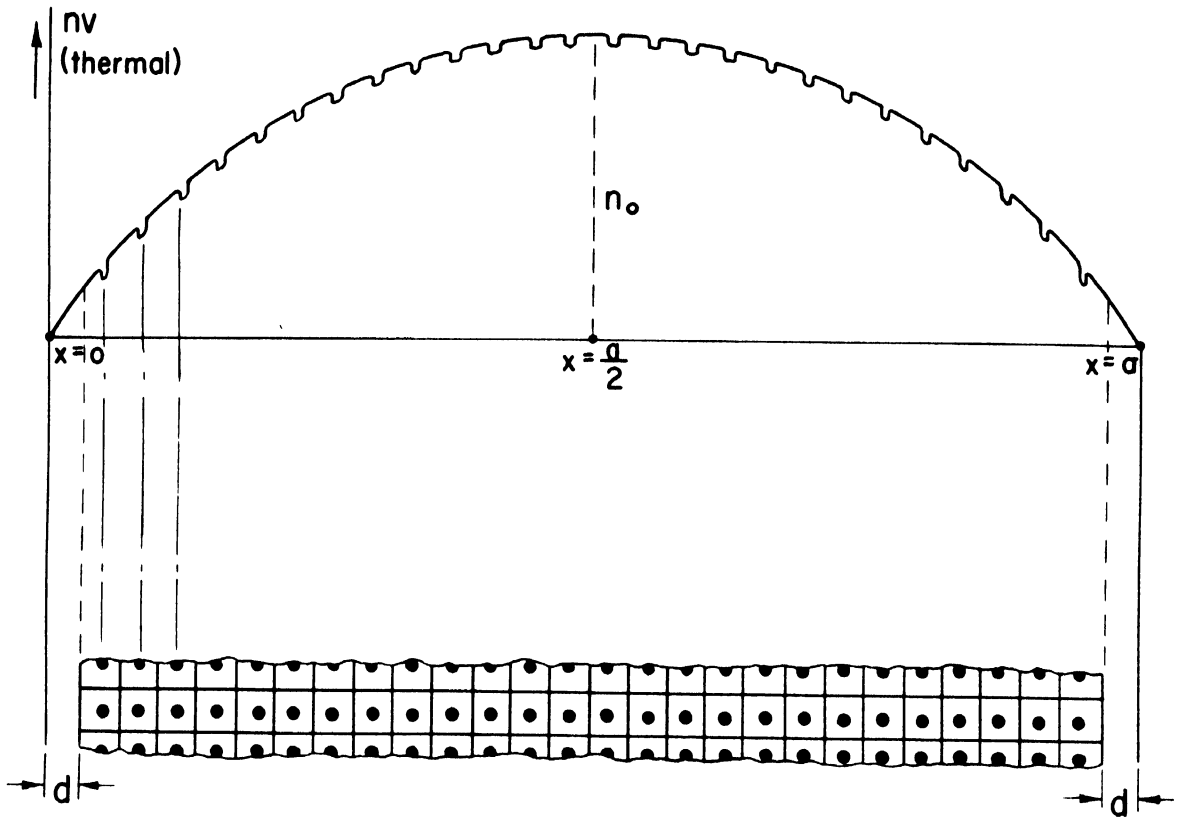


Figure 9-18. Neutron Flux Distribution Along Major Axis of a Cubical Reactor. The flux nv for neutrons of any given velocity v is a sinusoidal function of the distance x from the outer surface of the extrapolated volume of thickness d . The curve shows local dips in the thermal flux (and would show humps in the fast flux) in the immediate vicinity of the metal represented by black dots in the lattice projected below. The general distribution is not unlike a section across a Quonset hut. The flux or neutron density, of course, is a maximum at the center, $x = a/2$, $\sin(\pi x/a) = \sin(\pi/2) = 1$.

ability of a few per cent that the neutron will be absorbed by the fuel, in this case considered to be ordinary uranium, before its energy has been appreciably decreased. Such absorptions often lead to fast fissions of U^{238} . The slight increase in the fast flux at the periphery of the lump in Figure 9-20 is attributable partly to this effect and partly to the somewhat larger number of fissions per unit volume near the surface. Some of the fast neutrons are slowed down by inelastic collisions with uranium nuclei.

Upon escaping from the lump, the fast neutrons are rapidly moderated in energy by elastic collisions with the nuclei of the moderator. As seen

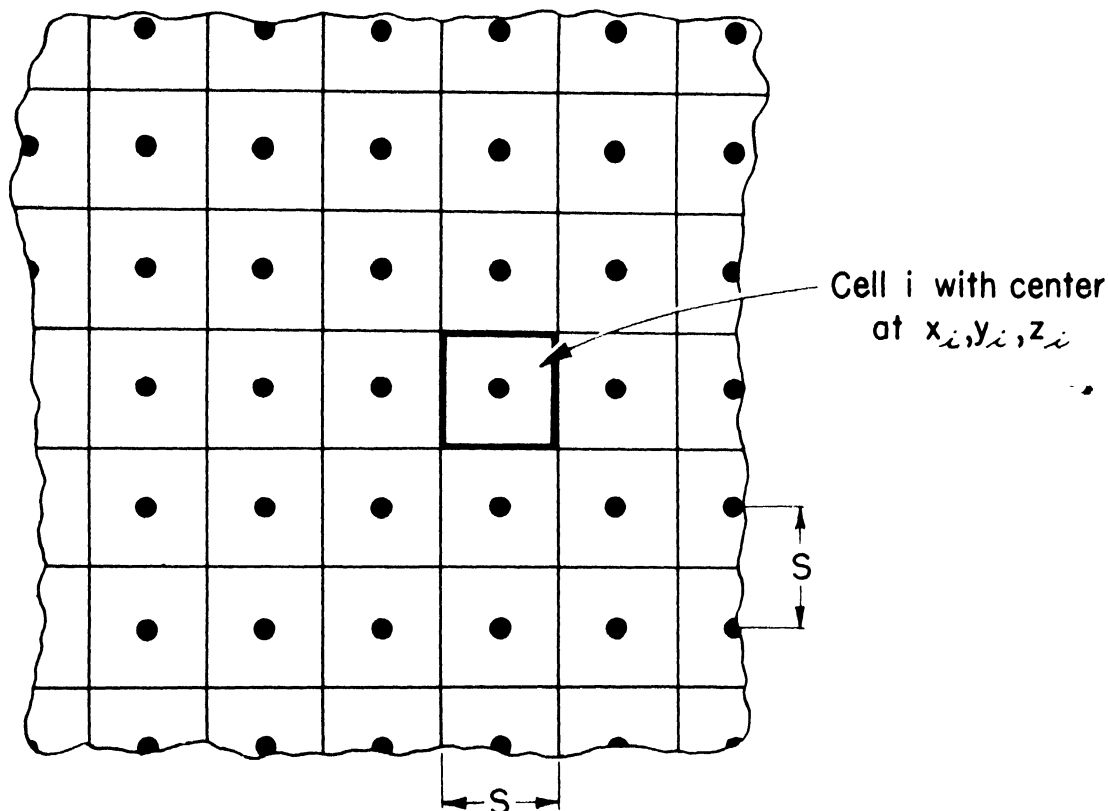


Figure 9-19. Enlarged Section of Lattice Shown in Figure 9-18. The dimensions and location of an individual cell in the lattice are indicated in this diagram. The fuel might be in the form of spheres or cylindrical rods immersed in a matrix of moderator (graphite, Be, D_2O , etc.).

in Section 1-27, an average of about 110 collisions with carbon nuclei are required to reduce the energy from 1 Mev to $1/40$ ev. Thus the fast flux decreases rapidly with distance from the fuel and joins on smoothly with the fast flux in the adjoining cells.

After the neutrons have been thermalized, they diffuse throughout the lattice until they are absorbed by either a C or U nucleus (ignoring impurities). Since the diffusion length in uranium is substantially less than in graphite, the thermal flux decreases with distance from the surface to the center of the fuel. A rough estimate of this attenuation can be obtained considering only neutrons that are incident normal to the surface. Since $N(U)\sigma_o(U) = 0.27 \text{ cm}^{-1}$, $n_{th}v_{th} \approx e^{-0.27t}$ which gives a fractional change of 0.97, 0.89, and 0.76 for $t = 0.1, 0.4$, and 1.0 cm respectively. Since

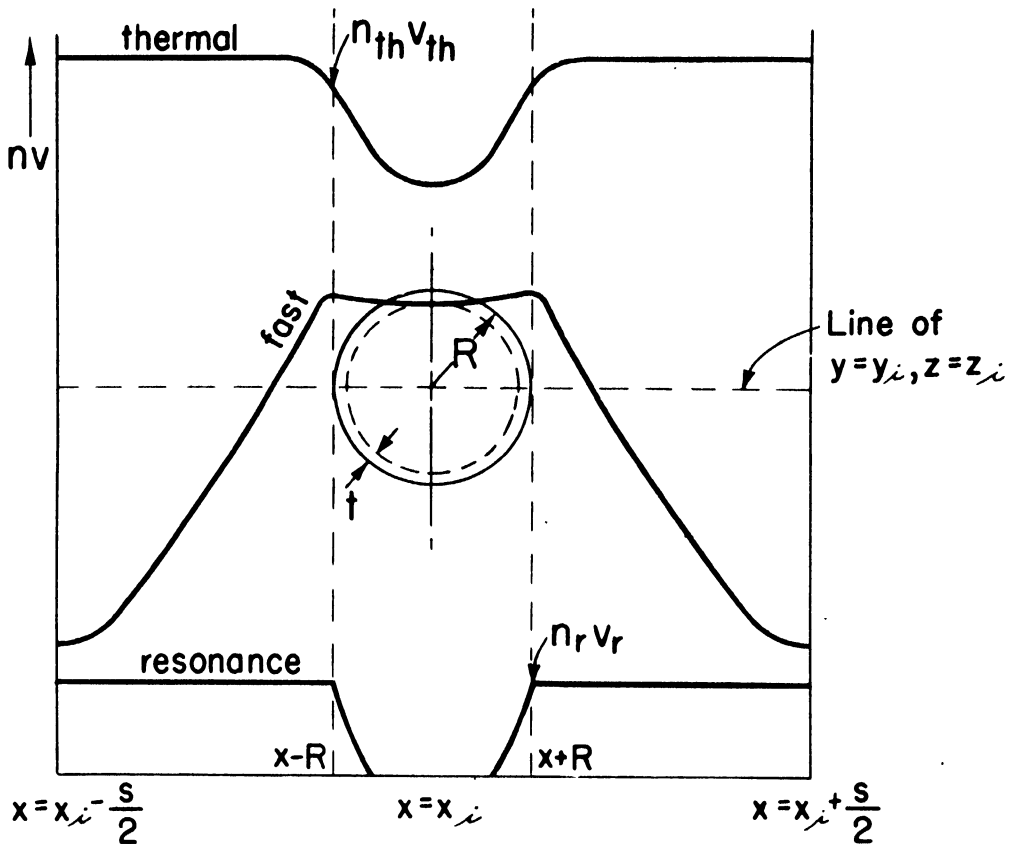


Figure 9-20. Schematic Representation of Flux Distribution Across a Single Cell. The lump or rod of fuel of radius R is located with its center at distances x_i , y_i , and z_i from the outer surfaces of the extrapolated cube as shown in Figure 9-17. Strictly the flux should show a net increase or decrease across the cell in accord with the sinusoidal distribution of Figure 9-18. However, for a cell of width $s \ll a$, to the first approximation this variation can be neglected. The relative heights of the curves of nv are not intended to indicate absolute orders of magnitude.

practically all neutrons strike the fuel at less than normal incidence, the attenuation will on the average be somewhat greater than these values.

However, this naive estimate is useful in comparing the attenuation of thermal neutrons with resonance neutrons. In Section 1-27, $\sigma_r(238)$ was indicated as several thousand barns at ~ 7 ev. If a modest value of only 2100 b. is taken for convenience, $N(238)\sigma_r(238) \approx 100 \text{ cm}^{-1}$. Hence, for normal incidence the fractional decrease in the resonance neutron flux will be $1/e$, .01, .0067, and .000045 for $t = .01$, .046, .05, and .1 cm respectively. Thus it is seen that a thin outer layer of the fuel is sufficient to reduce the resonance flux to a negligibly low value.

9-11 Reproduction in Heterogeneous Systems

In Sections 5-2, 5-4, and 5-18, two different thermal utilizations were defined and discussed. The thermal utilization f that has been used throughout the discussions of homogeneous thermal reactors is defined as the fraction of all thermal neutron captures taking place in fissionable isotopes. It is this quantity that enters the expression $k = pf\eta$ in which $\eta \equiv$ the number of neutrons released per fission. However, in heterogeneous reactors it is useful to express the reproduction as

$$(9-12) \quad k = \epsilon \eta_u f_u p_u$$

in which $\epsilon \equiv$ the fast effect, that is, the factor which takes into account the probability $(1-\epsilon)$ that a fission neutron will be absorbed, giving rise to fission before losing any appreciable amount of energy, $\eta_u \equiv$ the average number of neutrons emitted when a thermal neutron is captured by uranium, $f_u \equiv$ the thermal utilization in uranium, i.e., the probability that a thermal neutron is captured by uranium, and $p_u \equiv$ the resonance escape probability, i.e., the probability that a neutron is not absorbed before reaching thermal energy.

It can be shown that for small spherical lumps of radius R (in which $R < \lambda_g$), the average distance that a neutron produced in the lump must travel before reaching the surface is $3R/4$. In this case

$$(9-13) \quad \epsilon = 1 - 3R\sigma_{ff}(U)N(U)/4$$

in which $\sigma_{ff}(U) \equiv$ the average value of the fission cross section of uranium for fission neutrons and $N(U) \equiv$ the number of uranium nuclei per cm^3 in the lump. Fermi* cites $\epsilon = 1.03$ as an average value for a good lattice. The major uncertainty, as before, is the value of $\sigma_{ff}(U)$. However, taking 1.0 b as a very rough estimate based on the same reasoning as for Figure 9-9, a radius $R \approx 0.85$ cm for $\epsilon = 1.03$. In the subsequent sections this value will be used for purposes of discussion. For lumps of larger size, multiple collision processes become important, and both elastic and inelastic scattering play a considerable role. The latter effectively reduces the energy of the

*Fermi, Science 105, 28 (January 10, 1947)

neutrons below the fission threshold of U^{238} . In fact, Fermi has indicated that the "best approach to a practical solution is a direct measurement of neutrons absorbed by resonance in lumps of uranium of various sizes."

It is to be noted that $N(U) \tau_g(U)$ for thermal neutrons is about 1.5 $[N(238) \sigma_c(238) + N(235) \tau_f(235)]$. For this reason $n_{th} v_{th}$ is somewhat flatter through the lump than would be indicated by absorption alone, and an average value for the thermal neutron density in the lump $\equiv \bar{n}_u$ can be taken. Similarly, in the graphite part of the cell an average value $= \bar{n}_c$ is assumed. Fermi states that

"For practical purposes it is usually sufficiently accurate to calculate \bar{n}_c and \bar{n}_u , using the diffusion theory. The approximation is made to substitute the lattice cell by a spherical cell having volume equal to that of the actual cell, with the boundary condition that the radial derivative of the density of neutrons vanishes at the surface of the sphere. It is also assumed that the number of neutrons that are slowed down to thermal energies per unit time and unit volume is constant throughout the graphite part of the cell. This approximation is fairly correct, provided the dimensions of the cell are not too large. With these assumptions one finds the following":

$$(9-14) \quad f_u = \frac{N(U) \sigma_f(U) \bar{n}(u)}{N(U) \sigma_f(U) \bar{n}(u) + N(c) \sigma_c(c) \bar{n}(c)}$$

$$(9-15) \quad \therefore f_u = \frac{3a^2(1-a)(1+s)e^{-s+a} - (1+a)(1-s)e^{s-a}}{a^3 - s^3(a+b-ba)(1+s)e^{-s+a} - (a+b-ba)e^{s-a}}$$

where the unit of length is the diffusion length in graphite,

$$L_0 = \sqrt{\lambda_s(c) \lambda_c(c)/3}, \text{ and}$$

$$(9-16) \quad b = \frac{\lambda_s}{\sqrt{3}} \frac{1+\gamma}{1-\gamma}$$

where $\gamma \equiv$ reflection coefficient of uranium lump for thermal neutrons.

The corrected resonance escape probability p is considerably more difficult to calculate accurately, and unfortunately remains classified.

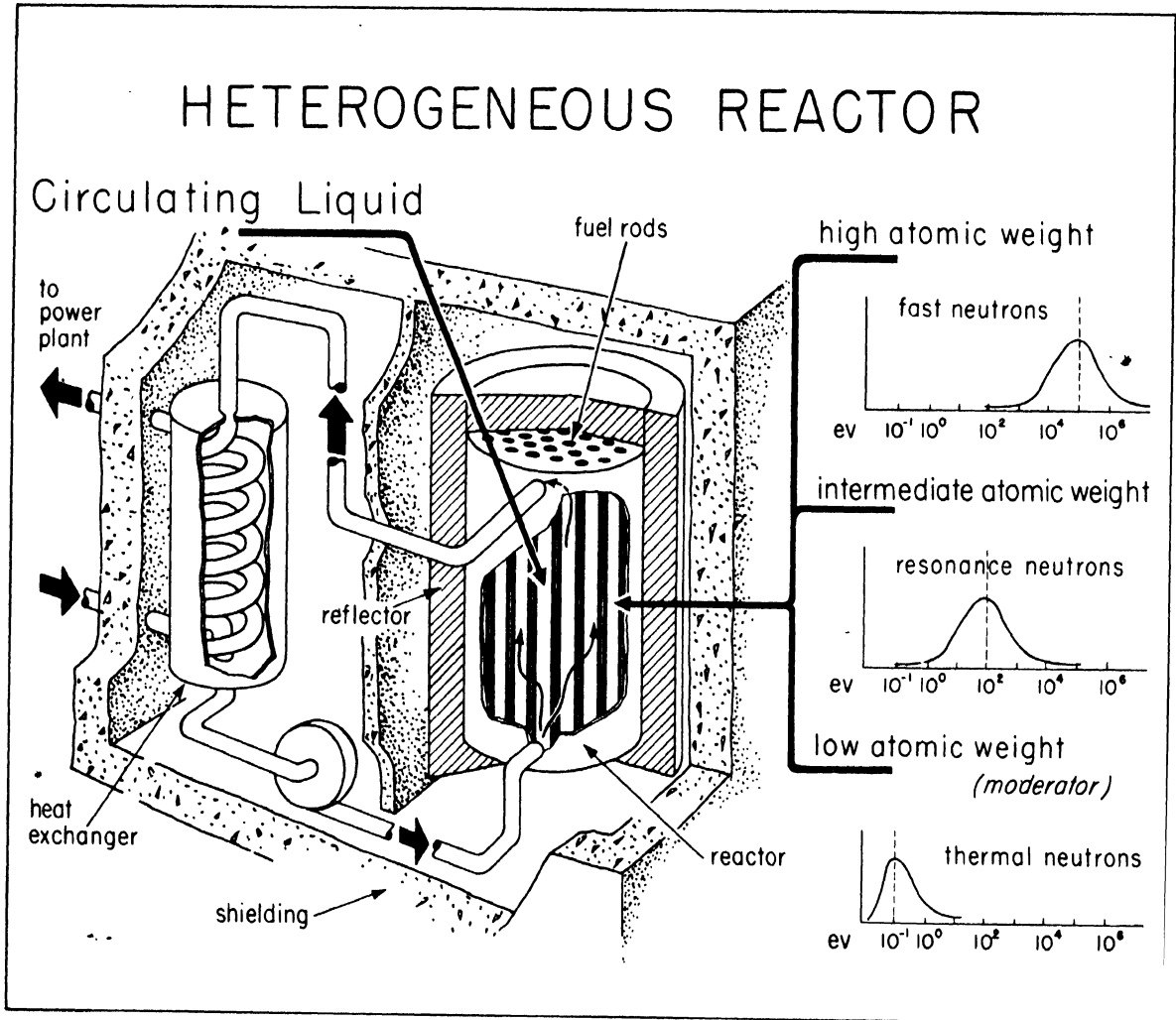


Figure 9-21. Heterogeneous Reactor with Circulating Liquid Diluent. This unit might use natural uranium and a liquid moderator which also serves as a circulating coolant, or with enriched fuels it could operate as a resonance or fast unit, depending on the atomic weight of the liquid diluent. It would probably be quite difficult to provide ready replacement of fuel rods in this design of reactor. In the drawing, the shield around the heat exchanger and pump is indicated as being equal in thickness to that around the reactor proper. With a suitable choice of diluent, the former shielding could be substantially reduced, more like that in Figure 9-12.

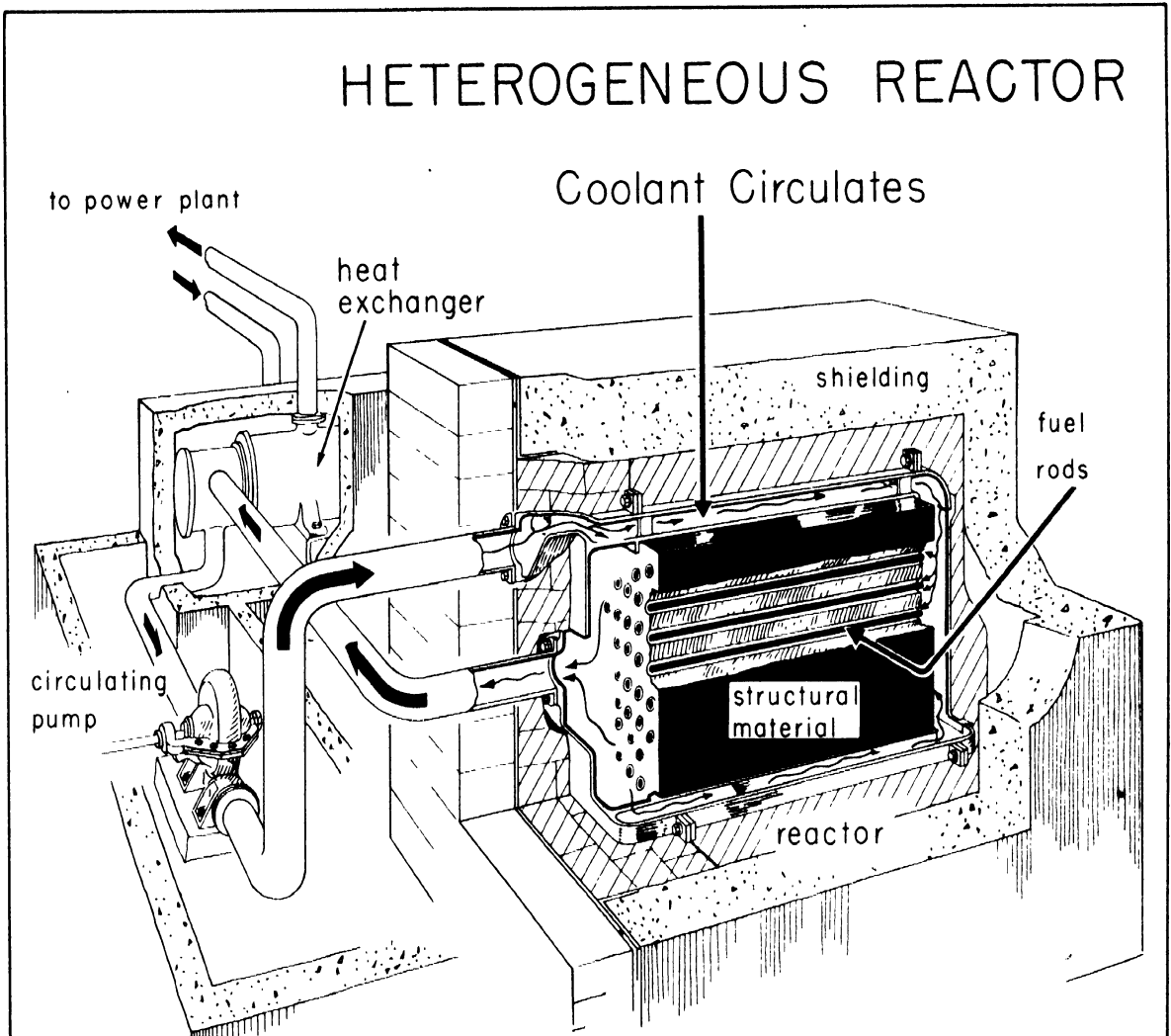


Figure 9-22 Heterogeneous Reactor with Solid Diluent and Circulating Coolant. This drawing is an attempt to show somewhat more in the way of engineering details than in the other sketches. Solid fuel rods, clad with a non-corrosive metallic coating, are mounted horizontally in a structural material that serves as a moderator in a thermal unit, or as a diluent in a fast or resonance unit. A removable section of shielding allows the end manifold to be removed for replacement of fuel and other parts. Because of the intense radiations from the fission products, this work would have to be done by special devices operated by remote control. Because of the numerous engineering advantages, the coolant would probably be a liquid. However, for special purposes, a gas coolant might be used, in which case a substantially larger proportion of the reactor volume would be required for the coolant.

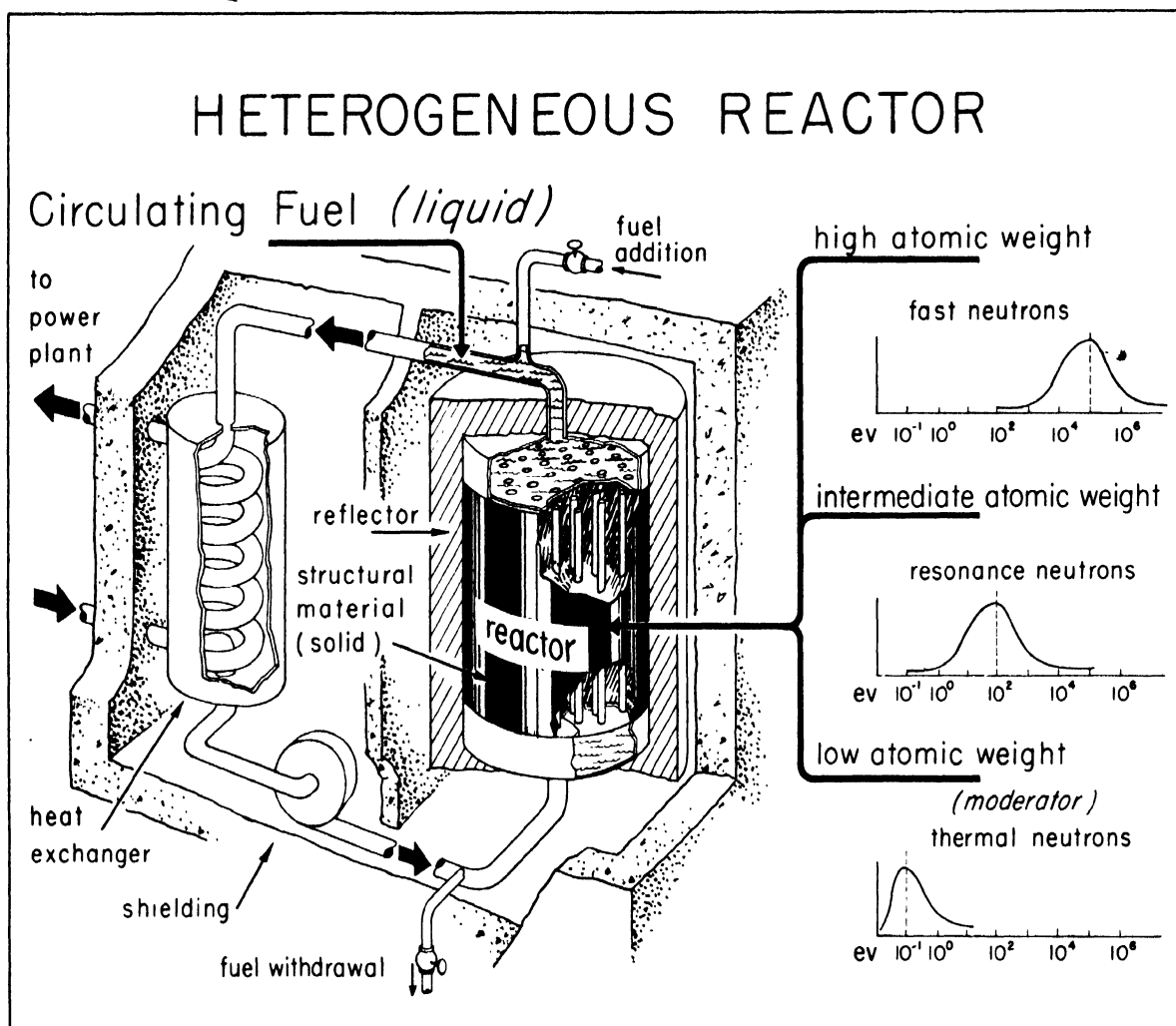


Figure 9-23 Heterogeneous Reactor with Circulating Liquid Fuel. In this scheme the solid structural material serves as moderator or diluent. The fuel, which could be ordinary uranium or enriched material, is contained in a solution, slurry, or fusible alloy. The heat developed in the fuel mixture and in the solid parts of the reactor is removed by circulating the liquid fuel. Arrangements are also provided for addition and withdrawal of fuel during operation. Since the heat exchanger and circulation system will be highly radioactive, heavy shielding must be provided throughout. This system has the same advantages and is subject to the same limitations as the circulating homogeneous reactor of Figure 9-14.

However, it is evident that if, as previously stated, k is to be increased from the optimum value of 0.84 for ordinary uranium plus graphite in a homogeneous mixture to the maximum value of 1.07 cited by Smyth for a heterogeneous system, p_u must be substantially greater than p since f_u is slightly less than f . For $k = 0.84$, based on the method and data of Chap. 6, $p = 0.77$. Using $\eta = \eta_u = 2.3$ as before:

$$(9-17) \quad k(\text{homo.}) = \eta p f = (2.3) (0.77) (0.475) = 0.84$$

This homogeneous system contains $N(c)/N(238) = 440$. If this ratio were maintained for a heterogeneous system the thermal utilization would be slightly less and the resonance escape probability would be substantially greater. However, because of the difference in definitions, f and f_u are not directly comparable. Instead, ηf and $\eta_u f_u$ must be considered. In Equation (9-17) $\eta f = 1.09$. For the equivalent homogeneous system, $\eta_u f_u \leq 1.09$ and $p_u > 0.77$ in order to obtain maximum of $k = 1.07$:

$$(9-18) \quad k(\text{hetero.}) = \epsilon \eta_u p_u f_u = (1.03) (>0.77) (\leq 1.09) = 1.07$$

In fact, p_u must be > 0.95 in order to satisfy this relation. It is unlikely that the optimum value of $N(c)/N(238)$ for a heterogeneous system would be the same as for a homogeneous mixture. With a decrease in the proportion of graphite, an increase in $\eta_u f_u$ above 1.09 could probably be achieved. Using the relation

$$(9-19) \quad L^2 = L_o^2 (1 - f_u) \quad \text{from Section 5-18.}$$

and the values $L^2 = 350 \text{ cm}^2$, $L_o^2 = 2500 \text{ cm}^2$ and $k = 1.06$ given by Fermi for a special lattice, values of $f_u = 0.86$ and $\eta_u f_u = 1.27$ are obtained. This value of f_u corresponds to $f = 0.52$ in the homogeneous case based on the fractional absorptions in various lattice materials given by Fermi. From this an estimate of $p_u = 0.81$ can be made.

9-12 Effect of Enrichment

The foregoing considerations are for ordinary uranium in a graphite moderator. Fermi cites as an example a cubical unit of critical side $a = 19.15$

feet. For a number of power purposes, it would be desirable to have more compact units, since the shielding will add at least another 8 feet of length to each side. The use of Be as moderator would allow some reduction in size, but the most obvious method is to use enriched uranium.

As the proportion of U(238) decreases, the nuclear benefits of lumping also decrease, not only because of the increase in p_u but also because of the decrease in f_u for a given size lump. Using the same approximate relations for estimating the skin thickness as in Section 9-10, the fractional decrease in $n_r v_r \approx e^{-100t \frac{U(238)}{U}}$ and $n_r v_r$ is reduced to $<1/e$ of initial value in a thickness t as follows:

$t(\text{cm})$	0.01	0.0125	0.02	0.04	0.1
$U(238)/U$	0.993	0.80	0.50	0.25	0.10
%U(235)	0.7	20.	50.	75.	90.

Similarly for a fractional decrease in $n_{th} v_{th}$ of $1/e$:

$t(\text{cm})$	3.7	0.21	0.083	0.055
%U(235)	0.71	20.	50.	75.

Thus it is evident that if rods of uranium are to be used, the diameter must decrease as the enrichment increases in order to maintain a desirable level for the thermal utilization. Of course, an alternative is to establish an optimum diameter for mechanical and thermodynamic reasons and dilute the enriched uranium with a material with low $N\sigma_c$ and favorable physical, mechanical and metallurgical properties.

While the nuclear advantages of lumping are less important in enriched reactors, the engineering advantages of using fuel rods instead of a homogeneous mixture may justify retaining the lattice array. Examples of this type are given in Figures 9-21 and 9-22. If unenriched or only slightly enriched uranium were to be used, it might be advantageous to use a circulating liquid but retain the lattice structure. A device of this type is shown in Figure 9-23. Other permutations are also possible. The diluent might be liquid surrounding a liquid fuel contained in tubes. Either of these liquids could be circulated to serve as a heat transfer medium. The fuel could be a fusible alloy contained in vertical openings in a solid diluent, while a liquid or gaseous coolant circulates through horizontal tubes in the diluent. As discussed in a subsequent chapter, the heat transfer coefficient for liquid metals is particularly high.

CHAPTER 10

HEAT TRANSFER

by

E. R. Gilliland

10-1 General Considerations

The purpose of this section and the one which immediately follows is to consider the various methods of transferring heat and to evaluate these in terms of the problems which arise in removing heat energy from nuclear reactors. Since engineering units will be used throughout, a number of conversion factors are included in Table 10-1 which allow these units to be transferred to those used by the physicist and chemist.

In removing heat from a reactor, there are a number of considerations, but to an engineer, the chief one appears to be that the physicist prefers that he keep his equipment out of the reactor. Apparently, nearly any material used in the reactor is objectionable. If a gas like helium is used, while not objectionable from its nuclear properties, it is not a good moderator and hence increases the size of the reactor. Many of the liquids require structural materials for the passages through which they flow that are objectionable in thermal reactors. The main objective is to remove the heat without disturbing the physical characteristics of the reactor any more than is absolutely necessary.

There are a number of methods by which heat energy is transferred from one position to another, but for nuclear reactors five of these methods cover most of the cases, i.e., Conduction, Radiation, Convection, Boiling, and Condensation. The principles involved in each of these five methods will be briefly reviewed.

TABLE 10-1

CONVERSION FACTORS

$$1 \text{ Btu} = 252 \text{ cal} = 0.293 \text{ watt-hours}$$

$$\frac{1 \text{ Btu}}{\text{hr.ft}^2 \text{ } ^\circ\text{F}} = 0.42 \times 10^{-2} \text{ cal/sec. cm}^2 \text{ } ^\circ\text{C}$$

$$= 0.0176 \text{ watts/cm}^2 \text{ } ^\circ\text{C}$$

$$\text{Btu/hr ft}^2 \text{ } ^\circ\text{F} = 1.35 \times 10^{-4} \text{ cal/sec. cm}^2 \text{ } ^\circ\text{C}$$

$$= 5.7 \times 10^{-4} \text{ watts/cm}^2 \text{ } ^\circ\text{C}$$

10-2 Conduction

In conduction, heat flows from one position to another by molecular effects; in other words, there is no mass movement of the material. This method of heat transfer always occurs in solids and since there will almost invariably be solids in the nuclear units, conduction will be important. The simple conduction equation relates the rate of heat flow $dQ/d\theta$ to the temperature gradient:

$$(10-1) \quad \frac{dQ}{d\theta} = -kA \frac{dt}{dx}$$

where k = the thermal conductivity, which is a proportionality factor defined by the equation. A is the area for heat flow and $\frac{dt}{dx}$ is the temperature gradient. In actual reactor design there is three-dimensional heat flow and the basic differential equation that applies is:

$$(10-2) \quad \frac{1}{\rho C_p} \left[\frac{\partial}{\partial x} \left(k_x \frac{dt}{dx} \right) + \frac{\partial}{\partial y} \left(k_y \frac{dt}{dy} \right) + \frac{\partial}{\partial z} \left(k_z \frac{dt}{dz} \right) \right] = \frac{\partial t}{\partial \theta}$$

which reduces to the Laplacian equation when the thermal conductivity is the same in all three directions. For the steady state condition, the partial derivative, $\partial t / \partial \theta$, is zero. To determine the temperature gradient or heat flow is a matter of integrating this equation, and Fourier and many others have performed this operation for a number of cases. Actually, in a nuclear reactor, it is rather improbable that direct integration will be possible. In the case of homogeneous reactors (see Section 9-8) it should be possible to integrate the equation. However, in the heterogeneous reactors, boundary conditions become very complicated and it is probably necessary to solve it by graphical integration. A large number of graphical methods have been developed by which the heat flow can be evaluated for almost any shape and for media of variable conductivity. If one is willing to spend the time and effort necessary to perform the graphical operation, the whole temperature pattern of almost any reactor can probably be worked out. The only factors needed are the thermal conductivities and the physical properties of the materials of construction. For high rates of transfer of heat, a high thermal conductivity is desirable. Conversely, for a heat insulator, a low thermal conductivity is preferable. For purposes of orientation, Table 10-2 includes a list of thermal conductivities for a number of solids, liquids, and gases which cover a wide variation of k .

TABLE 10-2
THERMAL CONDUCTIVITIES

<u>Solids</u>			
	<u>k</u>		<u>k</u>
Ag	240	Pt	40
Cu	220	Fe, Ni, BeO	35
Au	170	Mild Steel	25
Al	120	Pb	20
Mg	92	18-8 steel	16
Be	90	Bi	4
Graphite	85 - 90	Carbon	2
Na	80	SiC ₂	10
Zn	65	Al ₂ O ₃	2.5
Cd	50	MgO	2
<u>Liquids</u>		<u>Gases</u>	
Na	48	H ₂	0.1
Hg	5	He and D ₂	0.075
H ₂ O	0.35	CH ₄	0.02
CCl ₂ F ₂	0.05	H ₂ O	0.012
		N ₂ and O ₂	0.014
		CO ₂	0.009
		CCl ₂ F ₂	0.005

In this table no attempt has been made to indicate which materials are good or bad in nuclear reactors. This factor depends on the type of reactor, the major difference being between reactors which operate with thermal neutrons and neutrons of higher energies.

Among the solids, aluminum is the first material that has a reasonably low macroscopic absorption cross section for thermal neutrons. However, this material has rather poor moderating properties and, consequently, while it is satisfactory as a heat transfer material, the amount which should be used in a thermal reactor should be made as small as possible. The first material listed which is really good as a moderator is beryllium. Graphite is likewise a good moderator, and it is observed that these two substances have fairly good conductivities. It is not certain that the thermal conductivity of graphite is isotropic, because of its plate-like character.

Sodium has a low cross section for absorption, but it is not particularly good as a moderator, and it would probably not be used as a solid because of its low melting point. Iron, nickel, and beryllium oxide have values of thermal conductivity of about 35. Iron and nickel together with chromium are some of the best materials of construction, particularly for high temperature operation.

Continuing down the list, bismuth, alumina, and magnesia have relatively low values, and there are a number of porous solids which have thermal conductivities as low as .01, largely the result of the presence of air.

The liquid metals have relatively good thermal conductivities, sodium being substantially greater, however, than mercury, which in turn is considerably better than water, which is about the best of the non-metallic liquids. Nearly all of the organic liquids have values of the order of .05, i.e., they are poor for transferring heat by conduction. The gases, as a whole, have very low values of thermal conductivity. In building a nuclear reactor from blocks of graphite, one of the chief resistances to the flow of heat will be the gas films between the blocks, and the materials in the reactor. In such cases it may be desirable to fill the reactor with a gas of high thermal conductivity, such as helium, to improve the transfer across the gaps. Obviously, the best procedure is to keep the thickness of any gaps to a minimum.

10-3 Radiation

Heat can be transferred by means of radiant energy which follows the familiar Stefan-Boltzmann Law:

$$(10-3) \quad \text{Btu/hr-ft}^2 = 0.173 \epsilon \left(\frac{T_1}{100} \right)^4$$

in which $\epsilon \equiv$ emissivity and T_1 is \equiv the absolute temperature in degrees Rankine. In order to compare radiation with thermal conductivity, it is convenient to express the latter in terms of the heat transfer coefficient, h , which is equal to the heat transferred per unit area per unit time per unit temperature difference. Equation (10-1) is then written as:

$$(10-4) \quad \frac{dQ}{dt} = hA \Delta t; \quad \text{for solids} \quad h = k/\Delta x$$

in which $\Delta t \equiv$ overall temperature difference over the distance Δx . For example, a slab of copper 1 foot thick has an h of 220 as given in Table 10-2, and if it is 1 inch thick, $h = 2640$. If radiation is calculated on the same basis, for a surface temperature T_1 and a temperature difference between radiating surfaces of 100°F , the equivalent values of h , for $\epsilon = 1$, are as follows:

T_1 $^\circ\text{R}$	1500	2500	3500
h	20	90	220

From these values, it is seen that 4 feet of graphite will transfer more heat for a given temperature difference than can be radiated from a surface at 1500°R to a surface at 1400°R . The radiation increases as the fourth power of the temperature, but it requires a temperature of 3500°R in order to radiate as much heat per square foot per 100°F temperature difference as can be conducted through one foot of copper or silver.

It might be more significant to consider the radiation from the hot surface to a surface at constant lower temperature rather than use a constant difference of 100°F , since the temperature of the coolant surface is limited by engineering factors. The following table gives the heat radiated from a hot surface at T_1 $^\circ\text{R}$ to a surface at 1400°R for an emissivity of unity.

T_1 $^\circ\text{R}$	1,500	2,500	3,500
Btu/hr-ft ²	2,100	59,000	250,000
Btu/hr-ft ² for graphite*	8,500	93,000	178,000

Temperatures above 2500°F essentially rule out practically all materials of construction. Graphite, uranium carbide, and possibly some other materials might be used, but common materials of construction would melt or decompose. Transfer of heat by radiation would occur mainly between solid surfaces, since most of the gases have very little energy absorption at these levels, although CO_2 and water vapor have slight absorption bands. The amount of energy which can be absorbed by such gases is small. Of course, solids, such as carbon, could be suspended in the gases, and the reactor's

*For a thickness of one foot under the same temperature difference.

surfaces could radiate to these solids which, in turn, would transfer the energy to the gas. For example, powdered graphite suspended in helium could be blown through a tube, the sides of the tube radiating to the graphite, which in turn transfers the energy to helium. However, such an effect is ineffective, since the radiation could give a heat transfer coefficient of about 20, but by other procedures it is possible to obtain coefficients of several hundred, so that suspension of solids does not pay for the added difficulties.

Radiation is not likely to be of major importance in transferring heat in the normal operation of nuclear reactors.

10-4 Convection

The most important method of transferring heat to or from fluids is by convection. This method involves the motion of a fluid by means of which the heat is transferred from one place to another. Forced convection is divided into two types: streamline (or laminar flow) and turbulent flow. In streamline flow, any given boundary line continues in the same relative position to the wall. In turbulent flow, there is considerable motion of the liquid with eddies that move perpendicular to the net flow and no definite boundary lines are maintained.

One of the main objections to convection is that the heat transfer is obtained at the expense of pumping the fluid. For streamline flow, the viscosity causes a loss of energy as a result of the effect of one layer sliding over the other, since the inside layer is moving faster than the outside. The equation for this type of flow is as follows: (Poiseuille law)

$$(10-5) \quad \frac{dp}{dL} = \frac{32 \mu u}{gD^2}$$

where p = pressure
 L = length
 μ = viscosity
 u = velocity
 g = conversion factor
 D = diameter

In turbulent flow, the phenomenon is no longer essentially viscous - it is kinetic effects. Energy is wasted by creating eddies and the equation most commonly used is: (Fanning equation)

$$(10-6) \quad \frac{dp}{dL} = \frac{2f u^2}{gD}$$

where f is the friction factor, and it is a function of velocity, diameter, density, and viscosity as given by the Reynolds number, $(Du\rho/\mu)$. The factor f can be approximated by

$$0.046 / \left(\frac{Du\rho}{\mu} \right)^{0.2}$$

The Reynolds number is the criterion of whether the flow is turbulent or streamline. A value of this group greater than 2000 - 3000 usually indicates turbulent flow, while lower values correspond to streamline flow.

As would be expected, the two different types of flow result in different heat transfer coefficients. In the case of streamline flow, the heat transfer would be purely by thermal conduction through the fluid, and equations have been developed on this assumption. Actually, the equations assumed ideal conditions, i.e., no change of viscosity or density with temperatures. Since these physical characteristics for most fluids do vary with temperature, the flow conditions are not equivalent to those assumed, but it has been found that these theoretical developments serve as a valuable guide for correlating experimental data.

In the case of turbulent flow, the present accepted picture involves essentially no turbulence at the wall due to the stabilizing effect, but with increasing degrees of turbulence away from the wall. In this case, the heat is transferred through the layer near the wall essentially by thermal conduction and through the main body of the fluid essentially by turbulence, there being an intermediate region where both methods are important. In this case, heat transfer correlations have been developed by both theoretical and empirical approaches. The theoretical approaches have been largely based on the analogy between heat transfer and momentum transfer. Reynolds developed the first of such analogies using the turbulent core only. His equation agrees reasonably well with the data for gases, but is unsatisfactory for most liquids.

Prandtl modified the Reynolds' analogy by including a laminar film at the wall, and his equation is given below to illustrate the type of relationships obtained by these analogies. It is a fair quantitative equation, but there are other basic relations which are better.

Prandtl's equation is:

$$(10-7) \quad \frac{h}{C_p G} = \frac{f/2}{1 - r_v + r_v \frac{C_p \mu}{k}}$$

where h = heat transfer coefficient
 C_p = specific heat
 G = mass velocity = $u\rho$
 f = friction factor of Fanning Equation
 μ = viscosity
 k = thermal conductivity
 r_v = a function of the velocity at the boundary between the laminar film and the turbulent core.

The group $(1 - r_v)$ is the relative resistance of the turbulent core and the group $r_v(C\mu/k)$ that of the film. These relationships have been tested for fluids having values of $C\mu/k$ approximately unity or greater, and there may be doubt as to whether they apply to the liquid metals which have values of this group of the order of 0.01.

Empirical equations have been developed which correlate the available experimental data better than do the analogies, and these latter equations have their main value in indicating the important relationships. The empirical equations have been developed with the aid of dimensional analysis and for forced convection. They can usually be arranged to involve the Reynolds' number, the Prandtl number, and a dimensionless group involving the heat transfer coefficient. For fluid flowing inside a tube, the following equation is given by McAdams, "Heat Transmission":

$$(10-8) \quad \frac{hD}{k} = 0.023 \left(\frac{Du\rho}{\mu} \right)^{0.8} \left(\frac{C\mu}{k} \right)^{0.4}$$

where h = the heat transfer coefficient
 D = diameter of the tube
 k = thermal conductivity of the fluid
 u = linear velocity of the fluid
 ρ = density of the fluid
 μ = viscosity of the fluid
 C = heat capacity of the fluid

Any dimensionally consistent set of units can be used. This equation handles the data for gases and liquids (water and the various organic fluids, but not liquid metals). The published experimental data on liquid metals are

very meager, but a few experiments with mercury have indicated heat transfer coefficients several-fold lower than predicted by the foregoing equation.

This heat transfer equation can be condensed to the variables involved instead of employing dimension groups as follows:

$$(10-8a) \quad h = 0.023 \frac{k^{0.6} u^{0.8} \rho^{0.8} C^{0.4}}{D^{0.2} \mu^{0.4}}$$

In order to obtain a high coefficient, it is apparent that a high value of the thermal conductivity is desired. Materials of low thermal conductivities will, in general, give low values of the heat transfer coefficients. In other words, the heat transfer coefficients for gases will be relatively low. In all cases, the coefficients increase rapidly with the velocity and apparently there is no upper limit to this effect. High velocities are objectionable due to the fact that they involve high pumping costs and, if possible, it is usually more desirable to obtain a high heat transfer coefficient by other means. It is to be noted that the diameter of the tube has little effect on the value of h .

In order to indicate the magnitude of the coefficients obtained with gases, calculations were made with Equation (10-8) for a velocity equal to one-half the velocity of sound at 400° C. It should be emphasized that these velocities are much higher than normally employed for gases. With a velocity equal to one-half the velocity of sound, air gives a heat transfer coefficient of about 50 Btu per hr. per ft² per °F. Hydrogen at one-half the velocity of sound at 400° C has a coefficient of about 280 and helium around 170. However, as a whole, these coefficients are low as compared to those obtainable with liquids.

In the case of liquids, very high heat transfer coefficients are possible. Water flowing at a velocity of 10 feet per second gives a heat transfer coefficient of approximately 3,000 Btu per hr. per ft² per °F, which means that a large amount of heat can be transferred for a small temperature difference. If the velocity is increased to 50 feet per second, water gives a coefficient of about 10,000, and this is probably as high as would be desirable, since the other resistances would then become limiting.

On the basis of Equation (10-8), the liquid metals appear very good. For example, at about 10 ft/second, both liquid sodium and liquid mercury

give calculated heat transfer coefficients of over 20,000. There is a very serious question, in view of the present experimental data, whether the actual heat transfer coefficients are as high as those calculated, and it may be that the coefficients will be materially modified by whether or not the liquid metal wets the tube wall.

Assuming that the heat transfer coefficients for the liquid metal are as high as 20,000, it is doubtful that such high values would be particularly helpful due to the fact that with these materials a tube wall would be involved, and even with a thin tube, the wall resistance to heat transfer would probably be very much greater than corresponds to such high coefficients. Before liquid metals can be properly appraised, it will be necessary to have sufficient data to determine whether the metal wetting the tube wall is important. In the case of the chemically-active metals such as lithium, sodium, and potassium, it is probable that wetting will occur with the usual types of steel, but normally mercury does not wet steel. However, the data in the literature indicate that small quantities of other elements can be added to mercury which make the liquid wet the wall.

For the case of streamline flow in tubes, McAdams gives the following relationship:

$$(10-9) \quad \frac{hD}{k} = 1.86 \left[\left(\frac{Du\rho}{\mu} \right) \left(\frac{C\mu}{k} \right) \left(\frac{D}{L} \right) \right]^{1/3}$$

Nomenclature same as for Equation (10-8)

In general, this equation is of the same form as the one for turbulent flow, but the effect of velocity is much less, while the effect of thermal conductivity is about the same. Streamline flow is not widely used in industrial heat transmission problems, but in the case of the liquid metals it may be desirable, since such high coefficients can be obtained with these fluids even under low velocity conditions, which would save pumping power as compared to turbulent flow.

Besides forced convection, heat is also transferred by natural convection, in which case the circulation of the fluid is due to the fact that a temperature difference exists, and not due to any external pumping system. The fluid circulates due to the density differences produced as a result of the temperature difference. As a whole, natural convection gives low heat

transfer coefficients. Most gases give values of the heat transfer coefficients of 25 or less, and water gives coefficients up to approximately 300. There is very great uncertainty as to the magnitude of the heat transfer coefficients obtained with liquid metal.

The above equations were developed for flow inside tubes, and a limited amount of work has been carried out in conduits of other cross sections, such as annular spaces, square pipes, triangular pipes, elliptical pipes, etc. In general, it is possible to correlate the limited data available for these shapes with the equations for tubes by using four times the mean hydraulic radius instead of the diameter; where the mean hydraulic radius is defined as the cross section for flow divided by the wetted perimeter. Thus, for a circular tube, the mean hydraulic radius calculates to be one-fourth the diameter and reduces to the original relationship. For other shapes, the total perimeter is used in calculating the mean hydraulic radius regardless of whether the perimeter is all used for heat transfer.

10-5 Boiling Liquids

Another method of transferring heat that may be useful in nuclear reactors is the use of boiling liquids. Within the reactor itself, such systems may be objectionable since they tend to cause an irregular variation in the average density of the coolant, and this variation will probably reflect on the nuclear reaction. On the other hand, it is an excellent method of obtaining very high rates of heat transfer. The heat transfer coefficient for boiling liquids over fairly large temperature regions increases almost proportional to the square of the temperature difference between the tube wall and the fluid. At high temperature differences, the coefficient reaches a maximum and then drops off if still higher temperature differences are employed. At very high temperature differences, it undoubtedly increases again. This drop in the heat transfer coefficient is due to the fact that the temperature of the tube wall becomes so hot that the liquid no longer wets the metal. It is a case similar to a drop of water on a hot stove. This temperature difference that gives the maximum heat transfer coefficient varies with the systems employed but is usually of the order of 40 to 80° F. At the maximum, water at atmospheric pressure has a heat transfer coefficient of about 10,000. Thus, a boiling liquid is an excellent method of obtaining a high heat transfer coefficient without the necessity of paying a high price for pumping costs.

. . . If a fluid of the right physical and nuclear characteristics could be found, and if the problem of variable density within the reactor could be overcome, boiling appears to be one of the desirable methods of removing the heat. In any case, it is likely that it may be desirable to use the heat of a nuclear reactor in a steam turbine power unit, in which case, heat transfer by boiling would be involved in the secondary heat exchanger if not within the reactor itself.

10-6 Condensation

Another type of heat transfer that would be associated with boiling is condensation. It is not likely that condensation will be important within the nuclear reactor itself, but it may be important in the external power cycles. In general, heat transfer coefficients for condensation are high, and the main resistance is the film of liquid that forms on the condenser surface. For example, in the case of water, if the water films on the wall, coefficients of the order of 1,000 to 3,000 are obtained. However, if the water is made to condense drop-wise, coefficients of the order of 10,000 to 30,000 are possible. In the case of water, it is possible to add agents which will make it condense drop-wise, but with a great many other liquids, suitable agents for the production of drop-wise condensation have not been found.

10-7 General Considerations

This section will consider the application of the various methods of heat transfer to nuclear reactors reviewed in Sections 10-1 through 10-6. The following criteria are considered to be important in the design of the system for heat removal:

1. Minimum interference with nuclear reactions
 - a. Minimum volumes required for heat removal (that is the volume of material required to remove the heat and which has no bearing on the operation of the pile should be kept to a minimum);
 - b. Minimum introduction of undesirable components (that is the amount of extraneous materials should be kept as small as possible);
2. Lower power requirements for removing heat
3. Engineering feasibility (This includes such factors as the stability of the fluid under temperature and radiation. For example, most of the organic liquids are unstable above a temperature of 350° C. While some

of the fluorine compounds are stable above this temperature, few, if any, of the organic compounds offer promise as coolants in nuclear reactors. Other factors are corrosion, temperature level of operation, and other radiation effects. In the following discussion only the first two factors will be considered.)

10-8 External Methods of Heat Removal

Radiation. The best arrangement to satisfy the criteria of Section 10-7 would be to have a heat removal system that would occupy zero volume within the reactor. We might have a system such as that shown schematically in Figure 10-1.

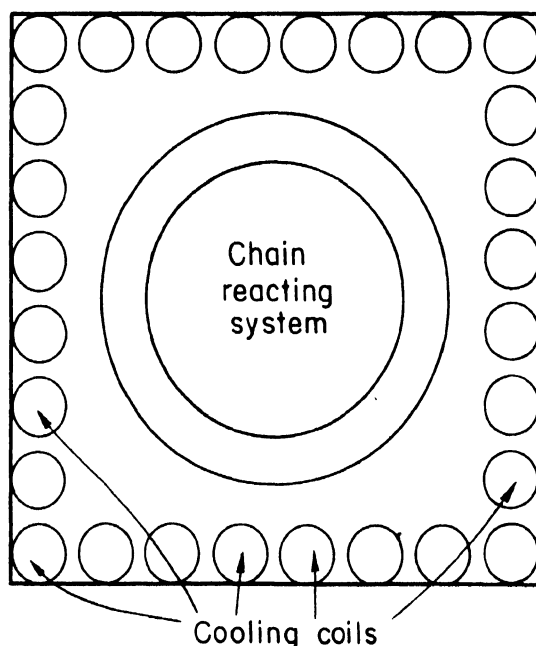


Figure 10-1. Heat Removal by Radiation

In order to obtain a concept of the problems involved in such a reactor, consider such a unit producing 10,000 horsepower, which corresponds to a heat production of approximately 100,000,000 Btu/hour when the efficiency of the heat cycle is included. Assuming that the average surface temperature of the cooling coil is 1400°R , what is the surface area of the radiating system as a function of the surface temperature necessary to transfer heat at this rate? Using the results given in the table of Section 10-3, the following values are calculated:

T_1 °R	1,500	2,500	3,500
Surface-ft ²	47,500	1,700	400
Diameter of Equivalent Sphere-Feet	120	23	11

Unless the temperature is very high, the radiating system will be very large and external surface radiation does not appear to be a desirable method of removing heat. In addition to the high surface temperature, there would be a very large temperature gradient through such a unit. Even if the average thermal conductivity of the solid sphere were as high as 100 Btu/hour/sq. ft/°F, the internal temperature drop would be several thousand degrees Fahrenheit.

Conduction. Another external method of removing heat would be to place the heat adsorbent surfaces in direct contact with the external surface of the reactor. This would of course eliminate the heat transfer resistance due to radiation. However, it would still require the very high temperature gradients within the reactor, and for most cases, these gradients are so great that this method does not appear practical.

External Heat Exchange. Another arrangement which could be employed to remove the heat without interfering with the reactor itself would be the use of a homogeneous reactor employing liquid media as was discussed in Section 9-8 (b). For example, a uranium salt could be dissolved in heavy water or uranium metal might be dissolved in one of the liquid metals. This active mixture would be circulated from the reactor through a heat exchanger and back to the reactor. In this case, the reactor itself is not altered to allow for heat removal, but there is a certain loss of delayed neutrons in the heat exchanger section which is not desirable. In order to minimize this loss, the most practical arrangement would be to make the volume of the active material in the heat exchanger as small as possible relative to that in the reactor. Thus, if the volume of the active liquid in the heat exchanger is kept down to 0.1 per cent of the volume of the liquid in the reactor, the neutron loss should not be over 0.1 per cent of the delayed

neutrons. It will probably be less than this value due to the fact that a considerable portion of the material will be returned to the reactor before the delayed neutrons are released.

The main problem in this liquid homogeneous reactor therefore is the volume of active fluid in the heat exchanger. In the following section, equations are developed for the relationship between the volume of the fluid in a heat exchanger and the dimensions of the exchanger, physical properties of the fluid, operating condition of the exchanger, and the power necessary for circulating the fluid through the exchanger. Equations (10-17) and (10-18) summarize these relationships for turbulent and streamline flow. For liquid reactants involving water or liquid metals, these equations indicate that it should be possible to design exchangers, for transferring 100,000,000 Btu/hour with a low power consumption, that have an active liquid volume of less than 0.1 cubic foot. It therefore appears feasible to keep the volume of liquid in the heat exchanger less than 0.1 per cent of the volume of the reactor. If suitable liquid mixtures can be developed for the nuclear reaction, this type of system appears very attractive.

10-9 Internal Methods of Heat Removal

In this method it will be assumed permissible to introduce some volume into the reactor for the purpose of heat removal. A variety of fluids might be used, and two flow conditions will be considered: (a) turbulent flow and (b) streamline flow.

10-10 Coolants

In considering the coolants irrespective of their nuclear properties, the two most important factors appear to be minimum power consumption and minimum volume required within the nuclear reactor for removing the heat. There are a large number of possible coolants, both gases and liquids. These would cover the various gases and vapors, water, organic liquids, molten salts, molten metals, etc. In order to attain a comparison of their heat-removing properties, it is instructive to study an idealized system. For example, consider a nuclear reactor in which the coolant flows through holes or tubes in the reactor and each stream of the fluid undergoes identical conditions. (This is undoubtedly not the case for a reactor with uniformly spaced passages

since the tubes near the wall probably receive less energy than those in the center.)

Heat Transfer and Energy Equations

In order to simplify the calculations and arrive at a useful working relationship, a number of assumptions will be made, but in no case do these appear to alter materially the picture. In the first place, it is assumed that the power required for pumping the fluid through the reactor can be calculated by:

$$(10-10) \quad W = \frac{V_c \Delta P}{J}$$

where W = the work required for pumping the fluid.

V_c = the volumetric flow rate of the fluid.

ΔP = the pressure drop of the fluid in passing through the reactor.

J = conversion factor.

This expression is correct when the fluid is incompressible and it should therefore be satisfactory for the liquids and for the case of gases when the pressure drop is small (in most cases, the feasible pressure drops with gases are small).

For turbulent flow, the pressure drop will be calculated by the Fanning equation and no allowances will be made for entrance or exit losses, or for changes in kinetic head of the fluid within the reactor. The Fanning equation is:

$$(10-11) \quad P = \frac{2fLu^2\rho}{gD}$$

where f = friction factor, and for the purposes of these calculations, is

$$\text{taken to be: } \frac{(0.046)}{\left(\frac{D\rho u}{\mu}\right)^{0.2}}$$

L = length of the fluid passage

u = average velocity of the fluid

ρ = average density of the fluid

g = conversion constant from pound mass to pound force

D = inside diameter of the passage

μ = viscosity of fluid

For viscous or streamline flow, ΔP will be calculated by Poiseuille's Law:

$$(10-12) \quad \Delta P = \frac{32L\mu}{g(D)^2}$$

The nomenclature is the same as in the Fanning equation. The volume of the reactor occupied by the coolant, V_h , is equal to $\frac{n\pi D^2 L}{4}$, where n is the number of passages.

The heat balance for the reactor (neglecting losses) is:

$$(10-13) \quad Q = wC_p \Delta T = V_c \rho C_p \Delta T$$

where Q = the rate of heat removal

w = the weight rate of flow of the coolant through the reactor

C_p = the heat capacity per unit weight of the coolant

ΔT = the temperature rise of the coolant in passing through the reactor

The rate of heat removal is also equal to the rate of heat transfer to the fluid. Thus:

$$(10-14) \quad Q = hA\Delta t = hn\pi DL\Delta t$$

where h = heat transfer coefficient

A = area for heat transfer

n = number of passages

Δt = average temperature difference between the tube wall and the bulk temperature of the coolant.

In order to evaluate the heat transfer coefficient, h , equations were taken from "Heat Transmission" by McAdams, and for flow inside tubes are:

For turbulent flow:

$$(10-15) \quad h = .023 \left(\frac{DG}{\mu} \right)^{0.8} \left(\frac{C_p \mu}{k} \right)^{0.4} \left(\frac{k}{D} \right)$$

For streamline flow:

$$(10-16) \quad h = 1.86 \frac{k}{D} \left[(DG/\mu) \left(\frac{C_p \mu}{k} \right) \left(\frac{D}{L} \right) \right]^{1/3}$$

where G = mass velocity = $u\rho$

k = thermal conductivity

These equations have been developed from experimental data on gases, water, and organic liquids. All of these materials have values of the Prandtl group, $C_p \mu/k$, from 0.6 up to several hundred. There may be some question in their use for liquid metals which have values of this group of the order of 0.01.

Combining Equations (10-10) through (10-16) and eliminating the variables that appear to be most dependent in the design of the unit (the elimination is somewhat arbitrary since the length was kept as an independent variable and the diameter was eliminated as a dependent variable), one obtains:

For turbulent flow:

$$(10-17) \quad \frac{W}{Q} = \left(\frac{1}{Jg} \right) \left(\frac{Q^2 L^2}{\Delta T^2 \Delta t V_h^2} \right) \left[\frac{\mu}{C_p^2 \rho^2 k \left(\frac{C_p \mu}{k} \right)^{0.4}} \right]$$

For streamline flow:

$$(10-18) \quad \frac{W}{Q} = \left(\frac{1.58}{Jg} \right) \left(\frac{Q^2 L^2}{\Delta T^{1.5} \Delta t^{1.5} V_h^2} \right) \left[\frac{\mu}{C_p^2 \rho^2 k} \right]$$

The above equations can be used in any set of consistent units. The left-hand side is a dimensionless energy ratio although the numerator is work energy and the denominator is heat energy. The following table lists suggested consistent units for each of the terms for both the engineer and the metric systems:

	<u>Engineering Units</u>	<u>Metric Units</u>
Q	Btu/hour	Cal/second
L	Feet	Centimeters
$\Delta T, \Delta t$	Degrees Fahrenheit	Degrees Centigrade
V_h	Cubic Feet	Cubic Centimeters
W	Btu/hour	Calories/second
μ	Lbs/ft/hour	Gms/cm/second (poise)
C_p	Btu/lb/°F	Cal/gm/°C
ρ	Lbs/cu.ft.	Gms/cu.cm.
k	Btu/hr-ft.°F	Cal/sec-cm.°C
J	778 ft.Lbs/Btu	$4.27 \times 10^4 \frac{\text{gm.cm.}}{\text{cal.}}$
g	$4.16 \times 10^8 \text{ft./hr}^2$	980cm/sec^2

It should be pointed out in using these equations that all the values of the physical constants should not be taken at the same temperature. The values of viscosity, heat capacity, and thermal conductivity were involved in the relationships pertinent to the reactor and should, therefore, be taken at some average values under the reactor conditions. One of the density terms relates to conditions within the reactor and the other relates to the density at the pump or compressor. Thus, the first should be evaluated at the reactor conditions and the second at pump conditions.

It will be noted that both of these equations consist of two main groups. The first group contains the rate of heat production, length of fluid passage, the volume of the reactor occupied by the heat transfer system and the two temperature differences. Thus, it is a design and operating variable group that can be altered by the choice of different combinations of the variables. The second group in both cases involves only the physical properties of the fluid and is therefore, chiefly, a function of the fluid, although to a minor extent it is a function of the operating conditions, since the physical properties may be a function of the temperature and pressures employed.

Physical Characteristics of Coolants. The desirability of a fluid for cooling a nuclear reactor from the heat viewpoint can be evaluated by this physical characteristics group. Since in general, it is desirable to

keep the power required at a minimum, and the volume of the heat transfer system at a minimum, small values of these groups are desired. Comparison for a number of the most common fluids is given in Tables 10-3, 10-4, 10-5.

In calculating the values given in Table 10-3 for the gases, the physical properties were taken at a temperature of 0° C and a pressure of one atmosphere.

In comparing the gases it is noted that there is a wide variation in the values, with hydrogen being the most desirable (lowest). The value of this physical characteristics group for gases can be approximated by considering the fact that the Prandtl group ($C_p \mu / k$), is essentially the same for all gases. Thus, for turbulent flow, the latter group becomes:

$$\frac{M \left(\frac{C_p \mu}{k} \right)^{0.6} R^2 T_p T_{av}}{(MC_p)^3 p^2}$$

and for viscous flow:

$$\frac{M \left(\frac{C_p \mu}{k} \right) R^2 T_p T_{av}}{(MC_p)^3 p^2}$$

where M = molecular weight of the gas

R = the gas constant

T_p = temperature of the gas at the pump condition

T_{av} = temperature of the gas under reactor conditions

p = absolute pressure

(MC_p) = molal heat capacity of the gas

Thus, for given conditions of temperature and pressure, the most important factor in determining the value of these groups for gases is the molecular weight divided by the cube of the molal heat capacity. High molal heat capacities are usually associated with complex molecules and for that reason some of the higher molecular weight gases appear more desirable than would be expected.

TABLE 10-3

Gases	Turbulent Flow	$\frac{x}{x_{H_2}}$	Streamline Flow	$\frac{x}{x_{H_2}}$
	$\frac{\mu}{c_p^{0.4} \rho^{0.4} k} = x$		$\frac{\mu}{c_p^{0.5} \rho^{0.5} k} = x$	
H ₂	652	1.0	576	1.0
D ₂	1,313	2.0	1,160	2.0
C ₂ H ₆	1,850	2.8	1,705	3.0
C ₂ H ₂	2,325	3.6	2,120	3.7
CCl ₃ F (Freon-11)	2,680	4.1	2,465	4.3
CH ₄	2,770	4.25	2,640	4.6
NH ₃	2,880	4.4	2,600	4.5
He	3,315	5.1	2,867	5.0
H ₂ O	5,040	7.7	5,425	9.4
CO ₂	6,560	10.1	6,115	10.6
H ₂ S	6,635	10.2	5,970	10.4
SO ₂	7,570	11.6	6,850	11.9
Air	8,150	12.5	7,190	12.5
N ₂	8,740	13.4	7,715	13.4
CO	9,030	13.8	8,150	14.1
NO	9,550	14.6	8,540	14.8
O ₂	9,600	14.7	8,490	14.7
HCl	11,540	17.7	10,200	17.7
Cl ₂	13,670	21.0	12,200	21.2
Xe	106,000	162.2	90,100	156.3
Hg	161,700	248.0	137,300	238.4

Since the average temperature of the reactor and the temperature at the pump will be above the 0°C assumed in calculating these groups, the values should be appropriately increased for actual calculations. The value of the Prandtl groups is essentially independent of temperature, but the molal heat capacity would be higher and should be evaluated at the average temperature of the reactor.

In comparing the values given in the table, it is noted that they do not follow the low molecular weight criterion and this is due to the fact that in many cases the effect of heat capacity offsets the molecular weight. H_2 , hydrogen and deuterium give low values of the physical property group as would be expected, but a more complicated structure such as ethane gives a surprisingly low value in spite of its high molecular weight. The same is true of Freon-11. Helium gives a surprisingly high value and this is due to the

TABLE 10-4

Liquids	Turbulent Flow	
	$\frac{\mu}{C_p^2 \rho^2 k \left(\frac{C_p \mu}{k}\right)^{0.4}} = x$	$\frac{x}{x_{\text{H}_2\text{O}}}$
H_2O	.0004425	1.0
*Na	.000877	2.0
*Sn	.00157	3.5
*Hg	.00335	7.6
*Bi	.0053	12.0
*Cd	.00583	13.2
$\text{NaNO}_2, \text{NaNO}_3, \text{KNO}_3$ (HTS)	.00628	14.2
*Pb	.00787	17.8
Acetic Acid	.00839	19.0
Glycol	.00919	20.8
CCl_2F_2 (Freon-12)	.00957	21.6
Aniline	.0157	35.5
Diphenyl	.0202	45.7
Naphthalene	.0286	64.6
Glycerol	.0398	90.0

*It is unlikely that the heat transfer equations used in these derivations can be used for correlating the behavior of liquid metals.

low molal heat capacity of the monatomic gas. It should be emphasized that this table has given no consideration to the nuclear characteristics or the chemical stability of the compounds under reactor conditions.

The table for the liquids gives the estimated values of the physical characteristics groups for several of the liquid metals, water, a few organic liquids, and one molten salt mixture. The physical properties of water were taken at 176° F, and moderately higher temperatures would give still lower values. However, temperatures approaching the critical cause the value of this group to decrease.

The available data on the physical properties of the liquid-metals are very limited. The values given in the tables are based on data from a number of different sources. In all cases, the temperatures were above the melting point of the metal, but frequently the physical properties employed for a given metal do not all correspond to a given temperature. Thus, the

TABLE 10-5

Liquids	Streamline Flow		
	$\frac{\mu}{c_p^2 \rho^2 k} = x$	$\frac{x}{x_{Na}}$	$\frac{x}{x_{H_2O}}$
*Na	.000136	1.0	0.2
*Sn	.000271	2.0	0.4
H ₂ O	.000612	4.5	1.0
*Hg	.00064	4.7	1.0
*Bi	.000929	6.8	1.5
*Cd	.000929	6.8	1.5
*Pb	.00149	11.0	2.4
NaNO ₂ , NaNO ₃ , KNO ₃ (HTS)	.01713	126.0	28.0
CCl ₂ F ₂ (Freon-12)	.01877	138.0	30.7
Acetic Acid	.0227	167.0	37.1
Aniline	.0646	475.0	105.0
Diphenyl	.0694	510.0	113.0
Glycol	.0696	512.0	114.0
Napthalene	.0996	732.0	163.0
Glycerol	.533	3920.0	871.0

*See Turbulent Flow

value of these groups is only approximate, but they should certainly be of the same order of magnitude and are probably within a factor of two of the true value.

The data on several of the organic liquids were likewise incomplete, and in these cases, values of the physical properties were estimated. In the case of the liquid salt mixture, data were available for all physical properties except thermal conductivity, which was estimated.

It will be noted that for turbulent flow, liquid water has the lowest value, but the use of water seriously limits the maximum temperature that can be employed in the reactor. Under these flow conditions, the liquid metals appear good, but it should be emphasized that the heat transfer equations employed have not been adequately tested for the liquid metals. In fact, the limited heat transfer data available for these metals indicate that the equations may give values several times the true values. If this is the case, the values for the liquid metals should be multiplied by five to ten, which greatly reduces their attractiveness. Whether this difference is due to the fact that the metals did not wet the tube wall in the experimental tests or whether it is an inherent characteristic of the metals, should be ascertained.

The organic liquids do not appear attractive from a heat transfer standpoint, and it is also likely that they are unattractive from thermal stability and nuclear viewpoints. The particular liquid-salt mixture given indicates that this type of fluid has reasonable attractive heat transfer characteristics. While this mixture may not be desirable for other reasons, it does indicate that other salt mixtures are worthy of consideration.

The values for the liquids in streamline flow are roughly in the same order as for turbulent flow except that water and the organic liquids appear less favorable relative to the liquid metals. In this case, the liquid metals should give values more in agreement with the heat transfer equations since they are based chiefly on conduction calculation.

In all the tables, a column is given comparing the value of the characteristic group for a substance to the lowest value for any substance in the table.

10-11 Design Variables

For a given fluid, the design variables can be altered to give the most desirable relationship. In general, the two most important considerations would be to have low values of the work, W , and low values of the volume of the reactor utilized for the removal of heat, V_h . (In examining the equation, it is obvious that these two considerations are contradictory and some type of balance must be made between them.) In general, for a given design, the value of the heat removed per unit time, Q , is fixed, and the designer therefore has only three variables that he can use to give low values of W and V_h , namely, the length of the heat transfer passage, the temperature rise of the fluid in passing through the reactor, and the temperature difference between the fluid and the reactor wall. Actually, the choice in the last two variables is not very great. The temperature rise of the fluid in passing through the reactor is defined by the characteristics of the power system utilizing the heat and by the maximum reactor temperature. The temperature difference between the wall and the fluid can be varied, but there are upper limits to this difference due to engineering factors. Thus, the main variable at the control of the design engineer is the length of the heat transfer passage and these equations would indicate that the shorter the length of the passage, the lower the value of the work and/or the volume occupied for heat transfer. It should be emphasized that when the length of the passage is varied for turbulent flow, the diameter of the passage is also varied to satisfy these relationships. The diameter can be calculated by the following equations obtained from Equations (10-14), (10-15), and (10-16):

For turbulent flow:

$$(10-19) \quad D^{1.2} = .092 \left(\frac{V_h^{0.2} L^{0.8} \Delta t}{Q^{0.2} \Delta T^{0.8}} \right) \left(\frac{k^{0.2}}{\left(\frac{C_p \mu}{k} \right)^{0.4}} \right)$$

For streamline flow:

$$(10-20) \quad D^4 = 412 \left(\frac{V_h^2 (\Delta t)^3 k^2}{Q^2 \Delta T} \right)$$

given by Section 10-10 would make the value of the characteristic group 12,600. Thus Equation (10-17a) reduces for these design conditions to:

$$\left(\frac{W}{Q}\right) = 4.8 \times \left(\frac{L^2}{V_h^2}\right)$$

The value of W is Btu/hour of work energy, while Q is Btu/hour of heat energy. Since it requires approximately 4 Btu's of heat energy for the cycle given to produce 1 Btu of work energy, using all of the power production as pressure drop in the reactor would correspond to a value of W/Q of .25. Practically, it would be undesirable to have a value of W/Q greater than .01, since there will be an approximately equivalent pumping loss through the helium-water exchanger and, correcting for the factor of 4 between heat and work, this would correspond to using about 8 per cent of the total energy produced for pumping the helium. Taking a value of W/Q of .01 gives $V_h^2 = 480 L^2$, or $V_h = 22 L$. If the heat transfer passages are made the length of the reactor namely, 10 feet, this would correspond to utilizing 220 cubic feet of the reactor volume for helium. This is probably excessive and some alternate method would have to be employed. The volume could be reduced by increasing the absolute pressure, which increases the density of the helium. For the conditions chosen, the value of V_h is inversely proportional to the pressure. Thus, a pressure of 10 atmospheres would reduce the volume of the helium within the reactor to 22 cubic feet.

Another method of reducing the volume of the helium within the reactor would be to use heat transfer passages shorter than 10 feet, and the volume required is directly proportional to the length of the passages. Thus, it would be ideal to use rather short passages except for the difficulty of arranging suitable manifolds and headers. In fact, the disadvantages of introducing such headers would probably be so great that it is doubtful whether passages any shorter than 5 feet would be desirable.

If some of the other gases, with lower values of the physical characteristic group, such as D_2 , were employed, it would allow slightly lower power and volume requirements. However, none of the gases have low enough values of the physical characteristic groups to make the problem of heat removal easy.

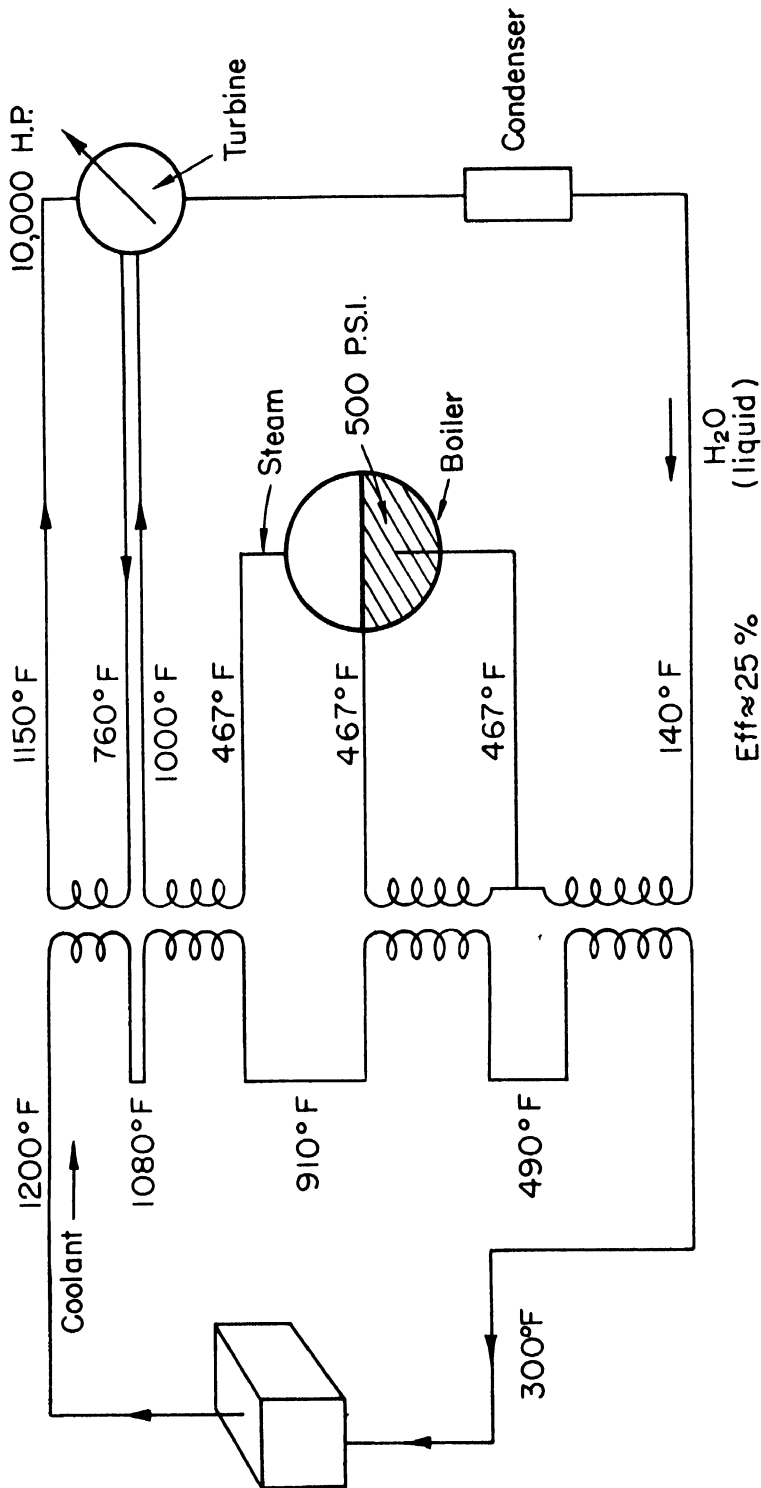


Figure 10-2
Illustrative power cycle

given by Section 10-10 would make the value of the characteristic group 12,600. Thus Equation (10-17a) reduces for these design conditions to:

$$\left(\frac{W}{Q}\right) = 4.8 \times \left(\frac{L^2}{V_h^2}\right)$$

The value of W is Btu/hour of work energy, while Q is Btu/hour of heat energy. Since it requires approximately 4 Btu's of heat energy for the cycle given to produce 1 Btu of work energy, using all of the power production as pressure drop in the reactor would correspond to a value of W/Q of .25. Practically, it would be undesirable to have a value of W/Q greater than .01, since there will be an approximately equivalent pumping loss through the helium-water exchanger and, correcting for the factor of 4 between heat and work, this would correspond to using about 8 per cent of the total energy produced for pumping the helium. Taking a value of W/Q of .01 gives $V_h^2 = 480 L^2$, or $V_h = 22 L$. If the heat transfer passages are made the length of the reactor namely, 10 feet, this would correspond to utilizing 220 cubic feet of the reactor volume for helium. This is probably excessive and some alternate method would have to be employed. The volume could be reduced by increasing the absolute pressure, which increases the density of the helium. For the conditions chosen, the value of V_h is inversely proportional to the pressure. Thus, a pressure of 10 atmospheres would reduce the volume of the helium within the reactor to 22 cubic feet.

Another method of reducing the volume of the helium within the reactor would be to use heat transfer passages shorter than 10 feet, and the volume required is directly proportional to the length of the passages. Thus, it would be ideal to use rather short passages except for the difficulty of arranging suitable manifolds and headers. In fact, the disadvantages of introducing such headers would probably be so great that it is doubtful whether passages any shorter than 5 feet would be desirable.

If some of the other gases, with lower values of the physical characteristic group, such as D_2 , were employed, it would allow slightly lower power and volume requirements. However, none of the gases have low enough values of the physical characteristic groups to make the problem of heat removal easy.

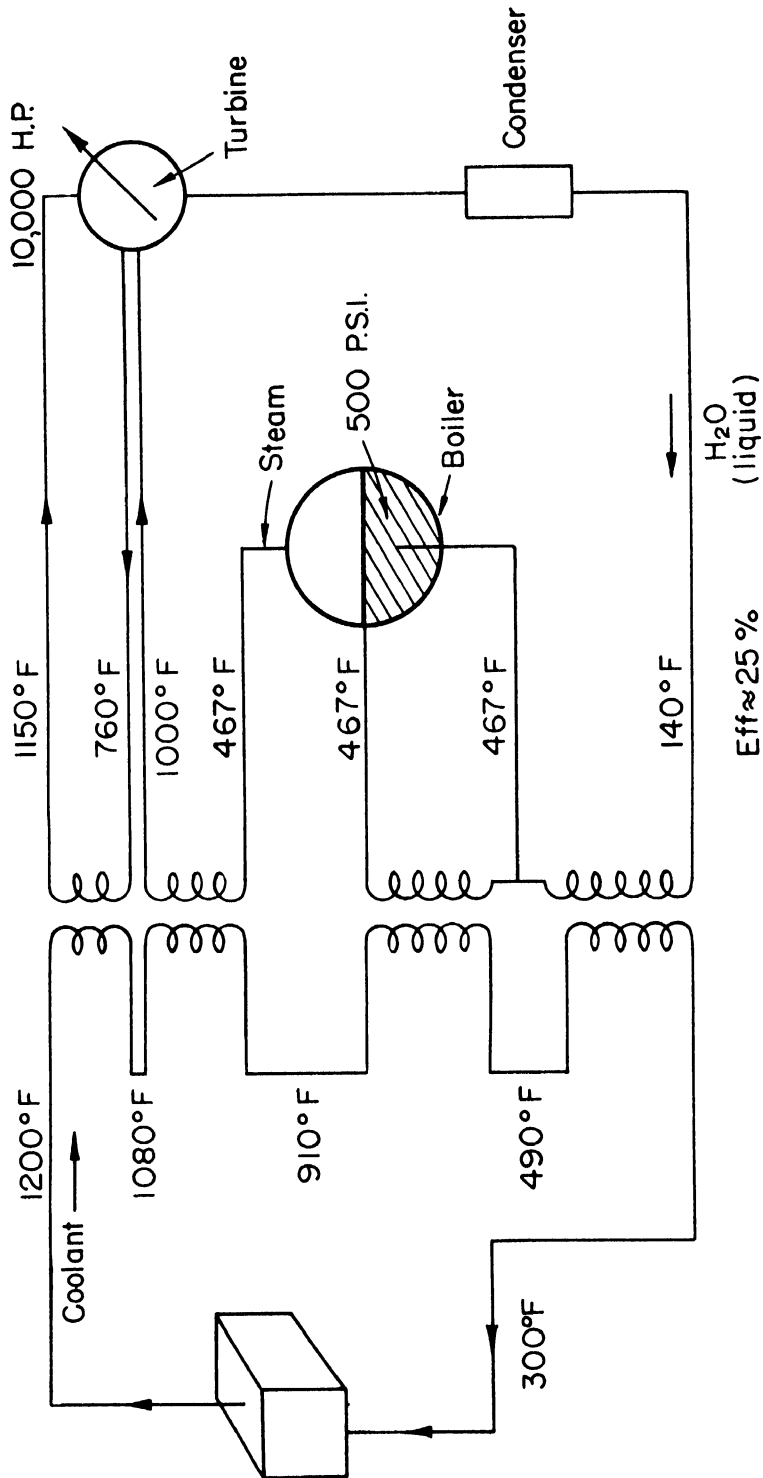


Figure 10-2
Illustrative power cycle

In fact, for reactors producing more energy per unit volume than the example considered here, the problem of using gases becomes very difficult.

Water Cooling. In this case, a water-cooled reactor will be considered in which liquid water will be circulated through the reactor under pressure and will be heated from 200° to 600° F. The other design conditions will be the same as before. For this case, Equation (10-17) becomes:

$$\left(\frac{W}{Q}\right) = 19.2 \times 10^{-4} \left(\frac{L^2}{V_h^2}\right) \left(\frac{\mu}{C_p^2 \rho^2 k \left(\frac{C\mu}{k}\right)^{0.4}}\right)$$

Using the value of the physical characteristics group given in Table 10-4 of 0.00044 without any corrections for temperature level, and using a length of heat transfer passage of 10 feet, gives:

$$\left(\frac{W}{Q}\right) = \frac{0.000084}{V_h^2}$$

In this case, very low values of W/Q and V_h are possible. For example, reducing the value of W/Q to 0.001, which would correspond to less than one per cent of the power for pumping, gives a value of V_h of less than 0.3 cubic feet.

CHAPTER 11

HEAVY ELEMENTS AND NUCLEAR FUELS

by

John W. Irvine, Jr.

Basic Chemistry of the Heavy Elements

11-1 Introduction

Heavy elements are defined for the purpose of this discussion as those elements whose atomic number is greater than 88. These are actinium, thorium, protoactinium, uranium, and the newly created transuranic elements neptunium, plutonium, americium and curium.

Before 1940 only thorium and uranium were of any commercial significance and the elements above uranium were unknown. Thorium has been used in Welsbach mantles since 1885 and much more recently as a catalyst and as an activating agent in tungsten filaments. Uranium has been used to a very limited extent in certain alloy steels and as a pigment in some yellow ceramic glazes and glass. As a result of the increased interest in radio-chemical and nuclear research, protoactinium is now available in quantities of a few grams at a price of about \$5,000 per gram.

The current interest in these heavy elements is due to the fact that the three known nuclear fuels are in this group. Also, four of the elements do not occur naturally and studies of their chemical and physical properties lead to a better understanding of the structure of matter.

11-2 Sources of the Heavy Elements

Figure 11-1 shows all of the isotopes of the heavy elements as they appear in the open literature.

The first element, actinium, has two isotopes. The principal one is Ac^{227} for which the element is named. It is a member of the naturally occurring $4n + 3$ radioactive series whose parent isotope is U^{235} . Normally, it is available in tracer amounts only.

Thorium is shown with seven isotopes of which Th^{232} is the common one, available in ton quantities. This isotope is the parent of the naturally occurring radioactive series, the thorium series, which is characterized by the mass relation $4n$. Th^{232} is the isotope from which U^{233} is synthesized by neutrons from a primary nuclear reactor. The first step of the synthesis is $\text{Th}^{232} (n, \gamma) \text{Th}^{233}$. The product isotope is a β -emitter decaying with a half-life of 23 minutes to Pa^{233} .

The next element, protoactinium, is named from its principal isotope Pa^{231} . This isotope was formerly known in milligram amounts but has recently

been made available in gram quantities. It is also a descendant of U^{235} and is the immediate parent of Ac^{227} . The 27-day Pa^{233} is important as an intermediate in the synthesis of U^{233} from Th^{232} .

Uranium has six isotopes, three of which occur naturally. Of these U^{238} is the most abundant and is the starting point in the synthesis of Pu^{239} by an $(n\gamma)$ reaction to give the β -active isotope U^{239} . Uranium (238) is the parent of the $4n + 2$ disintegration series, the uranium or radium series. Uranium (234) is an intermediate member of this series. Nuclear chain reactions are possible only because of the natural occurrence of U^{235} . This isotope is the primary nuclear fuel. In addition, it is the parent of the actinium series already mentioned. Uranium (233) is a secondary nuclear fuel synthesized from neutron capture by Th^{232} followed by two β -decay steps.

The first transuranic element to be discovered was neptunium. In Figure 11-1 are listed six isotopes of this element which are now known. In 1940, McMillan and Abelson identified the 2.3 day activity, which appears when uranium is bombarded with neutrons, as an isotope of element 93. Its mass number (239) was established by demonstrating its growth from the 23-minute isotope of uranium, U^{239} . Subsequently, Np^{237} was discovered and this isotope has been isolated from neutron reactor sources in quantities the order of 100 mg. It is formed by β -decay of U^{237} , which is the product of the reaction $U^{238}(n, 2n)$. The yield in nuclear reactors is approximately 0.1% that of Pu^{239} . In general, the isolation of macroscopic amounts of a radioactive isotope is contingent on that isotope having a relatively long half-life, the order of years at least.

Following the recognition of neptunium, plutonium was discovered in uranium sources bombarded with deuterons. In this manner Np^{238} was synthesized by a $(d, 2n)$ reaction on U^{238} and the 50-year Pu^{238} grown from it by β -decay. After the chemical properties of plutonium were established, using Pu^{238} as a tracer, Pu^{239} was isolated from solutions containing Np^{239} . This isotope, Pu^{239} , is the third nuclear fuel.

Americium, the third transuranic element, is made by bombardment of uranium and plutonium with helium ions of 44 Mev. The isotope Am^{241} has been isolated and studied in microgram quantities.

Curium, which has an atomic number of 96, the highest known, is made by helium ion bombardment of plutonium. It is known only in tracer quantities,

but its chemical properties have been well established by standard radiochemical techniques.

Since macroscopic quantities (micrograms) of Am^{241} have been isolated, there is a possibility of producing element 97 by helium ion bombardment. Whether elements with still higher atomic number can be produced is an unanswerable question at this time.

11-3 Tracer Chemical Methods

Prior to the discovery of radioactivity, two of the eight heavy elements were known as ordinary chemical elements. Uranium had been discovered by Klaproth in 1789 and thorium by Berzelius in 1829, and by the use of normal chemical methods, the properties of these elements were fairly well established.

The work of the Curies on polonium and radium established the principles of radiochemical tracing techniques. The ionizing power of the radiations from radioactive isotopes makes possible quantitative measurement of those isotopes at concentrations of 10^{-8} to 10^{-20} molar. By the use of these methods, Debierne and Giesel discovered and worked out the chemical properties of actinium in 1899. Hahn and Meitner discovered protoactinium through radiochemical studies in 1917, and from the knowledge of the chemical properties thus gained, Grosse was able to isolate a few milligrams of the element in 1927.

The validity of radiochemical studies at tracer concentrations is clearly shown by the successful design of the Hanford plutonium separation plants. These plants were designed to carry out a separation process for an element which had never been seen, and which did not occur naturally in the earth's crust. Before construction was completed, the process had been verified on an ultramicrochemical scale and later on a gram scale, but the original designs were substantially correct. This was a scale-up factor of about 10^{10} . Methods of such power deserve a more careful study.

At tracer concentrations, precipitates cannot ordinarily be formed because the concentration of the trace ions will not exceed the equilibrium concentration for the precipitate desired. In this case, solubilities can be determined approximately by co-precipitation methods. For example, U^{+4} forms an insoluble precipitate with F^- , UF_4 . If the concentration of U^{+4} is

smaller than its equilibrium value, it can be removed quantitatively by precipitating macroscopic amounts of a fluoride such as ThF_4 , or LaF_3 . The U^{+4} is carried as a solid solution in the precipitate. On the other hand, U^{+6} exists in solution as the uranyl ion UO_2^{++} . Uranyl fluoride is soluble. If the same insoluble fluorides are precipitated in the presence of UO_2^{++} the uranium remains in solution. Studies of an element, such as uranium, whose chemical properties are known, serve to establish the laws governing reactions at tracer concentrations.

To illustrate in more detail the working of the method, some of the experiments with neptunium and plutonium are described in the following paragraphs.

In the case of element 93, neptunium, an activity with a 2.3-day half-life, was found in uranium irradiated with neutrons. After removal of the fission products, it was found that this activity precipitated quantitatively with CeF_3 from an acid solution which had been treated with a reducing agent, SO_2 . When a strong oxidizing agent, HBrO_3 , was present, the activity did not precipitate with the CeF_3 . If $\text{NaUO}_2(\text{C}_2\text{H}_3\text{O}_2)_3$ was precipitated, the activity did not follow the uranium from the reduced solution but did follow it from the oxidized solution. From this evidence, it can be concluded that neptunium has at least two oxidation states and that in the higher state the neptunium probably has an oxidation number of +6 and exists as the ion, NpO_2^{++} . This conclusion is based on the fact that the formation of $\text{NaUO}_2(\text{C}_2\text{H}_3\text{O}_2)_3$ is a highly selective reaction for UO_2^{++} . In the lower oxidation state, the neptunium might be Np^{+2} , Np^{+3} or Np^{+4} , since these simple ions would be expected to co-precipitate with the insoluble CeF_3 . Further tests established that the activity co-precipitated with $\text{Th}(\text{IO}_3)_4$. Since this behaviour is characteristic of +4 ions, the neptunium must have been present as Np^{+4} . If a reducing agent stronger ^{than} SO_2 is used, for example metallic zinc, the neptunium activity does not co-precipitate with the iodates but does follow LaF_3 quantitatively. Thus, an oxidation state of +3 can be established. Similar experiments have established the existence of a +5 oxidation state.

The chemistry of plutonium was worked out in a similar manner using the 50-year α -active plutonium isotope, Pu^{238} . The behaviour of plutonium in reduced solutions was similar to that of neptunium, except that with

plutonium the +3 state was more stable relative to the +4 state. In HBrO_3 solutions, however, the plutonium did not behave as though it was present as PuO_2^{++} . The activity followed the fluoride precipitates rather than the $\text{NaUO}_2(\text{C}_2\text{H}_3\text{O}_2)_3$ precipitate. When a stronger oxidizing agent was used, the plutonium activity then behaved in the same manner as the neptunium activity. Thus acid solutions of persulfate ($\text{S}_2\text{O}_8^{=}$) with Ag^+ as catalyst, oxidize plutonium to PuO_2^{++} . Since the standard oxidation-reduction potential for the couple $\text{SO}_4^{=}\parallel\text{S}_2\text{O}_8^{=}$ is -2.05 v, and for the $\text{Br}^-\parallel\text{BrO}_3^-$ couple is -1.42 v, the oxidation-reduction potential for the $\text{Pu}^{+4}\parallel\text{PuO}_2^{++}$ couple must fall between these limits.

By experiments of this type, the chemical properties of all the heavy elements, except thorium and uranium, were first worked out. From such information, it has been possible to demonstrate the presence of plutonium in pitchblende and carnotite in concentrations of about 10^{-14} g Pu/gU. This would have been impossible to detect if the chemical properties had not first been worked out on a tracer scale. (The presence of Pu^{239} in U ores is attributed to neutrons from the spontaneous fission of U^{238} , $T_{1/2} = 10^{16}$ years.)

11-4 The Heavy Elements and the Periodic Table

Before the discovery of the transuranic elements the position of the heavy elements in the periodic table had not been seriously questioned. The possibility of a second rare earth-like transition group was anticipated but the chemical properties of the heaviest members of the periodic table did not indicate where such a transition might start.

In Figure 11-2 the position of actinium in Group IIIa is in strict accord with its chemical properties. Like other members of the group, it is exclusively tri-positive, forms an insoluble fluoride, and it is a slightly stronger base than its lower homologue, lanthanum.

Likewise, thorium belongs in Group IVa. It differs from hafnium and zirconium in having no lower oxidation states, and it has no acidic properties.

Protoactinium is definitely a homologue of tantalum. Its chemistry is almost exactly as might be predicted from its position in the table. Its oxide Pa_2O_5 is slightly more basic than Ta_2O_5 and it forms similar complex fluorides.

With uranium, deviations from expected properties are observed, but in the absence of elements beyond uranium it is not possible to determine

[illegible]

The atomic weights are on the chemical scale; i.e. (normal isotopic mixture of oxygen)=16.000

Figure 11-2
Periodic Table of the Elements

140.13	140.92	144.27	(147)	150.43	152.0	156.9	159.2	162.46	164.94	167.2	169.4	173.04	174.99	* <u>Rare Earth Elements</u>
Ce	Pr	Nd	Pm	Sm	Eu	Gd	Tb	Dy	Ho	Er	Tm	Yb	Lu	
58	59	60	61	62	63	64	65	66	67	68	69	70	71	

the significance of the deviations. The lower oxidation states of uranium are better characterized than those of tungsten. In the +6 oxidation state uranium forms two series of compounds of the basic UO_2^{++} ion and the polymeric acidic group $(\text{U}_n\text{O}_{3n+1})^=$. The latter resembles tungsten in some respects, but the uranyl ion is unique.

The first conclusive evidence that a new transition group was in the making came with the discovery of neptunium. Here, there is a definite break in the homologous series of Group VIIa. As previously noted, the chemical properties of neptunium show a very strong resemblance to those of uranium. If the chemical properties of neptunium resembled those of rhenium it would have formed a stable anion in the +7 state, formed an insoluble sulfide in strongly acid solutions and been readily reduced to the metal by zinc. None of these properties are attributable to neptunium. This indicates a departure from the expected regular addition of electrons in 7p shell.

The chemistry of plutonium confirms the observations on neptunium. The oxidation states and their chemical properties show strong uranium-like properties, but with an increasing tendency to form stable lower oxidation states.

Americium and curium have added their evidence towards the presence of a rare earth-like transition group starting in the heavy elements. The former exists largely in the +3 oxidation state with a +4 state questionable, while the latter exists exclusively as Cm^{+3} insofar as can be determined by tracer methods.

Table 11-1 and Table 11-2 summarize the relationships between the oxidation states of the heavy elements and show some of the chemical properties characteristic of the four oxidation states exhibited by these elements.

11-5 Heavy Element Transition Group

In the rare-earth transition group, inner orbitals are filled as the atomic number increases. After xenon with its completed 5p shell the electrons go to the 6s shell in cesium and barium. The next electron does not go to the 6p shell but drops back to the 5d in lanthanum and then to 4f in cerium. The more or less regular filling of the 4f shell is characteristic of the rare-earth transition until lutecium is reached, when the 4f shell is complete with fourteen electrons (see Table 11-3). This group of elements, sometimes called the lanthanide series, is known for the great similarity of the chemical properties of the elements and the high stability of its +3 oxidation state.

TABLE 11-1

PRINCIPAL OXIDATION STATES OF THE HEAVY METALS

		III	IV	V	VI
89	Ac	a*	-	-	-
90	Th	-	a	-	-
91	Pa	-	-	a	-
92	U	c	b	?	a
93	Np	c	ab	d	ab
94	Pu	c	a	d	b
95	Am	a	?	-	-
96	Cm	a	-	-	-

*a > b > c > d = decreasing order of stability of oxidation state in aqueous solution. (?) = existence uncertain (-) = not known in solution.

TABLE 11-2CHARACTERISTIC CHEMICAL PROPERTIES OF THE
PRINCIPAL OXIDATION STATES OF THE HEAVY ELEMENTS

		III	IV	V	VI
F^-		i*	i	s	s
IO_3^-		s	i	h	s
OH^-		i	i	i	$M_2X_2O_7(i)$
H^+		X^{+++}	X^{++++}	i	XO_2^{++}

*i = insoluble

s = soluble

h = completely hydrolyzed

TABLE 11-3

ELECTRONIC CONFIGURATION OF THE RARE-EARTH ELEMENTS

	K 1s	L 2s 2p	M 3s 3p 3d	N 4s 4p 4d 4f	O 5s 5p 5d 5f	P 6s 6p 6d	Q 7s 7p
Xe 54	2	2 6	2 6 10	2 6 10	2 6		
Cs 55						1	
Ba 56						2	
La 57	54 Xenon Core					2	
Ce 58					1	2	
Pr 59					1	2	
Nd 60						2	
Pm 61					(5)	2)	
Sm 62					6	2	
Eu 63					7	2	
Gd 64					7	1 2	
Tb 65					8	1 2	
Dy 66					10	2	
Ho 67					11	2	
Er 68					12	2	
Tm 69					13	2	
Yb 70					14	2	
Lu 71					14	1 2	

TABLE 11-4

POSSIBLE ELECTRONIC CONFIGURATION OF THE HEAVY ELEMENTS

	K 1s	L 2s 2p	M 3s 3p 3d	N 4s 4p 4d 4f	O 5s 5p 5d 5f	P 6s 6p 6d	Q 7s 7p
Rn 86	2	2 6	2 6 10	2 6 10 14	2 6 10	2 6	
At 87							1
Ra 88							2
Ac 89	86 Radon Core					1	2
Th 90						2	2
Pa 91						3	2
U 92						4?	2?
Np 93					1?	4?	2?
Pu 94					2?	4?	2?
Am 95					5?	2?	2?
Cm 96					7	1	2
Nt 118	2	2 6	2 6 10	2 6 10 14	2 6 10 14	2 6 10	2 6

G. T. Seaborg has suggested that the heavy element transition series is analogous to the lanthanide series and has proposed the name of actinide series for this transition. Here the 7s shell is filled at radium (see Table 11-4), and by analogy the next electron would drop back to the 6d or 5f shell. Subsequent electrons go to the 5f shell until the very stable configuration of 7-5f electrons is reached at curium. This would correspond to gadolinium in the lanthanide series. The failure of all of the members of the actinide series to exhibit pronounced and characteristic +3 oxidation states had been explained on the basis of small energy differences between the different levels being influenced by the energy of compound formation.

C. D. Coryell has suggested an alternative scheme in which the heavy element transition group is not a pure 5f transition but is a mixed 5f and 6d transition. Table 11-4 shows a possible arrangement of electrons on the basis of this hypothesis. This arrangement has the merit of explaining the chemical properties of elements 90 to 94 more satisfactorily than does Seaborg's.

Both suggestions are based largely on chemical evidence which is not sufficiently strong to make unequivocal assignments of electron configurations. The answer must await careful analysis of spectrographic data where such analysis is extremely difficult.

The time has not yet come when "The End" can be put on the periodic table of the elements. With macroscopic amounts of americium available it should be possible to make element 97 by helium ion bombardment. If some long-lived isotope of curium can be synthesized and isolated, another step up to 98 is possible. However, it seems reasonable to conclude that the effects of the law of diminishing returns are being felt in the efforts to extend our knowledge of the heaviest of the heavy elements.

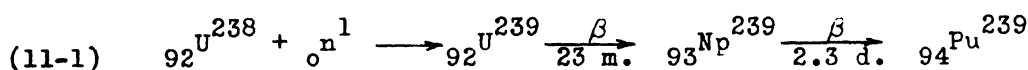
Technology of Nuclear Fuels

1-6 Introduction

Uranium (235) is the primary nuclear fuel. Of all the isotopes occurring in nature, this one is unique in that it undergoes fission with slow neutrons and in the fission process liberates more than one secondary neutron. By virtue of this property, it is possible to have a chain-reacting

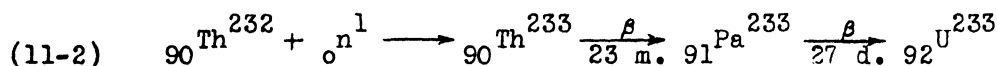
system. The number of fission neutrons in excess of the one necessary to maintain the chain reaction is approximately 1.3 per fission. These excess neutrons can be utilized to create new isotopes, at least two of which also undergo fission with slow neutrons and can be used as secondary nuclear fuels.

Plutonium (239) is the first of the secondary nuclear fuels. When U^{238} is present in a primary nuclear reactor, a large fraction of the excess neutrons is absorbed in the reaction $U^{238}(n, \gamma)U^{239}$. The product of this reaction then goes through two beta decay steps to form Pu^{239} . The process can be summarized by the nuclear equation:



The product of this series of reactions is not stable, but undergoes alpha-decay with a half-life of 2.4×10^4 years. However, because the half-life is so long, it is possible to make and separate this secondary fuel in kilogram quantities when a primary nuclear reactor is available.

The other secondary nuclear fuel is U^{233} . This isotope is made when Th^{232} is incorporated into a primary nuclear reactor. The series of reactions leading to its formation is:



Like Pu^{239} , the product U^{233} is not stable but decays by alpha emission with a half-life of about 1.6×10^5 years, which is sufficiently long to allow the preparation of large amounts of the isotope.

Although no technical information on the details of manufacturing or processing of U^{233} has been released, it has been noted that it undergoes fission with slow neutrons and is a potential nuclear fuel. This is particularly important since thorium from which it is made is more abundant than uranium. In the interest of economy of our nuclear fuel resources, it will undoubtedly receive more attention in the future. For this reason it has been discussed on the same basis as Pu^{239} .

11-7 Basic Problems in the Preparation of Nuclear Fuels

In order to operate a compact stationary or mobile chain-reacting unit for the production of power, it is necessary to have the nuclear fuel

highly concentrated. If the power reactor is to operate efficiently, the fuel and materials of construction must be free of isotopes which have high neutron absorption cross-sections.

The preparation of each of the nuclear fuels in a pure form presents individual problems. Uranium (235) occurs at a concentration of 0.72 per cent in the normal isotopic mixture of uranium. Thus, the problem of separating U^{235} is one of removing a large amount of the isotope U^{238} . In the production of Pu^{239} the concentration of the isotope is very small in the uranium delivered from the primary reactor, and the presence of a tremendous amount of radioactivity from the fission products makes the isolation difficult and hazardous. Uranium (233) will be present in concentrations of only a few grams per ton of Th after irradiation. Consequently, it is necessary to reduce the uranium to less than 10^{-6} gU/gTh before irradiation, so that the final product will not be contaminated with natural uranium.

It is evident that the basic problems involved in isolating pure nuclear fuels fall into two classes. The first is a problem of isotope separation, U^{235} from U^{238} , which is best attacked by physical methods, and the second is the separation of low concentrations of one element from high concentrations of other elements. The second problem is best carried out through the use of chemical techniques. In addition to these two main problems, there is a host of auxiliary problems, the solutions of which are necessary to achieve the desired goal.

Before going into the unit operations of nuclear fuel technology, It will be well to mention briefly the general methods of physical and chemical separation processes.

11-8 Physical Separation Processes

The methods developed for the separation of the isotopes of uranium are based largely on the difference in mass of the nuclei U^{235} and U^{238} . (Although U^{234} is normally present at a concentration of 0.0052 per cent, it will not be considered here.) Other methods based on chemical reactivity, such as electrolysis of solutions and chemical exchange reactions, have been used successfully with light elements, but they are not satisfactory for separating the isotopes of the heavy elements.

Four methods that have been investigated sufficiently to demonstrate their feasibility are: gaseous diffusion, thermal diffusion, electromagnetic,

and centrifugal. The first three have been carried through to full-scale plant operation, while the centrifugal method was carried through the pilot plant stage before being dropped.

In the gaseous diffusion separation process, a volatile compound of uranium is allowed to diffuse at reduced pressure through a porous barrier. Because the lighter isotope diffuses more rapidly than the heavier one, it is concentrated in the gas passing through the barrier. The only uranium compound whose physical properties are satisfactory for gaseous diffusion is uranium hexafluoride, UF_6 . This compound has a vapor pressure of one atmosphere at 56°C .

This method of isotope separation gives small separation factors but is well adapted for setting up in cascade operation. Thus, a high over-all separation factor can be obtained. The amount of UF_6 tied up in the system is very high when at equilibrium operation. Also, the length of time necessary to reach equilibrium is great. In spite of these limitations, a large plant has been constructed and operated at better than expected performance.

Thermal diffusion separation of the isotopes of uranium is effected by using liquid UF_6 under pressure between two surfaces, one hot and one cold. Due to the difference in mass of the uranium isotopes, and to complicated intermolecular forces, a separation of the isotopes occur. Because of the relative simplicity of construction and operation of equipment for this method, it was used before completion of the gaseous diffusion plant to furnish enriched feed to the electromagnetic separation plant. Like the gaseous diffusion process, thermal diffusion gives small separation factors per unit but can be run in cascade to give any enrichment desired. One serious drawback to the method is a large power consumption.

The electromagnetic separation plant was the first to achieve large-scale separation of the uranium isotopes. This method differs from the other two methods in giving a very high separation factor in each unit. This factor approaches 100 per cent, but the through-put per unit is small. Total production can be increased linearly by increasing the number of units and increasing the concentration of U^{235} in the feed material. The method depends on the fact that two gaseous ions having the same energy but different masses will be focussed at different points in a plane when the ions traverse a uniform magnetic field perpendicular to their path. By arranging an ion

source at the center of a uniform magnetic field so that several ion beams come out in different directions, efficient use can be made of large magnets. The collectors are so arranged that they intercept each beam and collect the two main isotopes, U^{238} and U^{235} , in a state of high isotopic purity.

The centrifugal method of separation of isotopes depends on the difference of mass of the isotopes. The feasibility of this method was demonstrated in pilot plant operation but the method never reached full-scale operation.

Other methods of isotope separation, such as distillation, exchange reactions, and electrolysis, are not well suited for use with the heavy elements.

11-9 Chemical Separation Process

One of the most fundamental chemical operations is precipitation of an insoluble compound from solution. Because of the low concentration of Pu^{239} in the irradiated uranium and of U^{233} in the irradiated thorium, this process is not directly adaptable to the raw material at hand. Although the term "insoluble" is widely used, it is only a comparative term. Every substance has a finite solubility and the concentration of the elements here desired is so low that the solubility product of their compounds would not normally be exceeded. In order to use a precipitation process, it is necessary to take advantage of the property of co-precipitation described in Section 11-3.

Other chemical separation processes less generally used are solvent extraction, ion exchange, and volatilization. Distillation of liquids is not feasible in this case.

Solvent extraction operates on the principle that a compound has different solubilities in two immiscible liquids. Consequently, when the compound is present in the two-solvent system, it is distributed between the two phases in the ratio of its solubility in each phase.

Some simple ionic compounds, particularly the chlorides, nitrates, and thiocyanates, are soluble in organic solvents of the ether, ester, and alcohol types. In such cases that the distribution ratio is favorable, these compounds can be extracted from aqueous solutions with a suitable organic solvent. For example, uranyl nitrate can be extracted into diethyl ether. The solubility in the ether phase can be increased by adding a "salting out"

agent such as ammonium nitrate. These agents decrease the solubility of the uranyl nitrate in the aqueous phase and consequently make the distribution ratio ($C_{\text{ether}}/C_{\text{aqueous}}$) larger, since the ammonium nitrate is not very soluble in the ether. Another well known example is the extraction of ferric chloride from strong hydrochloric acid solutions with diethyl or diisopropyl ether.

Grahame and Seaborg have shown that in the case of GaCl_3 , the distribution ratio between hydrochloric acid and diethyl ether is independent of the total concentration between the limits of 10^{-1} M and 10^{-14} M. They also have shown that FeCl_3 can be quantitatively extracted from 10^8 times as much MnCl_2 or CoCl_2 .

While the examples just cited supposedly involve simple ionic compounds, the extractability into an organic solvent may well be due to some unidentified coordination compound with the solvent. The solvent extraction method can be greatly extended by first introducing into the aqueous phase some organic material that selectively forms definite coordination compounds with the element to be extracted. Thus, small quantities of zinc and lead can be extracted into chloroform or carbon tetrachloride if "Dithizon" (diphenylthiocarbazone) is introduced as a complexing agent. This type of solvent extraction has not been fully explored either on a laboratory scale or on a plant scale of operation. It definitely deserves more attention because of the highly selective nature of some complexing agents. The scope of suitable solvents is enlarged by this method to include halogenated solvents and hydrocarbons.

Ion exchange resins have been defined as porous salts containing an insoluble anion and exchangeable cations. Certain resins contain active sulfonic acid and phenolic groups that are capable of forming salts with metallic ions. When the cations are fixed in the resin, advantage can be taken of the differences in the ratios of the equilibrium constants for the reaction between two or more cations and the resin, and the cations and a complexing agent to effect a separation of the cations. Thus, on a gram scale, separations of praseodymium and neodymium are readily made. These rare-earths are usually separated by laborious fractional crystallization, taking weeks of work. Using ion exchange resins, a 50-50 mixture of Pr^{+++} and Nd^{+++} can be made to yield 22 per cent of the Nd^{+++} spectroscopically

pure, and 50 per cent of the Nd^{+++} with a purity > 98 per cent in a single pass through a six-foot column over a period of three to four days. These resins are even better adapted to separation of trace elements. Their use also deserves much more extensive study.

Both of these general chemical methods of separating elements must be given serious consideration in nuclear fuel processing. They can be made highly selective in their action and, because of the simplicity of equipment, they are both well adapted to the type of remote control necessary in handling highly active radioactive sources.

Volatilization of solids at elevated temperatures and electrochemical methods do not appear too promising in the separation of nuclear fuels.

11-10 Technology of Nuclear Fuels

Figure 11-3 is a schematic representation of the basic operations necessary for the isolation of pure U^{235} , Pu^{239} , and U^{233} . The flow sheet is broken down into five sections, each representing a more or less separate operation, but all five interrelated as indicated.

Under each section, consideration will be given to special problems encountered, health hazards associated with the operation, and a very elementary discussion of chemical and physical processes that might be used.

Section 1. Uranium Metal from the Ore

Special problems in this operation involve separation of ore from gangue, removal of ordinary impurities, removal of impurities with high thermal neutron cross section, and the preparation of the pure uranium metal for use in the pile.

Gangue removal involves the use of standard ore processing techniques adapted to uranium ore. Low grade ores can be processed by differential leaching and by ore flotation.

The removal of ordinary impurities, such as common metals and silica, is effected by the use of standard chemical methods indicated below. The removal of traces of impurities with high thermal neutron cross section presents a very special problem. Such elements as boron, cadmium, indium, and some of the rare earths, must be reduced to concentrations of $<10^{-6}$ g/gU. This is accomplished in a final purification step in which the uranyl nitrate is extracted with diethyl ether. This process furnishes tons of a product with

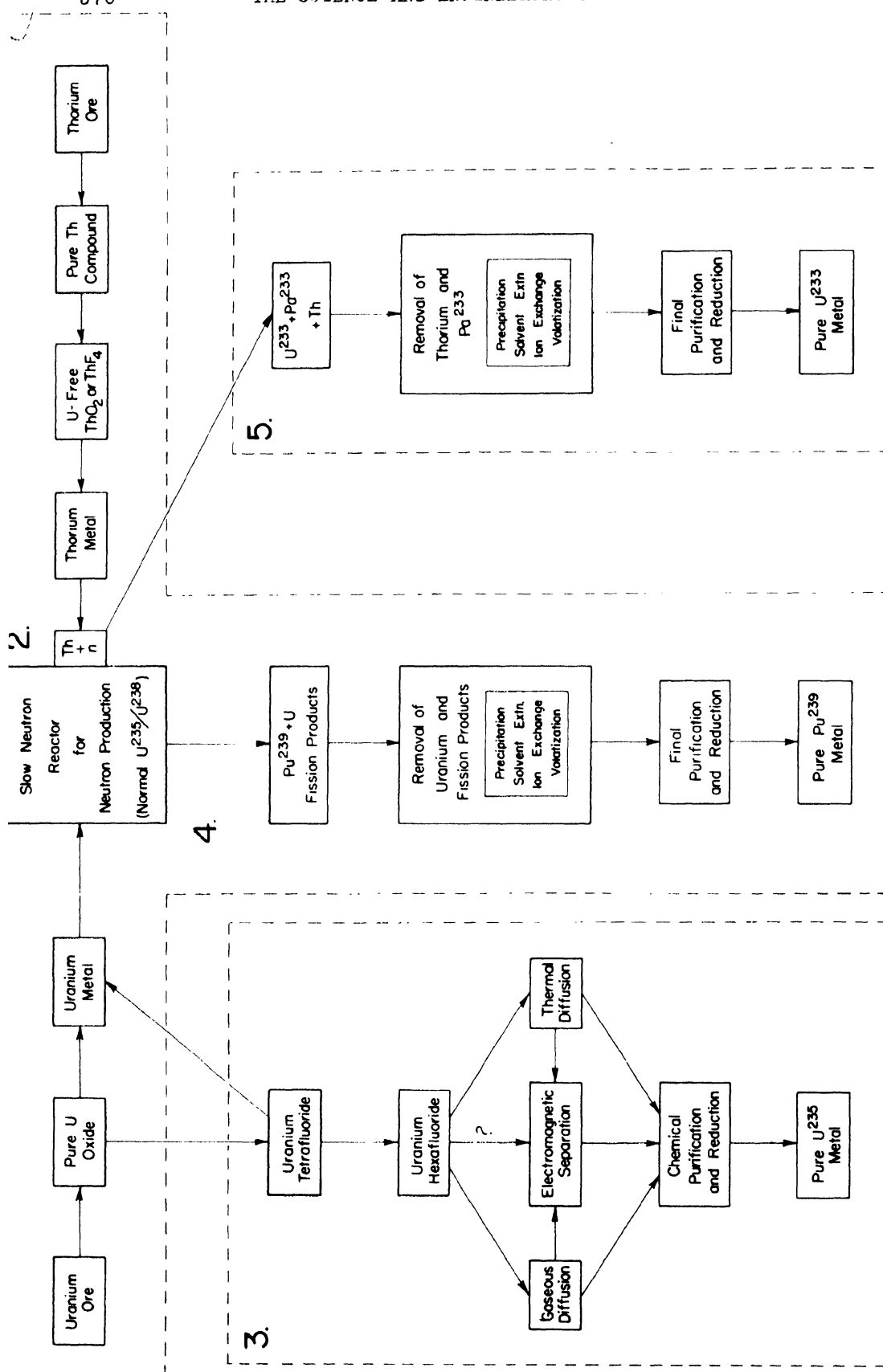


Figure 11-3
Flow Sheet for the Isolation of U^{235} , U^{239} , U^{233}

a purity higher than usually found in laboratory reagent chemicals.

An apparently trivial problem that nearly prevented the operation of the high power nuclear reactors was one of "canning." This consists of coating the uranium metal with aluminum to prevent corrosion of the uranium metal and contamination of the coolant with plutonium and fission products.

Health hazards associated with this section of operation are those due to Ra^{226} and its decay products and the radiation resulting from the operation of nuclear reactors. These are controlled through careful supervision of operating personnel, by remote control operation and by shielding.

Uranium generally occurs in deposits of pitchblende (uranium oxide) and carnotite (complex uranium vanadate). The ore concentrate can be opened up with a mixture of HNO_3 and H_2SO_4 . The uranium goes into solution as UO_2^{++} and those metals forming insoluble sulfates (Pb, Ba, Ra, etc.) remain behind with silicious material insoluble in the acid mixture. Adding an excess of Na_2CO_3 will make the solution alkaline, holding the uranium in solution as a complex carbonate, and precipitating elements that form insoluble carbonates, hydroxides, or basic carbonates (Fe, Al, Cr, Zn, etc.).

Acidification of the solution with HNO_3 gives a solution of uranyl nitrate (frequently called UNH-uranyl nitrate hexahydrate, after the formula of the solid salt, $\text{UO}_2(\text{NO}_3)_2 \cdot 6\text{H}_2\text{O}$), which is soluble in diethyl ether. Extraction with this solvent yields a product of exceptional chemical purity suitable for making uranium for use in nuclear reactors. When UNH is ignited, the mixed oxide, U_3O_8 , results.

This oxide can be reduced to the metal by a bomb reduction with Al, Ca, or Mg. Carbon reduction yields a product heavily contaminated with uranium carbide, while hydrogen reduction yields UO_2 . This lower oxide can be converted to UF_4 or UCl_4 by treatment with anhydrous HF or HCl at an elevated temperature. These tetrahalides can be reduced to the metal by Na or Ca. The halide salt KUF_5 prepared from UF_4 yields a very pure metal by electrolysis.

The metal obtained from the reduction of the oxides or halides is finally fabricated, canned, and used to start a thermal neutron reactor for the production of neutrons. The excess neutrons from the fission of U^{235} are absorbed by the U^{238} present to make Pu^{239} as indicated in Equation 11-1 or U^{233} as indicated in Equation 11-2.

Section 2. Thorium from the Ore

The special problems connected with this process are essentially the same as those encountered in processing uranium. One additional problem of importance is the reduction of the uranium content to a very low value. Since the U^{233} formed will be present in very small concentrations, it is necessary to have contamination from natural uranium much smaller than the expected concentration of the product to eliminate the necessity of a later isotope separation step. This means the final thorium should contain $<10^{-6}$ gU/g. The best way to achieve this would be to purify the thorium before irradiation, using the same process by which the U^{233} will be removed.

Radium (228) and Th^{228} are radioactive decay products of Th^{232} . These have long lives and constitute a radiation hazard comparable to that of Ra^{226} from uranium ores.

Thorium occurs most commonly as a complex phosphate ore, monazite. The ore is usually opened up by prolonged digestion with concentrated H_2SO_4 . With the development of techniques for the use of HF, it is possible that this gas at an elevated temperature would also be useful in the preliminary steps in recovering thorium.

After a solution of thorium is obtained, it is freed of gross contaminants by precipitation reactions with phosphoric acid and oxalic acid. A process to remove contaminants with large cross sections for thermal neutron capture would be necessary. In general, this step is less important for thorium than for uranium unless the thorium is to be irradiated in the high flux section of the reactor.

Uranium always occurs with thorium and it must be reduced to a very small concentration. A solvent extraction process should be effective for this step. Specific complexing agents might well be found that would facilitate the extraction of minute quantities of uranium from large quantities of thorium.

For irradiation of the thorium, a stable compound or the metal will be needed. The irradiated material should be readily soluble for the product removal step. Thorium basic carbonate, a low-temperature formed oxide, or ThF_4 might be suitable compounds. The metal can be reduced from ThF_4 or $ThCl_4$ by Na, Ca, or Mg.

After fabricating and canning the thorium compound or metal, it is

placed in the neutron reactor for irradiation. Such irradiations for either Pu^{239} or U^{233} should involve a neutron economy that produces more of the secondary fuel than is burned in its production. In this way, the relatively abundant U^{238} and Th^{232} can be utilized in such a manner that the primary fuel, U^{235} , will be conserved.

Section 3. Separation of Pure U^{235}

In addition to the special problems involved in making isotope separation processes work at all, there are certain general technical problems of importance to operation and overall economy. Both the gaseous diffusion and the thermal diffusion methods are dependent upon the compound UF_6 . This compound is a strong oxidizing agent and is highly corrosive. Its preparation involves the use of elementary fluorine, F_2 . Both materials require highly specialized techniques for handling with safety.

All three methods of isotope separation involve the use of equipment that does not leak. This involves the engineering design, construction, and testing of equipment of the most advanced nature. Leaks of such small size as to be unnoticed in ordinary equipment would prevent the operation of any of the three processes.

All of the methods of isotope separation involve the use of a tremendous amount of power. This has to be taken into account in studying the comparative economy of the various pure nuclear fuels. It has been stated that the isotope separation processes for U^{235} production cannot compete on an economic basis with the production of an equivalent amount of plutonium.

Both F_2 and UF_6 are extremely corrosive and poisonous. Handling these dangerous materials requires extraordinary precautions to prevent injury to operating personnel. Another hazard involves the handling of the pure U^{235} and its compounds. Because of the high purity of this isotope, the critical size for a chain reaction to start in the material is comparatively small. This necessitates design of final processing and storage facilities so the critical size is never approached. Although an explosion comparable to that of the atomic bomb probably would not occur, neutron intensities above the dangerous level might be encountered, and a large area would be contaminated with fission products for many years. This problem is common to all processes in which nuclear fuels of high purity are produced.

Starting with the pure oxide, UF_4 is produced by treatment with

anhydrous HF at elevated temperatures. This compound is converted to UF_6 by treatment with elementary fluorine. The UF_6 goes to the gaseous diffusion plant and to the thermal diffusion plant where the $\text{U}^{235}/\text{U}^{238}$ ratio is increased by many small increments in a cascade system. Material can be withdrawn at any desired value of enrichment up to approximately 100 per cent.

Electromagnetic separation, with its high separation factor per unit and low capacity, can handle the natural isotopic mixture of uranium. However, because the output per unit is directly proportional to the input concentration of U^{235} , it is very advantageous to use an enriched feed from one of the other two separation processes. This has been done successfully. The chemical form of uranium used in the electromagnetic separation has not been published.

After the pure isotope has been obtained, its processing, reduction to metal, alloying or compounding is the same as with the unenriched material. The greatly enhanced value of the enriched material and the dangers associated with its handling will undoubtedly modify the techniques used, but do not change its chemical properties.

Section 4. Separation of Pu^{239}

The first step in processing the irradiated uranium for removal of Pu^{239} involves removing the aluminum can. This must be done chemically since the mechanical operation would be too hazardous.

The actual processing of plutonium involves two major steps. Since the ratio U/Pu is very large, large amounts of uranium must be removed. Secondly, the fission products must be eliminated from the final product. Both of these operations result in a third major problem, the disposal of waste. The uranium must be recovered and the dangerous fission products, both gases and solutions, must be disposed of in such a way as not to present health hazards. The best methods seem to be brute force methods, namely, to carry out the operations remote from thickly settled areas and to build storage tanks large enough to store the major wastes. Minor wastes can be dissipated slowly by controlled dilution in streams that have a sufficiently large volume of flow.

The health hazards in plutonium separation are twofold. First is the tremendous radiation intensity from the fission products in the uranium. These radiation intensities are comparable to many tons of radium. This

makes remote control mandatory for all chemical operations. The second hazard is the extreme toxicity of the element, plutonium. Not only does it have a high chemical toxicity, but its high specific alpha activity makes it comparable to radium as an internal radiation poison. This means that micrograms of the element in the body will be fatal. Extraordinary precautions are needed to prevent such exceedingly small quantities becoming air-borne as dust and being inhaled or ingested. Constant monitoring of operating personnel can reduce the danger of injuries to a negligible level.

The first step in separating Pu^{239} from uranium is an aging period during which the shorter-lived fission products decay, thus reducing the radiation levels in the separation processes. This is important from a chemical point of view since, under intensely ionizing conditions, many peculiar chemical reactions occur. Corrosion is accelerated, peroxide formation in water solutions is large, organic materials dissociate and polymerize, and the energy of the radiations heat the solutions, rendering temperature control difficult.

After aging, the uranium slugs are "de-canned" and the uranium dissolved. As pointed out in 11-3, plutonium has an oxidation state of +6 in which it behaves much like uranium and probably exists as PuO_2^{++} in solution. This oxidation state is more readily reduced than the +6 state of uranium. In its lower oxidation states (+3 and +4) plutonium is co-precipitated with rare earth fluorides. By taking advantage of this oxidation-reduction cycle, it should be possible to free plutonium from both uranium and the fission products.

If the initial uranium solution is treated with an oxidizing agent sufficiently strong to oxidize plutonium to +6, many of the fission products can be precipitated with a rare earth fluoride carrier such as CeF_3 or LaF_3 . After removing the precipitate, the PuO_2^{++} can be reduced with a mild reducing agent to Pu^{+4} which will be co-precipitated as the fluoride with a rare-earth carrier. This leaves in solution uranium and fission products not precipitated with fluorides. After dissolving the second fluoride precipitate, the plutonium can be oxidized to the +6 state and the decontamination cycle repeated. These operations achieve a volume reduction and concentration of the Pu^{239} as well as decontamination. It has been reported that at least two different types of co-precipitation are used to achieve maximum decontamination.

It would probably be possible to effect a final clean-up of the plutonium by means of some other separation process such as solvent extraction or ion exchange.

The possibility also exists that an entire separation procedure could be designed around a process other than precipitation. For example, $\text{PuO}_2(\text{NO}_3)_2$ should be soluble in organic solvents in a manner similar to $\text{UO}_2(\text{NO}_3)_2$. This would enable the bulk of fission products to be removed. In the reduced state, plutonium would not be soluble in the organic phase while the uranium, still present at UO_2^{++} , could be extracted from the nitrate solution.

Published information on the properties of plutonium metal is nil. However, it might be expected to resemble uranium and be handled in a similar manner with due regard to its multifold greater toxicity.

Section 5. Separation of U^{233}

The obvious special problems in processing thorium for U^{233} are those associated with the separation of small amounts of uranium from large amounts of thorium, and the problem of handling Pa^{233} . This isotope represents both a radiation hazard and a hold-up of U^{233} . The simplest way to solve the problem is to age the irradiated thorium for five to six half-lives (four to six months) and allow the Pa^{233} to decay. This aging period will also allow most of the fission products from fast neutron fission to decay. This latter source of activity is not serious when a slow neutron reactor is used for irradiation.

For thorium exposed to a neutron flux of $10^{10} \text{ n/cm}^2 \text{ sec}$, the activity due to Pa^{233} at equilibrium is about 5 kilocuries per ton of Th. It also represents about 0.2 g. of U^{233} . Early separation and purification of Pa^{233} would allow the recovery of very pure U^{233} .

The health hazards in this separation operation are largely due to Pa^{233} radiation and the high alpha activity of U^{233} . Since the half-life of U^{233} is approximately six times that of Pu^{239} , its specific alpha activity will be about 1/6 as great. This activity is still great enough to be a very serious health hazard.

The problem of separating trace amounts of uranium from bulk thorium by precipitation reactions is practically impossible. U^{+6} does not form many insoluble compounds under conditions that thorium will stay in solution. In the +4 oxidation state, uranium resembles thorium so closely that no separation could be expected. It would be an extremely difficult task to precipitate tons of thorium and recover a few grams of uranium from the solution.

Solvent extraction methods seem to offer the best method of attack on this problem. If the thorium is converted to the nitrate, the presence of the large amount of nitrate ion in the aqueous solution would serve to salt out the $\text{UO}_2(\text{NO}_3)_2$ into the organic layer (possibly an ether). After the initial volume reduction and concentration step, any of several types of clean-up might be used.

If freshly irradiated thorium is to be processed for Pa^{233} , advantage could be taken of the tendency of Pa^{+5} to hydrolyze and form a radiocolloid. Under controlled conditions, the Pa^{+5} could be separated from thorium by coprecipitating with Ta_2O_5 or some scavenging oxide like MnO_2 which will precipitate from an acid solution. Solvent extraction methods might also be found that would work with protoactinium.

Final reduction to uranium metal and alloying with suitable material would be the same as for U^{235} .

(To anyone who is familiar with the actual processes in use for the separation of the pure nuclear fuels, this discussion may seem incredibly naive. There is no question at all that it is an extremely simplified version of the problems that might be encountered. However, it is hoped the basic ideas are sound and the speculations are reasonable in the absence of experimental data.)

BIBLIOGRAPHY OF THE HEAVY ELEMENTS

- McMillan, E. M., and Abelson, P. H. - "Radioactive Element 93" *Phys. Rev.* 57, 1185L (1940).
- Seaborg, G. T. - "The Chemical and Radioactive Properties of the Heavy Elements" *Chem. & Eng. News* 23, 2190 (1945).
- Seaborg, G. T. - "The Transuranium Elements" *Science* 104, 379 (1946).
- Joliot-Curie, I. - "Les Radioelements Naturels" Hermann and Cie., Paris (1946).
- Seaborg, G. T. - "The Heavy Elements" *Chem. & Eng. News* 24, 1192 (1946).
- Perlman, I. - "The Cyclotron in Atomic Energy Development" *Chem. & Eng. News* 24, 3032 (1946).
- Seaborg, G. T., McMillan, E. M., Kennedy, J. W., and Wahl, A. C., - "Radioactive Element 94 from Deuterons on Uranium" *Phys. Rev.* 69, 366L (1946).
- Seaborg, G. T., Wahl, A. C., and Kennedy, J. W. - "Radioactive Element 94 from Deuterons on Uranium" *Phys. Rev.* 69, 367L (1946).
- Kennedy, J. W. Seaborg, G. T. Segre, E., and Wahl, A. C. - "Properties of 94 (23)" *Phys. Rev.* 70, 555 (1946).
- Seaborg, G. T. - "Plutonium and the Other Transuranium Elements" *Chem. & Eng. News* 25, 358 (1947).

APPENDIX A*

The calculation of nuclear reaction energies is facilitated by the following table of precise masses. The principle involved is identical with that discussed in Section 1-14. Q values are obtained by simply subtracting two numbers selected from the appropriate columns of Δ . The neutral atomic masses M listed in the third column are known for the light elements 0 to 26 with a probable error, in the fifth decimal place, as given in the fourth column. The values in parentheses are estimated by semi-empirical methods. Based on the physical scale of $O^{16} = 16.00000$ atomic mass units (amu) and the conversion factor $931 \text{ Mev} = 1 \text{ amu}$, the excess mass Δ corresponding to each atomic mass is given in Mev in the fifth column. The addition of a neutron, proton, deuteron, or alpha particle gives a total excess atomic mass in Mev as listed under the columns headed Δ_n , Δ_p , Δ_d and Δ_α respectively. The last column gives the total binding energy E of the nucleus in Mev. When divided by the atomic number A , the binding energy per nucleon E/A is obtained, as discussed in Section 1-10.

*These data were compiled by the Cornell University Group under the supervision of H. A. Bethe.

Atomic Number Z	Nucleus	Neutral Atomic Mass M	Error	Δ (M-A)931	Δ_n	Δ_p	Δ_d	Δ_a	Binding Energy E	Binding Energy Per Particle E/A
0	¹ n ₁	1.00893	3	8.31	16.62	15.87	22.00	11.94	0.00	
1	H ₂	1.008123	0.6	7.56	15.87	15.12	21.25	11.19	0.00	
1	H ₃	2.014708	1.1	13.69	22.00	21.25	27.38	17.32	2.18	1.09
1	H ³	3.01700	3.4	15.85	24.16	23.41	29.54	19.48	8.33	2.78
2	³ He ₄	3.01700	4.	15.83	24.14	23.39	29.52	19.46	7.60	2.53
2	He ³	4.00390	3.	3.63	11.94	11.19	17.32	7.26	28.11	7.03
2	He ⁶	5.0137	35	12.75	21.06	20.31	26.44	16.38	27.30	5.46
2	He	6.0209	50	19.46	27.77	27.02	33.15	23.09	28.90	4.82
3	⁵ Li ₆	(5.0136)	(60)	12.66	20.97	20.22	26.35	16.29	26.64	5.33
3	Li ₇	6.01697	5	15.80	24.11	23.36	29.49	15.43	31.81	5.30
3	Li ₈	7.01822	6	16.96	25.27	24.52	30.65	20.59	38.96	5.57
3	Li ⁸	8.02502	7	25.29	31.60	30.85	36.98	26.92	40.94	5.12
4	⁶ Be ₇	6.0219	(100)	20.39	28.70	27.95	34.08	24.02	26.47	4.41
4	Be ₈	7.01913	7	17.84	26.15	25.40	31.53	21.47	37.33	5.33
4	Be ₉	8.00785	7	7.31	15.62	14.87	21.00	10.94	56.17	7.02
4	Be ₁₀	9.01503	6	13.99	22.30	21.55	27.68	17.62	57.80	6.42
4	Be ₁₁	10.01677	8	15.61	23.92	23.17	29.30	19.24	64.49	6.45
4	Be ¹¹	(11.0277)	-	25.79	34.10	33.35	39.48	29.42	62.62	5.69
5	⁹ B ₁₀	9.01620	7	15.08	23.39	22.64	28.77	18.71	55.96	6.22
5	B ₁₁	10.01618	9	15.06	23.37	22.62	28.75	18.69	64.29	6.43
5	B ₁₂	11.01284	8	11.95	20.26	19.51	25.64	15.58	75.71	6.88
5	B ₁₃	12.0190	70	17.69	26.00	25.25	31.38	21.32	78.28	6.52
5	B ¹³	(13.0207)	-	19.27	27.58	26.83	32.96	22.90	85.01	6.54

Atomic Number Z	Nucleus	Neutral Atomic Mass M	Error	Δ (M-A)931	Δ_n	Δ_p	Δ_d	Δ_a	Binding Energy E	Binding Energy per Particle E/A
6	¹⁰ C	10.0210	30	19.55	27.66	27.11	33.24	23.18	59.05	5.91
6	¹¹ C	11.01495	9	13.92	22.23	21.48	27.61	17.85	72.99	6.64
6	¹² C	12.00382	4	3.56	11.87	11.12	17.25	7.19	91.66	7.64
6	¹³ C	13.00751	10	6.99	15.30	14.55	20.68	10.62	96.54	7.43
6	¹⁴ C	14.00767	5	7.14	15.45	14.70	20.83	10.77	104.70	7.48
6	¹⁵ C	(15.0165)	-	15.36	23.67	22.92	29.05	18.99	104.79	6.99
7	¹² N	(12.0233)	-	21.69	30.00	29.25	35.38	25.32	72.78	6.07
7	¹³ N	13.00988	7	9.20	17.51	16.76	22.89	12.83	93.58	7.20
7	¹⁴ N	14.00751	4	6.99	15.30	14.55	20.68	10.62	104.10	7.44
7	¹⁵ N	15.00489	21	4.55	12.86	12.11	18.24	8.18	114.85	7.66
7	¹⁶ N	> 16.0065	-	6.05	14.36	13.61	19.74	9.68	121.66	7.60
7	¹⁶ N	< 16.011	-	10.24	18.55	17.80	23.93	13.87	117.47	7.34
7	¹⁷ N	(17.014)	-	13.03	21.34	20.59	26.72	16.16	122.99	7.23
8	¹⁴ O	(14.0131)	-	12.20	20.51	19.76	25.89	15.83	98.14	7.01
8	¹⁵ O	15.0078	40	7.26	15.57	14.82	20.95	10.89	111.39	7.43
8	¹⁶ O	16.000000	-	0.00	8.31	7.56	13.69	3.63	126.96	7.94
8	¹⁷ O	17.00450	6	4.19	12.50	11.75	17.88	7.82	131.08	7.71
8	¹⁸ O	18.0049	40	4.56	12.87	12.12	18.25	8.19	139.02	7.72
8	¹⁹ O	(19.0139)	-	12.94	21.25	20.50	26.63	16.57	138.95	7.31
9	¹⁶ F	(16.0175)	-	16.29	24.60	23.85	29.98	19.92	109.92	6.87
9	¹⁷ F	17.0075	30	6.98	15.29	14.54	20.67	10.61	127.54	7.50
9	¹⁸ F	18.0065	60	6.05	14.36	13.61	19.74	9.68	136.78	7.60
9	¹⁹ F	19.00450	26	4.19	12.50	11.75	17.88	7.82	146.95	7.73
9	²⁰ F	> 20.0042	-	3.91	12.22	11.49	17.60	7.54	155.54	7.78
9	²⁰ F	< 20.0092	-	8.57	16.88	16.13	22.26	12.20	150.88	7.54
9	²¹ F	(21.0059)	-	5.49	13.80	13.05	19.18	9.12	162.27	7.73

Atomic Number Z	Nucleus	Neutral Atomic Mass M	Error	Δ (M-A)931	Δ_n	Δ_p	Δ_d	Δ_a	Binding Energy E	Binding Energy per Particle E/A
10	¹⁸ Ne	(18.0114)	-	10.61	18.92	18.17	24.30	14.24	131.47	7.30
10	¹⁹ Ne	19.00781	20	7.27	15.58	14.83	20.96	10.90	143.12	7.53
10	²⁰ Ne	19.99877	10	-1.15	7.16	6.41	12.81	2.48	159.85	7.99
10	²¹ Ne	20.99963	22	-0.344	7.97	7.22	13.62	3.29	167.35	7.97
10	²² Ne	21.99844	36	-1.45	6.86	6.11	12.24	2.18	176.77	8.04
10	²³ Ne	(23.0013)	-	1.21	9.52	8.77	14.90	4.84	182.42	7.93
11	²¹ Na	(21.0035)	-	3.26	11.57	10.82	16.59	6.89	153.00	7.76
11	²² Na	21.9999	50	-0.0931	8.22	7.47	13.60	3.54	174.66	7.94
11	²³ Na	22.99618	31	-3.56	4.75	4.00	10.13	0.07	186.44	8.11
11	²⁴ Na	23.9975	45	-2.33	5.98	5.23	11.36	1.30	193.52	8.06
11	²⁵ Na	(24.9967)	-	-3.07	5.24	4.49	10.62	0.56	202.57	8.10
12	²² Mg	(22.0062)	-	5.77	14.08	13.33	19.46	9.40	168.05	7.64
12	²³ Mg	23.0002	40	0.186	8.50	7.75	13.88	3.82	181.94	7.91
12	²⁴ Mg	23.9924	60	-7.08	1.23	0.48	6.61	-3.45	197.52	8.23
12	²⁵ Mg	24.9938	90	-5.77	2.54	1.79	7.92	-2.14	204.52	8.18
12	²⁶ Mg	25.9898	50	-9.50	-1.19	-1.94	4.19	-5.87	216.56	8.33
12	²⁷ Mg	26.9928	150	-6.70	1.61	0.86	6.99	-3.07	222.07	8.22
13	²⁵ Al	24.9981	100	-1.77	6.54	5.79	11.92	1.86	199.77	7.99
13	²⁶ Al	25.9929	150	-6.61	1.70	0.95	7.08	-2.98	212.92	8.19
13	²⁷ Al	26.9899	80	-9.40	-1.09	-1.84	4.29	-5.77	224.02	8.30
13	²⁸ Al	27.9903	70	-9.03	- .72	-1.47	4.66	-5.40	231.96	8.28
13	²⁹ Al	28.9893	80	-9.96	-1.65	-2.40	3.73	-6.33	241.20	8.32
13	³⁰ Al	(29.9954)	-	4.28	4.03	3.28	9.41	-0.65	243.83	8.13
14	²⁷ Si	26.9949	90	-4.75	3.56	2.81	8.94	-1.12	218.62	8.10
14	²⁸ Si	27.9866	60	-12.48	-4.17	-4.92	1.21	-8.85	234.66	8.38
14	²⁹ Si	28.9866	60	-12.48	-4.17	-4.92	1.21	-8.85	242.97	8.38
14	³⁰ Si	29.9832	90	-15.64	-7.33	-8.08	-1.95	-12.01	254.44	8.48
14	³¹ Si	30.9862	60	-12.85	-4.54	-5.29	0.84	-9.22	259.96	8.39
14	³² Si	(31.9849)	-	-14.06	-5.75	-6.50	-0.37	-10.43	269.48	8.42

Atomic Number Z	Nucleus	Neutral Atomic Mass M	Error	Δ (M-A)931	Δ_n	Δ_p	Δ_d	Δ_a	Binding Energy E	Binding Energy per Particle E/A
15	²⁹ P	(28.9919)	(100)	-7.54	0.77	0.02	6.15	-3.91	237.28	8.18
15	³⁰ P	29.9873	100	-11.82	-3.51	-4.26	1.87	-8.19	249.87	8.33
15	³¹ P	30.9843	50	-14.62	-6.31	-7.06	-0.93	-10.99	260.98	8.42
15	³² P	31.9827	40	-16.11	-7.80	-8.55	-2.42	-12.48	270.78	8.46
15	³³ P	(32.9826)	-	-16.20	-7.89	-8.64	-2.51	-12.57	279.18	8.46
16	³¹ S	(30.9899)	-	-9.40	-1.09	-1.84	4.29	-5.77	255.01	8.23
16	³² S	31.98089	7	-17.79	-9.48	-10.23	-4.10	-14.16	271.71	8.49
16	³³ S	32.9800	60	-18.62	-10.31	-11.06	-4.93	-14.99	280.85	8.51
16	³⁴ S	33.97710	35	-21.32	-13.01	-13.76	-7.63	-17.69	291.86	8.58
16	³⁵ S	34.9788	80	-19.74	-11.43	-12.18	-6.05	-16.11	298.59	8.53
16	³⁶ S	35.978	100	-20.48	-12.17	-12.92	-6.79	-16.85	307.64	8.55
17	³³ Cl	(32.9860)	-	-13.03	-4.72	-5.47	0.66	-9.40	274.51	8.32
17	³⁴ Cl	33.9801	-	-18.53	-10.22	-10.97	-4.84	-14.90	288.32	8.48
17	³⁵ Cl	34.97867	21	-19.86	-11.55	-12.30	-6.17	-16.23	297.96	8.51
17	³⁶ Cl	35.9788	100	-19.74	-11.43	-12.18	-6.05	-16.11	306.15	8.50
17	³⁷ Cl	36.97750	14	-20.95	-12.64	-13.39	-7.26	-17.32	315.67	8.53
17	³⁸ Cl	37.981	300	-17.69	-9.38	-10.13	-4.00	-14.06	320.72	8.44
17	³⁹ Cl	(38.9794)	-	-19.18	-10.87	-11.62	-5.49	-15.55	330.52	8.47
18	³⁵ Ar	(34.9850)	-	-13.97	-5.66	-6.41	-0.28	-10.34	291.32	8.32
18	³⁶ Ar	35.9780	100	-20.48	-12.17	-12.92	-6.79	-16.85	306.14	8.50
18	³⁷ Ar	(36.9777)	-	-20.76	-12.45	-13.20	-7.07	-17.13	314.73	8.51
18	³⁸ Ar	37.974	250	-24.21	-15.90	-16.65	-10.52	-20.58	326.49	8.59
18	³⁹ Ar	(38.9755)	-	-22.81	-14.50	-15.25	-9.12	-19.18	333.40	8.55
18	⁴⁰ Ar	39.9756	60	-22.72	-14.41	-15.16	-9.03	-19.09	341.62	8.54
18	⁴¹ Ar	40.9770	60	-21.41	-13.10	-13.85	-7.72	-17.78	348.62	8.50
19	³⁷ K	(36.9830)	-	-15.83	-7.52	-8.27	-2.14	-12.20	309.05	8.35
19	³⁸ K	(37.9795)	-	-19.09	-10.78	-11.53	-5.40	-15.46	320.62	8.44
19	³⁹ K	(38.9747)	-	-23.55	-15.24	-15.99	-9.86	-19.92	333.39	8.55
19	⁴⁰ K	39.9760	100	-22.34	-14.03	-14.78	-8.65	-18.71	340.49	8.51

Examples:

$$\text{H}^2(\text{d}, \text{p})\text{H}^3; \Delta_{\text{d}} \text{ of } (\text{H}^2 + \text{d}) = 27.38, \Delta_{\text{p}} \text{ of } (\text{H}^3 + \text{p}) = 23.41 \text{ .} \cdot \text{. } Q = 27.38 - 23.41 = 3.97 \text{ Mev}$$

$$\text{Be}^9(\text{n}, 2\text{n})\text{Be}^8; \Delta_{\text{n}} \text{ of } (\text{Be}^9 + \text{n}) = 22.30, \Delta_{\text{n}} \text{ of } (\text{Be}^8 + \text{n}) = 15.6, \text{ adding } \Delta \text{ of extra n} = 15.62 + 8.31 = 23.93 \text{ .} \cdot \text{. } Q = 22.30 - 23.93 = -1.63 \text{ Mev}$$

$$\text{S}^{32}(\text{n}, \text{p})\text{P}^{32}; \Delta_{\text{n}} \text{ of } (\text{S}^{32} + \text{n}) = -9.48, \Delta_{\text{p}} \text{ of } (\text{P}^{32} + \text{p}) = -8.55 \text{ .} \cdot \text{. } Q = -9.48 - (-8.55) = -0.93 \text{ Mev}$$

Loss of Energy in Elastic Collisions

From Q-value equation, (15), p. 17

$$Q = E_2(1 + A_2/A_3) - E_1(1 - A_1/A_3) - 2 \cos \theta \sqrt{A_1 A_2 E_1 E_2}/A_3$$

For elastic scattering $Q = 0$ (conservation of KE) and $A_1 = A_2 = m$ while $A_3 = A = \text{mass of target}$. Then $E_1 = E_0 = \text{initial KE}$ and $E_2 = E = \text{final KE}$. In general for any angle of scattering θ ,

$$E(1 + m/A) - \sqrt{E} \cos \theta (2m \sqrt{E_0}/A) - E_0(1 - m/A) = 0$$

Therefore:

$$\begin{aligned} \sqrt{E} &= \frac{(2m \sqrt{E_0} \cos \theta) \pm \sqrt{4m^2 E_0 \cos^2 \theta + 4E_0(A^2 - m^2)}}{2(A + m)} \\ &= \left[m \sqrt{E_0}/(A + m) \right] \left[\cos \theta \pm \sqrt{(A^2/m^2) - \sin^2 \theta} \right] \end{aligned}$$

At $E = E_{\min}$, $\theta = 180^\circ$; $\cos \theta = -1$; $\sin \theta = 0$,

$$\begin{aligned} \sqrt{E_{\min}} &= \left[m \sqrt{E_0}/(A + m) \right] \left[-1 \pm \sqrt{A^2/m^2} \right] \\ &= (A - m) \sqrt{E_0}/(A + m) = E_0 - E_{\min} \\ &= E_0 \left[1 - (A - m)/(A + m) \right]^2 = (1 - \alpha)E_0 \end{aligned}$$

$$\text{where } \alpha = \left[(A - m)/(A + m) \right]^2$$

APPENDIX C

NEUTRON CROSS SECTIONS OF THE ELEMENTS

A Compilation*

by

H. H. Goldsmith, Brookhaven National Laboratory, Patchogue, L.I., N.Y.

H. W. Ibser, University of Wisconsin, Madison, Wisconsin

B. T. Feld, Physics Department and Laboratory for Nuclear Science and Engineering, Massachusetts Institute of Technology, Cambridge, Mass.

A collection of neutron cross sections of the elements, based on the prewar and wartime work of many investigators, was compiled during 1945 (by H.H.G. and H.W.I.) at the Metallurgical Laboratory, University of Chicago. This compilation was designed for use in the Manhattan Project Laboratories. It was declassified in June 1946, for publication in the Manhattan Project Technical Series.

Informal circulation resulted in widespread demand for the publication of such a collection. However, many of the original articles were then being prepared for appearance in the periodical literature. The publication of this collection was therefore delayed to permit as many as possible of these papers to appear in the normal fashion. During this delay, the original collection was completely revised (by B.T.F. and H.H.G.).

At the present writing, some of the data included in this compilation are still unpublished, mainly due to the pressure of other commitments on the original authors. In all such cases, we have made every effort to secure permission from the authors for the inclusion of their data in this collection.

The general plan of this survey has been to present the available cross section data for each element in two curves, the first containing the low-energy (0.001 - 1000 ev) values and the second the high-energy (0.001 - 100 mev). If one of the curves is not available a blank page is left, so that the cross sections may be plotted in when the data become available. The cross sections plotted are in barns (10^{-24} cm²) per atom of the normal element, except where otherwise indicated. In each case, the type of plot used has been chosen in order to allow the clearest representa-

*These curves, and the accompanying text, are reprinted from the October 1947 issue of the Reviews of Modern Physics, by permission of the editors. For the complete text and complete list of references, see the RMP.

tion of the data, and to bring out the most important features of the energy variation of the cross section. The notation used has the following meaning:

σ_t	total cross section					
σ_s	scattering cross section					
σ_r	cross section for the (n,γ) process					
σ_p	"	"	"	"	(n,p)	"
σ_a	"	"	"	"	(n,α)	"
σ_f	"	"	"	"	fission	"

In the curves herein reproduced, only those in the region below a few ev are well resolved, since it is only in this region that the resolution widths of the velocity selectors are smaller than the expected widths of the resonances. As the energy of the neutrons increases beyond a few ev, the resolution of the instruments becomes appreciably worse, so that measurements in this region merely represent average cross sections over an energy spread at least as great as the width of the resonance under investigation. Consequently, the maximum observed cross sections are much smaller than the actual cross sections at the peak of the resonance. Furthermore, what often appears to be a broad resonance may turn out, on more careful observation, to be a superposition of two or more adjacent resonances (as in the case of the 35 ev resonance in I).

The compilers are acutely conscious of the dubious validity of drawing solid curves of cross section vs. energy through points measured in the neighborhood of a resonance, when the resolution width of the measuring instrument exceeds the expected width of the resonance. Nevertheless, because of the nuclear physicist's interest in the variation of cross section with neutron energy, we have drawn such curves to serve as a visual aid in following those trends in this variation which are indicated at the present writing.

We again wish to express our thanks to the many scientists who, without exception, have granted us permission to use their unpublished data. We are especially indebted to the Columbia Velocity Selector Group, J.R. Dunning, W.W. Havens, Jr., L.J. Rainwater, and C.S. Wu, who have made available the

results of their experiments as soon as these were completed, and who have permitted us to publish a considerable body of data which have not appeared in print. We are similarly indebted to W.J. Sturm for his constant cooperation with regard to the Argonne Laboratory Velocity Selector results. The cross section data, due to Amaldi, et al, were transmitted to us by E. Amaldi during his recent visit in this country. These data have been published since this compilation was prepared.

We wish to thank R.S. Mulliken and W.H. Zinn for facilitating the publication of Manhattan Project declassified data prior to the publication of the MPTS.

Space limitations have prevented explicit reference, on the curves, to all of the workers concerned with particular sets of unpublished data. Toward this end, we include the following:

- 1) Argonne Crystal Spectrometer Group: G.P. Arnold, W.J. Sturm, S.H. Turkel, and W.H. Zinn.
- 2) Argonne Mechanical Velocity Selector Group: T. Brill and H.D. Litchenberger; also E. Fermi, L.W. Marshall, and J. Marshall.
- 3) Clinton Crystal Spectrometer Group: L.B. Borst, A.J. Ulrich, C.L. Osborne, and G.H. Hasbrouck; also E.O. Wollan, S. Bernstein, R.G. Peterson, and R.B. Sawyer.
- 4) Los Alamos Velocity Selector Group: E.E. Anderson, L.S. Lavatelli, B.D. McDaniel, and R.B. Sutton.
- 5) Los Alamos Linear Accelerator Group: C.L. Bailey, W.E. Bennett, T. Bergstralh, J.M. Blair, D.H. Frisch, O.A. Hanson, R.D. Perry, H.T. Richards, and J.H. Williams.
- 6) Los Alamos Radioactive Sources Group: M. Deutsch, G.A. Linenberger, T.A. Miskel, and E. Segre; also (for σ_r of Au) K.I. Greisen and J.H. Williams.

We gratefully acknowledge the aid of Grace Rowe, of the M.I.T. Laboratory for Nuclear Science and Engineering, who did the drafting work required in the revision of the original compilation and in the preparation of these curves for publication.

B.T. Feld and H.H. Goldsmith

June 1, 1947

INDEX OF CURVES

(Blank spaces indicate inadequate information for inclusion of curves for this element)

<u>ATOMIC NO.</u>	<u>ELEMENT</u>	<u>SYMBOL</u>	<u>LOW ENERGY</u>	<u>HIGH ENERGY</u>	<u>PAGE NO.</u>
89	Actinium	Ac			
13	Aluminum	Al	σ_t	σ_t	418, 419
95	Americium	Am			
51	Antimony	Sb	σ_t	σ_t	462, 463
18	Argon	A			
33	Arsenic	As			
85	Astatine	At			
56	Barium	Ba			
4	Beryllium	Be	σ_t	σ_t, σ_a	402, 403
83	Bismuth	Bi	σ_t	σ_t	498, 499
5	Boron	B	σ_a	σ_t, σ_a	404, 405
35	Bromine	Br			
48	Cadmium	Cd	σ_t	σ_t	456, 457
20	Calcium	Ca			
6	Carbon	C	σ_t	σ_t	406, 407
58	Cerium	Ce			
55	Cesium	Cs			
17	Chlorine	Cl	σ_t		426, 427
24	Chromium	Cr	σ_t		430, 431
27	Cobalt	Co	σ_t		436, 437
41	Columbium	Cb	σ_t		448, 449
29	Copper	Cu	σ_t	σ_t	440, 441
96	Curium	Cm			
66	Dysprosium	Dy	σ_t		476, 477
68	Erbium	Er			
63	Europium	Eu	σ_t		472, 473
9	Fluorine	F	σ_t	σ_t	412, 413
87	Francium	Fr			
64	Gadolinium	Gd	σ_t		474, 475
31	Gallium	Ga			
32	Germanium	Ge	σ_t		444, 445

Index of Curves (Cont'd)

<u>ATOMIC NO.</u>	<u>ELEMENT</u>	<u>SYMBOL</u>	<u>LOW ENERGY</u>	<u>HIGH ENERGY</u>	<u>PAGE NO.</u>
79	Gold	Au	σ_t	σ_t, σ_r	490, 491
72	Hafnium	Hf			
2	Helium	He		σ_s	398, 399
67	Holmium	Ho			
1	Hydrogen	H	σ_t	σ_t	394, 395
49	Indium	In	σ_t	σ_r	458, 459
53	Iodine	I	σ_t	σ_t, σ_r	464, 465
77	Iridium	Ir	σ_t		486, 487
26	Iron	Fe	σ_t	σ_t	434, 435
36	Krypton	Kr			
57	Lanthanum	La	σ_t		466, 467
82	Lead	Pb	σ_t	σ_t	496, 497
3	Lithium	Li	σ_t	σ_a	400, 401
71	Lutecium	Lu			
12	Magnesium	Mg	σ_t	σ_t	416, 417
25	Manganese	Mn	σ_t		432, 433
80	Mercury	Hg	σ_t		492, 493
42	Molybdenum	Mo			
60	Neodymium	Nd	σ_t		468, 469
10	Neon	Ne			
93	Neptunium	Np		σ_f	500, 501
28	Nickel	Ni	σ_t	σ_t	438, 439
7	Nitrogen	N	σ_t	$\sigma_t, \sigma_s, \sigma_p, \sigma_a$	408, 409
76	Osmium	Os	σ_t		484, 485
8	Oxygen	O	σ_t	σ_t	410, 411
46	Palladium	Pd			
15	Phosphorus	P	σ_t	σ_t, σ_p	422, 423
78	Platinum	Pt	σ_t		488, 489
94	Plutonium	Pu			
84	Polonium	Po			
19	Potassium	K		σ_t	428, 429
59	Praseodymium	Pr			

Index of Curves (Cont'd)

<u>ATOMIC NO.</u>	<u>ELEMENT</u>	<u>SYMBOL</u>	<u>LOW ENERGY</u>	<u>HIGH ENERGY</u>	<u>PAGE NO.</u>
61	Promethium	Pm			
91	Protactinium	Pa			
88	Radium	Ra			
86	Radon	Rn			
75	Rhenium	Re	σ_t		482, 483
45	Rhodium	Rh	σ_t		452, 453
37	Rubidium	Rb			
44	Ruthenium	Ru	σ_t		450, 451
62	Samarium	Sm	σ_t		470, 471
21	Scandium	Sc			
34	Selenium	Se			
14	Silicon	Si	σ_t		420, 421
47	Silver	Ag	σ_t	σ_t, σ_r	454, 455
11	Sodium	Na		σ_t	414, 415
38	Strontium	Sr			
16	Sulphur	S	σ_t	$\sigma_t, \sigma_p, \sigma_a$	424, 425
73	Tantalum	Ta	σ_t		478, 479
43	Technetium	Tc			
52	Tellurium	Te			
65	Terbium	Tb			
81	Thallium	Tl	σ_t		494, 495
90	Thorium	Th			
69	Thulium	Tm			
50	Tin	Sn	σ_t	σ_t	460, 461
22	Titanium	Ti			
74	Tungsten	W	σ_t	σ_t	480, 481
92	Uranium	U			
23	Vanadium	V			
54	Xenon	Xe			
70	Ytterbium	Yb			
39	Yttrium	Y			
30	Zinc	Zn	σ_t	σ_t	442, 443
40	Zirconium	Zr	σ_t		446, 447

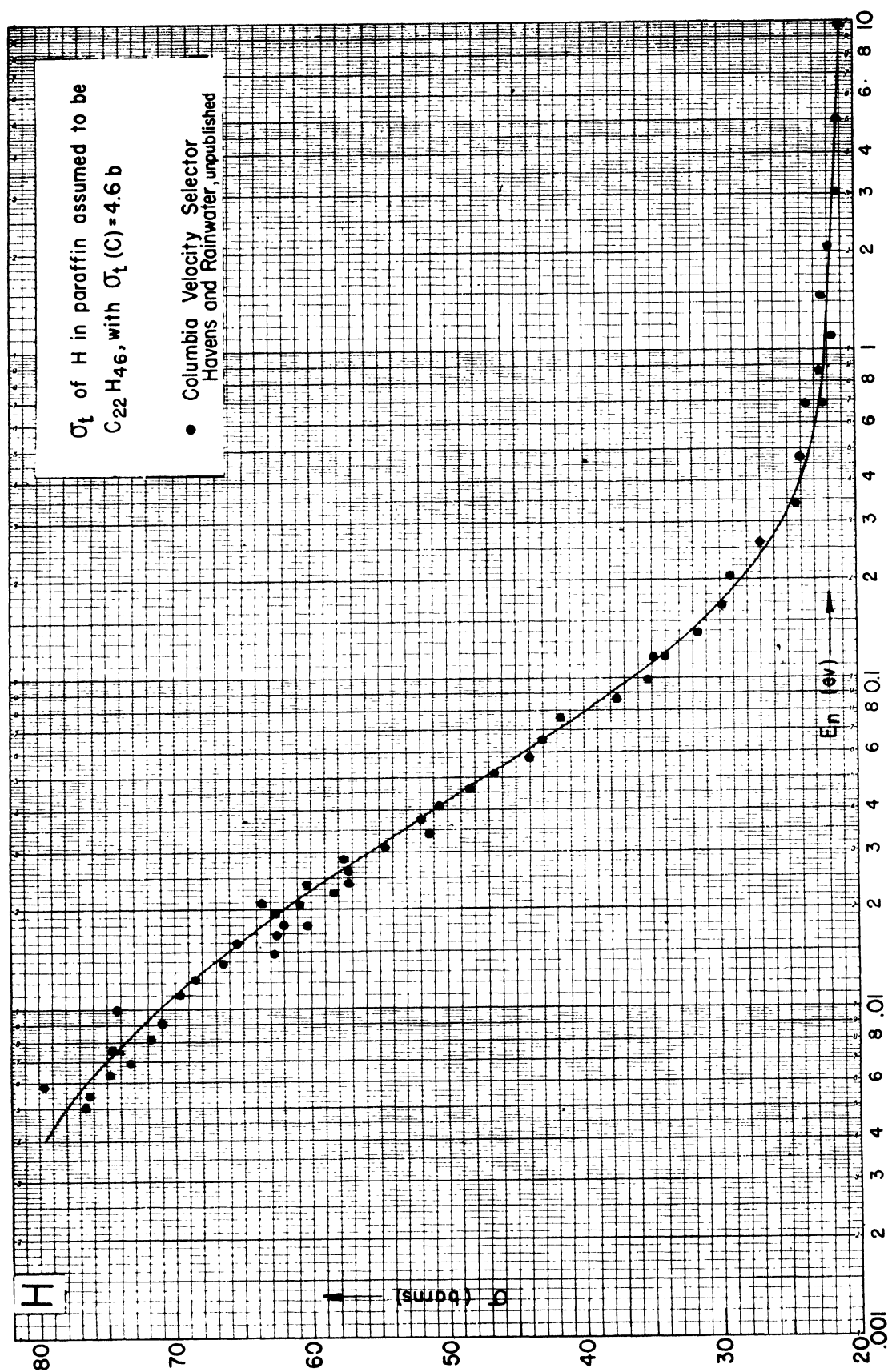
NEUTRON CROSS SECTIONS OF THE ELEMENTS

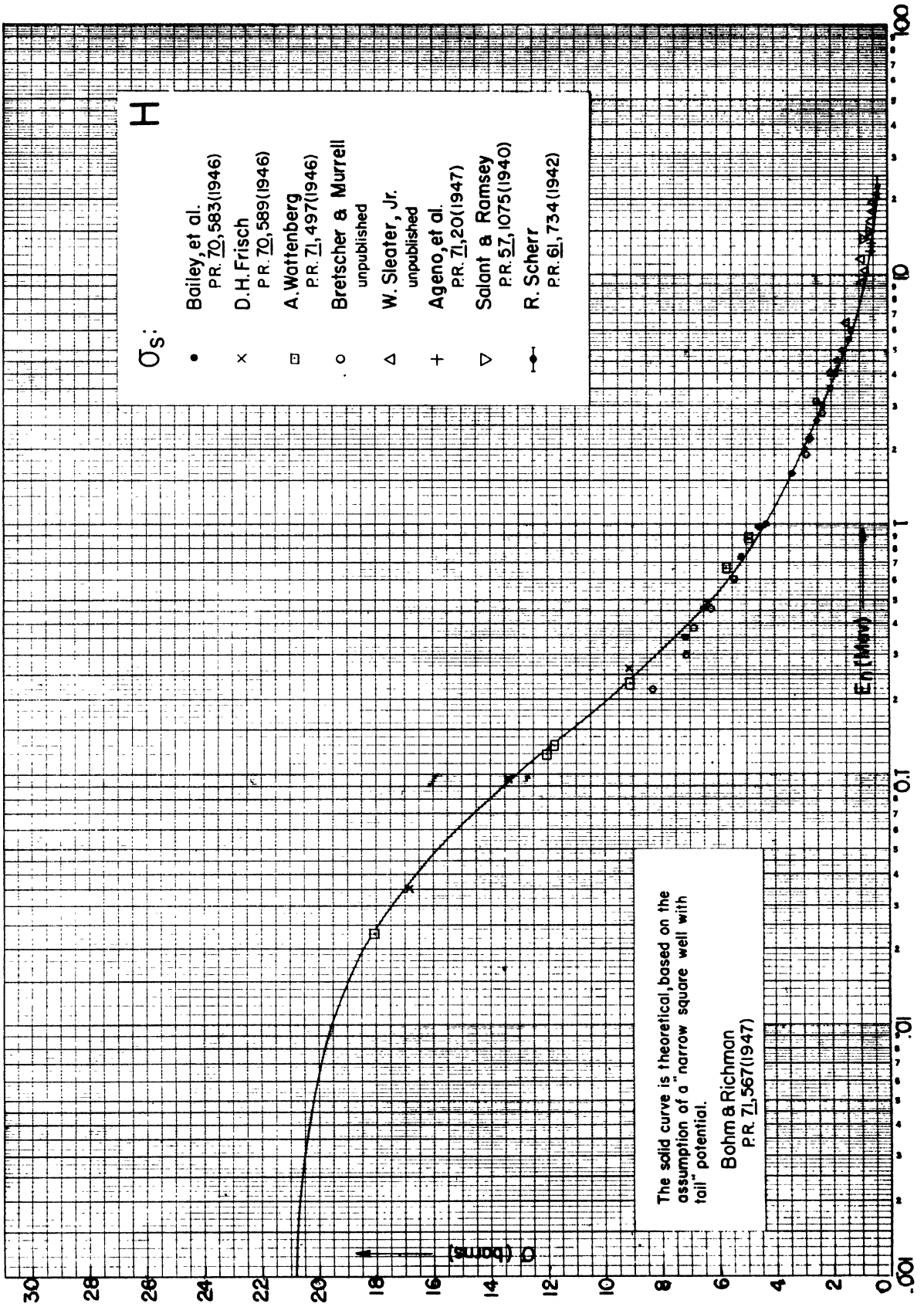
by

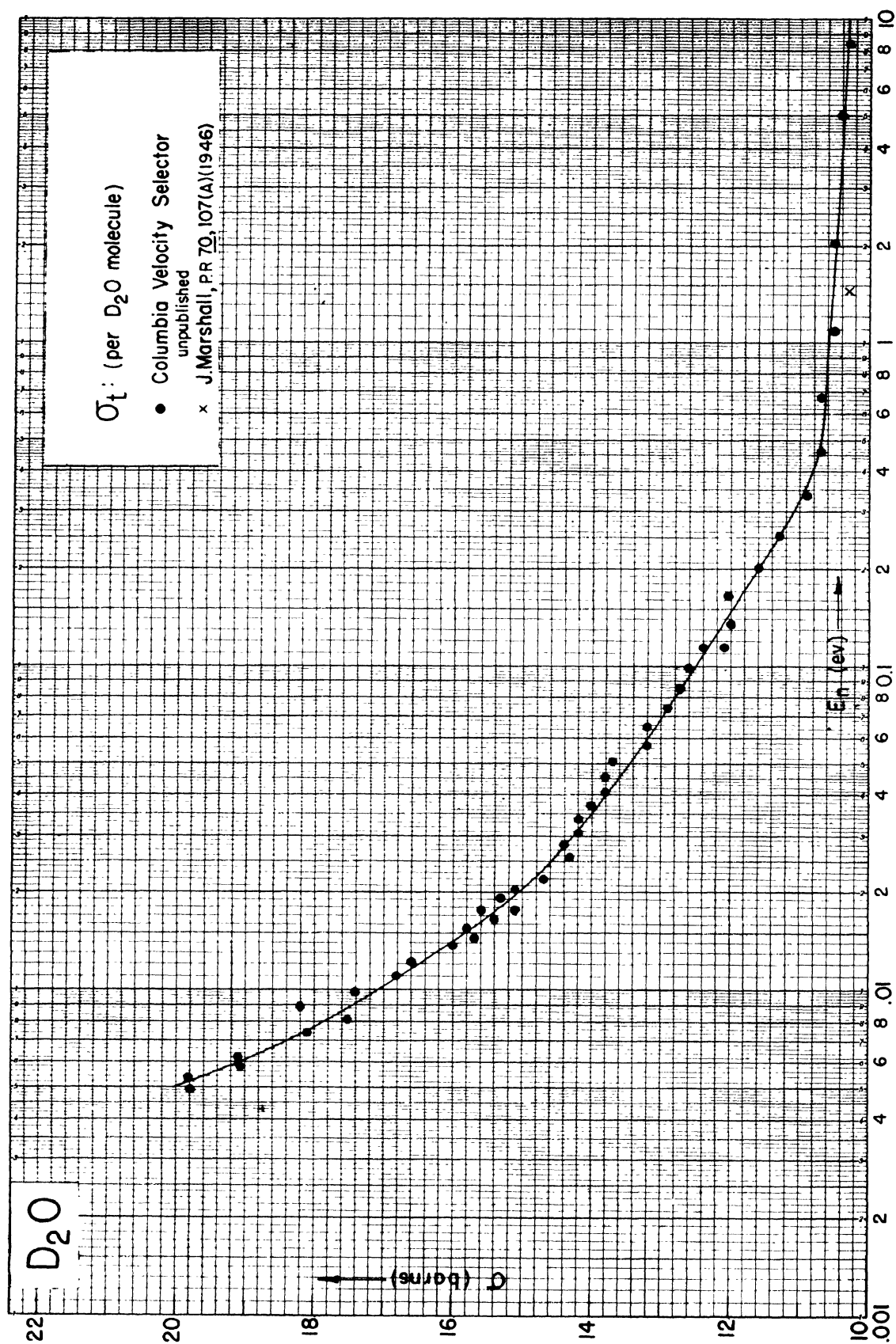
H. H. Goldsmith

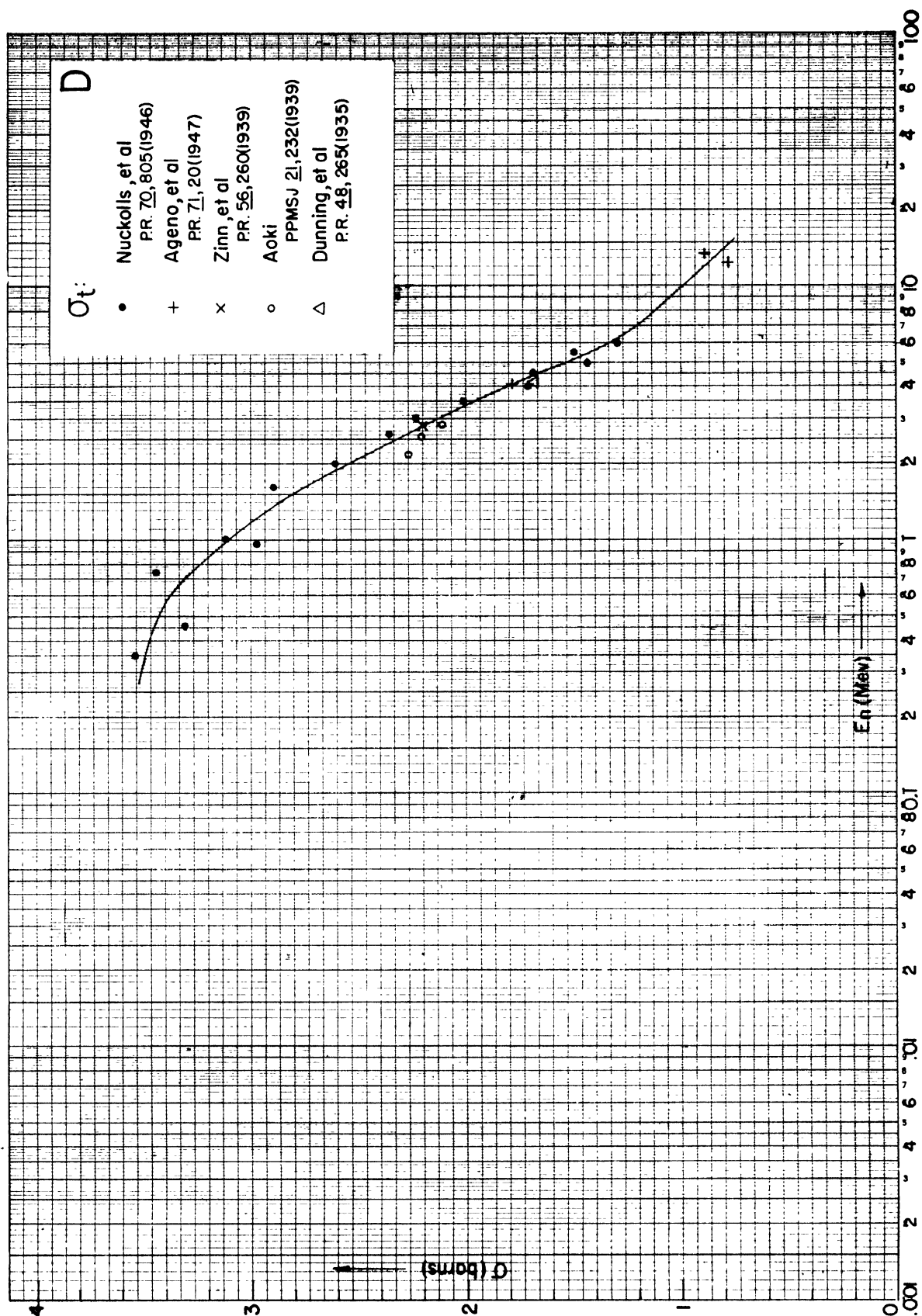
H. W. Ibser

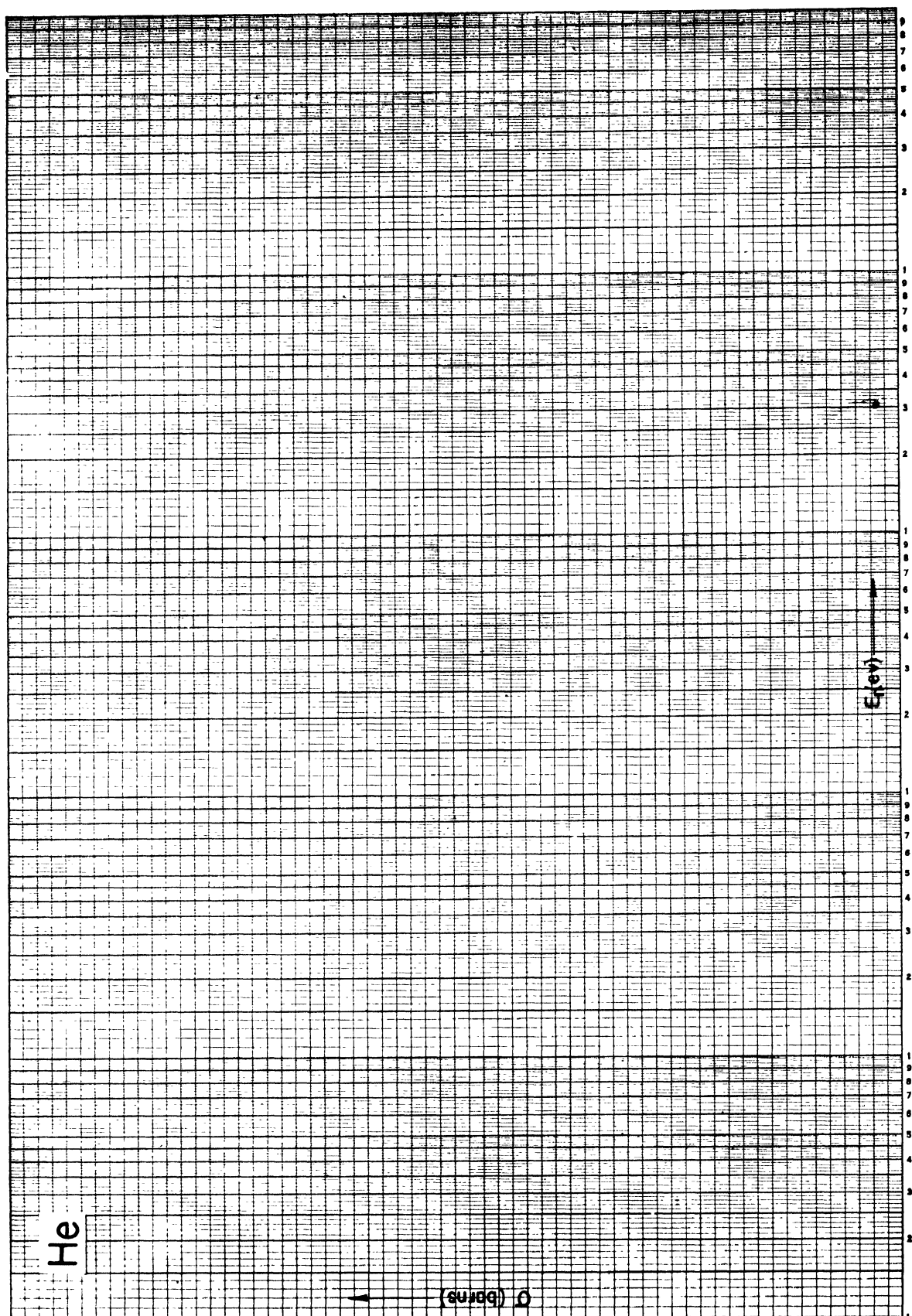
B. T. Feld

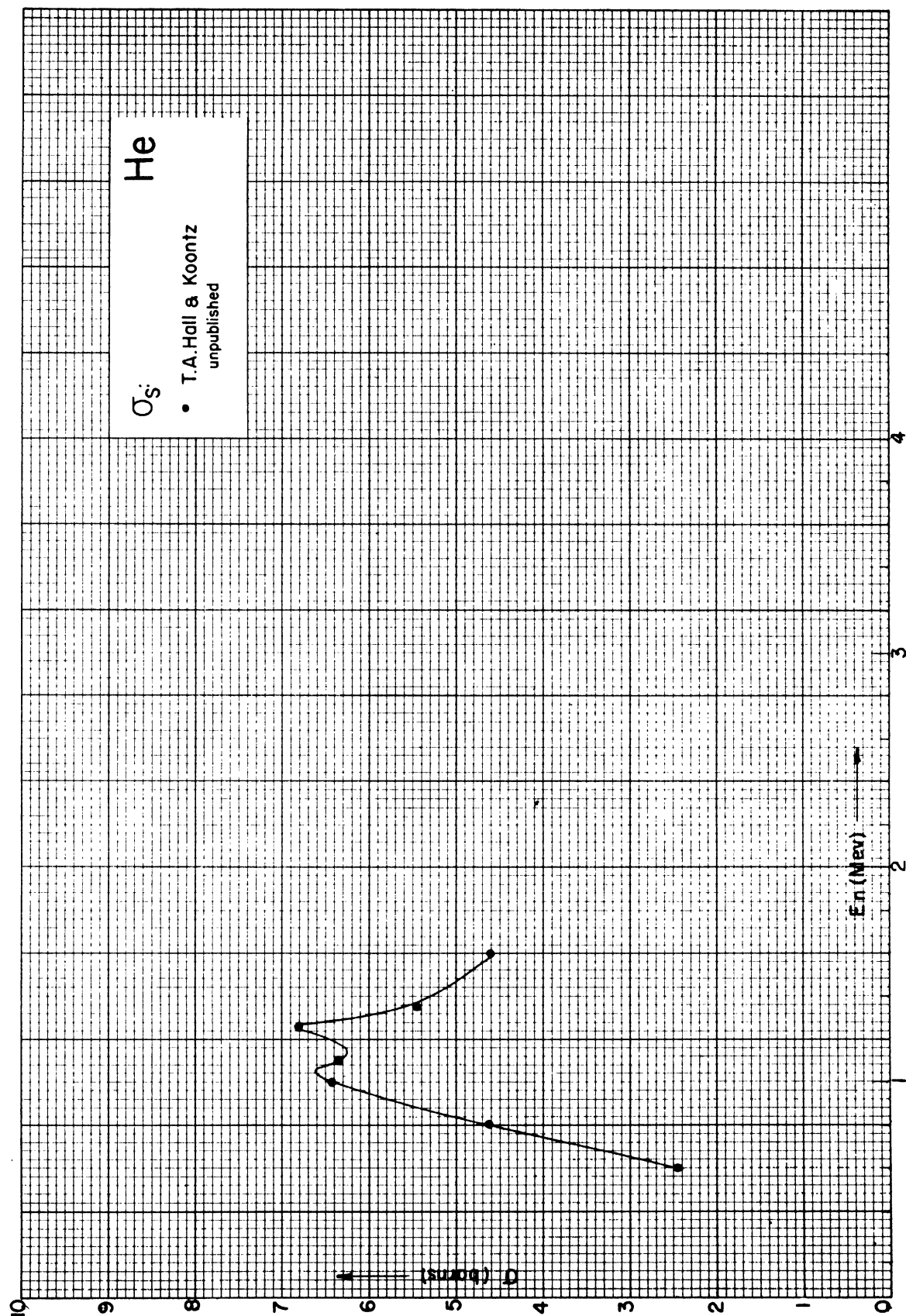


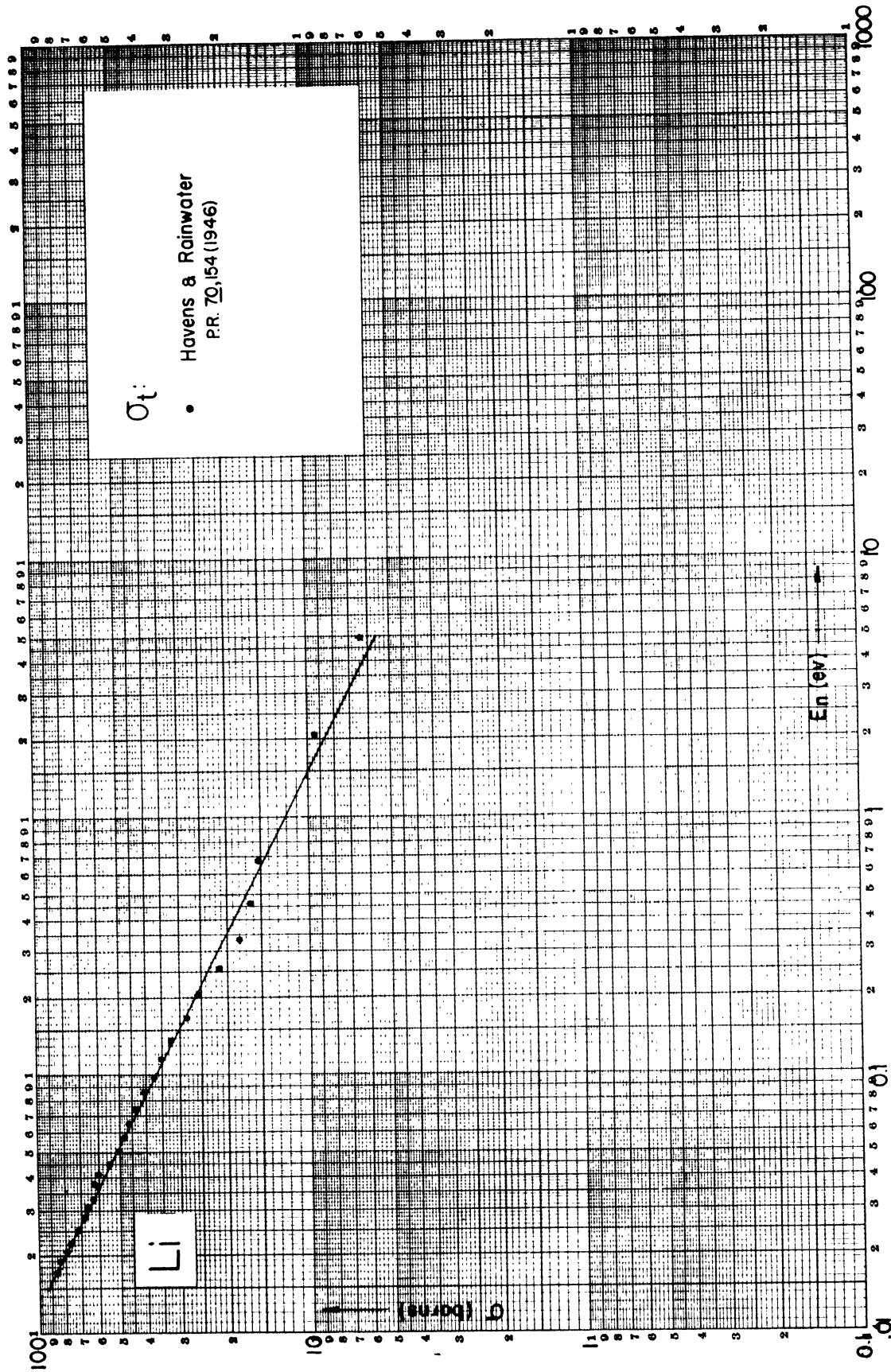


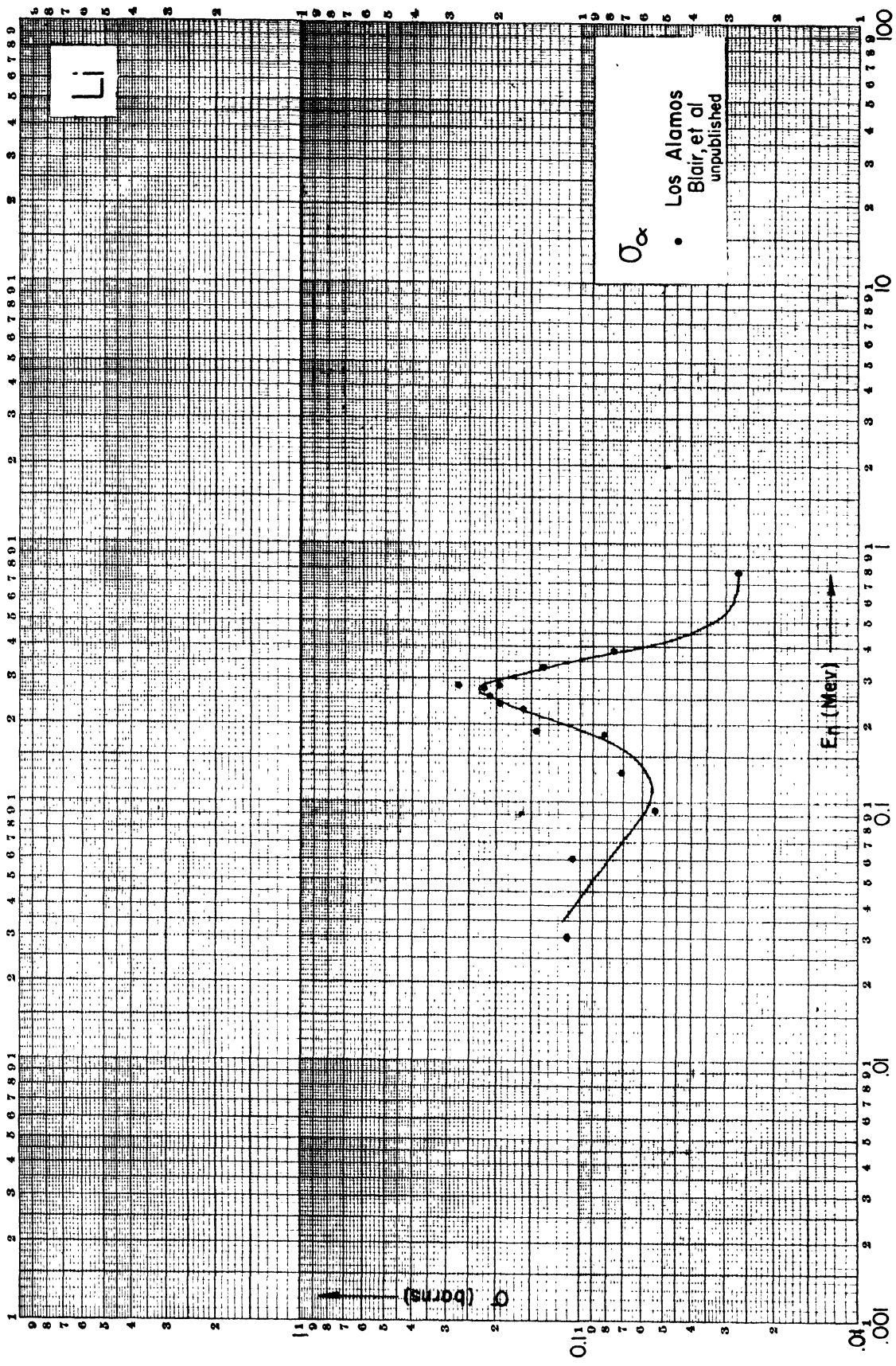


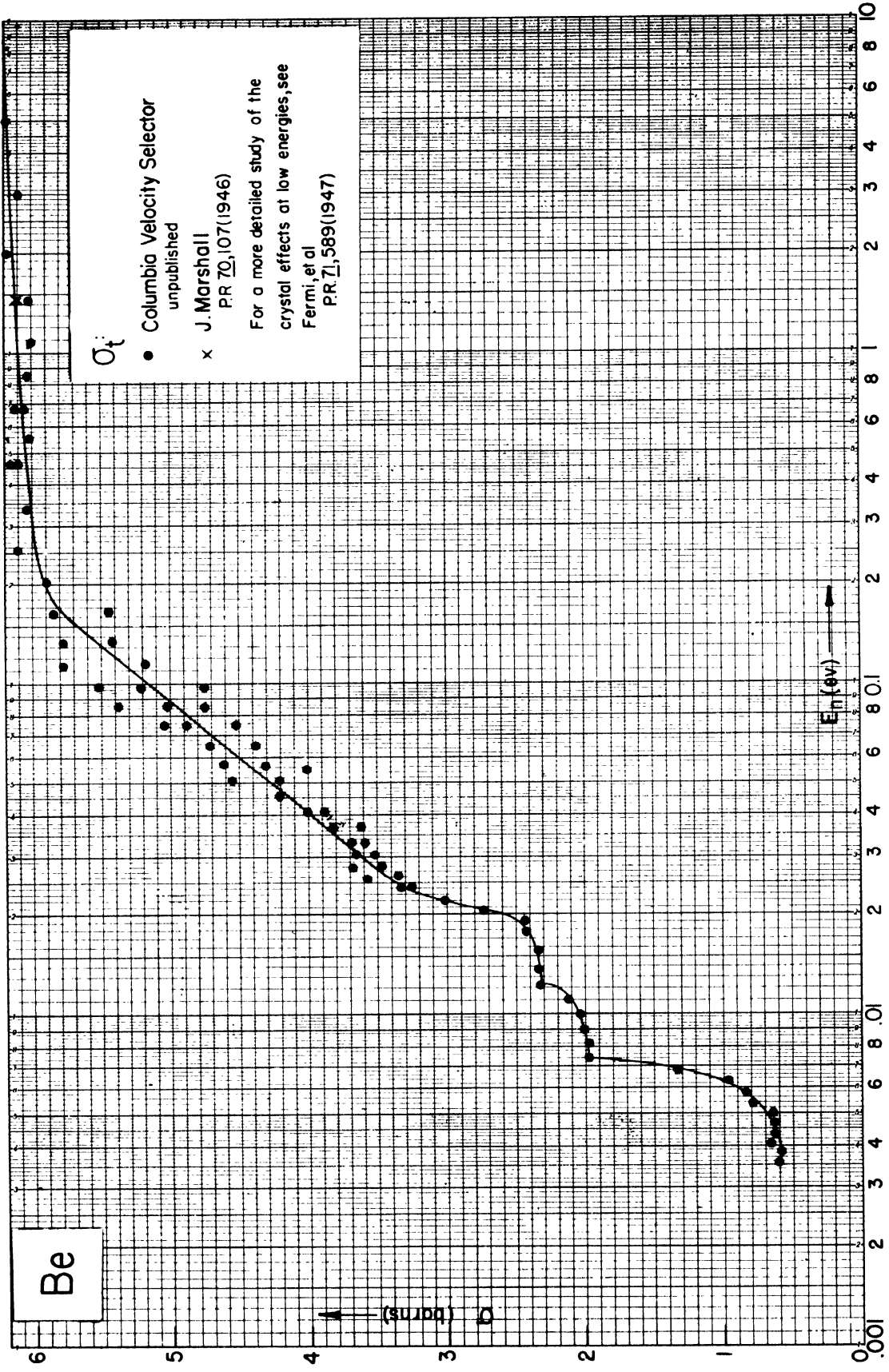








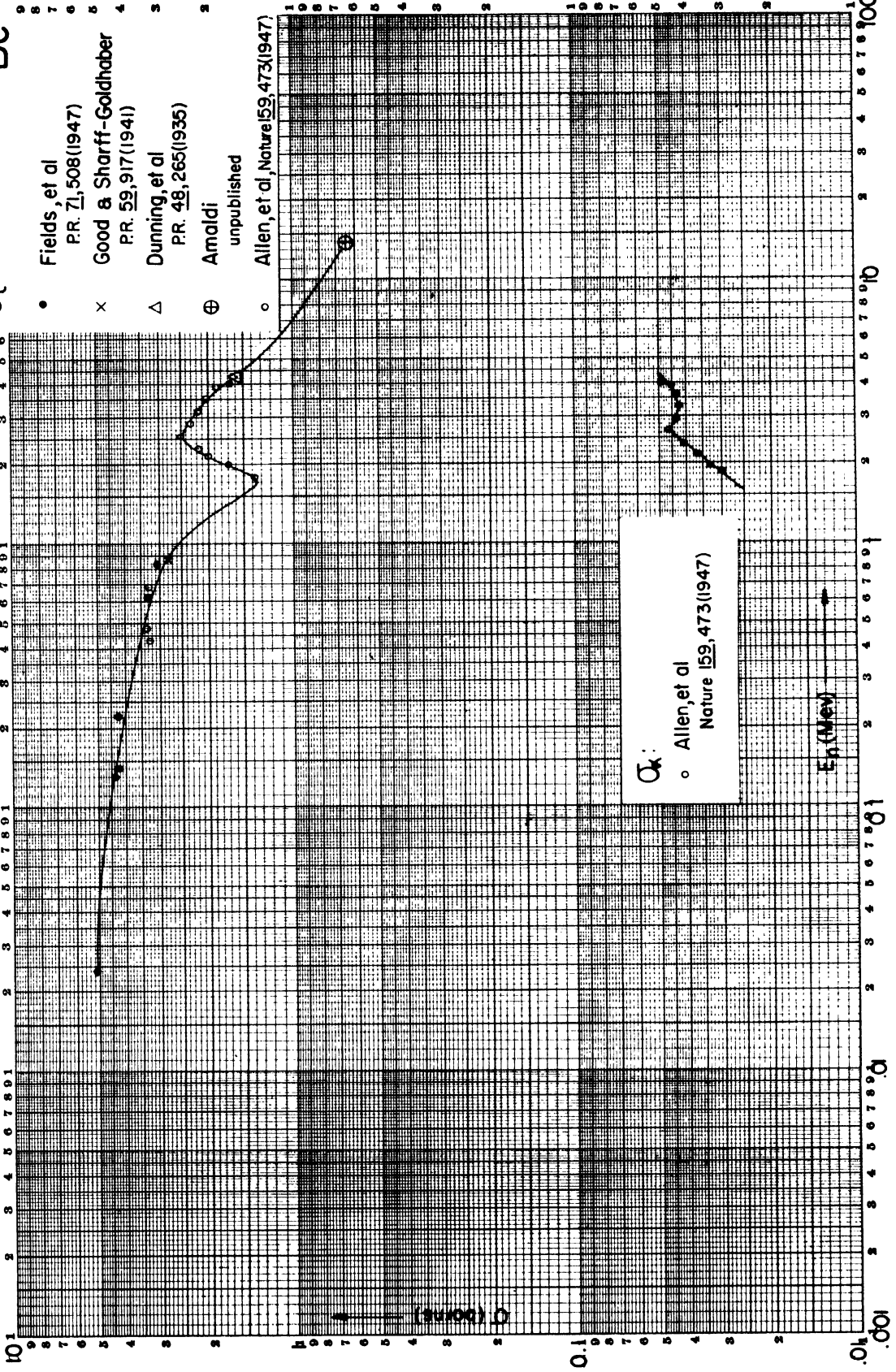


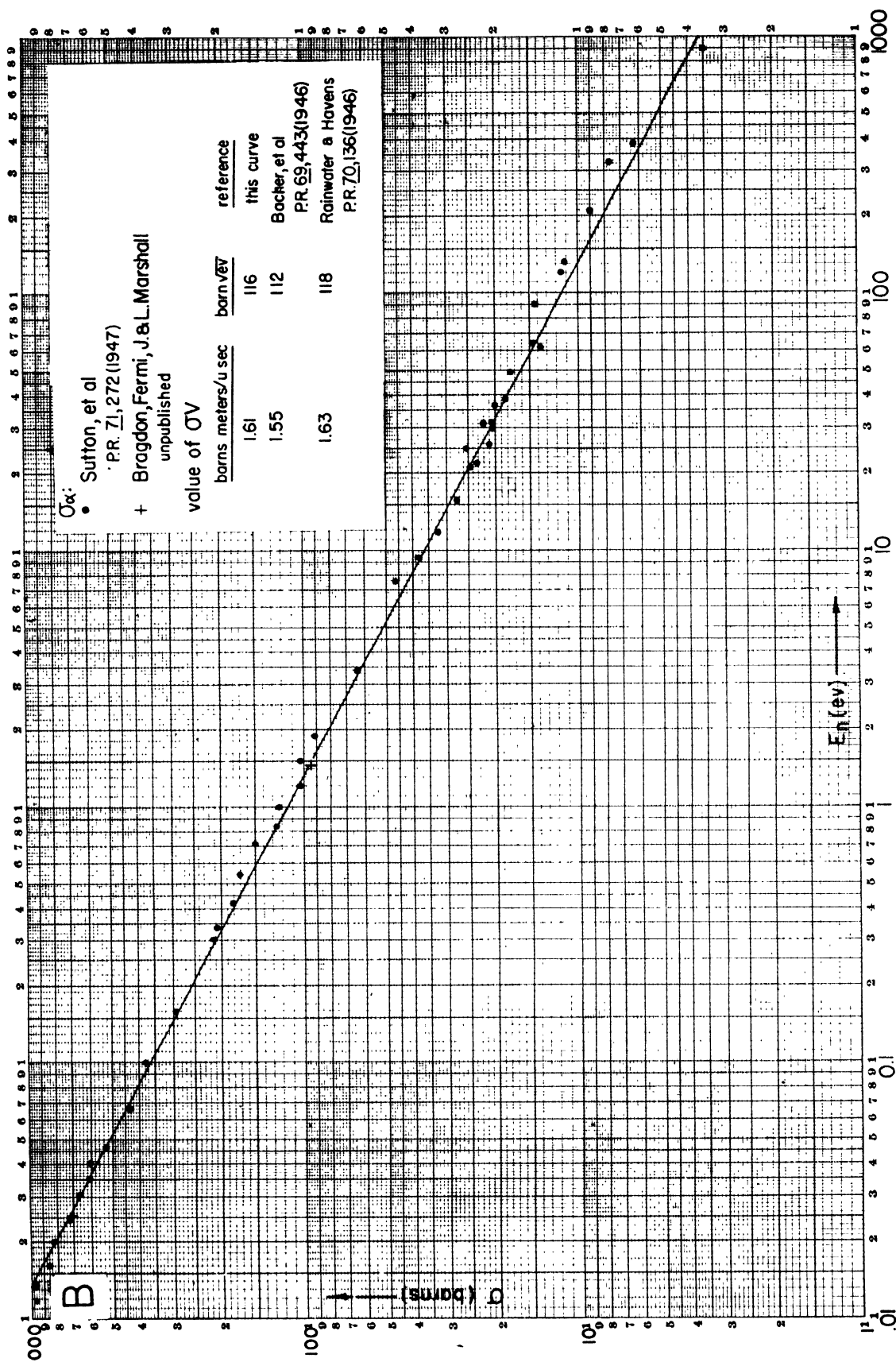


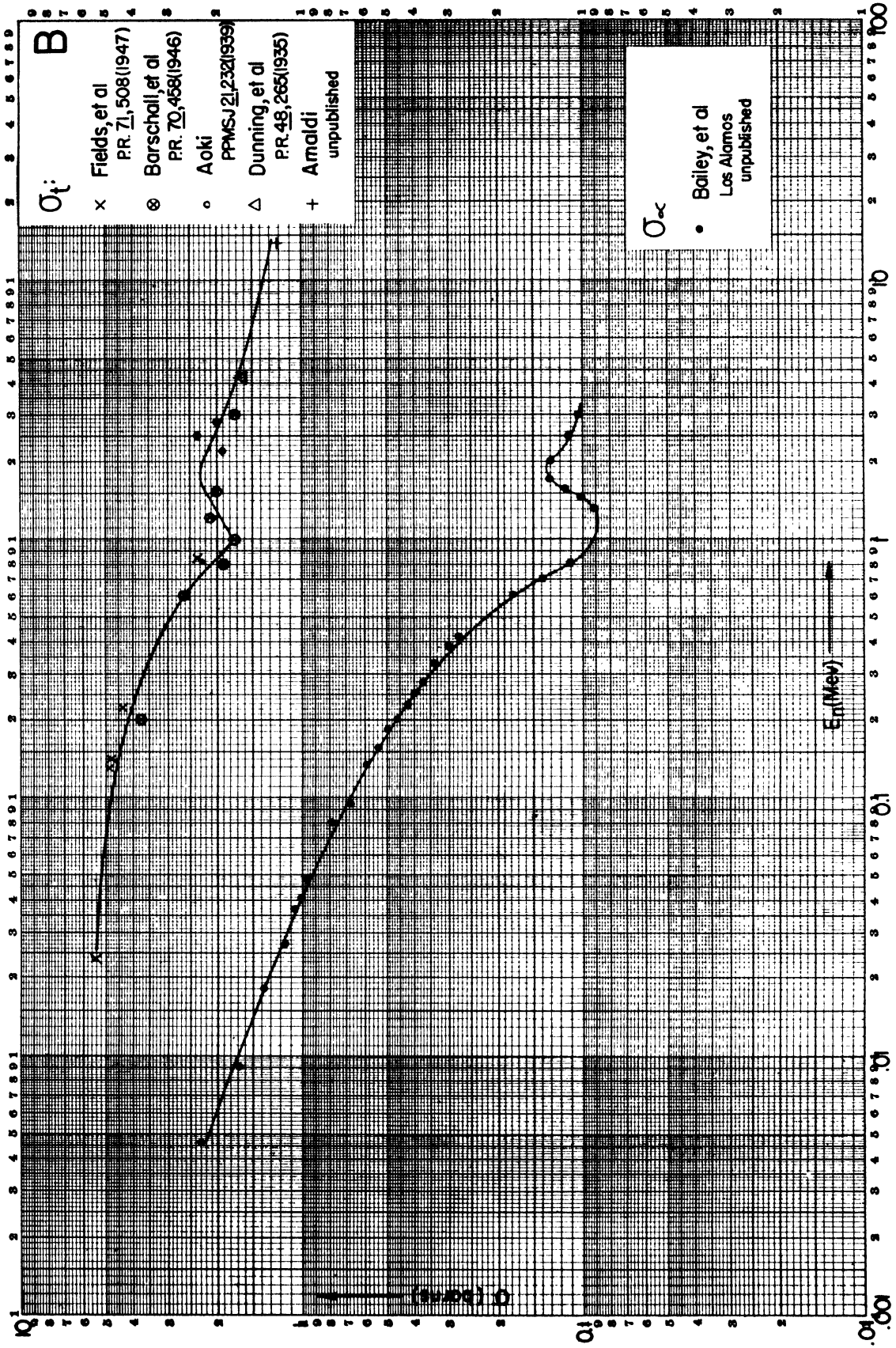
Be

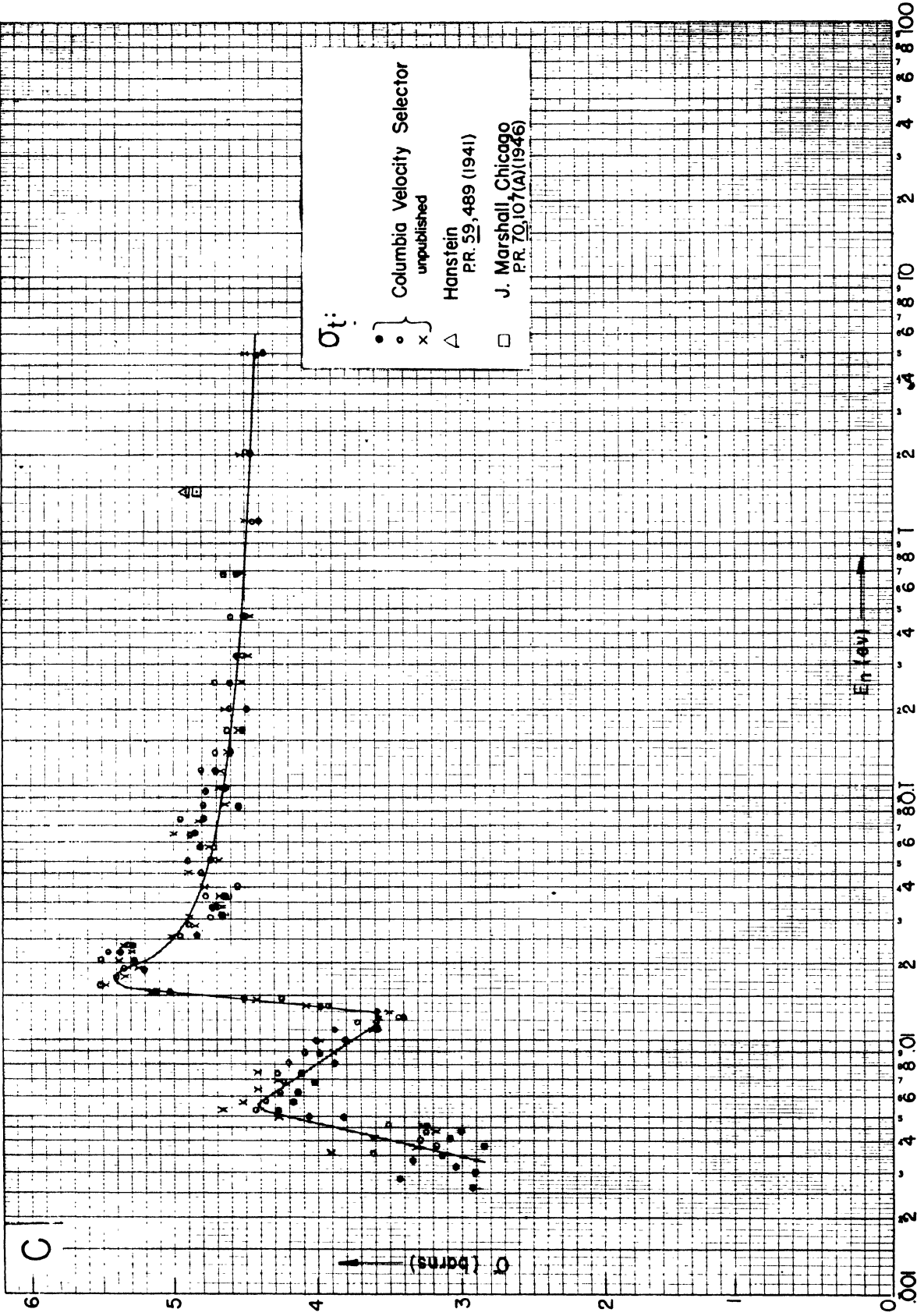
σ_t

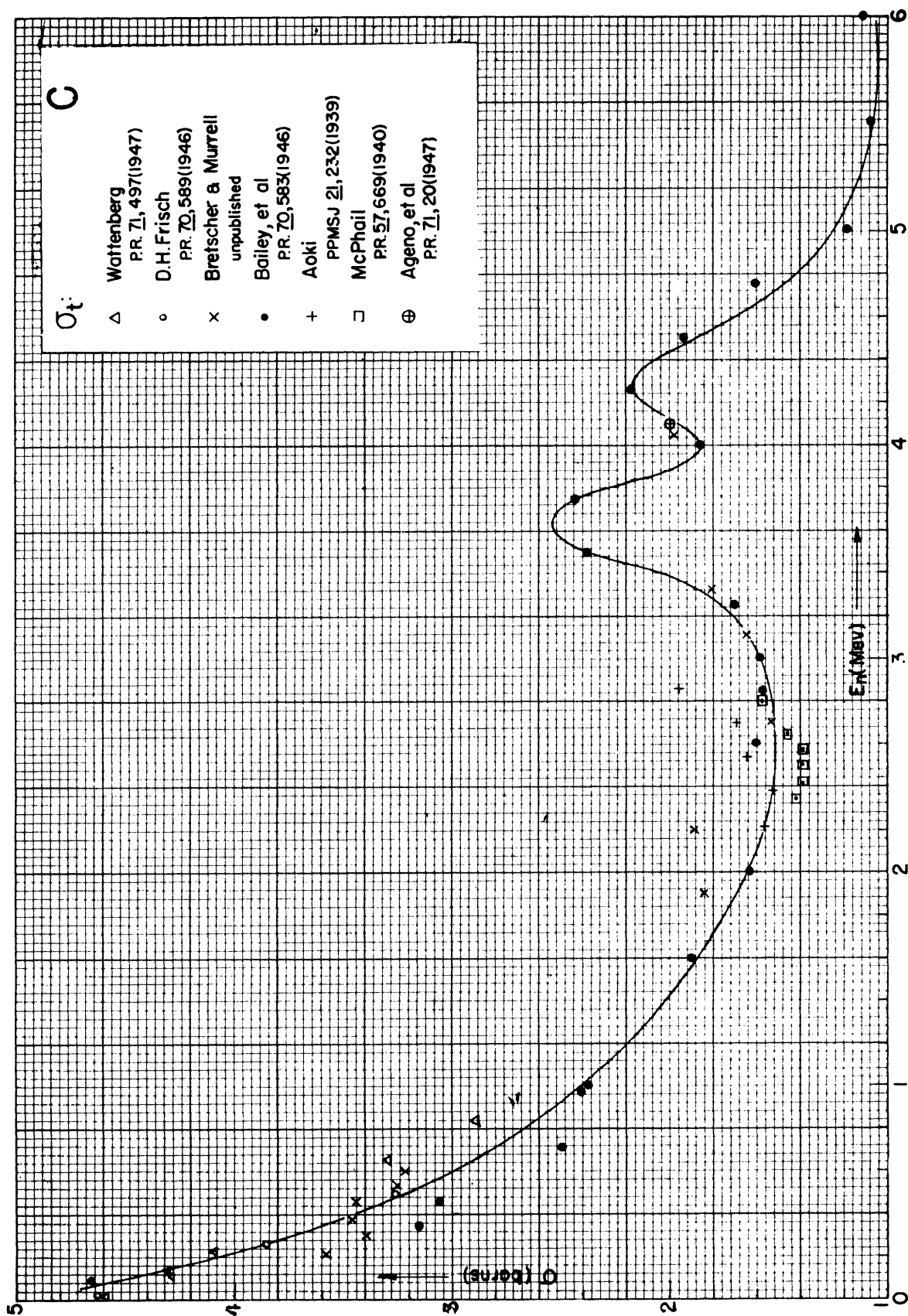
- Fields, et al
PR. 71, 508 (1947)
- × Good & Sharff-Goldhaber
PR. 59, 917 (1941)
- △ Dunning, et al
PR. 48, 265 (1935)
- ⊕ Amaldi
unpublished
- Allen, et al, Nature 159, 473 (1947)

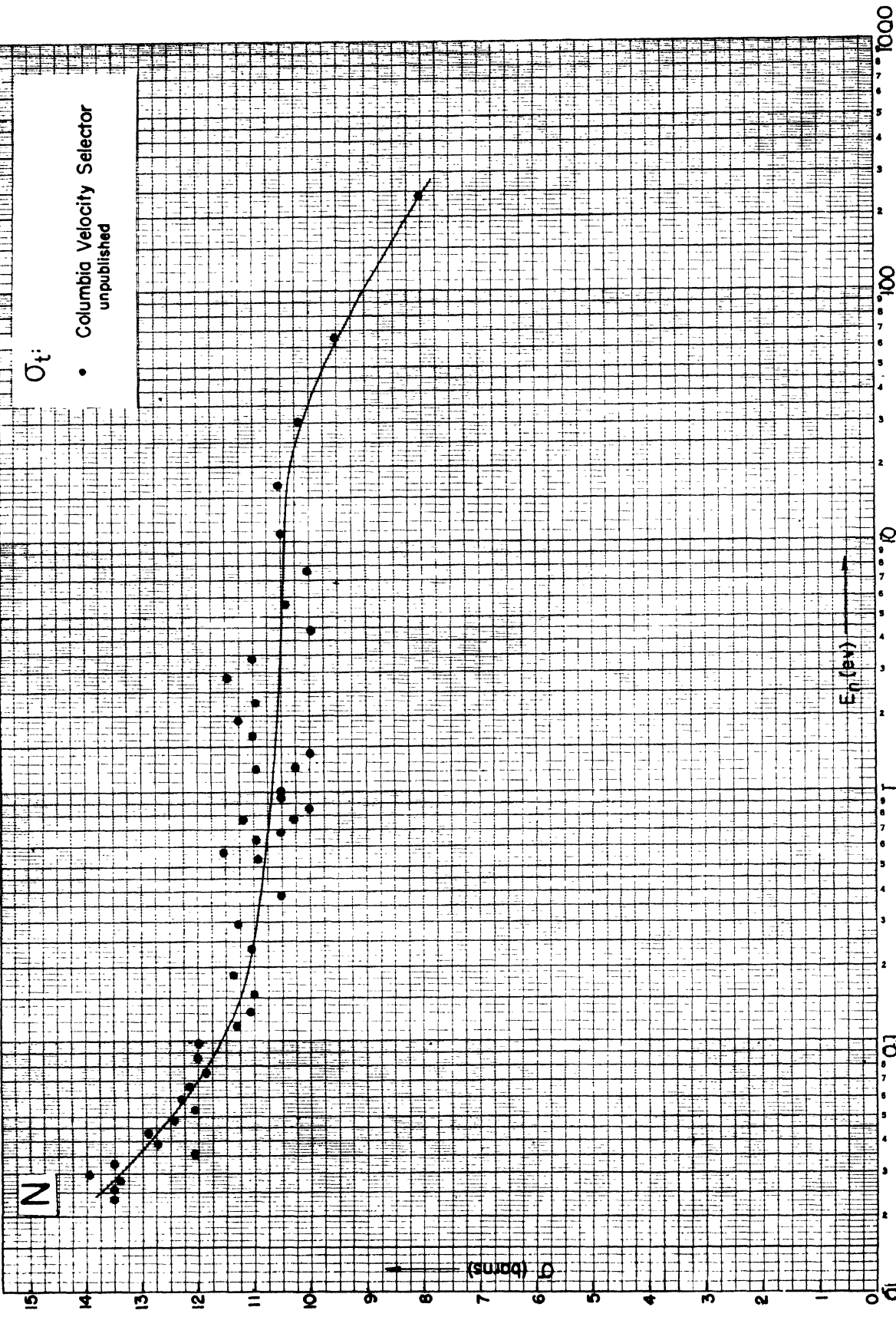


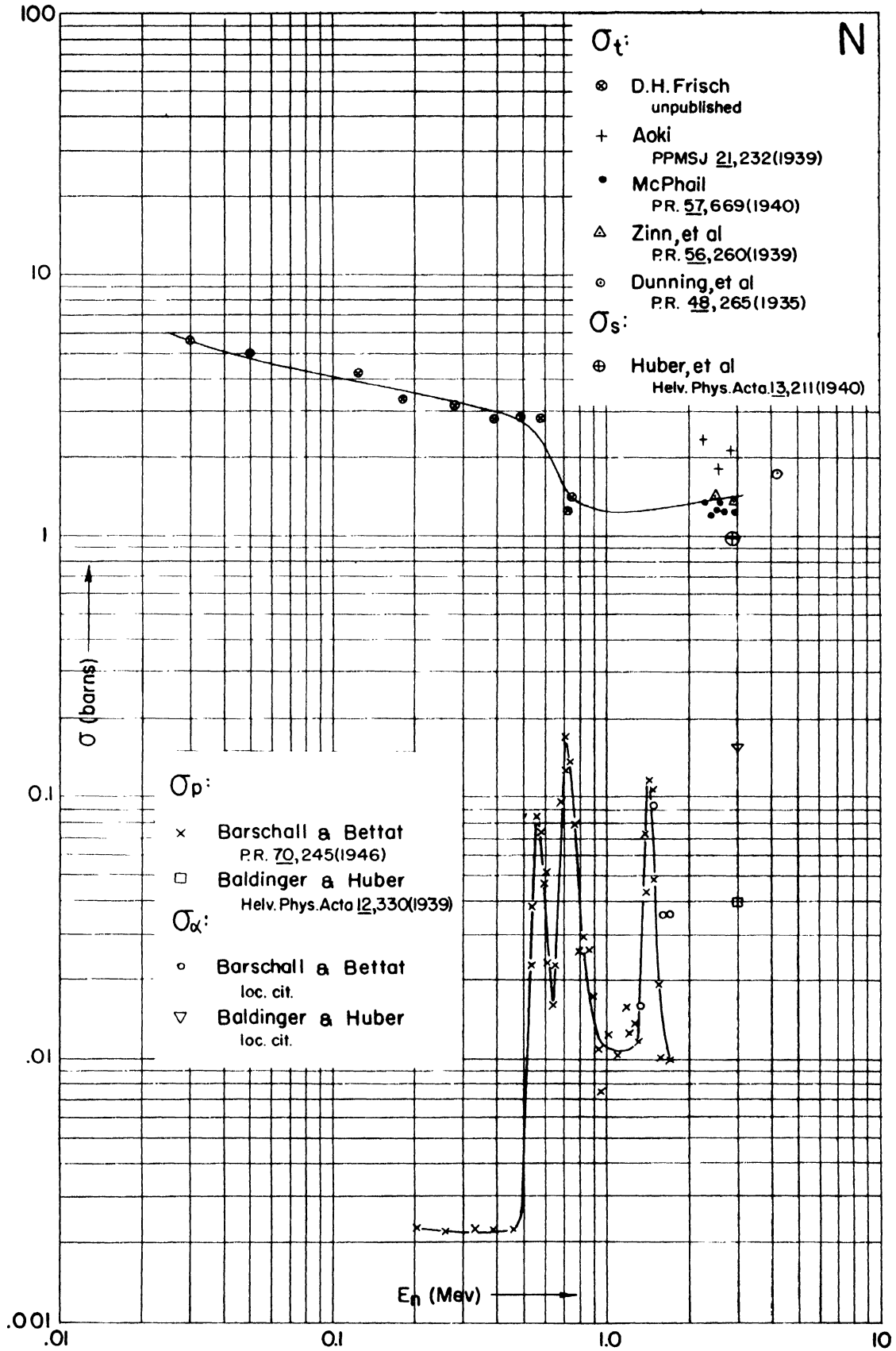


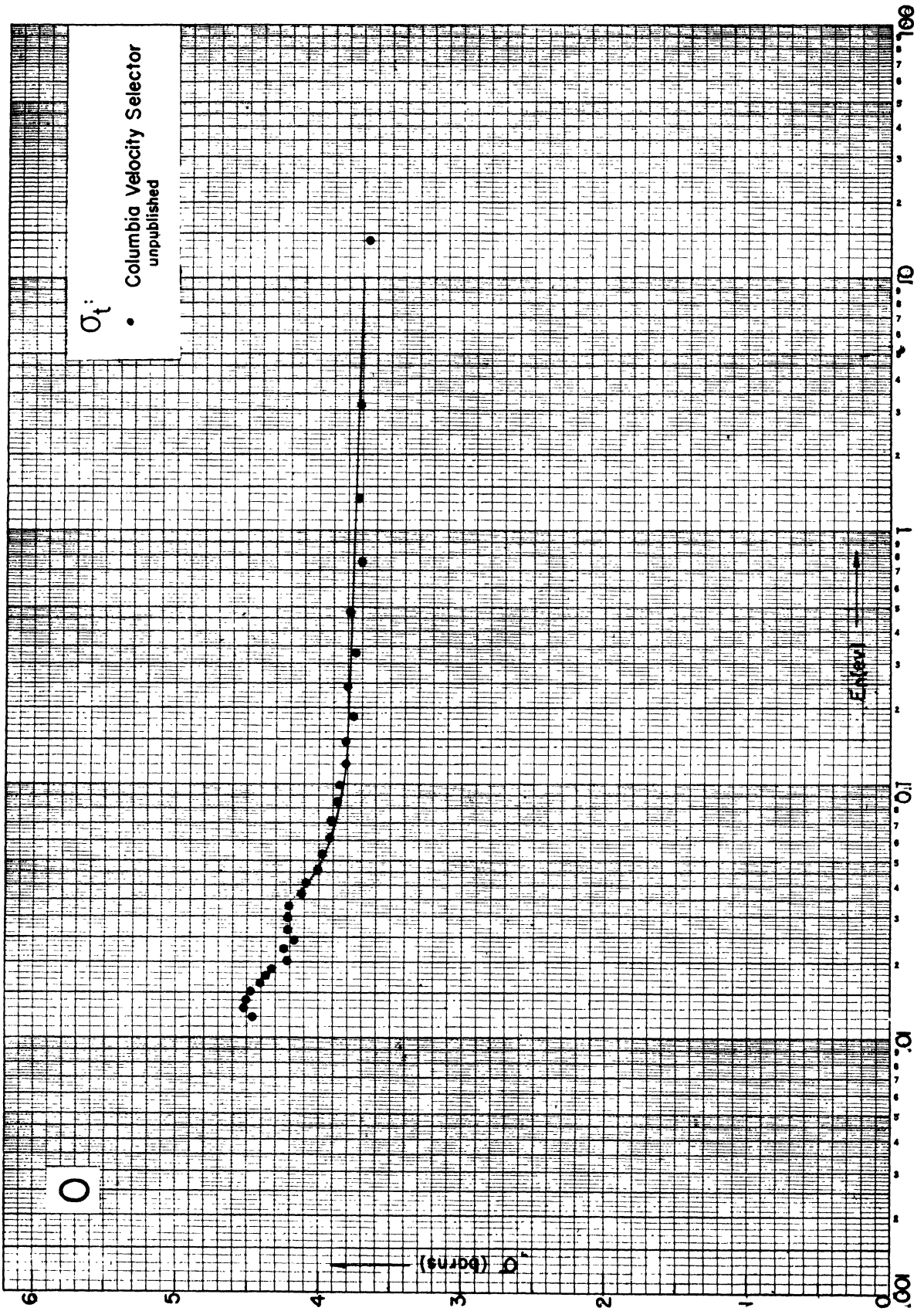


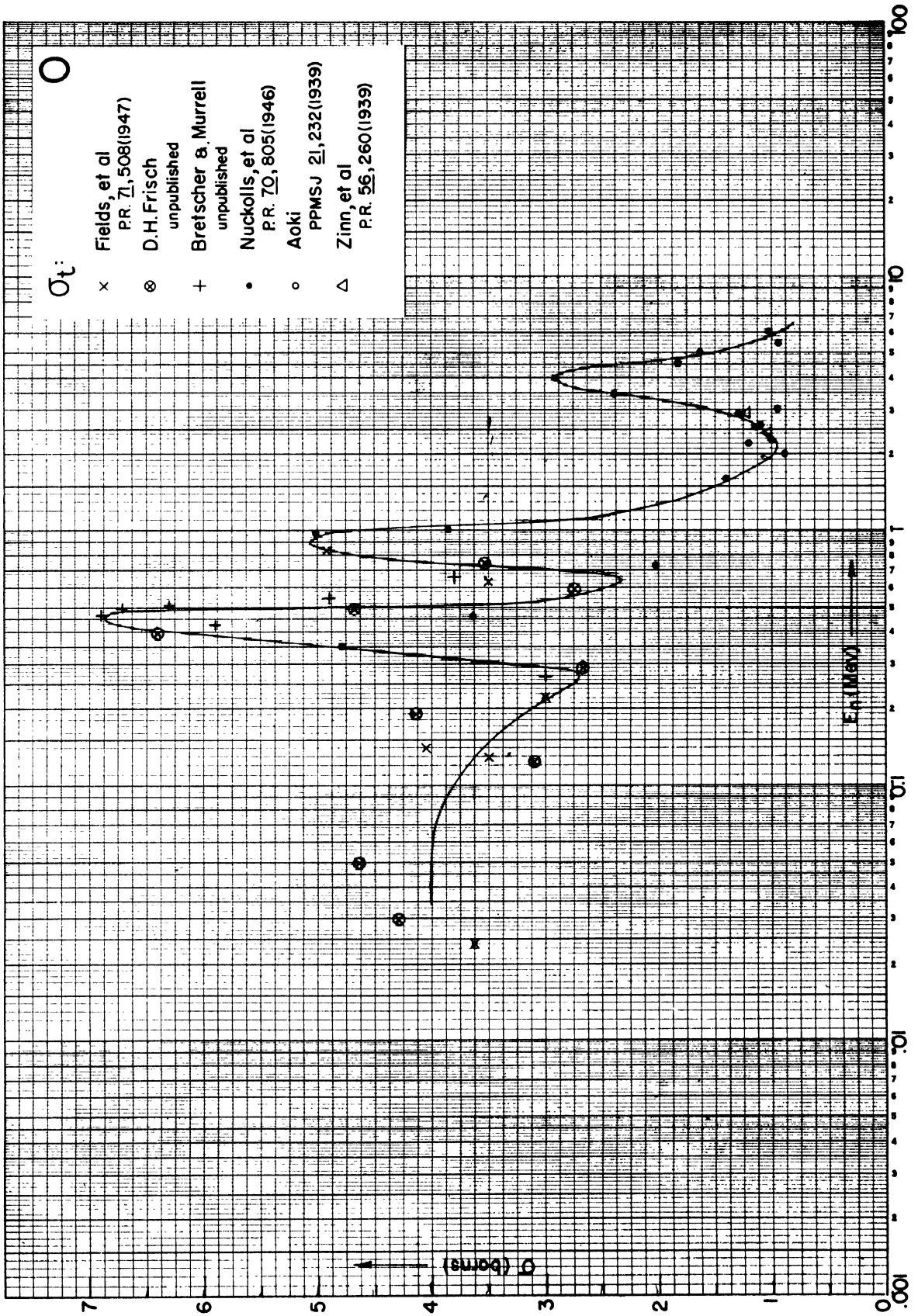


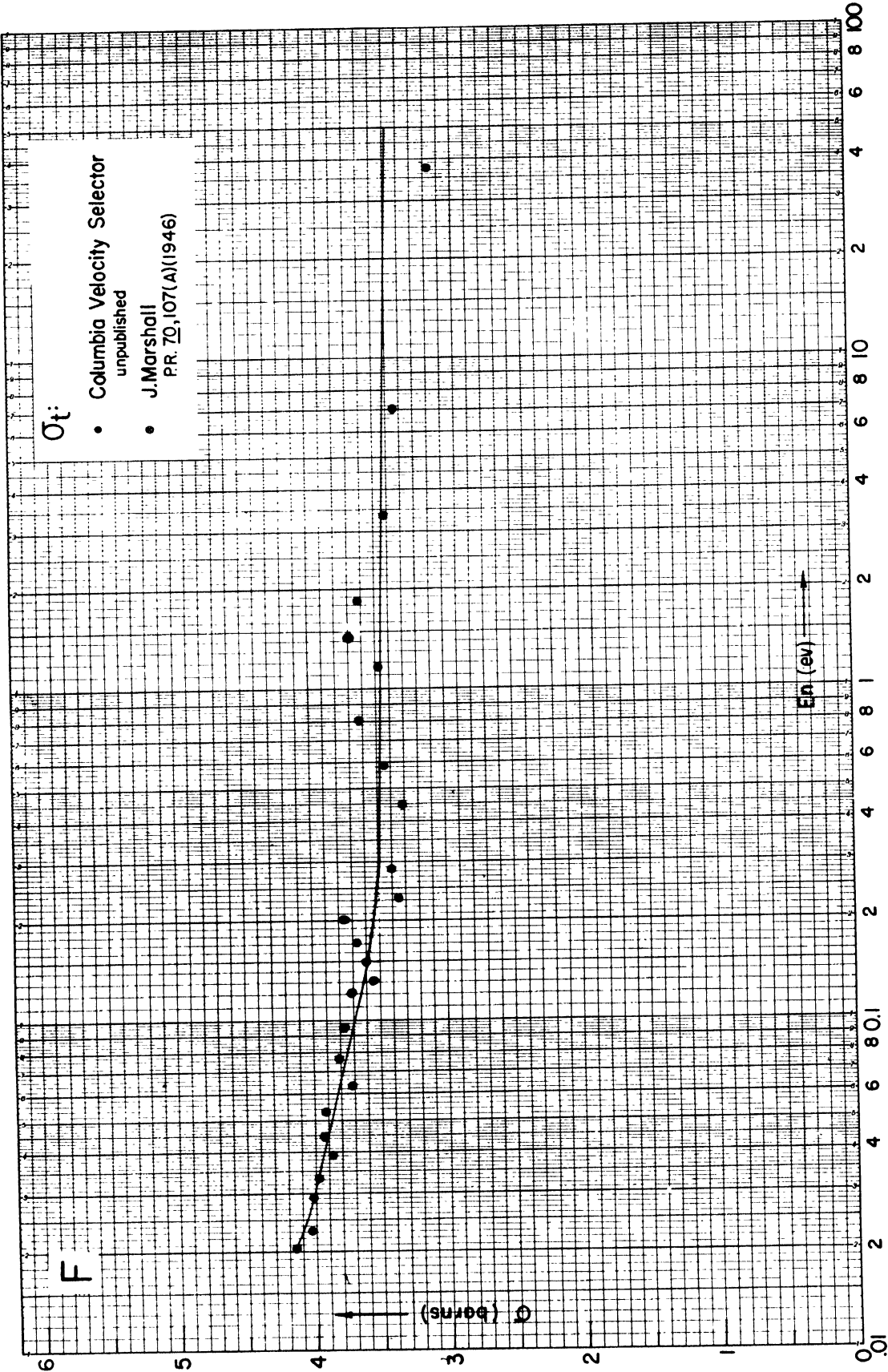


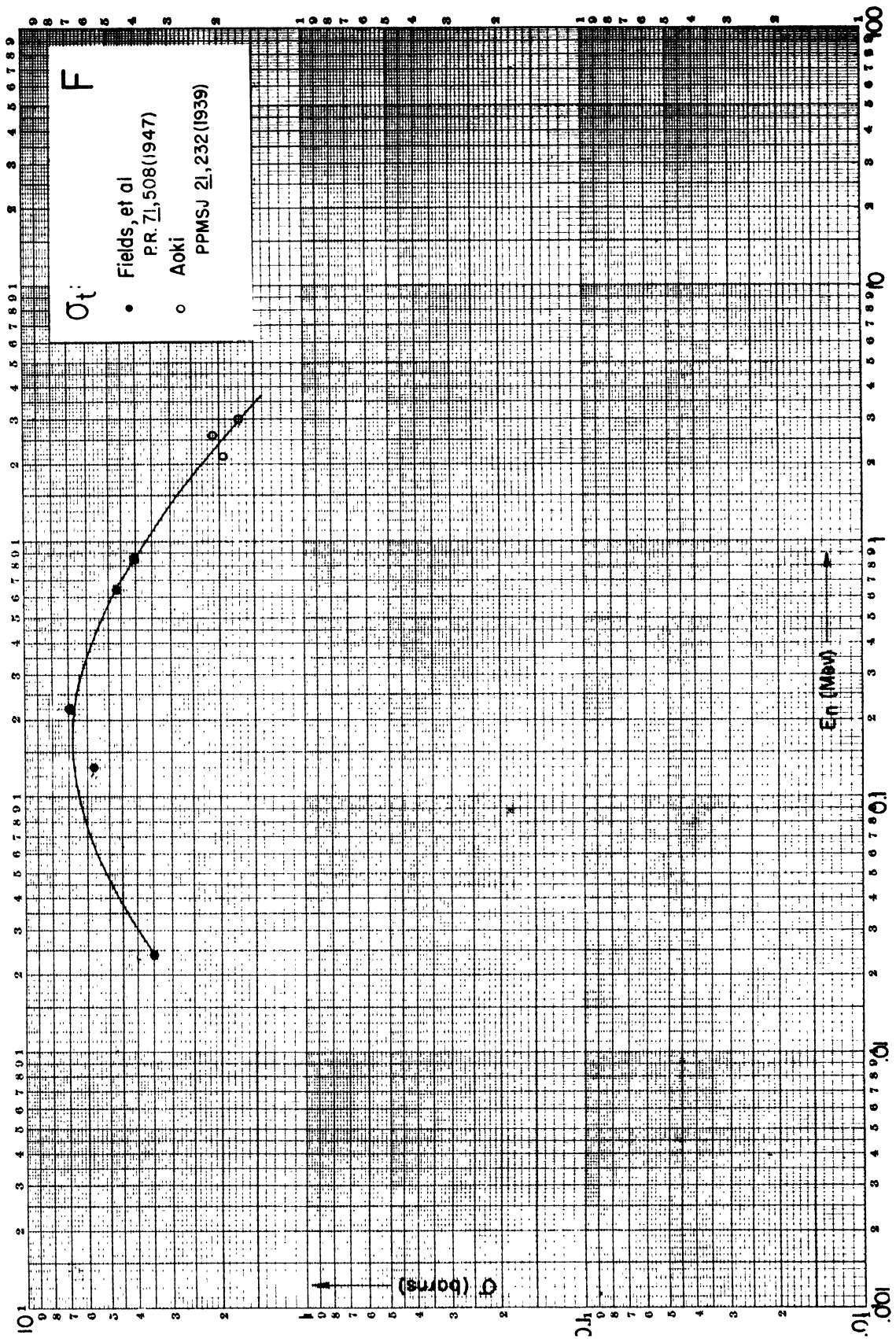








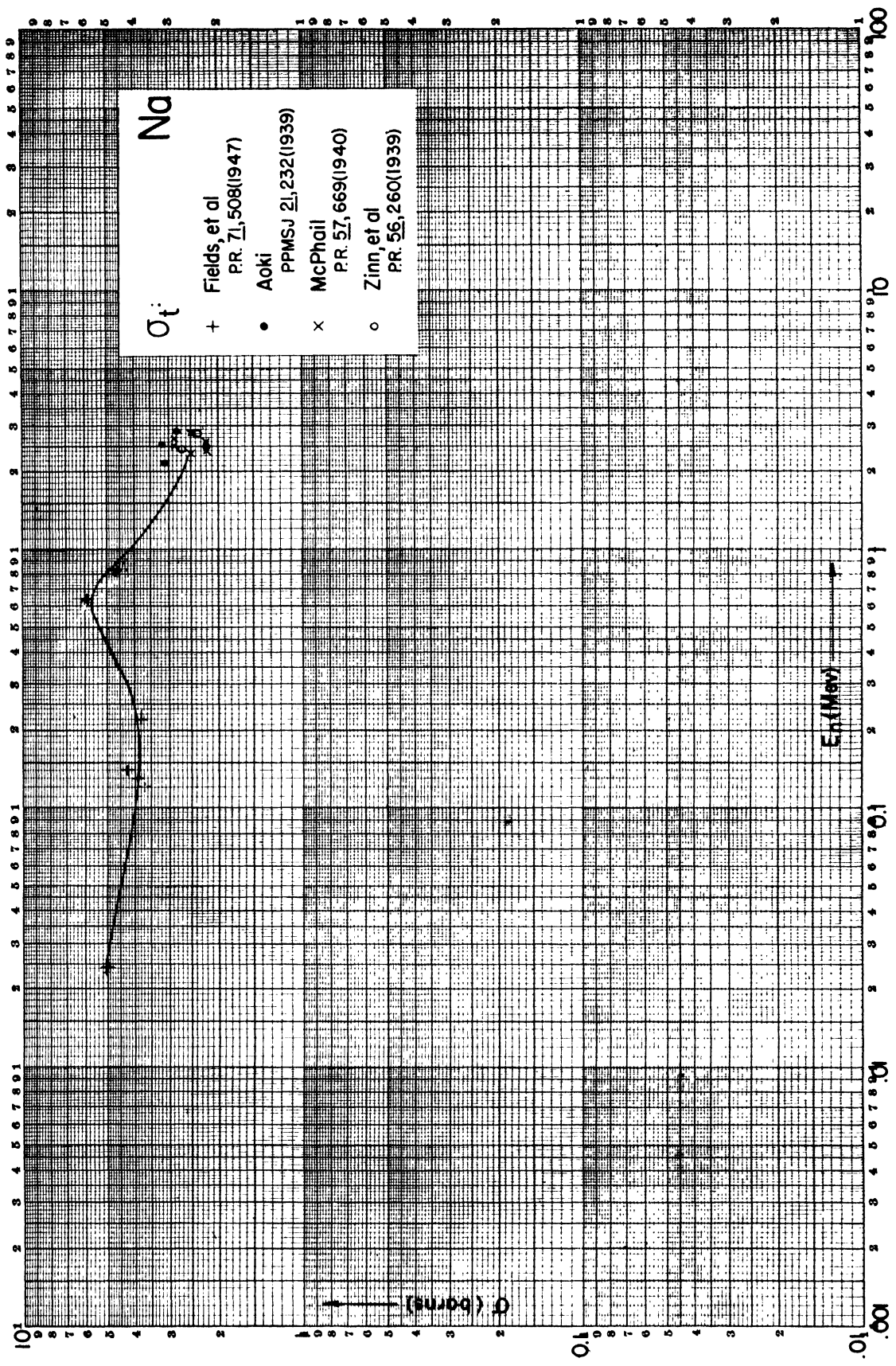


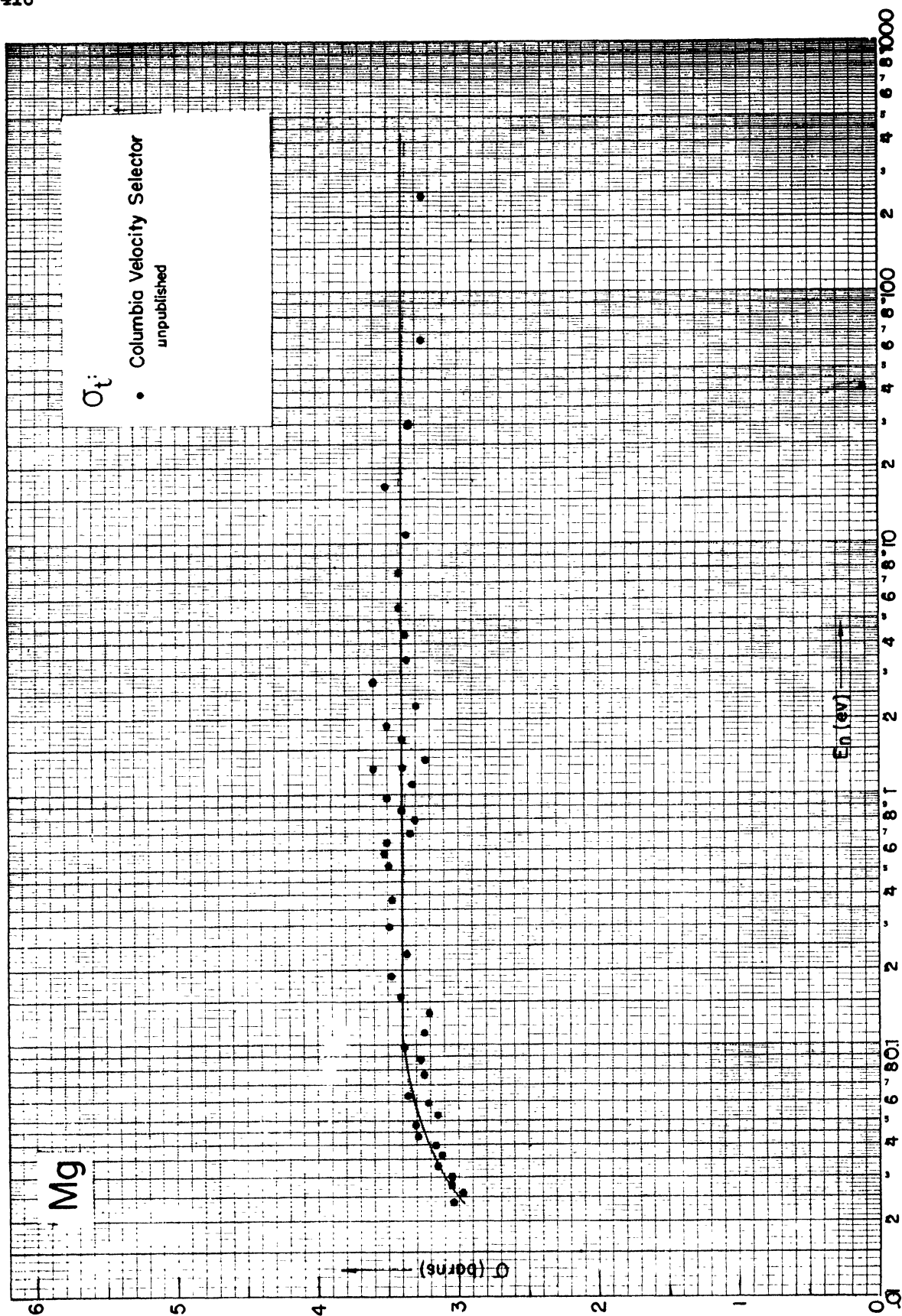


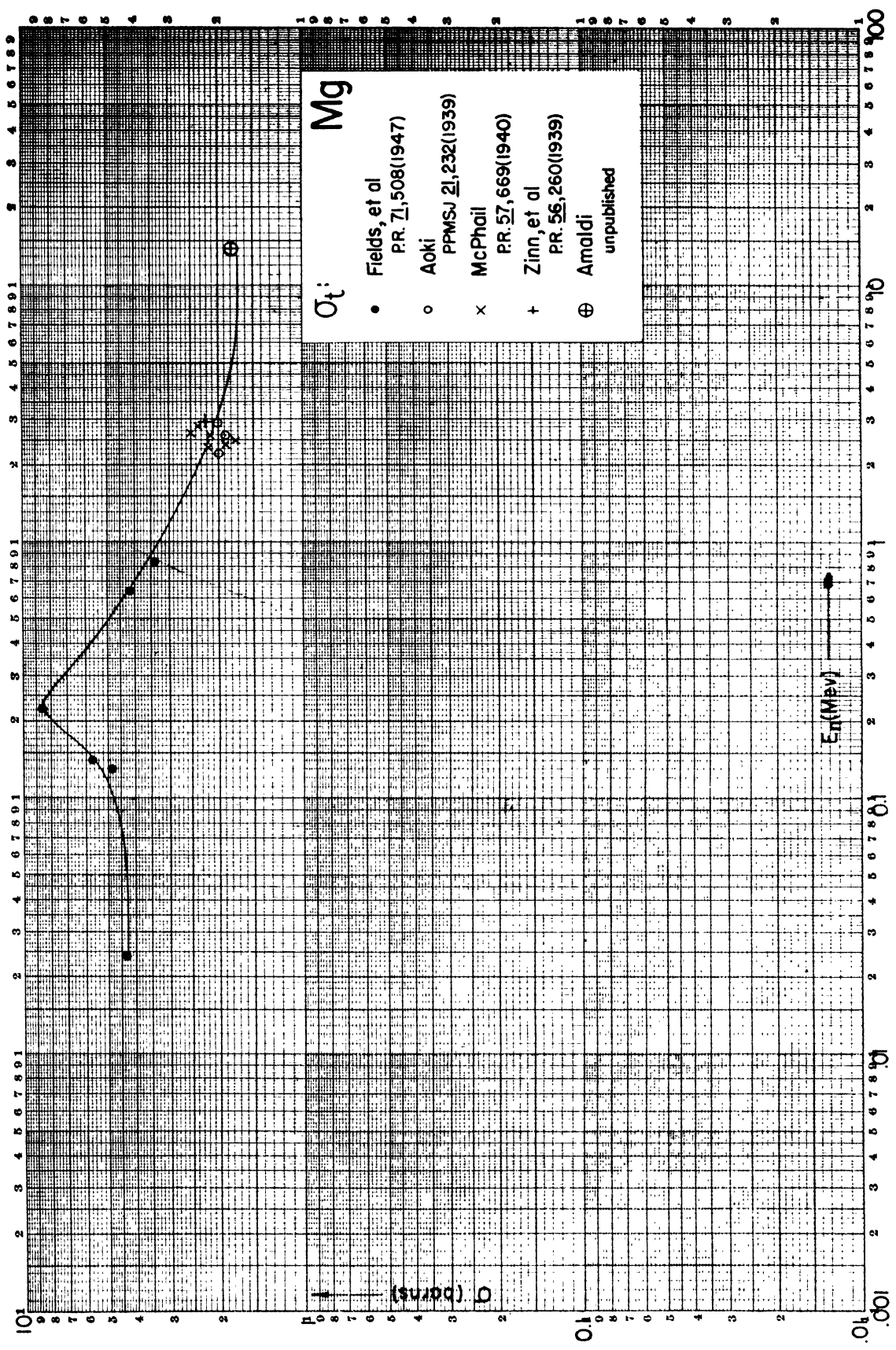
Na

0 (bars)

E_f (eV)







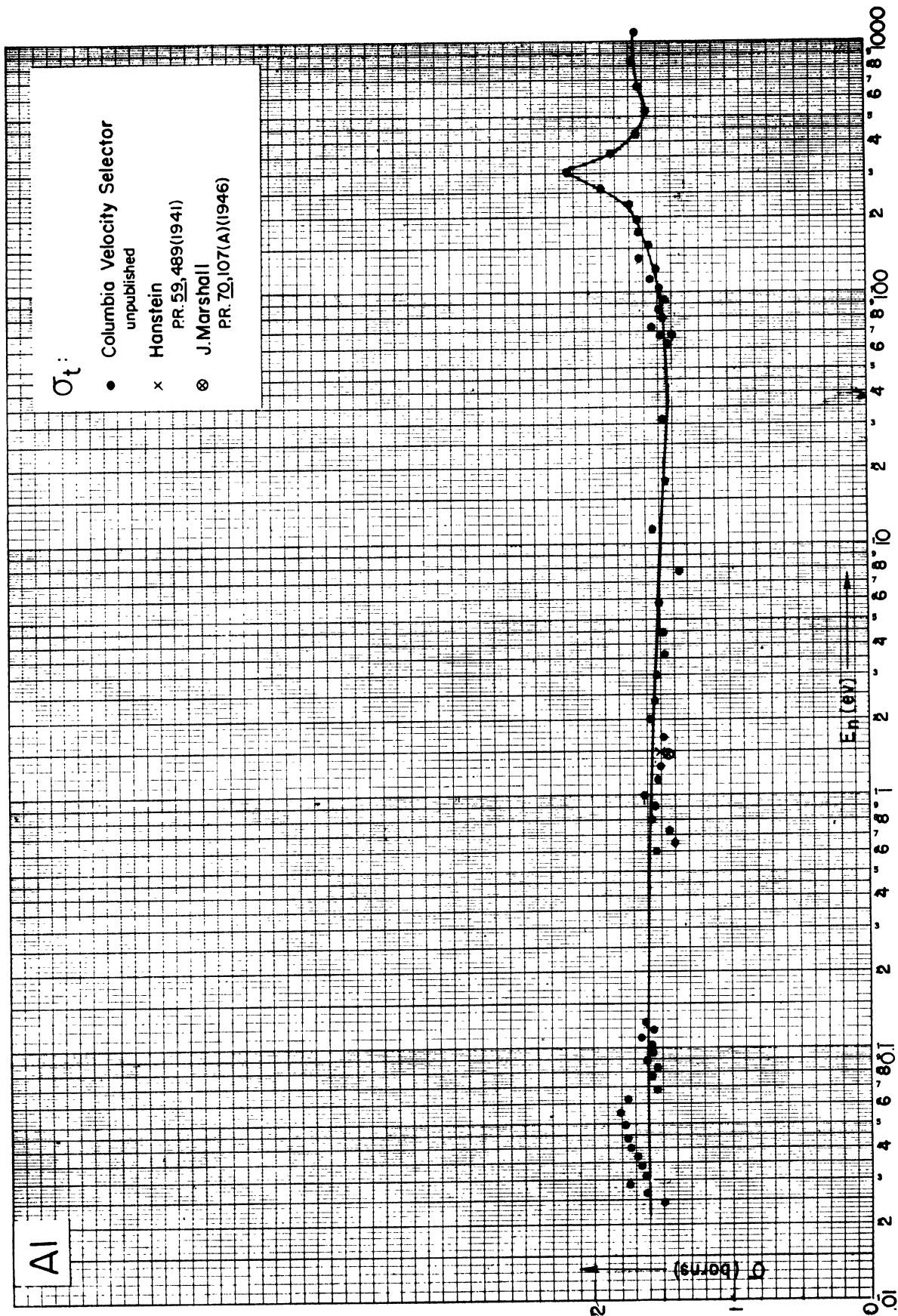
Al

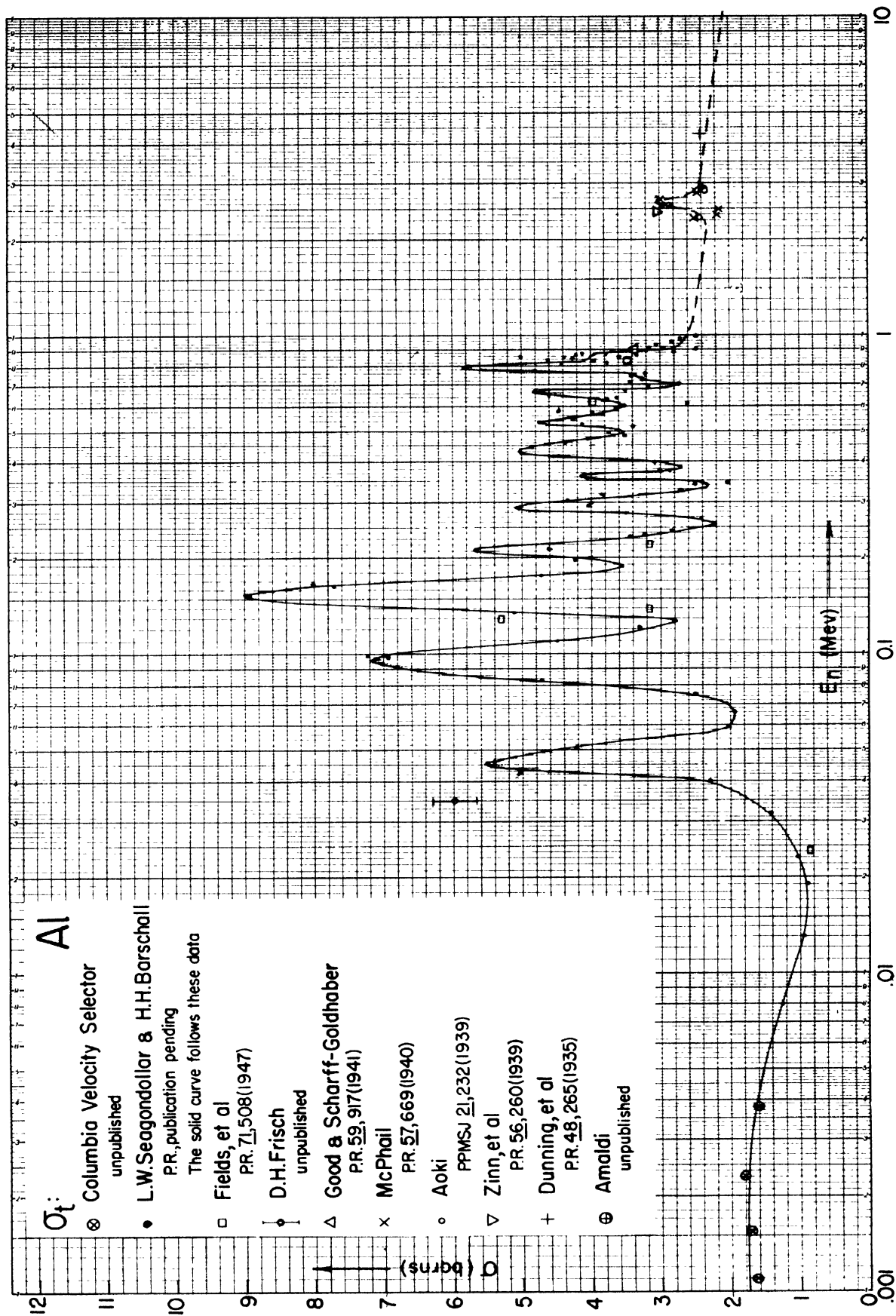
σ_t

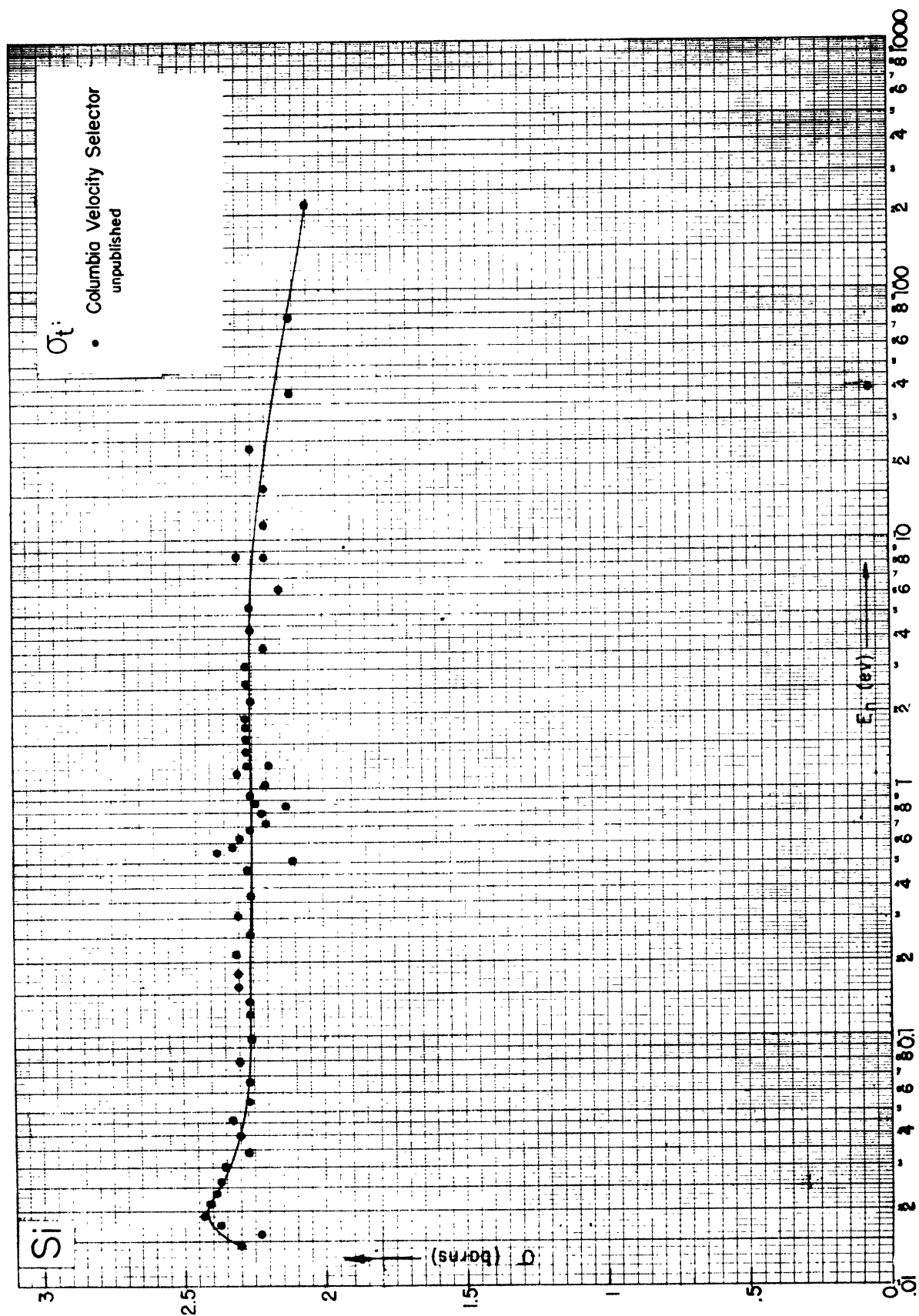
- Columbia Velocity Selector
unpublished
- x Hanstein
PR. 59,489(1941)
- ⊗ J. Marshall
PR. 70,107(A)(1946)

σ (barns)

E_n (eV)



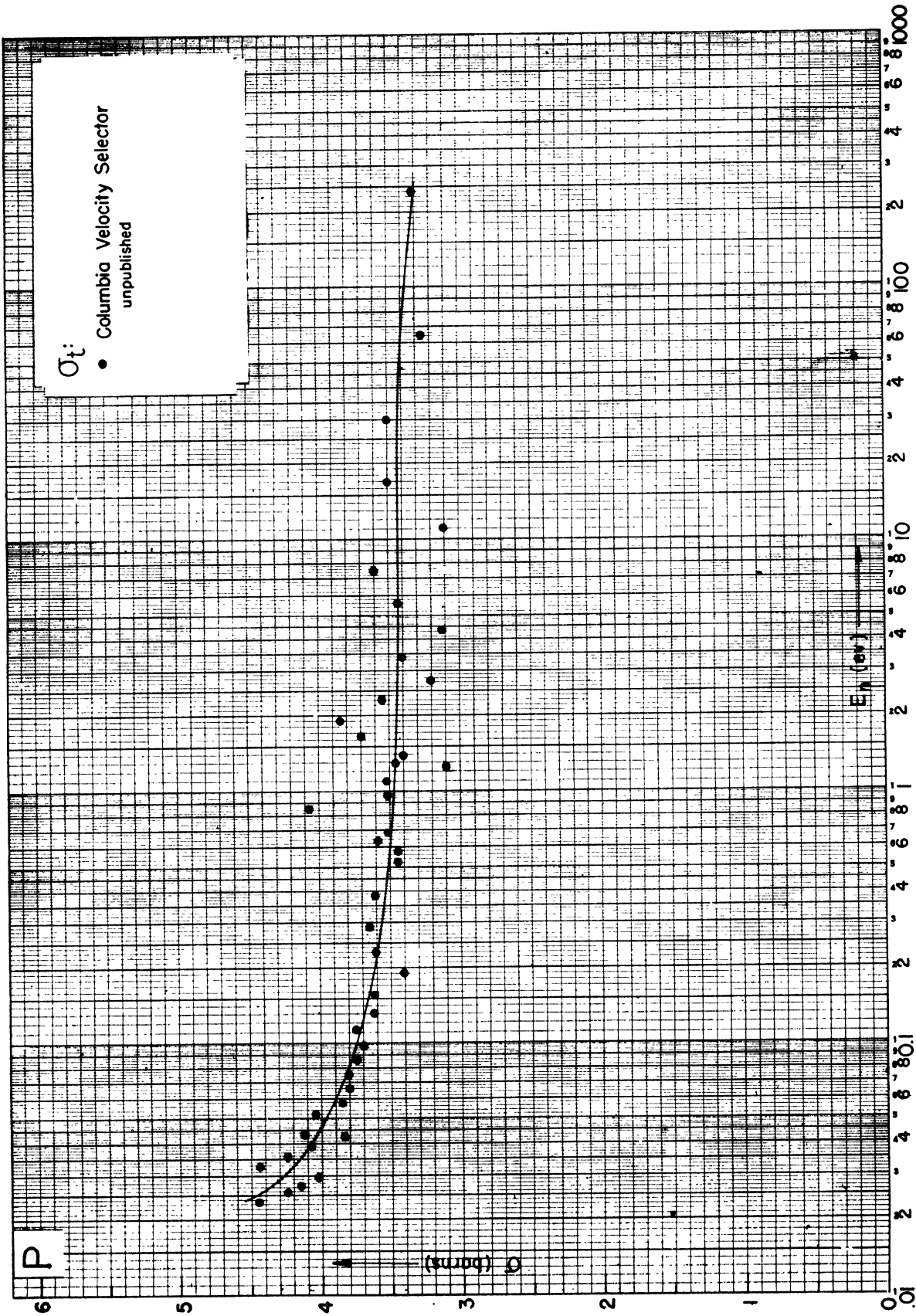


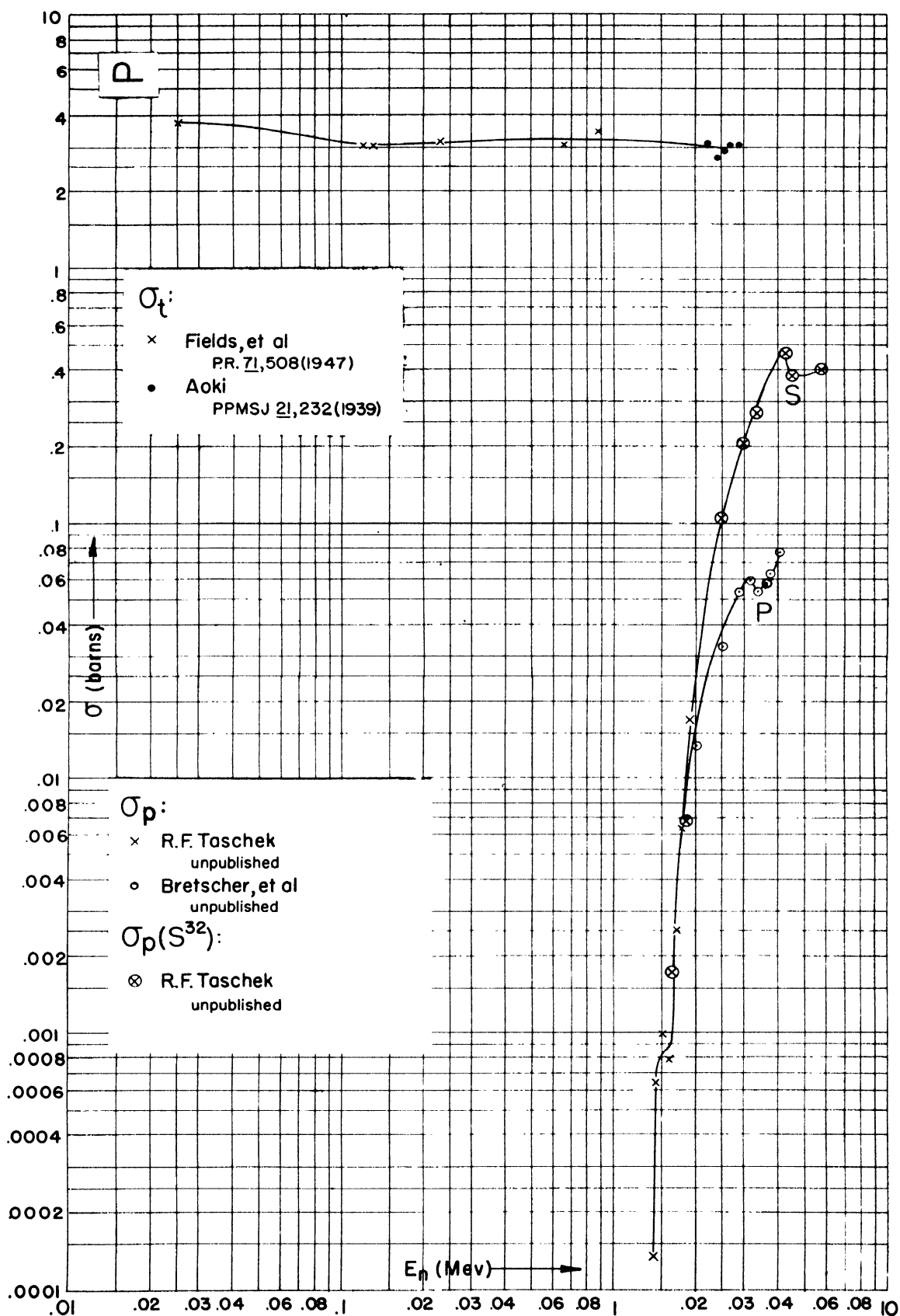


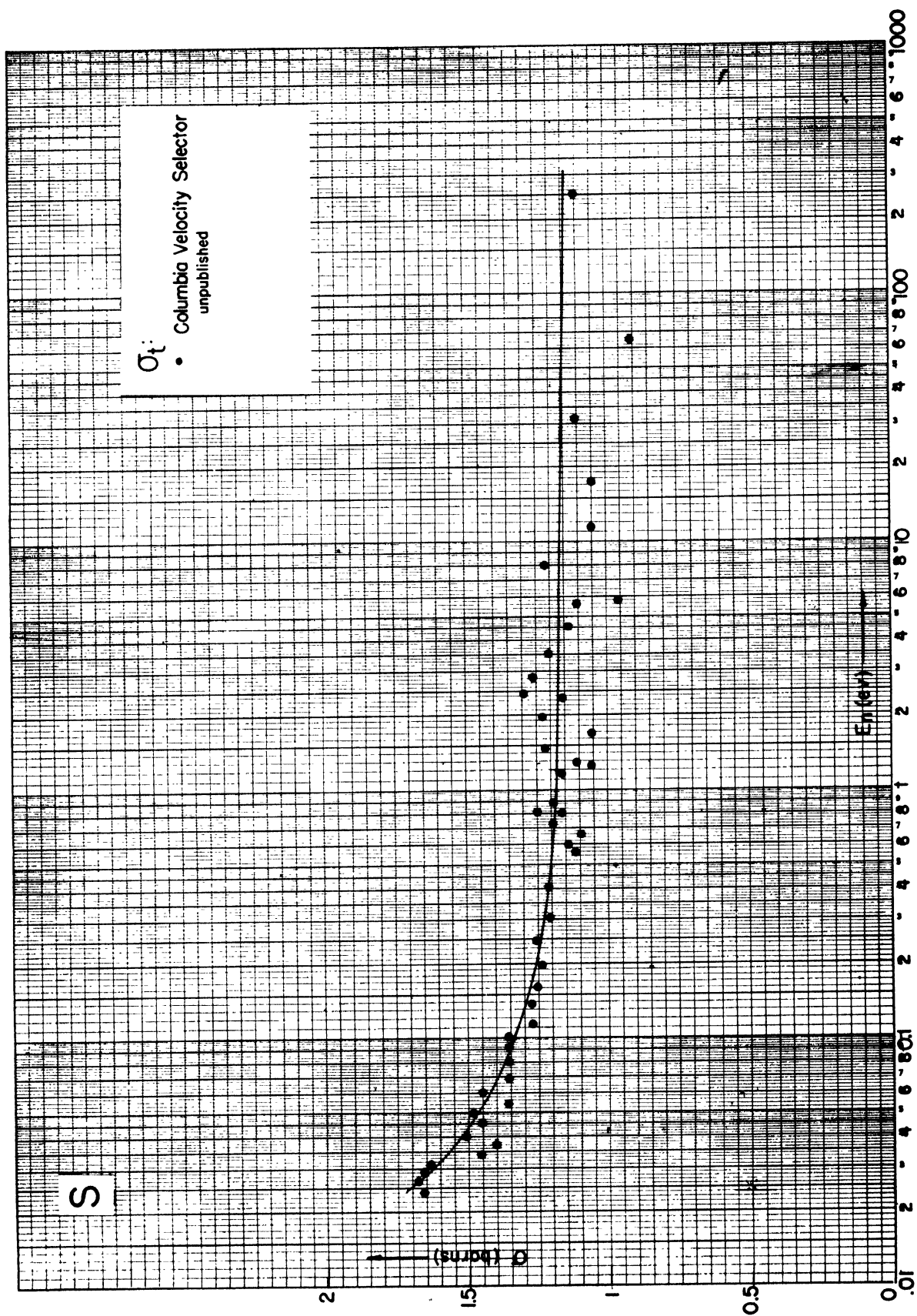
si

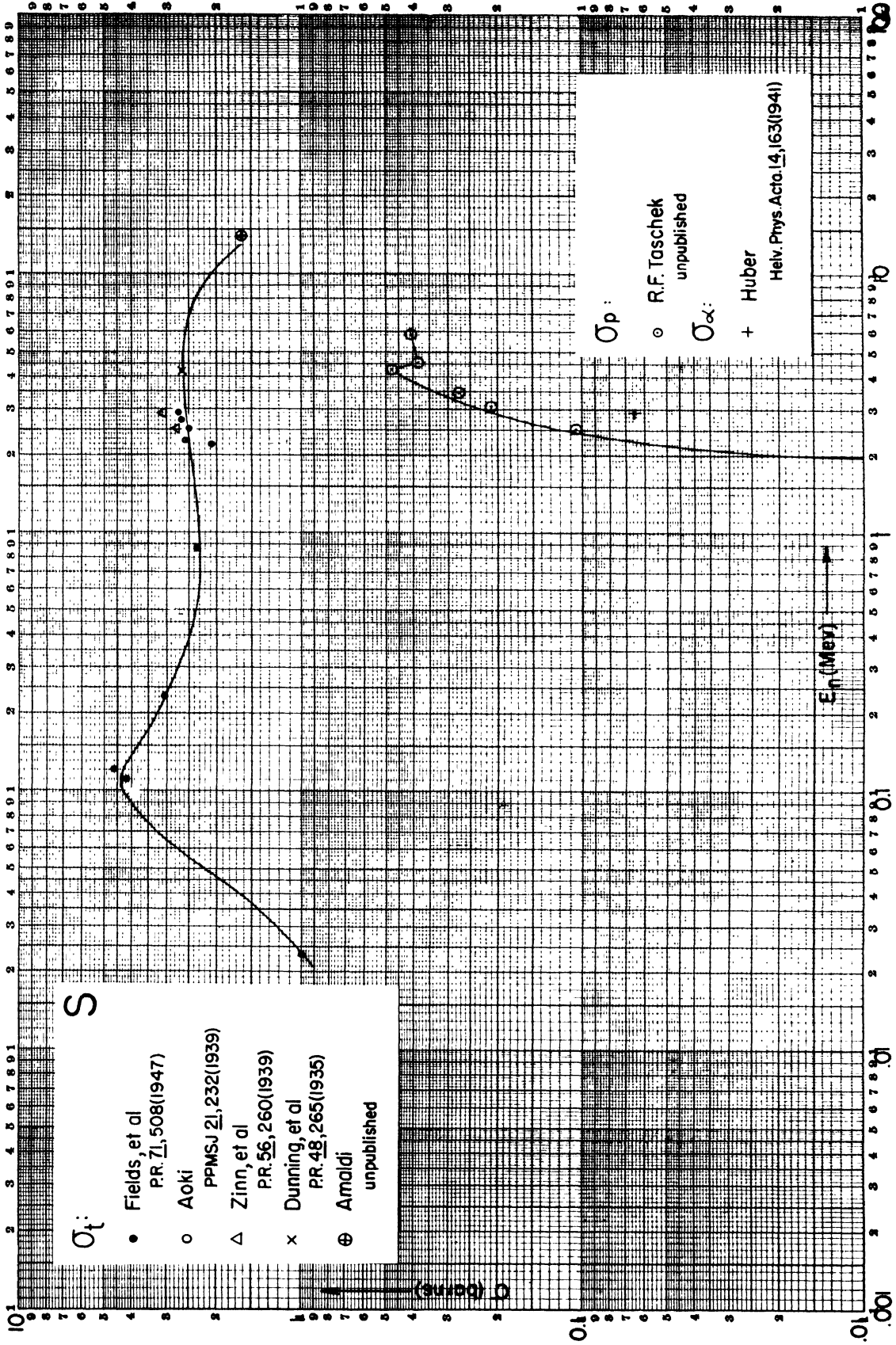
Er (Mev)

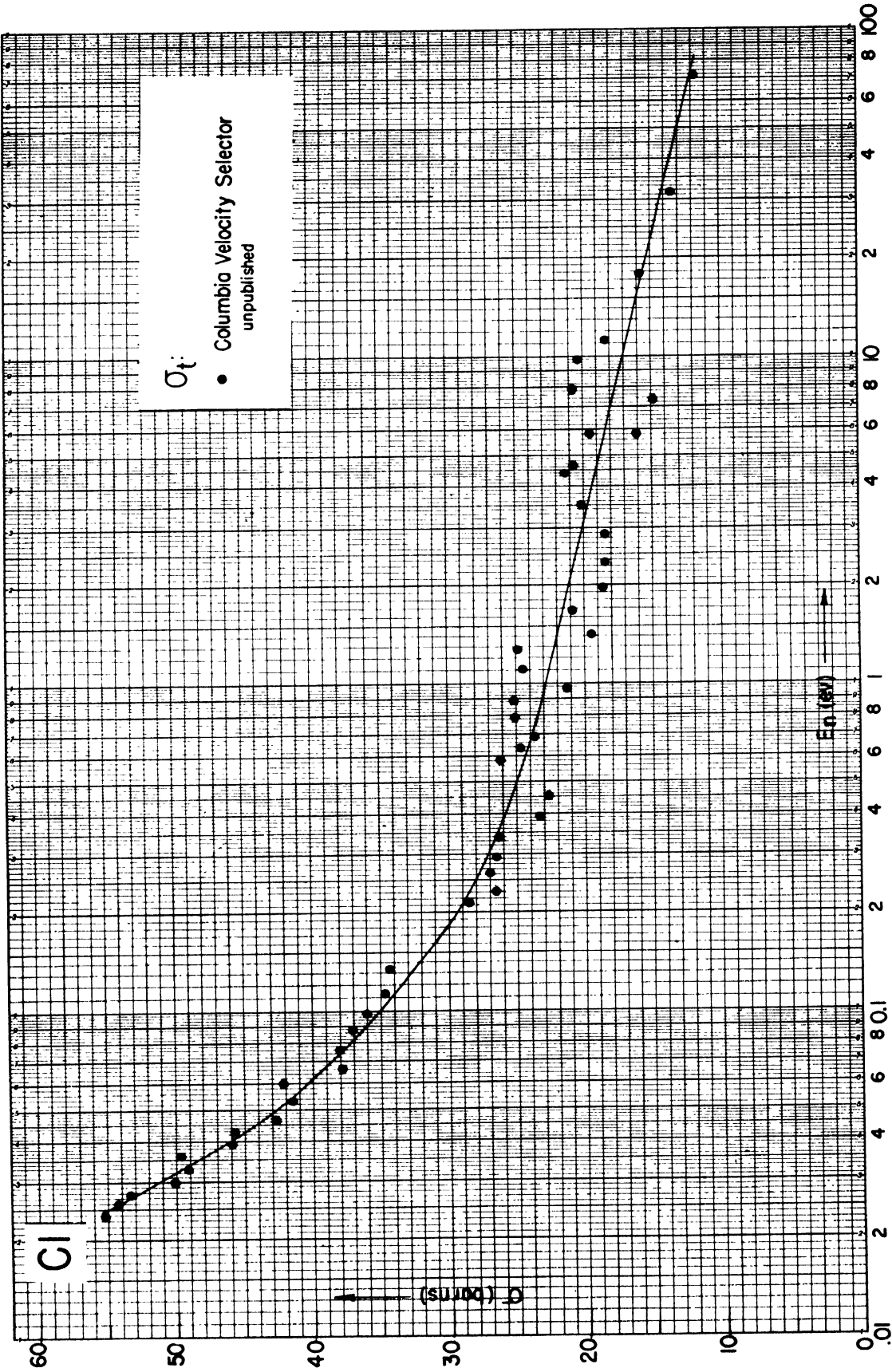
0 (ev) 100

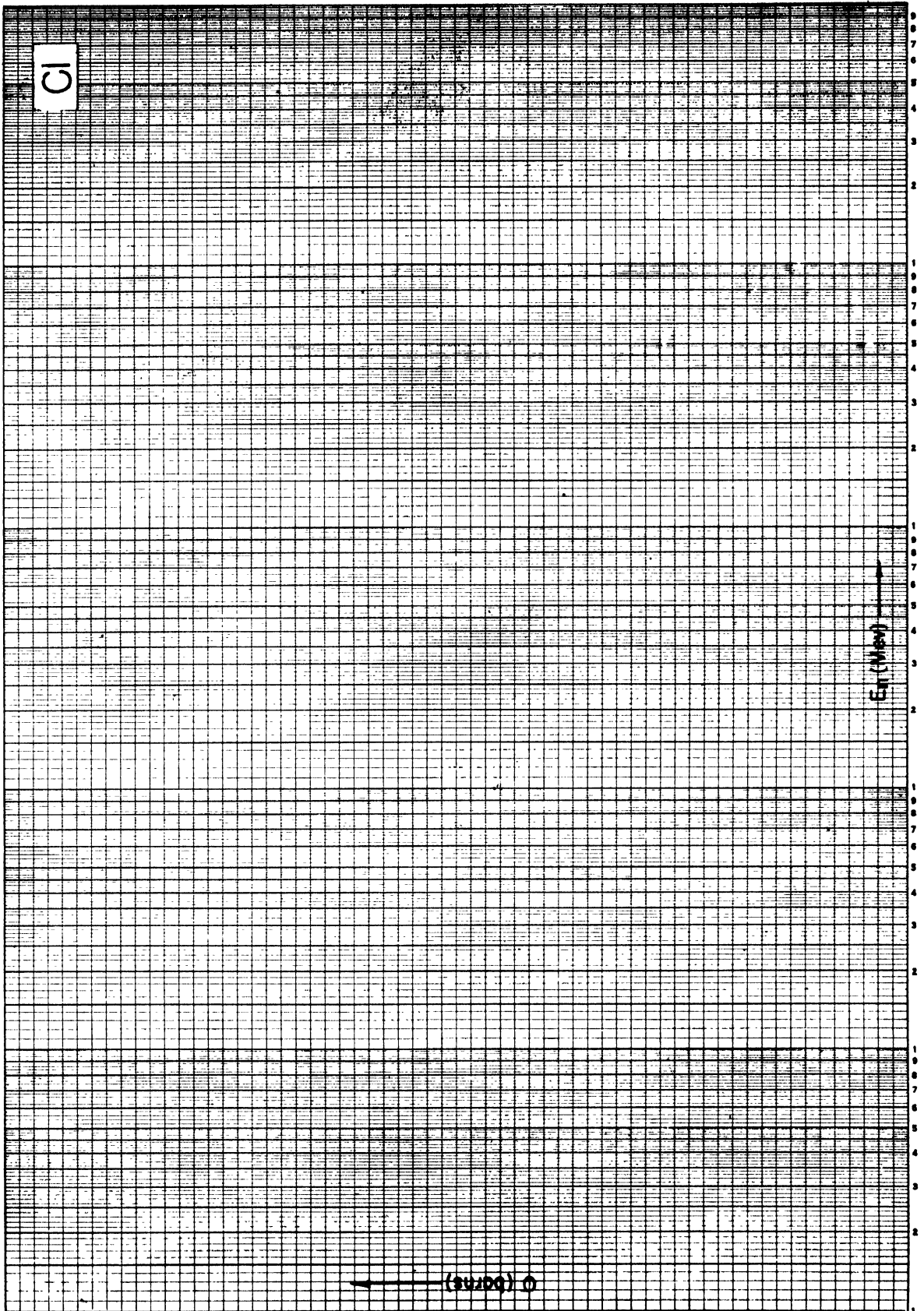


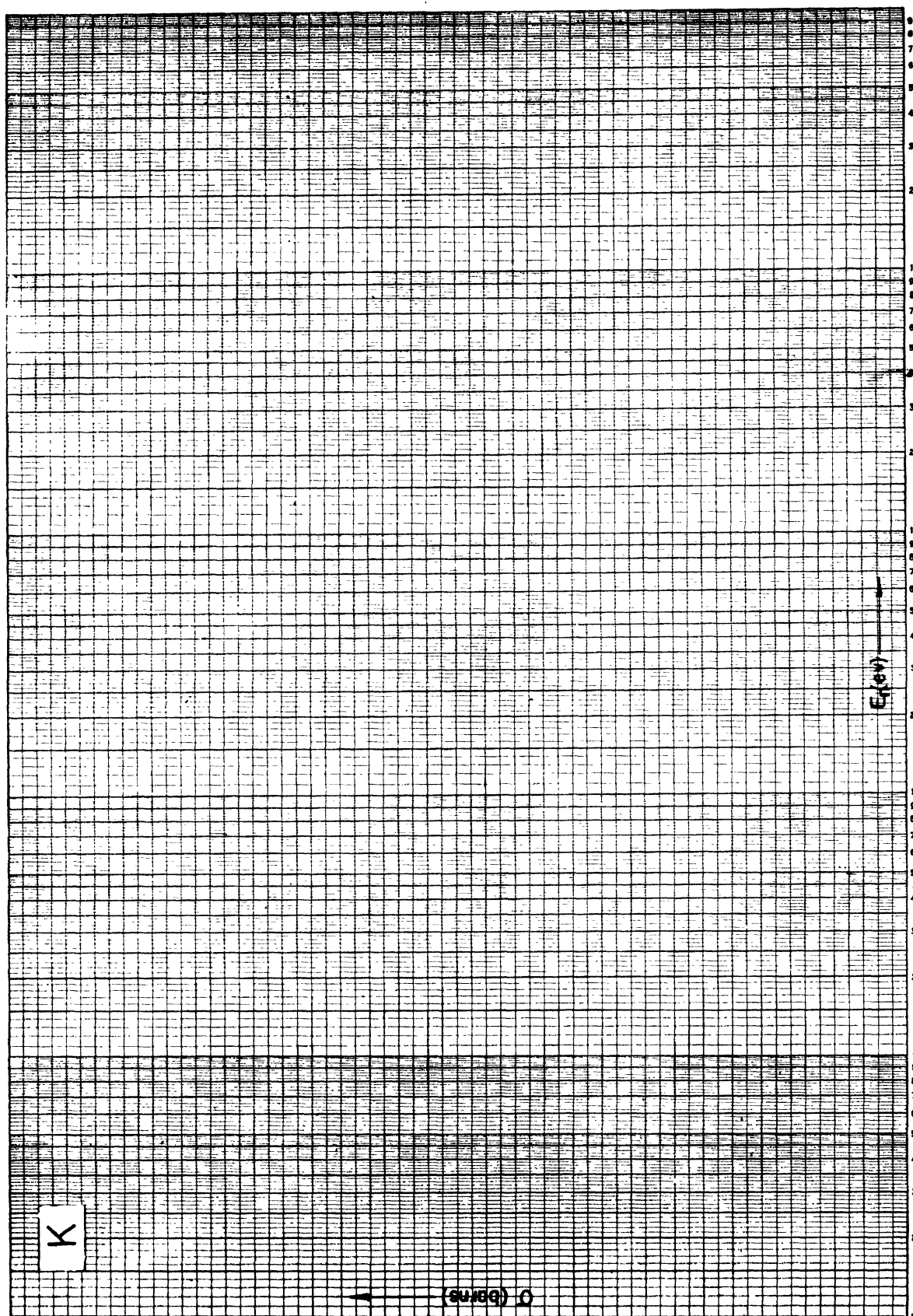


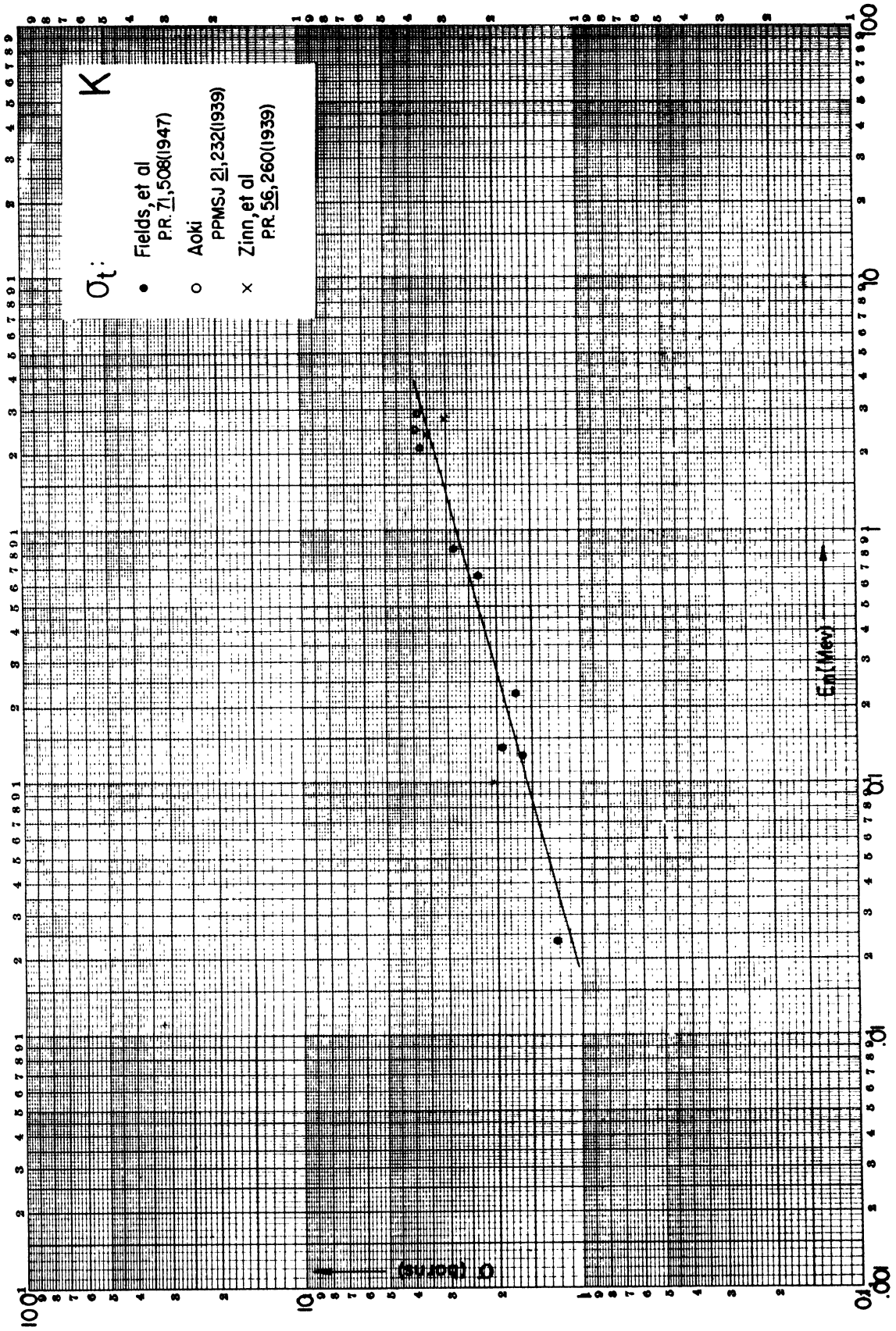


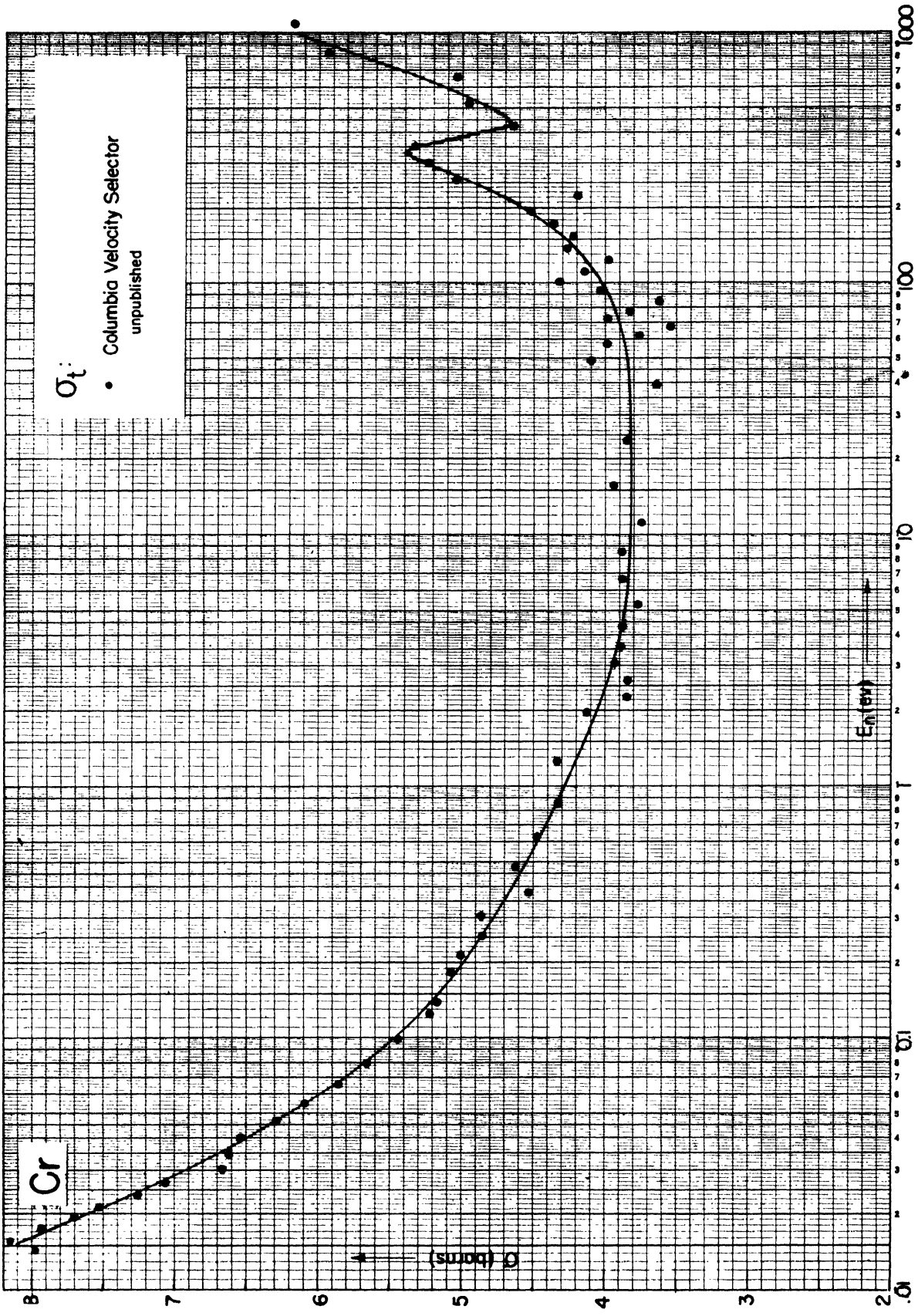


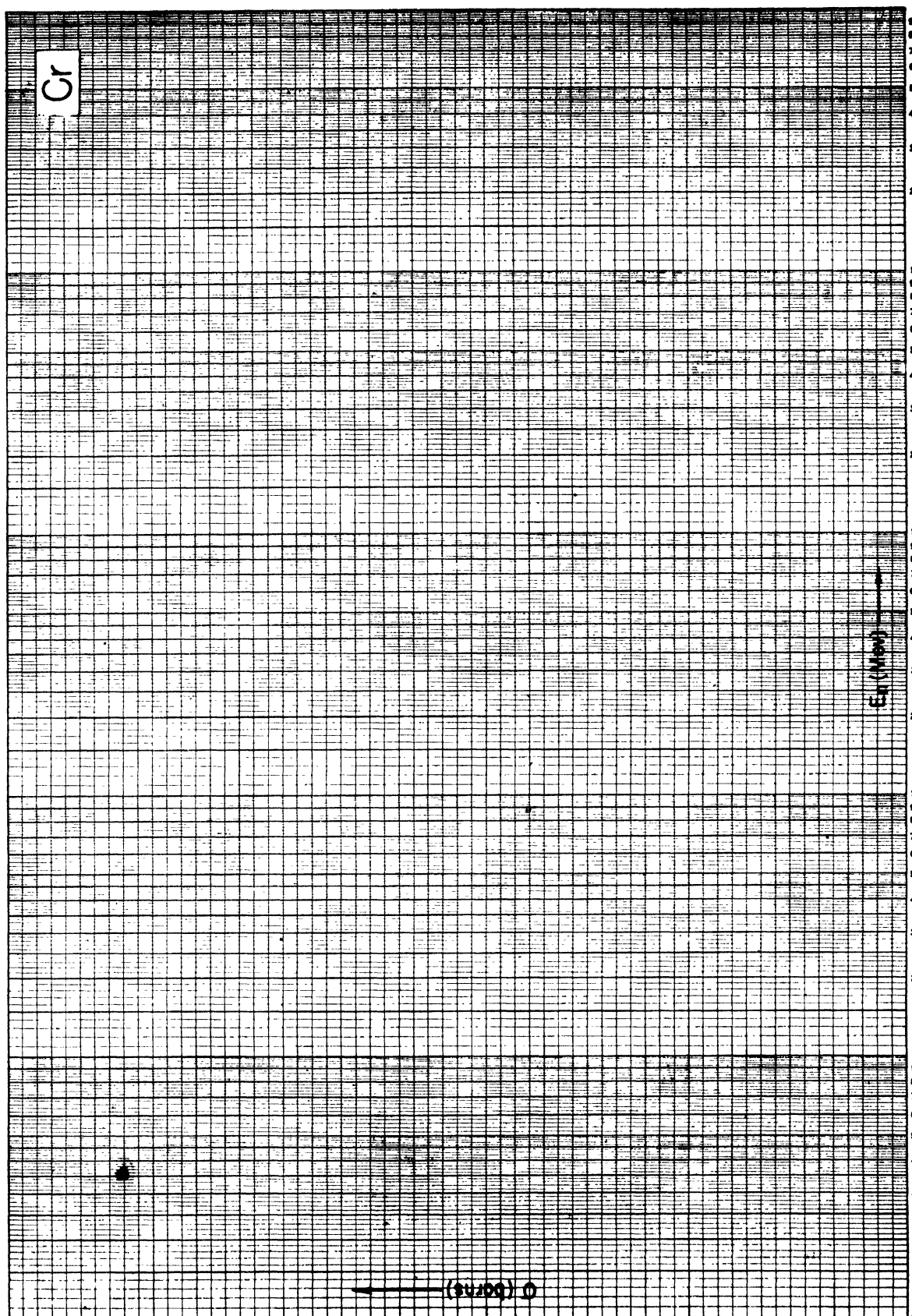


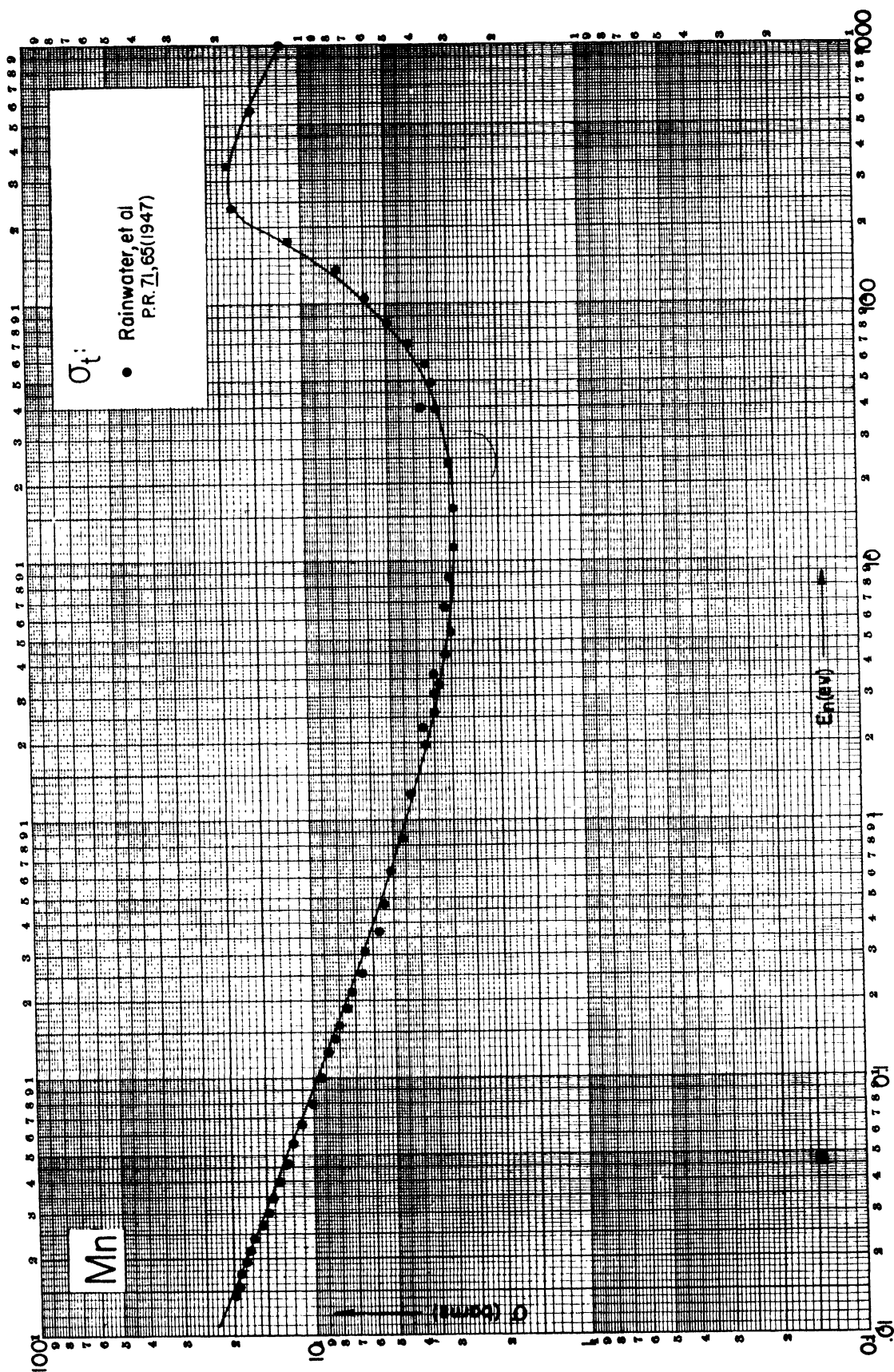








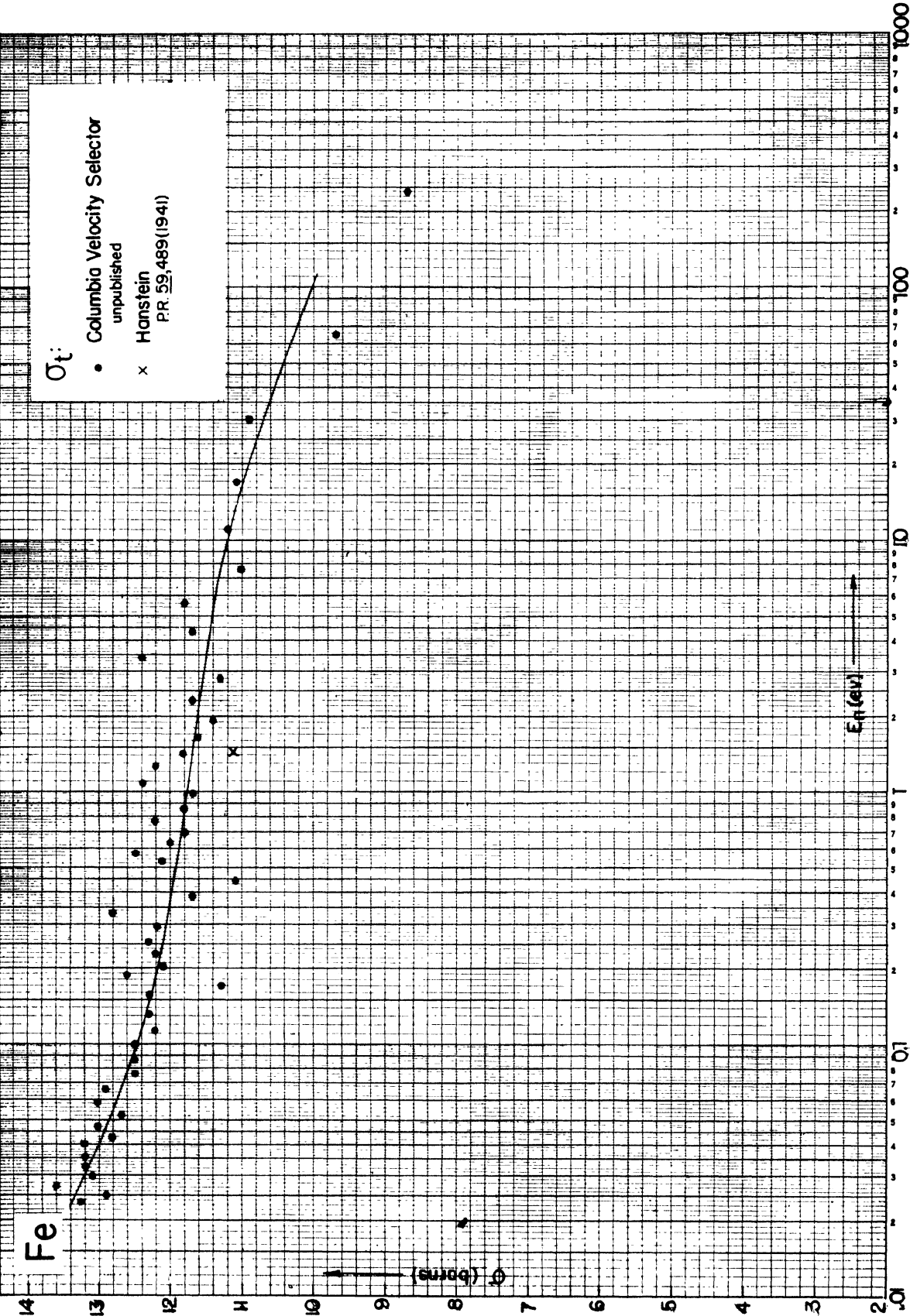


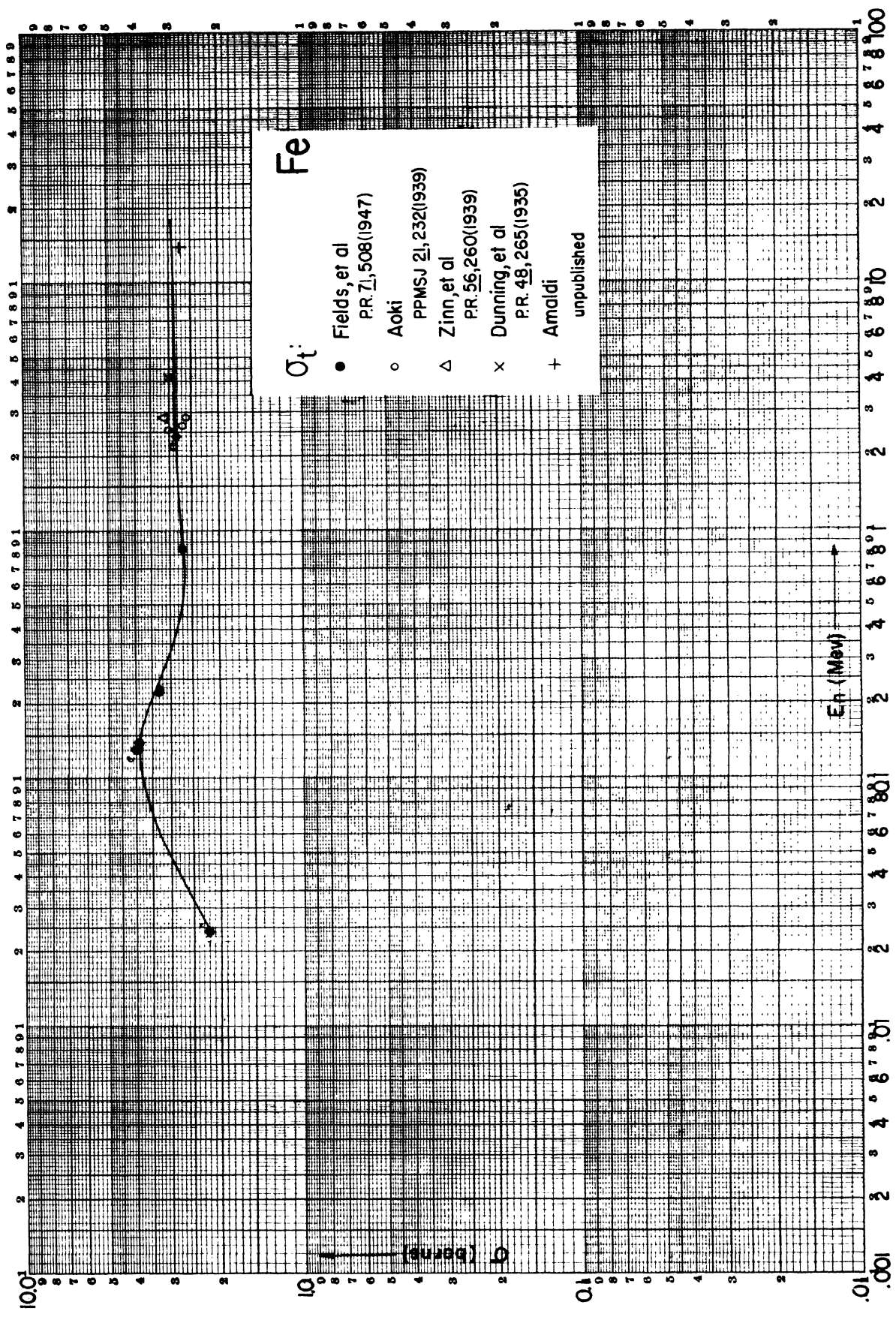


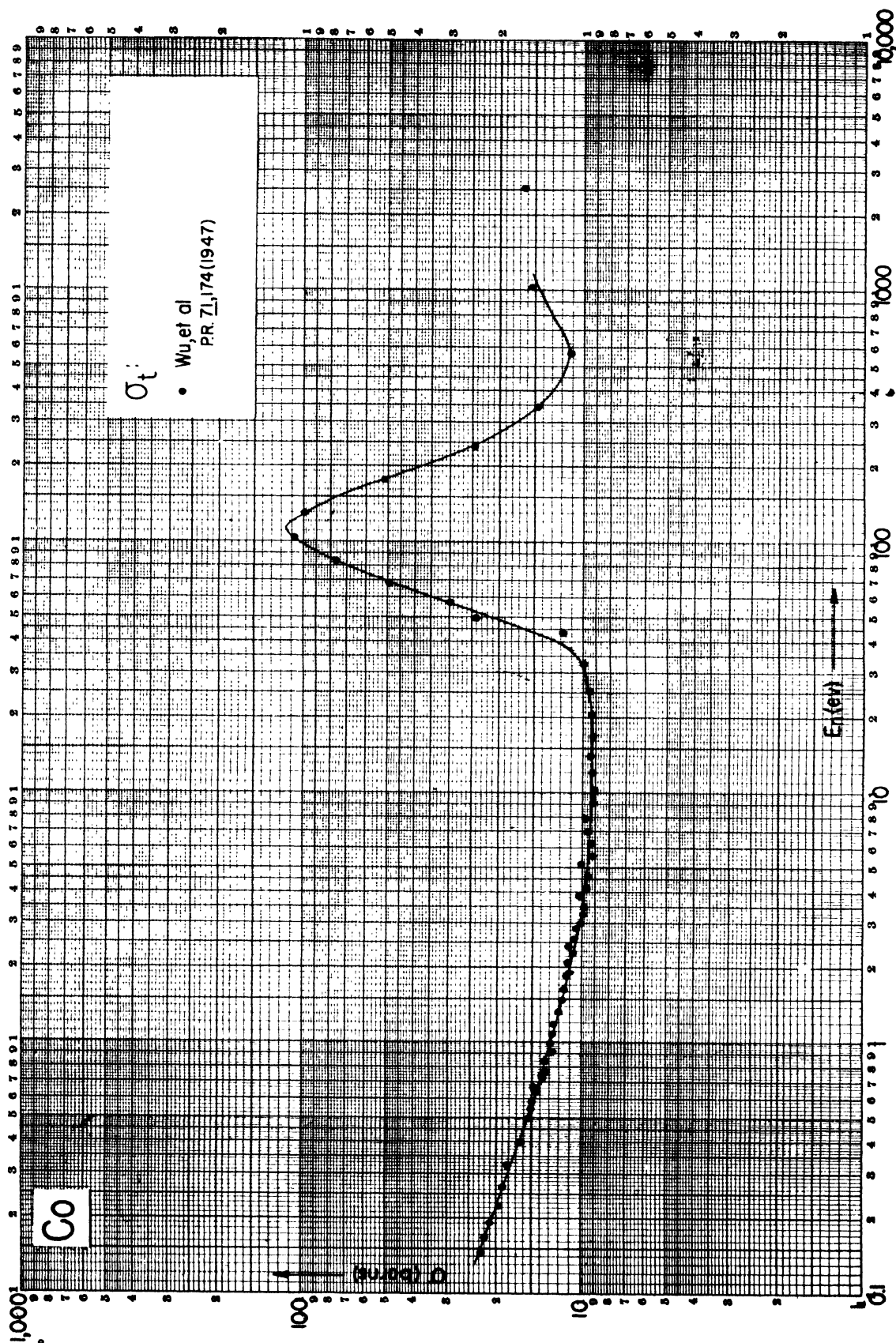
Mn

En (MeV)

(99200) 0



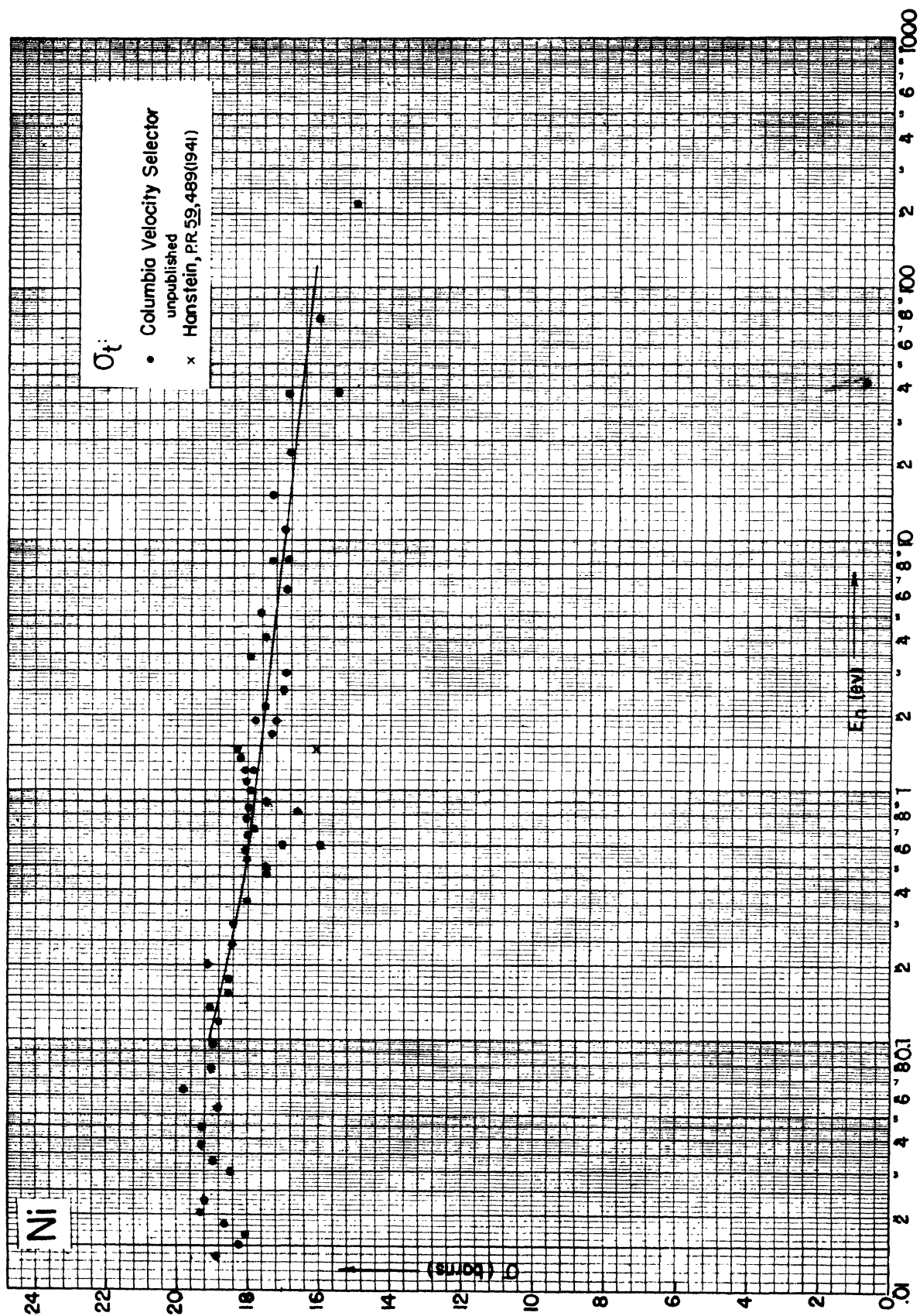


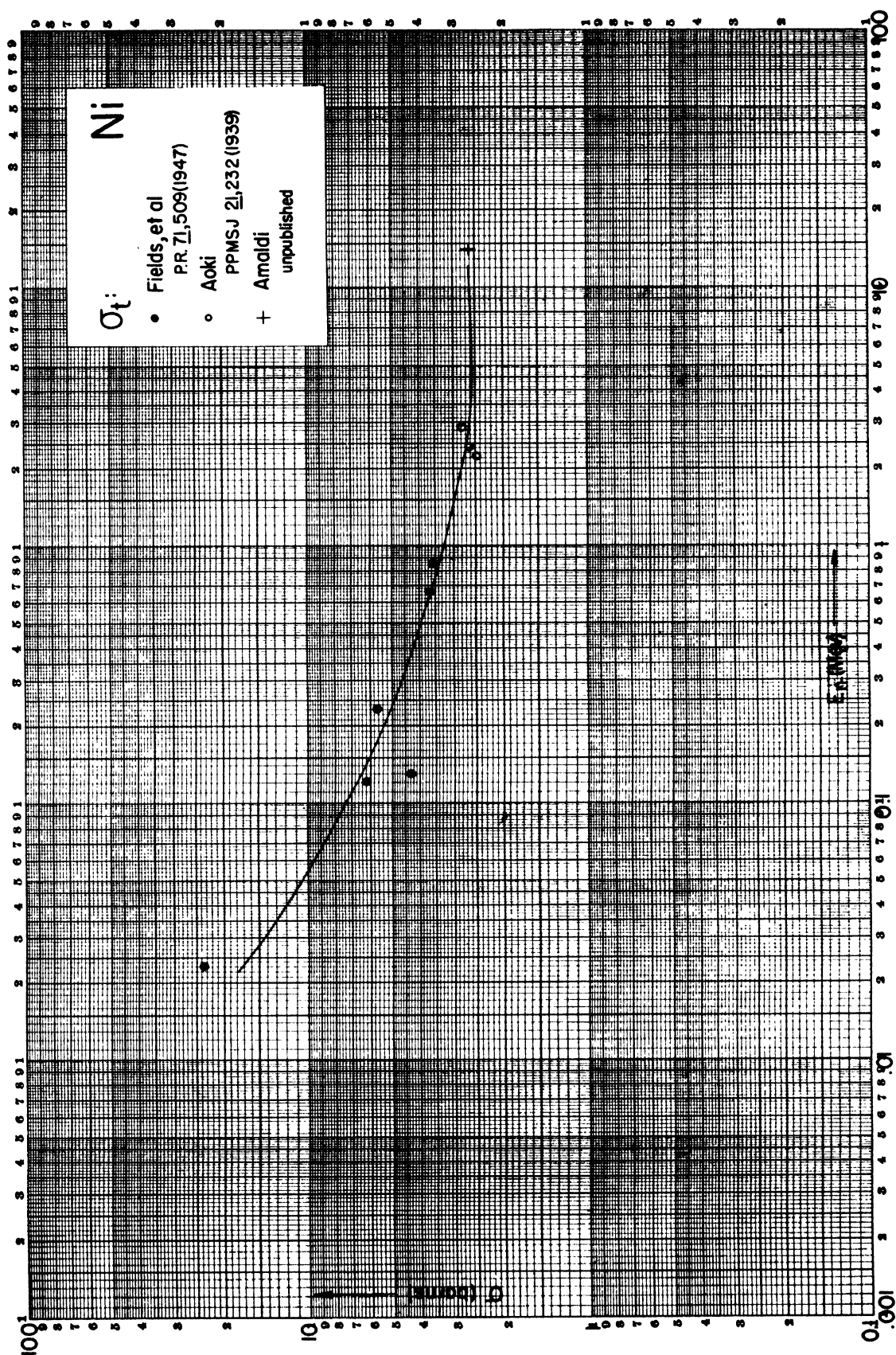


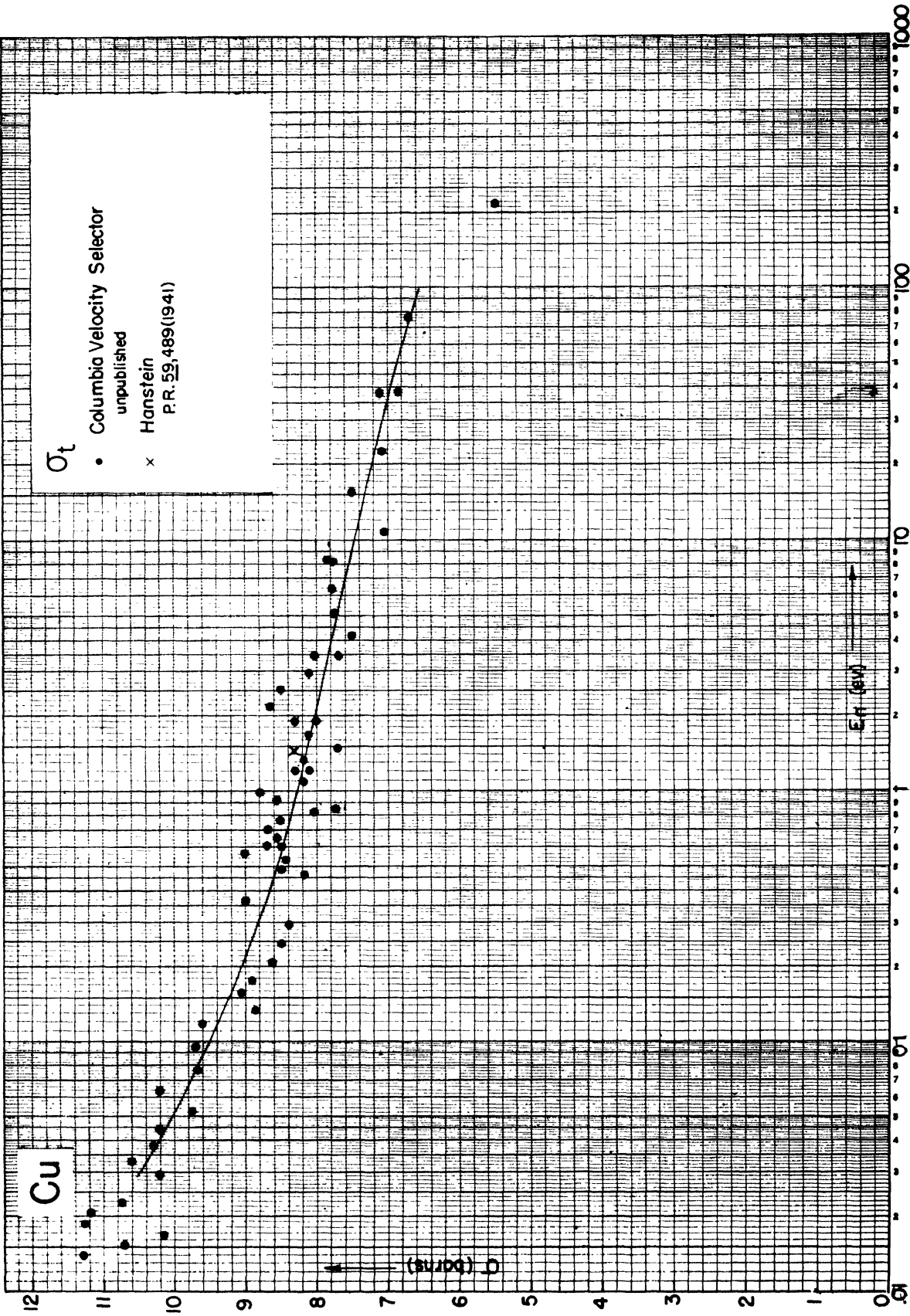
3

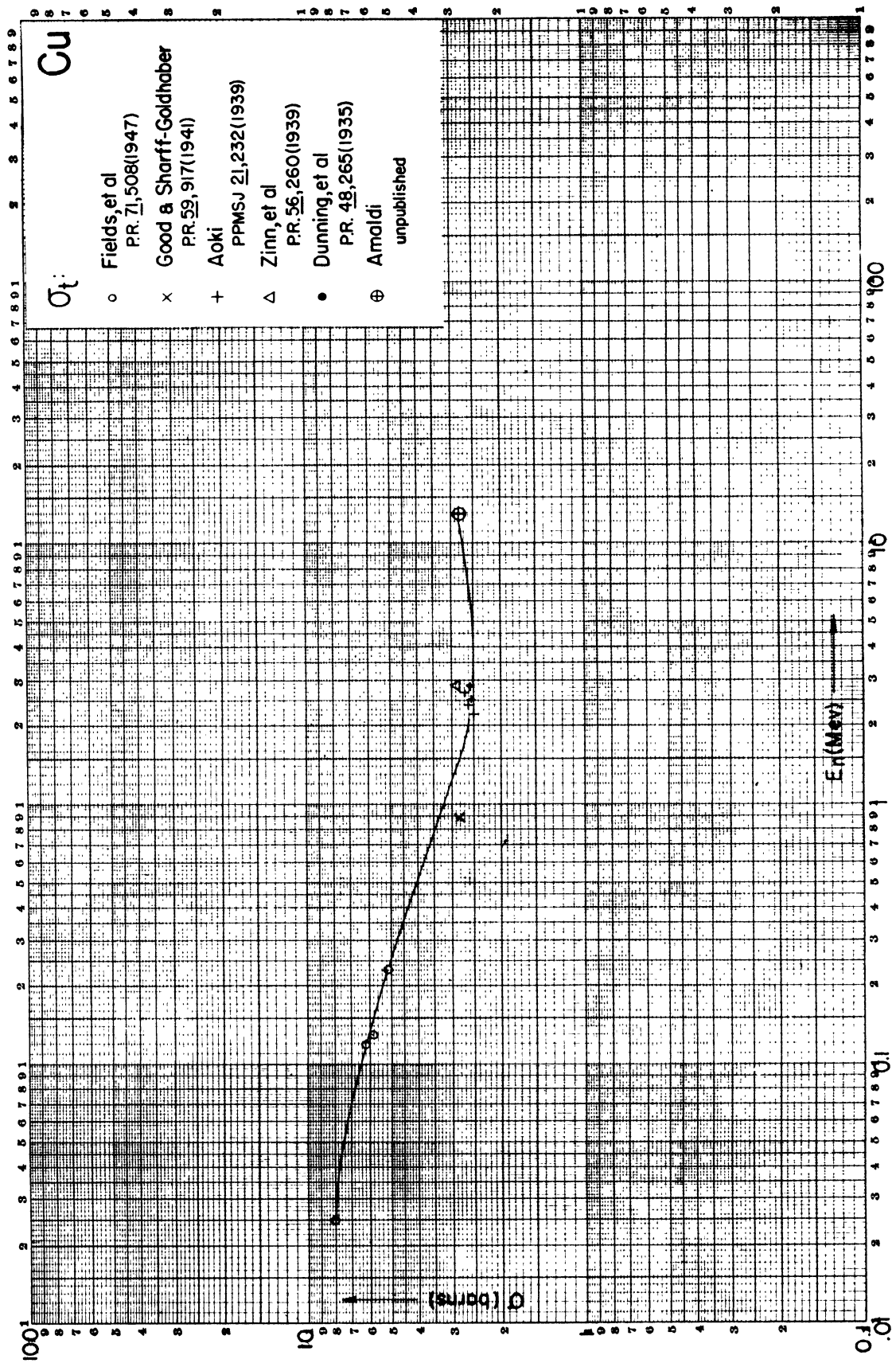
En (MeV)

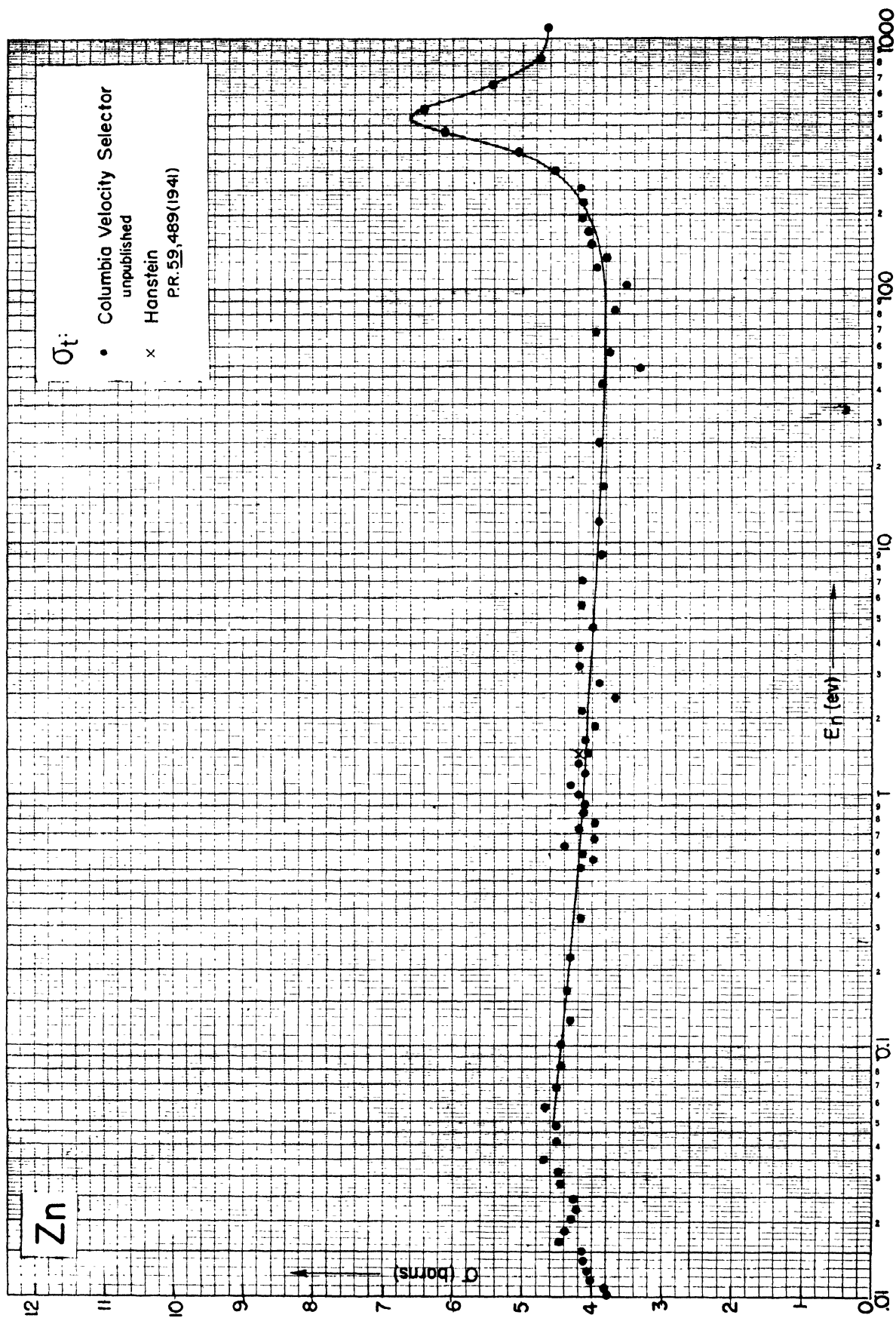
(su/eq) 0

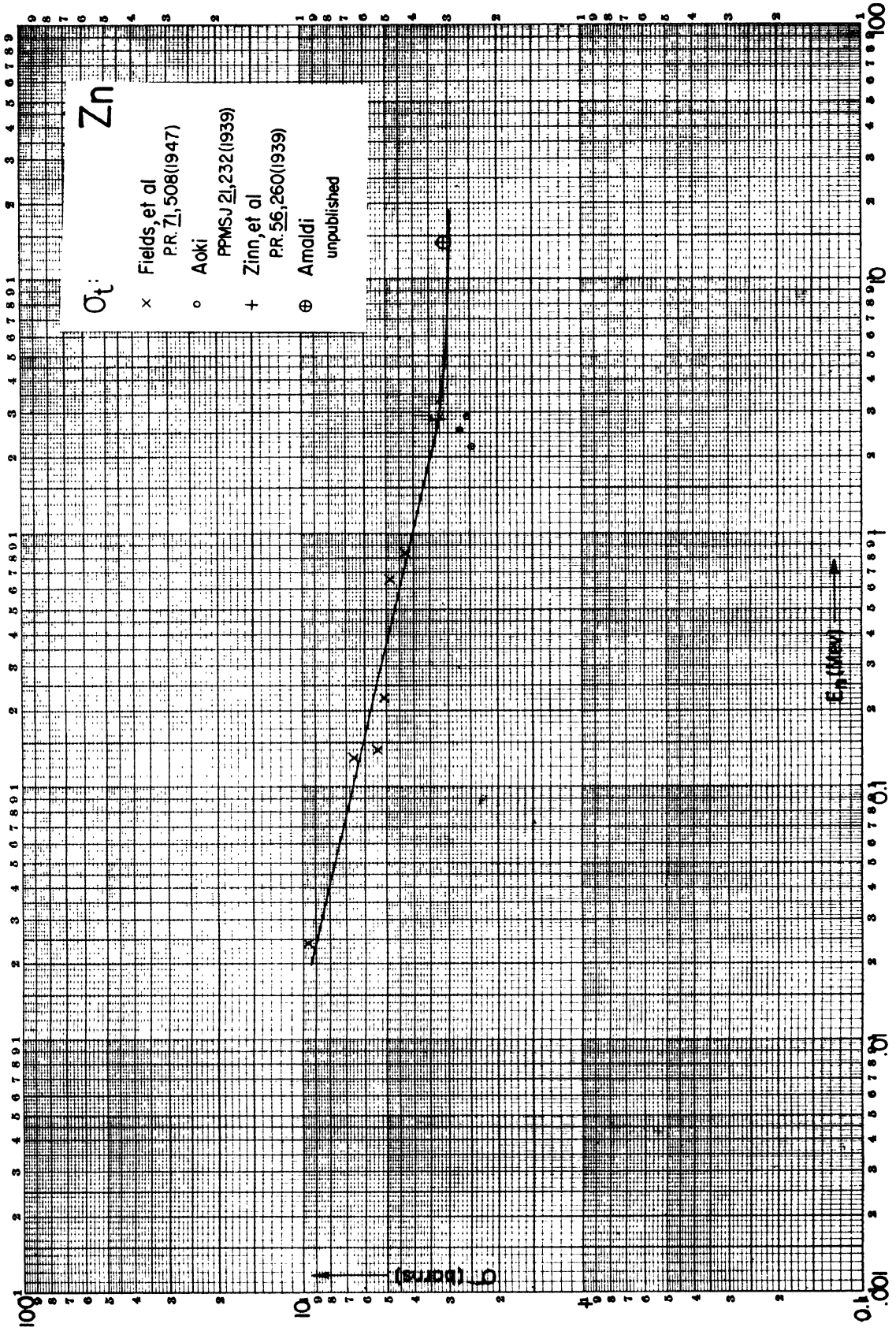


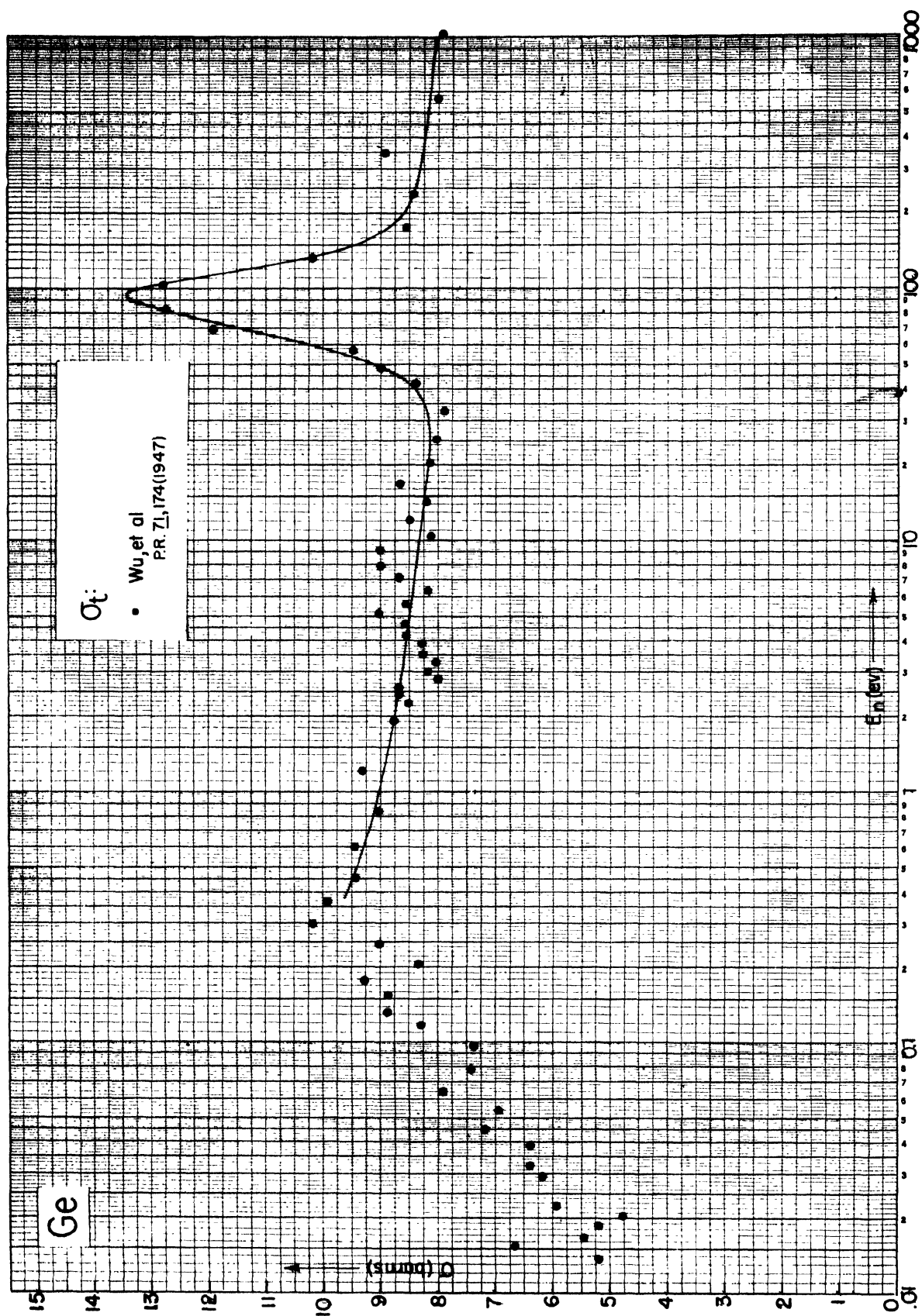


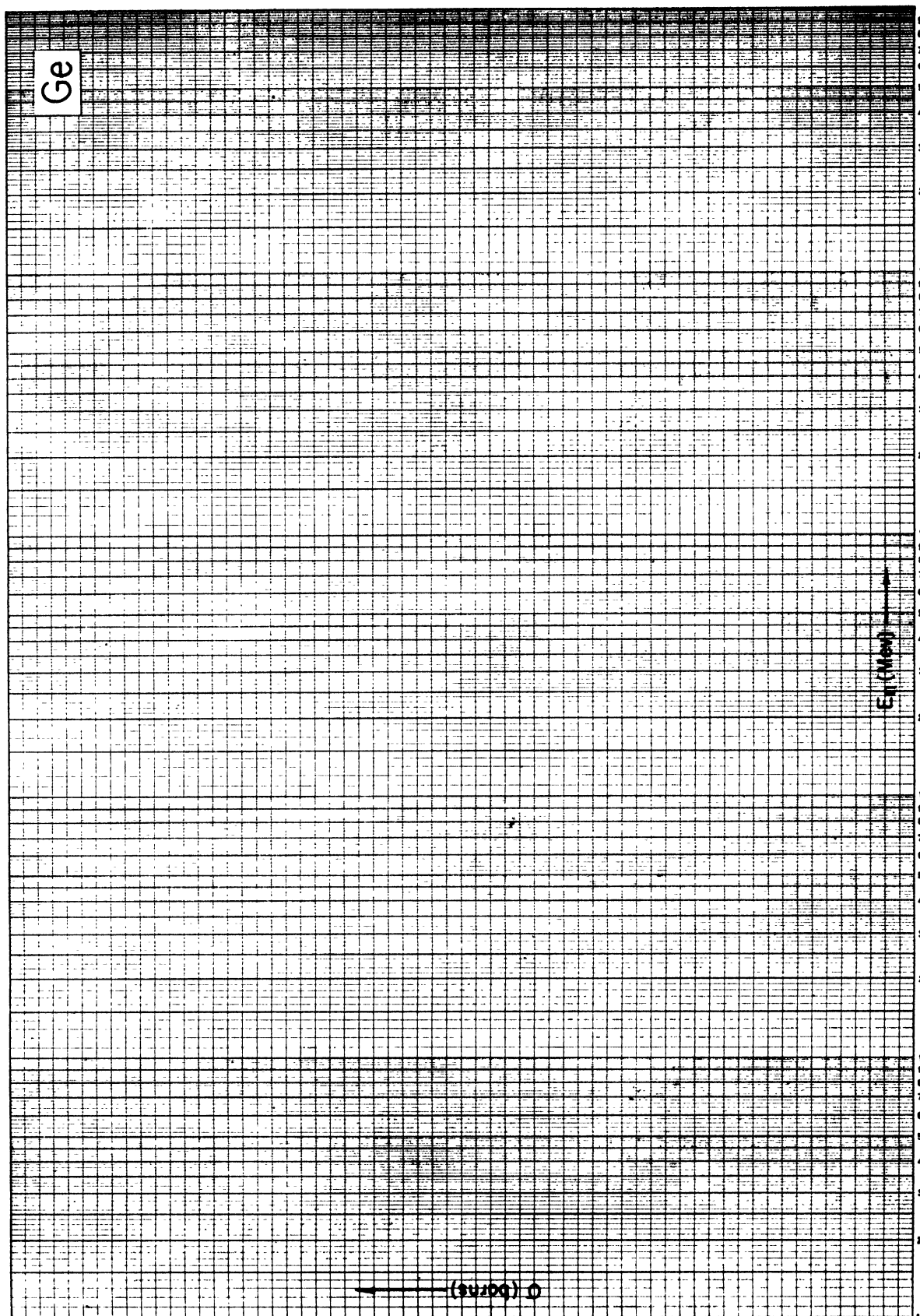


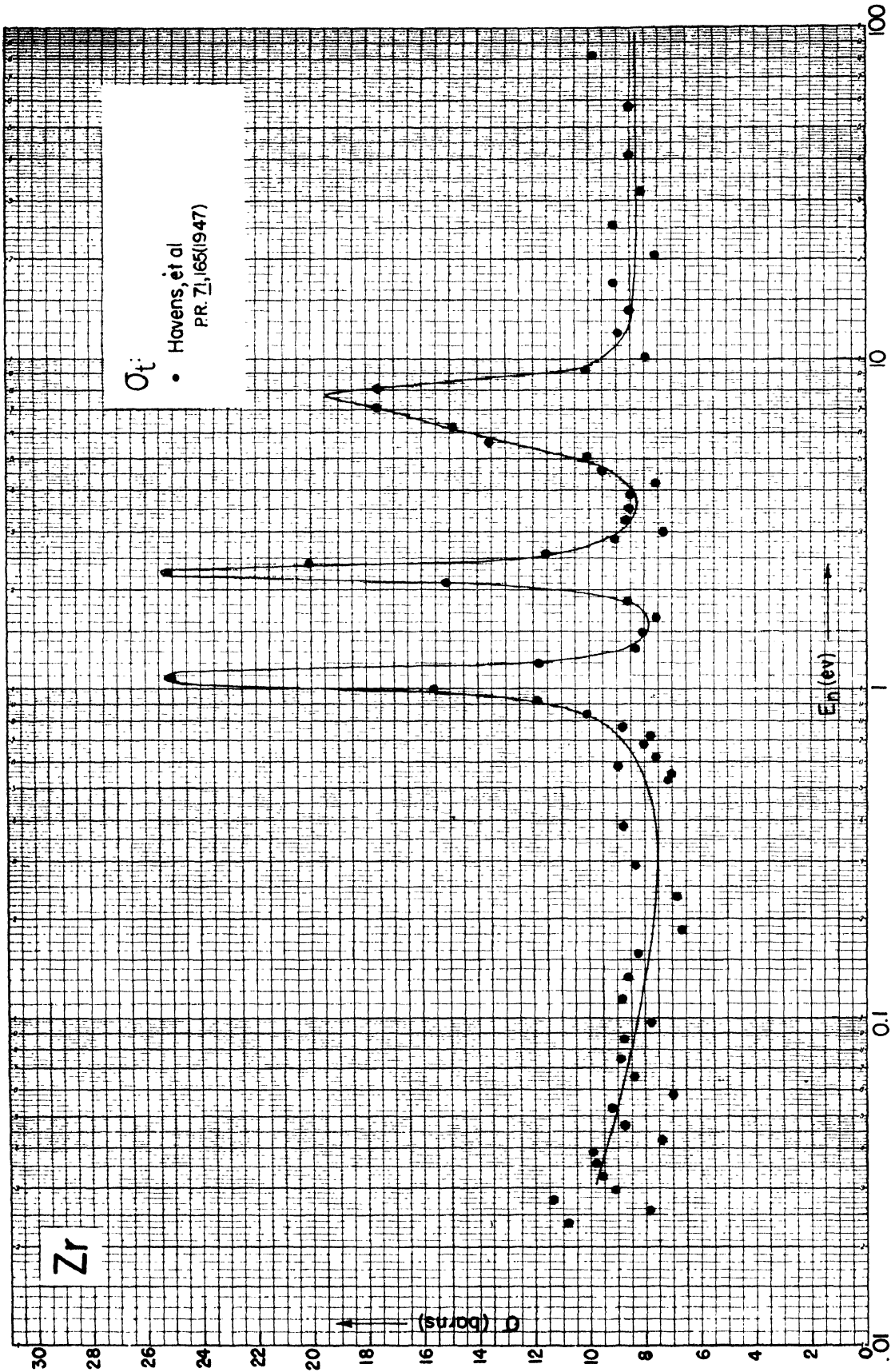


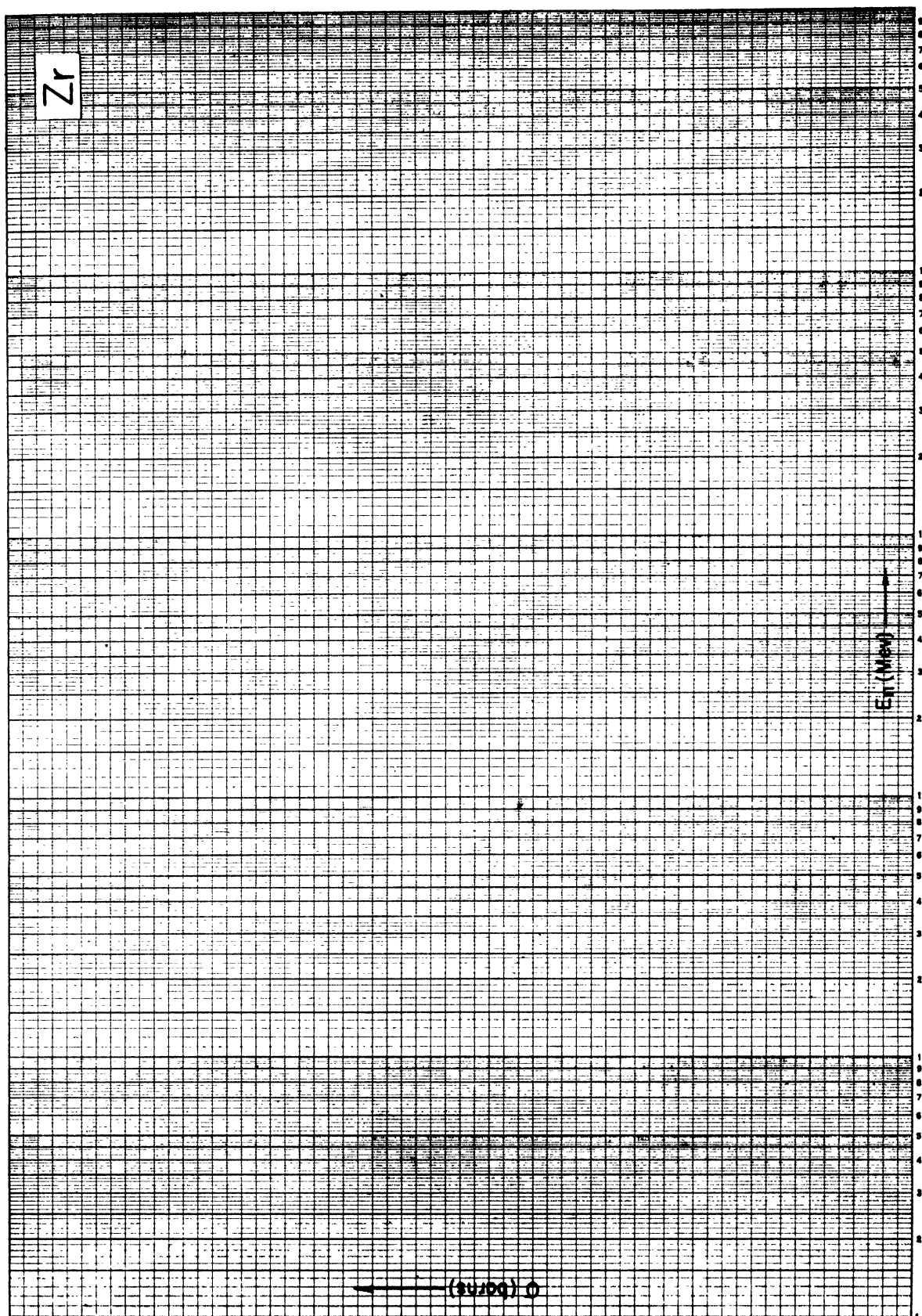


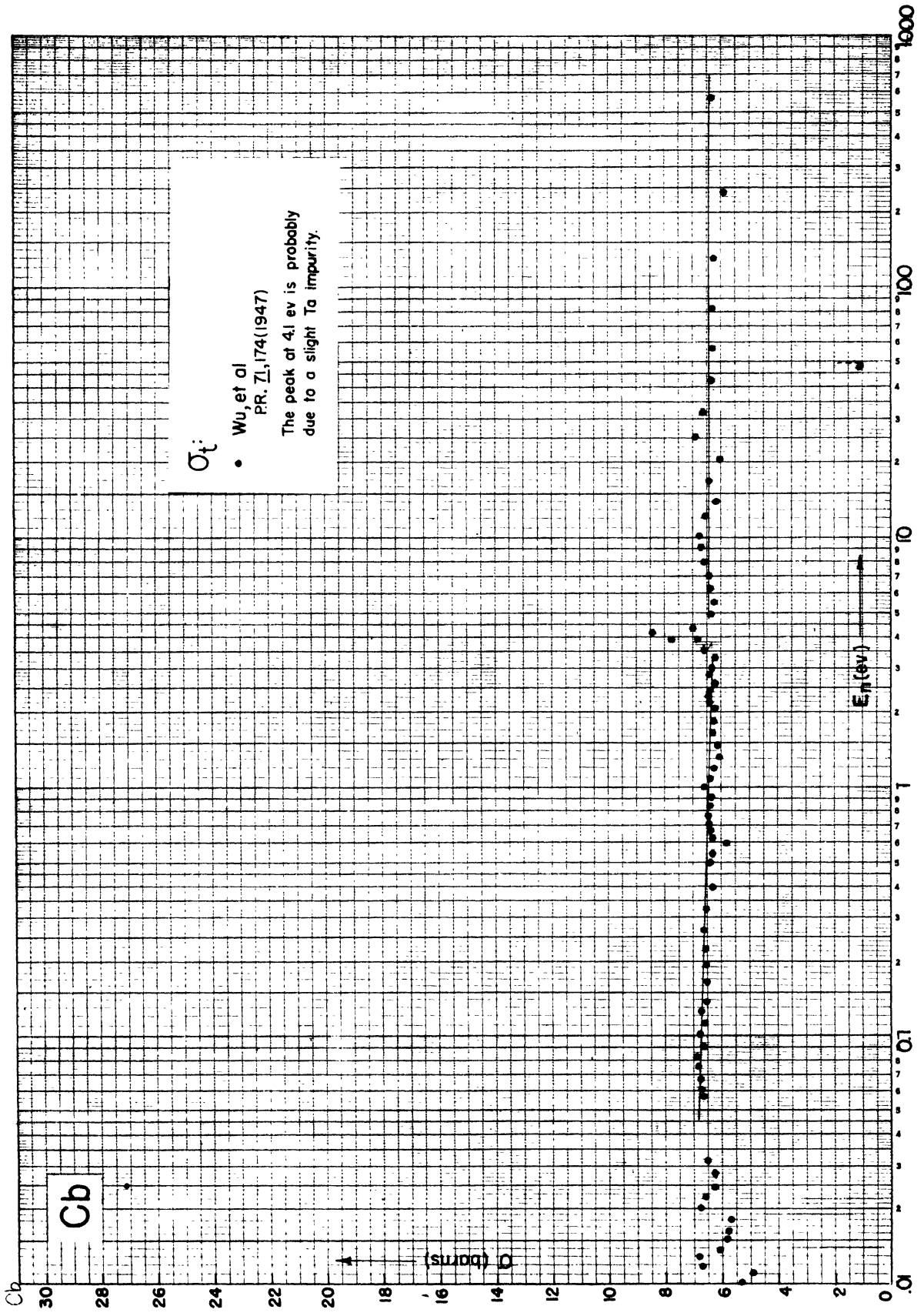


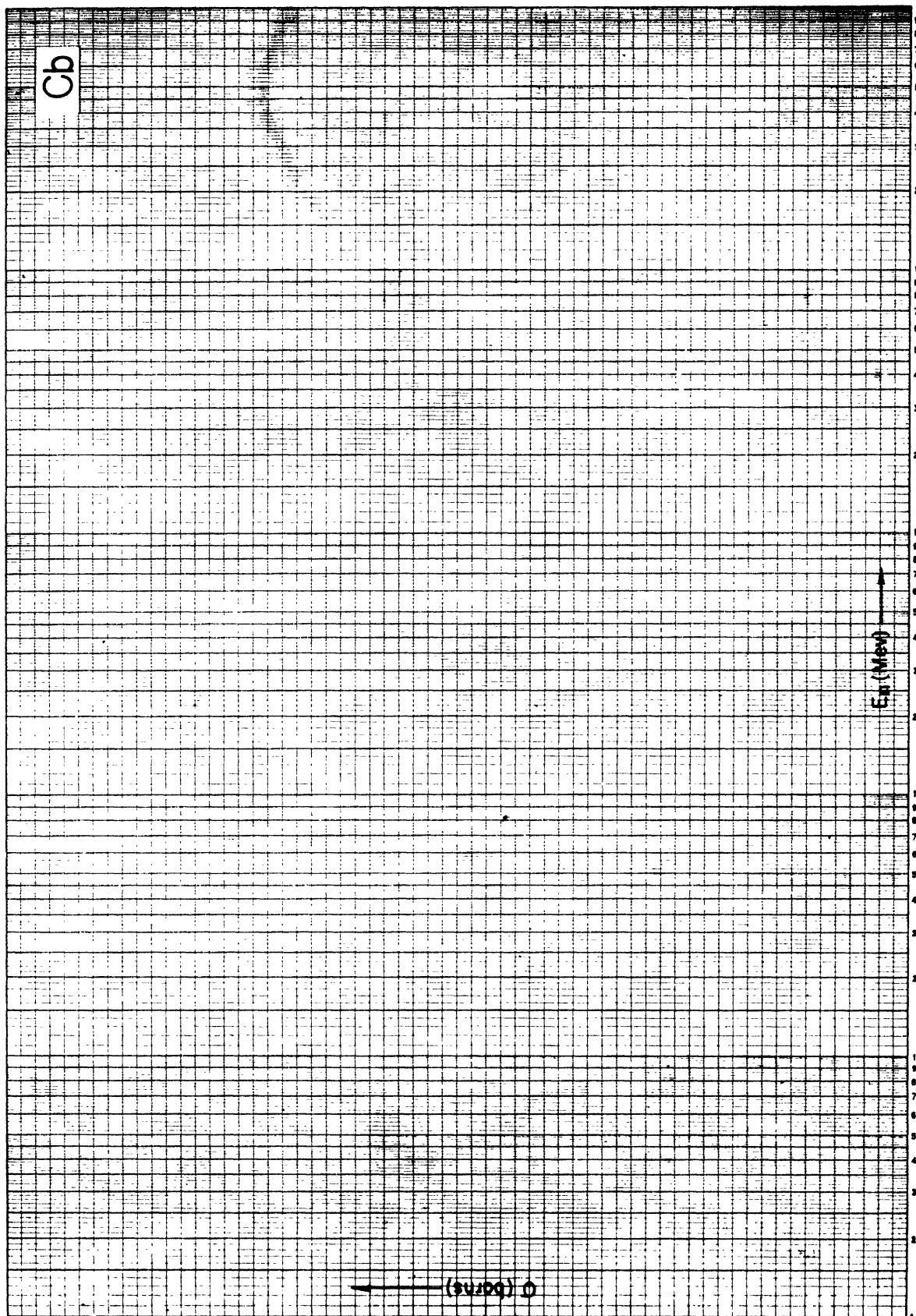


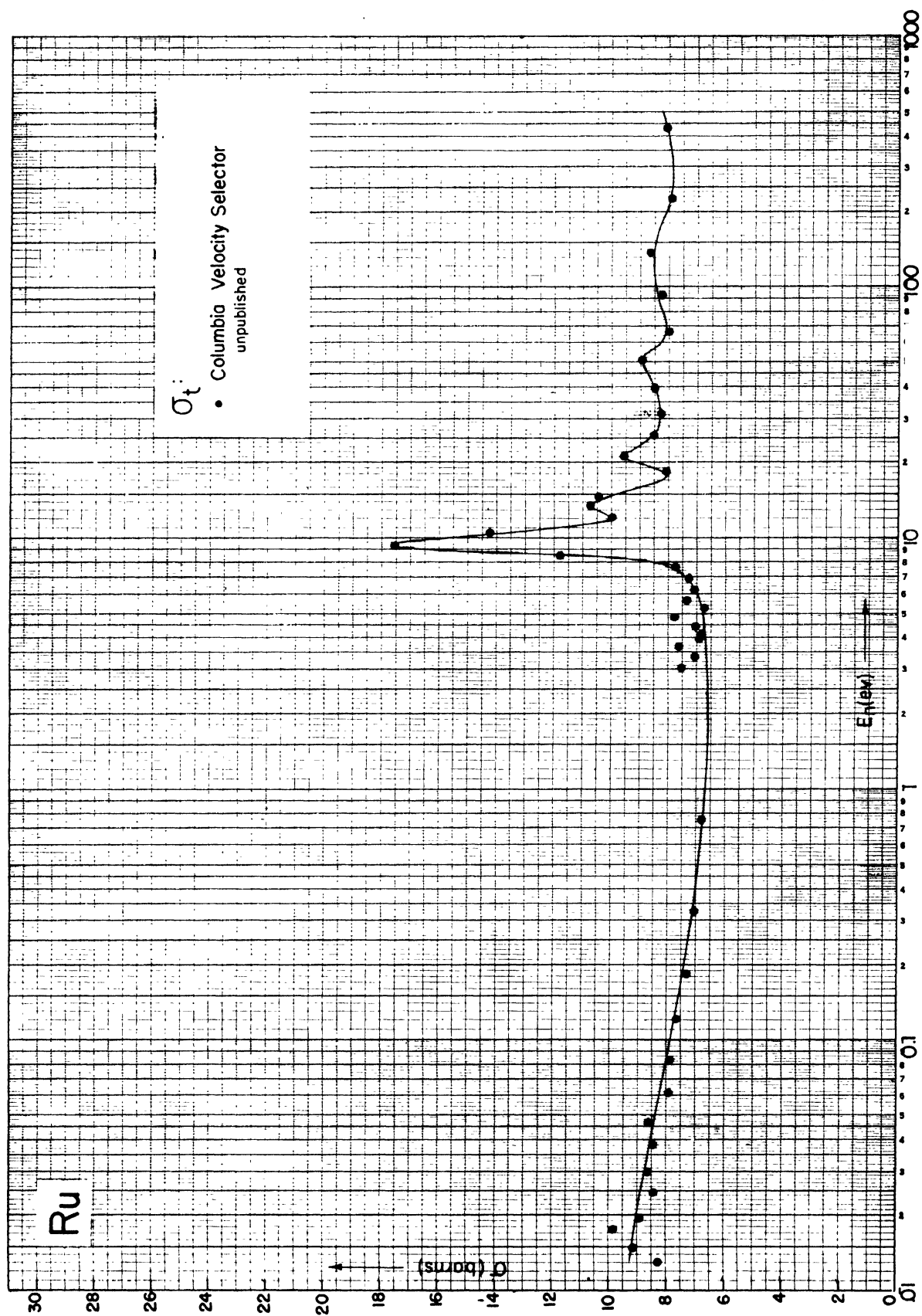


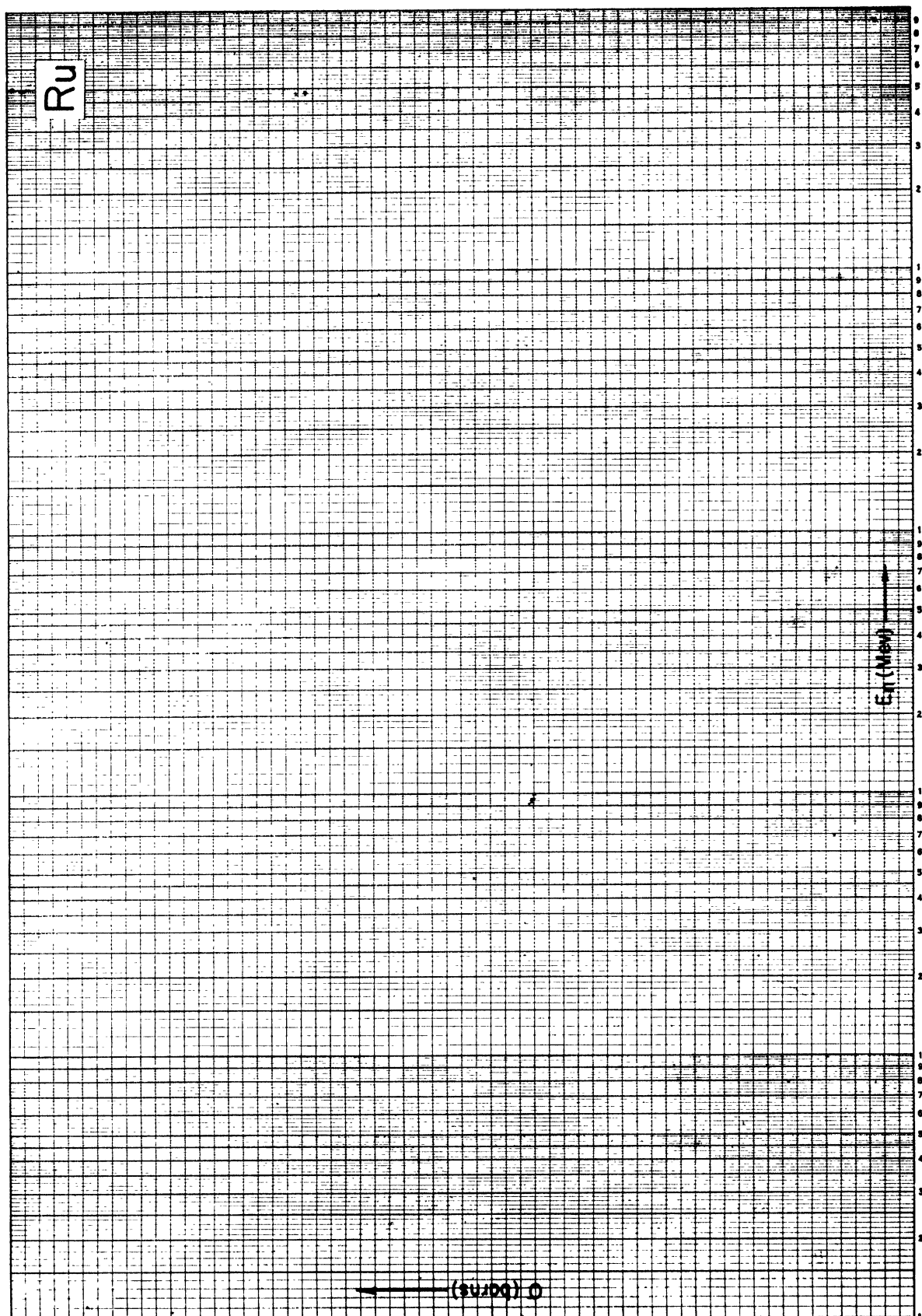


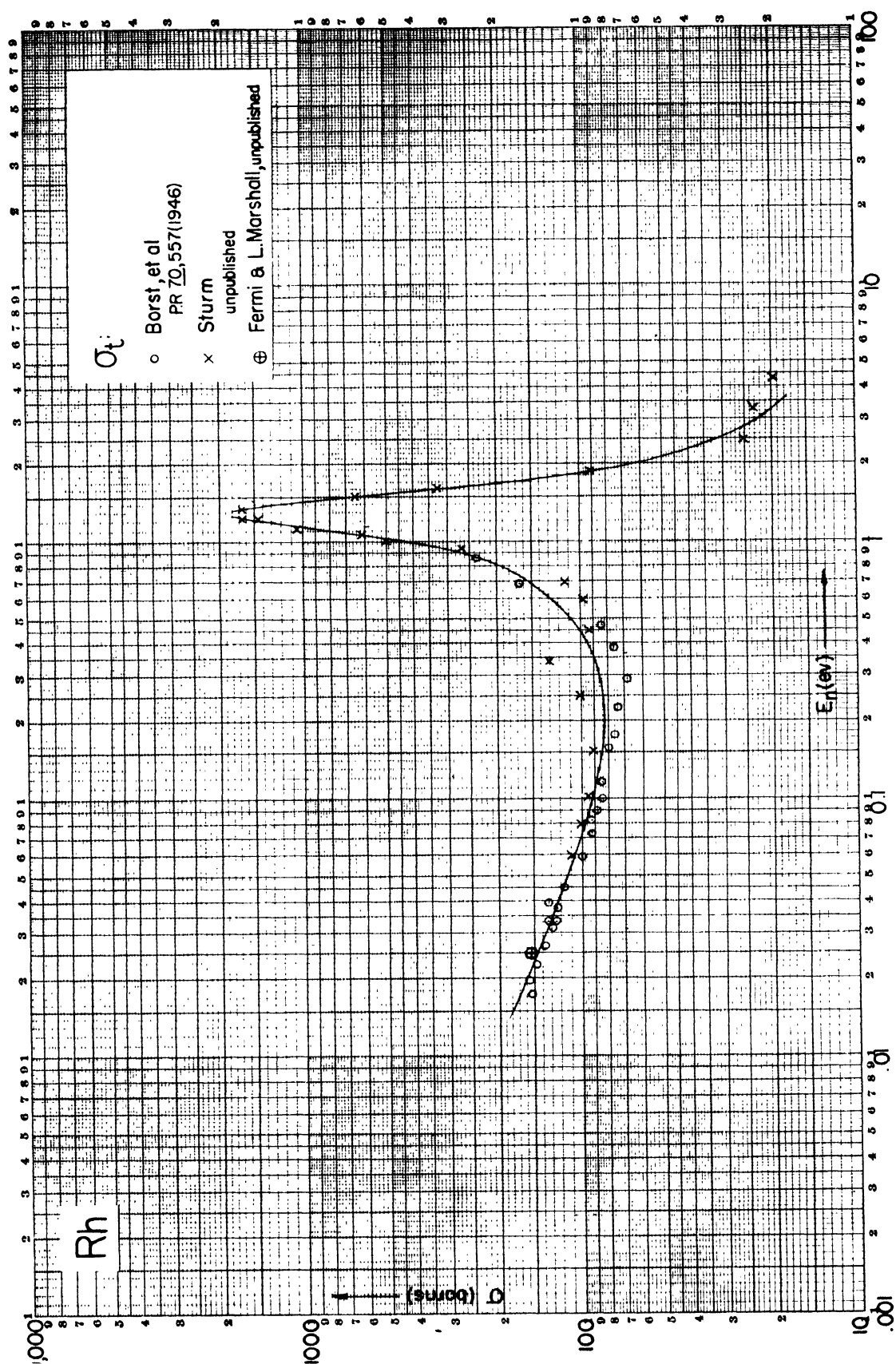


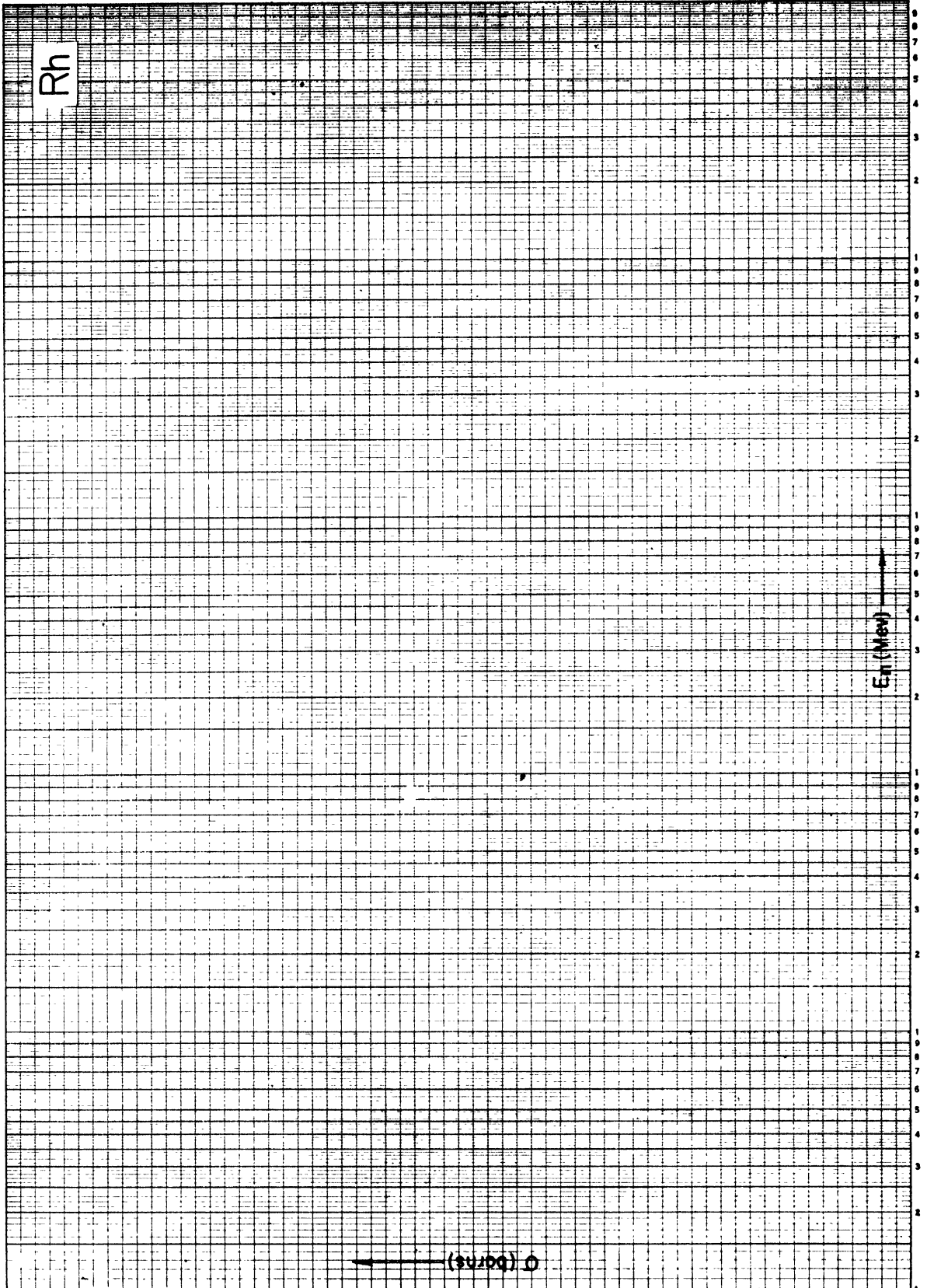


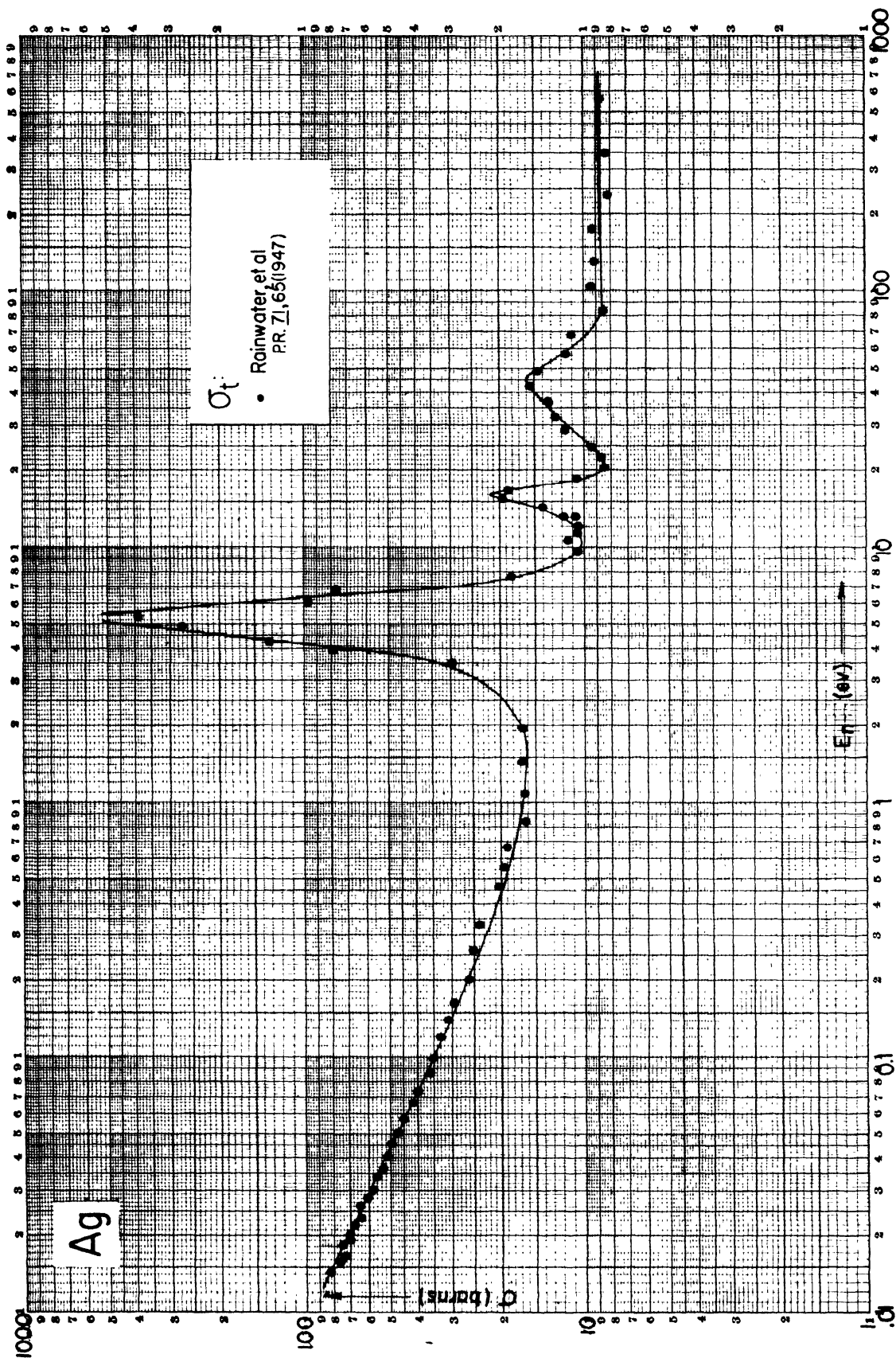


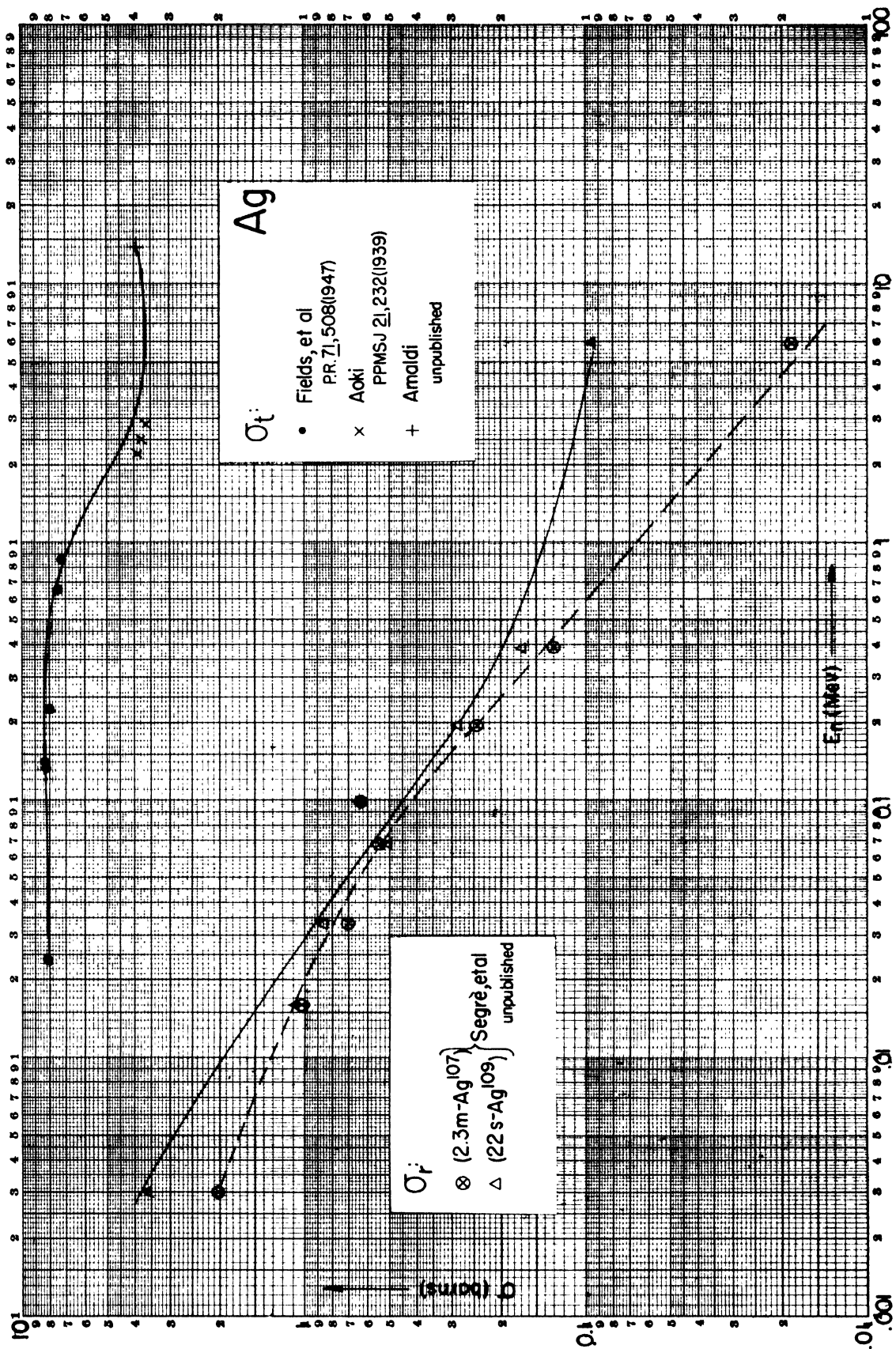


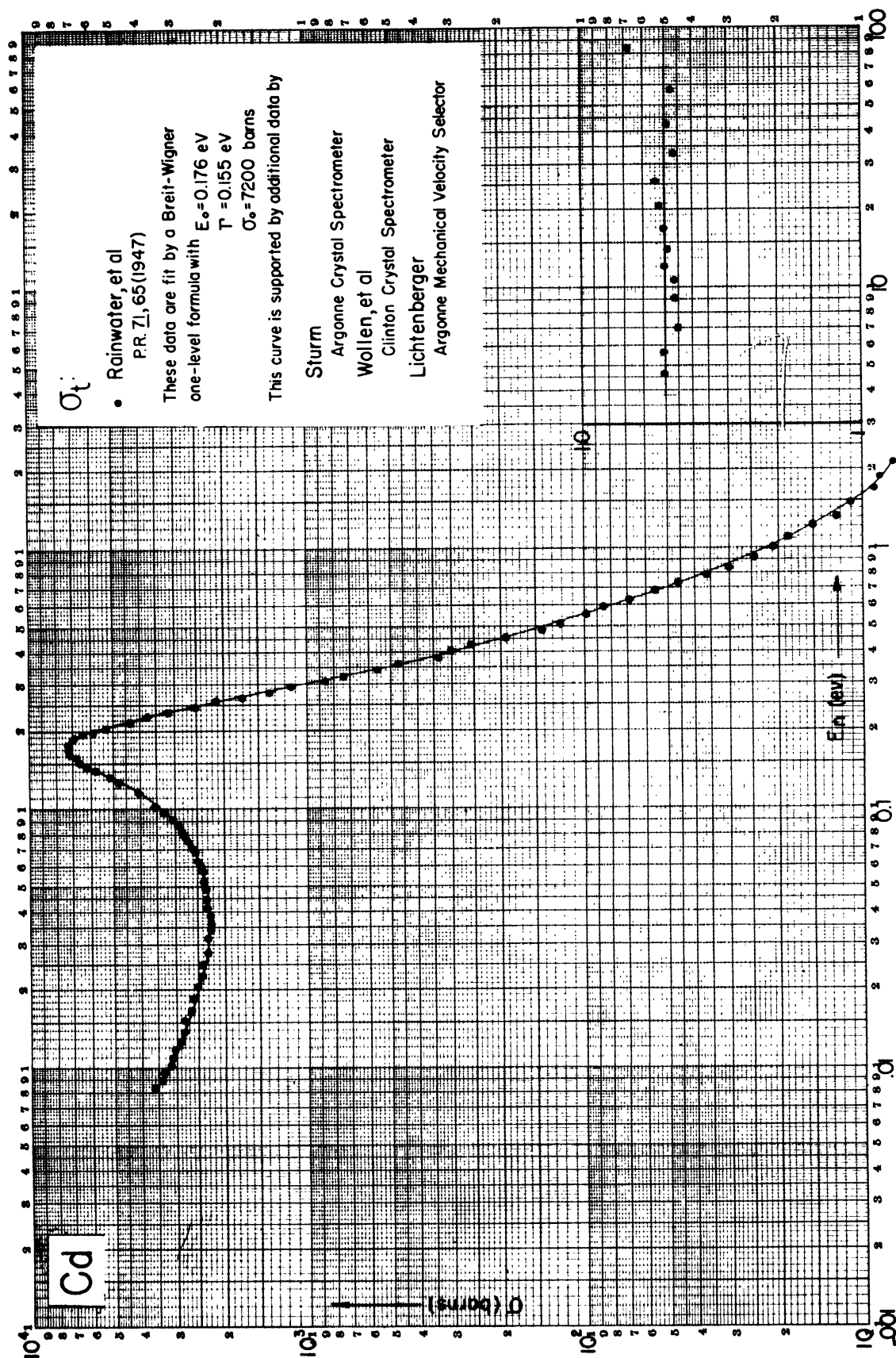


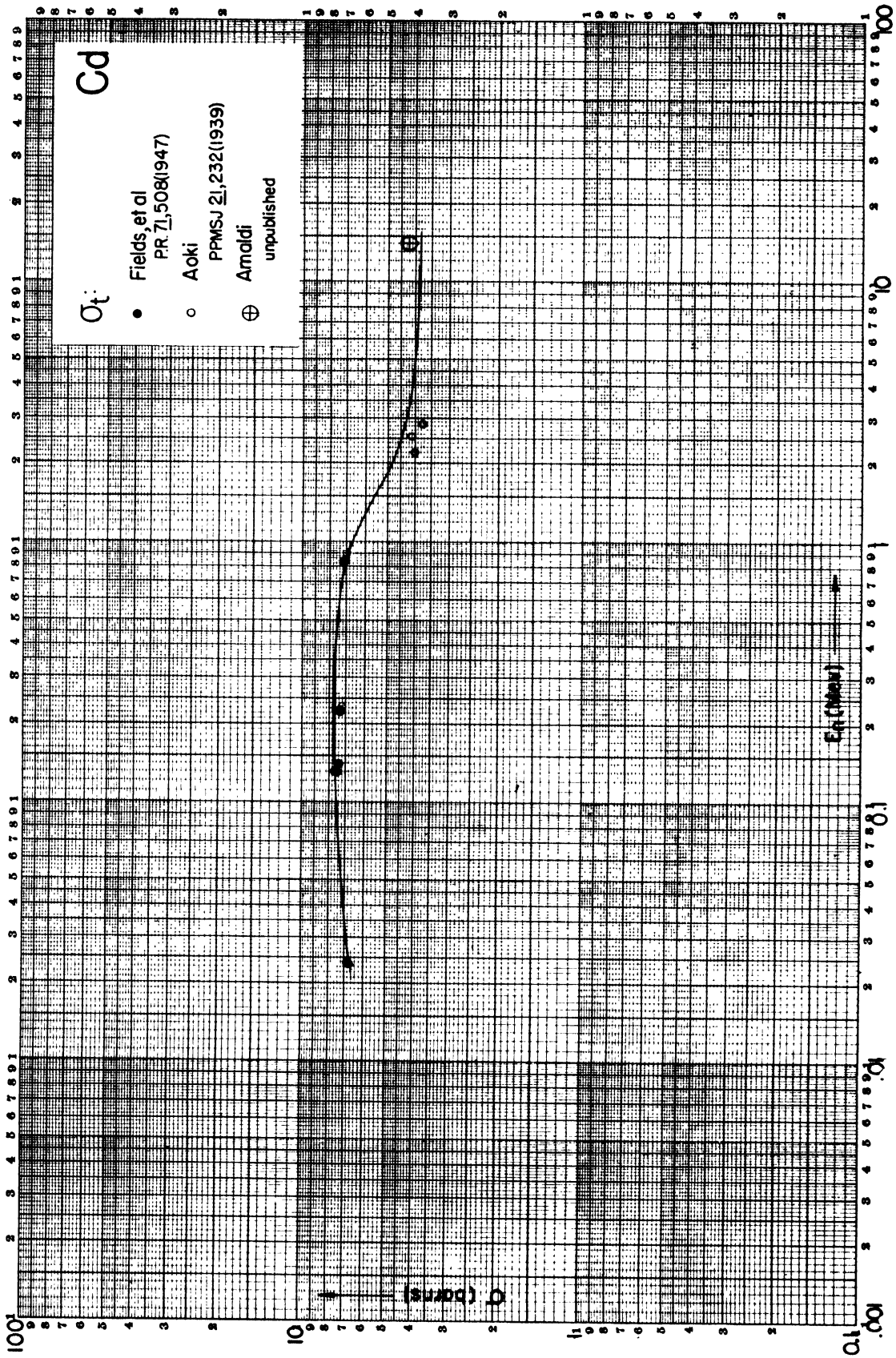


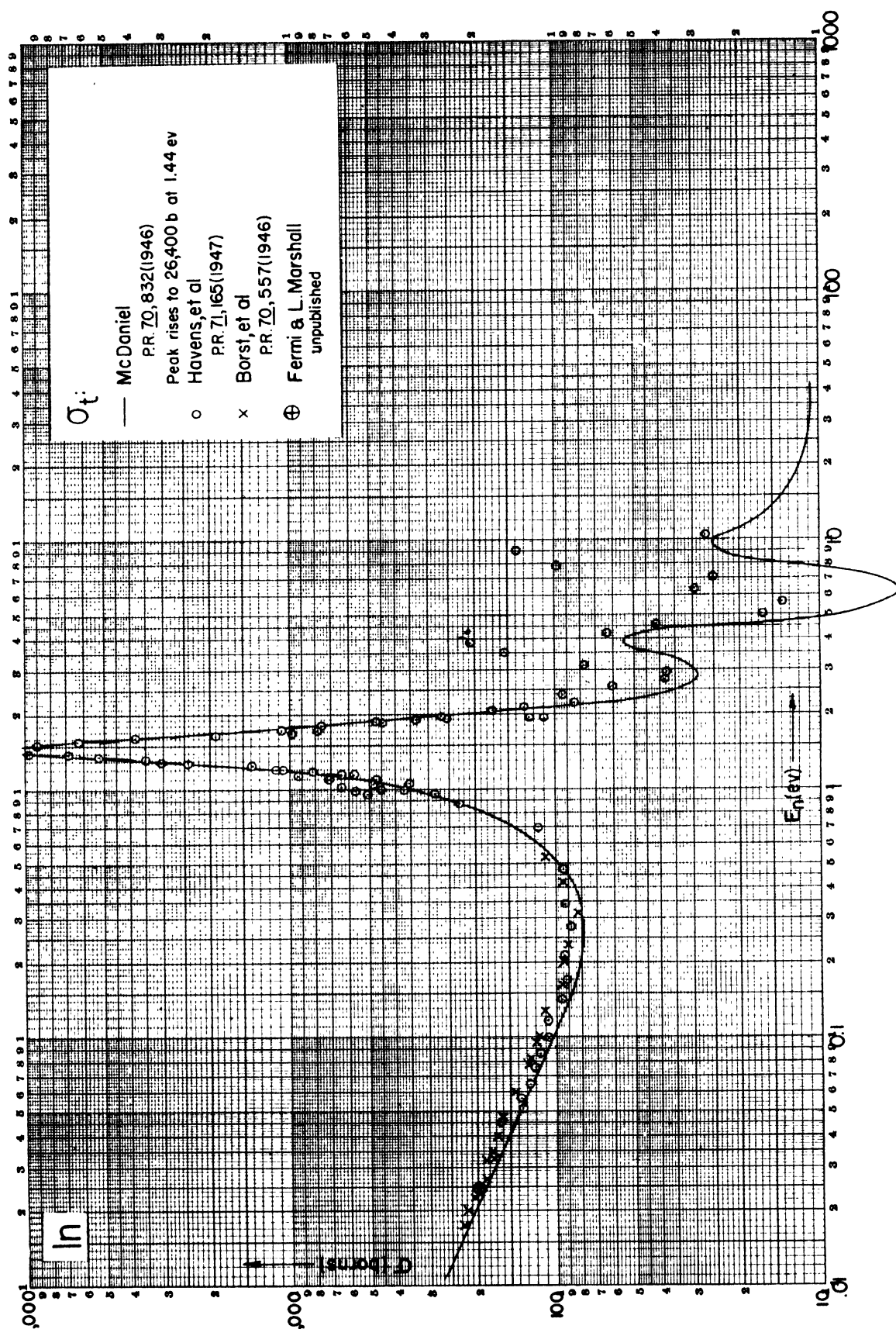


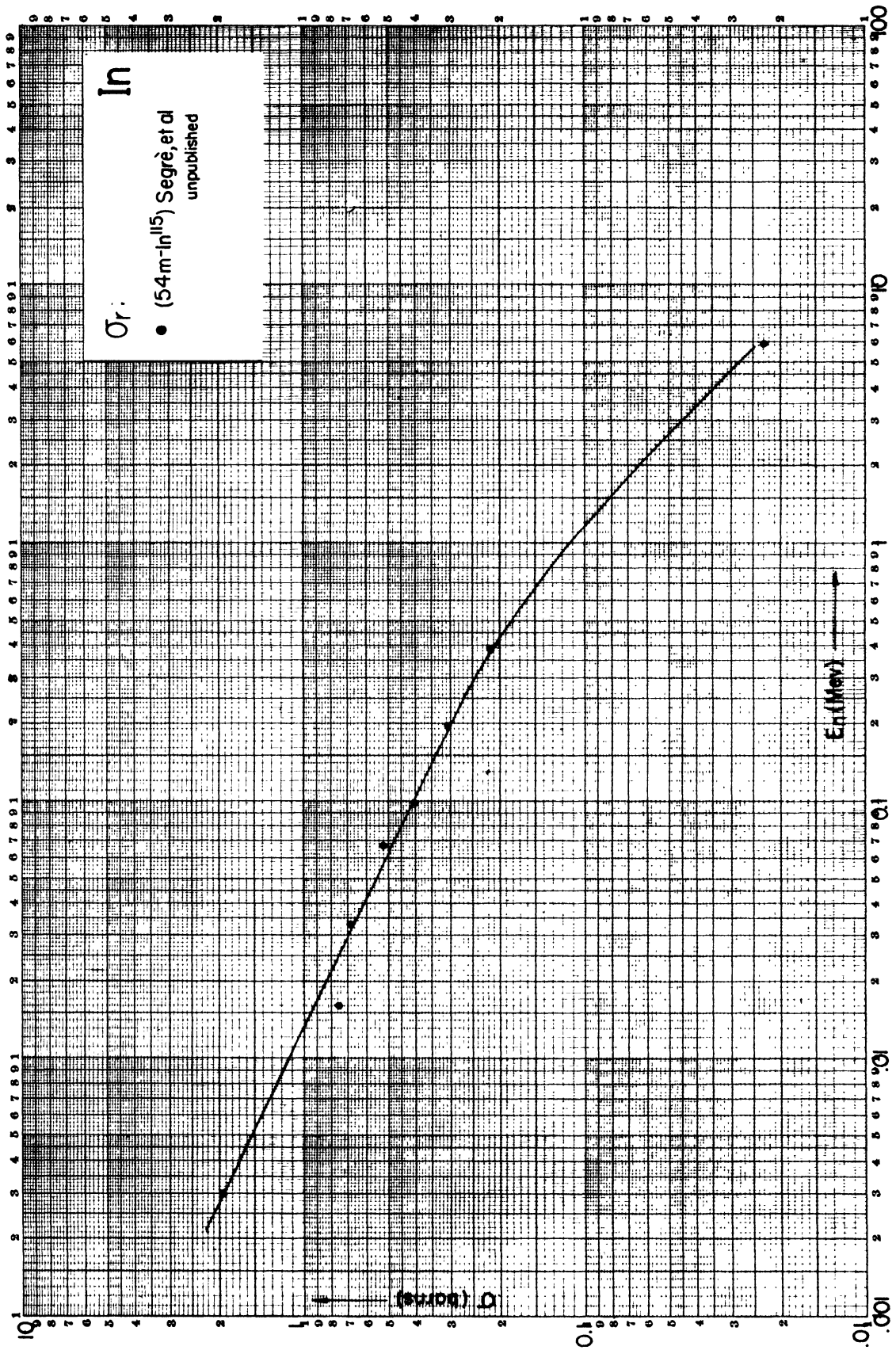


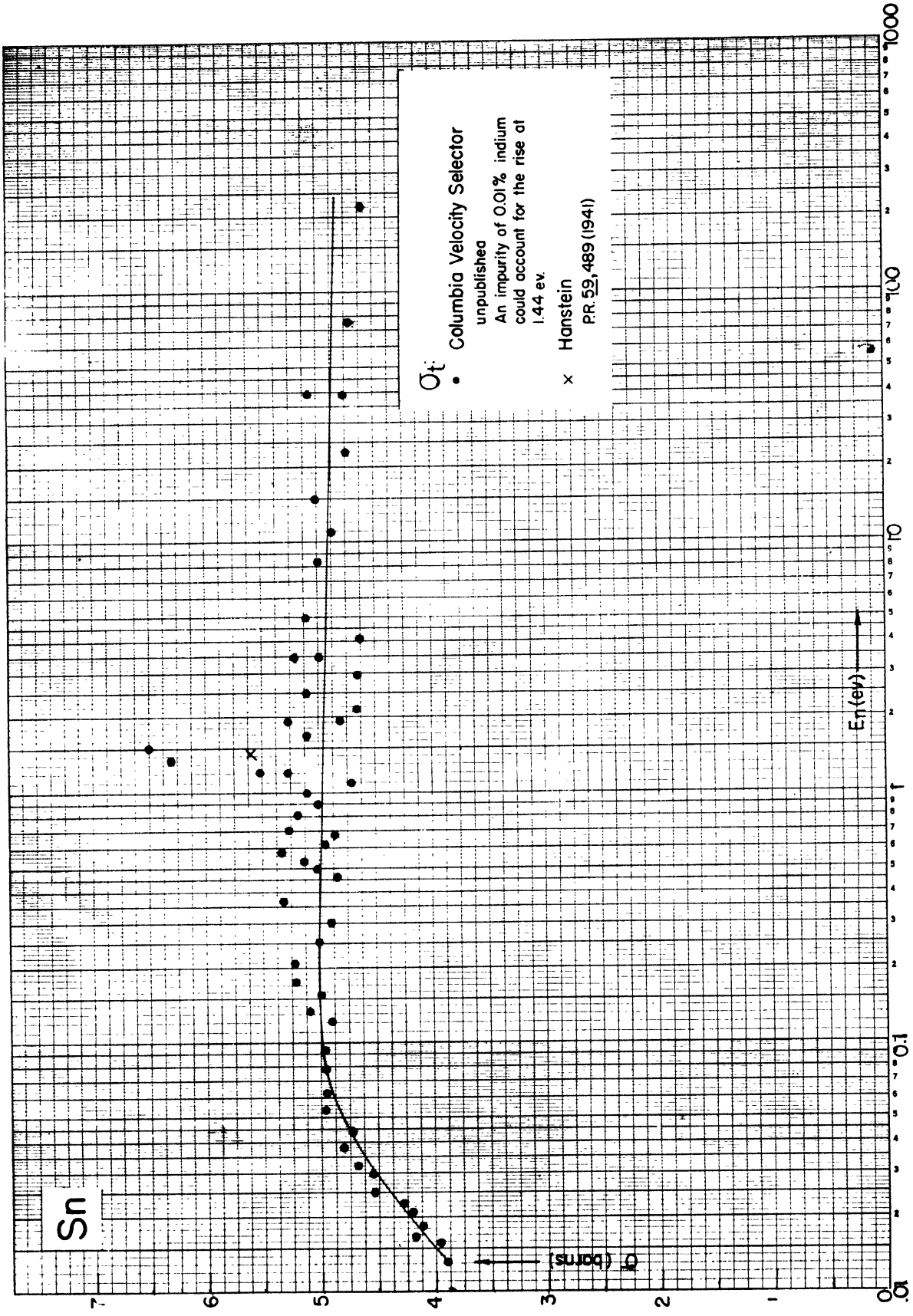


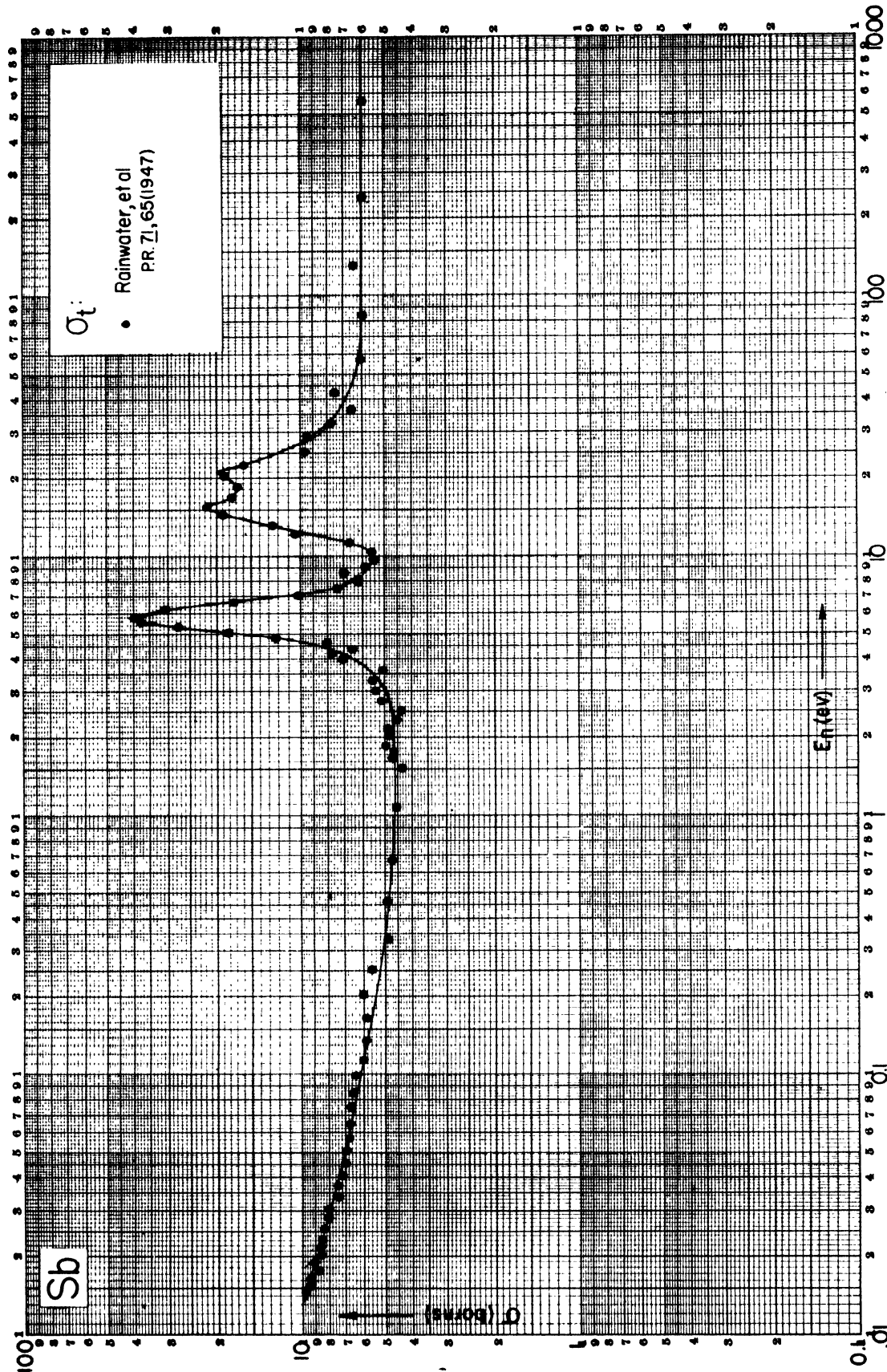


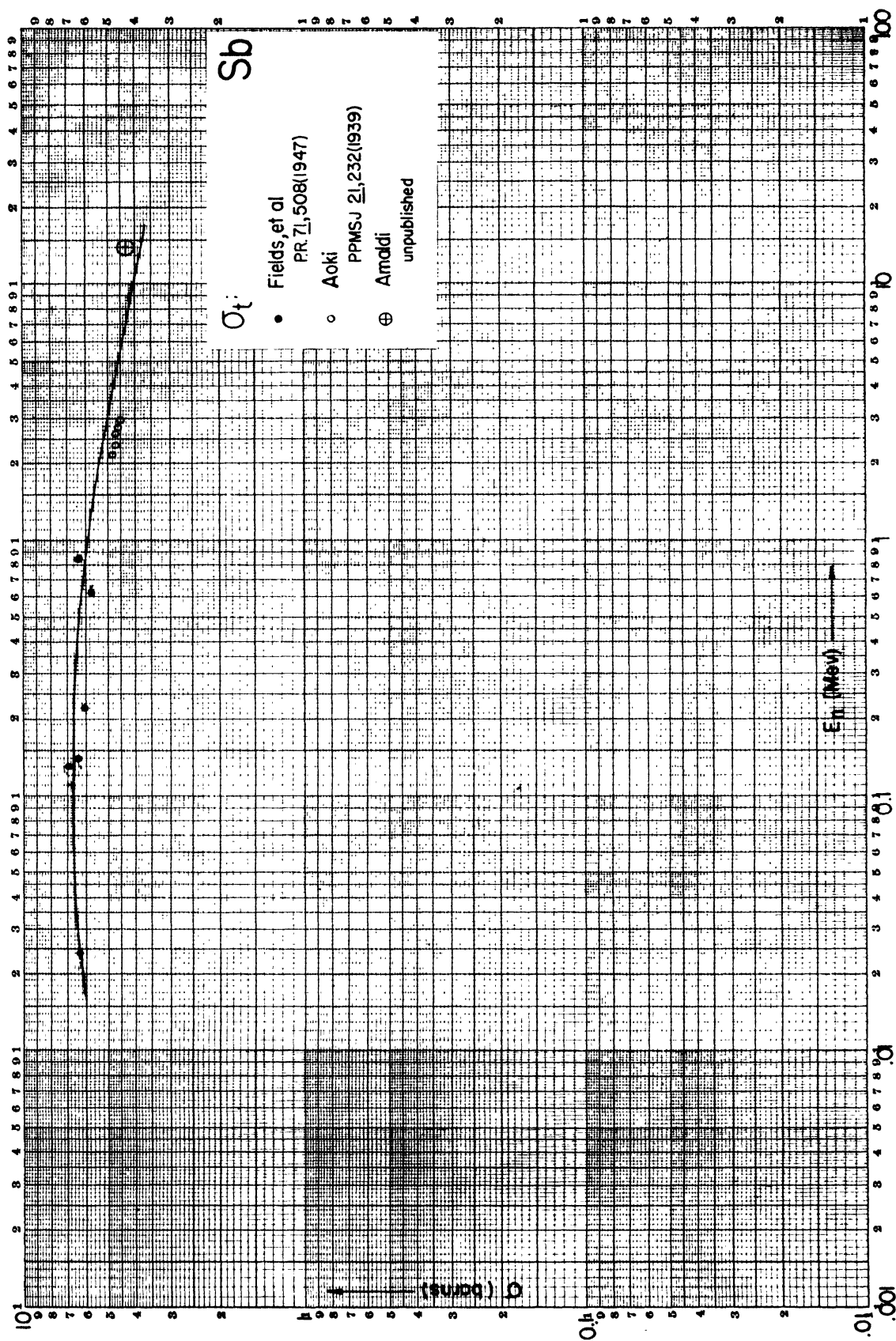


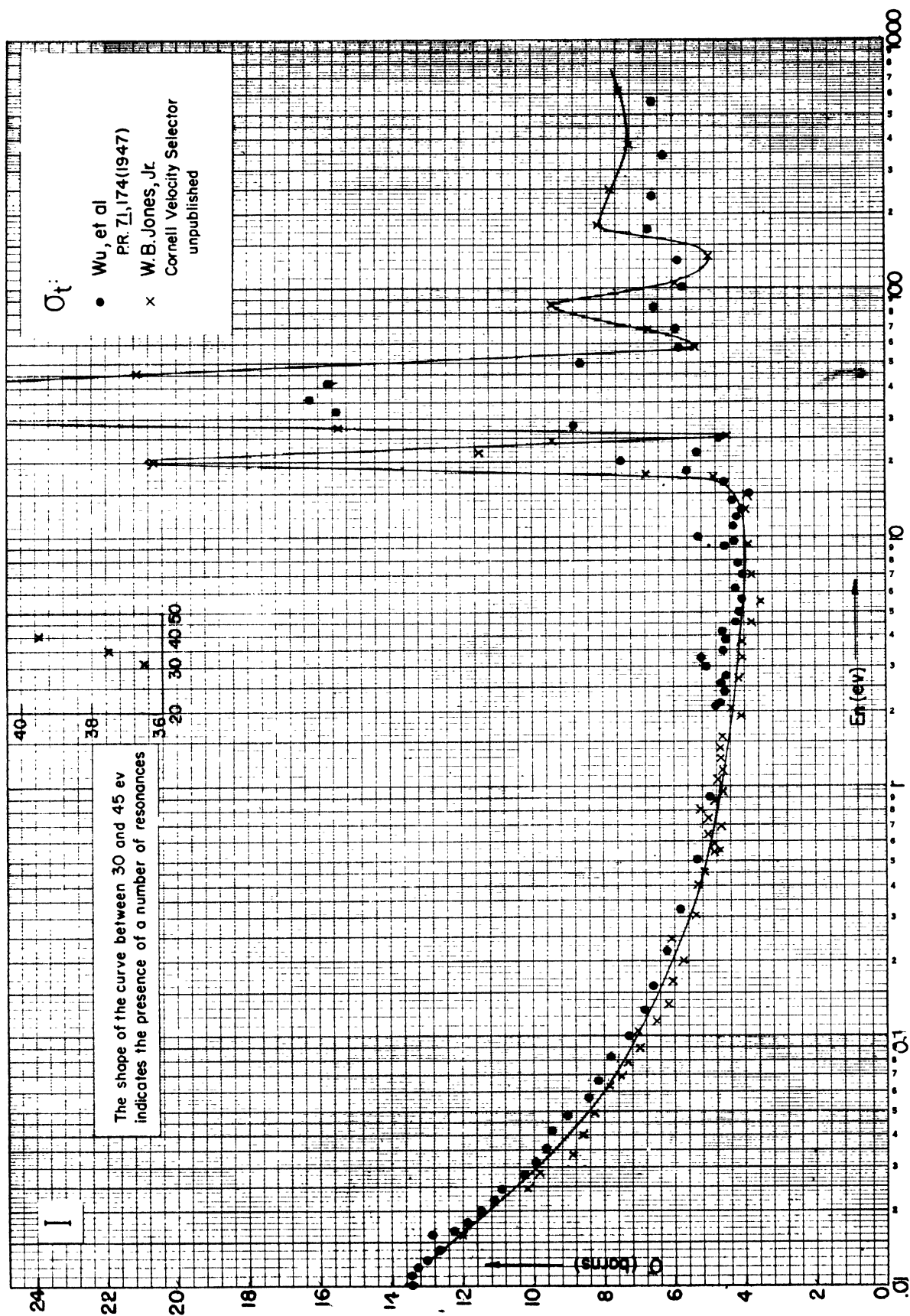


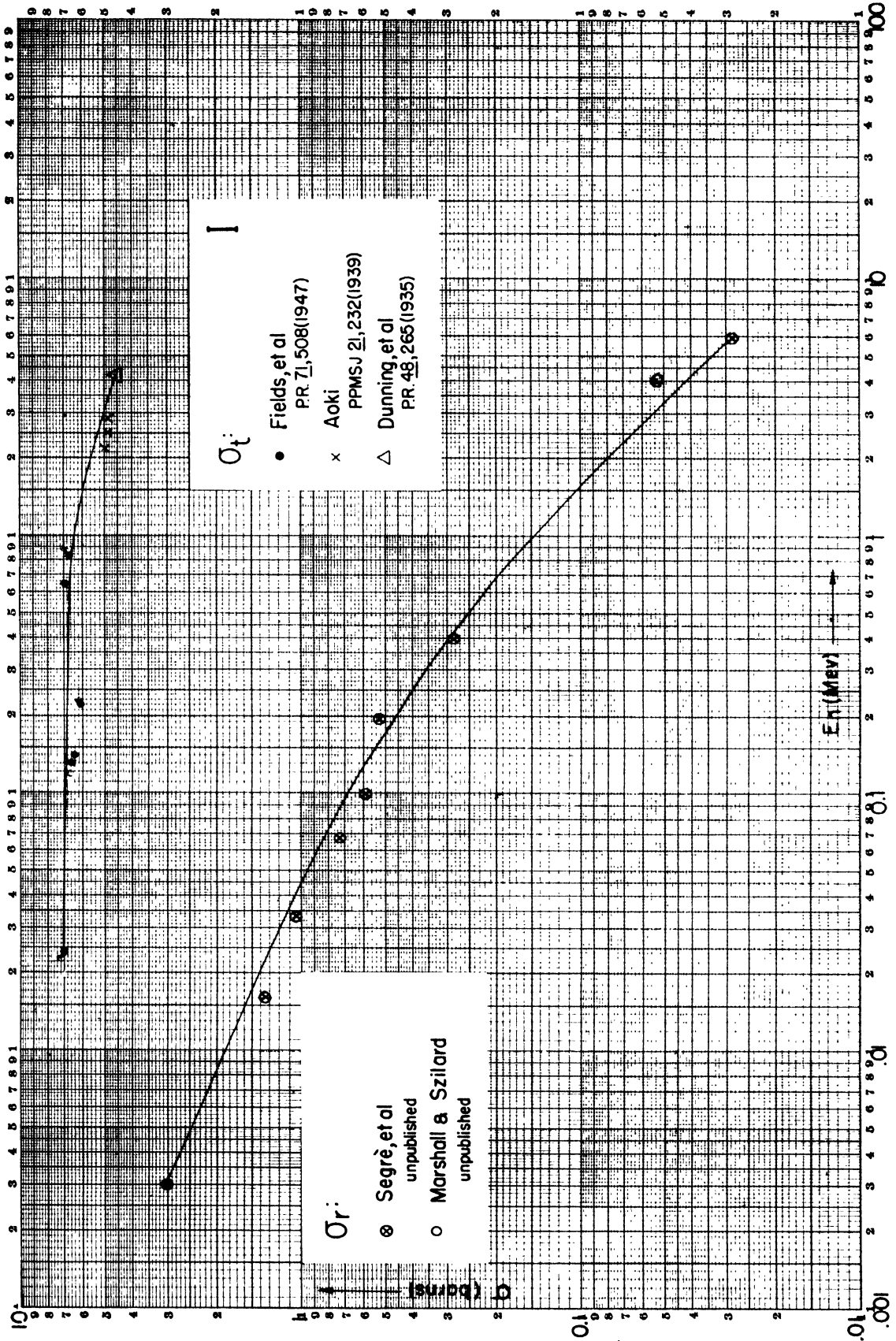


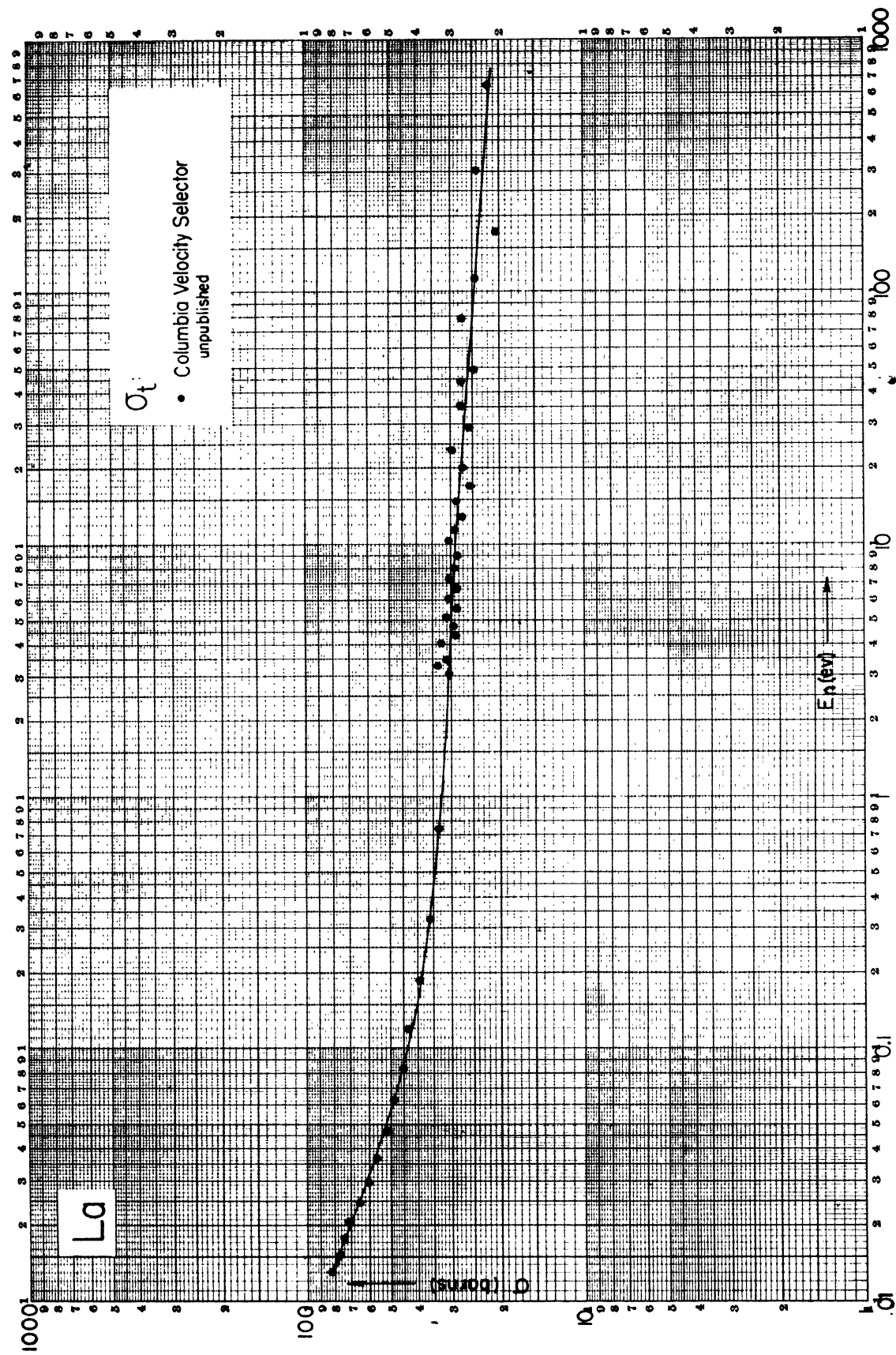








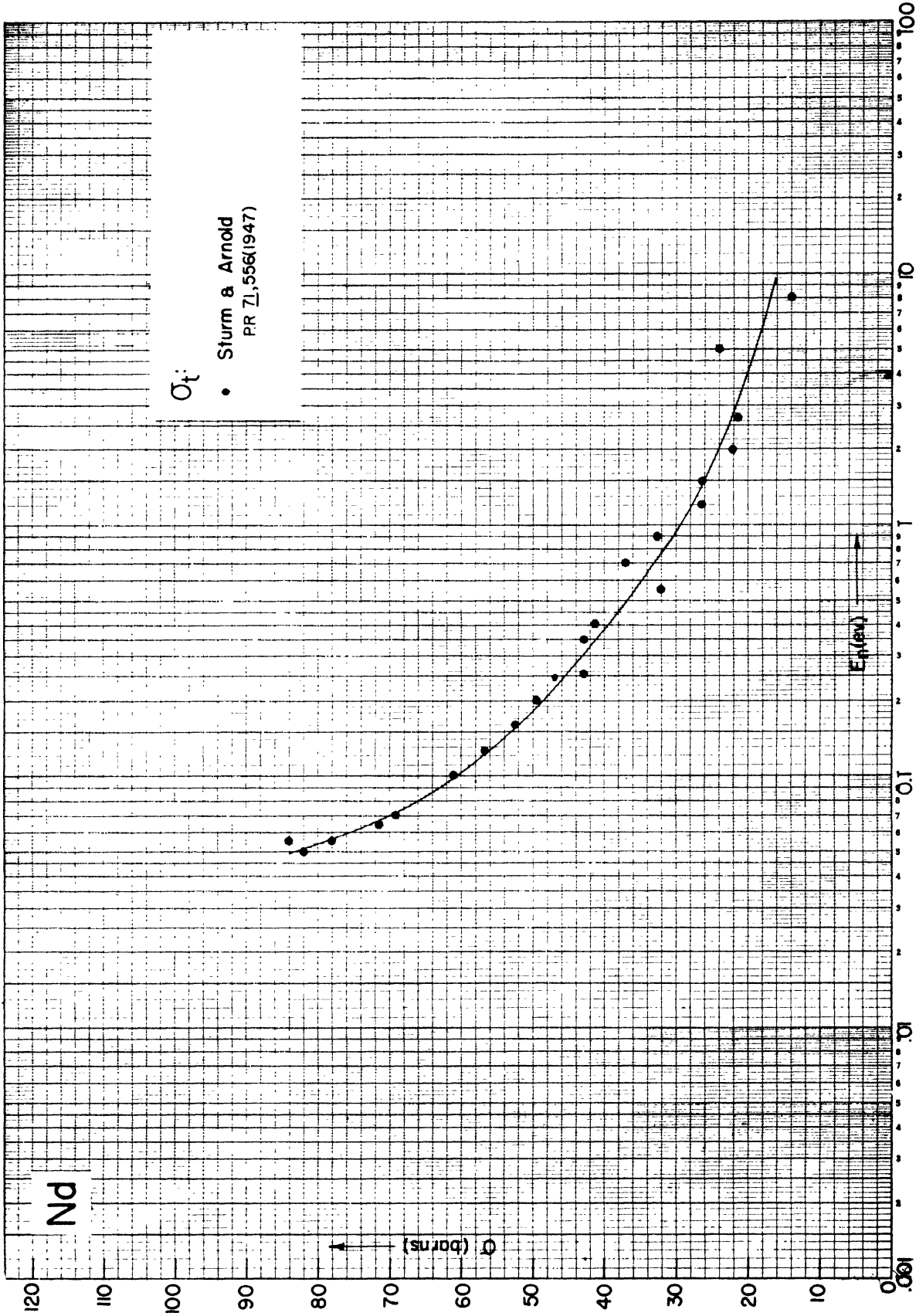


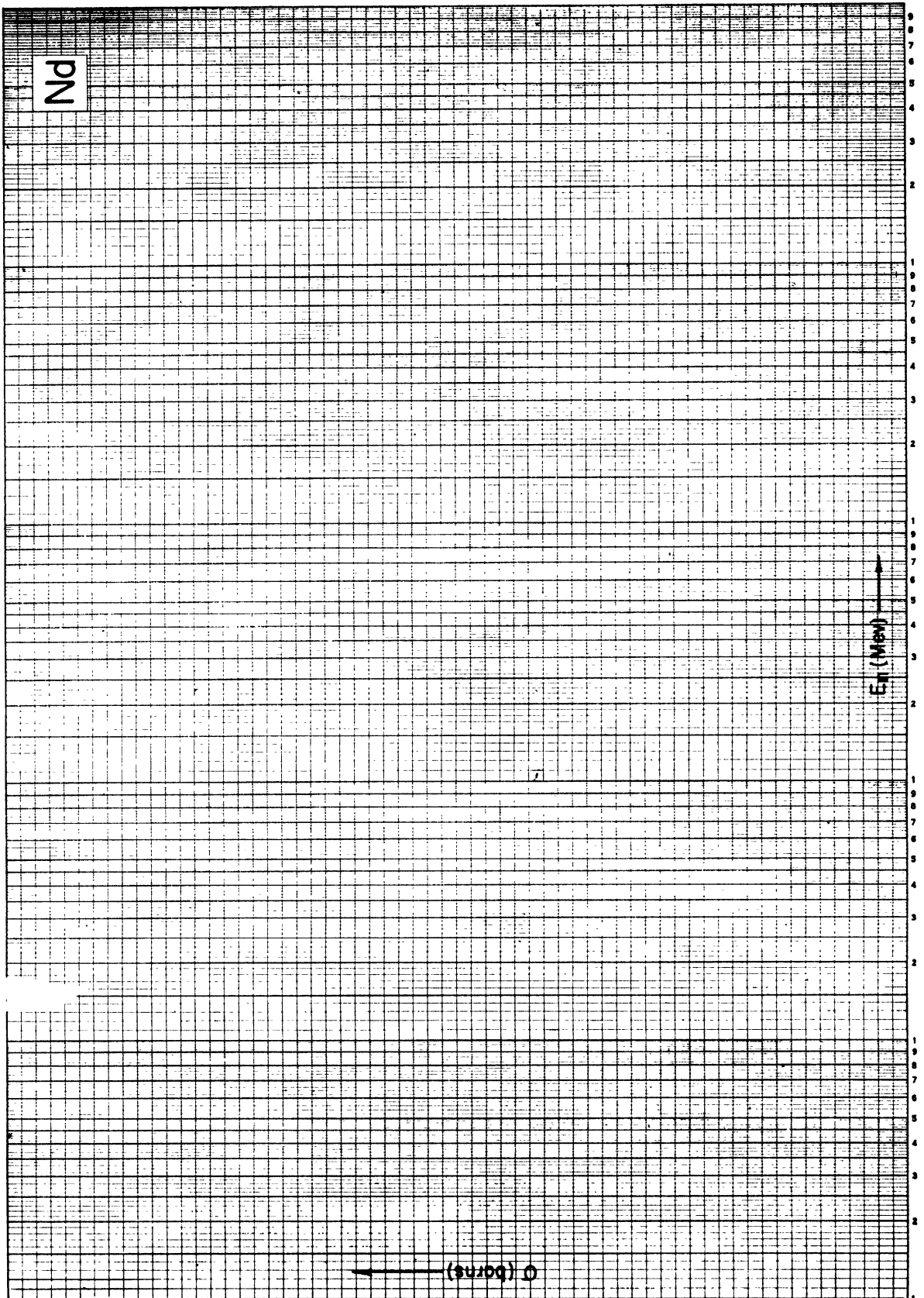


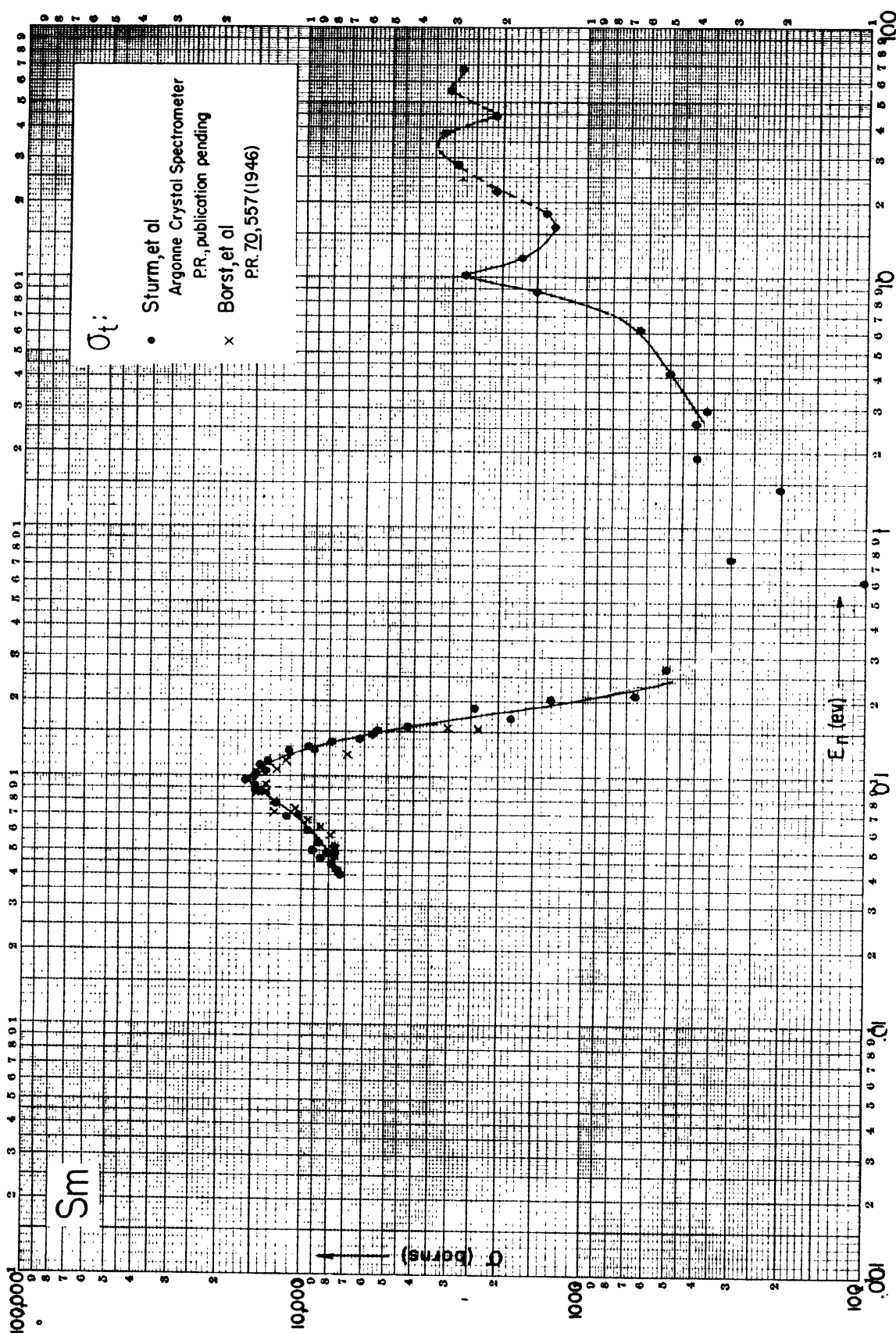
9

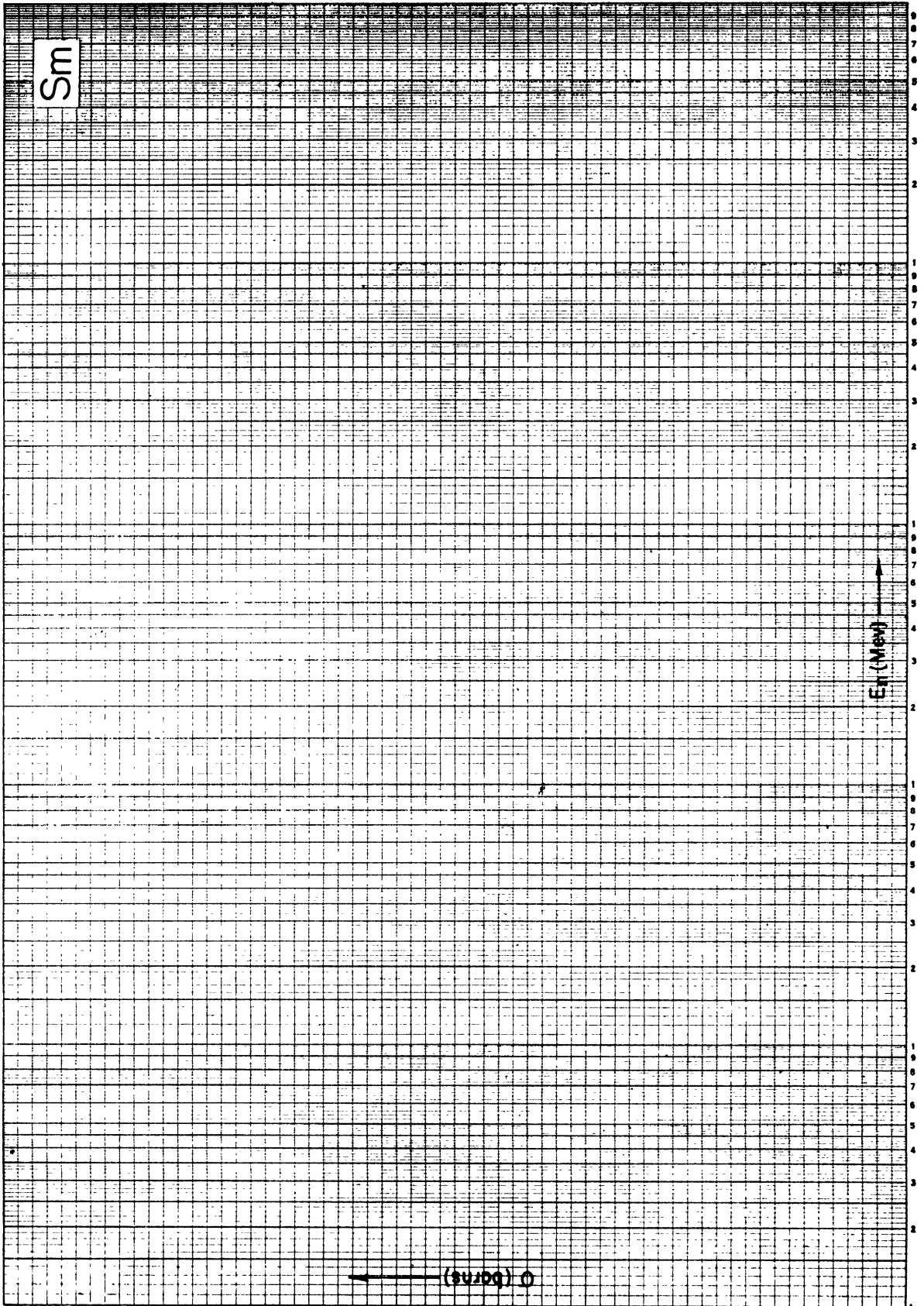
365

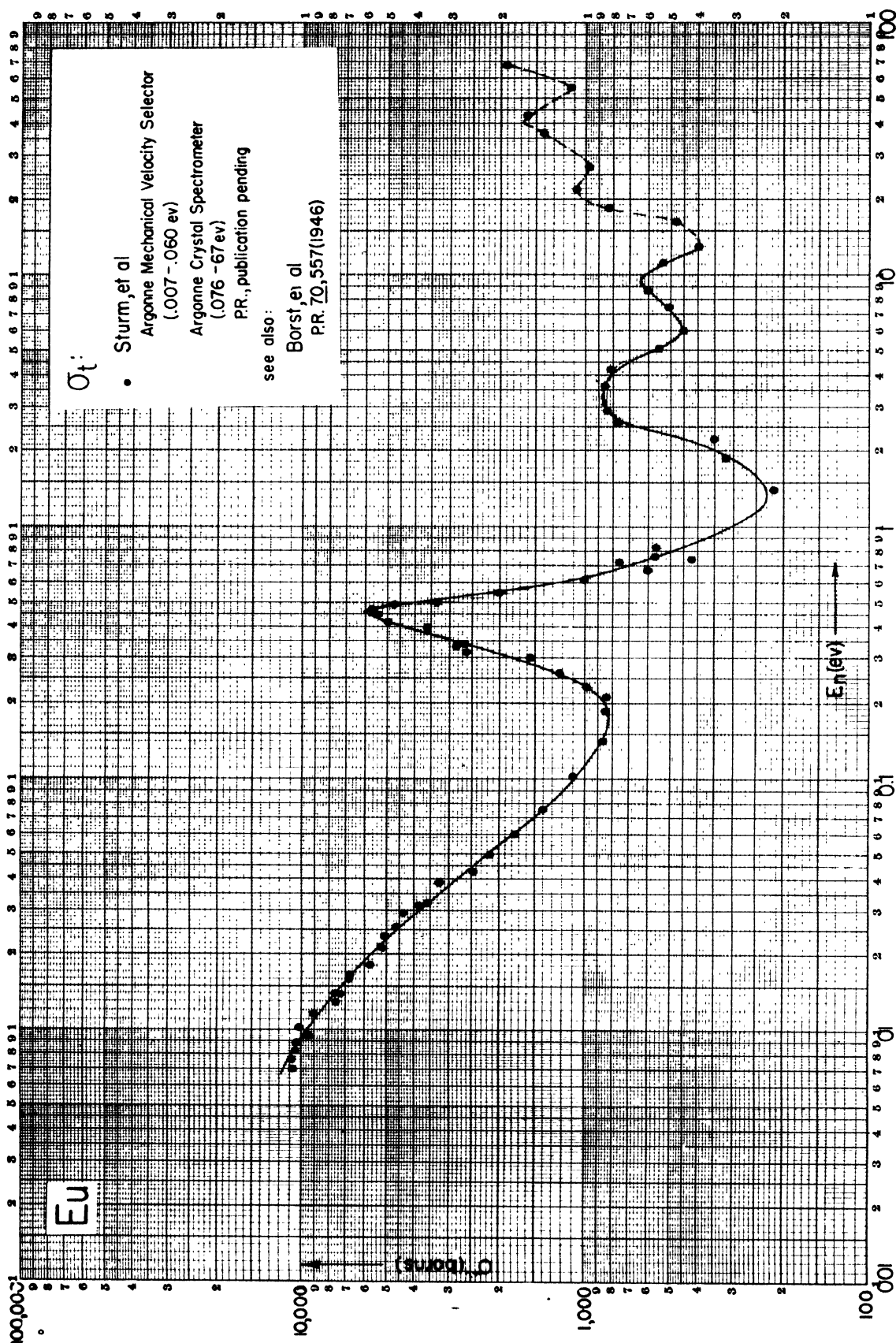
(b)(7)(D)

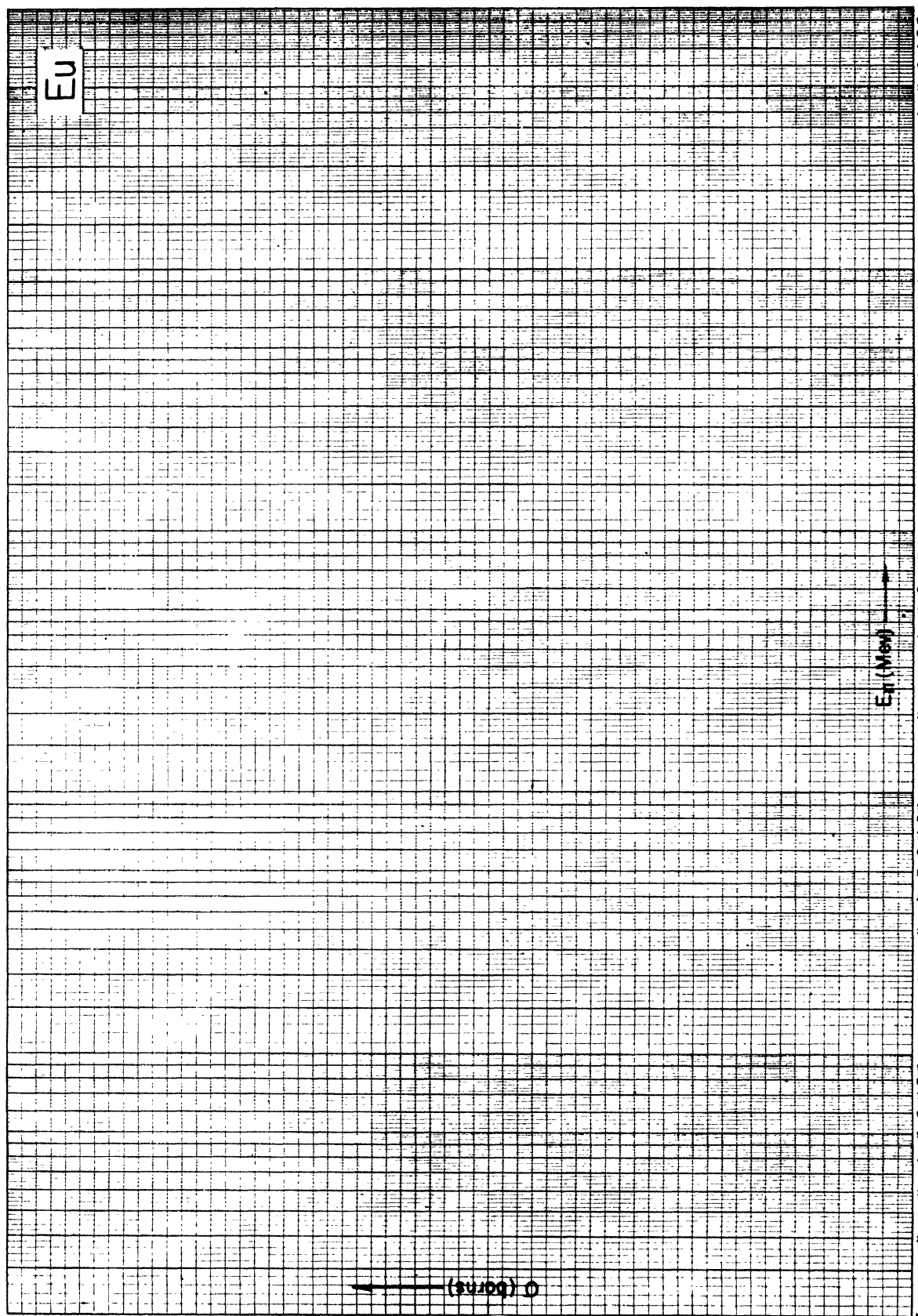


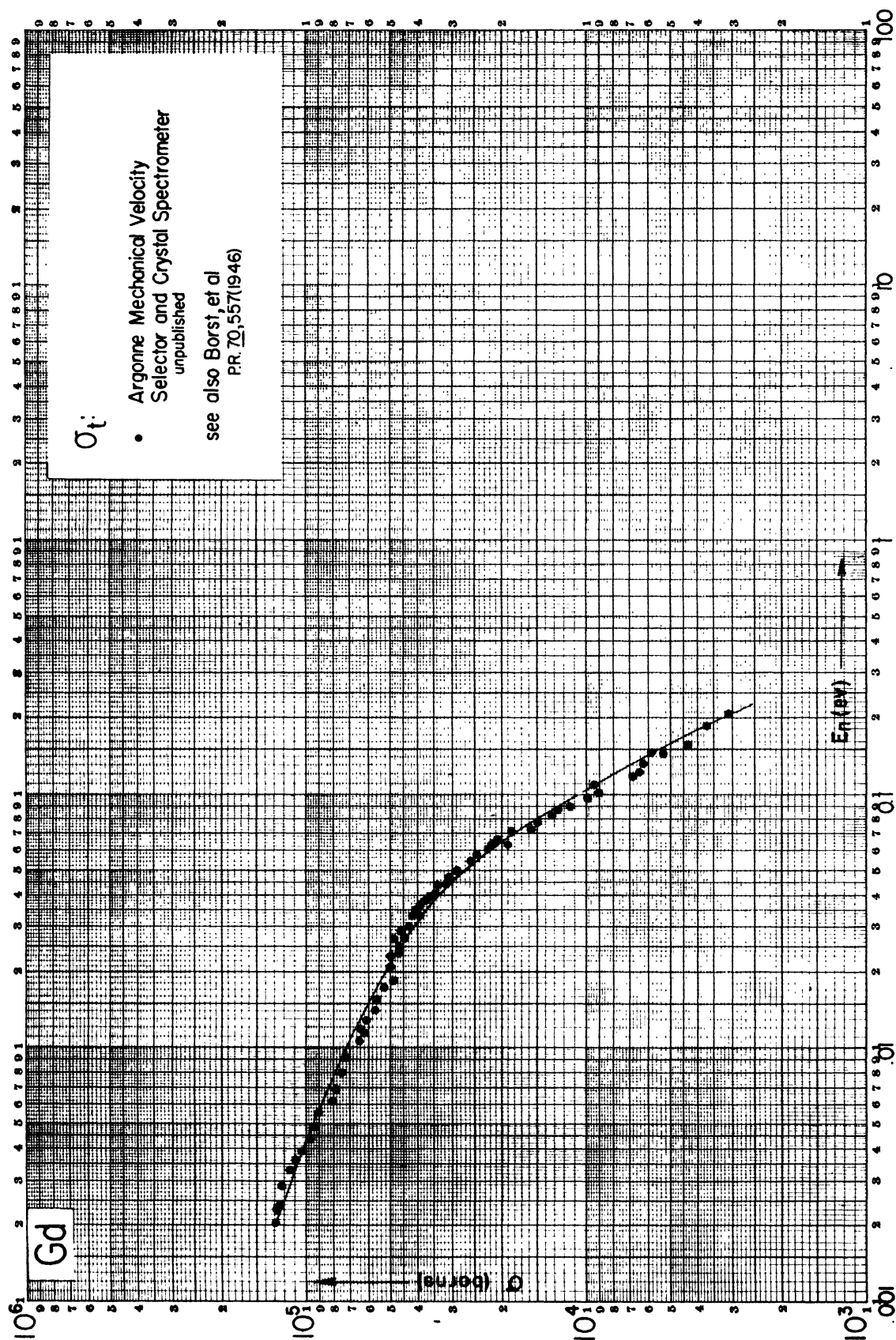


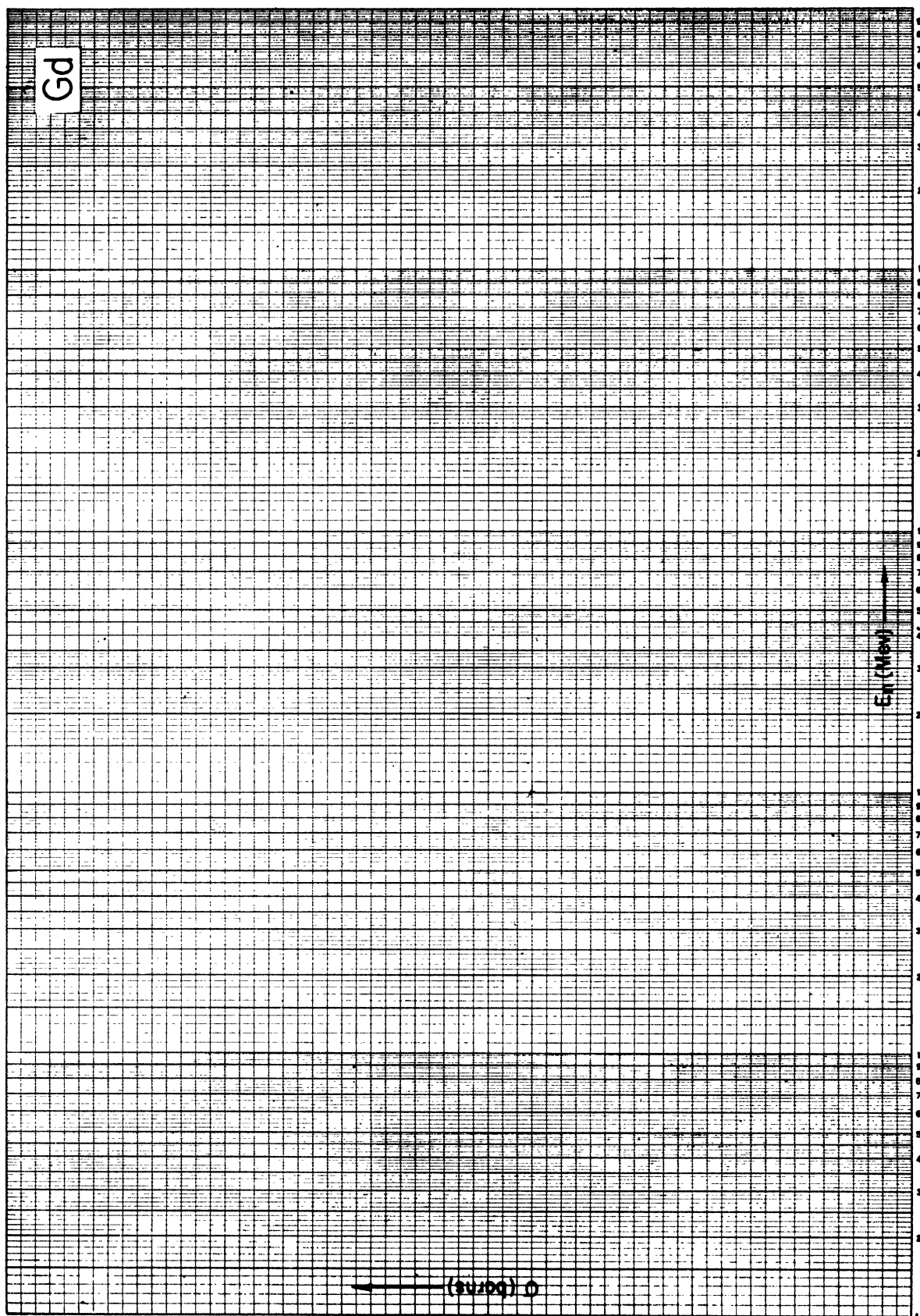


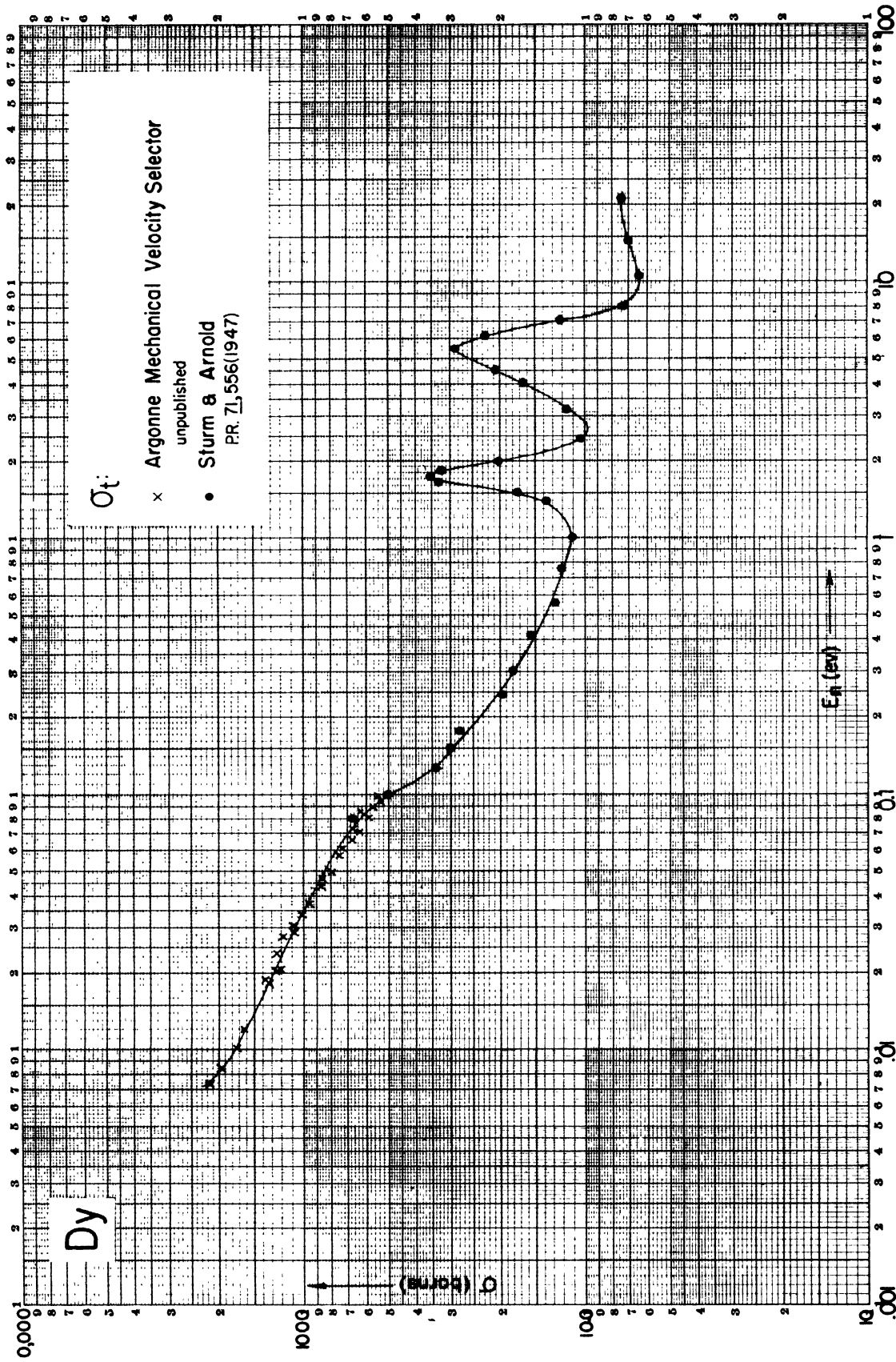








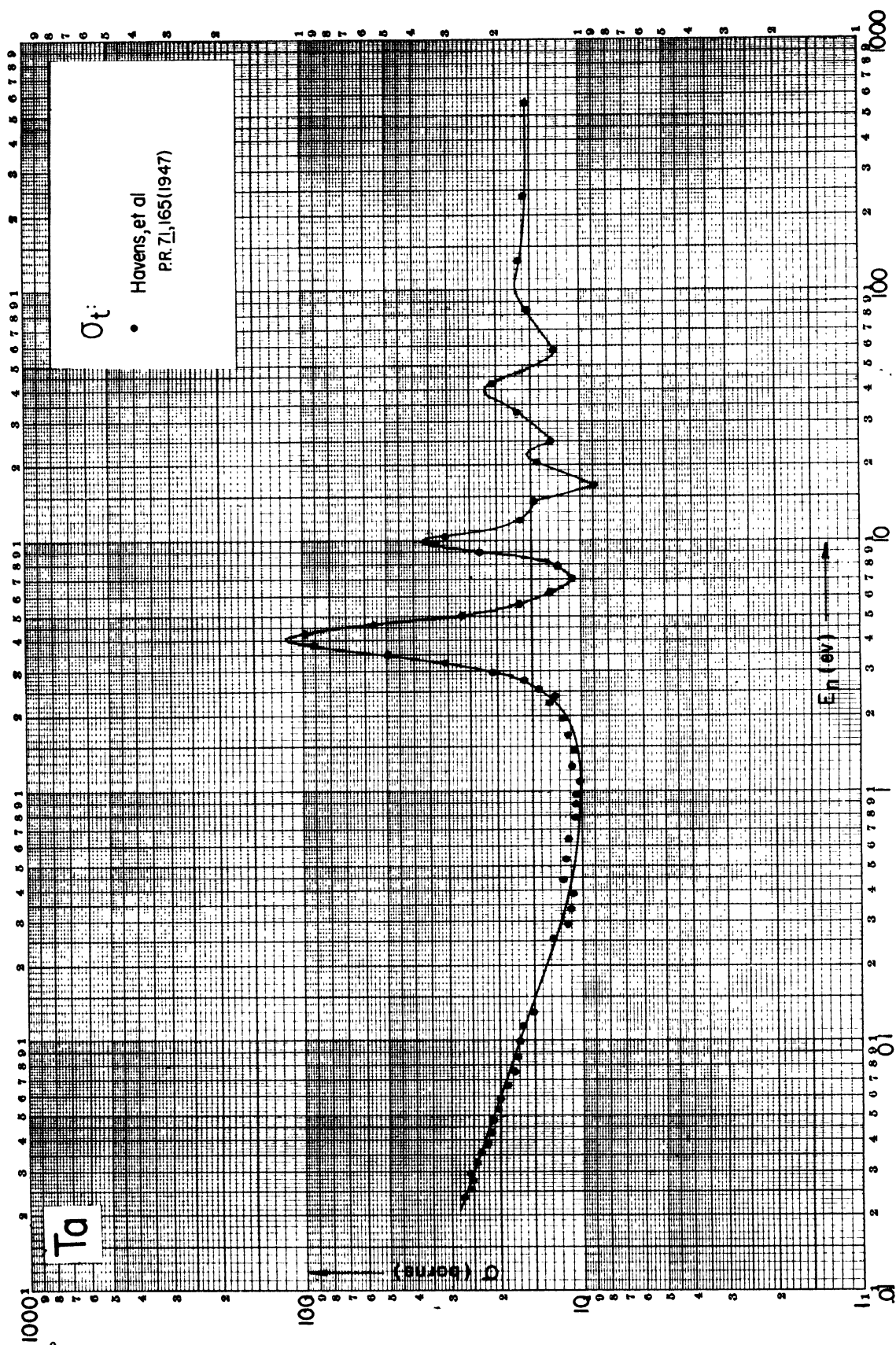


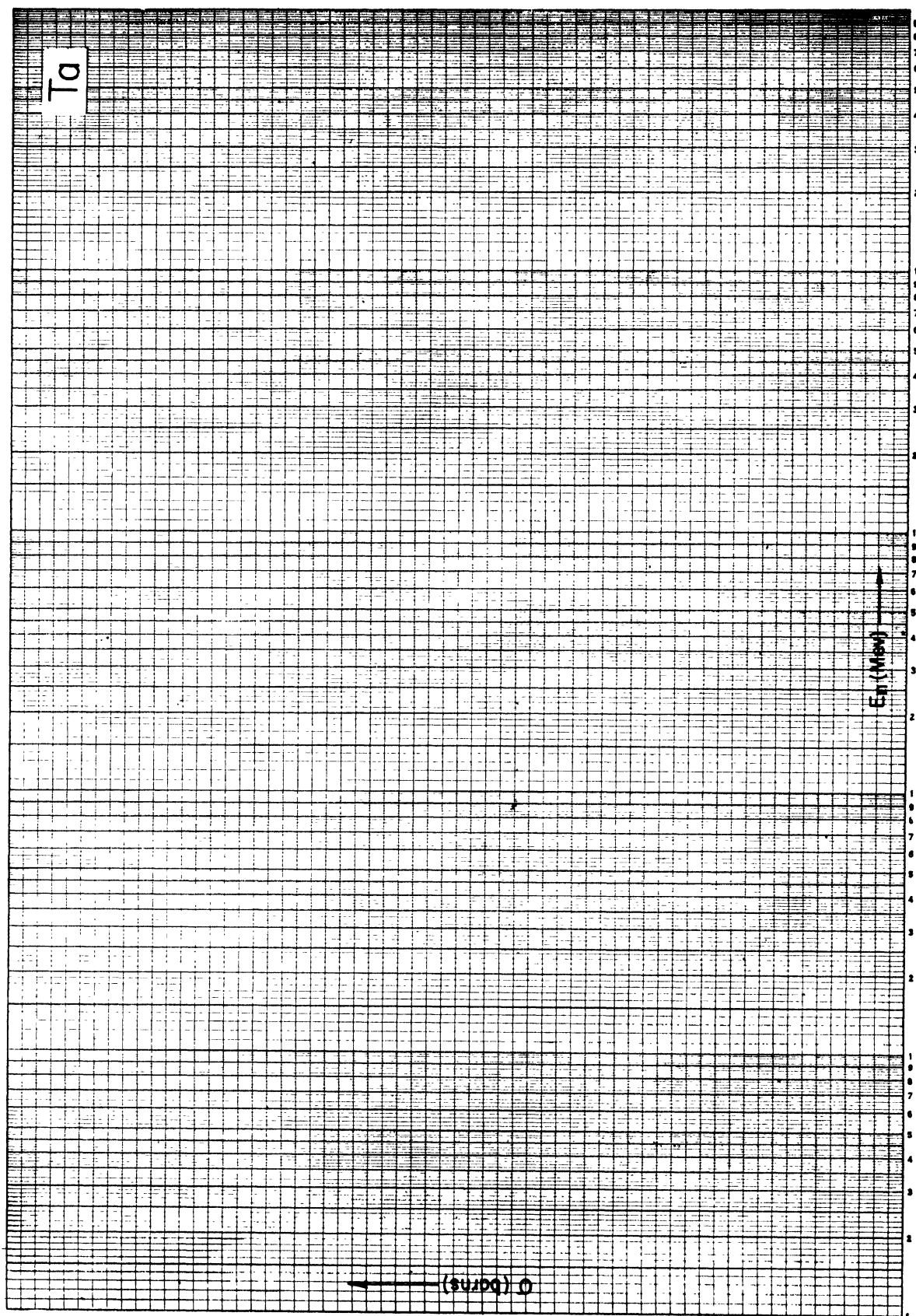


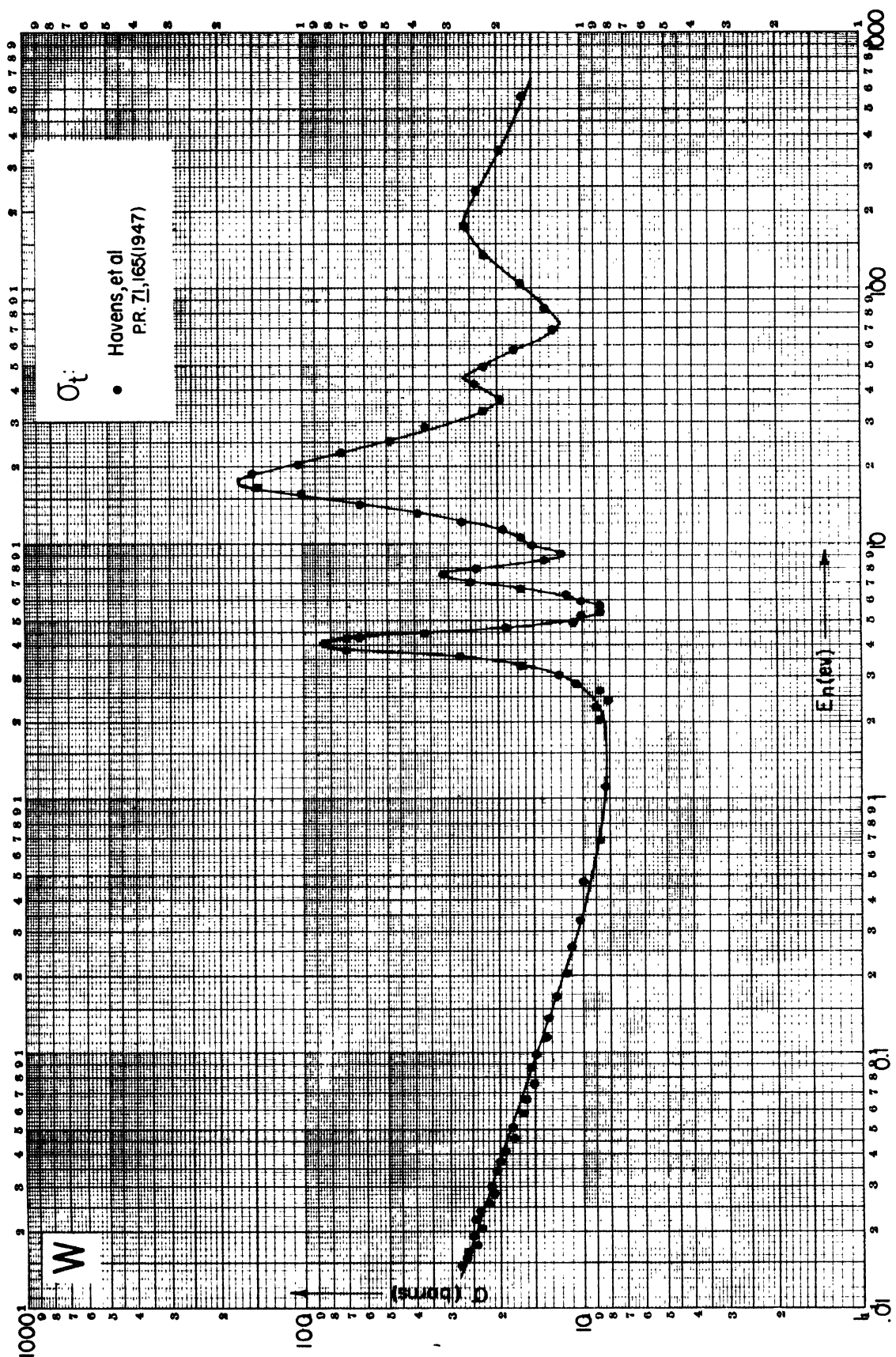
Dy

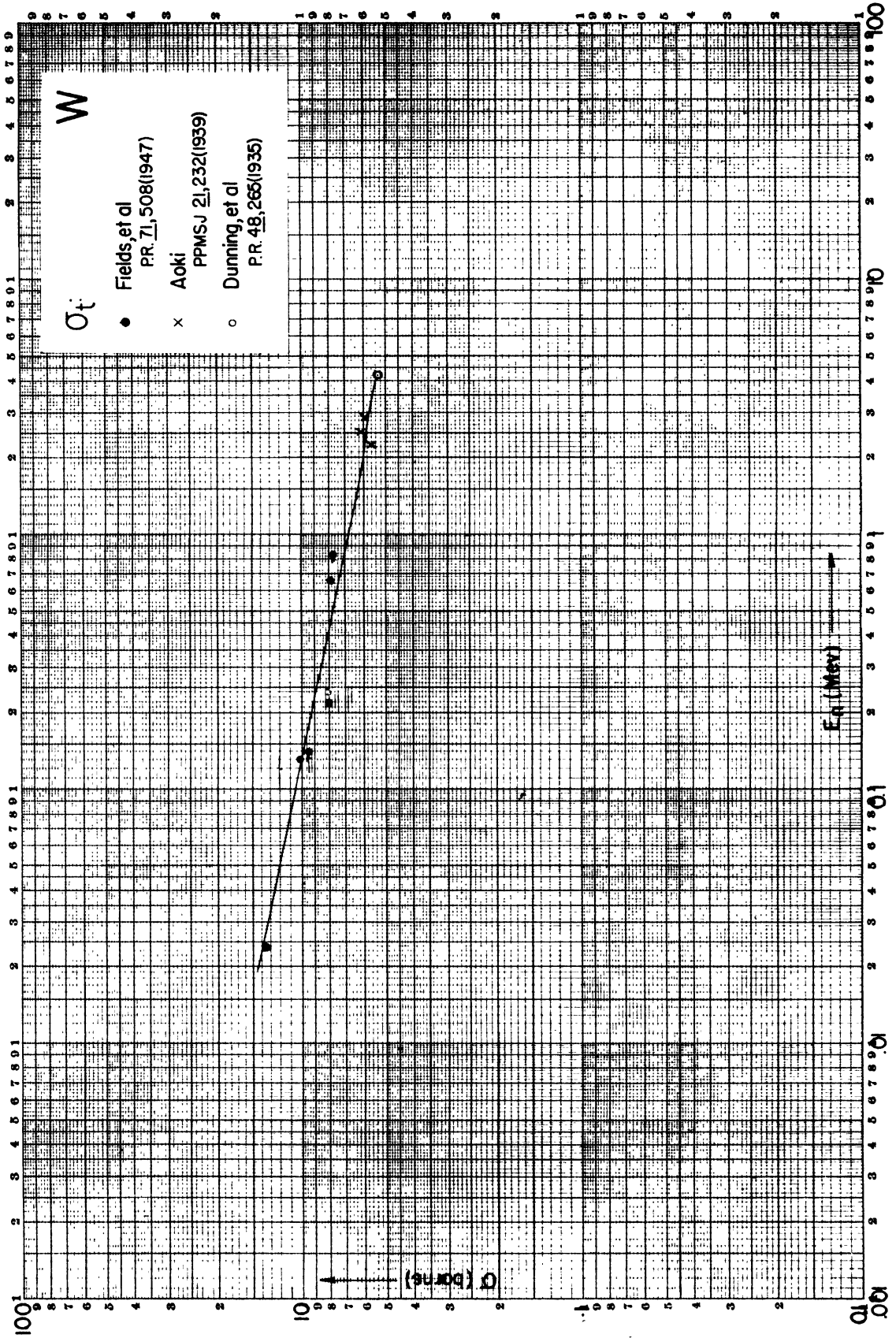
En (Mev)

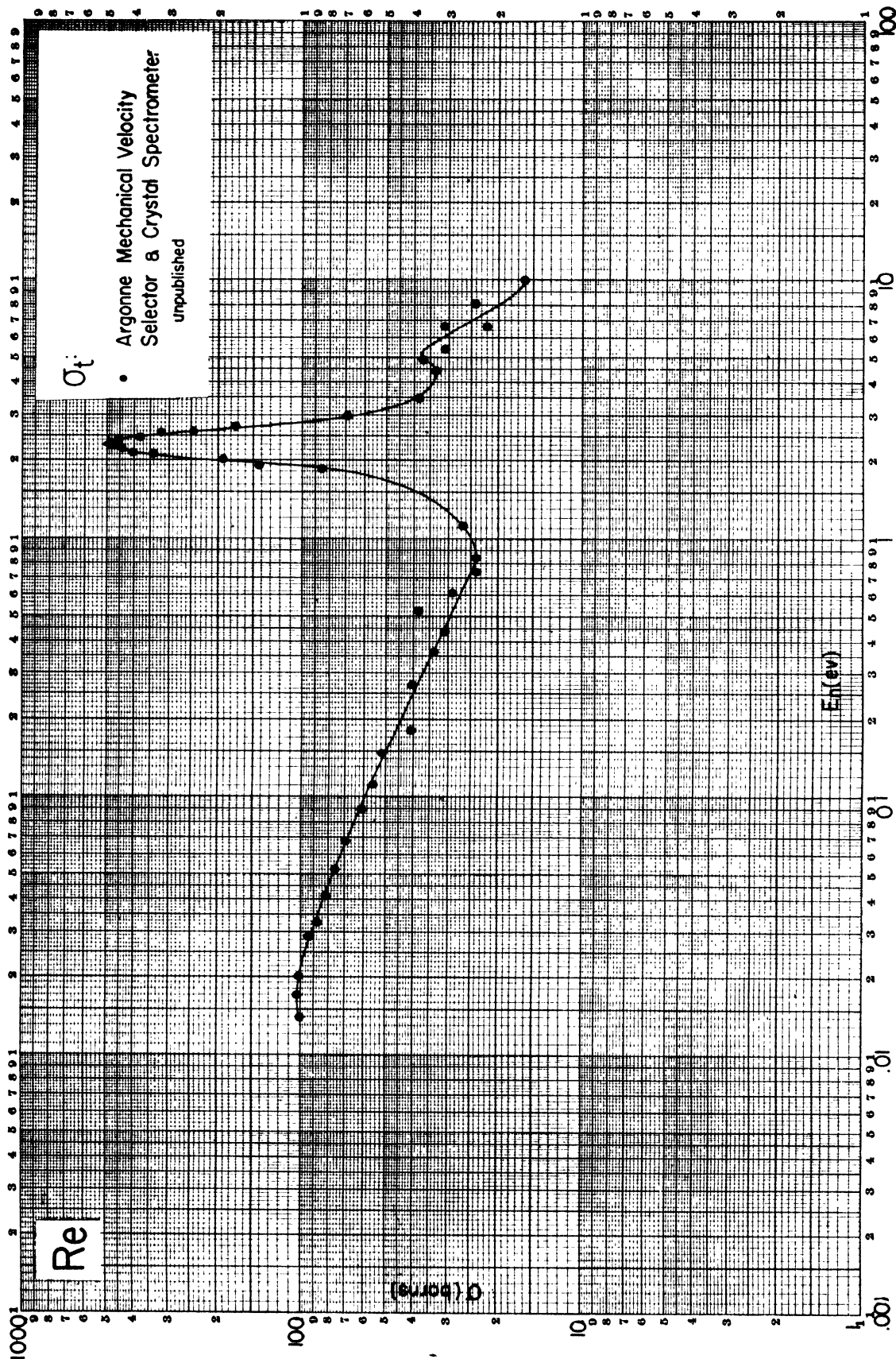
(europ) 0







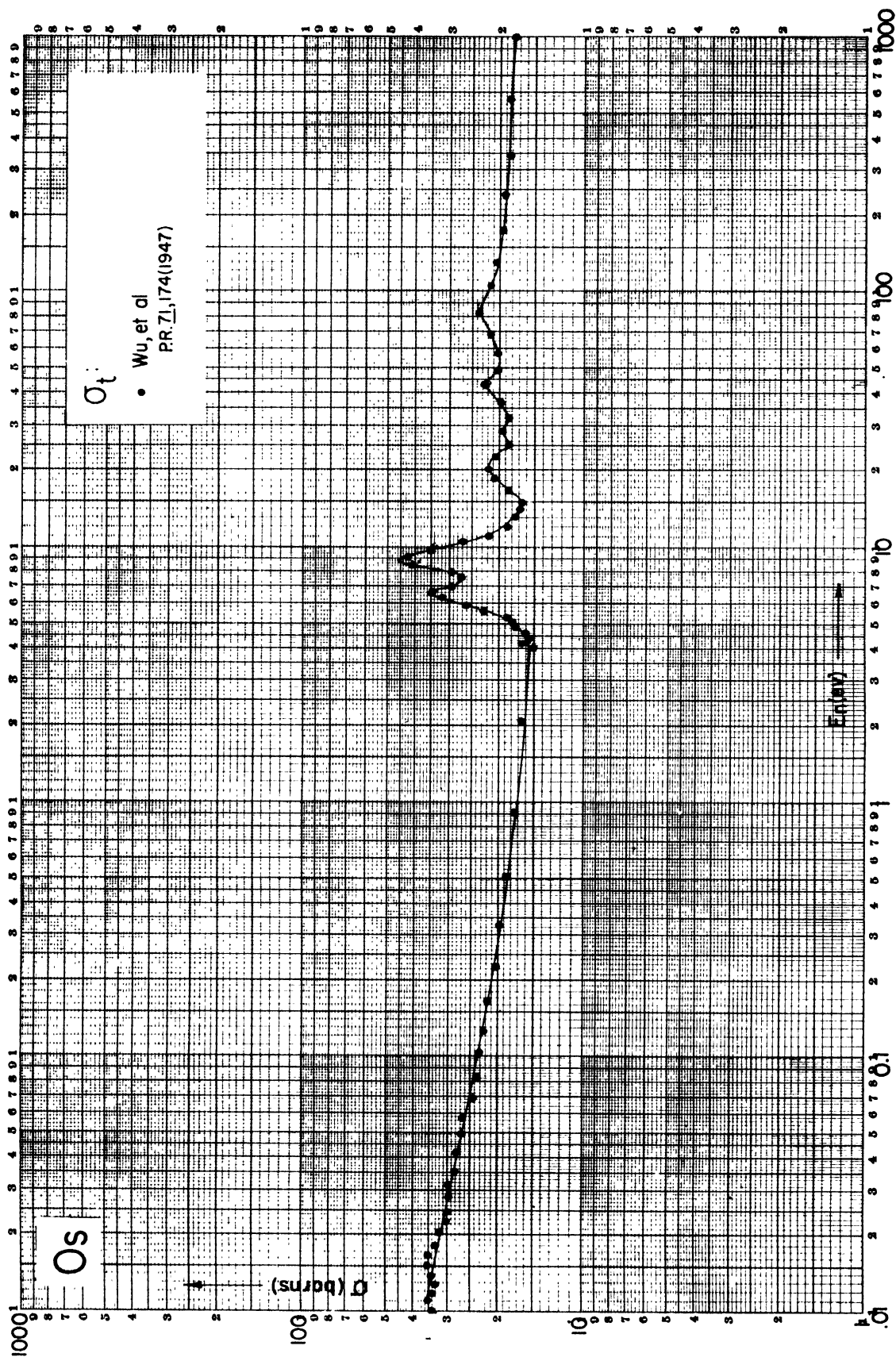


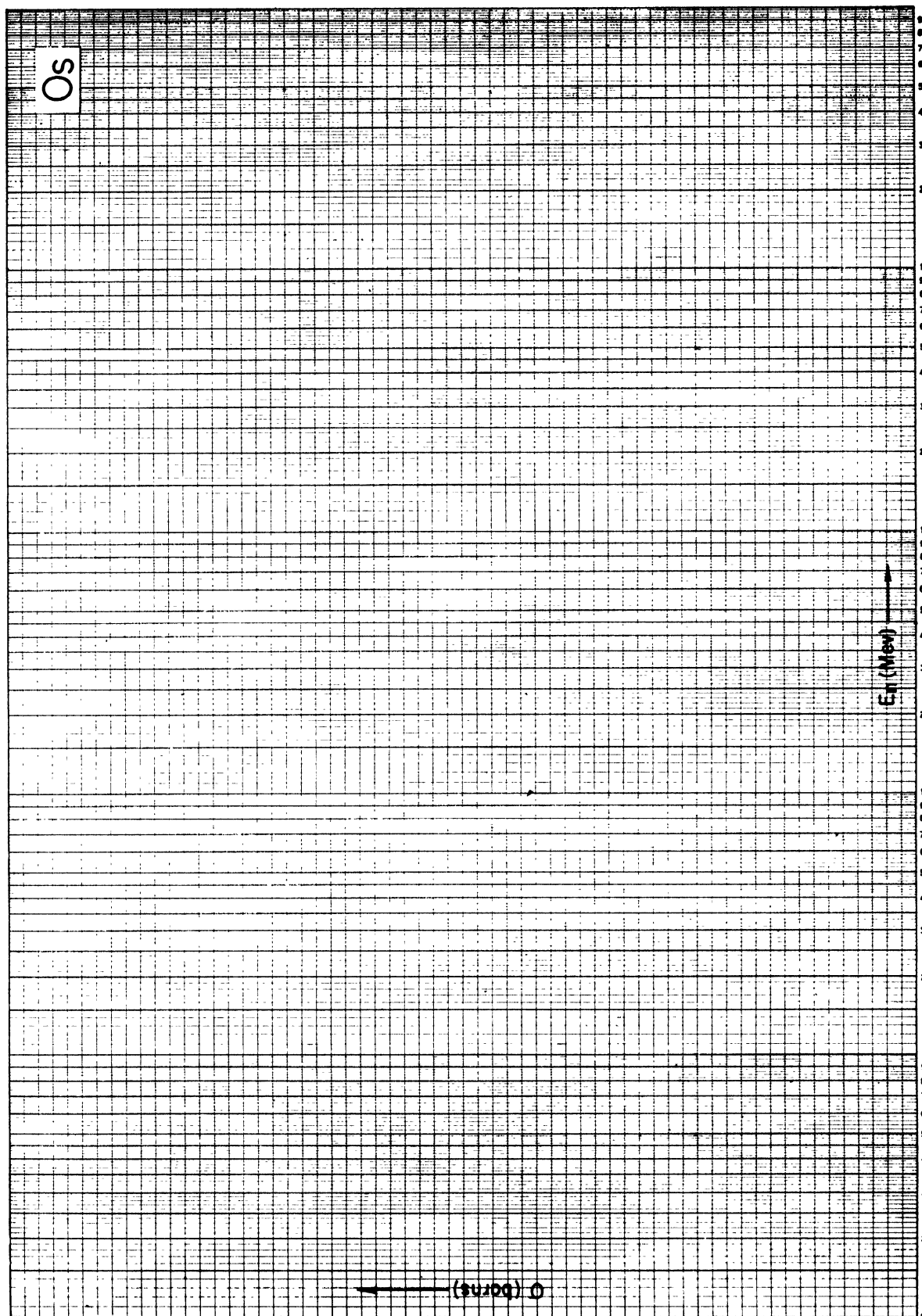


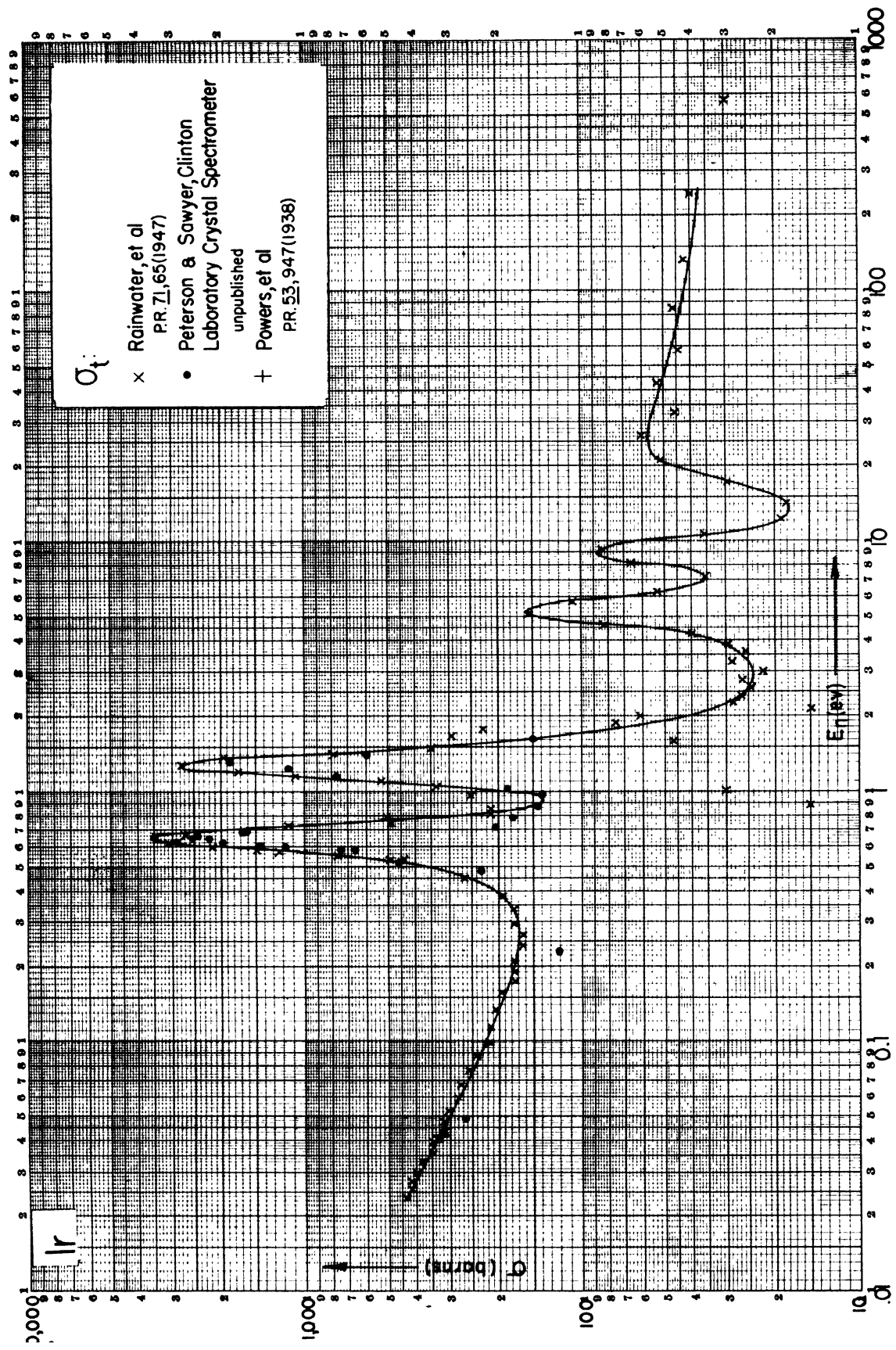
Re

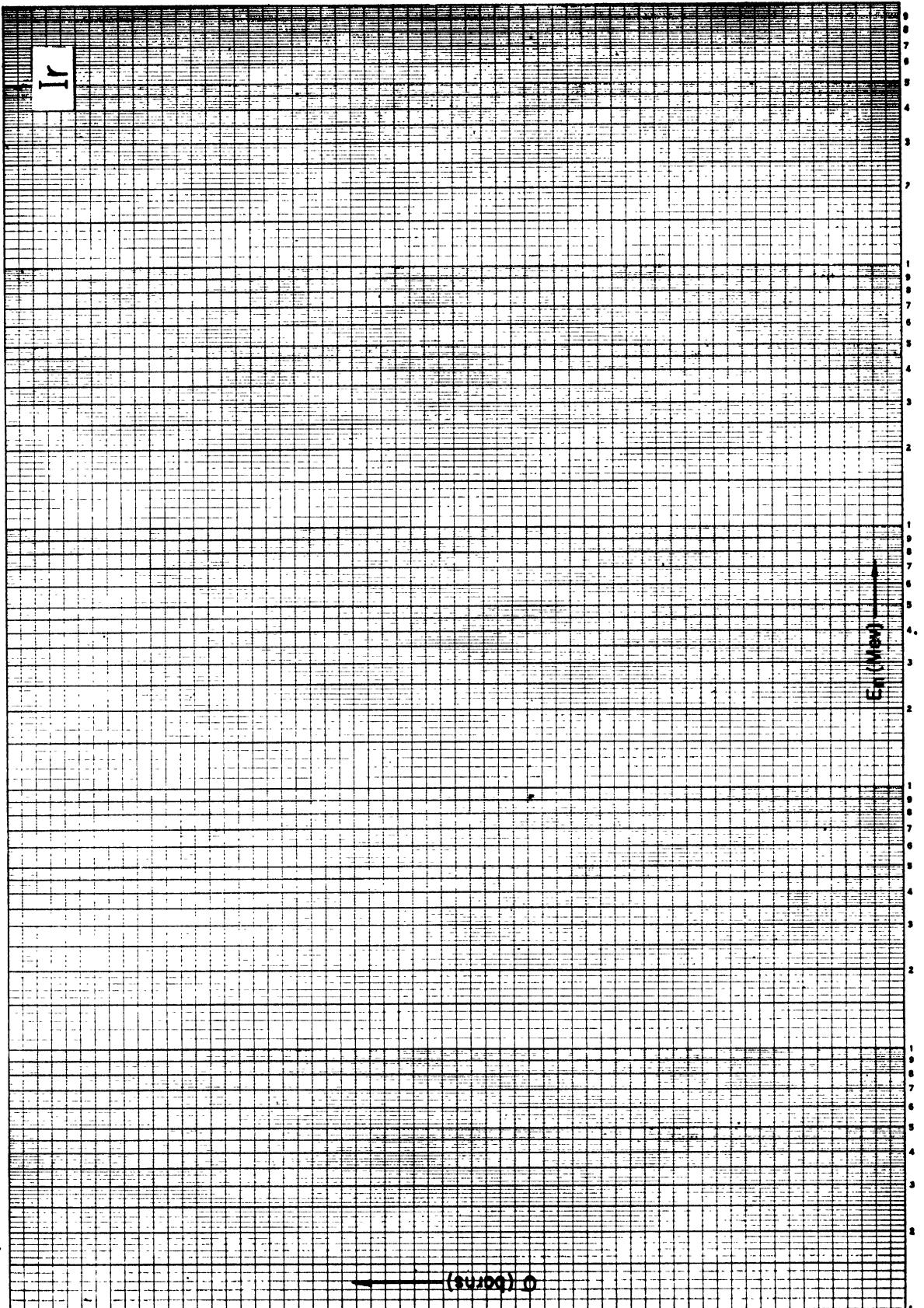
E_n (Max)

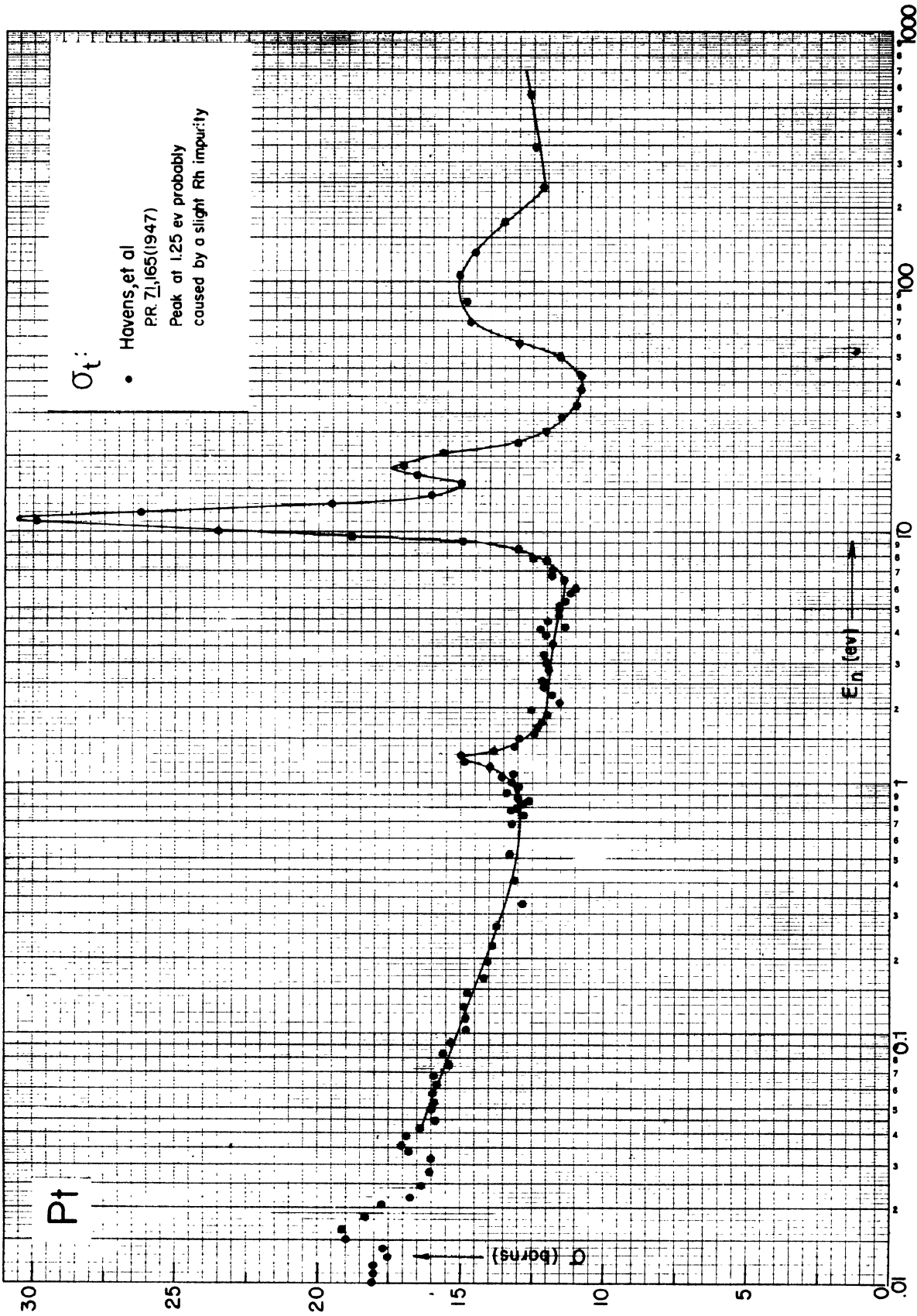
$(\sigma_{\text{avg}}) \phi$

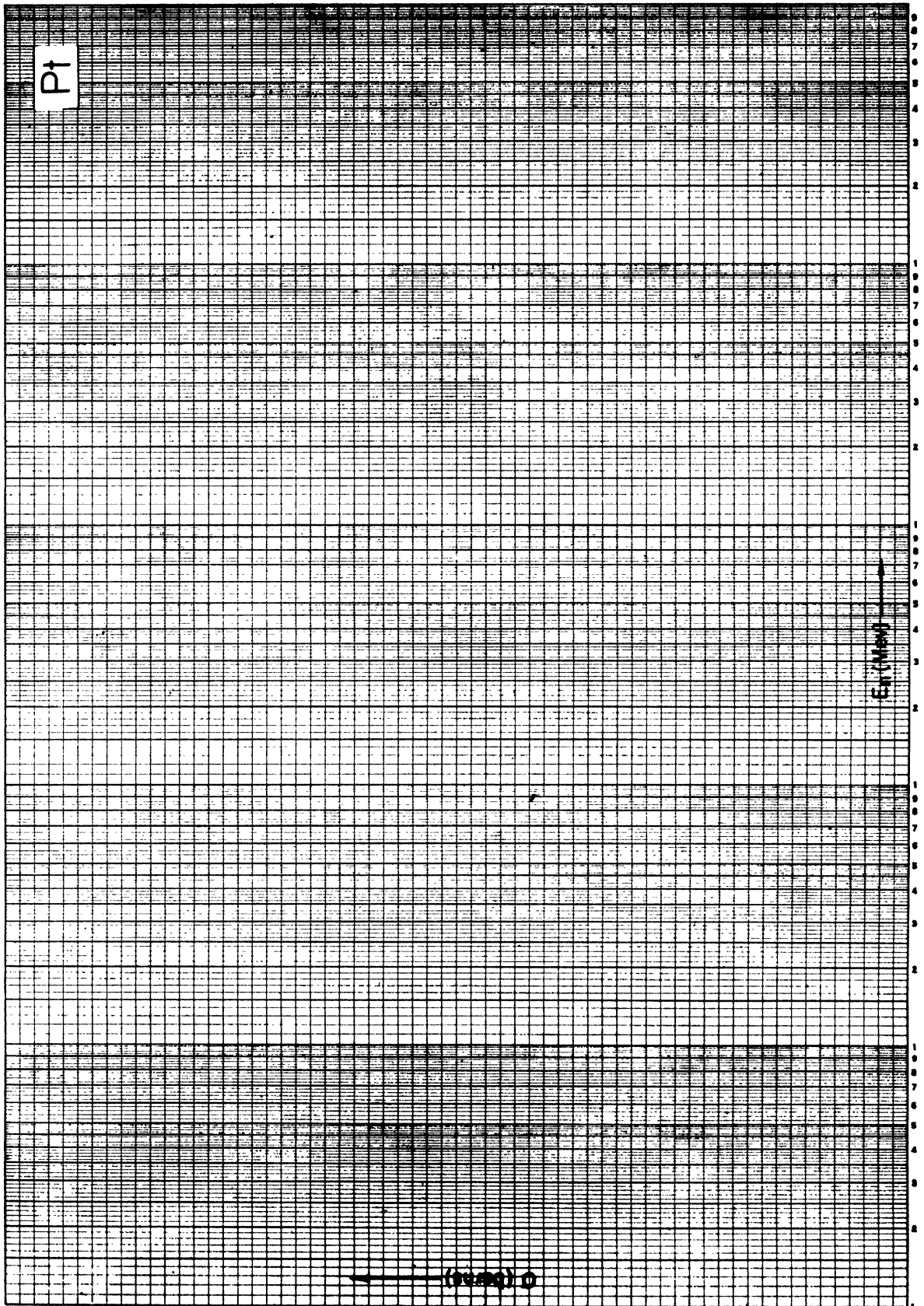


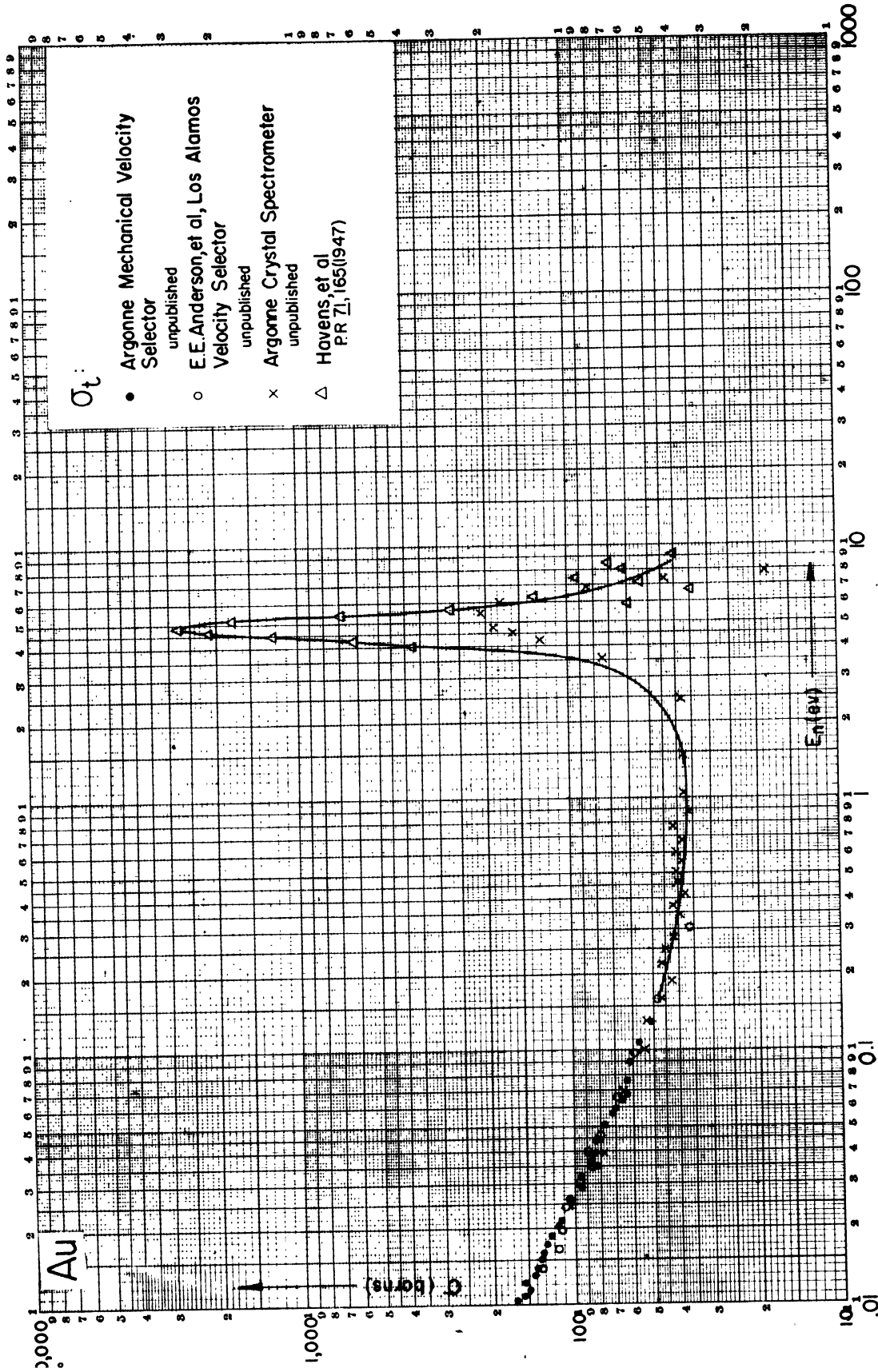


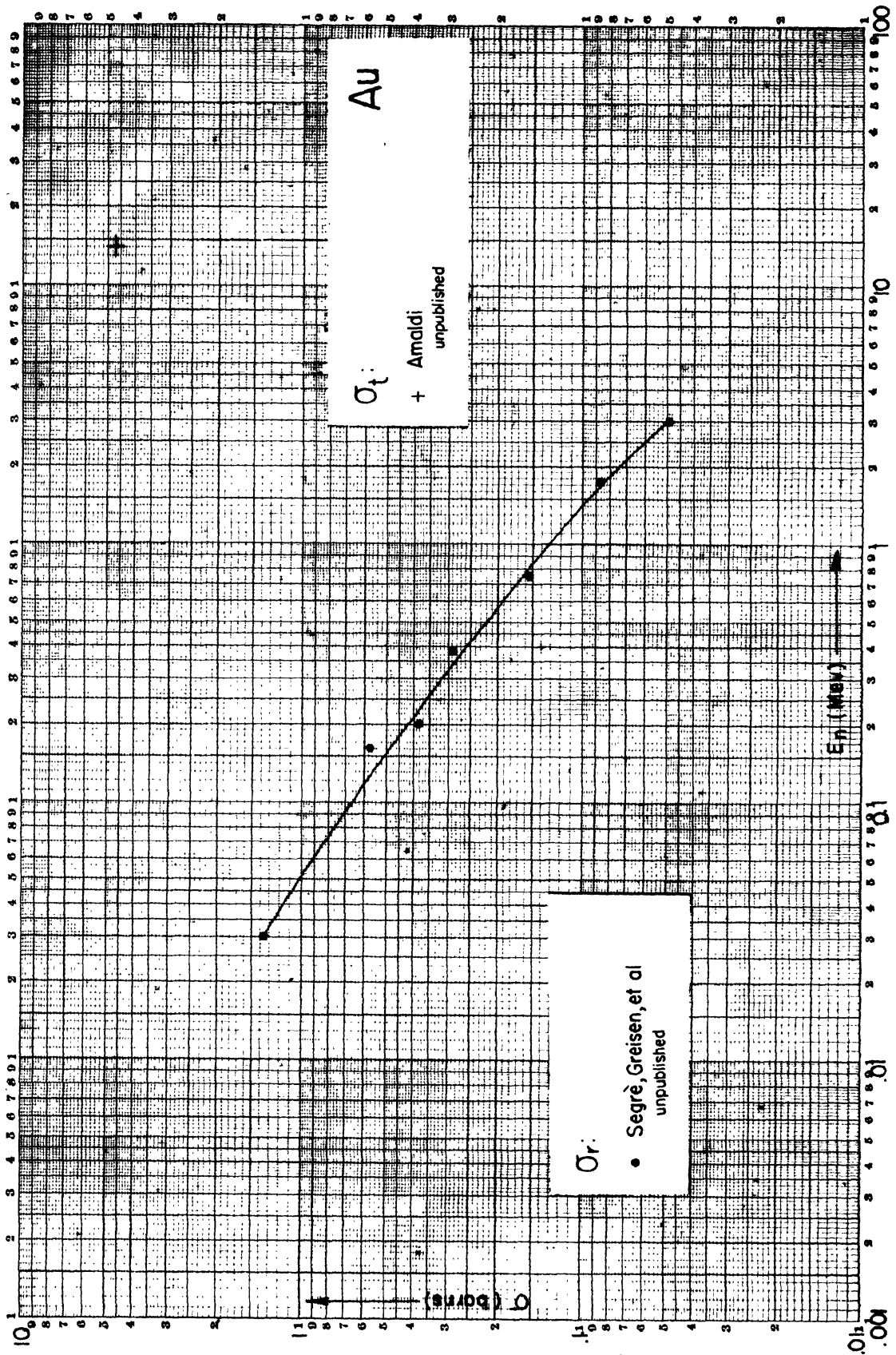


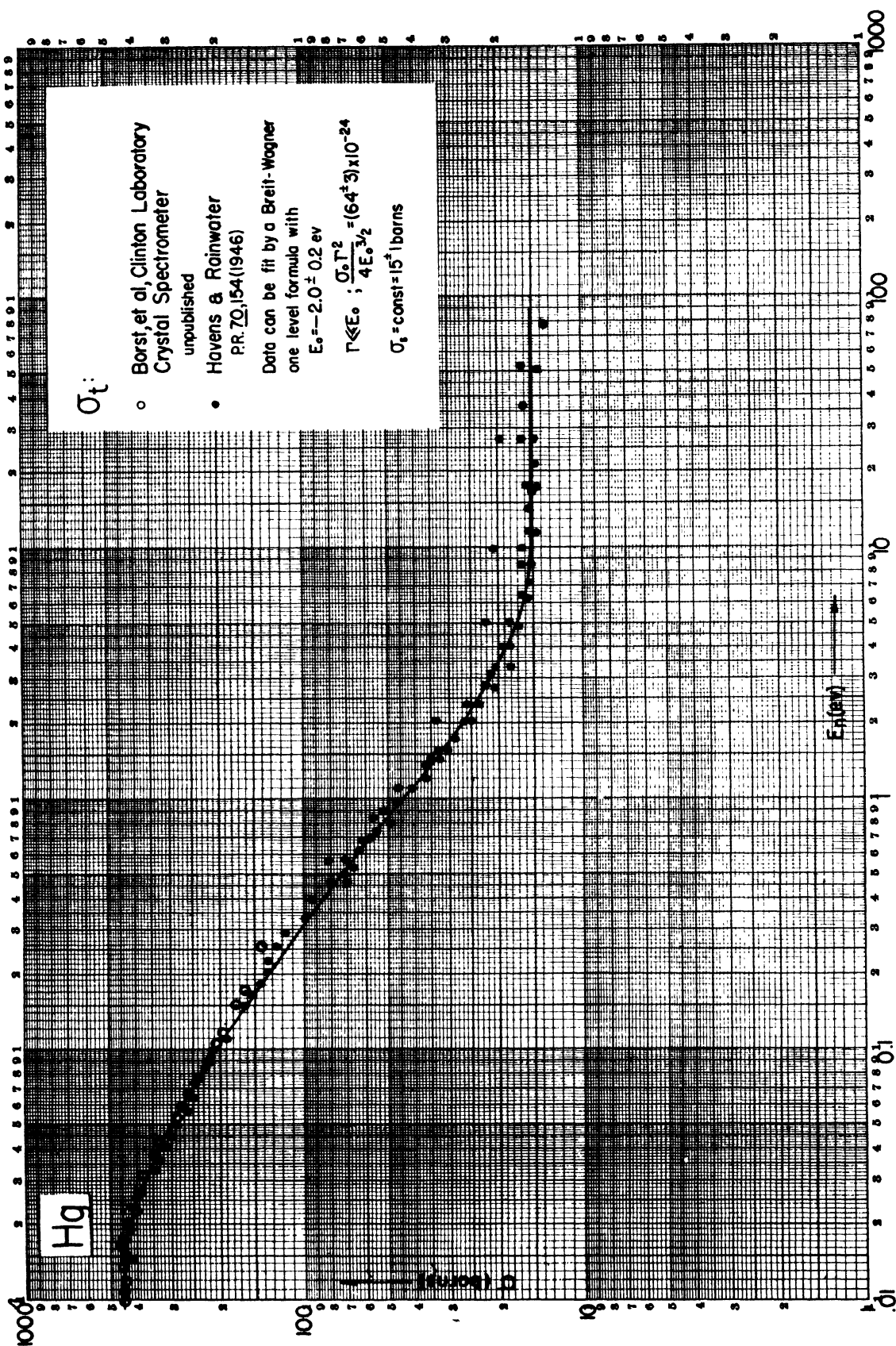


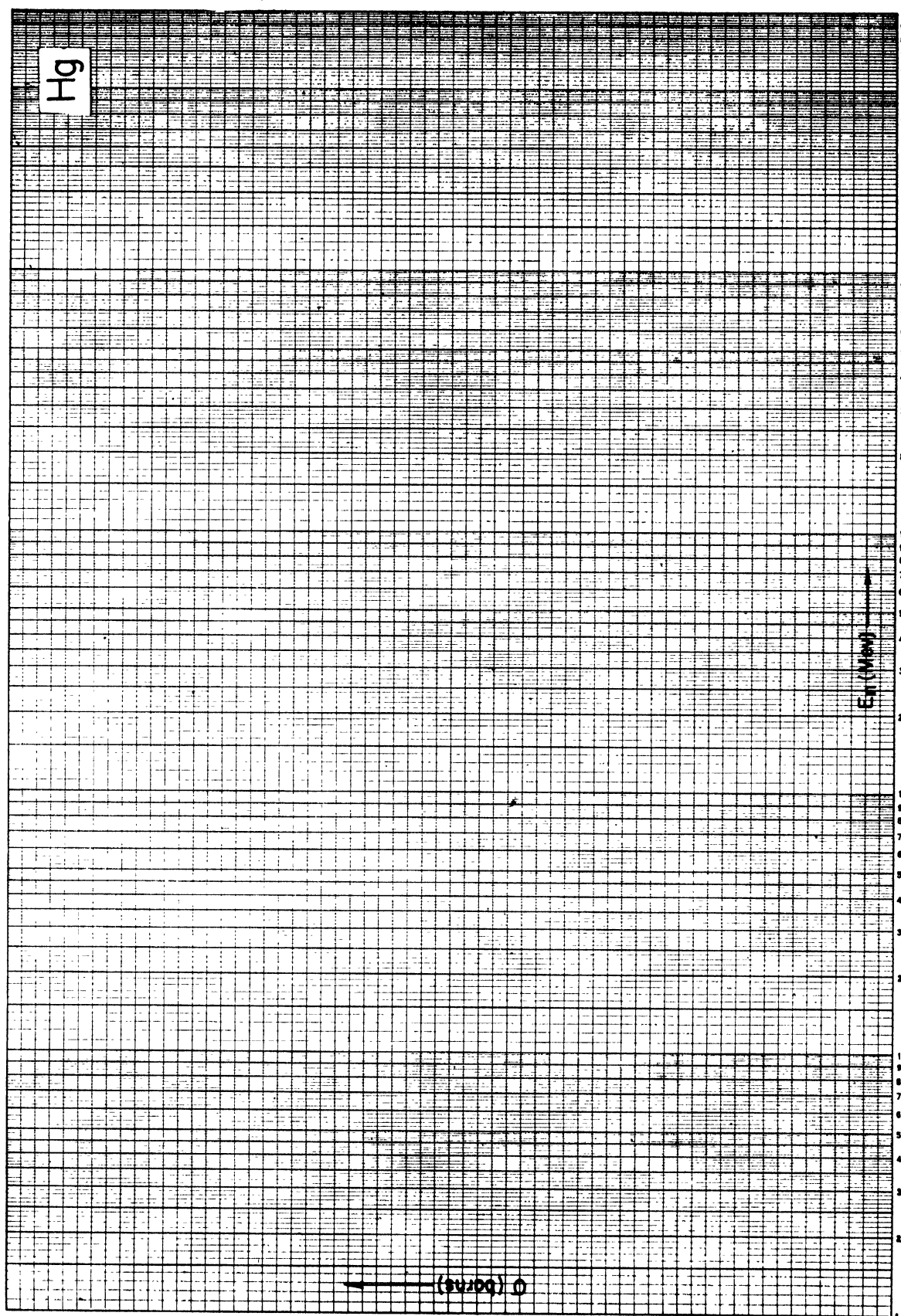


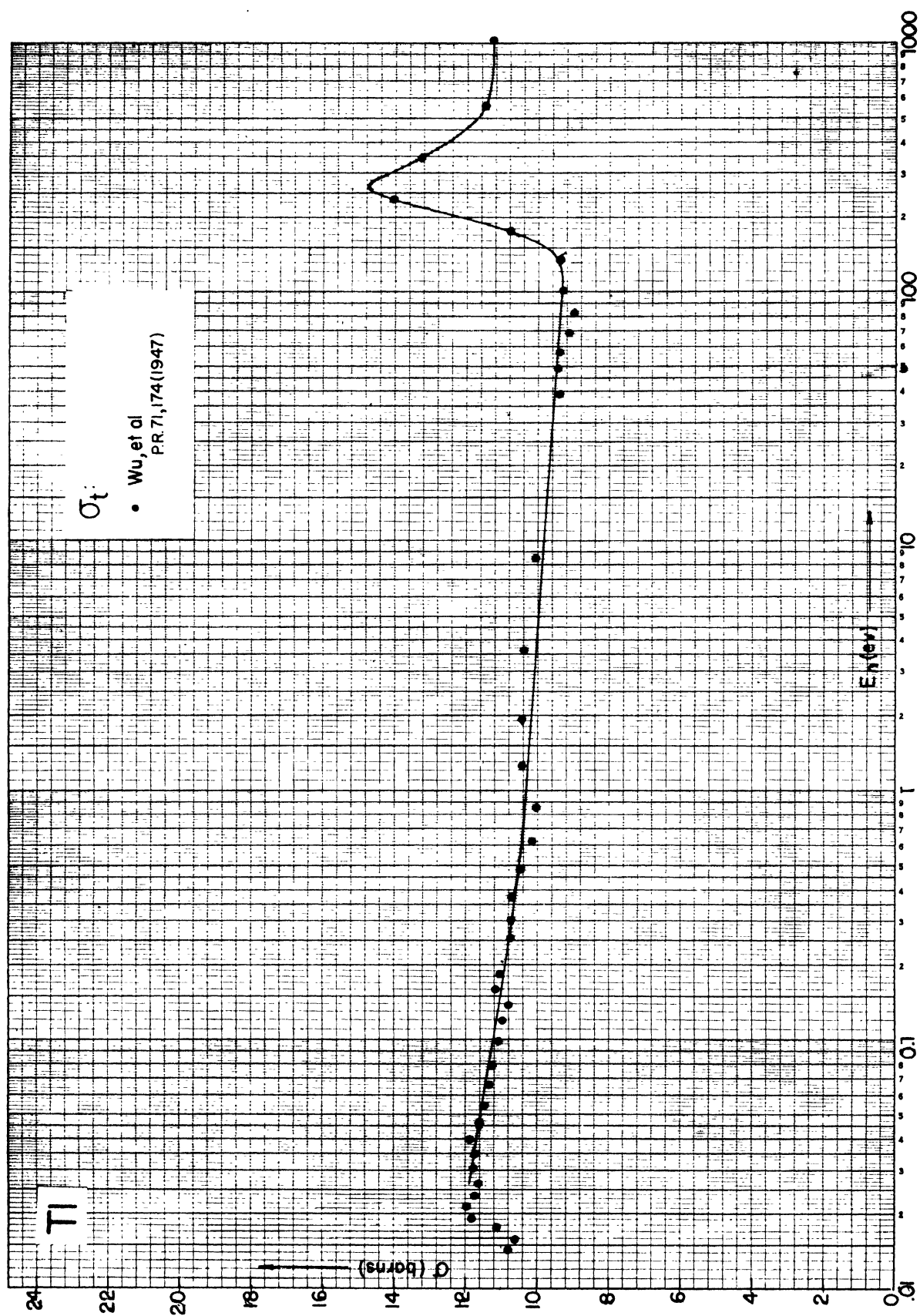


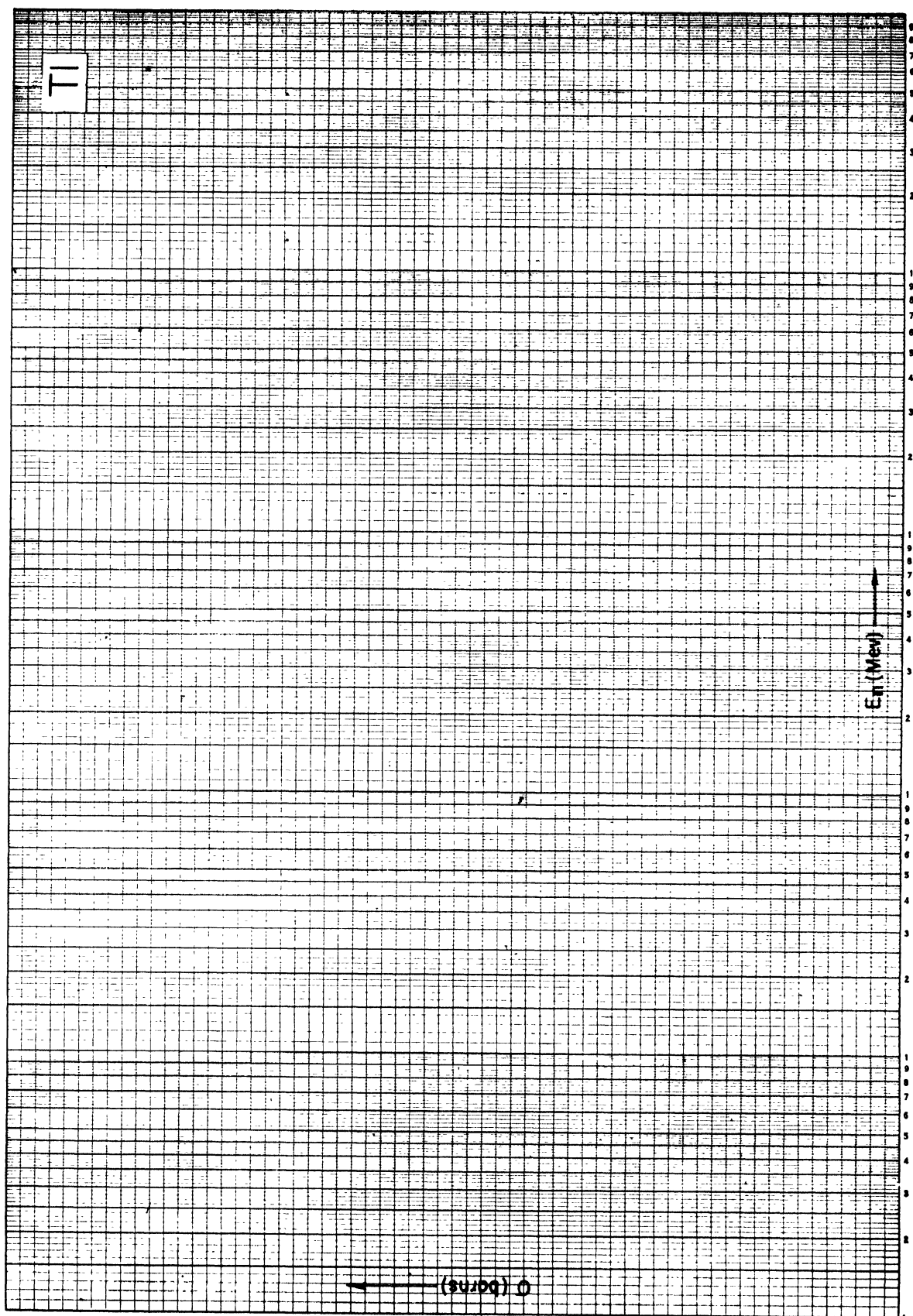


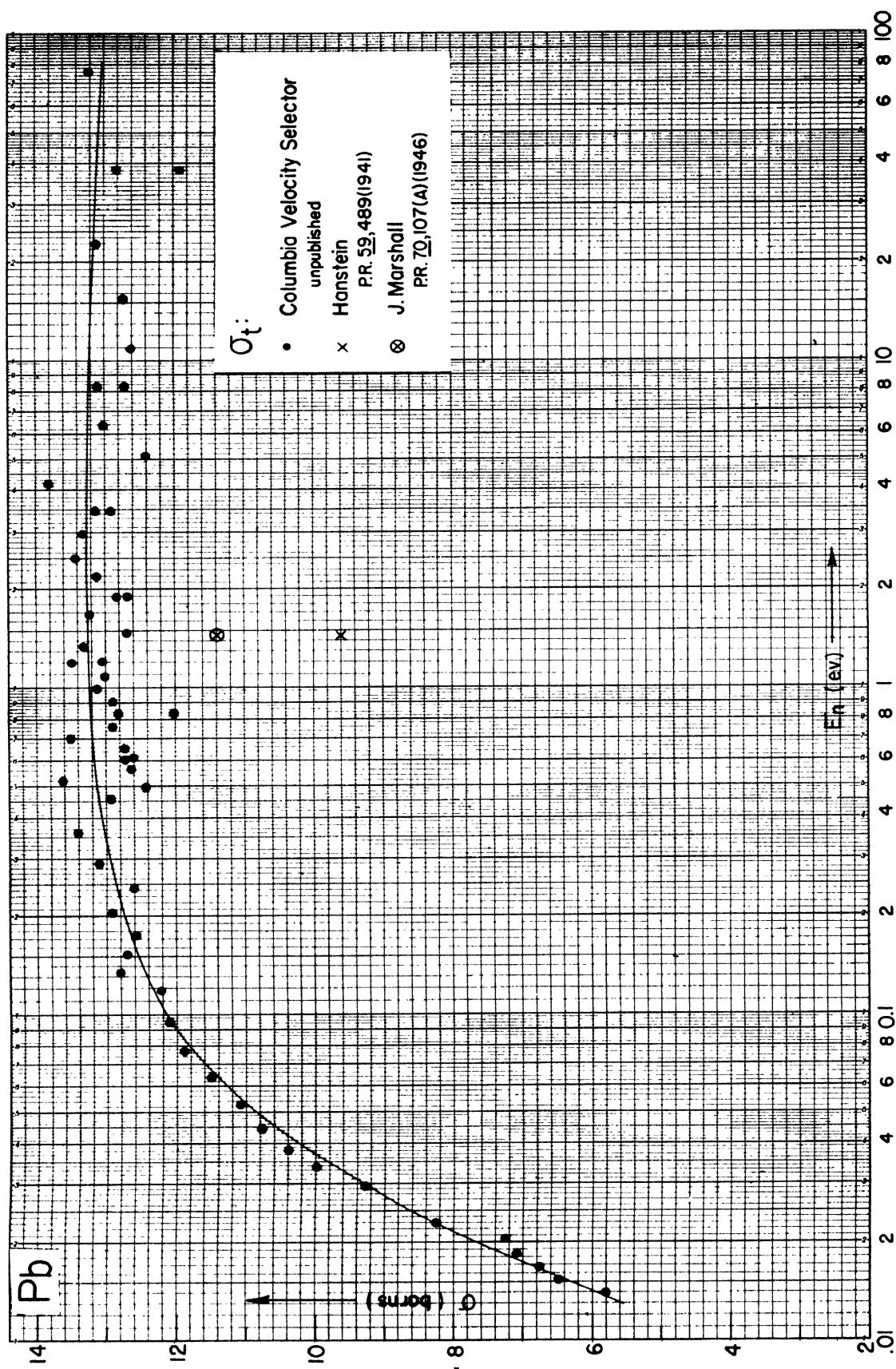


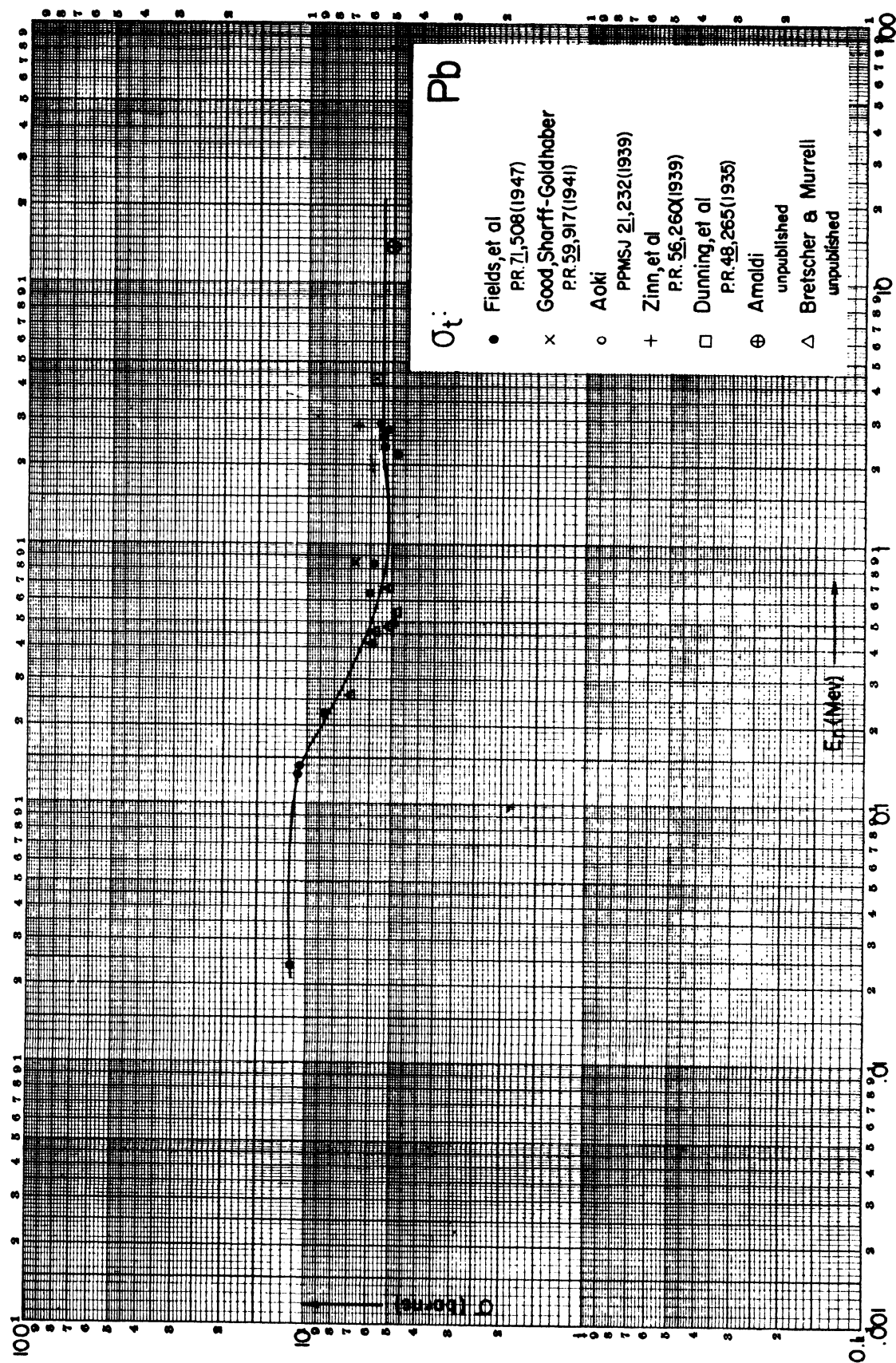


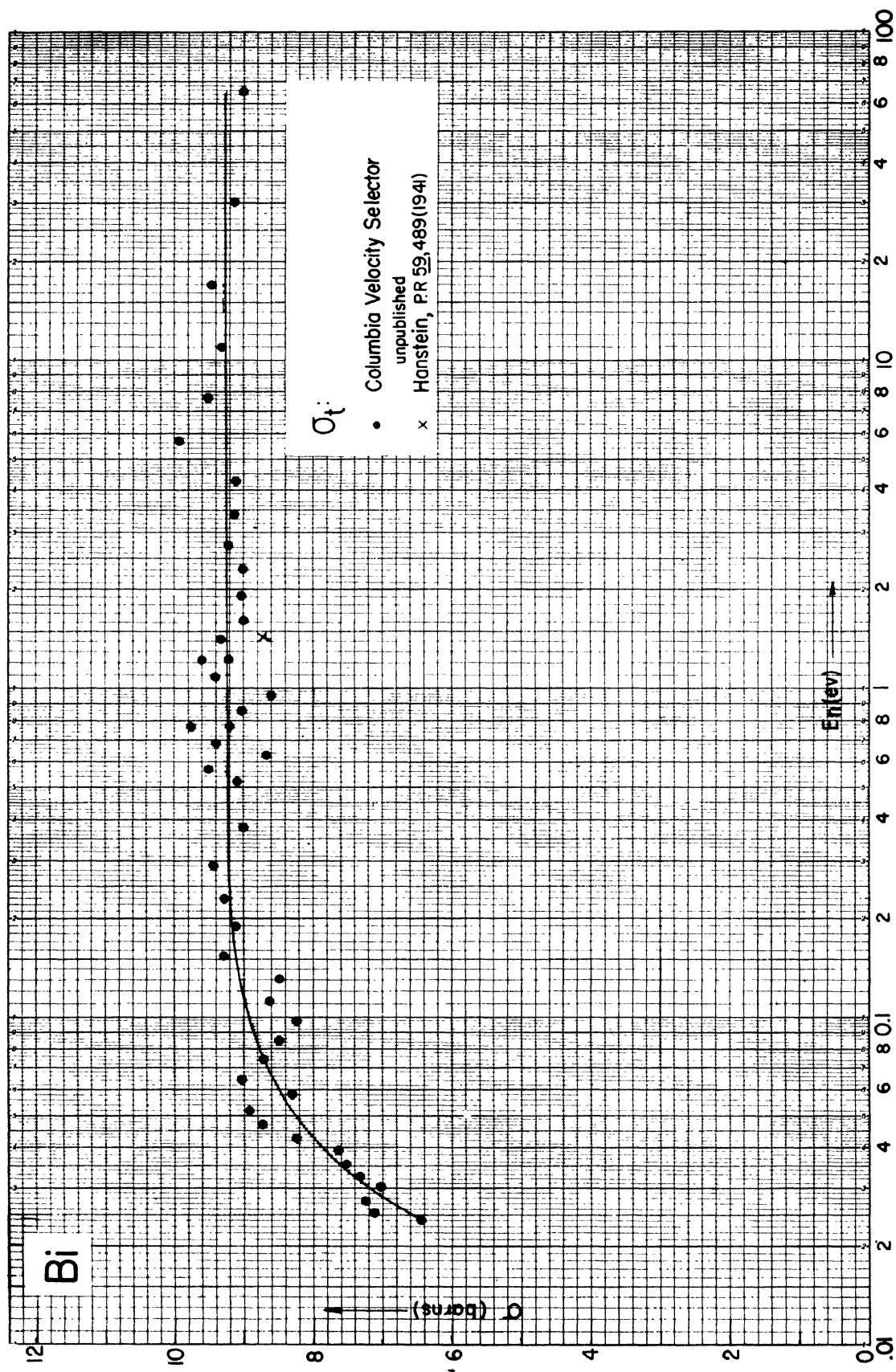


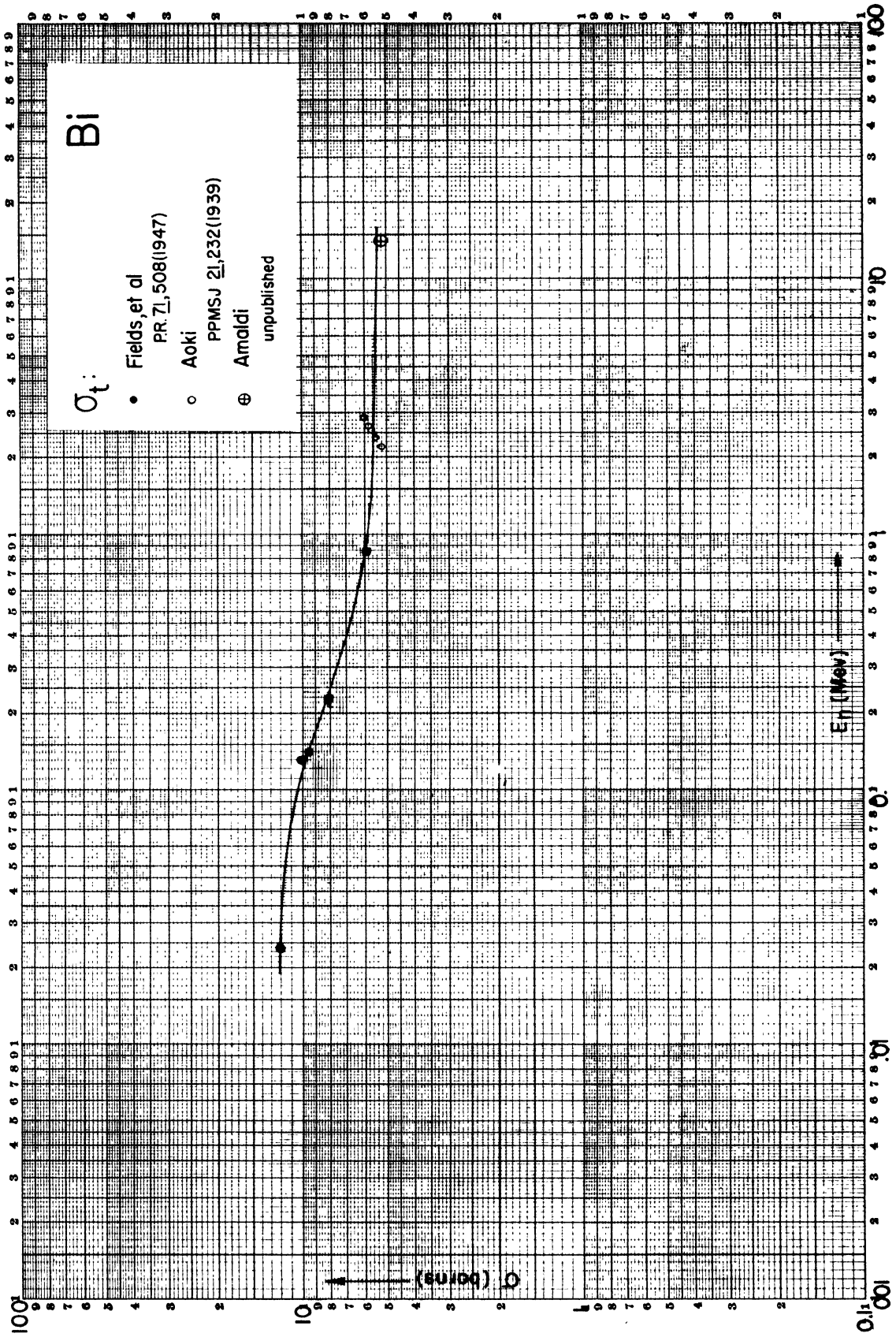


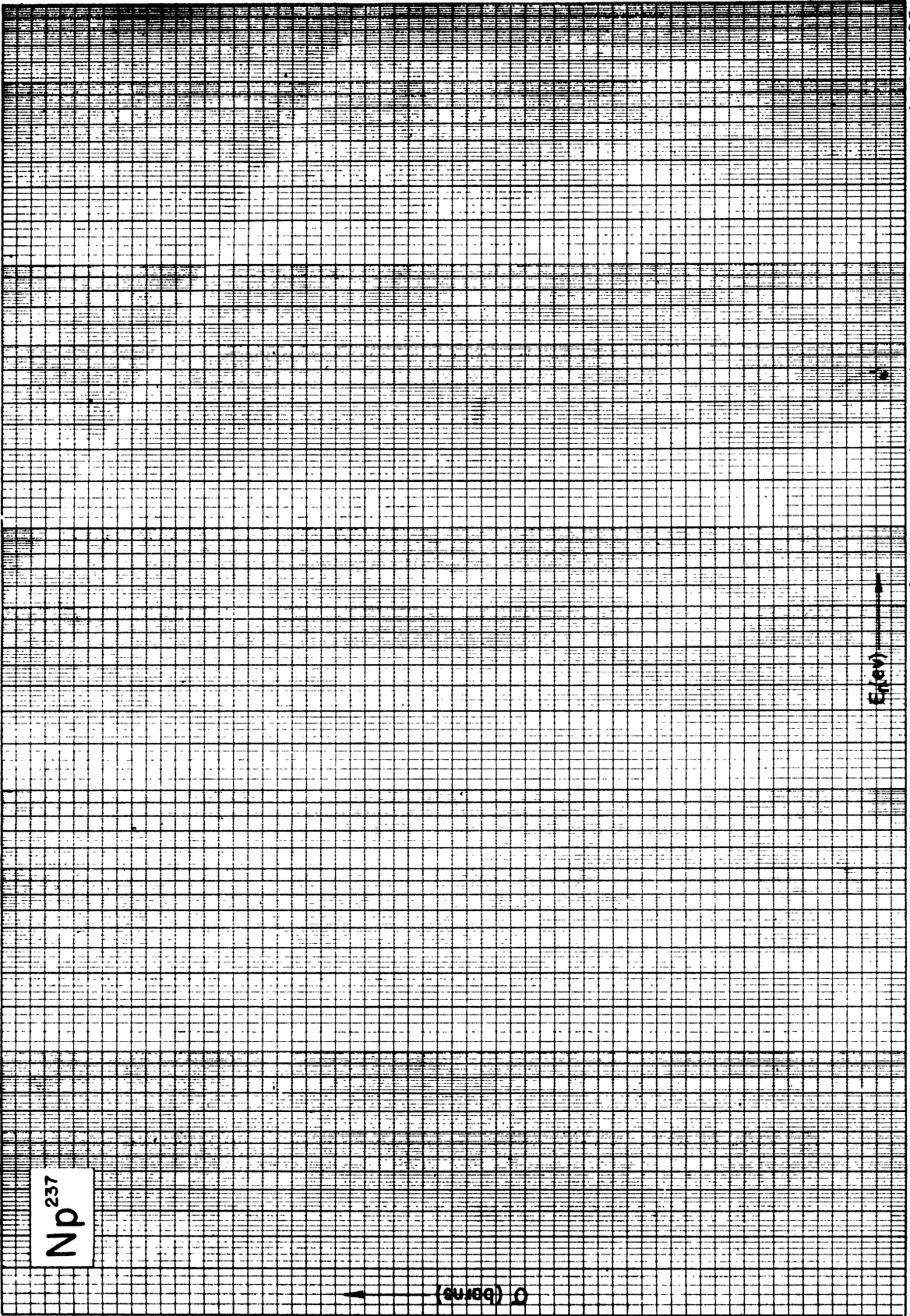


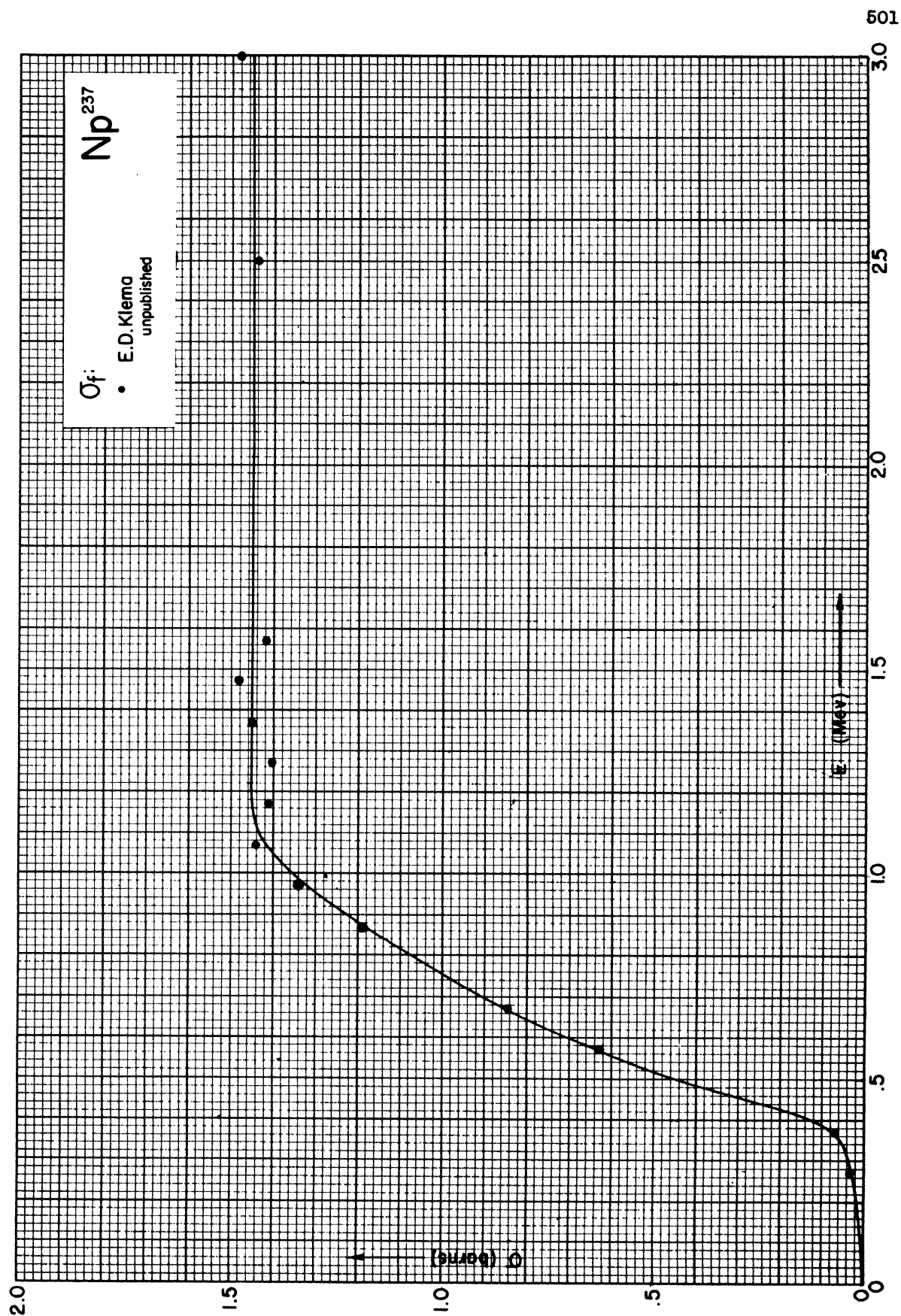












<u>Fig. No.</u>	<u>Caption</u>	<u>Page</u>
1-1	Naturally Occurring Nuclei	2
1-2	Binding Energy of Nuclei	10
1-3	Nuclear Potential Barrier for Posi- tively-Charged Particles	13
1-4	Nuclear Potential for Neutrons	14
1-5	Schematic Diagram of Neutron Beam	15
1-6	Segré Chart	22-23
1-7	Isotope Chart	24
1-8	Natural Radioactivity Disintegration Series . . .	25
1-9	Typical β^- Spectrum	26
1-10	Energy Levels in Beta-Ray Spectrum of Br^{87}	27
1-11	Energy Level Diagram of Mn^{52}	29
1-12	Exponential Decrease of Activity	31
1-13	Exponential Build-Up	31
1-14	Activity Relations between Ba^{140} and La^{140}	33
1-15	Schematic Representation of a Gamma-Ray Photon . .	37
1-16	Photoelectric Effect	38
1-17	Absorption Coefficients of γ -rays in Lead	39
1-18	γ -ray Absorption in Lead	40
1-19	Schematic Diagram of Compton Collision	41
1-20	Absorption Coefficients of γ -rays in Aluminum . .	43
1-21	Pair Production Process	44
1-22	Momentum-Energy Relationship	47
1-23	Typical Absorption Curve for Homogeneous Electrons	51
1-24	Range-Energy Relationship for β -rays	52

<u>Fig. No.</u>	<u>Caption</u>	<u>Page</u>
1-25	Typical Absorption Curve for Continuous Spectra	54
1-26	Range-Energy Relationship for β -rays	55
1-27	Range-Velocity Relation for Alphas	58
1-28	Statistical Straggling of Alphas	58
1-29	Specific Ionization by Alphas	59
1-30	Range-Energy Relationships for α Particles	61
1-31	Yield Curve	63
1-32	Range-Velocity Relationship of Fission Fragments	65
1-33	Rate of Energy Loss as a Function of Range	66
1-34	Schematic Drawing of Fission Track	66
1-35	Maxwellian Distribution of Thermal Neutrons	70
1-36	Capture Cross Section of U^{238} (n, γ)	73
1-37	Fission Cross Section of U^{235} (n, f)	73
1-38	Capture Cross Section of B^{10} (n, α)	74
1-39	Capture Cross Section of Cd (n, γ)	74
2-1	Coulomb Energy E_c and Symmetrical Fission Energy E_0 versus A	78
2-2	Nuclear Energy E as a Function of Distance r between Fission Fragments	79
2-3	Ionization Chamber Used for Measurement of Fission Fragments	82
2-4	Distribution of Masses Produced in the Fission of U^{239}	83
2-5	Statistical Distribution of the Kinetic Energies of the Fragments in the Fission of U^{239}	83
2-6	Energy Distribution of the Heavy and Light Fragments in the Fission of U^{239}	83

<u>Fig. No.</u>	<u>Caption</u>	<u>Page</u>
2-7	Distribution of Masses Produced in the Fission of U^{236}	83
2-8	Statistical Distribution of the Kinetic Energies of the Fragments in the Fission of U^{236}	83
2-9	Energy Distribution of the Heavy and Light Fragments in the Fission of U^{236}	83
2-10	Distribution of Masses Produced in the Fission of Th^{233}	83
3-1	Schematic Representation of Neutron Diffusion . .	88
3-2	Neutron Distribution in Nonabsorbing Half-Space	94
5-1	Schematic Neutron Densities and Absorption Cross Sections	137
5-2	Typical Curves of the Spatial Distribution of Neutrons Slowing Down from a Point Source . . .	150
5-3	Schematic Solution of Inhour Equation	169
5-4	Neutron Density Distributions in a Cylindrical Pipe	174
6-1	Electroscope	203
6-2	Ionization Chamber and Associated Circuit	204
6-3	Pulse Ionization Chamber	206
6-4	Pulse Height-Voltage Relationship	208
6-5	Pulse Rate-Voltage Relationship	210
6-6	Mechanical Velocity Selectors	224
6-7	Time of Flight Velocity Selector	226
6-8	Crystal Velocity Selector	227
7-1	Apparatus for Fission Yield Determinations	233
7-2	Yield Curve	235
7-3	Distribution of Half-Lives of Fission Products . .	238
7-4	Radioactive Power Dissipation	246

<u>Fig. No.</u>	<u>Caption</u>	<u>Page</u>
8-1	Schematic Pile and Controls	251
8-2	Neutron Flux in Pile with Control Rod	252
8-3	Operation of Control Rod	252
8-4	Neutron Flux Measurement	253
8-5	Electronic Control of Shut-Off Rod	254
8-6	Electronic Control of Shut-Off Rod	255
8-7	Coolant Monitoring Equipment	256
8-8	Current-Voltage Relationship for Ionization Chamber	257
8-9	Self Absorption of Boron Alphas	259
8-10	Electrode Separation for Boron Coated Ion Chamber	261
8-11	Type TPD Ion Chamber	262
8-12	Type TPA Ion Chamber	265
8-13	D. C. Amplifier	267
8-14	Plate-Filament Current Relationship, D. C. Amplifier	268
8-15	Principle of Logarithmic Amplifier	269
8-16	Commercial Tube as Logarithmic Amplifier	269
8-17	Counting Rate Meter	270
8-18	Calibration of Low Current Amplifiers	271
8-19	Calibration of Low Current Amplifiers	271
9-1	Hypothetical Ram Jet Engine	277
9-2	Nuclear-Powered Pseudo Rocket	279
9-3	Transmission through Aluminum of Fission Fragments from U^{235}	280
9-4	Transmission through Various Materials of Fission Fragments from U^{235}	280

<u>Fig. No.</u>	<u>Caption</u>	<u>Page</u>
9-5	Hypothetical Fission EMF	282
9-6	Power Versus U^{235} Consumption	284
9-7	Cross-Section Versus Energy for Fission of ${}_{93}\text{Np}^{237}$ by Neutrons	288
9-8	Qualitative Energy Relation for Symmetrical Fission of ${}_{93}\text{Np}^{238}$	288
9-9	Assumed Fission Energy Relationship for U^{235} . .	289
9-10	ξ Versus A Relationship	295
9-11	Schematic Diagram of Projected Oak Ridge Power Installation	297
9-12	Schematic Diagram of a Homogeneous Reactor Containing a Solid Fuel Mixture	304
9-13	Diagram of Circulating Homogeneous Fluid Fuel	307
9-14	Homogeneous Reactor with Circulating Fuel Mixture	308
9-15	Neutron Density Along the Diameter of a Spherical Reactor	310
9-16	Neutron Density Along the Axis and Radius of a Right Circular Cylindrical Reactor . . .	310
9-17	Neutron Density Along Major Horizontal Axes of a Rectangular Parallelepipedal Reactor . .	311
9-18	Neutron Flux Distribution Along Major Axis of a Cubical Reactor	313
9-19	Enlarged Section of Lattice	314
9-20	Schematic Representation of Flux Distribution Across a Single Cell	315
9-21	Heterogeneous Reactor with Circulating Liquid Diluent	318
9-22	Heterogeneous Reactor with Solid Diluent and Circulating Coolant	319
9-23	Heterogeneous Reactor with Circulating Liquid Fuel	320

<u>Fig. No.</u>	<u>Caption</u>	<u>Page</u>
10-1	Heat Removal by Radiation	335
10-2	Illustrative Power Cycle	351
11-1	Isotopes of the Heavy Elements	354
11-2	Periodic Table of the Elements	359
11-3	Flow Sheet for the Isolation of U^{235} , U^{239} , U^{233}	370

INDEX
(References are to page numbers)

A

- Abelson, P. H., 353,377
Absolute temperature, 326
Absorbed neutron energy, 85
Absorber thickness, electron, 51
Absorption, 54
 aluminum, 53
 half value for electron, 53
 internal, 53
 maximum range, 53
 resonance, 101,114,134,137,309
 thickness, 50
Absorption coefficient, 45
 aluminum, 45
 Compton, 45
 copper, 45
 lead, 45
 mass, 45,53
 pair production, 45
 photo, 45
 total, 45
Absorption cross section, 14,15,18,
 42,87,91,95,97,127,137
 macroscopic, 135
 measurement, 127,230
 photoelectric, 38
 resonance, 113,115,154,229
Absorption curve, beta-ray
 spectra, 53
 continuous spectra, 54
 homogeneous electrons, 51
Absorption mean-free-path, 96
Abundance, isotopic, 22-23
Actinide series, 363
Actinium, 353,354
Activation, 112,115,136,138,210
 cadmium difference, 214,215,
 218,228
 cross section, 114,213
 fast neutron, 112
 foil, 210,211,212,213
 indium, 214,218,219,228
 resonance, 215
 cross section, 216
 detector, 228
 neutron, 112
 standardization, 213
 thermal neutron, 112,215,216
Activity units, 22
 curie, 22
 International Radium Standards
 Commission, 22
 Rutherford, 23
Age, Fermi, 148,152
Ageo, M., et al, 395,396,407
Air-cm, 60
Alamogordo, nuclear reactor, 274
Alarm circuit, 256,257
Alder, R. L., 270
Allen, K. W., et al, 403
Alpha decay, 21
Alpha particles, Born approxima-
 tion, 57,58
 capture and loss of charge, 59
 columnar ionization, 60
 critical velocity, 58
 delta rays, 67
 energy loss, 57
 interaction with matter, 54,66
 ion pairs, 59
 mean range, 58
 monokinetic, 58
 photographic method, 201
 production of fission, 81
 range, 57,58,59,60,261
 range-velocity relations, 58
 residual range, 58
 short-range, 108
 specific ionization, 59
 statistical fluctuation in
 range, 58
 stopping power, 263
 straggling, 58
 ultimate range, 58
Aluminum
 absorption, 53
 coefficient, 45
Amaldi, E., 389,405,417,419,425,
 435,439,441,443,455,457,461,
 463, 491,497,499
 et al, 389
American Physical Society, 274
Americium, 353,354,355
Amplifier, direct current, 253,
 254,258,265,266,267
 input current, 266
 insulation, 272
 logarithmic, 255,269,270
 low current calibration, 271,272
 pulse, 233
 stabilization, 265,266

INDEX

- Anderson, E. E., 389
 - et al, 490
- Anderson, H. L., 101,109,188
- Angular momentum, 36
 - conservation, 5,23
 - neutrons, 67
 - nuclear, 7
 - orbital, 5
 - spin, 5
 - total, 5,7
- Anisotropic scattering, 153
- Annihilation radiation, 27,28,46
- Antiparallel spin, 11
- Aoki, H., 397,405,407,409,411,
 - 413,415,417,419,423,425,
 - 429,435,439,441,443,455,
 - 457,461,463,465,481,497,499
- Area, fast migration, 148
 - migraticn, 114,163,172,193
 - slowing-down, 150,192
 - thermal diffusion, 148,192
 - total migration, 149
- Argonne, crystal spectrometer,456,
 - 470,472,474,482,490
 - group 389
 - Laboratories, 224
 - mechanical velocity selector,
 - 389,456,472,474,476,482,490
 - group 389
 - nuclear reactors, 274,300
- Arnold, G. P., 389,468,476
- Associated source strength, 151
- Atomic abundance, 286
- Atomic mass, 76
 - stable isotopes, 77
 - table, 380,381,382,383,384,385
 - unit,4,379
- Atomic number, 1,291,292,293
 - most stable, 77
- Atomic weight, chemical,291,292,293
- Auger electrons, 29,38
- Avogadro's number, 290

- B

- Bacher, R. F., et al, 404
- Bailey, C. L., 389
 - et al, 395,405,407
- Baldinger, E., 409
- Band spectra, 3

- Bardeen, J., 105,109
- Barn, 15,290
- Barschall, H. H., 409,419
 - et al, 405
- Battat, M. E., 409
- Bennett, W. E., 389
- Bentley, E. P., 269
- Bergstrahl, T., 389
- Bernstein, S., 389
- Beryllium target, 64
- Berzelius, 356
- Bessel function, 142,303
- Beta-counting, efficiency, 234
 - rate, equation, 233
 - standardization, 234
- Beta decay, 23,26,27,30,46,85
 - energy release, 77
 - gamma-ray accompaniment, 26
 - maximum energy, 26
 - neutrons, 68
- Beta-ray absorption, internal, 53
- Beta-ray emission, 30
- Beta-ray energy, table, 22-23
- Beta-ray spectra, absorption curve,53
- Beta-ray spectrum 26,51,247
 - Br⁸⁷,27
 - continuous spectrum, 51
 - line spectrum, 51
 - maximum value, 51,53
 - mean energy, 26
 - modal value, 26
 - probable error, 53
- Beta rays, photographic method, 201
- Bethe, H. A., 57,379
- Bikini, nuclear reactors, 274
- Binding energy, 1,9,10,11,37,58,62,72
 - 75,76,287,379
 - neutrons, 77,84,85
 - per nuclear particle, 9
 - nuclei, 10
 - per nucleon, 9,10
 - prompt neutrons, 84
 - table, 380,381,382,383,384,385
- Biological shield, 251,256
- Blair, J. M.,389
 - et al, 401
- Block, F., 57
- Bøggild, J. K., 64,277
- Bohm, D., 395
- Bohr, N., 64,67,80,101
- Bohr magneton, 8,54
- Bohr-Wheeler, 80
- Boiling, 323,333

INDEX

Born approximation, 57,58
 B₁₀, capture cross section, 74
 Boron lining, thickness, 260
 Borst, L. B., 389
 et al, 452,458,470,472,474,492
 Bosé, 7
 Boundary condition, 97,105,142,177,
 180,324
 Bradbury, N. E., 290
 Bragdon, E., 404
 Bragg, W. L., 226,227
 Bragg, angle, 227
 condition, 229
 curve, 59,66
 reflections, 229,230
 relation, 226,227
 scattering, 37
 gamma rays, 37
 reflection angle, 37
 Bragg-Kleeman rule, 60
 Breit, G., 71,188,229,289,290,309,
 456,492
 Breit-Wigner formula, 71,188,229,
 289,290,309,456,492
 Bremsstrahlung, 49
 Bretscher, E., 395,407,411,497
 et al, 423
 Briggs, G. H. 290
 Brill, T., 389
 British thermal unit, 323
 Brookhaven National Laboratory, 387
 Brostrom, K. J. 277
 Brownian motion, 148
 Bubbling, 303
 Burton, M., 107

C

Cadmium, 18
 capture cross section, 74
 difference, 214,215,218,228
 shield, 223,227
 Cahn, 108
 Calibration, low current ampli-
 fiers, 271
 neutron sources, 220
 Canning, 371, 372
 Capture, electron, 28,29,34
 K, 29
 mean-free-path, 294
 neutron, 71,115
 resonance, 101,102,128,132,137
 Capture cross section, 72,73,96,114,
 115,222,291,299
 B₁₀, 74
 Cd, 74
 macroscopic, 291,292,293,299,300,
 301
 table, 22-23
 thermal, 113
 U²³⁸, 73
 Carmichael, H., 257,261,262,265
 Cellular method, 101
 Center-of-mass coordinates, 13
 Centrifugal separation, 366,367
 Chain reacting pile, 111
 Chain-reacting system, control, 27
 properties, 115
 Chain reactions, elementary
 theory, 99
 Chalk River, Canada, 20,257,261,266,
 274,300
 nuclear reactor, 261,274,300
 Chang, W. Y., 108,109
 Characteristic equation, 160
 Charge, capture and loss, 59,60
 fission products, 62
 ionic, 64
 fission fragments, 64
 nuclear, 1,3,46,67
 Chart, isotope, heavy elements, 24
 nuclear reactions, 21
 Segré, 22-23,189,290,300
 Chemical atomic weight, 291,292,293
 Chemical binding, 134
 effect, 103
 forces, 163
 Chemical reprocessing, 298,302
 Chemical separation, low concentra-
 tion, 365
 Chemical separation processes, 367
 ion exchange, 368,369
 precipitation, 367,376
 solvent extraction, 368,377
 volatilization, 368,369
 Chemical yield, 233
 Chemistry, heavy elements, 353
 Chicago, University of, 387,406
 nuclear reactor, 274
 Christy, R. F., 101,107,274
 Cladding, 319

INDEX

- Clinton Laboratories, 68,99,111
 - crystal spectrometer, 456,486,492
 - Group, 389
 - nuclear power plant, 296,297
- Clinton pile, 19
- Closed cycle, 308
- Cloud chamber method, momentum
 - measurement, 202
 - range, 202
- Cloud chamber track, fission
 - fragments, 66
- C neutrons, 74
- Coagulation, 305
- Coefficient, absorption, 45
 - Compton, 44
 - diffusion, fast neutrons, 157
 - heat transfer, 322,326,328,329, 330,334,339
 - gases, 333
 - liquid metal, 331,332,333
 - streamline flow, 329
 - table, 343
 - turbulent flow, 329
 - linear absorption, 15,38,44
- Cohen, V. W., 188
- Coherent scattering, 37
- Coincidence counting, 28
- Columbia Project, 290,388,394,396,402, 406,408,410,412,416,418,419,420, 422,424,426,430,434,438,440,442, 450,460,466,496,498
- Columnar ionization, 60
- Committee on Radioactive Standards,23
- Competitive mode, 34
- Compound nucleus, 12,70
- Compton, A. H., 41
- Compton, absorption coefficient, 45
 - coefficient, 44
 - collision, schematic diagram, 41
 - effect, 36,41,45
 - conservation of energy, 41
 - conservation of momentum, 41
 - Klein and Nishina, 41
 - electron, 42
 - process, 42
 - recoil, 210
 - wave length, 41
- Condensation, 323,334
 - drop-wise, 334
- Conduction, 323,324,336
- Conductivity, thermal, 303,324,325, 330,340,341,346
- Conductivity, thermal (Cont'd)
 - fluid, 330
 - gases, 325
 - gas films, 326
 - liquids, 325
 - liquid metals, 326
 - organic liquids, 326
 - solids, 325
- Conservation, angular momentum,5,23
 - energy, 12,37,41
 - mass-energy, 23
 - momentum, 12,37,41,62
 - parity, 6
 - statistics, 23
- Continuity, equation, 152
- Continuous spectrum, 51
- Continuous x-ray spectrum, 49
- Control, 194
- Control rods, 106,174,175,194,217, 251,252,254,255,298
 - cooling, 298
 - effectiveness, 174
 - geometry, 174
 - location, 174
 - safety, 298
- Convection, 323,328,332
 - forced, 328
 - laminar flow, 328
 - natural, 332
 - streamline flow, 328,330
 - turbulent flow, 328, 330
- Coolants, 251,274,327
 - circulating, 319,320
 - contamination, 305
 - fluid fuel, 307
 - gases, 297,304,319,322,348
 - helium, 349
 - liquids, 304,318,322,348
 - liquid metals, 304,336,337,346
 - nuclear properties, 337
 - organic compounds, 335
 - physical properties, 341
 - secondary, 305
 - water, 352
- Cooling water, 255
- Coordinates, center of gravity, 153
- Copenhagen cyclotron, 64
- Copper, absorption coefficient, 45
- Co-precipitation, 370
- Cornell University, 379
 - velocity selector, 464
- Corrosion, 303,305,319,335,373

INDEX

- Coryell, C. D., 84,231,363
- Coulomb barrier, 56,68
 - energy, 78,80
 - field, 3,11,13,44,49,79
 - forces, 76
 - repulsion,9,75,76,78
- Counters, efficiency, 112,209,210, 212
 - Geiger-Mueller, 208,209,212,214, 230
 - proportional, 206,208,209,221, 223,227
- Counting rate, beta, 233
 - fission,233
 - meter, 270
- Coupled diffusion model, 167
- Coupling, 5
- Creutz, E., 101
- Critical conditions, 181
- Critical mass, 93,95,96
 - effect of reflector, 97
- Critical radius, 95,96,142,193
- Critical size, 99,111,139,142, 146,155,156,158,160,167, 173,177,191,192,193,322
 - cubic, 193
 - extrapolated length, 193
 - materials required, 195,196
 - reflector, 195
 - spherical, 193,194
 - temperature considerations, 162
- Critical volume, 97,143
- Cross section, absorption, 14,15, 18,42,87,91,95,97,127,137
 - macroscopic, 135
 - measurement, 127,230
- activation, 114,213
- capture, 72,73,96,114,115,222, 291,299,301
 - B10, 74
 - Cd, 74
 - table, 22-23
 - thermal, 113
 - U238, 73
- elastic scattering, 71
- electronic, 42
- fission, 15,91,114,115,289, 388
 - plutonium, 289
 - uranium, 289
 - U235, 73
- linear absorption, 44
- macroscopic, 15,220,290,291, 292,293
- Cross section, macroscopic (cont'd)
 - capture, 291,292,293,299,300, 301
 - scattering, 291,292,293,299, 301
 - microscopic, 15
 - (n, α) process, 388
 - (n, γ) process, 388
 - (n,p) process, 388
 - neutron absorption, 223
 - index,390,391,392
 - measurement, 221,222,223,228, 230
 - table, 388
 - nuclear, 14
 - pair production, 44
 - photoelectric absorption, 38
 - resonance, 115,189,388
 - absorption, 113,115,154,229
 - activation, 216
 - scattering, 229
 - scattering, 14,15,42,87,90,115, 116,131,222,230,291,299,301,388
 - inelastic, 15
 - measurement, 230
 - thermal neutron measurement, 228
 - total, 14,71,114,222,291,388
 - measurement, 227,229,230
 - neutron, 230
 - table, 22-23
 - transport, 15,87,90,153
- Crystal effect, 103,222,230
- Crystal spectrometer, 226,227,228
 - Argonne, 456,470,472,474,482,490
 - Group, 389
 - Clinton Laboratories, 456,486,492
 - Group, 389
- Crystal spectrometer velocity
 - selector, 226
- Cubic lattice, 141
- Cubic pile, critical conditions, 181
 - critical dimension, 142,145,192, 193
- Cubical nuclear reactors, 141,142,308 312,313
- Curie, 356
- Curie unit 23,240
- Curium, 353,354,355
- Cyclotron, 12,224,225
 - Copenhagen, 64
- Cylindrical nuclear reactors, 142, 174,308
- Cylindrical pile, critical radius, 142

INDEX

D

Dancoff, S. M., 101,108
 Darwin, C. R., 56
 Debierne, 356
 de Broglie wave length, 14,48
 Decay, alpha, 21
 beta, 23,27,28,30
 energy release, 77
 exponential, 31,32
 radioactive, electron
 capture, 29
 Decay constant, 31,32,34
 Decay period, radioactive
 nucleus, 115
 Decay probability, 34
 Decontamination, 232,245
 Degraded radiation, 42
 Delayed neutrons, 27,62,85,112,115,
 123,124,125,126,128,140,188,
 197,198,239,256
 control, 194
 density, 112,118,123
 mean life, 115
 percentage, 85
 period, 198,307
 possible loss, 306,307
 stationary state, 141
 Delayed neutron periods, 85,86,123,
 168
 Delta rays, 67
 Demers, P., 281
 Dempster, A. J., 245
 Density, element, 291, 292,293
 fictitious, fast neutrons, 157
 fissionable material, 116
 fluid, 330,338
 neutron, 91,92,93,94,95,96,97,
 106,107,114,116,137,194,311
 average, 106,196,197
 boundary condition, 142
 control, 194
 control rod, 252
 cylindrical, 310
 delayed, 112,118
 distribution, 174,180,196,312,
 313
 exponential decay, 119
 extrapolated distance, 178
 extrapolation, 142
 falling, 122
 fictitious, 157

Density, element, neutron (Cont'd)
 free, 171
 harmonic expansion, 178
 interface, 94
 latent, 112,118,165,171
 measurement, 210,211,216,
 217,221
 radial, 310
 schematic, 137
 slope, 94
 slowing-down, 171
 spherical, 310
 thermal, 114,138,155,165,
 210
 time dependence, 117,
 118, 119, 197, 198
 nuclear, 1,114,290,291,299
 radiation, 107
 saturated, 211
 slowing-down, 114,132,149,155,
 158,165,215,216
 measurement, 215
 source, 90
 fast neutrons, 157
 thermal neutrons, 157
 Design variables, in heat transfer,
 347
 Detection of charged particles,
 199
 cloud chamber, 202
 electroscope, 202
 Geiger-Mueller counters,208
 ionization chambers, 204
 Lauritsen electroscope, 203
 Lindemann electrometer, 204
 photographic method, 200
 proportional counters, 206
 scintillation method, 200
 Detection of neutrons, radioactiva-
 tion of foils, 210
 Detector, resonance neutron,136,
 137
 thermal neutron, 136,137,215
 Deuterium, 300
 heavy hydrogen, 300
 heavy water, 300
 Deuteron, electric quadrupole
 moment, 8
 ground state, 11
 interaction with matter, 54
 production of fission, 81
 range,58
 triplet state, 11

INDEX

- Deutsch, M., 28,75,389
 - Differentiator, 255
 - Diffraction, electron, 48
 - neutron, 67, 108
 - Diffusion, gaseous, 365,373
 - neutron, 87
 - critical mass, 95,96
 - dimensional considerations, 92
 - effect of reflector, 97
 - elementary theory, 87
 - hydrogenous material, 87
 - infinite mass, 91
 - monoenergetic, 103
 - schematic representation, 88
 - thermal, 148
 - thermal, 365,366,373
 - Diffusion area, thermal, 148,192
 - Diffusion coefficient, 141
 - fast neutrons, 157
 - Diffusion constant, 89,112
 - Diffusion equation, thermal neutrons, 155,158,165,181
 - Diffusion length, 91,92,104,105,147, 161,162,163,192,317,321
 - thermal, 114,161,162
 - Diluent, 294,296,299,304,305,318,319, 320
 - Dipole moment, electric, 36,67
 - magnetic, 7,8,54
 - Dirac, P. A. M., 7,23,67
 - Dirac electron theory, 8
 - Disintegration constant, 25
 - Dispersion, optical,70,72
 - Dispersion theory,single resonance, 70
 - Displacement law, 1
 - Dissociation energy, 70
 - Dissociation limit, 70
 - Distance, mean square, 114,147
 - relaxation, 114
 - Distribution, exponential
 - frequency, 167
 - frequency, 128
 - Gaussian, 149,150,151,157
 - Maxwellian, 69,70,84,137,144,163
 - neutron, 88,93,94,310,311,315
 - average, 197
 - extrapolated endpoint, 95
 - fast, 315
 - non-absorbing half-space,94
 - radial, 303
 - Distribution (Cont'd)
 - resonance, 315
 - sinusoidal, 310
 - spherical harmonic, 93
 - thermal, 315
 - neutron density, 174,180,196,312, 313
 - neutron energy, 312
 - neutron flux, 312,313,315
 - number-energy, 69,84
 - slowing-down, 147,149,150,152
 - spatial,150
 - thermal,69
 - velocity, 143
 - Dithizon, 368
 - Dunning, J. R., 188,388
 - et al, 397,403,405,409,419,425, 435,441,461,465,481,497
- E
- Effect, Compton, 36,41,45
 - conservation of energy, 41
 - conservation of momentum,41
 - Klein and Nishina, 41
 - photoelectric, 36,37,38
 - conservation of energy, 37
 - conservation of momentum, 37
 - Einstein relation, 4
 - Einstein-Bosé statistics, 7
 - Elastic collision, angular
 - distribution, 386
 - Q values, 386
 - Elastic scattering, 48,56,68,69,71, 294
 - cross section, 71
 - electron, 48
 - Electric dipole moment, 36,67
 - Electric field, non-uniform, 206
 - Electric quadrupole moment, 8,36
 - deuteron, 8
 - Electric vector, 36,38
 - Electrode, collecting, 260,264
 - separation, 260,261
 - spacing, 263
 - Electromagnetic pulse, 34
 - Electromagnetic radiation, 35
 - Electromagnetic separation, 365,366, 367,374

INDEX

- Electrometer, 82
 - Lindemann, 204
- Electron, absorption, 50
 - capture, 28,29,34
 - cosmic ray, 50
 - diffraction, 48
 - extrapolated range, 51
 - homogeneous, 51
 - ionization, 50,51
 - chamber, 204
 - line spectra, 51
 - microscope, 48
 - multiplication, 209
 - pairs, 44
 - radiative losses, 50
 - range, 50
 - rest mass, 4
 - scattering losses, 51
 - straggling, 50
 - volt, 4
 - wave length, 48
- Electrons, Auger, 29
 - internal conversion, 30
 - production of fission, 81
- Electronic configuration, heavy
 - elements, 362,363
 - neptunium, 360
 - rare-earth elements, 362,363
- Electronic cross section, 42
- Electroscope, 202,203,204
 - Lauritsen, 203
- Electrostatic energy, 79
- Elements, periodic table, 359
- Emissivity, 326
- Energy, absorbed neutrons, 85
 - beta-ray, table, 22-23
 - conservation, 12,37,41
 - Coulomb, 78,80
 - dissociation, 70
 - electrostatic, 79
 - excitation, 81
 - fission, 192,240
 - statistical distribution, 82, 83
 - fission fragments, 64,67,82,83, 85,287
 - fission products, 240
 - gamma-ray, table,22-23
 - neutron, 67,216
 - distribution, 312
 - mean value, 285
 - measurement, 228
- Energy, neutron (Cont'd)
 - prompt gamma rays, 85,240
 - prompt neutrons, 85
 - radioactive series, 85
 - relativistic kinetic, 46
 - thermal neutrons, 192
 - threshold, 81
- Energy balance, fission, 85,240
 - fission fragments, 84
- Energy barrier height, 79
- Energy continuum, 44
- Energy interval, logarithmic, 216
- Energy levels, 12
 - beta-ray spectrum of
 - Br87,27
 - mean life of nuclear, 33
 - transition probability of
 - nuclear, 33
 - width of nuclear, 33
- Energy level diagram, 22
 - Mn52, 28,29
- Energy loss, alpha particles, 57
 - fission fragments, 66
 - logarithmic, 69,115,116,148, 189,294,295,299
 - approximate equation, 295
 - graphical relation, 295
 - neutrons, 68,69
- Energy spectrum, neutrons, 103
- Energy state, negative,44
- Engelkemeir, D. W., 234
- Engineering units, 323
- Enriched fuel, 274,278,300,318, 320,321
- Enriched uranium, 274,278,300,320, 321,322
- Entropy, 275
- Epithermal nuclear reactors, 275
- Epithermal region, 157
- Equation of continuity, 152
- Equilibrium, thermal, 103, 112, 131,134
 - transient, 32
- Esterline-Angus recorder, 254
- Evans, R. D., 1,187,263,270
- Exchange forces, 10
- Excitation energy, 81
- Excited level, 34
- Excited state, 35
- Exponential build-up, 31,32
- Exponential decay, 31,32
- Exponential frequency
 - distribution, 167

INDEX

Exponential relaxation distance, 104

Extrapolated end point, 95

Extrapolated length, 193

Extrapolation distance, 112,193

F

Fanning equation, 328,330,338,339

Fast effect, 285,286,316

Fast fission, 100,313

effect, 285

Fast flux, 313,314

Fast migration area, 148

Fast neutrons, activation, 112

diffusion coefficient, 157

distribution, 315

fictitious density, 157

mean life, 157

source density, 157

Fast nuclear reactors, 274,275,278, 302,303

Fast-period nuclear reactors, 170

Feld, B. T., 187,251,252,387,389

Fermi, E., 7,23,57,67,75,99,100, 101,102,103,104,105,109,111, 151,162,188,189,224,289,309, 312,316,321,389,452,458

et al, 402

Fermi age, 114,148,150,151,152,163, 172,192

Fermi-Dirac statistics, 7,23,67

Feshbach, H., 290

Fields, R. B., et al, 403,405,411, 413,415,417,419,423,425,429, 435,439,441,443,455,457,461, 463,465,481,497,499

Filter, slow neutron, 214

Fissile material, 233,244

Fission, asymmetry, 81

decay chain, 85

deuteron-induced, 86

distribution of energy, 83

distribution of masses, 81

electromotive force, 282

fast, 100,313

fast effect, 285

ionization, 82

mean-free-path, 96,294,296

Fission, asymmetry (Cont'd)

neutron-induced, 78,81,86

neutrons, 68,112,113,115,192,218

nuclear, 9,35,78

probability, 80

production, 81

alpha particles, 81

deuterons, 81

electrons, 81

gamma rays, 81

neutrons, 81

photons, 81

spontaneous, 80,86,358

symmetrical, 236,287,288

symmetry, 81

Th233, distribution of

masses, 83

threshold energy, 81

types, 86

U236, distribution of masses, 83

energy distribution of heavy and light fragments, 83

statistical distribution of total energy, 83

U239, distribution of masses, 83

energy distribution of heavy and light fragments, 83

statistical distribution of total energy, 83

Fission chamber, 205,218,233

efficiency, 233

Fission counting rate, 233

Fission cross section, 15,91,114,

115,289,388

Np237,288

plutonium, 289

uranium, 289

U235,73

Fission energy, 10,62,192,240,275

balance, 85, 240

statistical distribution, 82

symmetrical, 78

Fission fragments, 60,79

absorption, 281

atomic number, 64

atomic weight, 64

beta emission, 85

charge, 62

cloud chamber track,66

critical separation, 287

energy, 64,67,82,83,85

balance, 84,85

INDEX

Fission fragments, energy, (Cont'd)
 loss, 66
 and mass, 82
 entropy, 275
 excitation, 84
 gamma emission, 85
 heavy, 62
 initial velocities, 62,64,65
 ionic charge 64
 ionization chambers, 204
 kinetic energy, 287
 light, 62
 magnetic rigidity, 64
 masses, 78,82,83
 mean range, 64,282
 measurement, with ionization
 chamber, 82
 neutrino emission, 85
 neutron emission, 84
 nuclear charge, 67
 nuclear collision, 66
 number-energy distribution, 84
 photographic method, 201
 Plutonium Project, 64
 range, 279
 in aluminum, 280
 in gases, 65,66
 in various materials,280,281,
 282
 range measurement, 279,280,281
 range-velocity relations, 65
 recoil momentum, 277
 residual range, 65,66
 separation, 288
 specific ionization, 66
 transmission, 280
 Fission neutrons, 68,112,113,115,
 218,236,364
 delayed, 112
 energy, 192, 240
 measurement, 218
 number, 218
 Fission particles, interaction with
 matter, 60
 Fission process, 75
 chemistry, 231
 liquid-drop model, 80
 semi-empirical relations, 75
 source of power, 275
 symmetrical, 78,81
 Fission products, 20,27,31,32,35
 activity, 241

Fission products, (Cont'd)
 chains, 232
 charge, 62
 chemistry, 232
 consumption, 245
 decay constant, 31,32
 decay rate, 237,238
 decontamination, 245
 distribution of half-lives, 237,
 238
 energy, 240
 exponential build-up, 31,32
 exponential decay, 31,32
 fission yield, 248
 half-period, 31,32
 identification, 231
 long-lived, 239,248,249
 mean life, 31,32
 power dissipation, 242,243,244,
 246
 precipitation, 375
 radiation, 319
 radioactive wastes, 249
 radioactivity, 241,242,243,245
 series, 31,32
 series relations, 31,32
 short-lived, 249
 statistical survey, 236,237
 tabulation by Plutonium Project,
 232
 technological importance, 248
 volatile, 248,249
 Fission threshold, 100,287,317
 Fission track, 82
 Fission yield, 62,234,236,241,248
 determination, 232,233
 Fizeau, 224
 Fissionable material, 93,274
 density, 116
 loss, 256
 Flow, laminar, 328
 streamline, 328,329,332,337,339,
 340,343,345
 turbulent, 328,329,332,337,340,
 342,343,346
 viscous, 339,342
 Flow sheet, production nuclear fuel,
 370
 Fluid, density, 330,338
 heat capacity, 330
 thermal conductivity, 330
 velocity, 330,338

INDEX

- Fluid, density (Cont'd)
 - viscosity, 330,339
 - Flux, fast, 313, 314
 - neutron, 97,140,253
 - average, 196
 - distribution, 312,313,315
 - measurement, 210,211,213,214
 - power, 252
 - thermal, 211,212,213,214
 - Foils, activation, 210,211,212,213
 - Forced convection, 328
 - Fourier series, 36
 - superposition, 36
 - Fraction of fission neutrons,
 - delayed, 112
 - Fractional crystallization, 368
 - Franck, J., 107
 - Freedman, M. L., 234
 - Free neutron density, 171
 - Free neutrons, 119,120,122,123,130, 166,172
 - Frequency distribution, 128
 - Friction factor, 329,338
 - Friedman, F. L., 106,111
 - Frisch, D. H., 287,389,395,407,409, 411,419
 - Fuel, circulating liquid, 320
 - enriched, 274,278,300,318,320,321
 - fusible alloys, 322
 - nuclear, 353
 - chemical separation, 367
 - ether extraction, 368
 - flow sheet, 370
 - isolation, 365
 - processing, 369
 - production, 355,364,365,370, 373
 - purification, 365,373
 - purity,369
 - salting out, 367
 - solvent extraction, 367
 - technology, 363,365,369
 - reprocessing, 244,245,302
 - spherical lumps, 316
 - uranium, 273,274,278,300,320
 - Fuel consumption, 197,283,284
 - rate, 197
 - Fuel mixture, 320
 - circulating, 308
 - fluid, 305
 - liquid, 306,307
 - mean atomic weight, 308
 - Fuel mixture, (Cont'd)
 - solid, 305
 - Fuel replacement, 319
 - Fuel rod, 319
 - Fusible alloys, 320,322
- ## G
- Gabus, G. H., 266
 - Gamma-ray energies, table, 22-23
 - Gamma rays, 22,35
 - Bragg reflection angle, 37
 - detection by Geiger counters, 210
 - ionization chamber, 204,264
 - (n,γ), 35
 - photographic method, 201
 - production of fission, 35,81
 - prompt, energy, 85,240
 - radioactivity, 35
 - Gamow, G., 108,109
 - Gamow's theory, 108
 - Gas constant, 342
 - Gaseous diffusion, 365,373
 - Gases, physical characteristics,343
 - thermal conductivities, 325
 - Gauss' lemma, 146
 - Gaussian, 149
 - distribution, 149,150,151,157
 - hydrogenous material, 149,150
 - non-hydrogenous material,150
 - normalization condition, 149
 - Geiger-Mueller counter, 208,209, 212,214,230
 - efficiency, 209,210,212
 - thin window, 234
 - Ghiorso, A., 287
 - Giesel, 356
 - Gilliland, E. R., 276,307,323
 - Goldberger, M., 107,108
 - Goldhaber, M., 228,290
 - Goldsmith, H. H., 188,221,387,389
 - Good, W. E., 403,419,441,497
 - Goodman, C., 273
 - Grahame, D. C., 368
 - Greisen, K. I., 389
 - et al, 491
 - Grosse, A. V., 356
 - Ground state, 70
 - deuteron, 11

INDEX

Group velocity, 35
Grummitt, W. E., 234

H

Hahn, O., 231,356
Haigerloch, Germany, nuclear
 reactor, 274
v. Halban, H., 99
Half-life, table, 22-23
Half-space, 93
Hall, T. A., 399
Hanford, 356
 piles, 18,115,273,274,302,356
Hanson, O. A., 389
Hanstein, H. B., 406,418,434,438,
 440,442,460,496,498
Harmonic amplification factor, 185
Harmonic expansion, 178,180
Harmonics, sequence, 113
Hasbrouck, B. H., 389
Havens, W. W., Jr., 290,388,394,
 400,404,492
 et al, 446,458,478,480,488,490
Haxby, R. O., 109
Health hazards, 371,372,374,375,376
Health monitoring, Lauritsen
 electroscope, 203
 photographic method, 200
 separation of plutonium, 375
Health physics, 256,258
 instrumentation, 257
Heat, specific, 330
Heat capacity, 341
 fluid, 330
 gas, 342
 molal, 342
Heat exchanger, 308,336,337
 liquid content, 337
Heat flow, 324
Heat removal, conduction, 336
 control rods, 298
 radiation, 335,336
Heat transfer, 305,323
 boiling, 323,333
 boundary condition, 324
 condensation, 323,334
 drop-wise, 334
 conduction, 323,324

Heat transfer, (Cont'd)
 convection, 323,328
 forced, 328
 laminar flow, 328
 natural, 332
 streamline flow, 328,329,332
 turbulent flow, 328,329,332
 design variables, 347
 engineering factors, 347
 engineering units, 323,341
 equation, 330,331
 gas, 304
 general criteria, 334
 graphical integration, 324
 illustrative power cycle, 351
 liquid, 304
 coolant, 318
 metals, 304,346
 salt, 346
 metric units, 341
 organic liquids, 346
 radiation, 323,326,327,328
 steady state, 324
 temperature pattern, 324
Heat transfer coefficient, 322,326,
 328,329,330,334,339
 gases, 333
 liquid metal, 331,332,333
 streamline flow, 329
 table, 343
 turbulent flow, 329
Heavy elements, bibliography, 377
 chemical properties, 361
 chemical separation, 367
 chemistry, 353
 co-precipitation, 357
 electronic configuration, 362,363
 isotopes, 354,355
 oxidation, 357
 number, 357
 states, 357,360,361
 sources, 353
 table, 355
Heavy hydrogen, 300
Heavy particles, photographic
 method, 201
Heavy water, 300
Heisenberg, W., 274
 uncertainty principle, 33,36
Heterogeneous nuclear reactors, 274,
 275,309,312,316,318,319,320,324
Hiroshima, nuclear reactor, 274

INDEX

Homogeneous mixtures, 159
 Homogeneous neutron beam, 223
 Homogeneous nuclear reactors, 139,
 144,274,275,278,296,298,300,
 302,303,304,307,308,312,321,
 324,337
 Homogeneous thermal neutron pile,
 139
 time behavior, 144,197
 velocity distribution, 143
 Huber, P., 409,425
 et al, 409
 Hydraulic radius, 333
 Hyperfine structure, 3

I

Ibser, H. W., 387
 Ideal nuclear paint, 139
 Ideal resonance detector, 136,137,
 138,139,149
 Indiana, University of, 101
 Indium resonance, 151,218,219
 Induced fission, 81
 Induced radioactivity, 35
 Inelastic scattering, 48,56,68,100
 cross section, 15
 Infinite lattice, 102,104
 Infinite pile, 100,104
 neutron density, 197
 Inhour, 168,170
 equation, 168,169,170,171,173,
 179
 Integral equation, 159
 Internal conversion electrons, 30
 International Radium Standards
 Commission, 22
 Inverse-square law, 92
 Iodine resonance, 151
 Ion exchange resins, 368
 Ionic charge, fission fragments, 64
 Ionization, 48,49,53,57,59,60,65,66,
 199
 alpha particle, 57
 columnar, 60
 loss, 261
 measurement, 53,62
 specific, alpha particles, 59
 fission fragments, 66
 Ionization chamber, 82,207,251,253,
 257
 boron-filled, 205,217,258,264
 boron-lined, 20,258,261,263
 capacity, 272
 Chalk River pile, 261,262,264,265
 design, 262,265
 detection of charged particles,
 204
 electric field, 206
 electron, 204
 multiplication, 209
 fission fragments, 82,204
 gamma-ray, 204,264
 health physics, 258
 helium-filled, 264
 hydrogen-filled,264
 insulators, 264
 neutron measurement, 258
 parallel plate, 206
 pulse, 206
 height, 209
 resolving time, 207
 saturation, 217
 sensitivity, 217
 slow neutrons, 204
 type TPA, 265
 type TPD,262
 Ionization current, 259,263
 measurement, 266
 saturated, 257
 Ionization process, 200
 Irvine, J. W., Jr., 353
 Isomeric nuclear levels, 37
 Isomeric state, 29,36,49
 Isomeric transition, 28,30,37
 Isomers, 30
 Isotopes, 3
 heavy elements, 354,355
 stable, atomic mass, 77
 Isotope chart, heavy elements, 24
 Segré,22-23, 189
 Isotope separation, 300
 centrifugal method, 366,367
 electromagnetic method, 365,366,
 367,374
 gaseous diffusion method, 365,373
 thermal diffusion method, 365,366,
 373
 Isotope separation processes,
 physical, 365
 Isotopic abundance, table, 22-23

INDEX

Isotopic mass, 4
 table, 22-23
 Isotopic ratio, 300
 Isotropic scattering, 89, 130

J

Jentschke, W., 82, 234
 Joliot-Curie, I., 377
 Jones, W. B., Jr., 464
 Journal of Applied Physics, 99
 Jupnik, H., 101

K

K-capture, 29
 k delayed, 113
 k prompt, 113
 Kennedy, J. W., 377
 Kinetic energy, relativistic, 46
 Klaproth, 356
 Kleeman, 60
 Klein, 41
 Klema, E. D., 501
 Koontz, P. G., 399

L

Laboratory for Nuclear Science
 and Engineering, 387, 389
 Laminar flow, 328
 Lanthanide series, 360
 Lanthanum, 358, 360
 Laplacian, 113, 141, 145
 heat equation, 324
 Lapp, R. E., 245
 Lassen, N. O., 64
 Latent neutrons, 118, 119, 120, 122,
 123, 130, 166, 168, 172
 Latent neutron density, 112, 118, 171
 Lattice, 314, 316
 cell, 314, 315
 cubic, 141

Lattice (Cont'd)
 finite, 104
 infinite, 102, 104
 optimal, 102
 uranium, 103
 Lauritsen, T., 277
 electroscope, 203
 Lavatelli, L. S., 389
 Lead, absorption coefficient, 45
 Legal considerations, 256
 Level, excited, 34
 nuclear resonance, 34
 width, 34, 188, 223
 excited, 71
 partial, 34, 71, 72
 resonance, 72
 total, 34, 71
 Levinger, J. S., 239
 Lichtenberger, H. D., 389, 456
 Light elements, as moderators, 301
 Lind, S. C., 107, 109
 Lindemann electrometer, 204
 Line spectra, 51
 Linear absorption coefficient, 15,
 38, 44
 Linear absorption cross section, 44
 Linear accelerator, 12, 225
 Los Alamos Group, 389
 Linenberger, G. A., 389
 Liquid-drop model, 80
 Liquids, thermal conductivity, 325
 Logarithmic amplifier, 255
 Logarithmic energy interval, 216
 Logarithmic energy loss, 69, 115,
 116, 148, 189, 294, 295, 299
 approximate equation, 295
 graphical relation, 295
 Lorentz force, 38
 Los Alamos, Linear Accelerator Group
 389
 nuclear reactor, 274
 Radioactive Sources Group, 389
 University, 75, 111, 188, 401, 405
 velocity selector, 490
 Group, 389
 water boiler, 18, 273
 Lumping, 309
 Lutecium, 360

INDEX

Mo

MacPhail, M. R., 407,409,415,417,419
 McAdams, W. H., 330,332,339
 McDaniel, D. D., 309,458
 McMillan, E. M., 355,377

M

Macroscopic absorption cross section, 135
 Macroscopic cross section, 15,220, 290,291,292,293
 capture, 291,292,293,299,300,301
 scattering, 291,292,293,299,301
 Macroscopic pile theory, 106
 Magnetic dipole moment, 7,8,36,54
 Magnetic moment, 8
 table, 22-23
 Magnetic quadrupole moment, 36
 Magnetic vector, 36
 Magnetron, Bohr, 8,54
 nuclear, 7,8
 Magnusson, L. B., 287
 Manhattan Project, 187,273,387
 Marshall, J., 389,396,402,404,406, 412,418,465,496
 Marshall, L. W., 389,404,452,458
 Mass, absorption coefficient, 45,53
 critical, 93,95,96
 effect of reflector, 97
 isotopic, 4
 table, 22-23
 Meson, 10
 neutron, 11,112
 nuclear, 112
 number, 3
 relativistic, 46
 statistical distribution,
 fission products, 62
 Mass-energy equivalent, 35
 Mass spectrometer, doublet
 method, 4
 Mass velocity, 330,340
 Massachusetts Institute of Tech-
 nology, 387,389
 Maximum range, 53
 Maxwellian distribution, 137,163
 prompt neutrons, 84
 thermal neutrons, 69,70,144

Meagher, R. E., 269
 Mean-free-path, 88,89,90,92,93,95, 96,97,104,294
 absorption, 96
 capture, 294
 fission, 96,294,296
 scattering, 90,96
 transport, 89,90
 Mean life, 34,35,68,91,141,197
 delayed neutrons, 115
 fast neutrons, 157
 thermal neutrons, 115,197
 Mean slowing-down time, 115
 Mean square distance, 104,114,147, 148
 Measurement, ionization,
 calorimeter, 62
 ionization measurement, 202
 Measuring techniques, 216
 Mechanical velocity selector, 223, 224,228
 Argonne, 389,456,472,474,476, 482,490
 group, 389
 Meiners, E. P., 239
 Meitner, L., 356
 Meson, mass, 10
 potential, 10
 Metal utilization, 285
 Metallurgical Laboratory, 387
 Metastable state, 30,49
 Metric units, 323
 Metropolis, N., 103
 Microscopic cross section, 15
 Microscopic pile theory, 106
 Migration area, 114, 163,172,193
 fast, 148
 total, 149
 Miskel, T. A., 389
 Mitchell, A.C.G., 101
 Moderating ratio, 299,301
 Moderator, 18,100,274,301,320
 beryllium, 20,322,325
 carbide, 302
 gaseous, 305
 graphite, 191,274,302,325
 heavy-water, 20,274
 hydrogenous, 191
 liquid, 318
 oxide, 302
 ratio, 299
 sodium, 326
 thermal conductivity, 325
 water, 274

INDEX

Moment, dipole, electric, 36,67
 dipole, magnetic, 7,8,54
 magnetic, 8
 table, 22-23
 quadrupole, electric, 8,36
 Momentum, angular, nuclear, 7
 angular, total, 5
 conservation, 12,37,41,62
 relativistic, 46
 Monk, 101,102
 Monochromatic neutron source, 17
 Monoenergetic neutrons, 67
 Monoenergetic neutron beam, 223
 Monoenergetic neutron diffusion,
 103
 Monokinetic alpha particles, 58
 Monokinetic neutrons, 116,139
 Morrison, P., 103
 Moshinsky, M., 108
 Motion, Brownian, 148
 Mulliken, R. S., 107,389
 Multiplication, neutron, 20, 99
 Multiplication constant, 99,102,106,
 132,139,159,189,190,191,193,
 194,285,299,312,316
 effective, 100,102,105,106,113,
 167,171,252
 excess, 113,168,171,194,296
 infinite, 100,101,102,105
 measurement, 127
 optimum, 159,299,300,301,312,
 321
 temperature effect, 199
 variation with isotopic
 ratio, 191
 Murray, F., 106
 Murrell, E. B. M., 395,407,411,497

N

Nagasaki, nuclear reactor, 274
 National Bureau of Standards, 23
 National Research Council, 23
 National Research Council of
 Canada, 234,261,262,265,266
 Natural convection, 332
 Negative Laplacian, 141
 Negatron, 27,47
 decay, 27,28
 Neodymium, 368

Neptunium, 3,287,288,289,305,353,
 354,355,357,360
 Neutrino, 23,28,29,35,54,85
 continuous spectrum, 29
 Neutrons, absorbed, fission energy
 balance, 85
 age, 104,105,114,148,150,151,152
 average velocity, 144
 beta decay, 68
 binding energy, 77,84,85,287
 Np²³⁷, 287
 U²³⁶, U²³⁷, U²³⁸, 77
 C, 74
 delayed, 27,62,85,112,115,123,
 124,125,126,128,140,188,196,
 198,239
 control, 194
 density, 112,118,123
 associated with fission, 115
 mean life, 115
 period, 198,307
 possible loss, 306,307
 stationary state, 141
 diffraction, 67,108
 diffusion length, 91,92,104,105,
 147
 effective temperature, 103
 elastic collision, 68
 elastic scattering, 68,69
 energy loss, 68,69
 energy spectrum, 103
 epithermal, 285
 exponential relaxation dis-
 tance, 104
 excess, 125
 fast, 157
 diffusion coefficient, 157
 fictitious density, 157
 flux, 314
 mean life, 157
 source density, 157
 filter, 214
 fission, 68,112,113,115,218,
 236,364
 delayed, 112
 energy, 192,240
 free, 119,120,122,123,130,166,
 172
 frequency distribution, 128
 Gaussian distribution, 149, 150
 151,157
 half-period, 68
 indeterminacy, 70

INDEX

Neutrons (Cont'd)

- inelastic scattering, 68
- k delayed, 113
- k prompt, 113
- latent, 118,119,120,122,123,130, 166,168,172
- logarithmic energy loss, 69,115, 116,148,189,294,295,299
- Maxwellian distribution, 69
- mean-free-path, 85,92,95,104
- mean life, 68,91,141,197
- mean square distance, 104
- modal velocity, 69
- moderation, 130
- monoenergetic, 67
- monokinetic, 116,139
- nuclear potential, 14
- number released per fission, 112,115,218
- physiological effects, 19
- point source, 180,181,182
- production of fission, 81
- prompt, 62,84,85,112,118,124,126, 166,170,197
 - fission energy balance, 85
 - Maxwellian distribution, 84
 - multiplication, 197
 - source, 84
- radiative capture, 3
- reflector, 97,251,273,277,298,310
- resonance capture, 132
- scattering angle, 90
- slow, ionization chambers, 204
- slowing-down distribution, 147, 149
- spatial distribution, 150
- thermal, 69,73,102,103,104,106, 107,111,116
 - activation, 112,215,216
 - diffusion equation, 155,158, 165,181
 - distribution, 69
 - energy, 192
 - equilibrium, 105,112,131,134, 137, 163
 - high energy, 69
 - Maxwellian distribution, 69,70
 - mean life, 115,197
 - source density, 157
- transmutation, 68
- velocity distribution, 144
- Neutron activation, fast, 112
- resonance, 112

- Neutron beam, homogeneous, 223
 - monoenergetic, 223
- Neutron capture, 71,113,115
 - thermal, 113
- Neutron capture cross section, table, 22-23
- Neutron cross section, absorption, 223
 - index, 390,391,392
 - measurement, 221,222,223,228,230
 - scattering, 230
 - table, 387
 - thermal, measurement, 228
 - total, 230
- Neutron current, 88,94
- Neutron cycle, 124
- Neutron density, 91,92,93,94,95,96, 97,106,107,114,116,137,194,311
 - average, 106,196,197
 - boundary condition, 142
 - control, 194
 - rod, 252
 - cylindrical, 310
 - delayed, 112, 118
 - distribution, 174,180,196,312,313
 - exponential decay, 119
 - extrapolated distance, 178
 - extrapolation, 142
 - falling, 122
 - fictitious, 157
 - free, 171
 - harmonic expansion, 178
 - infinite pile, 197
 - interface, 94
 - latent, 112,118,165,171
 - measurement, 210,211,216,217,221
 - radial, 310
 - schematic, 137
 - slope, 94
 - slowing-down, 171
 - spherical, 310
 - thermal, 114,138,155,165,210
 - time dependence, 117,118,119, 197,198
- Neutron detection, activation of foil, 210
 - proportional counters, 207
 - special techniques, 228
- Neutron detector, resonance, 136, 137,228
 - thermal, 136,137,215
- Neutron diffraction, 67,108

INDEX

- Neutron diffusion, 87
 - critical mass, 95,96
 - dimensional considerations, 92
 - effect of reflector, 97
 - elementary theory, 87
 - hydrogenous material, 87
 - infinite mass, 91
 - monoenergetic, 103
 - schematic representation, 88
 - thermal, 148
- Neutron dispersion, 70
- Neutron distribution, 88,93,94, 310,311,315
 - average, 197
 - extrapolated end point, 95
 - fast, 315
 - non-absorbing half-space, 94
 - radial, 303
 - resonance, 315
 - sinusoidal, 310
 - spherical harmonic, 93
 - thermal, 315
- Neutron emission, 49,84
- Neutron energy, 67,216
 - distribution, 312
 - mean value, 285
 - measurement, 228
- Neutron flux, 97,140,253
 - average, 196
 - distribution, 312,313,315
 - logarithmic energy interval, 216
 - measurement, 210,211,213,214
 - power, 252
 - thermal, 211, 212,213,214
- Neutron-induced fission, 81,86
- Neutron interactions, 67
- Neutron leakage, 100,104,140,144, 146,165,172,252
- Neutron mass, 11,112
- Neutron measurement, 258
- Neutron multiplication, 20,99
- Neutron periods, delayed, 85,86,123
- Neutron production, 91
 - prompt, 166
- Neutron reactions, 18
- Neutron reflection, 67,118
- Neutron reflector, 97,251,273,277, 298
- Neutron reproduction, prompt, 172
- Neutron scattering, 89
- Neutron sources, 94,138
 - calibration, 220
- Neutron sources (Cont'd)
 - fast, 157
 - Ra-Be, 138,151
 - thermal, 219
 - column, 219
- Neutron species, 1
- Neutron statistics, 67
- Neutron transmission, 67
- Neutron velocity, 71,221
 - average thermal, 196
 - measurement, 225,228
- Neutron wave, 71
 - length, 67,70,226,229
- Nishina, Y., 41
- Noncritical pile, time behavior, 164
- Nordheim, L. W., 106,107,168
- Nottingham, W. B. 269
- Nuckolls, R. G., et al, 397,411
- Nuclear angular momentum, 7
- Nuclear chain reactions, elementary theory, 99
- Nuclear charge, 1,3,46,67
- Nuclear collision, fission
 - fragments, 66
- Nuclear constants, 187
 - delayed neutrons, 188
 - graphite (C), 189
 - U235, 187
 - U238, 188
- Nuclear cross section, 14, 71,88,95
- Nuclear density, 1,114,290,291,299
- Nuclear energy levels, Heisenberg
 - uncertainty principle, 33
 - mean life, 33
 - transition probability, 33
 - width, 33
- Nuclear engineering, 273
- Nuclear excitation, 48
- Nuclear fission, 9, 35,78
- Nuclear forces, 75
 - range, 10
- Nuclear fuels, 353
 - chemical separation, 367
 - ether extraction, 368
 - flow sheet, 370
 - isolation, 365
 - processing, 369
 - production, 355,364,365,370,373
 - purification, 365,373
 - purity, 369
 - rate of consumption, 284
 - reprocessing, 370

INDEX

Nuclear fuels (Cont'd)

- salting out, 367
- solvent extraction, 367
- technology, 363, 365, 369
- uranium, 363
- Nuclear levels, isomeric, 37
- Nuclear magneton, 7, 8
- Nuclear mass, 46, 112
- Nuclear paint, ideal, 139
- Nuclear potential barrier, 12, 13
- Nuclear potential for neutrons, 14
- Nuclear power, basic requirements, 283

Nuclear radius, 3, 8, 11, 46, 75, 79

Nuclear reactions, 11, 12, 16, 21

- charts, 21

- (n, α), 19

- (n, γ), 18

- (n, f), 20

- (n, 2n), 20

- (n, p), 19

- (γ , n), 20

- types, 18

Nuclear reactors (see also pile), 26,

35, 60, 72, 87

- active volume, 310

- active zone, 277

- aircraft, 309

- Alamogordo, 274

- Argonne, 274, 300

- average temperature, 344

- Bikini, 274

- Chalk River, 261, 274, 300

- characteristic constant, 113

- characteristic size, 153

- class, 274, 275

- construction, 273, 278, 296, 298

- control, 106, 173, 217, 251, 253, 255,

296, 297, 298

- critical size, 155, 177, 195

- cubical, 141, 142, 308, 312, 313

- cylindrical, 142, 174, 308

- declassified information, 273

- economic advantage, 283

- economics, 283

- enriched uranium, 274, 278

- epithermal, 275

- extrapolated boundaries, 142

- fast, 274, 275, 278, 302, 303

- fast period, 170

- gas coolant, 297

- gaseous, 163

Nuclear reactors (Cont'd)

- graphite-moderated, 104

- Haigerloch, Germany, 274

- Hanford, 18, 115, 273, 274, 302, 356

- heterogeneous, 274, 275, 309, 312,

316, 318, 319, 320, 324

- high temperature, 278, 302

- Hiroshima, 274

- homogeneous, 139, 144, 274, 275, 278,

296, 298, 300, 302, 303, 304, 307,

308, 312, 321, 324, 337

- horse power, 283, 284

- instrumentation, 199

- kinetics, 197

- limitations, 278

- Los Alamos, 274

- mobile, 309

- Nagasaki, 274

- neutron distribution, 310, 311

- Oak Ridge, 274

- operation, 251, 253

- period, 198, 199

- perturbation theory; 177, 178

- power, 197, 274, 275, 283

- power level, 174, 196, 217, 253

measurement, 216, 217

- power utilization, 297

- rectangular, 311

- reflector, 173, 177

- resonance, 275, 278, 302, 303

- servicing, 307, 308, 309

- shape, 105, 173

- size, 105, 173

- spherical, 143, 308

- subcritical, 177

- temperature, 275

dependence, 143

- thermal, 274, 275, 278, 302, 303

- time behavior, 144

- types, 274, 285

- University of Chicago, 274

- water-moderated, 104

Nuclear resonance levels, 34

Nuclear rocket, 277, 279

Nuclear scattering, 56

Nuclear spin, 8

Nuclear stability, 79, 239

Nuclei, size, 1

- statistics, 6

Nucleon, 1, 3, 37

- average density, 75

- binding energy, 37, 75

INDEX

Nucleus, Coulomb energy, 80
 compound, 12
 radioactive, decay period, 115
 spherical, 80
 surface energy, 80
 Number-energy distribution, 69,84

O

Oak Ridge, nuclear power plant, 296
 nuclear reactor, 274
 Optical dispersion, 70,72
 Optimal conditions, 111
 Optimal lattice, 102
 Orbital angular momentum, 5
 Organic solvents, 376
 Osborne, C. L., 389
 Osborne, R. K., 28
 Oscillation method, 126,127
 Oxidation, 373
 reduction potential, 358
 states, heavy elements, 357,360,
 361
 Ozeroff, W. J., 251

P

Packing fraction, 9
 Pair production, 36,42,44,46,49
 absorption coefficient, 45
 cross section, 44
 process, 44
 Paraffin radiator, 208
 Parallel spin, 11
 Parity, 5,6,36
 conservation, 6
 Partial level width, 34
 Pauli exclusion principle, 7,11
 four-shells, 9
 Peabody, C. O., 266
 Peaslee, D. C., 290
 Penetration probability, 14
 Perry, R. D., 389
 Periodic table, 359
 Perlman, I., 377
 Persulfate, 358
 Perturbation theory, Schrödinger, 176

Peterson, R. G., 389,486
 Phase velocity, 35
 Photo absorption coefficient, 45
 Photodisintegration, 20, 37
 Photoelectric absorption cross
 section, 38
 Photoelectric effect, 36,37,38,210
 conservation of energy, 37
 conservation of momentum, 37
 Photoelectric emission, 38
 Photoelectron, 38
 Photofission, 81,86
 Photographic method, 200,201,202
 alpha particles, 201
 beta rays, 201
 fission fragment, 201
 gamma rays, 201
 heavy particles, 201
 Photons, 36
 detection by Geiger counters, 210
 production of fission, 81
 Physical separation processes, 365
 Physiological effects of neutrons, 19
 Pile (see also nuclear reactor)
 Argonne, 274,300
 chain-reacting, 111
 Chalk River, 261,274,300
 Clinton, 19
 control, 106,173,217,251,253,255
 296,297,298
 critical size, 155,177,195
 calculation, 191
 characteristic equation,
 156,158,160
 temperature considerations, 162
 cubic, critical conditions, 181
 critical dimension, 142,145,
 192,193
 cylindrical, critical radius, 142
 description, 251
 finite, 100,104
 Hanford, 18,115,273,274,302,356
 infinite, 100,104
 neutron density, 197
 instrumentation, 199
 kinetics, 197
 noncritical, time behavior, 164
 operation, 251,253
 oscillator, 108
 power, 197,274,275,283
 power level, 174,196,217,253
 measurement, 216,217
 shielding, 247

INDEX

Pile (Cont'd)

- spherical, critical radius, 142, 193
- critical size, 192
- thermal neutron, homogeneous, 139
- time behavior, 144, 197
- velocity distribution, 143
- Pile material, reprocessing, 244
- Pile period, 115, 125, 198, 199
 - fast, 126
 - transient, 125, 126
- Pile perturbation theory, 177, 178
- Pile theory, elementary, 111, 187
 - experimental basis, 199
 - macroscopic, 106
 - microscopic, 106
 - symbols and definitions, 112, 113, 114, 115
- Pitchblende, 371
- Placzek, G., 101, 103, 109
- Planck's constant, 226
- Plass, G. N., 101, 102, 105
- Plutonium, 3, 107, 274, 289, 301, 302, 353, 354, 355, 357, 364, 371
 - alloys, 302, 304, 305
 - alpha activity, 375
 - co-precipitation, 375
 - decontamination, 375
 - fabrication, 374
 - health hazards, 374, 375, 376
 - ion exchange, 376
 - oxidation states, 375
 - purification, 374
 - slurries, 303
 - solubility, 376
 - solvent extraction, 376
 - toxicity, 375
 - valuable compounds, 303
- Plutonium Project, 102, 232, 234, 237, 241
 - fission fragments, 64
- Poiseuille law, 328, 339
- Polarization, 36
- Polonium, 19
 - alpha rays, 19
 - half-period, 19
 - as heat source, 19
- Pool, M. L., 266
- Positron, 46
 - annihilation radiation, 27
 - decay, 27, 28
 - emission, 4, 28, 29
 - gamma-ray accompaniment, 28

Positron (Cont'd)

- spectrum, annihilation radiation, 28
 - maximum energy, 28
- Potential barrier, 12, 13, 79, 287
 - height, 14
- Np238, 288
 - nuclear, 12, 13
- Power, 197, 274, 275, 283
 - fission products, 242, 243, 244, 246
- Power considerations, 196
- Power cycle, efficiency, 284
 - illustrative, in heat transfer, 351
- Power level, 116, 174, 196, 253
 - measurement, 216, 217
- Power supply, stabilized, 269
- Powers, P. N., et al, 486
- Poynting vector, 36
- Praseodymium, 368
- Prandtl's equation, 329, 330
 - group, 340, 342, 344
 - number, 330
- Precipitation, 303, 367, 376
- Princeton, 101, 108
- Probability of penetration, 14
- Prompt gamma rays, 85
 - energy, 85, 240
- Prompt neutrons, 62, 84, 85, 112, 118, 124, 126, 166, 170, 197
 - energy, 85
 - fission energy balance, 85
 - Maxwellian distribution, 84
 - multiplication, 197
 - source, 84
- Proportional counters, 206, 208, 209
 - alpha, 206
 - background, 206
 - boron-filled, 221, 223, 227
- BF₃ gas-filled, 20
 - fission, 206
 - neutron detection, 207
 - noise, 206
 - resolving time, 207
- Protoactinium, 353, 354, 358, 377
 - health hazards, 376
- Protons, interaction with matter, 54
 - range, 58
 - recoil, 208
- Pulse amplifier, 233
 - ionization chamber, 206

INDEX

Q

Quadrupole moment, electric, 8,36
 Quadrupole radiation, 36
 Quantized excited levels, 13
 Quasi-stationary state, 70,72
 Q values, 4,11,12,15,16,17,19,21,
 379,386
 table, 380,381,382,383,384,385

R

Radar pulse, 35
 Radiation, 49,323,326,327,328,335,
 336
 annihilation, 27,28,46
 biological effects, 256
 chemical effects, 250
 degraded, 42
 density, 107
 electromagnetic, 35
 fission product, 319
 interaction with matter, 35
 measurement, 247,253
 quadrupole, 36
 shielding, 247
 tolerance, level, 247,249
 Radiation chemistry, 107,250,303,
 305
 Radiation effects, 107
 Radiative losses, 56
 Radioactive beta-ray spectra, 53
 Radioactive decay, electron
 capture, 29
 Radioactive nucleus, decay
 period, 115
 Radioactive recoil, 21
 Radioactive series, fission
 energy balance, 85
 Radioactive series relations, 30
 Radioactive Sources Group, Los Alamos,
 389
 Radioactive wastes, 249,255
 Radioactivity, alpha decay, 21
 Ba¹⁴⁰, 33
 beta decay, 23,26
 beta spectrum, 26
 cooling, 241
 disintegration constant, 25

Radioactivity, (Cont'd)

 electron capture, 28
 fission products, 248
 half-period, 25
 induced, 35,305,308
 isomeric transition, 28
 La¹⁴⁰, 33
 natural disintegration
 series, 25
 principles of, 21
 Th²³², 25
 U²³⁵, 25
 U²³⁸, 25
 Radiochemical contamination, 232
 Radiochemical decontamination, 232
 Radiochemical purity, 232
 Radiochemistry, 231,358,360,373
 co-precipitation, 356,357
 oxidation states, 361
 persulfate, 358
 tracer methods, 356
 Radium-beryllium source, 138,151
 Radium E, 19
 Radius, critical, 95,96,142,193
 hydraulic, 333
 nuclear, 3,8,11,46,75,79
 Rainwater, L. J., 290,388,394,400,
 404,492
 et al, 432,454,456,462,486
 Ram jet engine, 276,277
 Ramsey, N. F., 395
 Range, alpha particle, 58,59,60
 deuteron, 58,59
 maximum for electrons, 53
 nuclear forces, 10
 proton, 58,59
 Range-velocity relations, alpha
 particles, 58
 fission fragments, 65
 Rare earth, carrier, 375
 elements, electronic
 configuration, 362,363
 transition group, 358
 Rasetti, F., 109
 Rayleigh-Schrödinger method, 106
 Reactions, charged particles, 20
 neutron, 18
 nuclear, 11,12,16,21
 charts, 21
 (n, α), 19
 (n, γ), 18
 (n,f), 20

INDEX

Reactions, nuclear (Cont'd)

(n, 2n), 20

(n,p), 19

(γ ,n), 20

types, 18

Reactivity, 168,303,305

excess, 194,296

Reactors, nuclear, 26,35,60,72,87

aircraft, 309

active volume, 310

active zone, 277

Alamogordo, 274

Argonne, 274,300

average temperature, 344

Bikini, 274

Chalk River, 261,274,300

characteristic constant, 113

characteristic size, 153

class, 274,275

construction, 273,278,296,298

control, 106,173,217,251,253,

255,296,297,298

critical size, 155,177,195

cubical, 141,142,308,312,313

cylindrical, 142,174,308

declassified information, 273

economic advantage, 283

economics, 283

enriched uranium, 274,278

epithermal, 275

extrapolated boundaries, 142

fast, 274,275,278,302,303

fast period, 170

gas coolant, 297

gaseous, 163

graphite-moderated, 104

Haigerloch, Germany, 274

Hanford, 18,115,273,274,302,

356

heterogeneous, 274,275,309,312,

316,318,319,320,324

high temperature, 278,302

Hiroshima, 274

homogeneous, 139,144,274,275,

278,296,298,300,302,303,304,

307,308,312,321,324,337

horse power, 283,284

instrumentation, 199

kinetics, 197

limitations, 278

Los Alamos, 274

mobile, 309

Reactors, nuclear, (Cont'd)

Nagasaki, 274

neutron distribution, 310,

311

Oak Ridge, 274

operation, 251,253

period, 198,199

perturbation theory, 177,178

power, 197,274,275,283

power level, 174,196,217,253

power level measurement, 216,

217

power utilization, 297

rectangular, 311

reflector, 173, 177

resonance, 275,278,302,303

servicing, 307,308,309

shape, 105,173

size, 105, 173

spherical, 143,308

subcritical, 177

temperature, 275

temperature dependence, 143

thermal, 274,275,278,302,303

time behavior, 144

types, 274,285

University of Chicago, 274

water-moderated, 104

Recoil momentum, 277

Recoil protons, 208

Rectangular nuclear reactors, 311

Reducing agent, 357

Reflection angle, Bragg, 37

Reflection coefficient, 317

Reflectors, 97,173,177,251,273,

277,304

neutron, 97,251,273,277,298,310

Reflector materials, 276

Relative resonance integral, 113

Relativistic kinetic energy, 46

Relativistic mass, 46

Relativistic momentum, 46

Relaxation distance, 114

Reprocessing, 298,302

Reproduction constant, 99,102,106,

132,139,159,189,190,191,193,

194,285,299,312,316

effective, 100,102,105,106,113,

167,171,252

excess, 113,168,171,194,296

infinite, 100,101,102,105

measurement, 127

INDEX

Reproduction constant (Cont'd)
 optimum, 159,299,300,301,312,321
 temperature effect, 199
 variation with isotopic ratio, 191
 Resins, ion exchange, 368
 Resonance, 72
 absorption, 101,114,134,137,309
 cross section, 113,115,154, 229
 activation, 215
 cross section, 216
 capture, 73,101,102,128,132,137
 cross section, 115,189,388,389
 detector, 228
 ideal, 136,137,138,139,149
 escape probability, 101,104,114, 132,135,153,154,190,191,312, 316,317,321
 integral, 189
 relative, 113
 levels, nuclear, 34,101
 single, dispersion theory, 70
 neutron activation, 112
 neutron detector, 136,137,228
 neutron distribution, 315
 nuclear reactors, 275,278,302,303
 scattering cross section, 229
 width, 135
 Review of Modern Physics, 387
 Reynolds number, 329
 Richards, H. T., 389
 Richman, C., 395
 Rocket, nuclear, 277,279
 Roentgen, 256
 Rowe, G., 389
 Rutherford, E., 56,200
 Rutherford, unit, 23

S

Safety rods, 298
 Salant, E. O., 395
 Sampson, M. B., 239
 Sargent, B. W., 239
 Saturated density, 211
 Sawyer, R. B., 389,486
 Scattering, 11
 angle, 90

Scattering, (Cont'd)
 anisotropic, 153
 Bragg, 37
 gamma rays, 37
 reflection angle, 37
 coherent, 37
 cross section, 14,15,42,87,90, 115,116,131,222,291,299,301, 388
 inelastic, 15
 macroscopic, 291,292,293,299, 301
 measurement, 230
 resonance, 229
 elastic, 48,56,68,69,71,294
 electron, 48
 experiments, 76
 inelastic, 48,56,68,100
 isotropic, 89,130
 mean-free-path, 90,96
 neutron, 89
 nuclear, 56
 Rutherford, 56
 total, 48
 Scharff-Goldhaber, G., 403,419,441, 497
 Scherr, R., 395
 Schmidt, 269
 Schrödinger equation, 57
 perturbation theory, 176
 Rayleigh-, method, 106
 Schweinler, H., 108
 Scintillation method, 200
 Seaborg, G. T., 287,363,368,377
 Seagondollar, L. W., 419
 Secondary coolant, 305
 Segré, E., 279,280,377,389
 et al, 455,459,465,491
 chart, 22-23,189,290,300
 Seitz, F., 107,108,109
 Selection rules, 6
 Separation processes, chemical,367
 physical, 365
 Sequence of harmonics, 113
 Shape factor, 142
 Shearing strength, 303
 Shield, biological, 251,256
 Shielding, 247,304,307,371
 biological, 256
 circulation system, 305,320
 concrete, 309
 heat exchanger, 305,308,318, 320

INDEX

- Shielding (Cont'd)
 - lead, 309
 - pump, 318
- Short-range alpha particles, 108
- Short-range exchange forces, 9
- Shoupp, W. E., 109
- Single resonance levels, 70
- Singlet force, 11
- Size, critical, 99,111,139,142,146,155,156,158,160,167,173,177,191,192,193,322
 - cubic, 193
 - extrapolated length, 193
 - materials required, 195,196
 - reflector, 195
 - spherical, 193,194
- Slater, J. C., 48
- Sleater, W., Jr., 395
- Slow neutrons, ionization chambers, 204
- Slow neutron filter, 214
- Slowing-down area, 150,192
 - density, 114,132,149,155,158,165,215,216
 - measurement, 215
 - distribution, 147,149,150,152
 - power, 115,138,153,216,299,301
 - time, 171, 198
 - mean, 115
 - with resonance capture, 132
 - without resonance capture, 128
- Slurries, 303,320
- Smyth, H. D., 100
- Smyth Report, 100,115,159,274,275,309,312,321
- Snell, A. H., 239
- Snyder, T. M., 101
- Solar energy, 10
- Solenoid, 254
- Solids, thermal conductivity, 325
- Solvent extraction, 367,370,377
- Soodak, H., 106
- Source, prompt neutrons, 84
- Source density, 90,140
 - fast neutrons, 157
 - thermal neutrons, 157
- Source strength, 114
- Sources, neutron, calibration, 220
- Spatial distribution, 150
- Specific heat, 330
- Specific ionization, alpha particles, 59
 - fission fragments, 66
- Specifically nuclear force, 10
- Spectra, continuous, absorption curve, 54
 - line, 51
- Spectrometer, crystal, 226,227,228
 - Argonne, 456,470,472,474,482,490
 - Group, 389
 - Clinton Laboratories, 456,486,492
 - Group, 389
- Spectrum, beta-ray, 26
 - Br⁸⁷, 27
 - continuous spectrum, 51
 - line spectrum, 51
 - maximum value, 51,53
 - mean energy, 26
 - modal value, 26
 - probable error, 53
 - continuous, 51
 - energy, neutrons, 103
 - x-ray, 49
- Spherical harmonic, 93
- Spherical nuclear reactor, 143,308
- Spherical pile, critical radius, 142,193
 - critical size, calculation, 192
- Spin angular momentum, 5
 - antiparallel, 11
 - nuclear, 8
 - orientation, 5
 - parallel, 11
 - table, 22-23
- Spontaneous fission, 80,86,358
- Standard air, 263
- Stationary state, 95,141
- Statistical fluctuation, alpha particles, 58
- Statistics, 6
 - conservation, 23
 - Einstein-Bosé, 7
 - Fermi-Dirac, 7,23,67
 - nuclei, 6
- Steady state, 324
- Stefan-Boltzmann Law, 326
- Stephens, W. E., 109
- Stephenson, 102
- Straggling, alpha particles, 58
 - electron, 50
- Strassmann, F., 231
- Streamline flow, 328,329,332,337,339,340,343,345

INDEX

Structural materials, 290,319
 Sturm, W. J., 389,452,456,468,476
 et al, 470, 472
 Sulfide precipitate, 231
 Surface tension, 10
 temperature, 327,335,336
 Sutton, R. B., 389
 et al, 404
 Szilard, L., 99,100,111,188,465

T

Tantalum, 358
 Taschek, R. F., 423,425
 Taylor expansion, 159
 Teller, E., 103
 Temperature, absolute, 326
 coefficient, 297
 coolants, 327
 dependence, nuclear re-
 actors, 143
 difference, 327, 332,347
 gradient, 276,303,324
 surface, 327,335,336
 Thermal capture cross sec-
 tion, 113
 Thermal column, 219,223,229
 Thermal conductivity, 303,324,325,
 330,340,341,346
 fluid, 330
 gases, 325
 gas films, 326
 liquids, 325
 liquid metals, 326
 organic liquids, 326
 solids, 325
 Thermal diffusion, 365,366,373
 area, 148,192
 equation, neutrons, 155,158,165,
 181
 length, 114,161,162
 Thermal equilibrium, 103,112,131,134,
 137,163
 Thermal expansion, 303
 Thermal neutron, 102,103,104,106,107,
 111,116
 activation, 112,215,216
 capture, 113
 cross section, measurement, 228

Thermal neutron, (Cont'd)
 density, 114,138,155,165,210
 detector, 136,137,215
 diffusion, 148
 distribution, 315
 energy, 192
 flux, 211, 212,213,214
 Maxwellian distribution, 69,
 70,144
 mean life, 115,197
 source density, 157
 sources, 219
 Thermal neutron pile, homo-
 geneous, 139
 temperature dependence,
 143
 time behavior, 144,197
 velocity distribution,
 143
 Thermal nuclear reactors, 274,275,
 278,302,303
 Thermal stresses, 276
 Thermal utilization, 101,103,113,
 116,117,126,127,161,174,189,
 190,191,285,312,316,317,321
 measurement, 127,136,138,162
 Thin coupling, 236
 Thomas-Fermi, 57
 Thorium, 353,354,376
 canning, 372
 compound, 372
 co-precipitation, 377
 fabrication, 372
 fluoride, 370
 health hazards, 372,376
 metal, fabrication, 372
 ore, 370
 oxidation states, 376
 oxide, 370
 precipitation, 376
 purification, 372
 Th²³², radioactivity, 25
 Threshold energy, 81
 fission, 100,287,317
 Time behavior, homogeneous thermal
 neutron pile, 144,197
 noncritical pile, 164
 Time dependence, neutron density,
 117,118
 Time-of-flight velocity selector,
 223,225
 Total absorption coefficient, 45

INDEX

Total angular momentum, 5
 Total cross section, 14,71,114,222,
 291,388
 measurement, 227,229,230
 table, 22-23
 Total level width, 34
 Total migration area, 149
 Total neutron cross section, 230
 Tracer methods, 356
 Transient equilibrium, 32
 Transition, isomeric, 28,30,37
 Transmission, electron, 51
 measurement, 222,230
 method, 229
 Transport cross section, 15,87,90,
 153
 Transport mean-free-path, 89,90
 Transuranic elements, 79
 Trigger circuit, 254,255,269
 Triplet state of deuteron, 11
 Turbulent flow, 328,329,332,337,
 340,342,343,346
 Turkel, S. H., 389

U

Uchiyamada, H. C., 102
 Ulrich, A. J., 389
 Uncertainty principle, Heisenberg,
 33,36
 Univeristy of Chicago, 387,406
 nuclear reactor, 274
 University of Indiana, 101
 University of Wisconsin, 387
 Uranium, 353,354,355,363
 alloys, 302,303,304,305
 de-canned, 375
 enriched, 274,278,300,320,321,322
 ether extraction, 369
 health hazards, 371,374,376
 hexafluoride, 366,370,374
 lattice, 103
 lumping, 309
 metal, 370
 canning, 371
 fabrication, 371
 ore, 369,370
 processing, 369
 oxidation states, 360,375,376

Uranium, (Cont'd)
 oxide, 370
 precipitation, 375
 production, 371
 purification, 369
 rod, diameter, 322
 slurries, 303
 valuable compounds, 303
 vanadate, 371
 U235, 187
 radioactivity, 25
 U236, binding energy, 77
 U237, binding energy, 77
 U238, 188
 binding energy, 77
 capture cross section, 73
 radioactivity, 25
 Uranyl fluoride, 357

V

Vacuum-tube voltmeter, 270,271
 Van Horn, J. R., 245
 van der Waal's forces, 9
 Vector, electric, 36,38
 magnetic, 36
 Poynting, 36
 Velocity distribution, 143
 Velocity, fluid, 330,338
 group, 35
 mass, 330,340
 neutron, 71,221
 average thermal, 196
 measurement, 225,228
 phase, 35
 Velocity selector, 223,224,225
 Columbia, 388,394,396,402,406,
 408,410,412,416,418,419,420,
 422,424,426,430,434,438,440,
 442,450,460,466,496,498
 Cornell, 464
 crystal spectrometer, 226,227,
 228
 cyclotron, 225
 linear accelerator, 225
 Los Alamos, 490
 mechanical, 223,224,228
 Argonne, 389,456,472,474,476,
 482,490
 Group, 389

INDEX

Velocity selector, (Cont'd)
 resolution, 223,388
 time-of-flight, 223,225
 Virtual excited level, 70
 Viscosity, 328,329,330,341,
 fluid, 330,339
 Viscous flow, 339,342
 Volatilization, 368,369
 Voltmeter, vacuum-tube, 270,271
 Volume, critical, 97,143

X

X-rays, 29,30,35,38,49
 X-ray spectrum, 49
 continuous, 49

Y

Yield-Mass Curve, 234,235

W

Wahl, A. C., 377
 Waste disposal, 249,255
 Water boiler, Los Alamos, 18,273
 Wattenberg, A., 395,407
 Wave function, 5,101,105
 Wave length, Compton, 41
 de Broglie, 14,48
 electron, 48
 neutron, 67,70,226,229
 Wave model, 34
 Wave, neutron, 71
 Wave penetration, 287,288
 Wave properties, 13
 Wave train, 34,35
 Way, K., 243
 Weinberg, A. M., 101,106,108
 Weinstock, R., 108,109
 Weisskopf, V., 87,111,251,290
 Wells, W. H., 109
 Wheeler, J. A., 80,102,106
 Wick, G. C., 103,109
 Wiegand, C., 279,280
 Wigner, E. P., 71,99,111,188,229,
 289,290,309,456,492
 Wilkins, J. E., 103,107
 Wilkinson, R. G., 234,239
 Williams, J. H., 389
 Wilson, R. R., 101
 Wisconsin, University of, 387
 Wollan, E. O., 389
 et al, 456
 Wu, C. S., 388
 et al, 436,444,448,464,484,494

Z

Zinn, W. H., 188,389
 et al, 397,409,411,415,417,419,
 425,429,435,441,443,461,497

